

**UNCLASSIFIED**

**AD 416474**

**DEFENSE DOCUMENTATION CENTER**

**FOR**

**SCIENTIFIC AND TECHNICAL INFORMATION**

**CAMERON STATION, ALEXANDRIA, VIRGINIA**

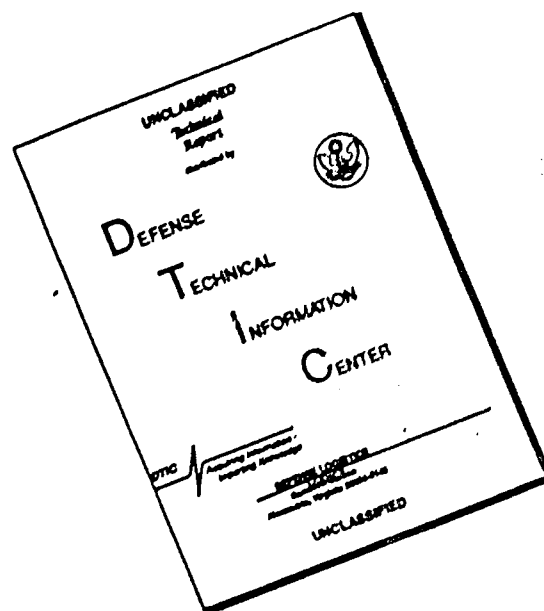


**UNCLASSIFIED**

NOTICE: When government or other drawings, specifications or other data are used for any purpose other than in connection with a definitely related government procurement operation, the U. S. Government thereby incurs no responsibility, nor any obligation whatsoever; and the fact that the Government may have formulated, furnished, or in any way supplied the said drawings, specifications, or other data is not to be regarded by implication or otherwise as in any manner licensing the holder or any other person or corporation, or conveying any rights or permission to manufacture, use or sell any patented invention that may in any way be related thereto.



# DISCLAIMER NOTICE



THIS DOCUMENT IS BEST QUALITY AVAILABLE. THE COPY FURNISHED TO DTIC CONTAINED A SIGNIFICANT NUMBER OF PAGES WHICH DO NOT REPRODUCE LEGIBLY.

416474  
— CATALOGED BY DDC  
AS AD 113.  
416474

PROCEEDINGS OF THE ARMY CONFERENCE ON

## **DYNAMIC BEHAVIOR OF MATERIALS AND STRUCTURES**

held at

Springfield Armory

Springfield, Massachusetts

26-28 September 1962

With Abstract Supplements of Symposia

on

STRUCTURAL DYNAMICS UNDER HIGH IMPULSE LOADING

and

DYNAMIC BEHAVIOR OF MATERIALS



Engineering Sciences Division

U. S. ARMY RESEARCH OFFICE—DURHAM

Durham, North Carolina

PROCEEDINGS  
ARMY CONFERENCE  
ON  
DYNAMIC BEHAVIOR OF MATERIALS AND STRUCTURES

Springfield Armory  
Springfield, Massachusetts  
26 -28 September 1962

With Abstract Supplements of  
SYMPOSIUM ON STRUCTURAL DYNAMICS UNDER HIGH IMPULSE LOADING  
17 -18 SEPTEMBER 1962 - DAYTON, OHIO

Co-sponsored by the Aeronautical Systems Division  
and

Office of Aerospace Research

AND

SYMPOSIUM ON DYNAMIC BEHAVIOR OF MATERIALS  
27-28 SEPTEMBER 1962 - ALBUQUERQUE, NEW MEXICO

Co-sponsored by the University of New Mexico  
and

Rocky Mountain District, A. S. T. M.

ENGINEERING SCIENCES DIVISION  
U. S. ARMY RESEARCH OFFICE-DURHAM  
DURHAM, NORTH CAROLINA

## FOREWORD

The area of "Dynamic Behavior of Materials and Structures" has always been one of great interest to Army engineers and scientists. It is important for a better understanding of the design and performance of all Army materiel including guns, armor, explosives, military vehicles, and bridges. A conference on "High Loading Rate" was conducted in March 1959 by Mr. James J. Murray at the Army Research Office-Durham. In 1961 a group of Army engineers, during a meeting of "Operation Crossfire" conducted by this office, unanimously voiced the necessity for a meeting on dynamic behavior. As a result, the 1962 conference on this subject was held at Springfield Armory.

In its role of responsibility for Army scientific symposia, the Army Research Office-Durham organized the conference for the benefit of all Army scientific agencies. Participation from academic institutions and industry was obtained. More than one hundred and fifty participants from Government, universities, and industry attended the conference.

The Army Research Office-Durham is most appreciative to Springfield Armory for acting as host for the conference, and for the excellent arrangements which were made. Special mention should be made of the efforts of Dr. Alexander Hammer and his Commanding Officer, Colonel C.L.P. Medinnis. Dr. Sudhir Kumar of this office acted as General Secretary of the conference, and has edited these proceedings. Thanks are also due Messrs. J.N. Crenshaw, Harry O. Huss, Frederick J. Lindner, J. Nelson Daniel, Charles J. Kropf, Joseph I. Bluhm, and Robert E. Weigle for serving on the Planning Committee of the conference.

We are grateful for the special addresses presented by The Honorable Finn J. Larsen, Major General F.H. Britton, Major General Alden K. Sibley, and Dr. L.W. Wallace. Finally, I should like to thank all the authors and participants for the high technical standards which made the conference a success.

*Nils M. Bengtson*  
NILS M. BENGTSON  
Colonel, GS  
Commanding

## PREFACE

The Army Conference on Dynamic Behavior of Materials was held at the Springfield Armory, Springfield, Massachusetts on 26-28 September 1962. It was sponsored and conducted jointly by the Army Research Office-Durham and Springfield Armory.

As desired by the Planning Committee, this conference was held with emphasis on design criteria. However, a cross fertilization of different disciplines with common interest in dynamic behavior of materials, was considered desirable. With this in mind, the session headings were kept quite general so as to accommodate different points of view. Active participation from all quarters of the Army both as authors and attendees was obtained. As many as 156 attendees took part in the conference.

Unfortunately, due to an accident, Dr. G.G. Quarles, the programmed General Chairman of the Conference, could not come and the undersigned filled in for him, and opened the conference on Wednesday, September 26th. The Keynote Address was then given by Major General F.H. Britton on U.S. Army Materiel Command Headquarters Organization. Five half day sessions, three in the mornings and two in the afternoons were held. Banquet gathering with an address by Honorable Dr. Finn J. Larsen on "Materials Research", two luncheon gatherings with addresses by Major General Alden K. Sibley and Dr. L. W. Wallace on "R & D for Army Mobility" and "Managerial Environment" respectively, highlighted the social gatherings. Ample time for individual discussion of papers was also provided after their presentations. Several movies on technical topics were shown as part of some paper presentations.

The program of the Conference was as follows:

### WEDNESDAY, SEPTEMBER 26

0800	Registration	
0900	Welcome by Commanding Officer, Springfield Armory, Springfield, Massachusetts	Dynamic Lower Yield Stress Versus Temperature Relationship
	COLONEL C. L. MEDINNIS	WILLIAM GRIFFEL, Picatinny Arsenal, Dover, New Jersey
0915	Introduction of Keynote Speaker	Instrumentation for Evaluation of Artillery and Rocket Launcher Performance at Rock Island Arsenal
	COLONEL NILS M. BENGTSON Commanding Officer, U.S. Army Research Office-Durham Durham, North Carolina	A.C. HANSON, Rock Island Arsenal, Rock Island, Illinois
	Keynote Address	Effects of Shock Waves on Underground Structures - a Survey of the Fundamental Problem
	MAJOR GENERAL F. H. BRITTON Director of Research and Development, Army Materiel Command	DIETRICH E. GUDZENT, U.S. Army Ordnance Missile Support Agency, Redstone Arsenal, Alabama
1000	Coffee Break	
1030	Remarks by DR. G.G. QUARLES, Chief Scientific Advisor, Office, Chief of Engineers, Washington, D.C., General Chairman of the Conference, followed by Introduction of Session Chairmen	1200 Lunch
	SESSION I - Problem Areas	1245 Introduction of Luncheon Speaker
	CHAIRMAN - MR. JOSEPH CRENSHAW, Dynamicist, U.S. Army Ordnance Missile Support Agency, Redstone Arsenal, Alabama	MR. JAMES J. MURRAY, Director, Engineering Sciences Division, U.S. Army Research Office-Durham, Durham, North Carolina
	CO-CHAIRMAN - MR. NELSON DANIEL, Chief, Systems and Equipment Division, Aviation Directorate, U.S. Army Transportation Research Command, Fort Eustis, Virginia	Luncheon Address
		MAJOR GENERAL ALDEN K. SIBLEY Commanding General, U.S. Army Mobility Command, Detroit Arsenal, Centerline, Michigan
1040	Some Problems Involved in Testing Materials at High Strain Rates	
	ULRIC S. LINDHOLM, Senior Research Engineer, Southwest Research Institute	

1330

SESSION II - Design Criteria

CHAIRMAN - DR. ALEXANDER HAMMER, Chief,  
Mechanical Research Branch, Springfield  
Armory, Springfield, Massachusetts

CO-CHAIRMAN - DR. HERMAN P. GAY, U.S. Army  
Ballistic Research Laboratories, Aberdeen  
Proving Ground, Maryland

Study of Shock and Vibration Effects on Vehicles Through  
Dynamic Simulations

FRED PRADKO, S. HEAL, and V. KOWACHEK, U.S.  
Army Tank Automotive Center, Detroit  
Arsenal, Centerline, Michigan

Rolled Armor Steel Brittle Fracture Temperatures and Design  
Significance

V.H. PAGANO, U.S. Army Tank-Automotive Center,  
Detroit Arsenal, Centerline, Michigan

Dynamic Stress Concentration Factors

RICHARD SHEA, Watertown Arsenal, Watertown, Massa-  
chusetts

1445 Coffee Break

1515 The Dynamic Behavior of Supercritical-Speed Shafts

JOHN E. VOORHEES, C.C. MELLOR, and  
R.G. DUBENSKY, Battelle Memorial Institute,  
Columbus, Ohio

Dynamic Response of Military Bridges

L.T. W. GENE CORLEY, Fort Belvoir, Virginia

Structural Design Criteria for Military Vehicles

CLARENCE WINFREY, Detroit Arsenal, Centerline,  
Michigan

1700 - 1830 Social Gathering

THURSDAY, SEPTEMBER 27

0900

SESSION III - Design Criteria

CHAIRMAN - MR. CHARLES J. KROPP, Army Tank-  
Automotive Center, Detroit Arsenal,  
Centerline, Michigan

CO-CHAIRMAN - MR. HARRY O. HUSS, Assistant to  
Chief Engineer, CBR Engineering Group,  
U.S. Army Edgewood Arsenal, Maryland

The Effect of High Rate Loading on the Mechanical Properties  
of Ordnance Materials

ALEXANDER HAMMER and HUBERT CADLE, Spring-  
field Armory, Springfield, Massachusetts

Determination of Yield Strengths of Engineering Materials at  
High Loading Rates

EARL H. ABBE, Springfield Armory, Springfield,  
Massachusetts

Explosive Deformation of Beams

E.N. CLARK, F.H. SCHMITT, and D.G. ELLINGTON,  
Picatinny Arsenal, Dover, New Jersey

1015 Coffee Break

1045 Photothermoelastic Determination of Gun Tube Stresses Due to  
Repetitive Firing

L.T. L.G. MILLKE and T.F. MACLAUGHLIN, Watervliet  
Arsenal, Watervliet, New York

Comparative Fanning Techniques for Titanium Helmet

HELEN AGEN, U.S. Army Quartermaster Research and  
Engineering Center, Natick, Massachusetts

1200 Lunch

1245 Introduction of Luncheon Speaker

DR. ALEXANDER HAMMER, Chief, Mechanical Re-  
search Branch, Springfield Armory,  
Springfield, Massachusetts

Luncheon Address

DR. L.W. WALLACE, Conference Leader, Top Manage-  
ment Seminar, OMET, Rock Island Arsenal,  
Rock Island, Illinois

SESSION IV - Instrumentation and Techniques

CHAIRMAN - DR. REINIER BEEUWES, JR., U.S. Army  
Materials Research Agency, Watertown  
Arsenal, Watertown, Massachusetts

CO-CHAIRMAN - MR. JOSEPH I. BLUHM, Watertown  
Arsenal, Watertown, Massachusetts

1330 Experimental Dynamics of Materials

GEORGE GERARD, Director of Engineering Sciences,  
Allied Research Associates, Inc., Boston,  
Massachusetts

A Method for Rapid Dynamic Evaluation of Large Weapon  
Components

THOMAS F. MACLAUGHLIN and JOHN P. PURTELL,  
Watervliet Arsenal, Watervliet, New York

Tensile Impact on Rubber and Nylon

MALCOLM N. PILSWORTH, JR., U.S. Army Quartermaster  
Research and Engineering Center, Natick,  
Massachusetts

1445 Coffee Break

1515 High Loading Rate Testing Machine; Development and  
Typical Materials Test Applications

T.M. ROACH, Picatinny Arsenal, Dover, New Jersey

A Medium-Speed Tensile Testing Machine

A.G.H. ANDERSEN, Watertown Arsenal, Watertown,  
Massachusetts

A New Concept for Studying Pressure Vessel Configurations  
Under Very High Pressures and Loading Rates

T.E. DAVIDSON and D.P. KENDALL, Watervliet Arsenal,  
Watervliet, New York

1900 Banquet

Toastmaster of the Evening

DR. RICHARD WEISS, Director, U.S. Army Research Office,  
Washington, D.C.

Banquet Address

DR. FINN J. LARSEN, Assistant Secretary of the Army  
(Research and Development)

0830

SESSION V - Fundamental Studies

CHAIRMAN - DR. ROBERT E. WEIGLE, Chief Scientist, Watervliet Arsenal, Watervliet, New York

CO CHAIRMAN - DR. S. DAVID BAILEY, Director, Pioneering Research Division, U.S. Army Quartermaster Research and Engineering Center, Natick, Massachusetts

Dynamic Behavior of Rock Under Confining Pressure

FRED A. DONATH, Associate Professor of Geology, Columbia University

Prediction of Metal Reaction to High Rate Loading from Standard Stress Strain Curves (U)

C.M. GLASS, R.B. POND, U.S. Army Ballistic Research Laboratories, Aberdeen Proving Ground, Maryland

Response of Cylindrical Shells Exposed to External Blast Loading (U)

WILLIAM J. SCHUMAN, U.S. Army Ballistic Research Laboratories, Aberdeen Proving Ground, Maryland

0945 Coffee Break

1015 Photoelastic Studies of Dynamic Stresses in Low Modulus Materials

DR. P.D. FLYNN, J.T. GILBERT, and A.A. ROLL, Frankford Arsenal, Philadelphia, Pennsylvania

A Method for the Study of the Dynamic Response of High Strength Materials

FRANCIS B. PACA, U.S. Army Engineer Research and Development Laboratories, Fort Belvoir, Virginia

Response to Thrust Buildup

J.N. CRENSHAW, U.S. Army Ordnance Missile Support Agency, Redstone Arsenal, Alabama

1200 End Conference

These proceedings have been edited quite carefully, however, there may still be several oversights and shortcomings, for which the Editor accepts full responsibility. For reasons of economy these proceedings were published at this office.

It is a pleasure to express our gratitude to Dr. Alexander Hammer, without whose untiring efforts this conference could not have been held so efficiently. We are also very appreciative of the help rendered by the members of the Planning Committee and the Review Committee and the many other individuals without whose help this conference could not have been possible.

In this volume, there is included in addition to the proceedings of this Army Conference a supplement of abstracts of papers, presented almost simultaneously at two other important conferences on the same subject. The three conferences were held in distant locations of the country for different audiences. While, there may be several participants who attended more than one conference, a large percentage could not, and it was felt desirable to have this consolidated presentation. For this reason a list of participants of the ASTM conference and a list of invitees (list of participants could not be supplied to us by the organizers) of the Air Force Conference have also been included. Acknowledgement and thanks are due to The Aeronautical Systems Division, the Office of Aerospace Research, University of New Mexico and The American Society of Testing Materials for making this material available and for granting permission to reproduce it.

*S. Kumar*

Engineering Sciences Division  
ARMY RESEARCH OFFICE(DURHAM)

SUDHIR KUMAR  
General Secretary of the Conference  
and Proceedings Editor

## TABLE OF CONTENTS

	PAGE
Forward	
Nils M. Bengston.....	II
Preface	
Sudhir Kumar.....	III
 <u>Special Addresses</u>	
Keynote Address - U. S. Army Materiel Command	
Headquarters Organization	
Major General F. H. Britton	
Director of Research and Development	
Army Materiel Command.....	I
Luncheon Address - Research and Development for Army	
Mobility	
Major General Alden K. Sibley	
Commanding General, U. S. Army	
Mobility Command, Detroit Arsenal.....	71
Banquet Address - Materials Research	
Dr. Finn J. Larsen	
Assistant Secretary of the Army	
(Research and Development).....	411
 <u>Technical Papers</u>	
Some Problems Involved In Testing Materials	
At High Strain Rates	
Ulric S. Lindholm.....	14
The Effect Of Static And Dynamic Loading And	
Temperature On The Yield Stress Of Iron And Mild	
Steel In Tension And Compression	
William Griffel.....	43
Instrumentation For Evaluation Of Artillery And	
Rocket Launcher Performance At Rock Island Arsenal	
J. C. Hanson.....	49
The Propagation Of Shock Waves Induced By	
Underground Explosions.	
Dietrich E. Gudzent.....	61



Study Of Shock And Vibration Effects On Vehicles Through Dynamic Simulations F. Pradko, S. Heal and V. Kowachek.....	81
Rolled Armor Steel Brittle Fracture Temperatures And Design Significance Victor H. Pagana.....	107
Dynamic Stress Concentration Factors Richard Shea.....	132
The Dynamic Behavior of Supercritical-Speed Shafts John E. Voorhees, C. C. Mellor, Jr. and R. G. Dubensky....	150
Dynamic Response Of Military Bridges W. G. Corley.....	170
Structural Design Criteria For Military Vehicles C. H. Winfree.....	198
The Effect of High Rate Loading On The Mechanical Properties Of Ordnance Materials Alexander Hammer and Hubert Cadle.....	222
Determination Of Yield Strengths Of Engineering Materials At High Loading Rates Earl H. Abbe.....	242
Explosive Deformation Of Beams E. N. Clark, F. H. Schmitt and D. G. Ellington.....	251
Thermal Stresses Arising In Gun Tubes During Repetitive Firing Lt. L. G. Mielke and T. F. MacLaughlin.....	290
Comparative Forming Techniques For Titanium Helmets Helen E. Agen.....	304
Introductory Comments By the Chairman, Session IV R. Beeuwkes.....	312
Experimental Dynamics Of Materials George Gerard.....	313

A Method For Rapid Dynamic Evaluation Of Large Weapon Components T. F. MacLaughlin and J. P. Purtell.....	315
Tensile Impact On Rubber And Nylon Malcolm N. Pilsworth, Jr.....	328
High Loading Rate Testing Machine, Development And Typical Materials Testing Applications T. M. Roach, Jr. ....	341
A Medium-Speed Tensile Testing Machine And Its Performance In Testing Of Some Ordnance Materials Dr. A. G. H. Andersen.....	359
A New Concept For Studying Pressure Vessel Configurations Under High Pressures And Loading Rates T. E. Davidson and D. P. Kendall	
Dynamic Behavior Of Rocks Under Confining Pressure Fred A. Donath.....	416
Correlation Of High Loading Rate Reactions With Low Rate Tests In Metals Coy M. Glass.....	438
Response Of Cylindrical Shells Exposed To External Blast Loading William J. Schuman, Jr. ....	454
Photoelastic Studies Of Dynamic Stresses In Low Modulus Materials P. D. Flynn, J. T. Gilbert and A. A. Roll.....	469
A Proposed Method For The Study Of The Dynamic Strength Of High Strength Materials Francis B. Paca.....	495
Structural Response To Missile Thrust J. N. Crenshaw.....	506
Abstracts From the Symposium On Structural Dynamics Under High Impulse Loading.....	516
Projection Techniques J. W. Gehring.....	517

Defects In Solids At High Velocities	
A. N. Stroh.....	517
Wave Propagation In Uniaxial Strain	
John H. Percy.....	518
Static Fracture	
George R. Irwin.....	518
Time Dependent Fracture	
C. C. Hsiao.....	519
Some Problems In Dynamic Response Of Two-Dimensional Structures	
W. H. Hoppmann II.....	519
Hypervelocity Impact Status Of Experiments	
Walter Herrmann .....	519
Dynamic Properties Of Matter Under High Stress- Thermodynamic Descriptions	
Harold L. Brode.....	520
Dynamic Analysis In Viscoelastic Media	
R. J. Arenz.....	520
Spall Fracture	
C. D. Lundergan.....	521
Uniaxial Stress Conditions	
Gordon L. Filbey, Jr.....	521
Oriented Solids	
J. L. Ericksen.....	522
Dislocation Concepts Of Strain Rate Effects	
J. E. Dorn and Frank Hanser.....	522
Abstracts From The Symposium On Dynamic Behavior Of Materials.....	523
High Speed Tensile Testing Of Selected Polymers	
R. R. Cosner.....	524
High Speed Compression Testing Of Thermoplastics	
Richard E. Ely.....	524

Impact Performance Of High Strength HT-1 And Nylon Parachute Materials To Mach 0.7 Robert J. Coskren, Chauncey C. Chu and Henry M. Morgan...	525
Report On Round Robin Testing Of Thermoplastics Gordon D. Patterson, Jr.....	525
An Investigation Of The Dynamic Mechanical Properties Of Polyethylene S. Matsuoka and C. J. Aloisio.....	526
The Behavior Of Filamentous Materials Subjected To High-Speed Tensile Impact Jack C. Smith.....	526
Production Of Strong Shocks In Plastics By Ultra-Short Impulsive Loading Arthur H. Guenther.....	527
Experiments On The Mechanism Of Spall Donald W. Blincow and Donald V. Keller.....	527
On Experimental Solid Dynamics George Gerard, Ralph Papirno and Herbert Becker.....	528
On The Measurement Of Dynamic Stress-Strain Curves With A Uniform Uniaxial Stress System P. C. Johnson, B. A. Stein and R. S. Davis.....	528
The Metallurgical Effects Of Explosive Straining Of Selected Metal Alloys Louis Zernow, Irving Lieberman, John Wilkin and Erik Henriksen.....	529
Theoretical Prediction Of Strain Distribution Under Impact Loading S. Rajnak, F. Hauser, and J. E. Dorn.....	530
Plastic Impacts On Short Cylindrical Specimens E. A. Ripperger and C. H. Karnes.....	530
The Three Low Pressure Spall Thresholds In Copper J. H. Smith.....	531
A Submicrosecond Technique For Simultaneous Observation Of Input and Propagated Impact Stresses W. J. Halpin, O. E. Jones and R. A. Graham.....	532

Fracture Of Single Crystals Under Explosive Loading C. M. Glass, S. K. Golaski and J. J. Misey.....	532
Residual Temperatures Of Shock-Loaded Iron R. G. McQueen, E. Zukas and S. Marsh.....	533
List Of Participants U. S. Army Conference On Dynamic Behavior Of Materials And Structures.....	534
List Of Invitees Symposium On Structural Dynamics Under High Impulse Loading.....	539
List Of Registrants Symposium On Dynamic Behavior Of Materials.....	548
Closing Comments By General Chairman, Dr. Sudhir Kumar.....	553

Keynote Address

U. S. ARMY MATERIEL COMMAND HEADQUARTERS ORGANIZATION

Major General F. H. Britton  
Director of Research and Development  
Army Materiel Command

May I express my thanks to Colonel C. L. Medinnis for his welcome and to Colonel Nils M. Bengtson for his kind introduction. Both are to be congratulated on co-sponsoring this conference which I believe will enhance the reputation of our Army laboratories, particularly those in the commodity commands.

The gentlemen who will speak to you during the course of this conference represent several disciplines in science and engineering. Most speakers come from Army laboratories. This is an admirable feature and helps in improving the coherency of our Army endeavors. The contributions of the speakers from our contractors and university associations add breadth and vision to the whole program.

The Planning Committee headed by Dr. Alexander Hammer has brought together design engineers and scientists who are working in the field of dynamic loading. This approach is a praiseworthy one and we hope that many more conferences of this sort will follow where Army engineers and scientists will mingle and exchange ideas about our needs and possible solutions.

The opportunity of participating in this conference on "Dynamic Behavior of Materials and Structures" offers an occasion to explore with you the dynamic changes in management resulting from the reorganization of the Army.

As all of you know, 1961 and 1962 have been years of great change for the Army. Weapons have become more and more complex and costly. Management of their research, development and production calls for new approaches so that cost, over-runs, reliability failures and schedule slippages will be sharply reduced and a better program balance achieved. The impetus for this increased attention to the management problems has come from Secretary McNamara. I believe a review of these changes will interest you.

One of the study projects which was assigned to the Army by Secretary McNamara was "Project 80," on the Army organization. Mr. L. W. Hoelscher, Deputy Comptroller of the Army undertook the study and was assisted by a team of Army officers and civilian employees. It was, as Secretary Iglaricus has pointed out "a critical self-examination of the Army, by the Army." The sweeping changes recommended by the Project 80 study group, and approved by the Secretary of the Army and the Secretary of Defense, thus take on more significance, perhaps than would have been the case had they been made by an outside group, unfamiliar with all the traditions and nuances of the way in which the Army works.

The changes which the Hoelscher Committee recommended in the organization of the materiel side of the Army are the most dynamic and certainly the ones of greatest interest to this audience.

First and foremost the Hoelscher Committee recommended that the materiel functions of the several technical services -- Engineers,\* Ordnance, Signal, Chemical, Quartermaster, and Transportation should be transferred to a new single command, with the commander reporting directly to the Chief of Staff and the Secretary of the Army. Even if this had been the only change recommended by the Hoelscher Committee, it would have been revolutionary for the technical services, which were so long a part of the Army picture, going back in some cases to the origins of the national government.

Essentially in the old system, complete integration among the technical services on the difficult task of weapons acquisition, development and production, was time consuming. In an aircraft, for example, the Transportation Corps had responsibility for the air frame, the Signal Corps for the electronics gear and Ordnance for any armament the plane carried. There was almost no large modern weapon systems that fell wholly within the technical bounds of a single technical service. Usually several were involved. And while primary responsibility was typically assigned to a specific technical service the problems of coordination were found to be acute. In addition, the division of authority between DCSLOG and CRD, also created some problems. It is seldom in a large modern weapon system, that we can draw a clear line between development and production of a system, and the transition period from development to production is often a critical phase in the life cycle of a weapon.

Coordination problems among the technical services and the problem of divided responsibilities between the development and procurement phase of a weapon system led many observers to the belief that the "lead-time" on Army weapons was excessive, that in some cases costs were higher

---

\* Not including the civil functions

than necessary, and that performance, once in the field, was not always equal to the needs of combat personnel. Briefly stated, such factors led the Hoelscher Committee to recommend a unified Army Materiel Command.

#### ORGANIZATION OF ARMY MATERIEL COMMAND

The headquarters organization of the Army Materiel Command is shown in Figure 1.

Within headquarters there is a strong supporting staff that can relieve the Department of Army staff personnel of much of the day to day activity that they have been forced to conduct in the past. This should permit the Army headquarters staff to focus increasingly on long-range plans, programs and policies. Also included is the Research and Development Directorate about which I will say more later.

#### AMC COMPTROLLER AND DIRECTOR OF PROGRAMS

Now let me direct your attention to the Office of the Comptroller and Director of Programs. This office, under General Bunker, combines two functions that are often separated in large organizations. We believe that the two functions of Programming and Funding belong together, and that their combination in this single office will add considerable strength and cohesiveness to the direction and control of operations.

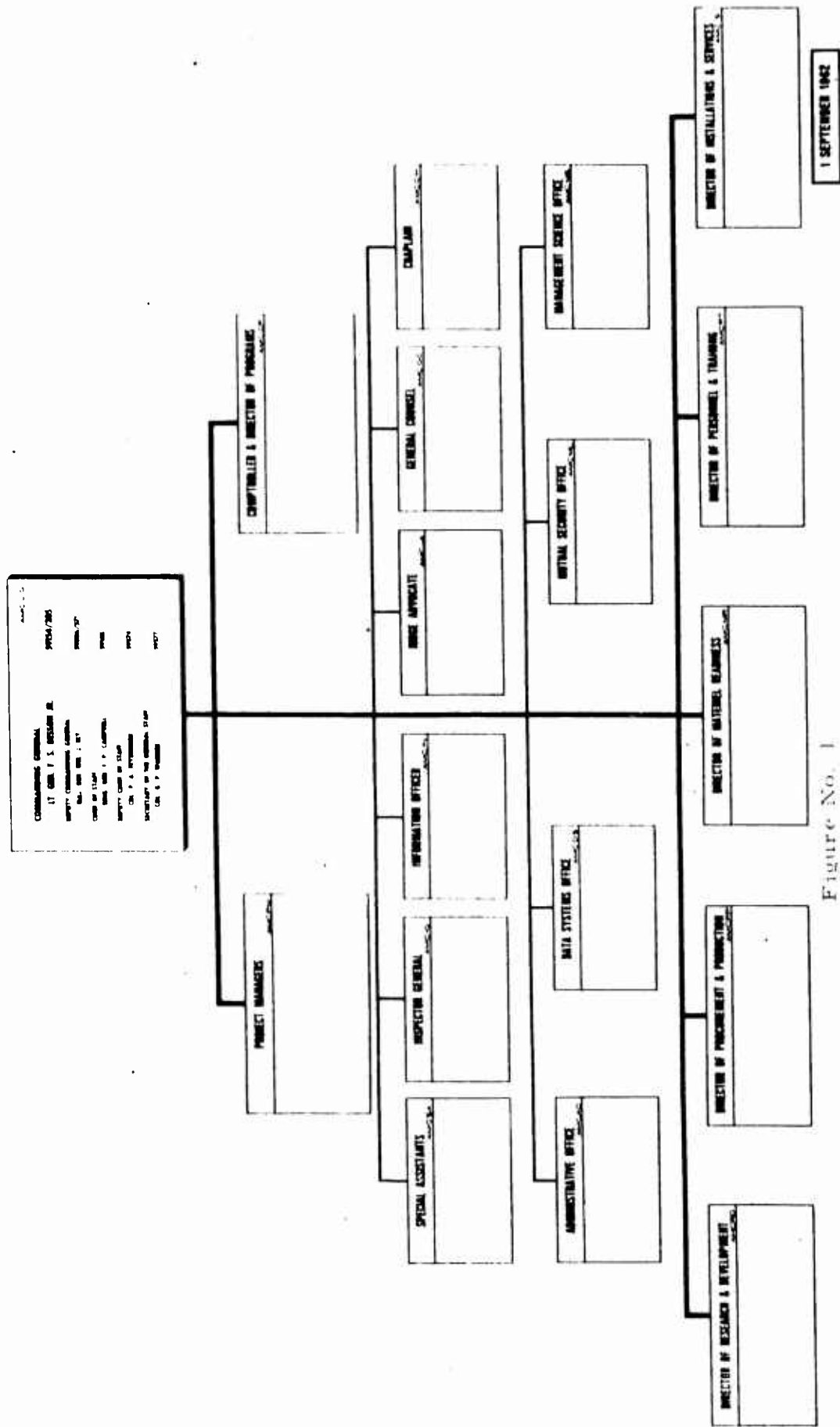
#### AMC PROJECT MANAGERS

Here we have "Project Managers." There are currently around thirty (30) large dollar value or critical programs that can be identified. These 30 some programs are a minute fraction of the total number of items which will be handled by AMC, but involve a large fraction of the funding. It is clear that if AMC is to discharge its overall mission satisfactorily, these programs must receive a major share of our attention and must be vigorously and effectively managed. For this purpose we have established as an integral part of the AMC structure a system of Vertical Program Management that will be applied to these programs. It should be stressed that this vertical management structure is basic to the concept under which AMC was established. It was not something hastily superimposed on a functional organization. It is, and will continue to be the main management pattern for about half of our total resources.

Before turning to a discussion of how this project management system works and how it interfaces with the AMC functional organization, let us try to define more precisely what we mean by vertical project management.



# HEADQUARTERS, U.S. ARMY MATERIEL COMMAND



This term means the vesting in a single individual, group or organization, of the sole line authority and responsibility for accomplishing the objectives of a program. The individual is charged exclusively with the accomplishment of his program objective and his attention and effort are not divided among a host of other tasks and programs.

Three things essentially identify the project manager approach. In the first place, he has an adequate project staff assigned to his immediate office and responsive directly to him. This staff consists in part of technical personnel who can follow the main problems of the weapon (whether they be developmental or production) and who can initiate proposals for solving technical problems, subject to approval by the project manager. The technical personnel will in addition initiate the technical development plan. The project manager also has a management or administrative staff immediately responsive to the needs of the project in such areas as programming, budgeting, financial management and the like. The project manager works closely with AMC staff in the programming and budgeting of the overall R&D program because he must participate in husbanding the resources of the Army.

A second feature of a project-oriented organizational structure is the fact that the project manager controls the dollar resources allotted to his project. These funds, plus his authority over a specific project, means that the project manager can "buy" a substantial amount of support and assistance, both from in-house laboratories and installations, and from contractors.

A third feature of project management in AMC is that each manager can communicate directly with the Commanding General of AMC.

#### COMMODITY AND OTHER COMMANDS

AMC has five commodity commands, a Supply and Maintenance Command and a Test and Evaluation Command as outlined in Figure 2. The Commands represent a regrouping of the former technical services along commodity lines. Thus the Missile Command replaces, on a somewhat expanded basis, the former Army Ordnance Missile Command at Huntsville, and has also been assigned Watertown Arsenal production facilities. Major General Francis J. McMorro is the Commanding General. Responsibilities include free rockets, guided missiles and associated equipment.

The Electronics Command under Major General Stuart S. Hoff at Ft. Monmouth includes among its responsibilities communications, electronic

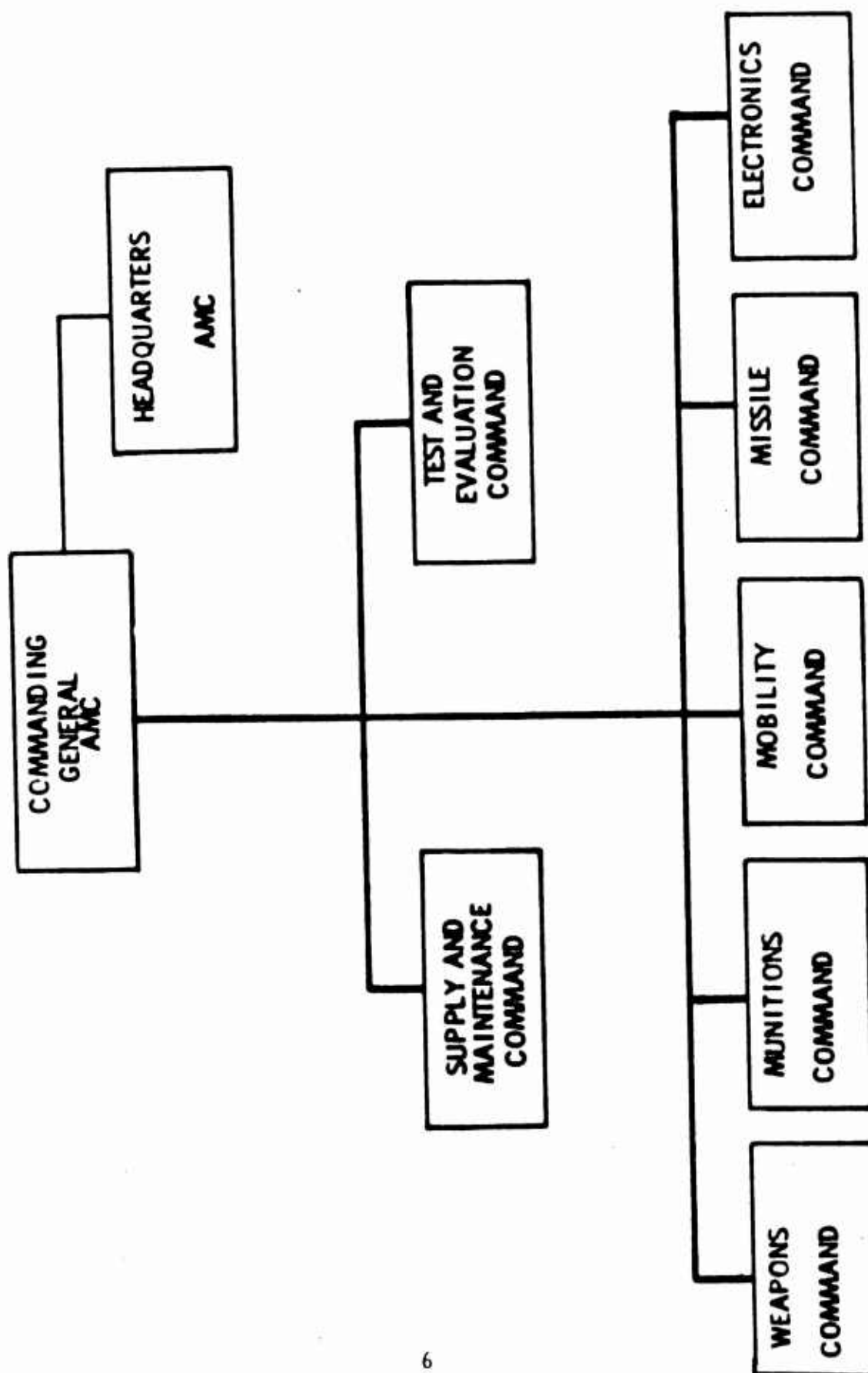


Figure No. 2

warfare, combat surveillance, automatic data processing, radar and meteorological materiel.

The Mobility Command at Detroit under the direction of Major General Alden K. Sibley is quite complex. Here responsibilities include among others, air and surface mobility, power generation, construction, barrier and bridging equipment, and general purpose vehicles.

The Munitions Command under Major General William K. Ghormley combines the Army Chemical Center, Fort Detrick, CBR Agency with Frankford and Picatinny Arsenals and Joliet, Pine Bluff and Rocky Mountain Arsenals, etc. Nuclear and non nuclear ammunition, rocket and missile warheads, chemical biological and radiological materiel and pyrotechnics are among the responsibilities of this command.

The Weapons Command at Rock Island under Major General Nelson M. Lynde, Jr. is assigned Watervliet and Rock Island Arsenals and Springfield Armory. Its responsibilities are specialized on small arms, gun type weapons and systems.

The Test and Evaluation Command under Brigadier General William F. Ryan is located at Aberdeen Proving Grounds. Activities include field engineering, service production and surveillance tests and evaluations, and supervision of troop tests conducted by the Combat Developments Command or CONARC.

The Supply and Maintenance Command in Washington, D. C. is under Lt. General A. Schomburg. It combines many functions of the Army through the wholesale level. Involved are stock control, storage, distribution, depot maintenance, transportation and disposal of Army controlled materiel and supplies.

The Commodity Commands undertake development, engineering, production planning and production work. In addition all commodity commands have laboratories where research directly associated with the respective commodity is accomplished. Where a capability already exists in the research area, and has been utilized by all Army agencies, it is expected that this capability will continue to be maintained and to be improved in quality for the betterment of the Army endeavor. A single example might be mentioned, namely the nonferrous capability at Frankford Arsenal in the Munitions Command. This is an important and nationally recognized endeavor useful to all Army Commands. There are many other examples but in order to save time I will not discuss them further.

## RESEARCH AND DEVELOPMENT DIRECTORATE

Returning now to the R&D Directorate of Headquarters Army Materiel Command, the Directorate consists of four divisions or offices as shown in Figure 3. They are as follows:

Research Division under Brigadier General J. G. Zierdt with responsibility for formulating and supervising all basic and applied research programs and directing seven Army laboratories.

Development Division under Brigadier General W. G. Merriam with responsibilities for directing and supervising the plans and activities of the Research and Development Directorate that translates the output of research into militarily useful components and end items of equipment.

Plans and Policy Division under Colonel J. W. Baum with responsibilities for formulating the Army Materiel Command Research and Development policy and plans and for evaluating program progress.

Technical Intelligence Office under Colonel J. T. H. Spengler with responsibilities for obtaining, producing and distributing technical intelligence.

There are several important factors which will interest you and should not be overlooked.

First of all, under the Research Division, there are seven Independent Army Laboratories as shown in Figure 4.

Each is a Class II activity although the program of the Coating and Chemical Lab is managed by AMRA. AMRA in addition is assigned the Watertown Arsenal Laboratories and the Materials Research Laboratory.

These Independent Army Laboratories are not associated with a specific commodity command but work in areas which cover important Army-wide requirements. They can however provide support to the Commodity Commands working in many areas of direct interest to them. In this respect their work might be considered as a contractor type operation for the commodity command concerned.

Research which is directly associated with a commodity area will be accomplished in Laboratories or Agencies within the commodity commands. The part of the activity in these commodity command laboratories, which

# DIRECTORATE OF RESEARCH & DEVELOPMENT

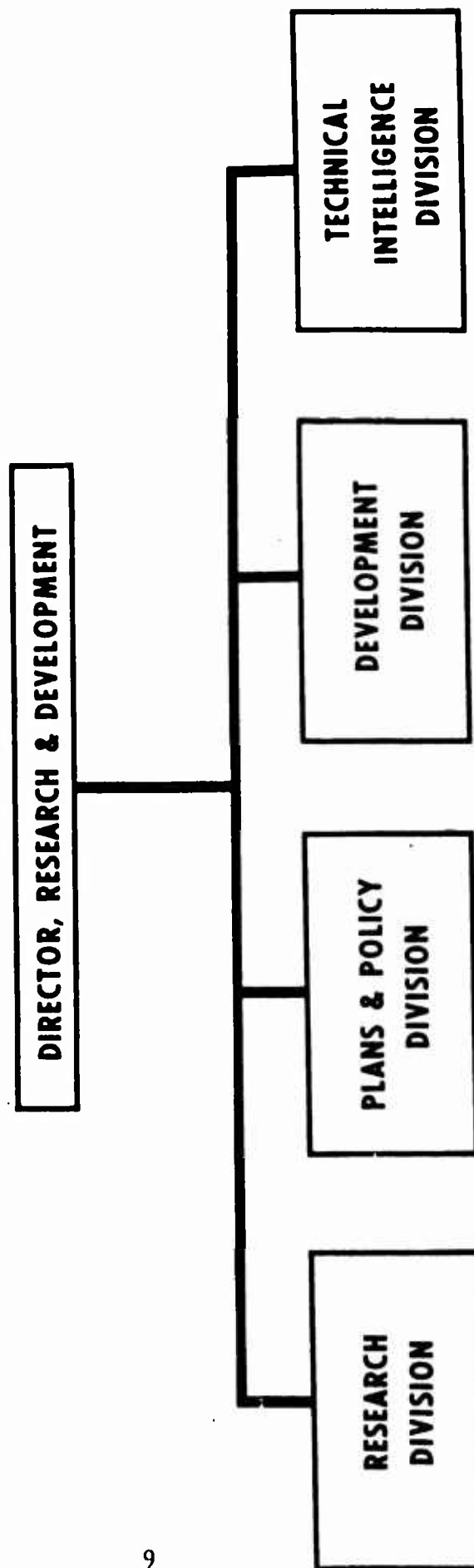


Figure No. 3

## ARMY RESEARCH LABORATORIES

ARMY MATERIALS RESEARCH AGENCY  
WATERTOWN ARSENAL, WATERTOWN 72, MASS.

BALLISTIC RESEARCH LABORATORIES  
ARMSTRONG PROVING GROUND, MD.

COATING & CHEMICAL LABORATORY  
ARMSTRONG PROVING GROUND, MD.

COLD REGIONS RESEARCH & ENGINEERING  
LABORATORIES  
HANOVER, N. H.

DIAMOND FUZE LABORATORIES  
WASHINGTON 25, D. C.

HUMAN ENGINEERING LABORATORIES  
ARMSTRONG PROVING GROUND, MD.

MATICE LABORATORIES  
MATICE, MASS.

Figure No. 4

are Army-wide in scope will also continue as has been previously mentioned.

A second feature is that the research programs of all organizations within the Army Materiel Command, including those of the Independent Laboratories and those of the major subordinate commands are authorized by the Research Division.

A third feature is in the area of materials research. The fields of materials are vast, the number of materials many, the number of independent investigators large and the number of reports immense. Complete coordination is essential. Here a real challenge exists in pulling together the whole activity into the materials program of AMC and integrating the product with the national effort. AMRA will be the focal point for this endeavor.

#### DEVELOPMENT DIVISION

The Development Division AMC will look to the field installations for detailed technical competence. Development as well as research is a necessary step in placing equipment in the hands of the troops, in effective quantities at the appropriate time. Let me here take time to mention with pride the significant contributions which Springfield Armory is making to the combat capability of the U. S. Army. The new family of infantry and tank weapons are examples including the M73 and M85 machine guns, M14 rifle and M79 Granade Launcher. It is important to recognize that these products are developed in-house at Springfield Armory by its own engineers. And I am confident that Springfield Armory and the Weapons Command will continue to bring about not only improvements in component life, reductions in weight and greater reliability but also unique weapons based on new concepts and new principles.

Example outside of Springfield Armory but within the Weapons Command might be cited. At Watertown the results of research at several laboratories including one outside of the Weapons Command, and their contractors were applied to the casting of large gun parts. Improved quality was obtained. This was the reason for the effort, and it was accompanied by not only savings in cost but also savings in production time. At the time the work was done Watertown was part of the Weapons Command.

At Rock Island Arsenal the Research and Development effort in rubber has resulted in the use of polycarboxylic elastomer for forearm, butt stock, pistol grip, cheek pad and carrying handle of the M60 machine gun. The materials were compounded based on research work and pilot production was worked out in-house.



## R&D PLANNING AND TECHNICAL FORECASTING

The facts of life are that it takes from 6 to 40 years after a new discovery to put weapons in the hands of troops that make use of that knowledge. Reduction of this lead time presents us a splendid opportunity in AMC to improve our management. This is in the field of technical forecasting and long range research and development planning. At the present time, the research and development cycle is in a large measure controlled by several factors such as funds, the results of basic and applied research, the quantitative materiel requirements which are established by the Combat Developments Command, the results of feasibility studies, Army war plans, Army capability plans, and the Army long-range development plans. These plans establish objectives and requirements for the Army and indicate certain problems to be solved. During our planning we must keep in mind other factors such as certain key times when advanced technology would indicate a time for introduction of something radically new into our system.

Our problem is to pull all this together, and here is the approach which we will take. We will consider our research program, the in-house work of our laboratories, that of their contacts in the academic world and industry, and the work of the laboratories within the commodity commands, to obtain the primary input for our longer-range technological forecasting. We intend that these laboratories not only participate in actual research, but in the planning for research to meet our objectives.

The commodity commands will provide inputs to our planning in the areas of technological improvements needed in various elements of weapons or equipment systems to meet stated objectives. The DA staff, the Combat Developments Command, and other such agencies will provide inputs such as tactical capability objectives, tactical materiel performance objectives and design objectives which will be required on the battlefield and in concepts of future warfare.

From the intelligence community we expect information and predictions on foreign scientific achievements.

We will weave all of these inputs into a planning matrix and definitively interrelate our development programs for the future with those of the current time frame. We will then be able to establish priorities, and subdivide assets and competence to work in certain predetermined areas.

### CAUTION

This has been a very brief review of the Army Materiel Command's organization for performing research and development, and I have touched briefly on the project managers and our proposed method for long-range research and development planning. However, I think it is only fair to put out here a word of caution.

As I mentioned in the beginning, we are in the act of merging and adjusting the former technical service organizations into this new organization. We are introducing new approaches -- for example our efforts to move out with more critical, specific definitive research and development planning, our establishment of a separate test agency, the separated independent Army laboratories directly under the Headquarters, and the overall control of key projects by the project managers. All of this is going to take time to have its full impact. However, given dedicated people, and the adequate knowledge, with real effort we will meet the objectives which have been established as desirable for the reorganization of the Army. You are assured that the Army Materiel Command will bring to the battlefield those weapons that are needed by our soldiers and which will give us the capability we must have for victory.

## SOME PROBLEMS INVOLVED IN TESTING MATERIALS AT HIGH STRAIN RATES

Ulric S. Lindholm\*

### ABSTRACT

An intensive effort is now being given to the determination of the rate dependence of the deformation of engineering materials. The difficulties associated with obtaining accurate and consistent experimental data on the mechanical response of a material at very high loading rates are becoming better known. These difficulties are primarily associated with inertial effects in the loading mechanism, in the measuring and recording system, and in the specimen itself. Other problems arise from size effects or specimen geometry, in assuring axiality of the loading and the change from isothermal to adiabatic test conditions. Some of these difficulties appear to be surmountable while others are inherent to the problem. A brief review of two typical dynamic testing methods is given in the light of the above-mentioned difficulties. Emphasis is given to methods which yield both instantaneous stress and strain data. The results, in terms of stress vs. strain and stress vs. strain rate, of several investigators are presented. There is a general need for further intensive experimental work aimed at defining basic material behavior.

### INTRODUCTION

The continuing and expanding need for quantitative information on the dynamic strength properties of materials has led to the large amount of experimental work in this area in recent years. However, we still cannot say at this time that the state of the art is such that dynamic material behavior is fully understood. This lack of understanding largely accrues from the inherent difficulties underlying the experimental problem. Although there is general agreement, with exceptions, that the basic material response is altered with changes in the rate of loading or deformation, quantitative information available on the magnitude of these changes is often dependent upon the particular testing technique employed. Recognition of the source of these discrepancies is essential both in designing an experimental test technique and in interpreting the results obtained from a given dynamic test. Most of the problems encountered in

---

\*Dr. Ulric S. Lindholm, Senior Research Engineer, Department of Mechanical Sciences, Southwest Research Institute, San Antonio, Texas

performing dynamic tests have been discussed to varying extent in the literature. It is the purpose of this paper, first, to review these problems and then to discuss two typical test techniques and some of the results obtained. The main emphasis will be on testing at very high rates and on establishing the influence of strain rate in the plastic deformation of metals.

### OUTLINE OF PROBLEM AREAS

Most of the problems associated with testing materials at very high deformation rates are associated, of course, with inertial effects. Inertial effects enter the problem in many ways: in accelerating the loading mechanism, in the ability of particular stress and strain measuring devices to follow the high rate of deformation, in the response time of the recording system, and, perhaps most important of all, in the nonuniform distribution of the variables to be measured over the volume of the specimen. Other items to be considered are the specimen geometry and size (closely related to the last item above), the uniformity of the loading, and the effect of heat generated within the specimen during the loading.

#### Loading Mechanism

As the desired rate of loading increases, the normal static or quasi-static testing machines soon become untenable because the forces required to accelerate the moving parts of the testing machine soon equal and surpass the forces required to deform the specimen, therefore, conventional testing machines have to be abandoned. For the higher strain rates, an impact machine or apparatus of some type is generally employed. There is an intermediate range in strain rates where a pressurized gas or hydraulic system can be employed, head speeds as high as 100 fps. being obtained. Our present discussion however, will consider only the impact type device as being applicable at the highest loading rates.

In impact loading devices, the load is transmitted to the specimen, either directly or indirectly, by a mass accelerated to the desired impact velocity. The manner in which the impact load is coupled to the specimen has been achieved by a variety of techniques. Figure 1 shows four different basic arrangements of the specimen, specimen support, and impacting mass. The large blocks denote assumed rigid masses, whereas the thin rods represent elastic elements (generally cylindrical bars) which may be used as either load transmission or measuring elements or both.

In Figure 1a, the specimen itself is accelerated to strike a rigid

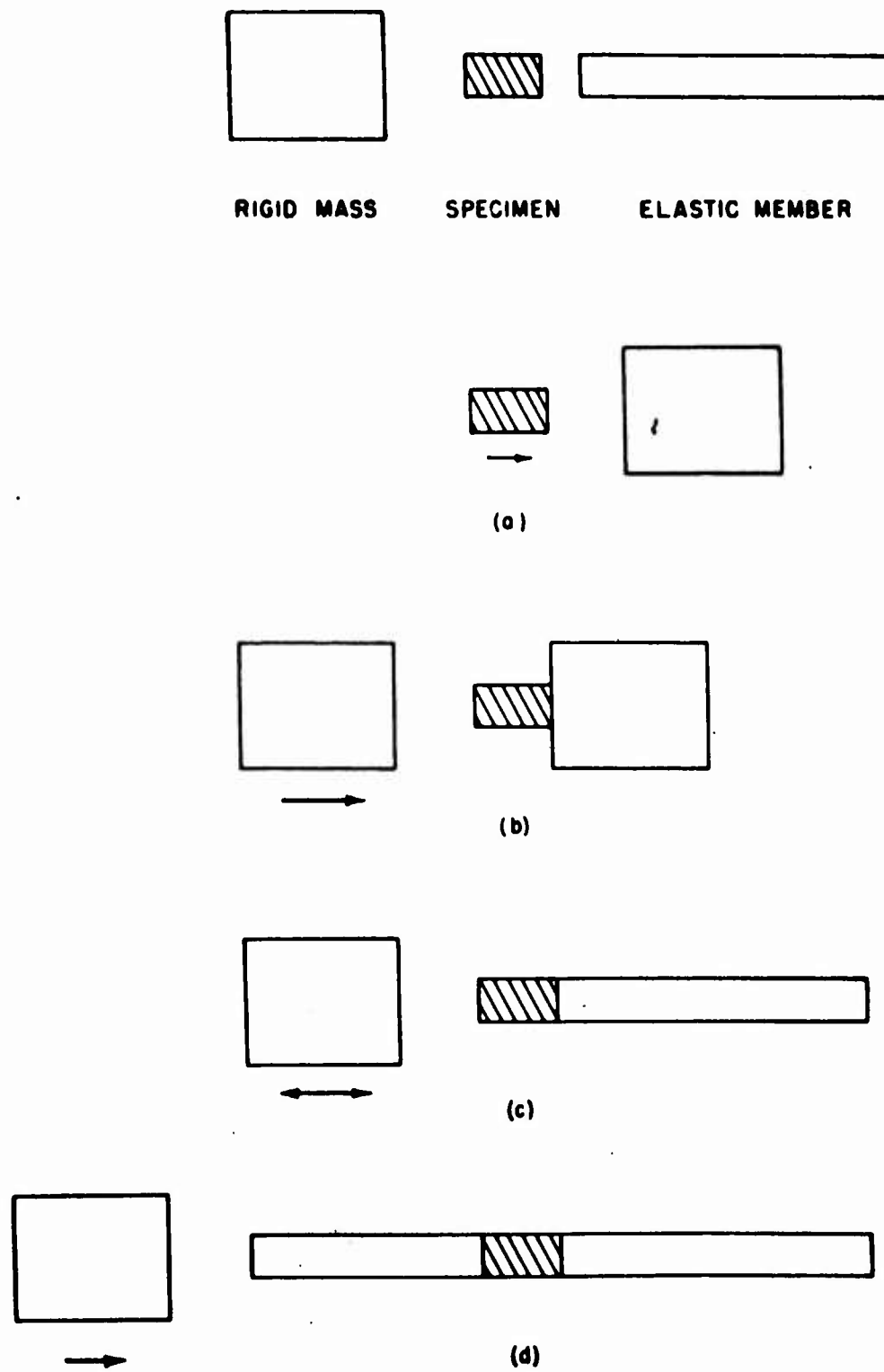


Figure 1. Schematic of impact loading arrangements

mass. This technique was used by Taylor and Whiffin (1)\* to determine dynamic yield stress from measurements of the final deformation in the specimen. Generally this technique has limited applicability because of the difficulty of making transient measurements on the test specimen. In Figure 1b, the test specimen is mounted on a rigid mass and is deformed upon impact from a second mass. Habib (2) has used this method in compression of copper cylinders, indirectly deriving the dynamic stress-strain curve from a large number of measurements of the energy absorbed and permanent deformation in similar specimens subject to varying impact velocities and impact masses. This method requires a large number of specimens to obtain a single stress-strain curve. Volterra, et al. (3) used the system of Figure 1b with the supporting mass suspended as a ballistic pendulum. The same type of arrangement as in Figure 1b and also 1c can be used in tension as well as compression, with the impacting mass moving in the opposite direction and contacting a tip or shoulder on the free end of the specimen. The impacting mass can be swung as a pendulum, as in modifications of the standard Charpy (4) or Izod (5) impact testing machines, or a rotating flywheel can be used (6, 7) to produce the impact.

In Figure 1c, an elastic element has been substituted for support of the specimen. This element is usually a dynamometer or weigh bar of varying length connected in series with the specimen and used to measure load. Arrangements of this type have been used in tension by Mann (6), Clark, et al. (4, 10), Manjoine and Nadai (7, 8, 9), and Baron (4). In compression, Turnbow and Ripperger (11) have utilized a Hopkinson pressure bar as the elastic element, while Alder and Phillips (12) have substituted two glass blocks for the elastic element, measuring the load by the birefringence created in the glass.

For several reasons it can be advantageous to separate the test specimen from the impacting mass by an elastic loading bar as in Figure 1d. This bar can aid in transferring the load uniformly to the specimen and also act as an elastic element in the measuring system. This type of split bar system has been used with various modifications by Kolsky (13), Krafft, et al. (14), Campbell and Duby (15), Hauser et al. (16) and the writer (17). In Kolsky's apparatus the impacting mass is replaced by an explosive charge to initiate the pressure wave in the bars.

---

\* Numbers in parentheses refer to References listed at the end of the paper.

An exception to the above axial impact arrangements is the technique of Clark and Duwez (18) who obtained dynamic loading of thin walled cylindrical specimens by impacting a highly incompressible internally contained fluid column. The cylindrical specimens were thus ruptured by the internal pressure pulse. This type of loading and thin walled specimen was designed in order to minimize wave propagation effects in the specimen. The attempt has also been made to derive information on material properties from measurements of the propagation of plastic deformation in long rods or wires. These methods are based on the plastic wave propagation theory of von Karman (19) and Taylor (20) where the velocity of propagation  $c$  of a strain increment is given by  $c = \sqrt{\frac{1}{\rho} \frac{d\sigma}{d\epsilon}}$ , where  $\frac{d\sigma}{d\epsilon}$  is the slope of the stress-strain curve at the

given strain level and  $\rho$  is the mass density of the material. This is a rate independent theory in that  $d\sigma/d\epsilon$  is taken from the static or an invariant stress-strain curve. Rate dependent properties of the material are thus derived from the use of a rate independent theory, which must lead to some inherent errors. Examples of this method are Campbell (21) and Johnson, Wood and Clark (22).

The problems associated with the loading mechanism are not in obtaining sufficient impact velocity; the impacting mass may be accelerated by means of free fall under gravity, rotating flywheels, spring or gas loaded guns or explosive charges. Rather, the problem lies in being able to fruitfully integrate the loading mechanism with the specimen configuration and the available methods of measuring the desired quantities. Care must also be taken to take into proper account the elasticity and inertia of the loading mechanism.

#### Measurement and Recording Devices

Measuring and recording devices are required which will respond to the fastest loading rates attainable. Thus, many very accurate devices used in static work cannot be employed because of their inherent inertia. The measurement of force is obtained most directly by means of an elastic dynamometer or force measuring bar connected directly in series with the specimen as indicated by the elastic elements in Figure 1. Indirect measurements of force may be obtained from energy (2) or acceleration measurements (3).

The design of a proper force measuring bar requires considerable care. In many cases short bars have been used. The maximum rate of loading that can be measured by the bar is limited by its resonant frequency. For example, if a force bar of 10 inches in length is made of steel, it will

have a resonant frequency of approximately 10,000 cps or a period of 100  $\mu$  sec. The total duration of a test employing this force bar must then be much greater than 100  $\mu$  sec. in order to prevent severe oscillations from occurring in the force records.

If the response for shorter time periods is required, as is the case at the higher strain rates, the length of the force measuring bar must be extended until the period of longitudinal oscillation becomes greater than the total time of the event to be recorded. This type of long force measuring bar is generally referred to as a Hopkinson pressure bar after B. Hopkinson (23) who first used it in impact studies. The length of the bar permits the force history at the loaded end to be completely recorded at a gauge station before a reflection returns from the far end of the bar. Pressure bars as long as 58 feet have been used. The theory of the Hopkinson pressure bar has been described in great detail by Davies (24). This device can be used with good accuracy to measure transients with effective wave lengths large in comparison with the bar radius. For shorter wave lengths, the pulse will suffer significant dispersion.

The force in the elastic dynamometer or pressure bar is usually measured by means of electrical resistance strain gages bonded directly to the bar; however, use has also been made of measuring the displacement of the free end of the bar, both by photoelectric (7) and capacitance gage (13) methods. Strain gages may be used in a bridge circuit so that only the direct stresses are recorded, the bending being cancelled. Many references to the use of resistance strain gages for dynamic measurements can be found in the literature.

Measurement of the instantaneous deformation or strain in the specimen is generally more difficult than stress. As in static testing, two techniques can be used; measurement of strain directly on the specimen or measurement of the motion or displacement of the loading surfaces. Direct measurements on the specimen impose severe difficulties. Mechanical type extensometers are, of course, inapplicable because of their inertia. Resistance strain gages may be bonded directly on the specimen but are limited in range to relatively low values of strain. They have been used, however, to study yield behavior (11). The frequency response of resistance strain gages properly bonded is limited only by their finite gage length. Bell (25) has developed an optical method for measuring plastic strains to 10% using very fine diffraction gratings ruled onto the specimen. This technique, although experimentally very difficult to use, has several advantages; relatively large strains may be measured



and gage lengths as small as 0.001 inch may be used, eliminating integration effects across the gage. Bell has used this technique to advantage in studying wave propagation in long rods. Ripperger and Yeakley (26) have described an electro-magnetic induction method for measuring particle velocities which might be employed to advantage in dynamic testing.

More often, the average strain across the specimen is determined by measurement of the displacement of the loading members. If the loading and support members are assumed rigid, the displacement of these members can be measured by means of streak or high speed photography (2) or photoelectric devices (7). At the highest strain rates, the displacement of the faces of the elastic supporting pressure bars in contact with the specimen can be measured either by integration of the strain-time records from strain gage stations on the bars (15, 16, 17) or directly from particle displacement measurements on the bars (13). This latter method will be described in more detail later.

The cathode ray oscilloscope is the only recording instrument with frequency response sufficient for transient measurements at the rates considered. Here the frequency response is only limited by the associated circuitry and amplifiers.

The choice of suitable stress and strain measuring devices is guided not only by their response characteristics, but also by their ability to allow simultaneous transient measurement of these two variables within as short a gage length of the specimen as possible, so that errors due to wave propagation in the specimen are minimized. The ideal situation, of course, is to be able to measure stress and strain independently as a function of time at the same point within the material. For other than this condition wave propagation within the specimen must be taken into account, as is discussed next.

#### Inertial Effects in the Specimen

The most difficult problems to overcome are those associated with the inertia of the specimen itself. The loads applied at one point or over a finite surface area of the specimen are propagated into the specimen at a finite velocity. This finite propagation velocity results in a nonuniform distribution of the stress, strain and particle velocity over the specimen at any instant of time. For uni-axial compression or tension specimens, two problems arise, the propagation of the deformation along the length of the specimen and the influence of the lateral inertia forces generated by the Poisson expansion or contraction on the measured forces.

If the specimen, or rather the gage length over which the variables are measured, is of such a length that the transit time for the disturbance to traverse this gage length is of comparable magnitude as the total duration of the test, then the results must be interpreted in terms of large amplitude wave propagation theory. The neglect of wave propagation effects can lead to spurious strain rate effects derived from average measurements made over the gage length (27). If the condition exists whereby the measured results must be interpreted in terms of a wave propagation theory, the problem arises as to the proper theory to use. Recourse is generally made to the rate independent theory. The adequacy of this theory is open to some question in that it neglects just that phenomenon which is under investigation, the dependence of the stress-strain curve on strain rate. Thus, before the equations governing wave propagation can be solved it is necessary to have first an accurate knowledge of the material behavior. An alternative approach available is to obtain measurements on the propagation of plastic waves and then attempt to determine what form of material property law will best describe the results obtained.

If the specimen is of such a length that a large number of internal reflections occur within the time interval when measurements are made, the distribution of the variables within the specimen can be considered uniform. Consider deforming the specimen to a maximum strain  $\epsilon$  at the strain rate  $\dot{\epsilon}$ . The time duration of this deformation is  $\epsilon/\dot{\epsilon}$ , during which the loading wave travels in the material a distance  $c\epsilon/\dot{\epsilon}$ , where  $c$  is the appropriate propagation velocity. Thus, the number of reflections occurring in a specimen of length  $l$  will be

$$N = \frac{c\epsilon}{l\dot{\epsilon}}$$

or upon rearranging,

$$l = \frac{\epsilon}{N} \frac{c}{\dot{\epsilon}}$$

If, for example, the specimen is aluminum for which we assume the plastic deformation propagates at approximately 1/10 the elastic wave velocity then  $c \approx 20 \times 10^3$  in/sec. If we further prescribe that 10 internal reflections per 1% of strain are necessary in order to approximate uniform conditions,  $l = \frac{20}{\dot{\epsilon}}$ . Thus, for this case, if the specimen is 1 inch long the maximum strain rate satisfying the conditions imposed is 20 per second. It is readily seen that to measure small strains at high strain rates, extremely short specimens would be required in order to be able to neglect propagation effects in the specimen. A specimen length of 0.20 inch would allow one internal reflection per 1% strain at a strain rate of 1000 per second which may be sufficient for the accurate measurement of large strains neglecting propagation. Compression specimens as short as 0.020 in. in

length have been used.

In addition to the axial motion of the specimen, radial expansion or contraction also occurs simultaneously due to the Poisson effect. The radial motion is resisted by radial inertia forces tending to constrain the specimen to its initial lateral dimensions. These lateral inertial restraining forces tend to increase the measured stress  $\sigma_m$  necessary to produce a given strain  $\epsilon$  in the specimen over that stress  $\sigma$  necessary to produce the same deformation when no kinetic energy is imparted to the specimen. For a cylindrical specimen with cross sectional area  $A$  and length  $l$ , the radial kinetic energy can be expressed as

$$K.E. = Al \int_0^\epsilon (\sigma_m - \sigma) d\epsilon$$

If we assume the specimen expands uniformly, the kinetic energy can also be expressed in terms of the radial particle velocity  $V_r$  of a point on the circumference of the specimen of radius  $r$ , as

$$K.E. = \int_0^{V_r} m \frac{V_r}{2} dV_r = \frac{1}{4} Al \rho V_r^2$$

where  $\rho$  is the density of the specimen. If  $\nu$  is Poisson's ratio

$$V_r = \nu r \frac{d\epsilon}{dt}$$

and

$$K.E. = \frac{1}{4} Al \rho \nu^2 r^2 \left( \frac{d\epsilon}{dt} \right)^2$$

Equating these two expressions for the radial kinetic energy and differentiating with respect to  $\epsilon$ , we obtain

$$\sigma_m - \sigma = \frac{1}{2} \rho \nu^2 r^2 \frac{d^2\epsilon}{dt^2}$$

This expression gives a correction to be applied to the measured stress to account for the radial inertia. If the variations in strain rate during the test are small, this correction may be negligible. It is assumed that the specimen is short and the radial deformation is uniform, and also that the static value of Poisson's ratio is valid under dynamic conditions.

As is seen from the above discussion, severe difficulties arise in trying to separate that part of the measured dynamic load due to basic mechanical properties of the specimen material and that which is produced solely by the inertial forces required to accelerate particle motion in the specimen. Inertial effects can not be eliminated in any measurements over a finite gage length, although they can be minimized by testing at a nearly constant strain rate, a difficult variable to control at very high testing rates. Some advantage can also be obtained by testing in pure torsion where radial motion is not present.

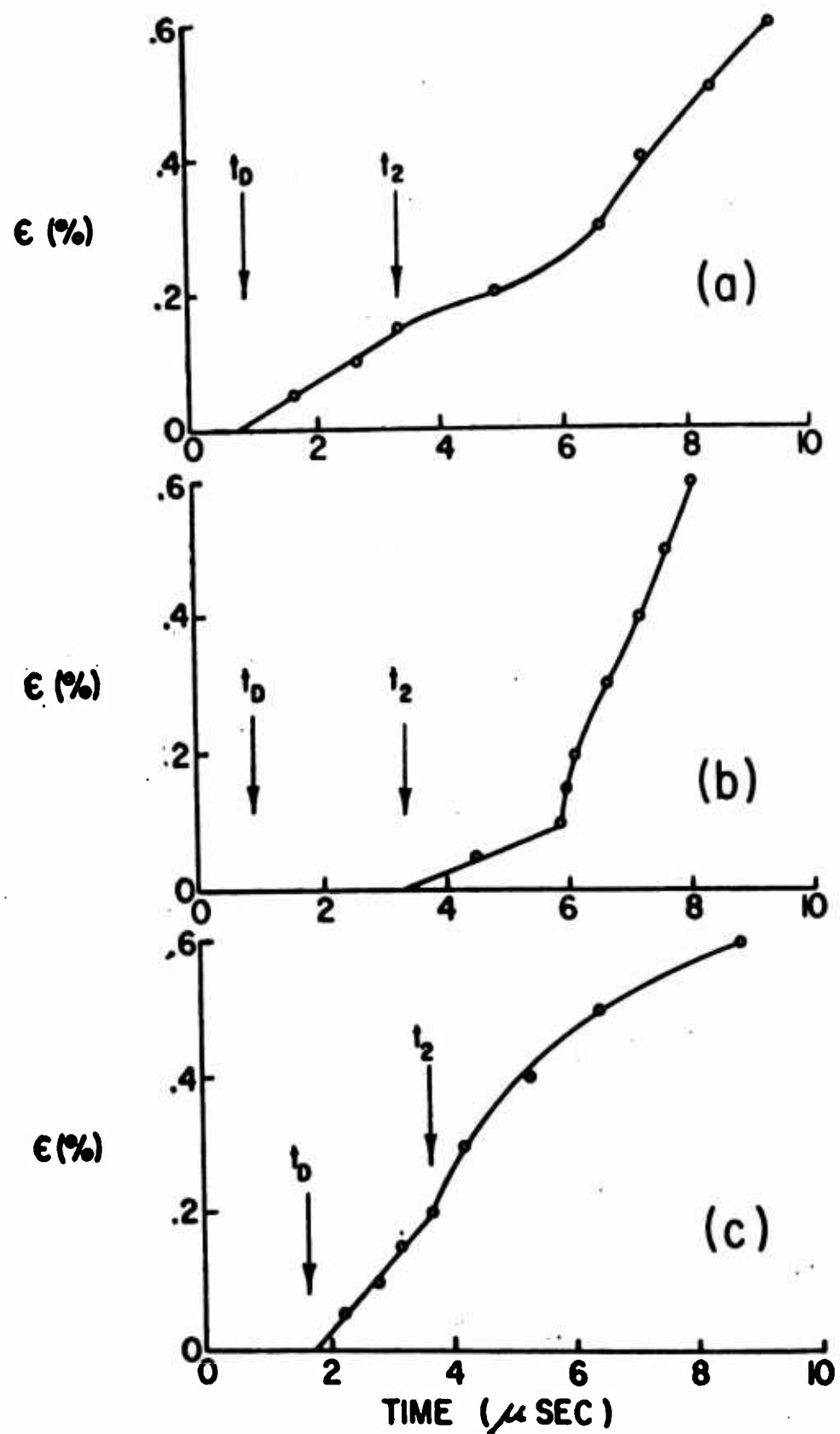


Figure 2. Strain-time records taken near the impact end of a cylindrical rod (from Ref. 28)

### Size Effects and Specimen Geometry

The overall size and shape of the specimen is determined by the manner of loading, either in tension, compression or torsion. In tension impact tests the specimen is generally similar to those used in the static test with a reduced section in the middle and provisions for gripping the specimen at each end. Because of difficulties in gripping the specimen and applying the load, tension specimens are of necessity of appreciable length and propagation nonuniformities across the length of the specimen cannot be avoided at very high loading rates. The compression specimen has some advantage in that it can be made of uniform cross section and quite short in length. For very short compression specimens, however, the influence of frictional restraining forces at the loading surfaces may become significant. These can be alleviated to some extent by proper lubrication.

In addition to considerations of specimen length, the lateral dimensions also have an influence, since errors caused by radial inertia forces increase with increasing radius. Thus, radial dimensions should also be kept small. For any precision testing technique, the influence of specimen size on the results obtained should be considered.

### Axiality of the Loading

The loading device should be designed so as to insure the uniformity and axiality of the loading. This is particularly important in the impact loading of short specimens where the strain does not have time to distribute itself uniformly over a cross section during the interval of measurement. This is illustrated in the strain-time records obtained by Bell (28) from axial impacts on long aluminum rods shown in Figure 2. If the strain development from the impact face is considered to emanate from an infinite number of point sources distributed over the surface a gage station at a fixed point on the lateral surface of the bar will feel first the shock arriving from the nearest point on the impact face. The shock from some further point, say on the opposite diameter of the bar, will arrive at some later time depending on the bar dimensions and the shock velocity  $D$ . In Figure 2,  $t_D$  is the time of arrival at the gage station of the wavelet from the nearest point on the face and  $t_2$  the arrival time from the far side of the impact face. (a) and (b) are measurements at  $1/4$  bar diameter from the impact face and (c) is at  $1/2$  diameter. Record (a) and (c) appear to represent uniform impact over the entire face while in (b) first contact appears to have been made at the far side of the impact face since the first recorded

signal occurs at time  $t_2$ . After some length of travel the wave front will tend to smooth out because of internal reflections from the side walls.

For direct impact of the specimen with a moving mass, precise alignment is difficult to control, thus, there is some advantage in the split pressure bar system shown in Figure 1 (d). With this system the surfaces may be lapped and prealigned.

The discussion heretofore has been concerned exclusively with assumed uniaxial tests. To the writer's knowledge, there has only been one investigation of biaxial dynamic stress-strain characteristics, that of Gerard and Papirno (29) using the rupture of thin circular diaphragms. Dynamic combined stress studies could prove useful in defining a dynamic yield surface and also a dynamic Poisson's ratio.

#### Thermal Effects in the Specimen

In the transition from static to dynamic testing, the test conditions go from isothermal to adiabatic. At high rates of straining, the heat produced by the process of inelastic deformation does not have time to be dissipated, causing a local increase in temperature. Nadai and Manjoine (8) have measured with thermocouples the increase in temperature of pure iron tensile impact specimens for which the test duration was less than 2 milliseconds. The temperature rise recorded at three stations along the specimen is shown in Figure 3. At the fracture cross section a temperature rise of almost 50°C was measured. Instantaneous temperature rises much greater than this undoubtedly occurred on localized slip and rupture surfaces. Since for most materials, temperature has the inverse effect from strain rate, such increases in temperature might be expected to soften the material and thus to flatten out the stress-strain curve at high strain rates and large strains. Although thermal conditions within the specimen cannot be controlled during the test, their influence on the material response should be considered.

#### TWO TYPICAL TEST TECHNIQUES

The high strain rate testing apparatus must take into account each of the items discussed in the previous section. There is, of course, a strong interdependence between the loading mechanism, the measurement techniques and the specimen design, each of which must be considered in terms of the integrated system. Two typical impact testing apparatus and some of the results obtained with them will now be reviewed in order to illustrate the above discussion.

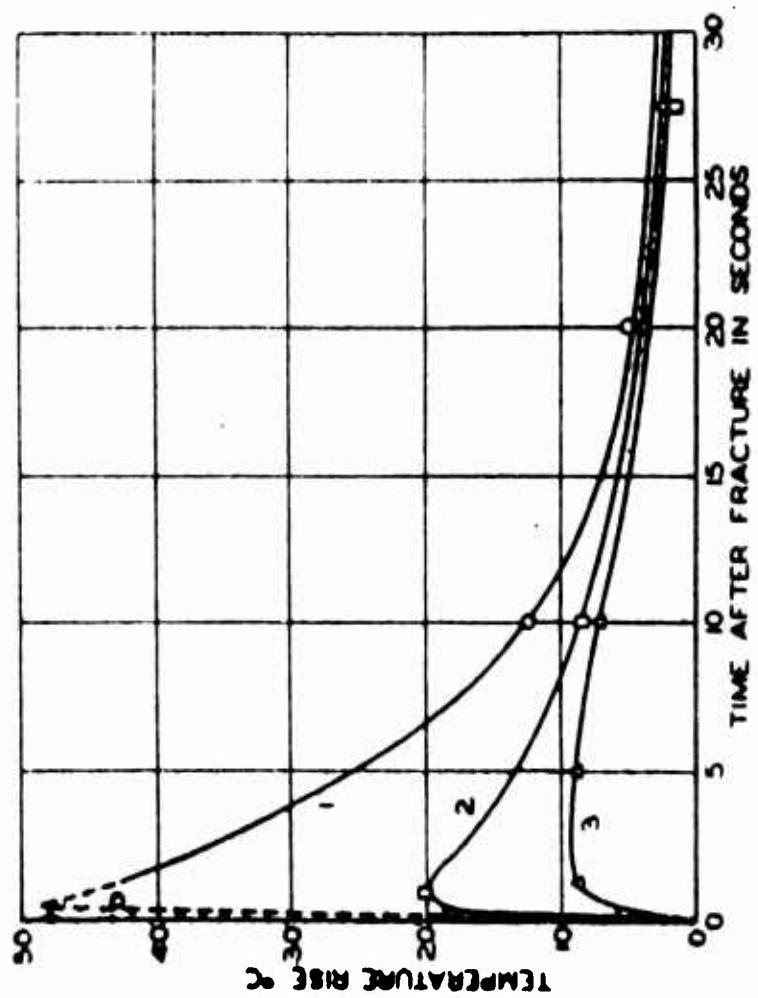
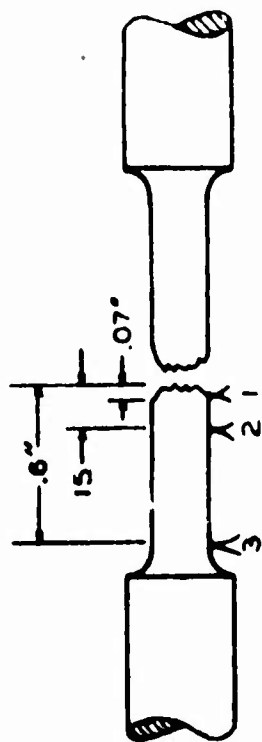


Figure 3: Temperature rise in a pure iron tensile impact specimen (from Ref. 8)

### Tension Tests of Manjoine and Nadai

The apparatus of Manjoine and Nadai (7) is typical of tensile impact testing devices and was one of the first to give complete stress-strain data. The high speed machine is shown in Figure 4. The tension test specimen *c* is suspended between two vertical columns by a force measuring bar *a* attached to the rigid crosshead. To the lower end of the specimen is attached an anvil *d*. The load is applied to the specimen by impact of two hammers *f* which contact the anvil. The hammers are attached to the flywheel *g* and are released by a solenoid operated pin. The load applied to the specimen is measured by the elastic extension of the force measuring bar. This extension is measured by the change in width of the narrow optical slit *h* which regulates the amount of light falling on the photo cell *o*. Strain is measured by the motion of the base of the anvil which is also recorded photoelectrically as shown. The output from each photo cell was fed directly to separate channels of an X-Y oscilloscope to give the stress-strain curve directly.

The test specimens were standard tensile test specimens with the diameter of the reduced section being 0.2 in. and the gage length of the reduced section 1 in. with 1/16 in. radius fillets. All the deformation recorded by the anvil movement is assumed to occur in this 1 in. gage length.

The natural frequency of the force-measuring bar was estimated to be around 15,000 cps and that of the force-measuring bar, test specimen and anvil together on the order of 10,000 cps. The duration of the fastest tests was 500 to 600 microseconds, thus 5 or 6 oscillations of the system occurred during these tests. The amplitude of these oscillations increased with increasing strain rate as shown in the actual test records given in Figure 5.

Some representative results of Nadai and Manjoine on the effect of strain rate on true stress at varying strains for mild steel are given in Figure 6. The shaded area represents the nearly constant stress maintained during elongation at the yield point. The yield point elongation increased with increase in rate of strain. These curves indicate an increasing influence of strain rate at the higher rates especially upon the yield point.

### Pressure Bar Technique of Kolsky

Typical, and perhaps most used of the pressure bar techniques of compression testing, is that of Kolsky (13). In this method, the specimen is compressed between two faces of a split Hopkinson pressure bar





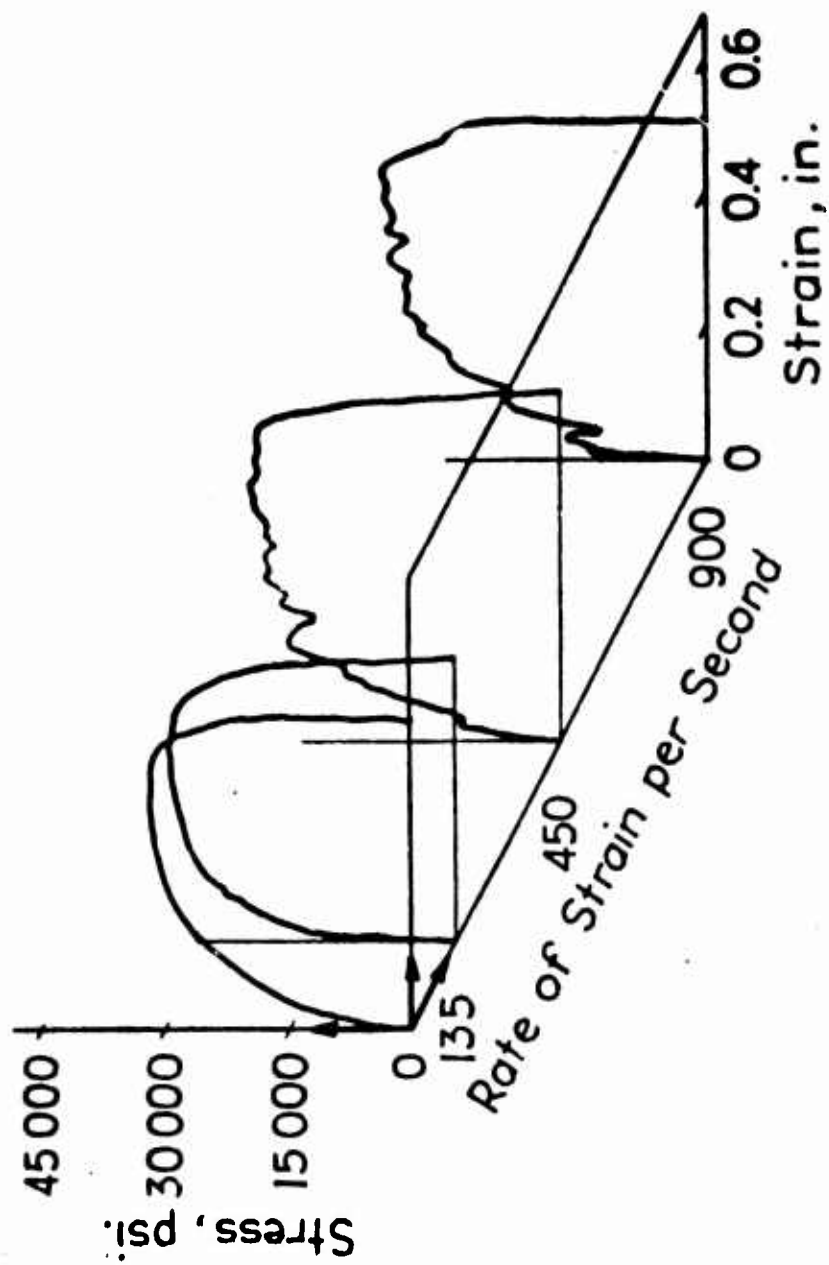


Figure 5. Stress-strain records for tensile impact of pure copper (from Ref. 7)

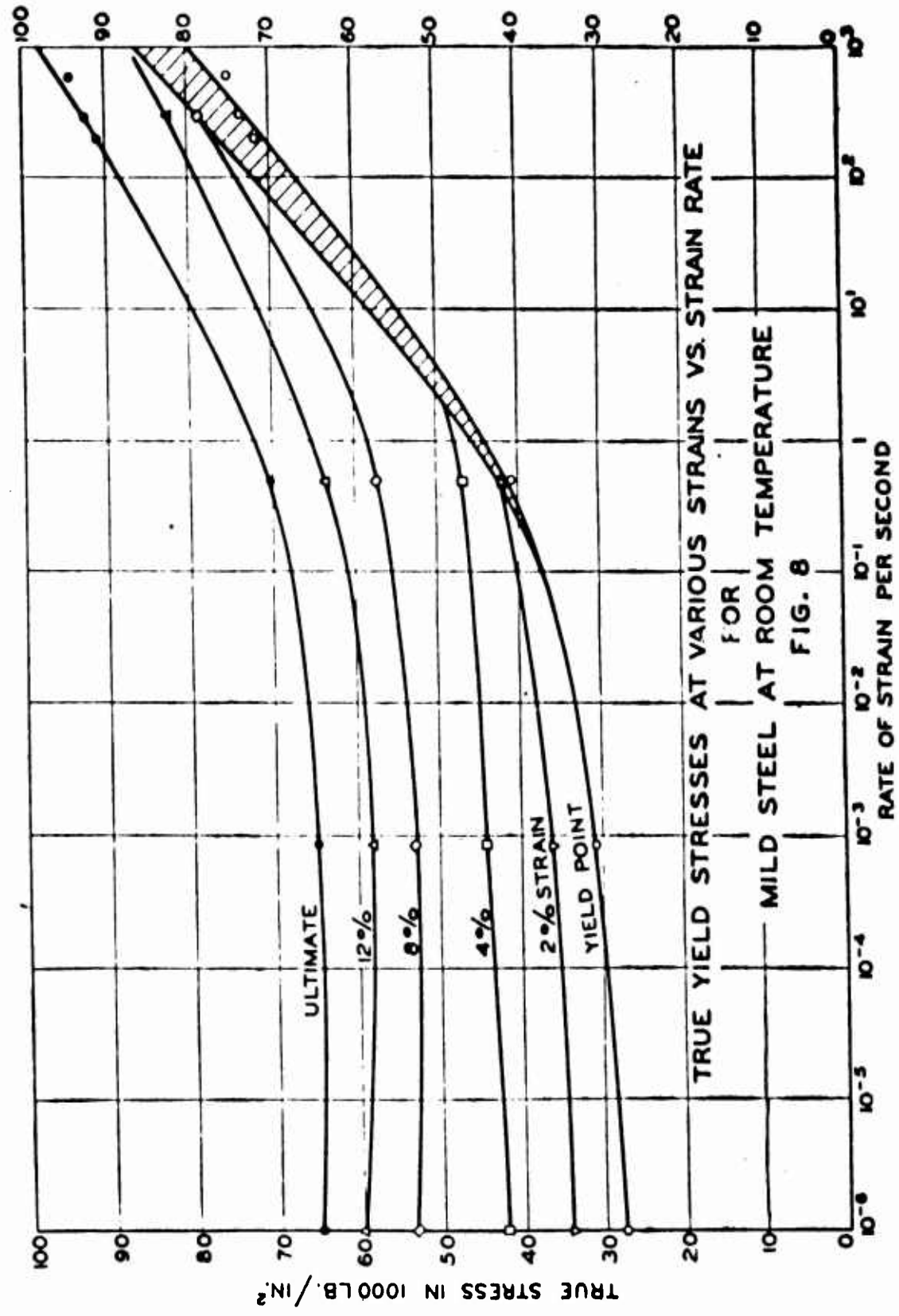


Figure 6. Stress vs. strain rate at constant strain for mild steel in tension (from Ref. 9)

by an elastic pressure pulse propagated in the bars. The original Kolsky apparatus is shown in Figure 7. The pulse is initiated by detonators fired against a hardened steel anvil which transmits the pulse to the first or incident steel pressure bar. When the incident pulse reaches the specimen, part of the pulse is reflected because of the mechanical impedance mismatch and part is transmitted through the specimen to the second or transmitter bar. The particle displacement produced by the pressure pulse is recorded both before and after it passes through the specimen by the cylindrical and parallel plate condenser microphones, respectively. In later work, both Lindholm (17) and Hauser, et al. (16) used resistance strain gages in place of the condenser microphones to record the pressure pulses. These investigators also initiated the pulse with a mechanical impact rather than the explosive charge. The gage stations are so placed and the pressure bars are of such a length that the loading of the specimen by the initial pulse is recorded before reflections return to disturb the strain or displacement readings. The two strain-time or displacement-time records are recorded simultaneously on the cathode ray oscilloscope.

Both the instantaneous stress and the strain in the specimen are derived from the displacement or strain readings on the pressure bars. Figure 8 shows schematically the loading of the specimen by the incident, reflected and transmitted pulses all of which can be recorded at the two gage stations. The displacement  $u_1$  of the face of the incident pressure bar in contact with the specimen is obtained from strain records by

$$u_1 = c_o \int_0^t (\epsilon_r + \epsilon_R) dt$$

and the displacement  $u_2$  of the face of the transmitter bar by

$$u_2 = c_o \int_0^t \epsilon_T dt$$

where  $c_o$  is the elastic bar wave velocity, and  $\epsilon_r$ ,  $\epsilon_R$ , and  $\epsilon_T$  are absolute magnitudes of the measured strains. The strain in the specimen  $\epsilon$  is then given by

$$\epsilon = \frac{u_1 - u_2}{l_o} = \frac{c_o}{l_o} \int_0^t (\epsilon_r + \epsilon_R - \epsilon_T) dt.$$

The instantaneous stress in the specimen is obtained directly from the force in the elastic bars. If displacements are recorded, as with the condenser microphone, strain in the specimen is obtained directly whereas a differentiation is required to obtain stress, which is somewhat less accurate than the integration procedure above. Figure 9 shows a typical oscilloscope record of the three recorded strain pulses. Both the incident and reflected pulses are recorded at the same gage station on the incident bar, the reflected pulse being tensile. The specimen in this record was

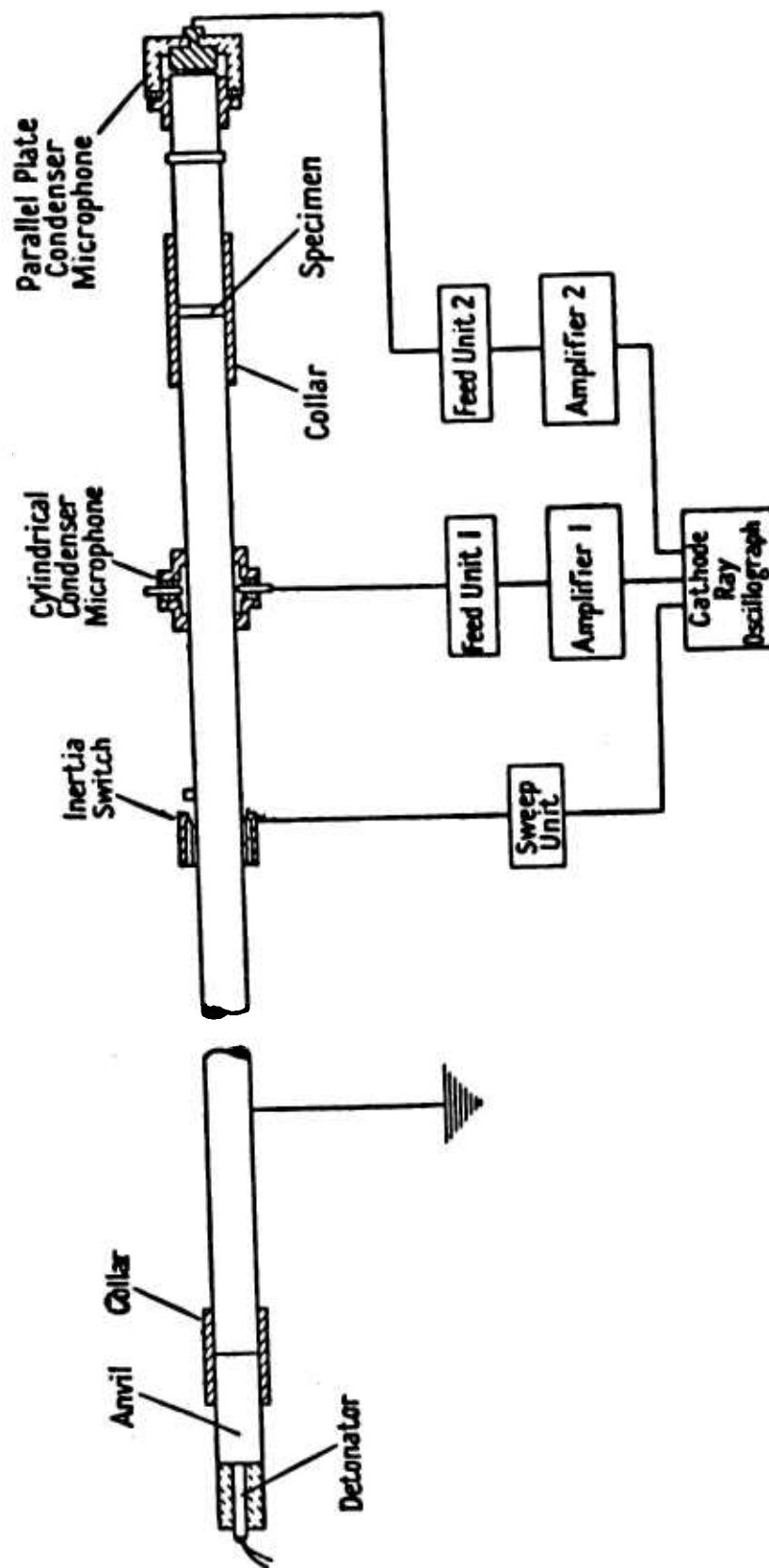


Figure 7. Pressure bar apparatus of Kolsky (from Ref. 13)

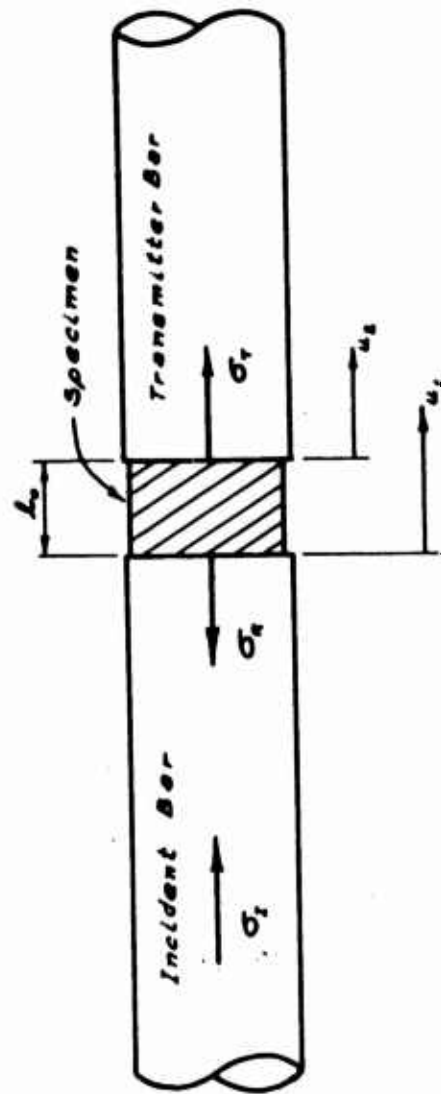


Figure 8. Schematic of Kolsky (from Ref. 13)

aluminum, 1/4 inch long and 1/2 inch in diameter. The total duration of the loading is seen to be about 125 microseconds. Slight oscillations are seen at the initiation of the transmitted and reflected pulses, corresponding to reflections within the specimen. Stress-strain curves derived from similar records for lead are shown in Figure 10. The curves at the three lower strain rates in this figure were obtained on a conventional testing machine.

Stress vs. strain rate curves at constant strain are shown in Figure 11 for aluminum from Hauser et al. (16) and for copper in Figure 12 from Lindholm (17) both using the Kolsky technique. In Figure 11 the average strain rate was varied by changing the length of the specimen; the results in Figure 12 were obtained on specimens of the same length but the lower strain rates were obtained on a standard static testing machine. Both show a logarithmic dependence of stress upon strain rate to approximately 1000 per second. At higher strain rates the data of Figure 12 indicates the possible existence of a limiting strain rate which the material can sustain, in the neighborhood of which the stresses increase sharply. Figures 11 and 12 also indicate an increase in strain hardening with increase in strain rate as evidenced by the increasing slope of the constant strain curves with increasing strain.

The two methods just described are typical of both tensile and compressive impact tests and serve to illustrate solutions to the problems discussed. Each method has its limitations and range of applicability and data obtained can only be compared accordingly. Despite the continued improvement in dynamic testing techniques, there is still a need for further intensive experimental work aimed at defining basic material behavior.

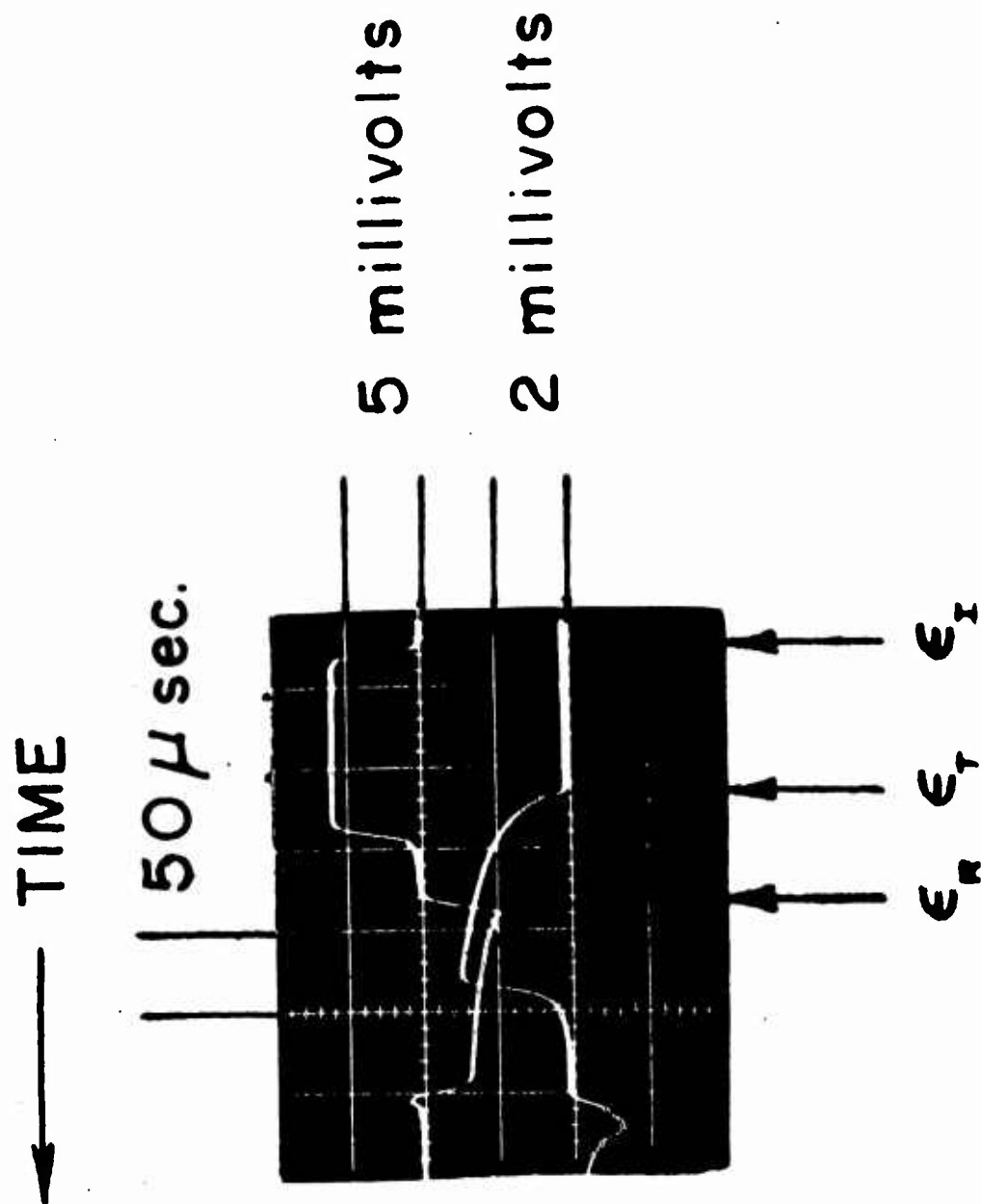


Figure 9. Typical oscilloscope records obtained from strain gage instrumented pressure bars.



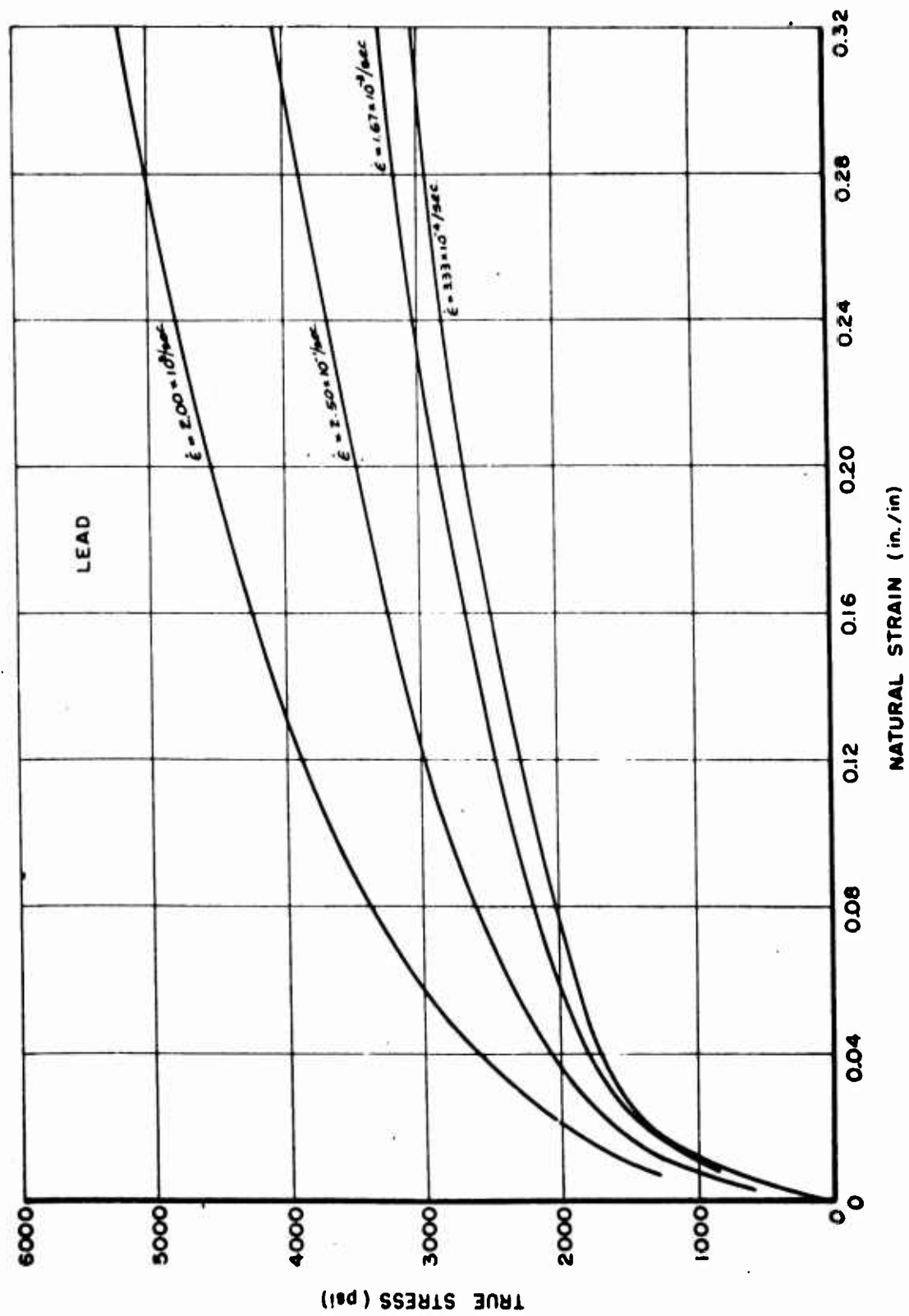


Figure 10. Stress-strain curves for lead at varying strain rates (from Ref. 17)

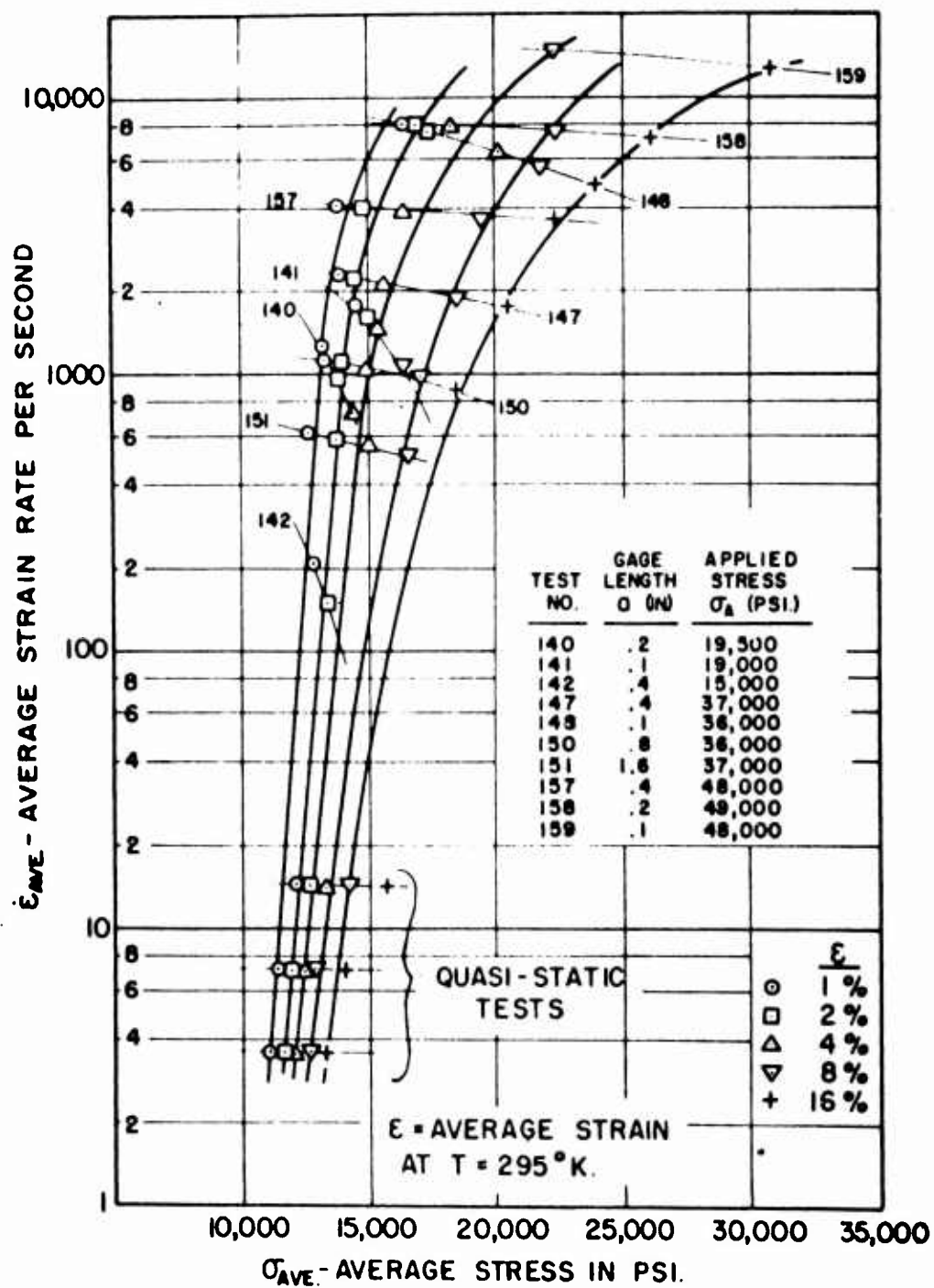


Figure 11. Stress vs. strain rate at constant strain for aluminum in compression (from Ref. 16)

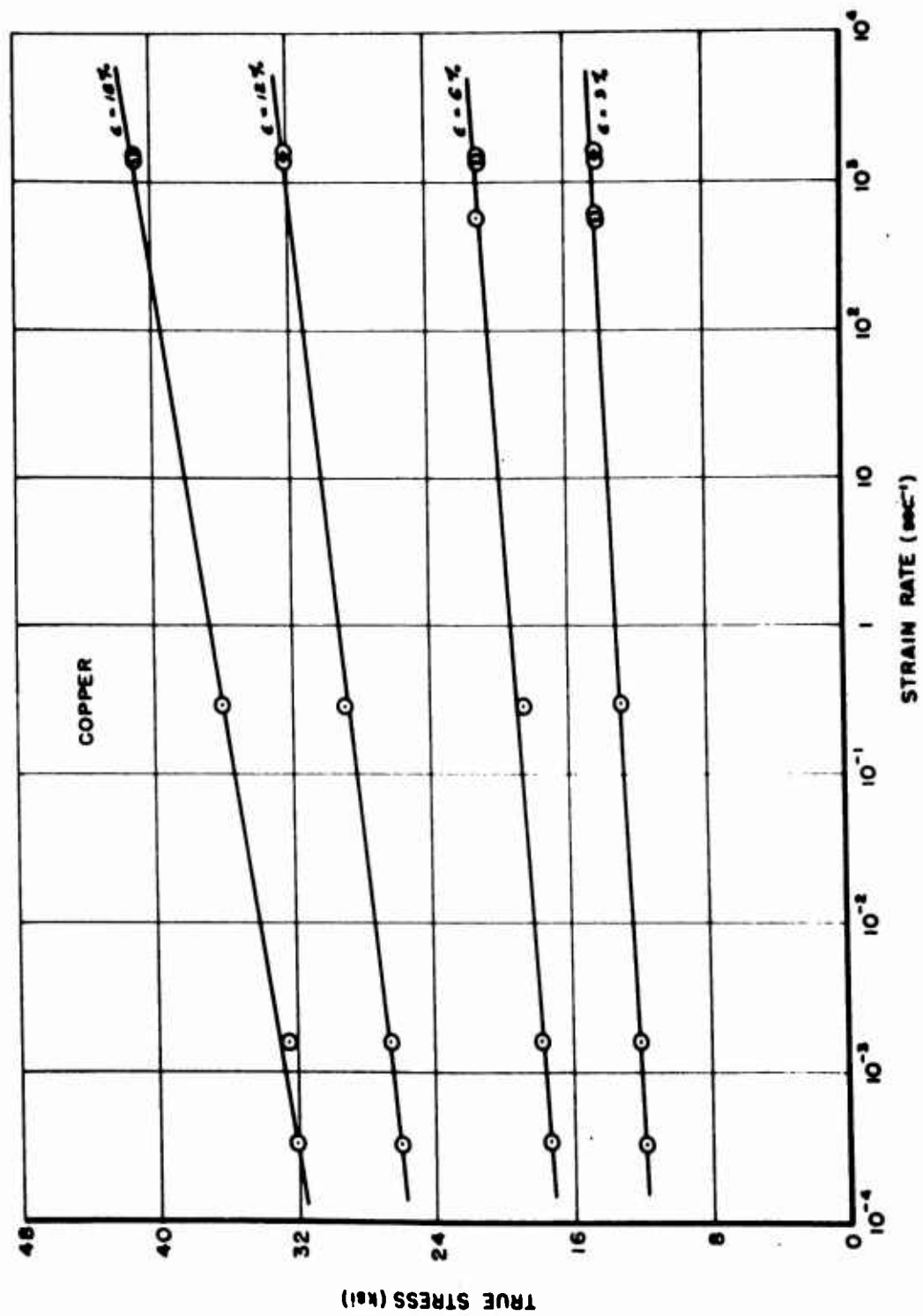


Figure 12. Stress vs. strain rate at constant strain for copper in compression (from Ref. 17)

## REFERENCES

1. Taylor, G. I. and Whiffin, A. C., "The use of flat ended projectiles for determining dynamic yield stresses," Parts I and II, Proc. Roy. Soc. Lond., 194, p. 289 (1938)
2. Habib, E. T., "A method of making high-speed compression tests on small copper cylinders," J. Appl. Mech., 15, p. 248 (1948)
3. Volterra, E., Eubanks, R. A., and Muster, D., "An investigation of the dynamic properties of plastics and rubber-like materials," Proc. Soc. Exp. Stress Anal., 13, p. 85 (1955)
4. Baron, H. G., "Stress-strain curves of some metals and alloys at low temperature and high strain rates," J. Iron and Steel, Inst. Lond., 182, p. 354 (1956)
5. Clark, D. S. and Datwyler, G., "Stress-strain relations under tension and impact loading," Proc. Am. Soc. Test. Mat., 38, p. 98 (1938)
6. Mann, H. C., "High velocity tension impact tests," Proc. Am. Soc. Test. Mat., 36, p. 85 (1936)
7. Manjoine, M. and Nadai, A., "High speed tension tests at elevated temperatures," Proc. Am. Soc. Test. Mat., 40, p. 822 (1940)
8. Nadai, A. and Manjoine, M., "High speed tension tests at elevated temperatures — Parts II and III," Trans. Am. Soc. Mech. Eng., 63, p. A77 (1941)
9. Manjoine, M. J., "Influence of rate of strain and temperature on yield stresses of mild steel," J. Appl. Mech., 11, p. A211 (1944)
10. Clark, D. S. and Wood, D. S., "The tensile impact properties of some metals and alloys," Trans. Am. Soc. Met., 42, p. 45 (1950)
11. Turnbow, J. W. and Ripperger, E. A., "Strain rate effects on stress-strain characteristics of aluminum and copper," Proc. Fourth Midwest Conf. on Solid Mech., Austin, Texas, Sept. 1959, Austin, Texas Univ. Press, p. 415

12. Alder, J. F. and Phillips, V. A., "The effect of strain rate and temperature on the resistance of aluminum, copper and steel to compression," *J. Inst. of Met.*, 83, p. 80 (1954-55)
13. Kolsky, H., "An investigation of the mechanical properties of materials at very high rates of loading," *Proc. Phys. Soc. Lond.*, 62B, p. 676 (1949)
14. Krafft, J. M., Sullivan, A. M., and Tipper, C. F., "The effect of static and dynamic loading and temperature on the yield stress of mild steel and iron in compression," *Proc. Roy. Soc. Lond.*, A221, p. 114 (1953)
15. Campbell, J. D. and Duby, J., "The yield behavior of mild steel in dynamic compression," *Proc. Roy. Soc. Lond.*, A236, p. 24 (1956)
16. Hauser, F. E., Simmons, J. A., and Dorn, J. E., "Strain rate effects in plastic wave propagation," in Response of Metals to High Velocity Deformation, ed. by P. G. Shewmon and V. F. Fackay, Interscience Pub., N. Y. (1961)
17. Lindholm, U. S., "An experimental determination of the stress-strain strain rate properties of several metals," Ph.D. Thesis, Michigan State Univ. (1960)
18. Clark, D. S. and Duwez, P. E., "The influence of strain rate on some tensile properties of steel," *Proc. Am. Soc. Test. Mat.*, 50, p. 560 (1950)
19. vonKarman, T. and Duwez, P. E., "The propagation of plastic deformation in solids," *J. Appl. Phys.*, 21, p. 987 (1950)
20. Taylor, G. I., "The plastic wave in a wire extended by impact load," The Scientific Papers of Sir Geoffrey Taylor, Cambridge Univ. Press, p. 467 (1958)
21. Campbell, W. R., "The determination of dynamic stress-strain curves from strain waves in long bars," *Proc. Soc. Exp. Stress Anal.*, 10, p. 113 (1952)
22. Johnson, J. E., Wood, D. S., and Clark, D. S., "Dynamic stress-strain relations for annealed 2S Aluminum under compression impact," *J. Appl. Mech.*, 20, p. 523 (1953)

23. Hopkinson, B., "A method of measuring the pressure produced in the detonation of high explosives or by the impact of bullets," *Phil. Trans. Roy. Soc. Lond.*, A213, p. 437 (1914)
24. Davies, R. M., "A critical study of the Hopkinson pressure bar," *Phil. Trans. Roy. Soc. Lond.*, A240, p. 375 (1948)
25. Bell, J. F., "Determination of dynamic plastic strain through the use of diffraction gratings," *J. Appl. Phys.*, 27, p. 1109 (1956)
26. Ripperger, E. A. and Yeakley, L. M., "Measurement of particle velocity," *SESA Spring Meeting Dallas Texas*, Paper No. 729, 1962
27. Lee, E. H. and Wolf, H., "Plastic-wave propagation effects in high-speed testing," *Trans. Am. Soc. Mech. Eng.*, 73, p. 379 (1951)
28. Bell, J. F., "Experimental study of the interrelation between the theory of dislocations in polycrystalline media and finite amplitude wave propagation in solids," *J. Appl. Phys.*, 32, p. 1982 (1961)
29. Gerard, G. and Papirno, R., "Dynamic biaxial stress-strain characteristics of aluminum and mild steel," *Trans. Am. Soc. Met.*, 49, p. 132 (1957)

## DISCUSSION

V. H. Pagano, U. S. Army Tank-Automotive Center:

What is the influence of the higher strain rate on the coefficient of the strain hardening exponent?

Dr. Lindholm: For a higher strain rate the slope would be increasing.

V. H. Pagano: You would be getting a larger strain exponent with the higher rate. This is of interest because of the significance implied, from a ballistic point of view, to the influence of strain hardening exponent on the ballistic resistance of a material; and some question has been brought up recently with regard to reduction in carbon content, actually bringing it further away from this resistance effect, because the strain hardening exponent decreases with decreasing carbon content. If this is the situation, actually these estimates are being made from static and not from dynamic results.

Mr. Crenshaw: Are there any more questions?

Question: Did you say anything about the temperature conditions?

Dr. Lindholm: Most of those which were shown on the slides here were at room temperature, but generally at elevated temperatures the rate effects will be more predominant.

Question: I meant with respect to isothermal versus adiabatic conditions.

Dr. Lindholm: Of course in all these tests the temperature is not monitored continuously during the test. Now we know that as the rate increased, and it is a higher rate shown here, essentially it has gone to an adiabatic condition. Test duration is of the order of maybe a hundred micro-seconds. I don't know if this answers your question.

Dr. Kumar: I would like to ask about the comparative view of the two techniques of testing the materials dynamically for strain rate characteristics especially; one is what you call the bar technique; the other is the short specimen. In your view, what would you say are the outstanding advantages of the short specimen and possible any outstanding advantages of the bar impact technique?

Dr. Lindholm: It is the higher strain we are talking about here. At the higher strain rate you're faced with the problem of the propagation within the specimen. You can minimize it by making the specimen as short as possible so you have many reflections during the time of interest. Of course this leads to another problem, which I didn't mention really, as how do you take into account the surface conditions? The bar technique has the advantage that you can use the bars as elastic members, may monitor the particle displacement on the faces of these bars and have at the same time the stress measurements. We are able to obtain from the integrated strain-time records agreement within 3 to 5% with the final deformation measurements in the specimen; so this gives us some indication of the accuracy. The tensile type test has the advantage that you can test the failure, but again if you work with tensile specimen you're faced with the problem of how do you grip the specimen and also how to minimize the length to eliminate rate propagation effect. Another approach to the problem, which we didn't mention, is to measure plastic wave propagation and then work backwards and try to determine what type of material parameters one can put into governing equations that will give the results one may obtain experimentally.

# THE EFFECT OF STATIC AND DYNAMIC LOADING AND TEMPERATURE ON THE YIELD STRESS OF IRON AND MILD STEEL IN TENSION AND COMPRESSION

William Griffel\*

## ABSTRACT

The elastic and plastic design of mild steel structures is based on the value of the lower yield stress, which is a measure of the resistance of the material to the propagation of yield into an unyielded material. On the other hand the upper yield stress has only a very limited application since its value is influenced by axially of loading and surface finish, factors difficult to control in actual structure.

As it is assumed that the value of the dynamic lower yield stress is determined by the dynamic properties of unyielded material, rather than those of plastically deformed material, how can we describe the relationship of this dynamic lower yield stress versus temperature utilizing criteria applicable to the dynamic upper yield stress?

## INTRODUCTION

A constant problem for an engineer, while evaluating the strength of a structure is to compare the resulting stresses with the dynamic yield stress of the material for a given temperature. Many investigations were made in this field. Most of them were on the effect of dynamic loading on metals in tension but the mechanism of deformation has yet to be determined. There is a general agreement that the yield of mild steel in tension may be raised to a value over 50% above that obtained in static test, while in most other metals the effect is slight.

Tensile tests of short duration at different temperature show that the yield stress increases with fall in temperature and that the time at a given stress required to initiate yield increases.

The purpose of this paper is to summarize some of the latest testing results of dynamic stress and deformation in a mild steel in tension at normal and low temperature and the effect of static and dynamic loading

---

\*Mr. William Griffel, Ammunition Group, Picatinny Arsenal, Dover, N. J.



and temperature on the yield stress of iron and mild steel in compression.

#### DYNAMIC STRESS AND DEFORMATION IN A MILD STEEL IN TENSION AT NORMAL AND LOW TEMPERATURE

Both the classical elastic and the modern plastic design of mild steel structures are based upon the value of the lower yield stress. The upper yield stress has only a very limited application since its value is considerably influenced by axiality of loading and surface finish, factors difficult to control in an actual structure.

Both these yield stresses, and particularly the upper yield stress, react markedly to the application of dynamic rates of strain, but, as in the case of design for dead loads, a design to resist dynamic loads is based entirely upon the dynamic lower yield stress.

D. B. C. Taylor of University of Cambridge, Cambridge, England, and L. E. Malvern of Michigan State University, East Lansing, Michigan, made a study of this dynamic lower yield stress, together with the associated plastic deformation, in a commercial quality mild steel under tension, particular attention being paid to the effect of temperature upon these two quantities. They argue that since the dynamic lower yield stress is that required for the continuous initiation of yield in unyielded material, its value is determined by the dynamic properties of unyielded material, rather than those of plastically deformed material. Assuming the correctness of this reasoning how is it possible to describe the dynamic lower yield stress versus temperature relationship by making use of criterion applicable to the dynamic upper yield stress?

In their research work, along the lines specified above, commercial mild steel was used. For more homogeneous behavior, the specimens were normalized in vacuum before testing. They were machined from 3/4 in. diameter bar, and the specification of the steel is given below:

#### COMPOSITION, PERCENT

C	Si	Mn	Ph	S	Ni	Cu
0.19	0.07	0.54	0.013	0.052	0.08	0.20

#### TENSILE PROPERTIES

Upper Yield Stress	53.8 kpsi
Lower Yield Stress	41.9 kpsi
Ultimate Tensile Stress	66.5 kpsi
Elongation on 2 in.	30 percent
Reduction in Area	65 percent

## CONCLUSIONS

The main conclusions from the above investigation may be briefly summarized as follows:

1. The effect of dynamic rates of strain up to 5/sec combined with temperatures down to  $-70^{\circ}\text{C}$ , upon a normalized mild steel of 0.19 percent carbon content is to increase the lower yield stress by amounts ranging up to 120 percent of the static room temperature value, that is 42 to 90 kpsi.
2. The increased value of lower yield stress which is a measure of the resistance of the material to the propagation of yield into an unyielded material, leads to a greater location and greater amplitude of nonuniform plastic strain. Local plastic strains of up to 14 percent were recorded at  $-70^{\circ}\text{C}$  as compared with the room temperature static value of 2 percent.
3. It is possible to describe the dynamic lower yield stress  $\sigma$  versus temperature  $T$  relationship by an equation of the form:

$$\sigma = K_1 - K_2 T^{1/3}$$

Where  $K_1$  and  $K_2$  are constants obtained by the investigators from a theoretical formulation for the activation energy.

## THE EFFECT OF STATIC AND DYNAMIC LOADING AND TEMPERATURE ON THE YIELD STRESS OF IRON AND MILD STEEL IN COMPRESSION

Cylindrical test samples were compressed statically and dynamically at temperatures ranging from  $+100$  to  $-195^{\circ}\text{C}$  and yield stress observed. Two materials were used for this experiment; one a high purity iron, and the other, a normal mild steel plate. The analyses are given below:

PURE IRON (%)    C < 0.01,    0 < 0.012,    N < 0.0002,    H < 0.0001

MILD STEEL (%)	C	Mn	S	P	Ni	Cr	Mo	V
	0.190	0.51	0.026	0.007	0.074	0.037	0.016	0.003

The steel was untreated. Cylindrical rods of the iron were heated at  $960^{\circ}\text{C}$  for 15 min. in vacuum and air cooled.

All the information obtained from these tests, performed by the Naval Research Laboratory, Washington, D. C., has been plotted in graphical form

in Figures 1 and 2. For the reasons that are beyond the Scope of this paper, there is some uncertainty with regard to the interpretation of the dynamic tests in that the stresses value in relation to strain may not be exactly comparable to that of the static test. The shape of the curves need not necessarily be affected and there is other evidence that the stress values are quantitatively approximately correct.

First, the dynamic yield stresses are all higher than the static, by an amount that varies with the temperature. At room temperature the ratio of dynamic versus static is about 2.5 for both the iron and steel. As the static and dynamic yield stress curves approach each other at lower temperatures, this ratio decreases. Similarly at higher temperatures, it would appear that the curves may eventually converge, probably at temperatures when the flat yield point in steel disappears. The temperature range of the tests is not wide enough in either material to prove that the two curves do, in fact, converge at both high and low temperatures, but the connection between the raising of the yield stress, a delay time in yielding and a flat yield were well established.

#### DISCUSSION

Mr. Zaroodny, BRL, APG: What about the ultimate stress?

Mr. Griffel: Well, the ratio of dynamic to static stress or ultimate strength is much lower than that of the yield stresses. To be specific, if my memory serves me right, for aluminum the ratio of dynamic to static ultimate stress is only 1.1.

Dr. Kumar: Aluminum is probably not an excellent choice to use as an example of the effect of strain rate on the ultimate stress because other materials, like copper, do show considerably more percentage of sensitivity than aluminum does.

Mr. Griffel: I agree but still less than for yield stress. The point I wanted to emphasize was that the ratio is larger for the yield than for the ultimate.

# IRON

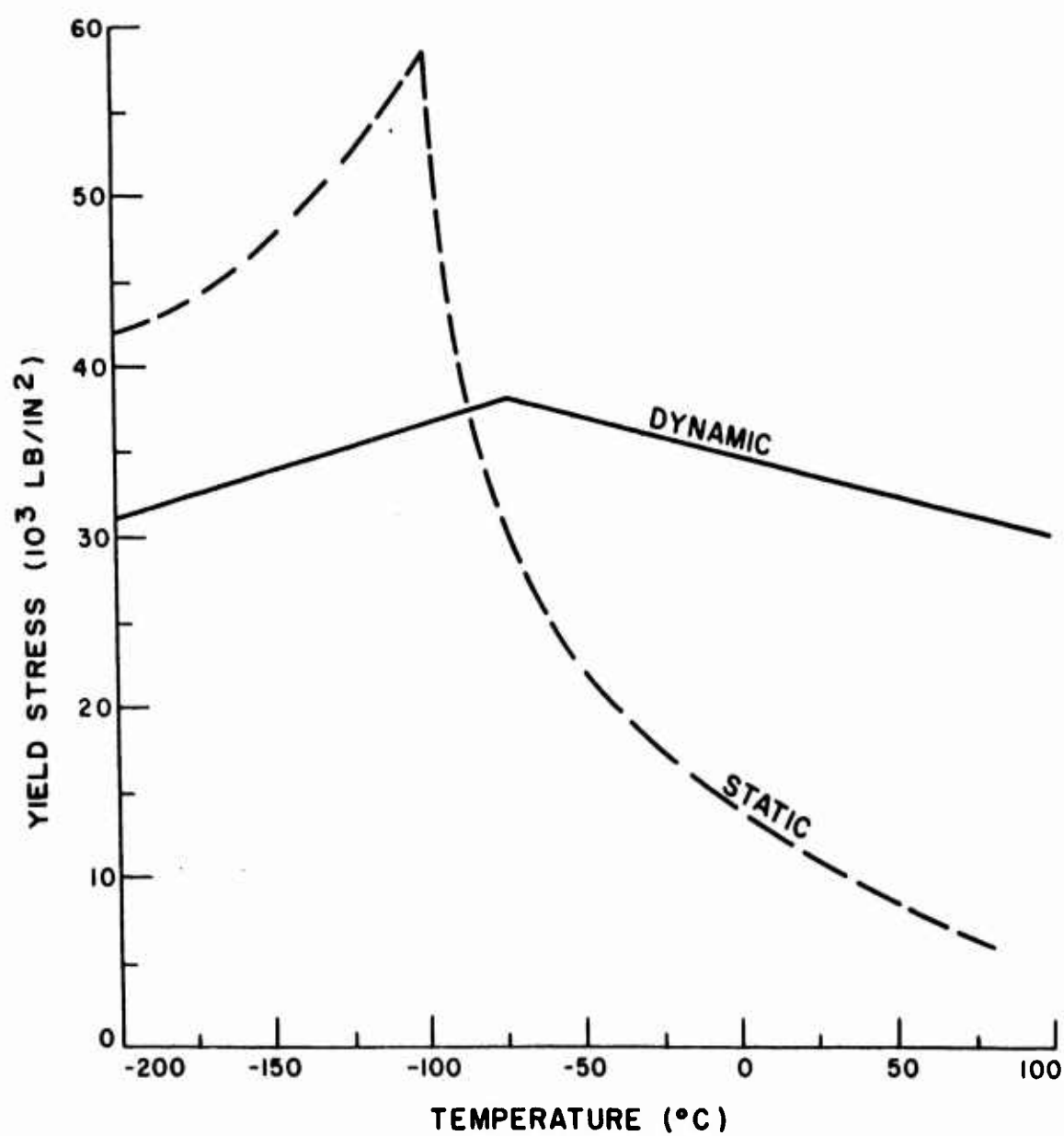


FIG.1 YIELD STRESS VERSUS TEMPERATURE CURVES

# STEEL

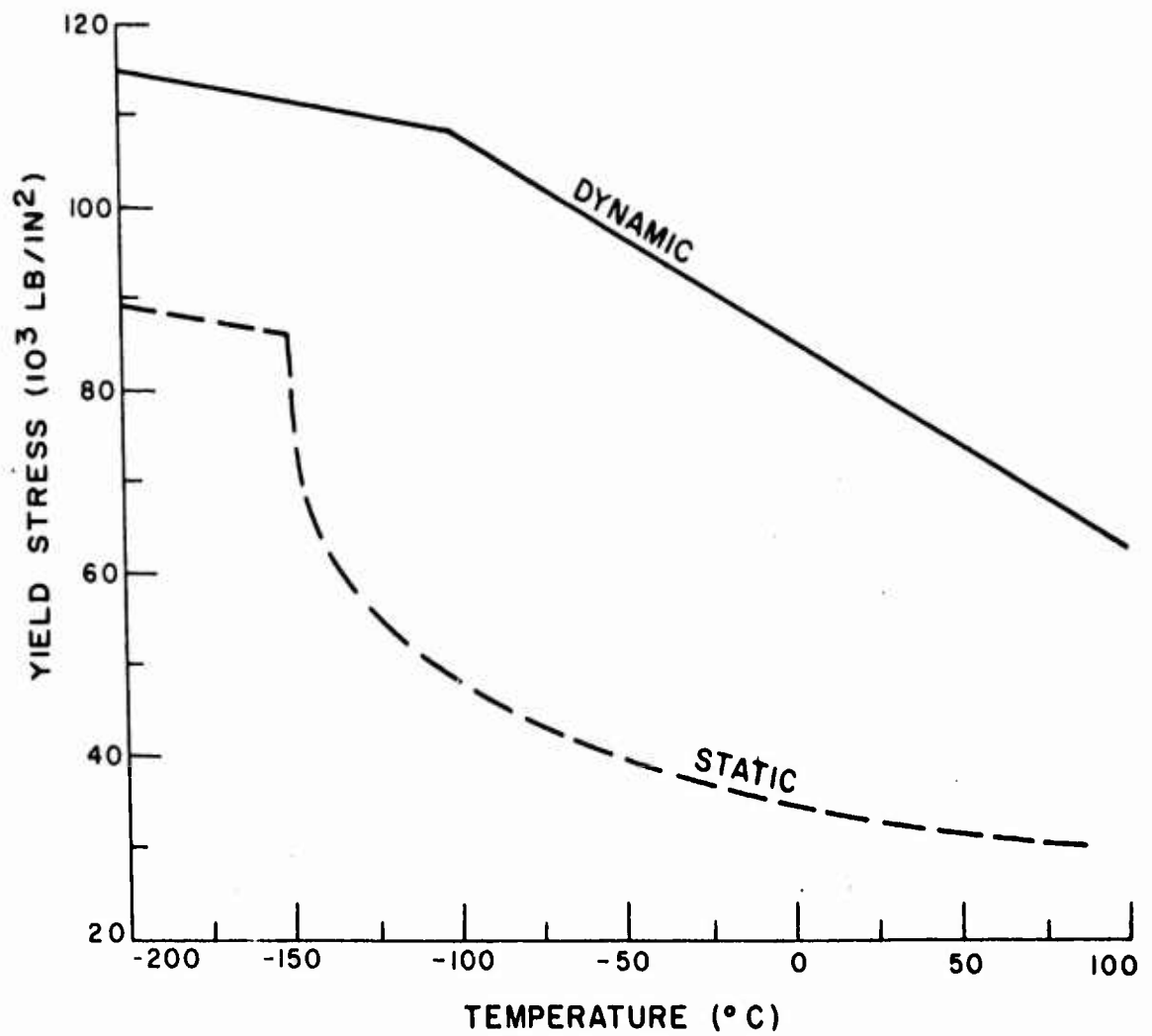


FIG.2 YIELD STRESS VERSUS TEMPERATURE CURVES

# INSTRUMENTATION FOR EVALUATION OF ARTILLERY AND ROCKET LAUNCHER PERFORMANCE AT ROCK ISLAND ARSENAL

J. C. Hanson\*

## ABSTRACT

All instrumentation measurements at Rock Island Arsenal under dynamic conditions have been utilized to obtain operating data on performance of research and development prototype weapons and assemblies during proof firing or functioning tests rather than on a specific material subject to a particular condition of loading.

The basic sensing device used for obtaining analogs of dynamic physical phenomena is the electromechanical transducer. Output signals from the transducers are usually recorded by means of optical galvanometer type oscillographs.

Commercial transducers are used for measuring fluid pressure, acceleration, displacement of moving parts and loads. Special transducers have been designed for measuring artillery recoil displacement, recoil rod and trunnion loads. Conventional strain gages are utilized to measure loads and surface strains on various components, movement of parts and projectile ejection from the barrel. (Transducers and methods used for mounting them are illustrated and explained.)

Recording equipment with a frequency response of zero to 600 cps has been found to be adequate for the majority of measurements. Multi-channel recorders equipped with time line apparatus are desirable. Chart speeds and types of recording paper used are selected on the basis of the test. Electrical noise in various instrument components such as cables and amplifiers present some problems which are explained.

Calibration of the transducers is performed with the complete system prior to each days firing. Methods are usually straight forward using static known quantities.

---

\* Mr. J. C. Hanson, Project Engineer, Mechanical and Electronics Unit, Rock Island Arsenal, Rock Island, Illinois.

Instrumentation problems are often encountered when measurements are required in areas of very limited access and when shock and vibration levels are excessive. (Specific problems are illustrated and explained.)

### Introduction

The design, selection, assembly and operation of instrumentation for dynamic data acquisition on Artillery and Rocket Launcher weapons is an important research and development function at Rock Island Arsenal. This paper is primarily concerned with the application of instrumentation to the evaluation of weapon performance rather than a determination of the ability of the materials used in these weapons to perform satisfactorily under certain loading conditions.

An instrumented performance test of a weapon under firing conditions is accomplished in seven steps as follows:

1. Design instrument system
2. Select instruments
3. Assemble instruments
4. Acquire data
5. Reduce data
6. Interpret data
7. Evaluate results

The average test setup requires from 8 to 12 channels of instrumentation. Some have required up to 21 separate channels of instrumentation in order to obtain the desired information.

The progression from idea to functioning hardware requires three basic steps, they are: design, fabrication, and testing. Instrumentation provides an important contribution to achieving design objectives when it is intelligently employed in testing.

### Transducers and Recording Equipment

The object of instrumentation in the context of this paper is to assist in the attainment of an optimum weapon with a minimum expenditure of time, funds, and effort. A good definition of the purpose of instrumentation has been stated by Dr. K. S. Lion of the Massachusetts Institute of Technology in his new book entitled, "Instrumentation in Scientific Research". He says, "The purpose of instrumentation is to obtain information about the physical or chemical nature of an investigated object or process, or to control an object or a process in accordance with such information."

Information is required or supplied either in a continuously variable form, such as the deflection of a meter (analogue systems) or in discontinuous steps, such as by counting (digital systems)." In order to have meaning, it is essential that recorded information be reduced to quantitative values or numbers. This is achieved by means of carefully established procedures for precise calibration of the transducers used for measuring the various physical quantities involved. When this has been accomplished, we have a measurement system and valid measurements can be made. The basic measurement chain consists of five elements:

1. The physical quantity to be measured.
2. The electrical input transducer.
3. Information acquisition and transmission.
4. Data analysis.
5. Interpretation of results.

One of the basic design requirements of prototype artillery and rocket launcher weapons is to achieve performance objectives with a minimum amount of hardware. In order to accomplish this, safety factors ranging from 1.5 to as low as 1.2 are used. It follows that as safety margins are decreased, instrumented measurement accuracy must be correspondingly increased and error tolerances held to a minimum. The necessity for high grade instruments and personnel thus becomes increasingly important.

It will be of interest to discuss the first three elements of the basic measurement chain as they relate to weapons testing at Rock Island Arsenal.

The majority of weapons tested involve measurement of one or more of the following:

1. Acceleration of components and assemblies.
2. Qualitative and quantitative measurement of mechanical strain in components.
3. Direct and indirect force or loads applied to components and assemblies.
4. Angular and translational velocity and displacement of components and assemblies.
5. Liquid and gas pressure in pneumatic, hydraulic and hydro-pneumatic systems such as equilibrators and recoil mechanisms.
6. Temperature of liquid, gas and solid materials in weapon components and assemblies.
7. Displacement of projectiles and missiles (position versus time).



Information is required or supplied either in a continuously variable form, such as the deflection of a meter (analogue systems) or in discontinuous steps, such as by counting (digital systems)." In order to have meaning, it is essential that recorded information be reduced to quantitative values or numbers. This is achieved by means of carefully established procedures for precise calibration of the transducers used for measuring the various physical quantities involved. When this has been accomplished, we have a measurement system and valid measurements can be made. The basic measurement chain consists of five elements:

1. The physical quantity to be measured.
2. The electrical input transducer.
3. Information acquisition and transmission.
4. Data analysis.
5. Interpretation of results.

One of the basic design requirements of prototype artillery and rocket launcher weapons is to achieve performance objectives with a minimum amount of hardware. In order to accomplish this, safety factors ranging from 1.5 to as low as 1.2 are used. It follows that as safety margins are decreased, instrumented measurement accuracy must be correspondingly increased and error tolerances held to a minimum. The necessity for high grade instruments and personnel thus becomes increasingly important.

It will be of interest to discuss the first three elements of the basic measurement chain as they relate to weapons testing at Rock Island Arsenal.

The majority of weapons tested involve measurement of one or more of the following:

1. Acceleration of components and assemblies.
2. Qualitative and quantitative measurement of mechanical strain in components.
3. Direct and indirect force or loads applied to components and assemblies.
4. Angular and translational velocity and displacement of components and assemblies.
5. Liquid and gas pressure in pneumatic, hydraulic and hydro-pneumatic systems such as equilibrators and recoil mechanisms.
6. Temperature of liquid, gas and solid materials in weapon components and assemblies.
7. Displacement of projectiles and missiles (position versus time).

These quantities are usually measured on a common time base in order to identify and compare the initiation and time duration of various related events.

The second element in the measurement system is the electrical input transducer. Its function is to transform the physical quantity to be measured, as existing in one form of energy, into some other physical quantity which can be more easily measured. In view of the fact that almost all recorded data must be in the form of electric analogs, it is necessary to use electrical input transducers. These are devices capable of converting any form of energy into an equivalent electrical current or voltage. The versatility of these devices is almost limitless and the state of the art at the present time is such that there is commercially available an electrical input transducer for measuring any or all physical quantities and they are available in a wide variety of ranges, shapes and sizes.

The types used, their physical and electrical characteristics, and physical quantities measured are of interest since experience has proven their complete suitability to weapons testing. The majority of transducers used are of the electric resistance strain gage type in which the sensing element is in the form of the conventional four arm wheatstone bridge. These are classified as nonself-generating transducers. They are divided into two groups, one having bonded wire strain gage arms and the other having unbonded strain gage arms. The former are more rugged than the latter and can better withstand high shock and vibration conditions. The unbonded strain gage types are generally a little more accurate and a little more linear. However, both types function in the same manner. The bridge arms are mechanically fastened to the sensing element flexure device which responds to the measured quantity. Thus changes in electrical resistance are produced which are directly proportional to the physical quantity to be measured. It is necessary of course to excite the bridge with either A.C. or D.C. current in order to obtain an output signal which by definition will be proportional to the measured quantity. Transducers based on this principle can be used to measure any or all of the physical quantities previously stated, within certain limits. A variant of this type of transducer uses inductive elements in place of resistive elements in the bridge arms and require A.C. current excitation. Generally, they have been used for measurement of acceleration, pressure and applied loads such as recoil mechanism rod pull during firing. Transducer type, quantities measured and operating range required in test work are as follows:

1. Load cells for measurement of tension and compression loads calibrated directly in pound units of force in the range of zero to 50,000

pounds. These devices are used on artillery to measure recoil rod load, trunnion load, elevating mechanism load, firing platform load, ground anchor load, and many other related special applications. On weapons classified as rocket launchers such as XM70, XM34, XM91, M386, XM92, XM80, and XM29, load cells have been effectively used to measure such things as weight distribution, center of gravity, and compression and tension loads in various components and assemblies under both handling and firing conditions. Operating range from 0 to 20,000 pounds have been required for tests of these weapons.

2. Accelerometers calibrated in "G" units for measurement of acceleration and deceleration of components and assemblies of artillery and rocket launcher weapons are used under various operating conditions such as firing tests, mobility tests and drop tests. Accelerometers are useful for measuring accelerations due to both gross motion, such as that associated with recoil of artillery tipping parts and vibratory motion resulting from high rate of loading. Piezoelectric type accelerometers are seldom used because they are not as easy to calibrate as the former type and are not readily adaptable to the type of information acquisition equipment used. Operating range from 0 to plus or minus 1000 "G" units have been used in tests.

3. Pressure transducers calibrated in pounds per square inch units are used primarily for measuring gas, and oil pressure in recoil and equilibrator mechanisms. The operating range is normally zero to 10,000 psi.

4. Linear and angular displacement transducers calibrated in units of .001 inch to 60 inches for the former and calibrated in degrees for the latter are used on artillery to measure displacement of recoiling parts, equilibrator motion, carriage hop, firing base motion and deflection of components due to vibration and shock. However, in addition to variable resistance transducers, variable inductance transducers are also used. Special solenoid type electro-mechanical transducers for measuring recoil displacements up to 60 inches have been developed at Rock Island Arsenal. With respect to rocket launcher materiel, these devices have been used to measure the deflection amplitude of components such as the launcher beam during simulated launching of the missile. Many other measurements of deflection and displacement produced by various conditions of loading have been made.

5. Velocity transducers have been used in connection with the measurement of vibratory motion of components in the range .001 to

approximately 1 inch double amplitude. However, these devices are seldom used since velocity is a physical quantity that does not indicate intensity of loading and thus would not indicate probability of failure.

6. Bonded wire and metal foil electric resistance strain gages are used extensively in two ways. The first is to directly measure mechanical strain and the second is to use them as transducer sensors by mounting them on special flexure devices which are calibrated in units of the particular quantity measured. The versatility of strain gage applications is limitless. They are indispensable in development work of all kinds.

7. Some conventional instruments have been used in a somewhat unusual manner. For instance, rate gyroscopes have been used successfully to measure the angular velocity of howitzer barrels and of M386 (Honest John) launcher beams during firing. The range of the instruments used was zero to 200 degrees per second.

8. Externally observed functional behavior ranging from specific components to entire weapons are monitored with normal and high speed movies. Gross displacement measurements are facilitated by the use of rectilinear coordinate grid boards as a backdrop. Both black and white and color film are employed.

9. Internal and external temperature measurements are recorded with both conventional thermocouple wire and with electric resistance temperature gages.

It should be noted that all of the transducers described have a linear frequency response range in excess of that required for the majority of weapons tested under firing conditions. Generally, this should be not less than 600 cps.

10. Artillery projectile velocity is measured by means of magnetized projectiles fired through large multi-turn coils of copper wire. The pulses of electric current generated in the coils are recorded.

Physical and electrical performance requirements for transducers are severe. They must be extremely rugged structurally to withstand the effects of severe shock and vibration conditions which are characteristic of all firing tests. For example, a fluid pressure transducer assembled on a recoil mechanism oil head must be physically and electrically immune to the complex time motion phenomena that it is subjected to in order to produce a faithful, relatively noise-free, signal. Accelerometers must withstand high accelerations in directions other than that for which they

are oriented to measure. Transducer function is generally limited by the operating environment and they must be protected from direct exposure to heat, blast and excessive shock loads. When it is necessary to use special mounting brackets, careful attention to stiffness and rigidity should be made, otherwise spurious signals may be generated and superimposed on those produced by the measured quantity.

The third element in the basic measurement system encompasses all electronic apparatus for information acquisition and transmission. In plain language, this is the equipment required to amplify, modify, and record transducer signals. Since the majority of transducers used are of the non-self-generating category, carrier type amplifiers are required. This type of amplifier contains circuitry designed to give output signals which are plus or minus with respect to a zero reference. Thus, not only continuous variations but also the polarity of measured quantities can be recorded. It is necessary to use either a built in or external oscillator and power supply. The former excites the transducer and the latter supplies energy to the amplifier. Provision for varying signal amplification in precise steps is of course essential. The transducer is electrically connected to the amplifier by means of conventional four conductor shielded cables in various lengths up to a maximum of approximately 160 feet.

Self generating piezoelectric transducers are generally connected to a cathode follower followed by a conventional single ended input amplifier. The function of a cathode follower is to serve as an impedance matching device to facilitate maximum transfer of energy from the high impedance piezoelectric transducer to the relatively low impedance of the amplifier.

Records of amplified signals are obtained by means of various types of direct writing oscillographic recorders and with cathode ray oscilloscopes equipped with photographic attachments. Recorders are selected on the basis of test conditions. Multi-channel direct writing light beam oscillographs are used for the majority of tests. Direct writing is accomplished by exposing light beam galvanometer traces on commercially available photo-sensitive paper. These recorders are ideally suited for weapons testing since the frequency range of most physical quantities measured on weapons is well within the capabilities of these instruments. Galvanometers and associate carrier amplifiers in the range zero to 600 cps. and zero to 3000 cps. are used. Systems of this type with a flat frequency response range from zero to 8000 cps. are now commercially available. The systems currently in use at Rock

Island Arsenal can accommodate up to 36 channels of information. Record chart speeds in increments from 1 to 100 inches per second are provided. Chart speeds in the range from 16 to 40 inches per second have been found adequate for the majority of tests.

Direct writing oscillographs which feature a heat stylus writing on heat sensitive paper have limited use in weapons testing due primarily to their relatively low frequency response. They are well suited, however, to static and quasi-dynamic tests under nonfiring conditions.

Cathode ray oscillographs equipped with photographic attachments are necessary for recording transient phenomena of extremely short time duration such as that produced by air blast, dynamic impact, vibration and other phenomena produced by high loading rate.

#### Calibration

Calibration of the transducers is performed with the complete system prior to each days firing. Methods are usually straight forward using static known quantities such as those produced by secondary standards. Circuitry for electronic calibration of each channel is built into the recording equipment. This is usually accomplished by switching a resistor across one active bridge arm of each transducer. The resulting signal is recorded as a step in the trace and it represents a fixed number of units of the measured quantity. The reduction of data is accomplished by ratioing the internal calibration signal to that produced by the secondary standard. It is necessary to obtain calibration signals frequently during test in order to compensate for small variations in signal amplitudes which occur due to variations in temperature, supply voltage and zero drift.

#### Applications

It may be of interest to describe some instrumented firing tests of weapons and components in process of development. Four investigations involving the development of disintegrating projectiles for use in howitzers of various calibers have been accomplished. The ultimate purpose of these investigations was to make possible the training of operating personnel, exercising of weapons and proof checking of recoil mechanisms and carriages in populated areas. The usual pretest procedure is first to determine what physical quantities should be measured and second to design the instrumentation system required to measure them. It is the practice in program planning to determine the

minimum number of measurements required to achieve the desired result. The instrumentation used in these investigations is typical for the majority of firing tests of artillery and boosted rocket launcher weapons at Rock Island Arsenal. The information acquisition and transmission equipment consisted of a multi-channel carrier amplifier system and optical galvanometer recording oscillograph. The transducers used consisted of the non-self-generating type previously described. The physical quantities measured and transducers used were as follows:

1. Recoil Rod Pull. - Measured by means of a load cell consisting basically of a steel cylinder with bonded wire strain gages oriented to sense tension load and calibrated in pound units. These devices are assembled directly on the recoil mechanism rod in place of the nut and are a special Rock Island Arsenal design.
2. Circumferential strain in the Howitzer barrel and bending strain in trails. - Measured by means of conventional electric strain gages.
3. Displacement of recoiling parts. - Measured by means of a special variable reluctance transducer developed at Rock Island Arsenal.
4. Acceleration of recoiling parts. - Measured by means of commercial transducer of the electric resistance strain gage type.
5. Recoil mechanism oil pressure. - Measured by same type of transducer as 4.
6. Motion analysis. - Monitored by means of high speed and conventional speed movie cameras.

Firing tests in connection with development work on a light weight 105 MM Howitzer designated the XM102 system has been in progress for several years. This weapon represents a radical departure from conventional artillery design in that the original weight of 5600 pounds is being reduced to 3000 pounds. This necessitates a great variety and quantity of recorded measurements. In addition to the measurements described previously, numerous qualitative and quantitative measurements of strain, deflection, displacement and load have been measured by means of either strain gages or flexure devices using strain gages. The point is that with a little ingenuity and perserverance it is usually possible by means of conventional or improvised transducers to measure any physical quantity associated with performance of weapons under firing conditions.

Artillery weapons development programs which have required rather extensive instrumentation are listed as follows:

1. Development of disintegrating projectiles for artillery weapons- previously discussed.
2. Development of light weight 105 MM Howitzer XM102- previously discussed.
3. Development of prototype auxiliary propelled carriages for 105 MM Howitzer and 155 MM Howitzer.
4. Research study on feasibility of firing 105 MM Howitzer material Out-Of-Battery.
5. Research study on feasibility of using braking rockets to provide counter-recoil force for 105 MM Howitzer material.
6. Development of firing platforms for artillery and boosted rocket launcher weapons.
7. Development of improved recoil mechanism control rod for 105 MM Howitzer materiel.

Due to limited range of the proof testing facilities, tests of weapons classified as rocket launchers have been limited to only a few weapons. These were weapons that could be fired directly into a sand pit. The quantities measured and instrumentation used on these weapons was generally the same as that used in firing tests of Artillery weapons. Most of the launcher weapons tested are research and development prototypes and have required, during the course of development work, extensive instrumentation. A brief discussion of some of the more novel instrumentation used on some of these weapons follows.

An interesting firing test program was conducted to measure the time-motion history of a 4.5 inch Multiple Rocket Launcher M21 during firing. A system of flexure devices consisting of cantilever springs with strain gages mounted on them were calibrated to measure deflection. They were oriented to measure vertical, lateral and longitudinal motion of the launcher. This test is a good illustration of the versatile use of the electric resistance strain gage for measuring physical quantities other than strain.



A tremendous amount of instrumentation has been utilized in connection with firing tests during the course of development work on the 115 MM Rocket Launcher XM70. This weapon fires a boosted rocket type artillery shell. Two accelerometers were mounted directly on the muzzle of the barrel during a series of firing tests in order to measure the deflection of the muzzle in the vertical and lateral directions. Deflections were obtained by electronic integration of the accelerometer signals.

Instrumentation has been used extensively in firing tests in connection with development of the spotting gun XM77 for the XM29 system (Davy Crocket Weapon). As previously mentioned, rate gyroscopes were used successfully to measure the angular velocity of the beam on a M386 Launcher during firing. A considerable amount of instrumented measurements have been made in connection with the development of the various launchers for Honest John and Little John Rockets, such as the M386 and the XM34. However, these were static and quasi-dynamic tests, not involving actual firing of rockets.

#### Instrumentation Problems

All technological effort is beset with problems and the acquisition of data on weapon performance is no exception. Instrumentation problems that arise fall into three general categories. The first includes those which are caused by the complex physical effects resulting from high loading rates imposed on weapon structures during firing. The second category includes those resulting from physical and environmental conditions which impose severe restrictions on measuring instruments, primarily the transducer itself. The third includes those problems due to functional limitations of instrument systems.

In so far as the first category is concerned, the firing impulse transmits complex shock and vibration phenomena which are sensed by transducers as corresponding variations in strain, deflection, force, pressure, and acceleration, to name a few. These secondary effects are superimposed on the primary effects and the result is often seen as a noise or "hash" in the recorded trace. However in dynamic work it is often important to take secondary effects such as strain into account, especially when the sum of the primary and secondary effect is sufficient to cause failure. For this reason it is generally not advisable to use electrical or mechanical filtering devices. Intermediate mounting devices are potential sources of trouble, since they may vibrate and produce spurious signals in the transducer which may be misinterpreted.

The second category involves some very formidable physical problems. The usual situation involves the measurement of some physical quantity in an inaccessible internal part or an external part with insufficient mounting space for the transducer.

The third category involves the usual well known difficulties associated with electronic equipment such as internally and externally generated noise, broken connections, feedback, high resistance soldered joints, system nonlinearity, failure of electrical components and many others.

It is hoped that this paper has been sufficiently comprehensive to give some insight into the important roll that instrumentation plays in weapons testing at Rock Island Arsenal.

### DISCUSSION

Question: Do you calibrate at rapid rates or do you calibrate under static conditions?

Mr. Hanson: We have calibrated accelerometers at rapid rate using a cathode ray oscilloscope with camera attachment but it was difficult. Generally we calibrate with static quantities and where we can we try to calibrate with dynamic quantities.

Questioner: I was just trying to find out if there were some means of calibrating this equipment under dynamic conditions.

Mr. Hanson: Well, maybe I could go into details on this subject with you later. I think time is a little short to go into details now.

## THE PROPAGATION OF SHOCK WAVES INDUCED BY UNDERGROUND EXPLOSIONS

Dietrich E. Gudzent\*

### ABSTRACT

This paper is intended to present the survey of the current status of investigations concerned with some of the fundamental problems involved in determination of efficient underground structures. The application of results from such studies is critical in the design of such things as bomb shelters, missile storage silos, highway construction, and mining operations. Information available has been drawn from many sources: explosions of mining operations, theoretical studies, earthquakes, experimental nuclear explosions, and many small-scale laboratory experiments.

Particular emphasis has been devoted to a study of the effects of soil properties such as mineral and moisture content, grain size, density, and cohesion. Shock waves passing through the earth have been measured and attempts to determine such things as particle acceleration, velocity, displacement, and peak pressure of the front of the wave have been made. In theoretical studies the slope of the acceleration vs. the distance from the explosion has been derived, i. e.  $A_r = A_0 \exp(-n \cdot \ln r)$ , where  $A_r$  is the acceleration at distance "r",  $A_0$  is the acceleration at the distance zero, "n" is the exponent which determines the rate of decrease of the acceleration with the distance "r" from the explosion. Attempts to predict shock wave intensity for full-scale explosions from the results of scale tests require use of a scaling formula. One commonly used is:  $W_s = W_L \cdot S^3$ , where  $W_s$  is the weight of the test explosive,  $W_L$  is the weight of the full-scale explosive, and S is the scale factor. This formula is satisfactory for air blasts but fails in application to underground explosions because the equation of state of soil conditions is not clearly defined. Other possible formulas for use in scaling may possibly be that used in deriving Newton's number or Hooke's number.

In addition to studies devoted predominately to soils and the nature of the transmission of waves through such a theoretical effort has been expended in attempts to establish equations of motion for the propagation of shock waves through solid bodies.

---

\* Mr. Dietrich E. Gudzent, Chief, Dynamics Characteristics Section, Dynamics Analysis Branch, Structures and Mechanics Laboratory, AMC, Redstone Arsenal, Huntsville, Alabama.

A number of theoretical approaches to the particular problem of establishing mathematical models for shock wave propagation will be discussed in this paper. Some discussion of experimental work in terms of tests and a determination of scaling laws will be given. Recommendations for future theoretical work and experimental research will be made.

## THE PROPAGATION OF SHOCK WAVES INDUCED BY UNDERGROUND EXPLOSIONS

I would like to give you a brief survey of the efforts devoted to the study of shock waves induced by underground explosion and their interaction with buried structures. I want also to show how this applies to the problem of sympathetic detonation of missiles housed in underground silos.

Let us assume that a certain number of silos are clustered to a nest, that the nests are a certain distance from each other, and that a number of nests are integrated into a system. It is possible that a missile blowup can occur. We require that in such a case only one nest may be destroyed while all other nests remain operational. Or, in other words, the radius of destruction,  $r_d$ , must be related to the inter-nest distance,  $l$ , by the inequality

$$r_d < l$$

This requirement may be achieved by

1. suitable design of silos and nests
2. choosing proper distance " $l$ " between two nests
3. using means to attenuate the propagating shock wave between adjacent nests.

We can try to achieve a solution in two different ways, either by experimental investigations or by theoretical considerations.

Let me first discuss experimental investigations.

Little has been done to date in full-scale experiments but numerous scaled experiments have been performed.

In 1946 Lampson published his very extensive and comprehensive report relating measured phenomena from underground explosions to damage on underground structures. Lampson derived a currently well known model law to extend the results of properly designed experiments over a range of scale factors.

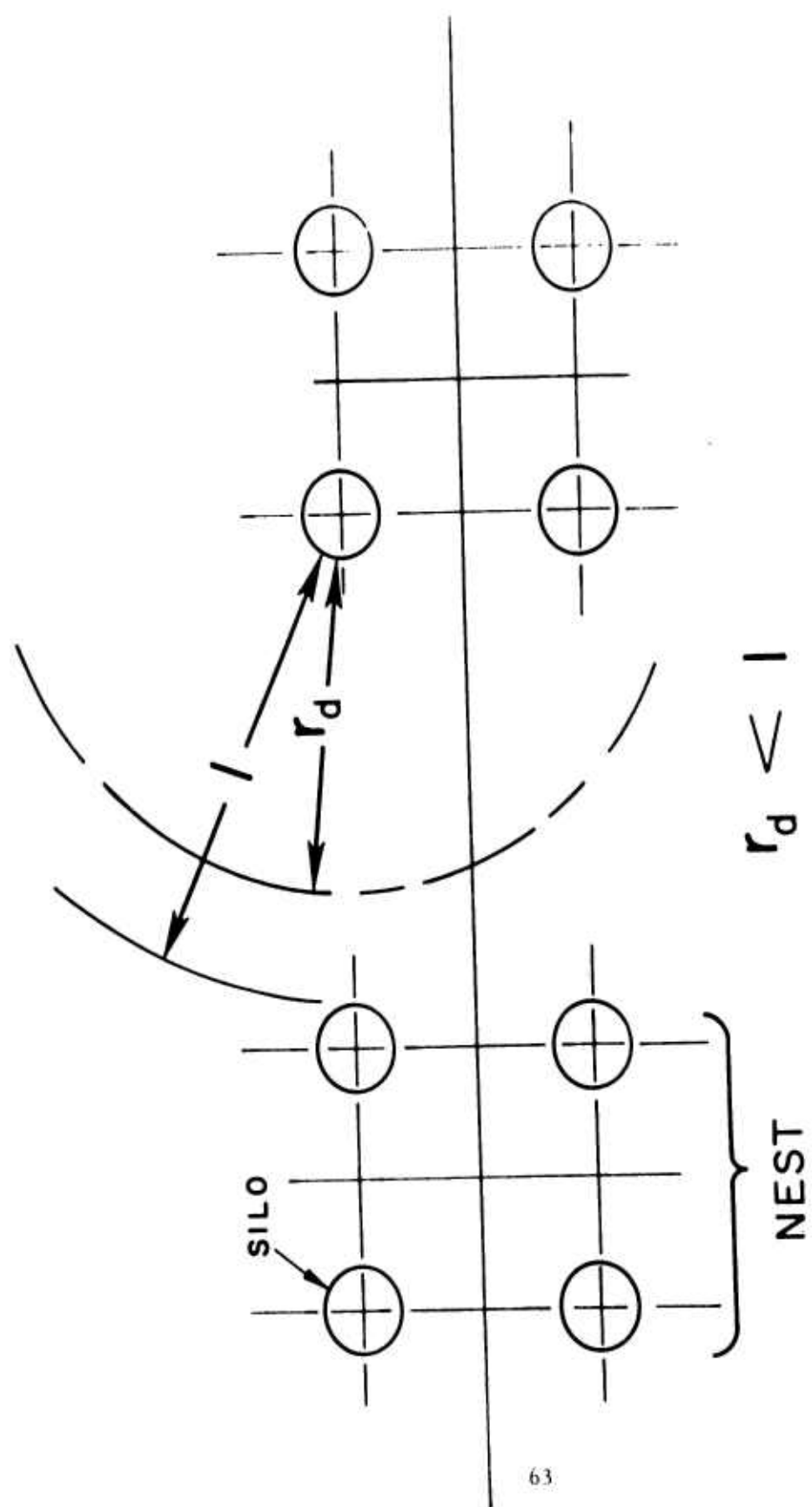


FIG 1

According to this law, if  $D_1$  is the distance from an explosion of a material of reference weight,  $W_1$ , with which a certain overpressure or dynamic pressure is attained, then for any weight of explosive,  $W$ , these same pressures will occur at a distance,  $D$ , given by

$$\frac{D}{D_1} = \left( \frac{W}{W_1} \right)^{1/3}$$

This law has been widely used in current literature despite the fact that many authors have found discrepancies between it and actual measurements. This is not too surprising because the law is well established only for a gaseous medium which follows the law of state of an ideal gas. We shall not expect that solid material behaves like an ideal gas. As long as we do not have a law of state for soil, we will have difficulties in establishing scaling procedures for investigation of explosions.

For this reason many scientists have developed empirical formulae for the attenuation of a shock wave versus distance. As an example, Townsend, Langseth, and Perkins published the formula

$$A_r = A_0 e^{-n \ln r}$$

where  $A_r$  is the acceleration at the distance,  $r$ , and  $A_0$  is the acceleration for the distance zero. The value of  $n$  has been found to be 4.3 in sand and 4.2 in clay, varying with distance.

Unfortunately, time is short so I must end the discussion of experiments in order to mention in the remaining minutes some theoretical consideration. This part of the discussion consists of a description of the requirements for the time-location relationship of the propagating wave after an underground explosion and its action upon the next nest, considering

1. type of wave,
2. frequency distribution,
3. kind of soil,
4. type of explosion or detonation, and
5. design criteria of silos and nests.

At the present time no general equation of such nature exists due to the complexity of the problem and the contributing unknown factors and functions. For certain aspects of the problem treatments are available.

In order to treat the propagation of waves through soil it is necessary to assume idealized behavior of the soil with regard to deformation. The

most common idealizations are represented by the model of the elastic medium and the locking medium. It is not necessary here to discuss the behavior of elastic medium except to note that in some cases rock may be considered as ideally elastic.

The locking medium is characterized by a certain behavior of the stress-strain relation of granular masses which may be described as follows:

First Stage: On initial compression a slightly non-linear elastic behavior exists.

Second Stage: Further compression may produce a plastic flow and some gradual breaking of grains resulting in a softening or plastic response.

Third Stage: Additional pressure produces a rather sudden rearrangement of granules into a less compressible state accompanied by large volumetric changes and by permanent strains, manifested by the upturning of the stress-strain curve.

The stress-strain relation can be idealized by various curves as shown in Fig. a, b, c, and d, the simplest being that of Fig. a, a case which we will consider later. This stress-strain diagram implies that upon initial loading the medium exerts no resistance until a critical value of the strain (or density) is reached. Beyond this critical strain the material becomes incompressible. Modifications affect either the initial behavior of the material, making it elastic (Fig. b) or elastoplastic (Fig. c), or they influence the behavior after the critical strain is reached by permitting a certain amount of residual elasticity, leading to the bi-linear model of Fig. d. At lower levels of compression, where the governing phenomenon is not that of incompressibility but rather that of a gradual but irreversible volume change, the behavior of the medium may be characterized by the stress-strain curve of Fig. e.

In some cases sand may be considered as an ideal locking medium. Other types of soil such as clay are located between the elastic and the locking medium.

Time limits a comprehensive discussion of famous mathematical treatments given by Hutton, Skalak, Salvadori, Weidlinger, and Wiedermann, to mention a few. I would like to present only one example: a very recently published paper by Jordan in England. He gives a thorough mathematical treatment and arrives at solutions which can be numerically evaluated. The detailed description of the theory is beyond the scope of my presentation

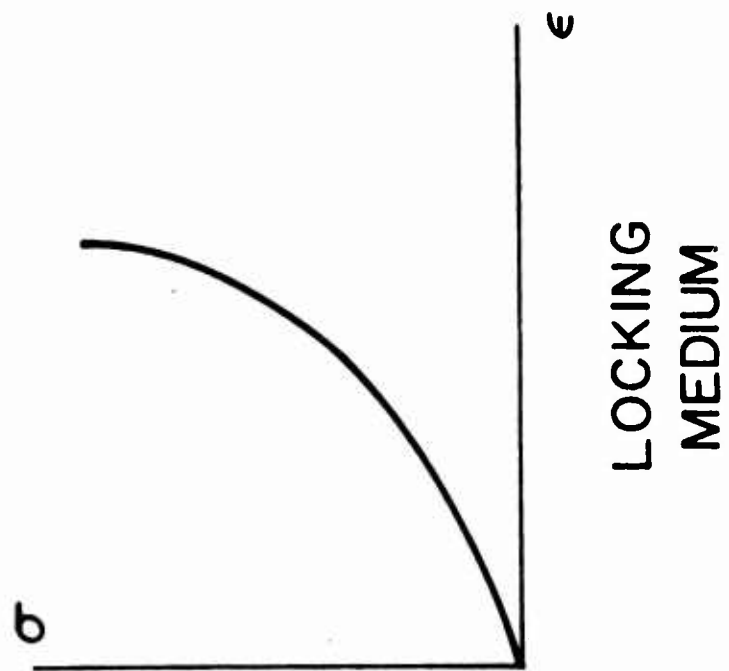
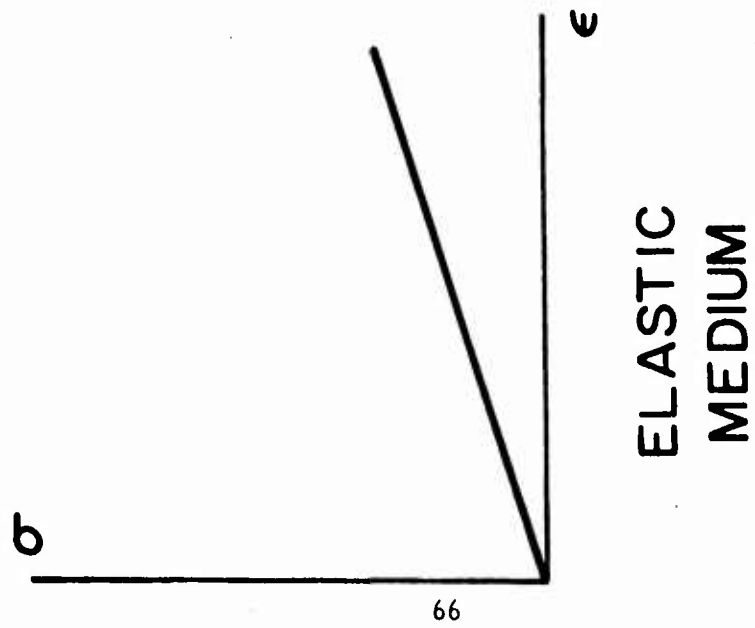
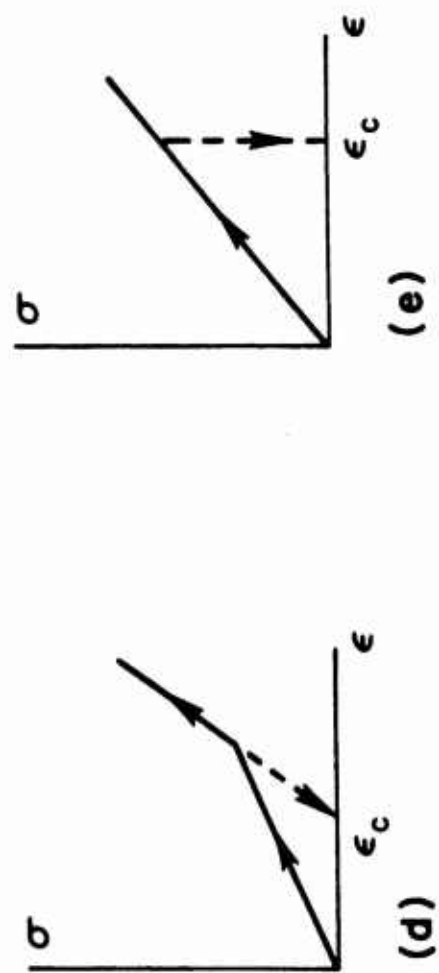
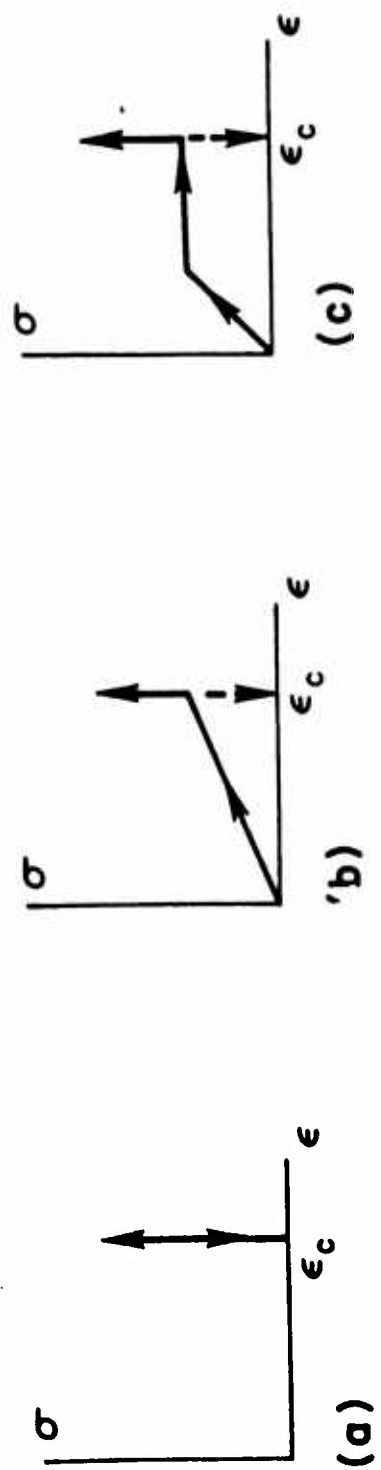


FIG 2





IDEALIZED STRESS - STRAIN CURVES

FIG. 3

today but to give an idea I will outline here the basis of his approach. Jordan assumes an infinite, cylindrical hole in the solid body, partially filled with explosives. The explosive is lighted on one end, the explosion travels through the material in the hole and a shock wave is created showing a certain time delay.

Cylindrical coordinates  $(r, \theta, z)$ , are used, with the origin of  $z$  at the center of the source.  $z$  extends along the axis of the hole. The radius of the infinite length cylindrical hole is  $a$ , the displacement components in the  $r$  and  $z$  directions are  $u_r$  and  $u_z$ , respectively, and component  $u_\theta$  is absent for reasons of symmetry. After introducing convenient non-dimensional coordinates, the general differential equations for the motion of a particle are

$$\frac{\partial^2 \frac{u_r}{a}}{\partial t^2} - \frac{\partial}{\partial \frac{r}{a}} \left[ \frac{1}{\frac{r}{a}} \frac{\partial}{\partial \frac{r}{a}} \left( \frac{r u_r}{a^2} \right) \right] - \frac{\partial^2 \frac{u_z}{a}}{\partial \frac{r}{a} \partial \frac{z}{a}} = 0$$

$$\frac{\partial^2 \frac{u_z}{a}}{\partial t^2} - \frac{\partial}{\partial \frac{z}{a}} \left[ \frac{1}{\frac{r}{a}} \frac{\partial}{\partial \frac{r}{a}} \left( \frac{r u_z}{a^2} \right) \right] - \frac{\partial^2 \frac{u_z}{a}}{\partial \left( \frac{z}{a} \right)^2} = 0$$

$$\frac{\lambda + 2\mu}{\mu} \frac{\partial^2 \frac{u_r}{a}}{\partial t^2} + \frac{\partial}{\partial \left( \frac{z}{a} \right)^2} \frac{\partial \frac{u_r}{a}}{\partial \frac{r}{a}} + \frac{\partial^2 \frac{u_z}{a}}{\partial \frac{r}{a} \partial \frac{z}{a}} = 0$$

$$\frac{\lambda + 2\mu}{\mu} \frac{\partial^2 \frac{u_r}{a}}{\partial t^2} + \frac{1}{r} \frac{\partial}{\partial \frac{r}{a}} \left[ \frac{r}{a} \frac{\partial \frac{u_z}{a}}{\partial \frac{r}{a}} \right] - \frac{\partial^2 \frac{u_r}{a}}{\partial \frac{r}{a} \partial \frac{z}{a}} = 0$$

We have two sets of two equations each for the two components,  $\frac{u_r}{a}$  and  $\frac{u_z}{a}$  for which we substitute  $u_r$  and  $u_z$  respectively. The reason is that the original equation

$$\frac{\partial^2 U}{\partial t^2} = \text{grad div } U - \frac{\mu}{\lambda + 2\mu} \text{Curl. curl } U$$

has, for simplicity, been split into two equations; hence, it is necessary to seek common solutions of the two systems.

The special form of the differential system suggests the use of a double Fourier transform from which the equation for the transformed functions results in the well-known Bessel equations. These equations are solved by Hankel-functions (Bessel-functions of third kind). The boundary conditions need careful consideration to determine their effects on the path of integration in order to avoid certain problems arising from branch points occurring in the problem. The task of obtaining a common solution to both systems can be achieved approximately by applying the method of "steepest descent" from calculus of variation. Having obtained the solutions, they are re-transformed by the appropriate inverse Fourier transforms. Exact solutions can not be obtained, but it is possible to adapt the integrals for an asymptotic expansion. Jordan has shown that these expansions with resulting approximations are valid for certain regions surrounding the source, but they cannot be applied to other regions, such as the region located near the free end of the exploding column energy source. Adapting the mathematical expressions to solution by numerical methods finally makes it possible to arrive at expressions of special wave forms with variations versus time and distance.

Based primarily on the material which I have presented here in addition to many more investigations not discussed today, we conclude that:

Publications on experiments to date do not give the desired answer to our specific problem, principally due to the following reasons:

a. Most of the experimental works were not intended to solve exactly the same problem with which we are concerned. Many neglect phenomena or circumstances which are vital to our task, i.e. (a) using spherically shaped instead of cylindrically shaped charges, or (b) directly burying the charges in the soil neglecting an air gap, or (c) using different type of explosives.

b. Most of the experimental works give too little consideration to the theory of similitude and so prevent satisfactory extrapolation to larger or smaller dimensions, i.e. application of a scaling law to underground explosions which is well established only for air blasts.

For that reason we are initiating at Army Missile Command a critical comparison of all important information dealing with experimental data in an effort to establish an integrated picture by inter-linking the more or less isolated data of independent reports. Furthermore, we will conduct our own experiments to fill existing gaps of information or to gain specific data for theoretical investigations.

The theoretical works do not present the desired answer to our specific problem due principally to the fact that one or more assumptions and/or simplifications necessary for mathematical treatment do not agree with the

conditions of our problem. For that reason we will conduct a critical investigation of the most important theoretical approaches to determine to what extent they are applicable to our problem, and we plan to apply the most promising approaches to our special requirements. Finally, we will compare theoretical results with the experimental data. We want to give attention to the development of equations of state for solids with the objective of establishing a theoretically well-founded scaling procedure for experiments in soils.

Finally, we are going to include studies of the interaction of a shock wave with buried structures in the above-mentioned investigations with the ultimate goal of establishing the design criteria for silos subjected to heavy dynamic loads from underground explosions.

Banquet Address  
RESEARCH AND DEVELOPMENT FOR ARMY MOBILITY

Major General Alden K. Sibley  
U. S. Army Mobility Command  
Springfield Armory  
Springfield, Massachusetts

Mr. Chairman, General Britton, Colonel Medinnis, Dr. Kumar, Dr. Hammer, members of Army Conference on Dynamic Behavior of Materials and Structures:

It is a pleasure to be with you this afternoon to participate in your conference. Your three-day program is impressive, and I was delighted to see that no less than 9 of your 46 participants are members of the research and development agencies of three of the Mobility Command's largest installations: the Detroit Arsenal and Army Tank-Automotive Command, located near my headquarters in Detroit; the Transportation Engineering Agency (TRECOM), at Fort Eustis, Virginia; and the Engineer Research and Development Laboratories at Fort Belvoir, Virginia.

I have had the opportunity to read the fine papers that will be presented by members of these installations, and was highly impressed by both their technical excellence and their very real contribution to the study of the dynamic behavior of materials and structures. I am confident that your conference will be of great value not only to the Mobility Command and to every Army installation represented here today, but to our domestic economy as well.

You are engaged in an area of research whose application has already revolutionized modern technology and which will continue to affect every aspect of modern life, particularly as the tools and techniques of your science become more and more powerful. Throughout my career as an engineer officer, I have watched your science grow. Your work permeates every field of modern technology. No matter where we look, whether to man's domination of his natural environment here on earth or to his mastery of outer space, the materials expert has set the pace of progress. I envy you for your great and challenging opportunity as scientists and engineers to work in one of the youngest and most exciting of scientific disciplines.

Progress made in developing new and better materials will affect directly attainment of total mobility for the Army of the future. In a very real sense the Army's ability to move - the primary mission of the new Mobility Command - will be affected profoundly by your efforts and your degree of success.

In the face of the stealthy encroachment of communism into free world areas since the end of World War II, we have at last fully realized the nature of the threat and have taken the steps necessary to halt the nibbling, "slice of salami" tactics of communist aggression. We have become fully aware of the war being fought against us. In building a greater capability for fighting limited, sub-limited and counter-guerilla warfare, highly mobile conventional forces have at last been given proper recognition and emphasis. The advent of nuclear energy, of absolute firepower, has changed forever the art of war. If we are to have a history this must be the last era in the history of mankind of the ascendancy of firepower. Therefore, it becomes evident that we are now at the dawn of the golden age of strategic and tactical mobility in the art of war. This will be the underlying philosophy of the art of war in the future. We can never go back to a strategy based on firepower. We must build our capabilities now for quick, lightening like thrusts to stamp out brushfire wars in any part of the world in a matter of hours.

Mobility will remain of overriding importance for as long as the freedom of Western Civilization is threatened by communist aggression. We must build mobile forces capable of a graduated response to any type of aggression. Our modern mobile Army must be able to respond even more rapidly, through use of both air and ground mobility, to a wide variety of conflict situations, from subversion and insurgency to major military operations.

Recognizing that we can no longer afford to subordinate mobility to firepower, our government has recently decided to create a single, expert mobility team to administer the Department of the Army program for research and development, production and procurement, as well as supply management of all types of mobility equipment and supplies. It has been fully realized that the leadership of the free world requires mobile forces adequate to support a determined national policy.

The Army's need for true strategic and tactical mobility must be met by the best possible efforts of our military - industry team. We must have tactical mobility on land, on water, and in the swamps and jungles of Southeast Asia, the deserts of the Middle East, the developed areas of Western Europe, in all conceivable types of terrain and climate. We must have the

capability to confront and defeat any type of military force, from the modern massive and mobile armies, to small hit-and-run guerilla bands. We therefore must have tactical mobility in all environments - vehicles that operate on the surface, those like the GEMS under development that travel a short distance above the nap of the earth, in and over water, and in the air. Ground vehicles must be able to traverse the roughest terrain, to operate in mud, ice, snow, water and sand, as well as on developed highways. We must continue to exploit with all the vigor and imagination at our command every significant scientific and technological breakthrough in the field of mobility.

We have thus far established here in Detroit a modest headquarters of 340 people in the Administration Building of the Michigan Ordnance Missile Plant. From now until the end of the calendar year, the Mobility Command headquarters will gradually be expanded to its full strength of some 600 key executive, administrative, and technical personnel.

The tremendous number and variety of products managed by the Mobility Command makes it by far the most complex of the seven commands that comprise the Army Materiel Command. The commodities managed from the new headquarters in Detroit will include electrical power and general equipment, construction and service equipment, bridging and barrier equipment, general mobility supplies, general purpose vehicles, all Army aircraft, aeronautical equipment, aerial delivery equipment, and surface transportation equipment.

The new Mobility Command will be composed of nine major field installations, including ATAC/Detroit Arsenal, operated by a total of over 13,000 military and civilian personnel. MOCOM will manage the whole spectrum of mobility equipment from research and development through production of over 346,000 separate items - well over half of all the items of the Army Materiel Command as a whole. The Mobility Command will operate on a budget exceeding \$2.0 billion annually, and in this fiscal year \$1.2 will be spent directly for hardware, and \$120 million for research and development.

Rapid progress in research and development, for bold new ideas and innovations, is one of the primary goals of the new Mobility Command. We must push back the frontier of knowledge to produce new materials, new methods, and new processes. Lead time in placing new equipment in the hands of troops must be reduced from the 7 year cycle of the past to 4 years. The job must begin at the R&D phase and be carried through with vigor and imagination to the production and distribution of new equipment to troops in the field.

Future advances in a great number of technological fields rests squarely upon the development of new materials. The range of materials with which we have been working for centuries will not suffice today. In our space and missile programs, we need rubber that can withstand both the high temperatures of the heat barrier and the icy breath of the stratosphere, lubricants that retain their properties on red hot surfaces, protective films that resist all-corroding acids, and propellants which will not crack under extreme shock and vibration.

The unprecedented demands for new materials are staggering - materials, for example, that can withstand conditions of extreme heat and pressure in the order of a half million pounds per square inch and 3000 degrees Centigrade. All the Armed Forces share the need, and are working jointly in this area on a variety of approaches - in plastics, in ceramics, in polymers, and in metals - spending many million dollars a year. The future of these techniques depends upon successful breaking of the materials barrier.

You are working in an exciting, relatively new, and challenging area of research of basic importance to all future progress in the development of equipment and materials for the modern Army. I was delighted to see the word "dynamic" emphasized in the announcement of this conference. We wouldn't have to go back too many years - in fact, well within the experience and memory of many of us in this room, when "static" analysis of the strength of materials would be the keynote of such a conference. This, I suppose, can be laid to the door of the civil engineer, since the whole field of materials research grew from his need to create better materials for his static construction. Curiously enough, the emphasis upon static phase of your study, and the dominance of the civil engineer in this work, has cast a long shadow. I would venture to say that the majority of texts used in our colleges and universities today in the strength of materials courses were written by civil engineers; and further, that these texts deal comprehensively with static analysis, treating dynamics as a special case.

Not until the development of steam propulsion in railroads and ships did our attention turn to the study of dynamic behavior, unfortunately as an extension of static behavior. I know that this was true in my own education in civil engineering at West Point some thirty years ago, and I'm sure that some of the texts I used then are still current in revised editions. Perhaps now is the time to reconsider the conventional approach to these studies and to dwell predominantly upon dynamics and to consider static analysis as a lesser and special case.

This early emphasis on the static behavior of materials forced reliance on empirical methods and use of the "safety factor," that is, a factor of



ignorance in designing machinery and vehicles. The degree to which these factors of ignorance have been cut is a good indication of the progress that has been made. Thirty years ago safety factors as high as 10 were not unusual. But with steadily increasing knowledge of size effects, surface finishes, heat treatment, notch effects, and analysis by wire-resistance strain gauges, and other modern techniques of analysis, the level of safety factors has been reduced to as low as 1.3. But continued reduction of "ignorance factors" in the field of materials as a whole rests squarely upon our efforts in basic, fundamental research.

In one sense our spectacular record of progress in technology clouds the fact that the technological explosion now taking place is triggered only by new scientific knowledge revealed through basic research.

Five years ago, almost to the day, launching of the Soviet satellite "Sputnik I" was headlined in every language and in every city in the world in which newspapers are printed. October 4, 1957 was given a place in the history books of our grandchildren as the beginning of the Age of Space. Since then spectacular achievements in manned space flight and in the flight of interplanetary probes from both sides of the iron curtain have rapidly pushed back the frontiers of space, and I have no doubt our stated goal of manned exploration of the moon will take place within the decade of the 60's. Technology is truly exploding. As we stand at mid-century we should be thankful for the privilege of living in an age when man's challenges and opportunities were never so great. We stand now at the threshold of space, in one of the true turning points in the history of man, when the accumulated knowledge of the ages presage events and accomplishment yet undreamed of. Victor Hugo, the great French novelist, once wrote, "in the sweep of the ages there come times when events constitute the hinges upon which the centuries swing." We are privileged to live in one of these fateful times, and how we face this challenge, both in space and here on earth, may well shape man's course in future centuries.

Just as we stand on this threshold of space, we also stand on the verge of all that science and technology promise for the future here on earth. Modern science is not yet 500 years old, and organized technology is less than half of that. During the past 100 years, just a small fraction of man's recorded history, he has achieved 90% of his technological progress. As evidence of the youth of science is the remarkable fact that of all men who have ever been educated and trained in the disciplines of science and technology the world over, 90% of them are alive today. Many of us here today have lived through and experienced the results of many milestones in the inexorable advance of scientific knowledge and its technological application. The oat barrier cracked with invention of steam locomotion, and

land locomotion made a quantum jump from the 35 mph maximum speed of the horse. Orville and Wilbur Wright flew their first plane at not much greater speed at the turn of this century, and just a few years later we broke the sound barrier. A man named Goddard spent his afternoons in his backyard in Springfield, Massachusetts, in the early 1930's horrendously disturbing the peace launching his small rockets. Orbiting satellites, manned space flights and multi-million mile interplanetary probes are now becoming almost daily affairs. At the same time Goddard was at work, Lise Meitner and Otto Hahn in Germany produced the first fission or uranium atoms on earth, and just a few years later World War II ended with the Nagasaki and Hiroshima fission bombs, and we entered the nuclear age.

No matter where we look, to speed of locomotion, on land, air, and in outer space, in materials research, the firepower of atomic and thermonuclear bombs, the harnessing of nuclear power for energy, preventive medicine, technology is truly exploding, reaching milestone after milestone at an exponential rate. The very number of scientific specialties themselves seem to be growing at a similar rate. In a recently published catalogue of existing scientific fields more than 1100 specialties are listed, ranging from acarology, a branch of zoology that deals with mites and ticks, to zymurgy, the chemistry of fermentation processes.

But we must pause to look more closely at the true source of this technological explosion, of our tremendous success in applied science, in developmental research and engineering. This source is the mind of the individual scientist whose ideas are the foundation upon which all technology rests. As an example, let us look for a moment at the pure research which led to construction of the first nuclear bomb.

Among these contributions were those of Henri Becquerel, a Frenchman, who first discovered the phenomenon of radioactivity; Niels Bohr, a Dane, and the Bohr model of the atom; Louis de Broglie, a Frenchman, the founder of modern wave mechanics, Werner Heisenberg, a German, with his elaborate matrix mechanics; Albert Einstein, a German, and the mass-energy relationship; Max Planck, a German, and the quantum theory; Pierre and Marie Curie in France and their researches in radium; Lord Rutherford, in England and the identification of alpha, beta and gamma rays; Robert Millikan, an American, and his classic oil-drop experiment with which he measured the charge on a single electron; F. W. Aston, an Englishman and the mass spectrograph; C. T. R. Wilson, an Englishman, who developed the Wilson Cloud Chamber for observing the tracks of high speed particles; P. M. S. Blackett, an Englishman, who photographed the first artificial transmutation of an element; Sir James Chadwick, an Englishman, who proved the existence of the neutron; and finally Lise Meitner and

Otto Hahn of Germany who succeeded in splitting an atom of uranium, thus producing the first nuclear fission.

From this point on, the making of a nuclear bomb was largely a technological problem, a now familiar story. The world first heard the word "fission" in August 1945 when Mr. Churchill released the story of the Hiroshima atomic bomb. With the release of the Smythe Report the story was told. But that does not bring the story quite up to date. A fission bomb can be made only so big and no bigger than the critical mass or it will blow itself up while being made. The trick is to make a ball of uranium isotopes just slightly smaller than the critical mass - then by squeezing it under the implosion of TNT, like squeezing a sponge-rubber ball, its density is increased and surface escape area reduced enough to trap the neutrons and make it explode. Hence it is impossible to build a fission bomb more than several times as powerful as the Hiroshima weapon. However, pure scientists had not been idle.

In 1938 an astrophysicist, Hans Bethe, at Cornell University, showed how energy radiated by the sun comes from the burning of hydrogen atoms into helium, a process he called the "carbon cycle". Two very light atoms can fuse together into a heavier one with loss of weight, according to Einstein's mass-energy relation, just as one extremely heavy atom can split into two lighter ones with loss of weight. But the two hydrogen atoms have to be subjected to the tremendous heat of the central regions of the sun before they can be made to fuse together. And in "Operation Greenhouse" on Eniwetok in 1952, Norris Bradbury, Edward Teller and others made enough heat with an ordinary atomic fission explosion to burn a container of hydrogen isotopes into helium for the first time on earth. Two years later, the March 1, 1954, shot at Bikini was the first man-made thermonuclear explosion. The literally world-shattering significance of this thermonuclear bomb, whose hydrogen atoms won't fuse at normal temperatures, is the absence of critical mass. Moreover, there are enough of the proper hydrogen isotopes in sea water to make a pound of heavy water sell for about twenty-eight dollars, or more bang for your buck.

The impact of these developments upon our concept of war as a means of dealing with international problems constitutes a subject in itself. And we can well search the writing of Clausewitz, Mahan, Douhet and MacKinder, for an age without precedent has real need for military guidance. Wars of the past have been fought for land, for wealth, for ideals, for blondes and brunettes for that matter. But wars of the future will be fought for none of these things primarily. The real war of today and tomorrow is the war of men's minds. What are our chances of survival? How are we doing in the race to train American minds to win the thinking war - the

war of pure science, of fundamental research?

A brief review of the state of science and technology in America may point to the answer. By science I mean what is usually called fundamental research: the free, uncharted probing into the unknown merely for the satisfaction of curiosity and the accumulation of knowledge, the development of basic scientific innovations from which technology springs. By technology I mean applied science, developmental or goal-oriented research, engineering, the systematic use of primary scientific knowledge for a purpose.

It has long been accepted that the United States has made a far greater contribution to the development of technology than any other nation in history. No other nation approaches us. Our closest competitor, the Soviet Union, has approximated only one-third of our technological advances as measured by relative productive capacity today. It is no mere whim of the European that has led him so often to characterize America as a nation of gadgeteers.

In contrast, our contributions to pure science have been far less impressive. You may remember that in our earlier review of the ideas, the theories that led to the development of nuclear energy only one American was mentioned. Americans tend to honor structure over design, the gadget more than the theory. Yet in the age of slow neutrons, radioisotopes, and nuclear fission, world girdling manned space flight and interplanetary probes, the nation which excels in pure science may well control the world.

There are reasons for the American penchant for gadgeteering, of course many of them fairly obvious. We have had at our disposal a vast geographic expanse containing an enormous wealth of natural resources. After three hundred years, great areas of our country still remain sparsely populated. We have always had room to move, resources to draw on. We have always been faced with the challenge to build - the challenge of engineering. We have been fortunate inheritors of the pragmatic spirit which brought the Pilgrims to our country and sent the pioneers across the western plains, relying on their common sense and ingenuity to cut a living from the raw and rugged continent they had chosen. Ingenuity born of necessity has led us inevitably to become a nation of gadgeteers. Like the Romans, we love to build things. We are the greatest skyscraper, road and bridge builders that the world has ever known. Today we continue this tradition, we build and produce empirically.

Although increasing quantities of our federal budget - over 8 billion dollars a year - are poured into research and development, this is research



and development of a very special kind. It is largely developmental research; applied science, technology, and engineering. Only about 10% of it is pure research. We research the hell out of everything, but we contemplate very little.

In the past this has been in many ways our strength. But it can be very strongly argued that we are moving into a different age--an age when respect for ideas, when respect for the basic contemplation of nature and society for the simple sake of seeking truth and satisfying curiosity may be much more necessary than we have previously realized.

It is a telling and disturbing fact that a similar situation does not exist in Soviet Russia. To compare the number of higher education graduates in engineering and science since the end of World War II and projected to 1970 is frightening not only on the basis of their superiority in number alone, but that probably about 20% of Russian graduates are fundamental researchers: pure physicists, mathematicians, chemists, and the like. In 1959, the Soviets graduated some 106,000 in engineering compared to our 40,000, and about 15 percent of these Soviet graduates were from correspondence extension courses. In addition to this output of engineering graduates, a great number of technicians are graduated yearly from their rapidly expanding system of two-year colleges, or junior colleges, called technicums. According to a recent report from the Soviet news agency, Tass, a total of 404,000 scientists are now at work in the Soviet Union - 40 times as many as there were under Czarist rule.

Perhaps the Russians are wrong in such a concentration of national effort in science. If they are wrong, they will have an overabundance of scientists. If we are wrong in developing too few scientists and high quality engineers, it may cost us our survival as a nation. It is hard to avoid the conclusion that the Federal government, industry, private foundations and each of us as individuals must come squarely to grips with this problem.

Some sort of incentive must be supplied to the young scientist to make a rewarding future in the laboratories of fundamental research. Tragically in our country the road to economic success and the presidencies of corporations leads not through the laboratory. A mathematician to be economically successful by American standards must forget mathematics, learn to sell soap, buy a house near the country club and drive two cars. Otherwise, he is a square, a queer sort of non-conformist whom "normal" Americans may secretly suspect of odd and strange tendencies.

In Soviet Russia a young man or woman who attains distinction over intense competition in mathematics or science automatically becomes a

member of the economic and social elite. Concessions by the State, fringe benefits and incentive awards place him in a kind of socialist aristocracy where he maintains his place by his mental fertility - his production of ideas.

We as scientists and engineers can help improve the lot of our meager and devoted corps of career thinkers in America by understanding and appreciating them and by applying the fruits of their contemplation to our own fields of technological development. We can encourage them, but we can't provide the broad economic challenge of the nuclear and space age - the challenge to think.

## STUDY OF SHOCK AND VIBRATION EFFECTS ON VEHICLES THROUGH DYNAMIC SIMULATIONS

F. Pradko\*, S. Heal\*\* and V. Kowachek\*\*\*

### ABSTRACT

This paper introduces a series of integrated research programs concerned with analytical and experimental investigation of vehicle reactions to impact forces. The program presents: (1) equations of vehicle dynamics, (2) techniques for generating random terrain profiles, (3) a unique motion Simulator and, (4) a "three screen" visual display system. The Simulator described is a high amplitude device that is capable of producing random motions of bounce, pitch, roll and yaw.

The paper summarizes research results and concludes that the work has led to a substantial improvement towards analytical and physical understanding of vehicle behavior. Mathematical models are presented with significant comparisons made between computer studies and experimental evidence.

---

The design of military vehicles is a rather complicated mixture of many technical activities. In each new development of a tank, truck or jeep, a substantial amount of engineering ideas are required to be blended together to bring forward vehicles possessing features and merit of advanced capability.

While each development is a separate and distinct program, there are development goals and problems that continually reappear and appear to be common. For example, it is always important to create a good suspension system and it is equally important to provide a dynamically stable vehicle.

The Suspension System is vital for it determines the vehicle ride and vibration behavior and it also establishes the tolerable speed limit of travel over various terrain surfaces, both of the man and the machine.

---

\* Mr. F. Pradko, Ch, Dynamic Simulations Laboratory, Army Tank-Automotive Center, Detroit Arsenal, Centerline, Michigan.

\*\* Mr. S. Heal, Electrical Engineer, Army Tank-Automotive Center

\*\*\* Mr. V. Kowachek, Mechanical Engineer, Army Tank-Automotive Center

Vehicle stability is a design area that also receives considerable attention, particularly in combat vehicle programs where large caliber weapons are expected to be fired from chassis of reduced weight and decreased size. Within military circles reference to vehicle stability differs from the usual automotive connotation. In place of steering behavior or directional control, vehicle stability pertains to pitch and roll movement, resulting from the gun recoil forces.

These two elements of vehicle design can be considered as perennials. They are always around and unfortunately they are rather "tough nuts" to handle. Individually they present major stumbling blocks to design engineers. Normally, useful study of these problems is beyond the level of developing a new layout or "cranking" through several equations on a desk calculator. As a result, the magnitude of each task has produced design specialists. These people, however, are not medicine men who consistently are able to generate successful answers. They need help; they need either physical or analytical means to guide and measure their design approaches. Consequently, knowledge of these systems must be consistently bolstered and expanded. This demand requires unique capability:

First, since all wheeled and tracked vehicles are earth bound, knowledge of road profiles or terrain contours upon which they move must be secured.

Next, detailed mathematical models are necessary that describe the vehicle and how it reacts to external disturbances or internal design changes.

Then, an accurate recording procedure is essential to transmit results from high speed computers in such format that their meaning may be assessed graphically, visually or physically.

The benefits of integrating these steps would be a complete capability for realistic design evaluation comparable to controlled tests at a proving ground.

Accordingly, the Army Tank-Automotive Command sought such a means to physically simulate the suspension performance and stability dynamics of a design while it was still in the blue-print stage, and to bring together the theory, mathematics and computer machinery to study each of these problems indoors in the laboratory. It was also the feeling that if this program was to be successful, it must produce the ability to



predict behavior and allow practicing engineers the opportunity to pre-test their designs before commitment to fabricate expensive wood mock-ups, experimental test rigs or engineering prototypes.

#### Suspension Simulation:

Simulation of vehicle suspension systems is basically the task of predicting the motion response of the vehicle to disturbances from the road. A thorough understanding of the elements that constitute this system and their interrelationship is essential to such study. Beginning with the road is perhaps logically the first step. The basic requirement is to present to the wheels, springs, and shock absorbers, the vertical displacement and frequency identical to those existing in road or terrain surfaces. For this purpose it is possible to construct a computer model of a road profile using either digital or analog computer techniques. The basic data profile information may be secured by conventional rod and transit means or automatic measuring instruments.

In real life the road is a stationary wave form over which the vehicle travels. The relationship between car velocity and the static road generates the suspension dynamics.

In a computer simulation the vehicle's forward movement cannot be faithfully reproduced. To conveniently maintain an order of reality the road is moved instead. The road profile is presented to the suspension components, as a continuous rearward velocity that normally would be road speed.

To accurately duplicate the physical case the road is presented to each wheel separately, properly phased so that the rear wheels "see" the same road irregularities as the front wheels, although at a later time. This phasing is governed by the wheel base and vehicle speed.

One successful procedure of road profile generation utilizes a digital computer and a digital-to-analog converter. The digital machine stores the road profile data in elevation increments. It selects the elevation that each wheel requires at a particular time and generates the time between elevations.

Several preliminary considerations which must be resolved before the construction of such a digital road function include:

1. The number of vehicle wheels.
2. The spacing between wheels.

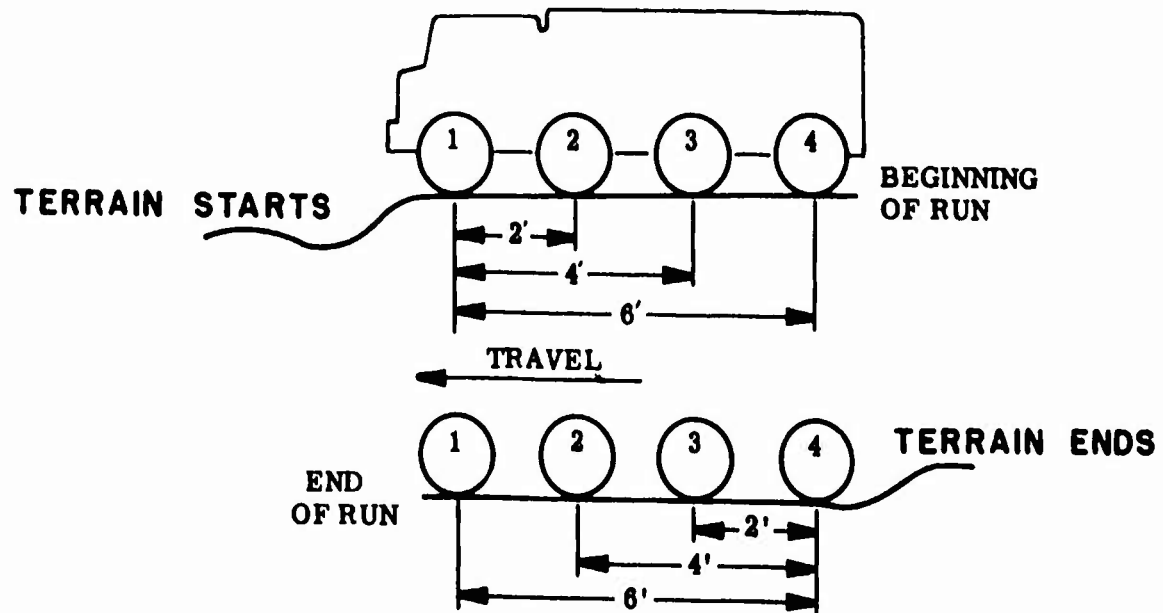
3. The starting road level.
4. The number of computer cells per road increment.
5. Overall length of the road profile.

The time at which a particular point on the road will arrive at each wheel is determined by the wheel spacing. This spacing is also considered in deciding how many elevation values will be equivalent to one linear foot of road. The following example will illustrate these points.

A vehicle suspension is set up on the analog computer; this simulation is for one side of the vehicle only, it being assumed that the other side is identical. The vehicle has four wheels on a side, spaced two feet apart. It will be driven over a Belgian Block type road. The road consists of 307 elevations spaced one foot apart. These things being known, it is possible to set up a scheme for generating the road function which will pass under each wheel in sequence. To rerun the road after once traversing it, a starting road level must be assumed, usually the initial starting elevation, or very near to it. For the conditions just outlined a situation similar to that shown in Figure 1 will exist.

**Preliminary assumptions:**

1. Vehicle is sitting on road level.
2. Start of road strikes 1st wheel
3. One computer word = 1 linear ft.



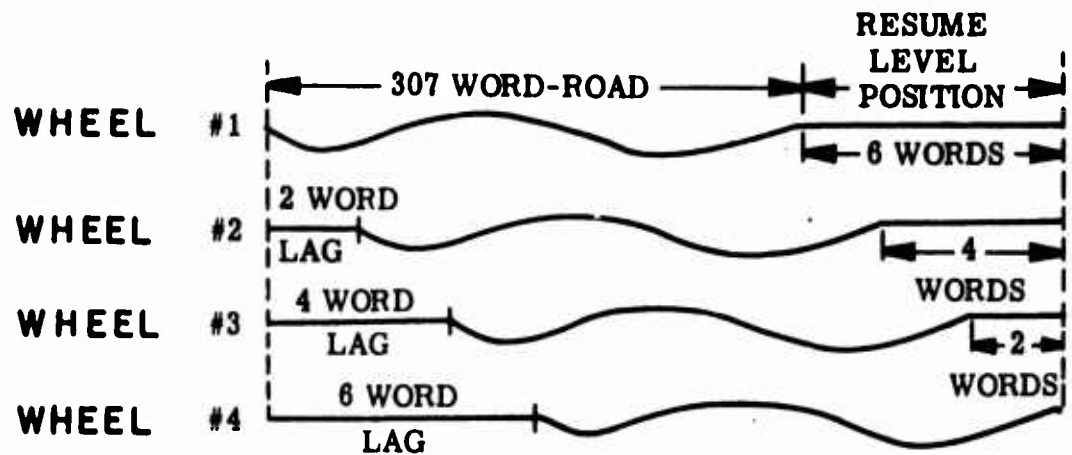


FIG. 1 ROAD PROFILE

The easiest scheme in this case is to let one foot of road be represented by one computer word. However, if the spacing between wheels is uneven, a scheme utilizing several words to the linear foot would be required.

After the preliminary road function details have been accounted for, the actual generation of the road function can be undertaken. This naturally divides into the following steps:

1. Preparation of the data tape.
2. Place road level data in computer memory.
3. Generation of the road function tape.
4. Transfer of the road function data to the digital-to-analog converter, etc.

Each computer "word" of information contains five channels, four of which are used for terrain simulation. Each of these channels can represent data. An algebraic representation of such a word is 1 aa bb cc dd 00, where each pair of letters represents one channel in the output of the Digital-Analog conversion system, while the number (1) in the sign position designates a particular group of D-A Converters, (Note that since the last channel is not used it is represented by 00, i. e. no information present). With proper scaling and programming, each channel can become a road-profile-wheel-terrain-function-generator (RPWTFG). Hence, there are

four RPWTFG's per computer word.

The time between data increments on the computer is generated by using a time control subroutine which increases or decreases the time between "calling up" the data increments. The speed of the road function is determined from the recorder tracings as follows:

$$\text{mph} = \frac{\text{actual length of road (ft)}}{\text{length of converted road (mm)}} \times \text{paper speed} \left( \frac{\text{mm}}{\text{sec.}} \right) \times \frac{30 \text{ mph}}{44 \text{ ft/sec}}$$

By this procedure vehicle road speed is established. Maximum road speed is only limited by the computers ability to call up data. Utilization of the time delay subroutine within the computer facilitates decreasing the speed. Also, greater speed can be attained by shortening the road, i.e. picking up every second or third road elevation. Oscillograph recordings, as generated by this sytem, are illustrated in Figure 2.

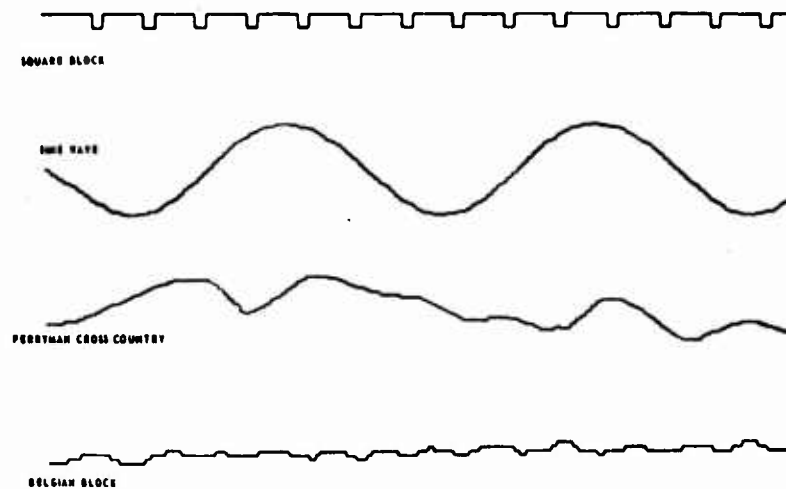


FIG. 2 ROAD PROFILE

A magnetic tape recorder and reproducer add convenience and efficiency to the system. By recording successive speeds on magnetic tape, the digital computer is used only once for a particular vehicle. In addition, velocity multiplication may be obtained by recording at one speed and reproducing at higher speeds.

Thus, any terrain that can be numerically described as increments of elevation with respect to horizontal distance, can be simulated with a digital computer for the analysis of vehicle behavior.

With the road prepared the simulation requires a model of the suspension system. For this purpose the Analog computer is best suited. The computer, as used, provides an accurate representation of the design. In a true sense the computer is an electronic model of the vehicle. The degree of realism achieved is naturally governed by the quantity of vehicle characteristics simulated.

As in any simulation, the system is first described by a mathematical model. The equations represent the dynamic system - the vehicle chassis, the suspension system and the road surface input.

Vehicular vibration components include the mass and inertia of the sprung components, the suspension springs, shock absorbers, road wheel masses, and the spring and damping characteristics of the wheel assembly.

The typical method of describing a vehicle to be simulated is shown in Figure 3 and Figure 4. From the diagrams, the equations of motion may be stated. These expressions are written as common linear differential equations with non-linear coefficients.

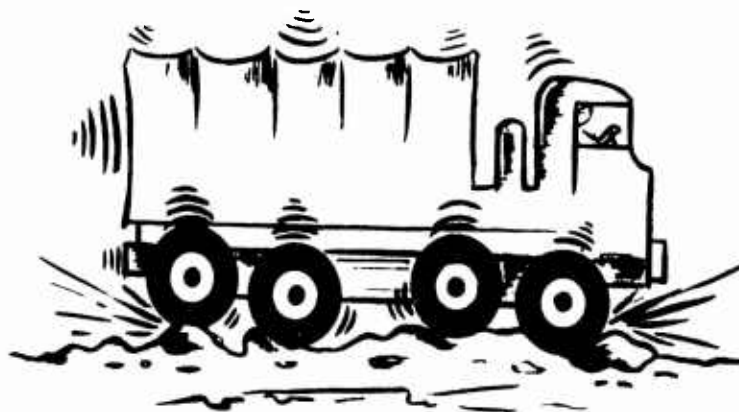


FIG. 3 VEHICLE CONFIGURATION

Non-linearities in the simulation exist normally due to non-linear spring characteristics, double acting shock absorbers, and the fact that wheels may leave the road surface.

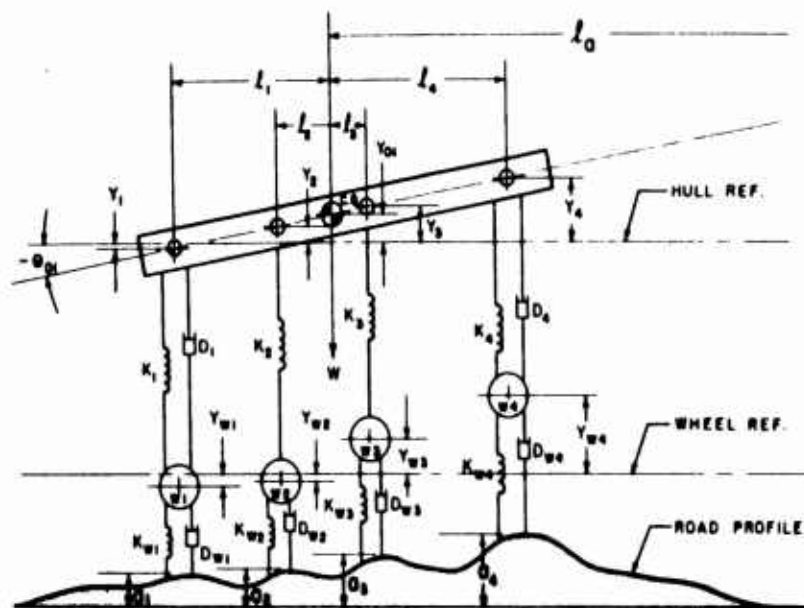


FIG. 4 VEHICLE SCHEMATIC

The equations result from linear and angular counterparts of Newton's second law of motion. The summation of the vertical forces on the chassis equals the mass of the chassis times its vertical acceleration; the summation of the torques about the center of gravity is equal to the polar moment of inertia times the angular acceleration of the hull. The forces and torques result from relative displacement and velocity of the springs and shock absorbers respectively. For example, the vertical force of the front wheel spring is equal to the spring constant ( $K_1$ ) times the relative displacement between the wheel and the chassis just above the wheel. Similarly, the torque is a product of this force times the distance from the center of gravity. The shock absorber force is a product of the damping coefficient and the relative velocity between the wheel and the chassis above the wheel.

Chassis, pitch and bounce equations may be developed using these relationships. Separate differential equations are written to describe the

motion of each wheel. Auxiliary equations are written to relate the pitch motion to the vertical motion so that the displacement and velocity of the chassis at each wheel station may be found.

Each wheel of the vehicle is considered a separate mass, spring, and damper system connected to the ground and to the chassis, the link to the chassis being the suspension spring and shock absorber. The force exerted on the wheel by the ground is equal to a product of the wheel rubber displacement and spring constant. This force can have only one sign since the ground cannot "pull" down on the wheel. The suspension spring force is also exerted on the wheel.

#### Simulation Equations:

##### Chassis Vertical Motion:

$$\ddot{Y}_o = \frac{\sum F_y}{M_o} \quad (\text{c. g. Bounce Acceleration})$$

$$\begin{aligned} \ddot{Y}_o = & -\frac{K_1}{M_o} (Y_1 - Y_{w1}) - \frac{K_2}{M_o} (Y_2 - Y_{w2}) - \frac{K_3}{M_o} (Y_3 - Y_{w3}) \\ & - \frac{K_4}{M_o} (Y_4 - Y_{w4}) - \frac{D_1}{M_o} (\dot{Y}_1 - \dot{Y}_{w1}) - \frac{D_4}{M_o} (\dot{Y}_4 - \dot{Y}_{w4}) + g \end{aligned}$$

##### Chassis Pitch Motion:

$$\ddot{\theta} = \frac{\sum T}{J_o} \quad (\text{c. g. Angular Acceleration})$$

$$\begin{aligned} \ddot{\theta} = & -\frac{K_1 l_1}{J_o} (Y_1 - Y_{w1}) - \frac{K_2 l_2}{J_o} (Y_2 - Y_{w2}) \\ & + \frac{K_3 l_3}{J_o} (Y_3 - Y_{w3}) + \frac{K_4 l_4}{J_o} (Y_4 - Y_{w4}) \\ & - \frac{D_1 l_1}{J_o} (\dot{Y}_1 - \dot{Y}_{w1}) + \frac{D_4 l_4}{J_o} (\dot{Y}_4 - \dot{Y}_{w4}) \end{aligned}$$

### Vertical Wheel Motion:

$$\ddot{Y}_w = \frac{F_w}{M_w}$$

$$\begin{aligned} \ddot{Y}_{w1} = & -\frac{K_{w1}}{M_{w1}} (Y_{w1} - a_1) - \frac{D_{w1}}{M_{w1}} (\dot{Y}_{w1} - \dot{a}_1) + \frac{K_1}{M_{w1}} (Y_1 - Y_{w1}) \\ & + \frac{D_1}{M_{w1}} (\dot{Y}_1 - \dot{Y}_{w1}) + g \end{aligned}$$

$$\ddot{Y}_{w2} = -\frac{K_{w2}}{M_{w2}} (Y_{w2} - a_2) - \frac{D_{w2}}{M_{w2}} (\dot{Y}_{w2} - \dot{a}_2) + \frac{K_2}{M_{w2}} (Y_2 - Y_{w2}) + g$$

$$\ddot{Y}_{w3} = -\frac{K_{w3}}{M_{w3}} (Y_{w3} - a_3) - \frac{D_{w3}}{M_{w3}} (\dot{Y}_{w3} - \dot{a}_3) + \frac{K_3}{M_{w3}} (Y_3 - Y_{w3}) + g$$

$$\begin{aligned} \ddot{Y}_{w4} = & -\frac{K_{w4}}{M_{w4}} (Y_{w4} - a_4) - \frac{D_{w4}}{M_{w4}} (\dot{Y}_{w4} - \dot{a}_4) + \frac{K_4}{M_{w4}} (Y_4 - Y_{w4}) \\ & + \frac{D_4}{M_{w4}} (\dot{Y}_4 - \dot{Y}_{w4}) + g \end{aligned}$$

### Auxiliary Chassis Equations:

$$Y_{1-4} = Y_0 + l_{1-4} \sin \theta \quad \dot{Y}_{1-4} = \dot{Y}_0 + l_{1-4} \dot{\theta}$$

The non-linearities are best described in graphical form, as is shown in Figures 5 and 6.



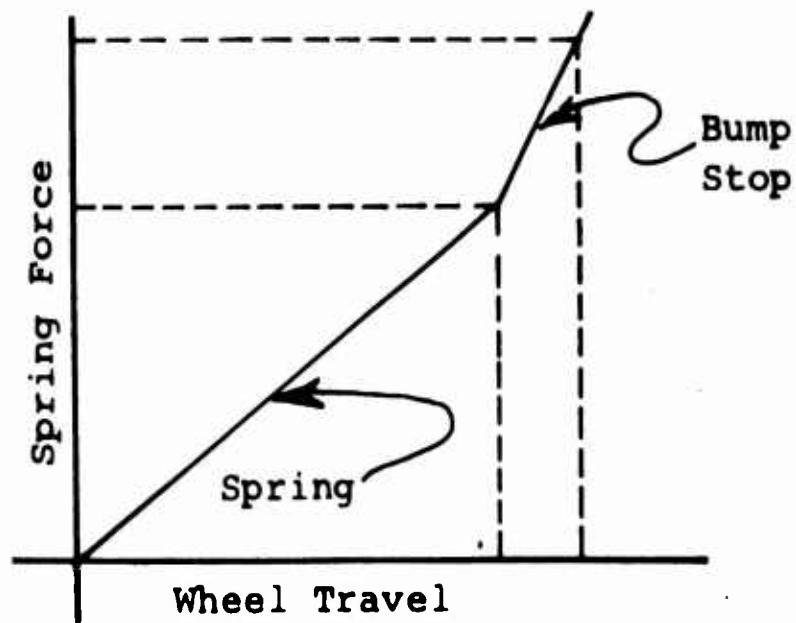


FIG. 5 SPRING LOAD VS WHEEL DEFLECTION

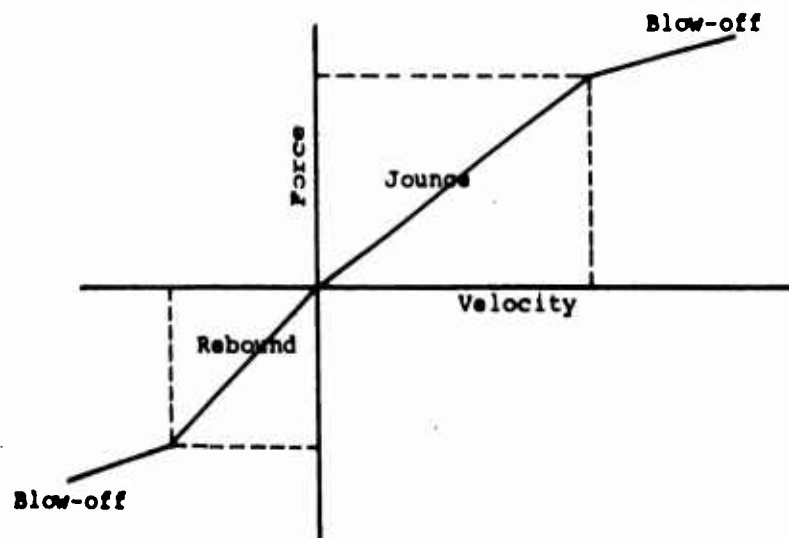
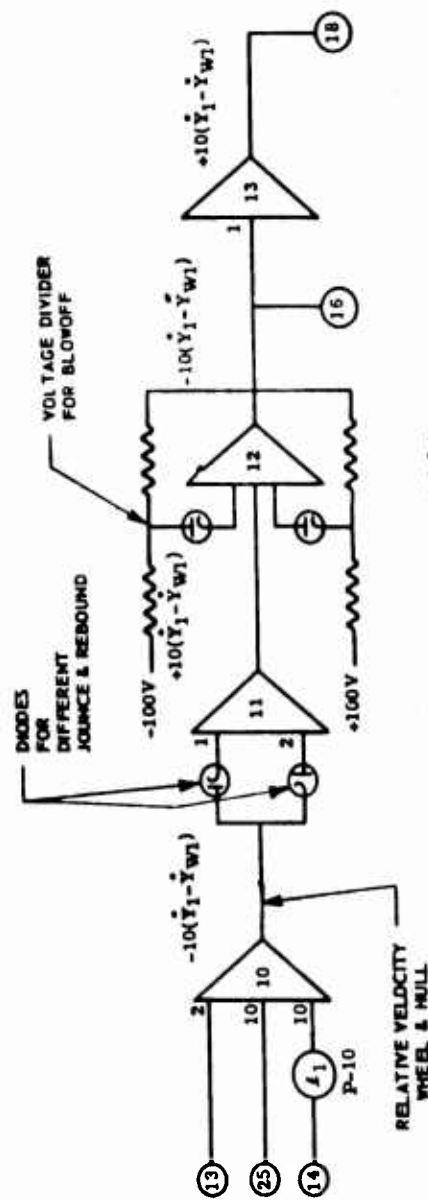


FIG. 6 SHOCK ABSORBER VS VELOCITY AT WHEEL

The non-linear suspension springing is composed of two linear segments, the one of lesser slope being the suspension spring, and the other the bump stop. The shock absorber non-linearity is shown in Fig. 6, which has four linear segments simulating different rates in compression and expansion with blow-off valves. The circuitry for creating the significant segments of a suspension simulation are shown in Figures 7 - 11. If a wheel leaves the ground, no spring force can exist between the ground and the wheel. To provide for this realistic action, a diode representing a unidirectional spring force is put in series with the wheel feedback loop, as is shown in the wheel circuit, Figure 9.

$$\dot{Y}_1 - \dot{Y}_{W1} = \dot{Y}_0 + L_1 \dot{\theta} - \dot{Y}_{W1}$$



$$\dot{Y}_4 - \dot{Y}_{W4} = \dot{Y}_0 - L_4 \dot{\theta} - \dot{Y}_{W4}$$

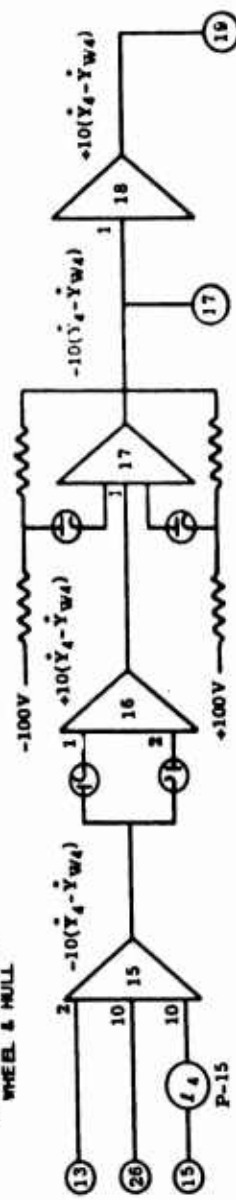


FIG. 7. SHOCK ABSORBER CIRCUITS

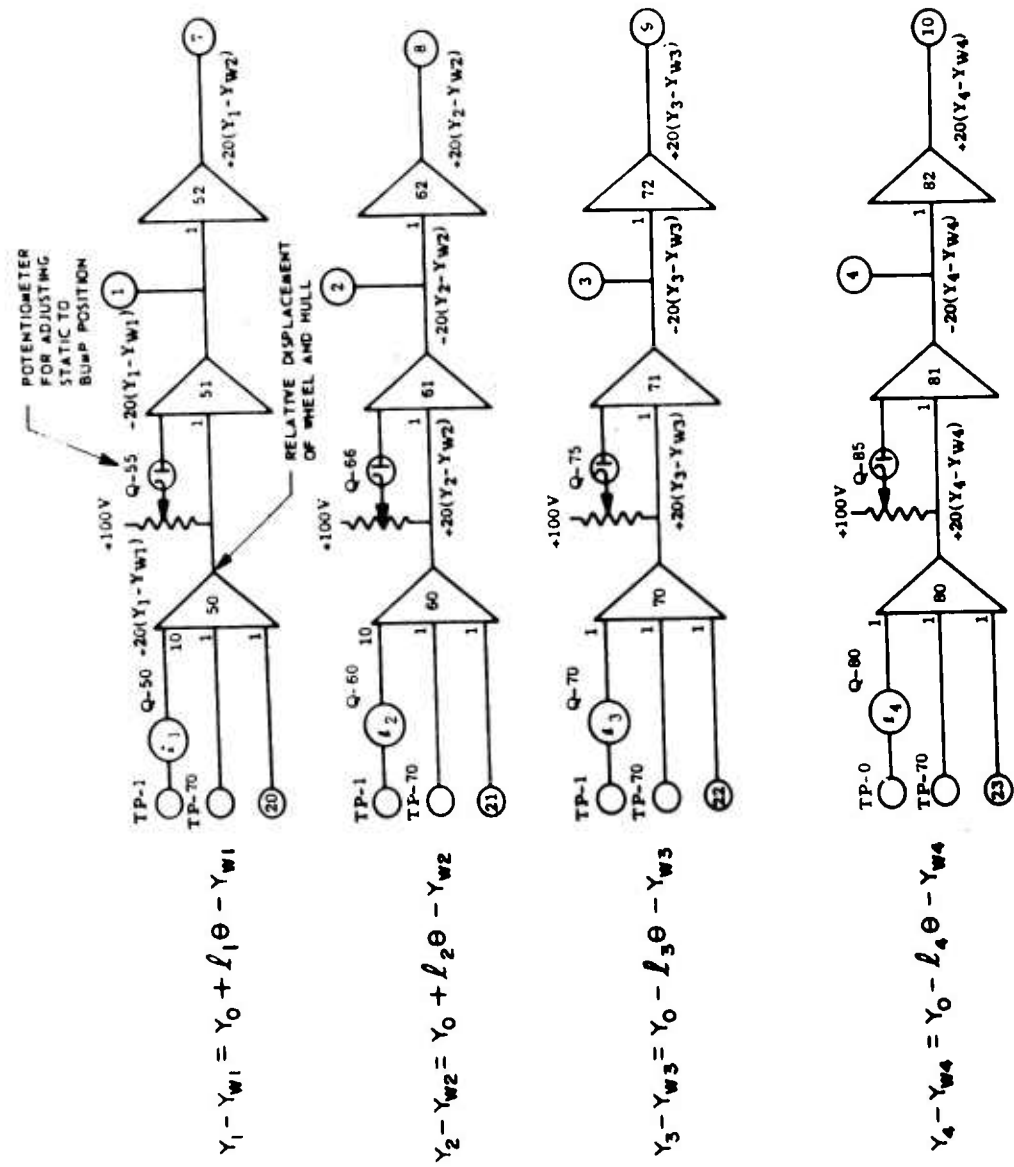


FIG. 8. SPRING CIRCUITS

$$\Sigma \frac{F_w}{M_w} = \ddot{y}_w$$

94

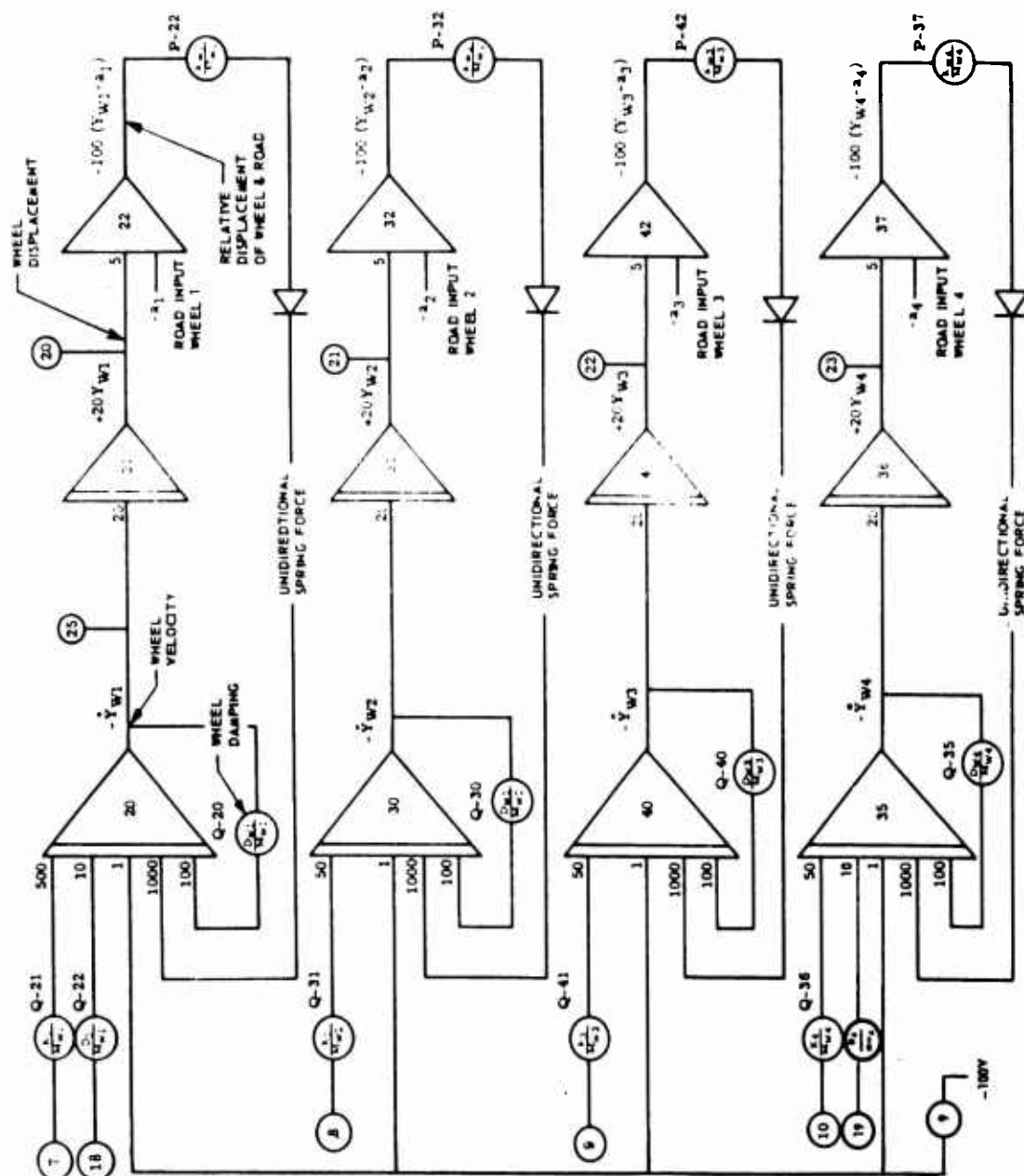


FIG. 9. WHEEL VELOCITY, AND DISPLACEMENT

$$\frac{\Sigma F_y}{M_0} = \ddot{y}_0$$

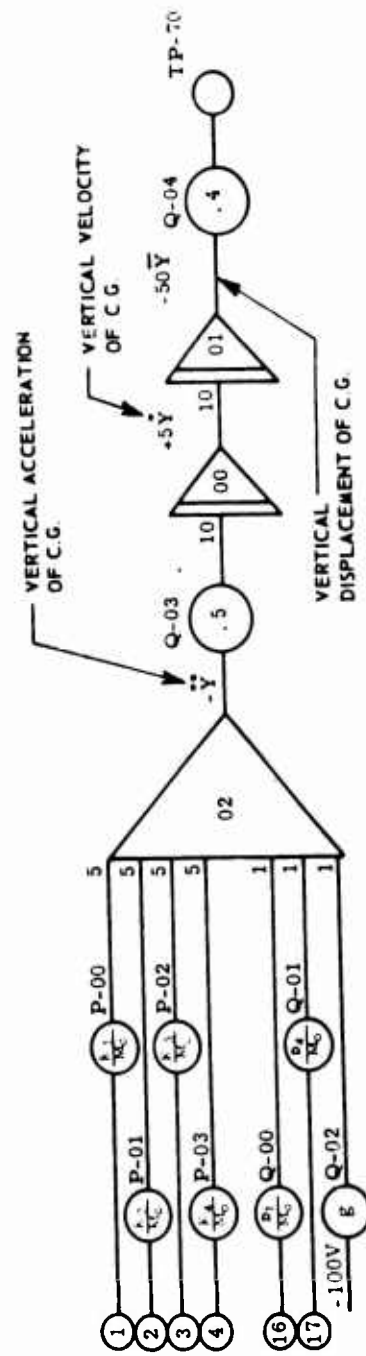


FIG. 10. C.G. VERTICAL ACCELERATION, VELOCITY, DISPLACEMENT

$$\frac{\Sigma T}{J_0} = \ddot{\theta}$$

96

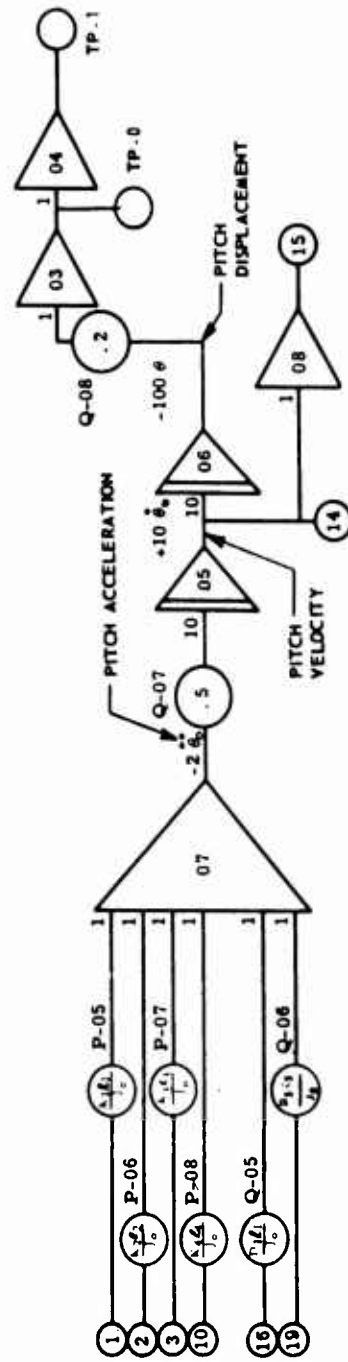


FIG. 11. C.G. PITCH ACCELERATION, VELOCITY, DISPLACEMENT

Simulation begins when the electronic version of a road and suspension system are brought together. Results are best analyzed using oscillographic or pen recorder output devices. Recorded paper tracings provide an excellent permanent record for lengthy detailed analysis. The oscillograph display system offers an opportunity to observe the simulation visually as an animated presentation. The dynamics of a complete vehicle or any component thereof may then be studied. This display system is used in conjunction with the analog computer. A cathode-ray-tube is used to convert the output voltages of the computer into a direct pictorial representation. Application of this system is shown in Figure 12. The series of photographs describe the motion of a tank that would be seen on the tube. The vehicle is shown negotiating at successive instances a 4" x 4" square obstacle.

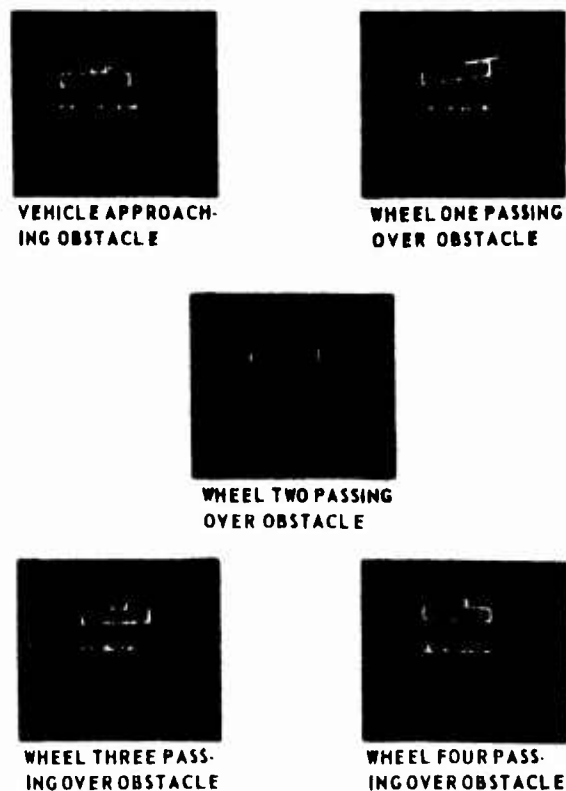


FIG. 12 VISUAL DISPLAY SYSTEM

This visual display provides a quick and easy method of conducting a preliminary analysis of new suspensions. It is also a good means of debugging a new simulation setup.

### Simulator:

Results of computer simulations may also be studied with the aid of a motion simulator. The value of the Simulator, Figure 13, lies in its ability to physically reproduce realistic "ride motion" that may be predicted by a computer simulation. Thus, by combining computer studies of new concepts with a simulator analysis, design merits may be judged in the laboratory by engineers, designers, and administrative people before a design is considered for fabrication. Each individual may ride a new suspension in the Simulator and personally evaluate his area of interest firsthand.

The Simulator described below is a four degree of freedom machine capable of providing bounce, pitch, roll and yaw motions.

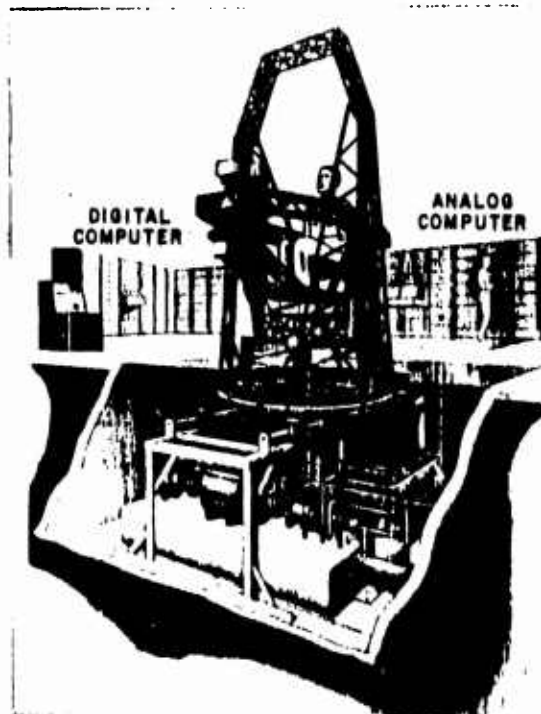


FIG. 13 SIMULATOR

The control of the machine is optional. The Simulator may be controlled from an instrument panel to produce either sine, square or triangular motions. Random motion inputs may be fed directly into the Simulator from an Analog computer simulation or by reproducing information previously recorded on magnetic tape.

This machine is hydraulically driven and electronically controlled. Each of the four motions may be used individually or simultaneously.



<u>Motion</u>	<u>Max. Tot. Travel</u>	<u>Max. Frequency</u>	<u>Acceleration</u>
Bounce	3 ft	10 cps	2 g's
Roll	40 deg	10 cps	30 radians/sec <sup>2</sup>
Pitch	40 deg	10 cps	30 radians/sec <sup>2</sup>
Yaw	20 deg	3 cps	15 radians/sec <sup>2</sup>

Perhaps the most significant claim that can be broadcast for the Simulator, at this time, is that it will make possible performance trials of designs prior to building of a design. In some instances it is the only economical approach, considering time and cost, particularly, where a new design is being investigated using many alternatives.

The creation of this Simulator provides the Army Tank-Automotive Command with a design tool that has been sought for some time. The need for an instrument of this kind has been in continuous demand for military suspension studies and other shock and vibration programs.

The immediate response to the Simulator was generally favorable, but reserved. Comments usually indicated that the vibratory motions were good. However, it was repeatedly stated that the laboratory environment around the Simulator degraded the intended realism. The common complaint was that the "out of doors" atmosphere seemed to be missing.

To compensate for this a visual display was created providing a 180 degree field of view horizontally and 48 degrees in the vertical plane. A 35mm motion picture format was used to produce a "three screen" presentation. This method was selected, based upon successful tryouts of a unique projection system developed and tailored to the Simulator.

The activity scene is photographed by three cameras and backprojected to the subject in the Simulator by three synchronized-interlocked projectors. This system presents to the observer a scene that compares favorably to a view from within a moving vehicle.

#### Vehicle Stability:

The Simulator was also used to simulate vehicle firing stability dynamics. The starting cue for this program was very forceably observed in vehicles like the Self-Propelled Artillery Weapon, M56.

In keeping with this indicated trend of big guns on small chassis platforms it was necessary to establish with greater accuracy, the stability of

contemplated designs.

The characteristic events describing fire stability were analyzed by charting the flow of events and establishing the equations of motion.

# Equations of Motion:

LONGITUDINAL TRANSLATION: GUN FORCE GROUND FRICTIONAL FORCE = MASS X ACCELERATION  $F_{gx} + F_{fx} = m (\ddot{x} - \dot{y} \dot{\theta}_z + z \dot{\theta}_y)$

LATERAL TRANSLATION: GUN FORCE + GROUND FRICTIONAL FORCE = MASS X ACCELERATION  $F_{gy} + F_{fy} = m (\ddot{y} - \dot{z} \dot{\theta}_x + \dot{x} \dot{\theta}_z)$

BOUNCE: GUN FORCE - SPRUNG WEIGHT SUSPENSION FORCES = MASS X ACCELERATION  $F_{gz} - W_{sc_z z} + \sum_{i=1}^n N_i = m (\ddot{z} - \dot{x} \dot{\theta}_y + \dot{y} \dot{\theta}_x)$

ROLL: GUN MOMENT + GROUND FRICTIONAL MOMENT + SUSPENSIONAL MOMENT = ANGULAR ACCELERATION X MOMENT OF INERTIA  $-\bar{z}F_{gy} + \bar{y}F_{gz} + (z + z_0) F_{fy} c_y Y + \sum_{i=1}^n N_i Y_i = \ddot{\theta}_x I_x - \ddot{\theta}_z I_{xz}$

$$(I_z - I_y) \dot{\theta}_y \dot{\theta}_z - I_{xz} \dot{\theta}_x \dot{\theta}_y$$

PITCH: GUN MOMENT - GROUND FRICTIONAL MOMENT - SUSPENSIONAL MOMENT = ANGULAR ACCELERATION X MOMENT OF INERTIA  $-\bar{x}F_{gz} + \bar{z}F_{gx} - (z + z_0) F_{fx} c_x X - \sum_{i=1}^n N_i x_i = \ddot{\theta}_y I_y + \dot{\theta}_x \dot{\theta}_x$

$$(I_x - I_z) + (\dot{\theta}_x^2 - \dot{\theta}_z^2) I_{xz}$$

YAW: GUN MOMENT GROUND FRICTIONAL MOMENTS = ANGULAR ACCELERATION X MOMENT OF INERTIA  $-\bar{y}F_{gx} + \bar{x}F_{gy} \sum_{i=1}^n$

$$x_i F_{fiy} c_y Y - \sum_{i=1}^n y_i F_{fix} c_x X = \ddot{\theta}_z I_z - \ddot{\theta}_x I_{xz} +$$

$$(I_y - I_x) \dot{\theta}_x \dot{\theta}_y + I_{xz} \dot{\theta}_y \dot{\theta}_z$$

The derived statements were for weapon systems free to move in three degrees of angular freedom - roll, pitch and yaw; and three degrees of translational freedom - fore and aft movement, bounce, and lateral slip. The equations define vehicle motion as effected by interrelated factors of gun firing force, gravity, terrain influence, and the resisting forces of the suspension.

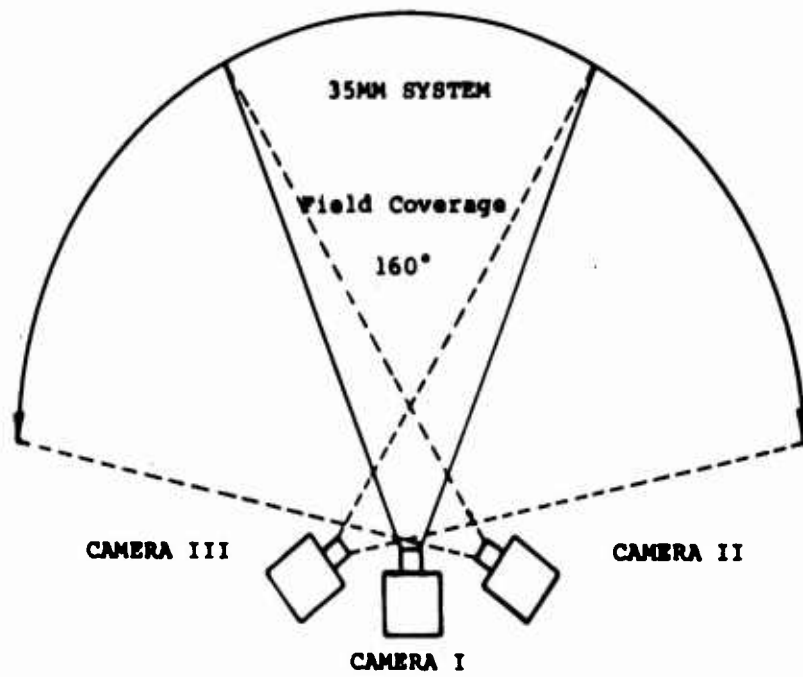


FIG. 14 CAMERA SYSTEM

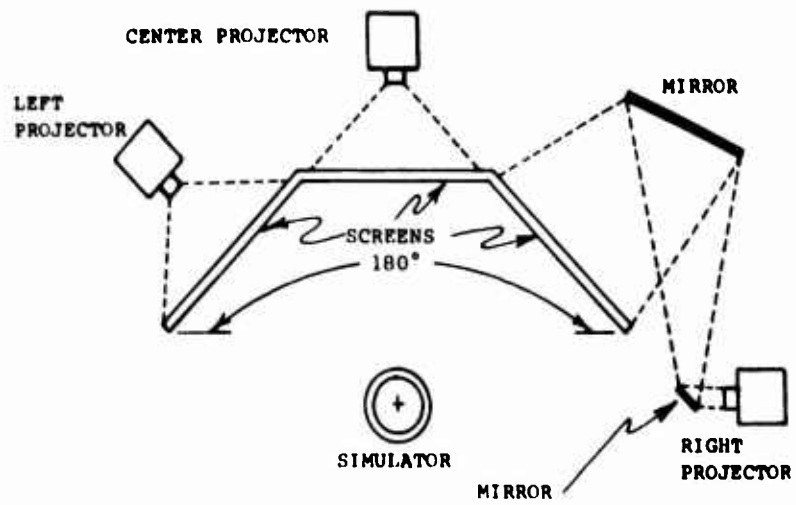


FIG. 15 PROJECTION SYSTEM

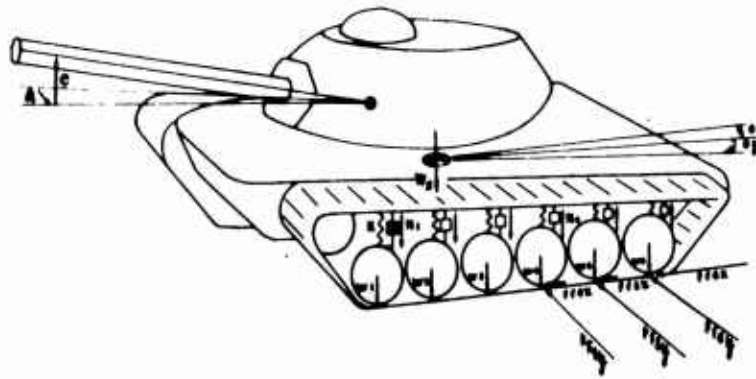


FIG. 16 VEHICLE SCHEMATIC

# VEHICLE FIRING STABILITY FLOW DIAGRAM

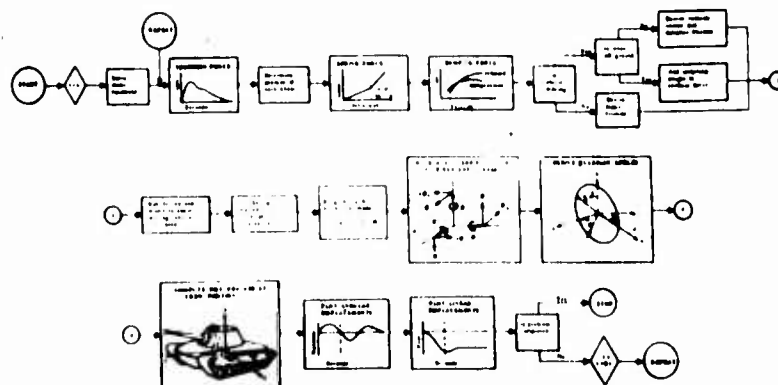


FIG. 17 FLOW DIAGRAM

The dynamics of firing stability are calculated on a digital computer. When this program is used in conjunction with the Simulator, the results are stored in computer memory. The physical arrangement of the Simulator permits the occupant to fire any weapon by merely pulling the usual trigger. The command to fire is completely controlled by the man in the seat.

The inputs to this problem consist of various vehicle measurements, weights, moments of inertia, gun recoil force, type of soil, and type of suspension (active or locked-out). The output consists of detailed information in tabular or graph form showing angular and translational disturbances and their respective displacements, velocities, and accelerations with respect to time. This information describing gun firing force impact on the vehicle and resultant vibrations is available for the C.G. of the vehicle with reference to earth-fixed axes and for any other point on or within the vehicle, such as gun muzzle, engine mounts and crew stations with reference to the vehicle axes.

#### Summary:

The combination of computers and simulation techniques at the Army Tank-Automotive Command has provided an effective and versatile designer's tool. Informative preliminary studies have been conducted of new suspension systems and stability characteristics, without the use of hardware units of the design. Probes of unique approaches have quickly established design direction and payoff areas.

#### SUSPENSION NOMENCLATURE

$\ddot{Y}_0$  = Vertical acceleration of the center of gravity.  
 $\dot{Y}_0$  = Vertical velocity of C. G.  
 $Y_0$  = Vertical displacement of C. G.  
 $\ddot{\theta}_0$  = Pitch acceleration about C. G.  
 $\dot{\theta}_0$  = Pitch velocity about C. G.  
 $\theta$  = Pitch displacement at C. G.  
 $(Y_1 - Y_{w1})$  = Relative displacement between hull and wheel at wheel 1.  
 $(\dot{Y}_1 - \dot{Y}_{w1})$  = Relative velocity of the hull and wheel at wheel 1.  
 $(Y_{w1} - a_1)$  = Relative displacement between wheel and input bump at wheel 1.  
 $J_0$  = Pitch Moment of Inertia.  
 $M_0$  = Sprung mass.  
 $M_w$  = Wheel mass.  
 $l$  = Distance from wheel centerline to C. G.  
 $K_{1-4}$  = Suspension spring constant.  
 $D_{1-4}$  = Shock absorber damping constant.  
 $K_w$  = Spring constant of road wheel rubber.  
 $D_w$  = Damping constant of road wheel rubber.  
 $a_{1-4}$  = Road inputs to wheel No. 1-4.  
 $Y_{1-4}$  = Chassis displacement.  
 $g$  = Acceleration of gravity

## VEHICLE STABILITY NOMENCLATURE

$F^g$  = Gun force.  
 $F_x^g$  = Frictional force.  
 $W_s$  = Sprung weight.  
 $M$  = Sprung mass.  
 $\bar{x}, \bar{y}, \bar{z}$  = Position of trunnion centerline.  
 $z_0$  = Static height of C. G.  
 $n$  = Number of wheels.  
 $\ddot{y}, \ddot{x}, \ddot{z}$  = Translational acceleration.  
 $\ddot{\theta}_x, \ddot{\theta}_y, \ddot{\theta}_z$  = Angular acceleration.  
 $\dot{y}, \dot{x}, \dot{z}$  = Translational velocity.  
 $\dot{\theta}_x, \dot{\theta}_y, \dot{\theta}_z$  = Angular velocity.  
 $I$  = Moment of Inertia  
 $K$  = Suspension spring constant.  
 $D$  = Shock absorber damping.  
 $a$  = Gun azimuth.  
 $e$  = Gun elevation.

## ACKNOWLEDGEMENTS

Acknowledgement is extended to the past and present members of the Dynamic Simulations Laboratory at the Army Tank-Automotive Command for their individual contributions which led to the completed development described in this paper, and to Mr. O. K. Till, F. Anderson and R. Armstrong for development of the experimental equipment and instrumentation. I am also indebted to Mr. J. Stanton and J. Lynch, Jr. for their art and photographic work in preparing the illustrations.

## REFERENCES

1. S. Heal, "Suspension Analysis", Army Tank-Automotive Command, Research Report No. RR-38.
2. M. Archambault, S. Heal, S. Staich, "Generation of Road Profiles for Vehicle Ride Simulations", Army Tank-Automotive Command, Research Report No. RR-44.
3. C. Fischer, "Mathematical Model and Digital Computer Program for Vehicle Firing Stability Analysis", Army Tank-Automotive Command, Research Report No. RR-27.
4. I. J. Sattinger, S. Sternick, "An Instrumentation System for the Measurement of Terrain Profile", University of Michigan Report No. 2948-36-F, December 1961.
5. "Operating and Maintenance Instructions for Simulation Display System", University of Michigan Report No. 2023-518-M, October 1955.
6. I. J. Sattinger, D. F. Smith, "Computer Simulation of Vehicle Motion in Three Dimensions", University of Michigan, May 1960.
7. R. Dean - Averbs, "Automobile Chassis Design".
8. V. Kowachek, Technical Notes, Firing Stability.

#### DISCUSSION

Dr. Hammer: The paper is now up for discussion.

Mr. Zaroodny, BRL, APG: In the mathematical formulation of any such thing, it seems to me that there often arises a need to simplify the mathematics. Did you use simplifications or did you tackle actual non-linear problems?

Mr. Pradko: We attempted to make the problems as non-linear as possible.

Mr. Whittlesey, QM, R&E Command, Natick: Will the facilities shown by you be available to others in the military who design vehicles?

Mr. Pradko: Yes sir. For Example, we have just recently completed a program with Redstone Arsenal and the Missile people from General Dynamics Corp.

Dr. Kumar: How many variables did you have to include in order to specify the laboratory characteristics of the vehicle, let's say for a four-wheel vehicle?

Mr. Pradko: For a four-wheel vehicle there would probably be about 15 pieces of data that go into the simulation.

Dr. Kumar: Is this essentially a spring dashpot arrangement?

Mr. Pradko: Yes, and mass distribution.



## ROLLED ARMOR STEEL BRITTLE FRACTURE TEMPERATURES AND DESIGN SIGNIFICANCE

Victor H. Pagano\*

### ABSTRACT

Determination of a steel's transition temperature can provide an invaluable basis for assessing whether "safe performance" of a structure can be expected in service. A single Charpy V-notch impact test will not suffice for this determination. A satisfactory estimate may be obtained from a complete Charpy V-notch transition curve; this, however, requires considerable cost and testing for adequate interpretation of the ductile to brittle transition point.

A more appropriate test for determining transition temperature is the Naval research Laboratory Drop Weight Test. This test, introduced in 1954, is the outgrowth of work by the Navy for an inexpensive and more expedient laboratory method to augment the established explosion bulge crack starter test. Extensive trials have shown that it provides a comparable means of identifying that temperature at which a given steel loses its ability to deform more than a minute amount in the presence of a sharp crack-like defect. This temperature has been defined as the nil-ductility transition (NDT) temperature.

An evaluation of the NDT temperature obtained from the Navy Drop Weight Test, and its comparison with the critical fracture transition temperatures as determined by the explosion bulge crack starter test, that is, NDT, FTP (fracture transition plastic) and FTE (fracture transition elastic), has led to design concepts by which the relative resistance to fracture of steels can be predicted. These concepts offer an economical and practical basis for materials selection in service applications requiring assurance of protection from brittle fracture.

This investigation evaluates the brittle fracture integrity of a high-strength, armor steel employed in the manufacture of light combat vehicles. Transition temperature determinations were made on thirty-two heats of 1/2" thick rolled armor steel plate of two chemical compositions and the same specification hardness range. The variation in Drop Weight

---

\*Mr. Victor H. Pagano, Supervisory Materials Engineer, Research and Engineering Directorate, Army Tank-Automotive Command, Centerline, Michigan.

Test NDT temperatures for the different heats of Mn-Cr-Mo armor was  $-50^{\circ}\text{F}$  to  $-110^{\circ}\text{F}$  and  $-80^{\circ}\text{F}$  to  $-130^{\circ}\text{F}$  for Mn-Mo armor. Also, FTE and FTP temperature values were obtained from limited crack starter explosion bulge tests, and used to interpret the safe operating temperature for anticipated service stressing of the armor structure. From an interpretation of all three transition temperatures, the steels investigated can be expected to perform safely under nominal elastic loads in the presence of notches down to operating temperatures of just above  $-90^{\circ}\text{F}$ . If the probability of exposing notch sites to crack initiating (plastic) loads is great, the operating temperature of the armor must be restricted to just above  $-30^{\circ}\text{F}$  to safely limit cracking within deformed metal regions.

### INTRODUCTION

The susceptibility of medium carbon, high hardness, low alloy armor plate to brittle fracture in the presence of weld cracks has been a topic of much discussion in terms of anticipated loads and temperature in service. It is generally acknowledged that three conditions are necessary for brittle failure to occur; a notch or stress raiser, yield point stress developed at the notch, and an operating temperature below the ductile to brittle transition temperature of the material. When all three conditions are present brittle fracture occurs. In the absence of one or more conditions, brittle fracture will not occur. If it is assumed that conditions of stress raiser and elastic load are almost always present or unavoidable in any welded armored vehicle structure, then determination of the material's transition temperature is required to interpret whether "safe operating" performance can be expected.

Of the many methods for transition temperature determination, the oldest and probably most widely used is the Charpy test. Both the V-notch and keyhole Charpy tests are currently employed. However, of the two, the V-notch test is now used almost exclusively in research studies, and acceptance specifications are gradually being changed to reflect only V-notch values. Unfortunately, use of the Charpy test for design specifications is limited by a lack of service correlation, the ultimate requirement of the designer. In addition, testing involves considerable cost and interpretation for establishing the ductile to brittle transition point. A more appropriate approach is to use the critical fracture transition temperature concept described in 1952 by Puzak, et al<sup>2</sup>, of the Naval Research Laboratory.

In this concept, three points on the temperature scale are established indicative of major changes in steel fracture behavior if certain conditions of loading are imposed. Design and service determine the

conditions of loading, while notches and temperature determine the response of the steel to the imposed conditions. These temperatures have been described<sup>5</sup> as follows:

1. NDT (Nil-Ductility Transition). At this temperature a given steel loses its ability to deform more than a minute amount in the presence of a sharp crack-like defect. Operation at or below this temperature must not result in yield stress loading at crack flaw positions; otherwise brittle fracture will occur. In other words, the structure must be free of design or manufacturing irregularities capable of concentrating normal elastic loads to yield point values. Above this temperature, "forcing" is required to initiate cracking.

2. FTE (Fracture Transition for Elastic Loading). Below this temperature propagation of brittle cracking can occur when imposed loads are within the elastic limits of the material, provided a "forced" start is obtained (loading capable of producing a small amount of deformation at position of crack initiator). Above this temperature, brittle cracking is not feasible in elastic loaded areas; in fact, cracking will be contained in that region subjected to deformation loads only.

3. FTP (Fracture Transition for Plastic Loading). Below this temperature propagation of a sharp crack will be limited to areas subject to deformation stresses during loading. Above this temperature, brittle fracture from a sharp crack source will not occur, even though material is plastically deformed severely by high over-stressing.

The temperature intervals between the NDT, FTE, and FTP transition temperatures have been found to be remarkably similar for many materials<sup>5</sup>. The addition of 30° to 50°F to the NDT temperature provides an estimate of the FTE temperature. The addition of 80° to 120°F will give the FTP temperature. Thus, it is possible to predict FTE and FTP temperatures by applying these appropriate rule of thumb temperature intervals to NDT temperature results.

The first of these three temperatures may be determined from either of two brittle fracture tests; the crack-starter explosion-bulge test or the drop-weight test. Both tests evaluate the behavior of steel in the presence of an "ultra-sharp" crack originated during testing in a hard-surfacing weld bead previously deposited on the surface of the specimen. The presence of an ultra-sharp crack was selected as the criterion for susceptibility to brittle fracture on the basis that sharp cracks and small amounts of plastic deformation at positions of unfavorable design do occur in large welded structures.

The explosion bulge test was the first of two crack starter tests developed by the Navy. It was used in early studies of the mechanical and metallurgical aspects of the catastrophic brittle cracking found in World War II welded ship plate. The test involves a large plate specimen loaded explosively over a circular die cavity; the die cavity permits the formulation of a rather deep circular bulge in the center of the plate specimen. By virtue of the varying plastic and elastic stresses in the specimen, appraisal of the propagation characteristics of the steel is readily accomplished. A "flat" multi-piece break (no bulging) of test plate is representative of the material's NDT temperature. When plate cracking just enters the region of the plate supported by the die (elastically stressed area), the plate is said to be at its FTE temperature. The temperature at which the steel shows complete refusal to propagate cracks emanating from the crack-starter weld bead is the material's FTP temperature. The identification of these critical fracture transition temperatures has led to design concepts for predicting the safe performance of steel without brittle fracture.

Later, another method of loading, using a relatively small test piece containing a brittle weld, was developed for laboratory use and termed the drop-weight test. In this test, which is simpler and cheaper to conduct, only NDT temperature is determinable. From the NDT temperature, however, the FTE and FTP temperatures can be predicted by the rule of thumb adjustments described earlier.

Investigations of ship plate failures have established brittle fracture temperature correlations between explosion crack-starter test results and Bureau of Standards Charpy V-notch data<sup>4</sup>. As a result, fracture energy data from the Charpy V-notch impact test have provided support to the significance of material performance evaluations by drop weight and explosion bulge crack starter tests. In general, the NDT temperature corresponds with Charpy V-notch energies found in the vicinity of the knee of the lower shelf, the FTE temperature with impact energies found in the lower part of the knee of the upper shelf and the FTP temperature with energies corresponding to those of the upper shelf.

This paper provides NDT temperature data on rolled armor steels obtained from the drop weight test, limited data on need for reheat treatment to nullify the influence of heat-affected zone (HAZ) on NDT temperature, and some data on armor fracture behavior by the crack-starter bulge test. An interpretation of NDT temperature results is also made in terms of safe operating temperature based on the NDT, FTE and FTP temperature concepts and anticipated service stressing.

## MATERIALS:

Thirty-two heats of 1/2 inch thick, cross-rolled, quenched and tempered (341 to 388 Brinell), medium-carbon alloy steel (Spec. MIL-A-12560) from four different steel manufacturers were investigated. The material was supplied in 3 x 3 foot plates and was representative of two chemical compositions--Mn-Mo and Mn-Cr-Mo analyses. The chemical compositions of the steel heats are shown in Table I. Twenty-five of these heats were heat-treated by the steel manufacturers. Seven of these heats (Nos. 20 through 26) were heat-treated by an independent steel supplier and fabricator. The complete heat-treat cycles used by individual sources to develop the "as-received" plate properties in both compositions are described in Table II.

Standard Charpy V-notch impact specimens from each heat were machined so that the notch was perpendicular to the plate surface. At least two specimens were tested for each of the following temperatures: room temperature, 0°, -20°, -40°, -60°, -80°, and -100°F.

Room temperature energy absorption values of 20 to 31 foot-pounds were obtained for all transverse Charpy specimens (Table III). If only the Mn-Cr-Mo steels (1 thru 26) are considered, the average room temperature energy value was 24 foot-pounds for transverse specimens. An insufficient number of Mn-Mo steels was tested in the transverse direction to provide a valid average. However, from the limited data obtained for heats produced by one manufacturer (27 thru 30) the upper-shelf energy value of Mn-Mo steels for the transverse direction tends to be lower than the Mn-Cr-Mo analyses. This may be explained by the differences in the extent of cross-rolling, as reflected in the ratios of energy values of transverse to longitudinal specimens. Figures 1 and 2 show Charpy V-notch energy versus temperature curves for both longitudinal and transverse directions from steels 12, 14, 18 and 21.

## SPECIMEN PREPARATION AND TESTING:

### Drop Weight Crack Starter Tests

Drop weight specimens were prepared and tested (Fig. 3) in two ways (non-standard and standard). The tests reflect some features of early Naval Research Laboratory practices<sup>2, 3</sup> and the changes<sup>9</sup> since that time.

The non-standard procedure<sup>2</sup> used during initial work conducted between 1954 and 1956 employed an excessive drop load and inadequate

TABLE 1  
STEELS AND CHEMICAL COMPOSITIONS

STEEL CODE NO.	HEAT NO.	ELEMENT (%) 1										2	
		C	MN	SI	S	P	CR	MO	ZR	B			
1	GL 0344	.31	.80	.48	.020	.020	.65	.23	.10	.001			
2	GL 0345	.32	.88	.49	.030	.018	.65	.21	.11	.001			
3	GL 0346	.30	.93	.50	.030	.021	.62	.17	.10	.001			
4	GL 0348	.32	1.07	.51	.023	.020	.74	.21	.12	.001			
5	GL 0351	.29	.85	.47	.022	.017	.60	.17	.07	.001			
6	GL 0354	.31	.85	.48	.022	.020	.65	.20	.07	.001			
7	GL 0359	.32	.99	.46	.025	.021	.68	.18	.08	.001			
8	GL 0368	.31	.98	.45	.030	.021	.62	.19	.12	.001			
9	GL 0370	.32	.96	.42	.024	.016	.65	.18	-	-			
10	GL 0372	.30	1.09	.53	.025	.024	.64	.18	.15	.001			
11	GL 0373	.30	.92	.42	.029	.021	.63	.17	.10	.001			
12	GL 0374	.28	.98	.42	.020	.016	.70	.17	.08	.001			
13	GL 0377	.33	1.00	.47	.021	.018	.71	.19	.12	.001			
14	GL 0389	.33	1.02	.50	.025	.021	.70	.18	.15	.001			
15	GL 0390	.29	.98	.50	.024	.019	.67	.17	.08	.001			
16	GL 0396	.32	.90	.49	.018	.020	.62	.21	.11	.001			
17	GL 0398	.32	.98	.48	.030	.020	.76	.20	.12	.001			
18	GL 0399	.29	1.02	.48	.020	.018	.68	.23	.11	.001			
19	GL 0410	.33	1.06	.49	.025	.020	.70	.26	.13	.001			
20	SCG 0385	.29	.77	.46	.024	.022	.61	.17	-	.001			
21	SCG 0386	.27	.76	.47	.024	.021	.58	.18	-	.001			
22	SCG 0387	.30	.85	.47	.022	.018	.64	.22	.09	.001			
23	SCG 0393	.29	.87	.43	.026	.019	.65	.20	.10	.001			
24	SCG 0395	.30	.95	.43	.028	.020	.58	.21	.12	.001			
25	SCG 0406	.31	.90	.45	.023	.022	.62	.22	.11	.001			
26	SCG 0407	.29	1.06	.50	.024	.022	.65	.20	.11	.001			
27	DB 13474-1	.28	1.83	.22	.021	.015	-	.54	-	-			
28	DL 13476	.31	1.50	.21	.013	.016	-	.45	-	-			
29	DL 13524-C	.20	1.55	.28	.011	.015	-	.46	-	-			
30	DL 13532-D	.28	1.58	.34	.011	.016	-	.47	-	-			
31	• USS	.23	1.60	.20	.018	.013	.15	.51	-	-			
32	JLJL 0990	.23	1.80	.15	.015	.010	-	.52	-	-			

\* HEAT NUMBER UNIDENTIFIED. RECORDED PLATE NUMBER IS 0123325-A1. COMPOSITION ALSO CONTAINS 0.40 NI.

1 TAKEN FROM ACTUAL TEST PLATE.

2 LADLE ANALYSIS.

TABLE II

## HEAT TREATMENTS

COMPOSITION AND MANUFACTURING SOURCE	HARDENING	TEMPERING <sup>1</sup>	APPROXIMATE A TEMPERATURE ° <sub>3</sub>
<b>Mn-Cr-Mo</b>			
(a) GL	Water quench from 1580° F after 80 min- utes <sup>2</sup> .	Air cool from 900° F after 81 minutes <sup>2</sup> .	1525° F
(b) SCG	Water quench from 1625° F after 90 min- utes <sup>2</sup> .	Water quench from 925° F after 30 minutes.	
<b>Mn-Mo</b>			
(a) DB	Water quench from 1625° F after 30 min- utes.	Air cool from 850° F after 75 minutes.	1420° F
(b) DL	Water quench from 1625° F after 30 min- utes.	Air cool from 850° F after 75 minutes.	
(c) USS	Water quench from 1560° F after 24 min- utes.	Water quench from 900° F after 30 min- utes.	
(d) JLJL	Water quench from 1650° F after 30 min- utes.	Water quench from 860° F after 75 min- utes.	

<sup>1</sup> Varies within 25° F compatible with as-quenched hardness (carbon content) and allowable hardness range.

<sup>2</sup> Heating and soaking time

TABLE III  
CHARPY V-NOTCH IMPACT DATA

STEEL CODE NO.	BRINELL HARDNESS (AVERAGE)	SPECIMEN AXIS DIRECTION <sup>1</sup>	FOOT POUNDS (AVERAGE) <sup>2</sup>						
			70 F	0 F	-40 F	-60 F	-80 F	-100 F	
1	363	T	22.5	19.5	17.5	16.5	14	13	
2	363	T	23	20	16	14	13	11	
3	363	T	24	21	16.5	15.5	14.5	15	
4	363	T	21	18	15.5	14	13.5	11	
5	352	L	31	26	18.5	16	13	11	
6	363	T	25.5	23.5	19	16	16.5	14	
7	363	T	21.5	20.5	17	14	14	11	
8	352	T	25	23	17.5	16.5	16	15	
9	352	T	22.5	21	18.5	14	13	14.5	
10	363	L	33	28.5	23	19	21	18	
11	363	T	24	20	17	17	14	14.5	
12	352	T	25	21	15	13	13	12	
13	363	T	26.5	25.5	23	20.5	19.5	17	
14	363	L	37	36	31	28	22	21	
15	352	T	26	26	18	17	15.5	15.5	
16	363	T	22.5	19.5	16.5	14	12.5	11	
17	363	L	32	28	17.5	18	14	12	
18	363	L	38	36	26	24	20	18	
19	363	L	35.5	34	24	20.5	20	19	
20	341	T	20	17.5	15	13	15	12.5	
21	341	T	24	18.5	14.5	14.5	14	13	
22	363	L	36	27	20	18	17	16.5	
23	341	T	27	22.5	17.5	17.5	15	16	
24	341	L	46	45	36.5	33.5	27	26	
25	363	T	27.5	28.5	22	20.5	18.5	18.5	
26	352	L	39	36	30	26	20	20	
27	363	L	37.5	33.5	29.5	23.5	20	19	
28	341	T	23.5	21	17.5	17.5	16.5	15.5	
29	363	T	26	24	22	19	17	15.5	
30	352	T	25	23	18.5	17	16.5	16	
31	341	L	27.5	25.5	19	17	15.5	14.5	
32	341	T	41.5	31	24.5	22	22	20	
		L	20	17.5	12.5	12	12	11	
		T	40	35	24	22	20	21.5	
		L	20	18	13.5	12.5	12	9.5	
		T	61	53	33	26.5	23	22	
		L	31	28	23	19.5	16	13	

1-T AXIS NORMAL OR TRANSVERSE TO PRIMARY DIRECTION OF ROLLING. L AXIS PARALLEL OR LONGITUDINAL TO PRIMARY DIRECTION OF ROLLING. 2-MINIMUM OF TWO SPECIMENS RECORDED TO NEAREST 0.5 FOOT POUNDS.



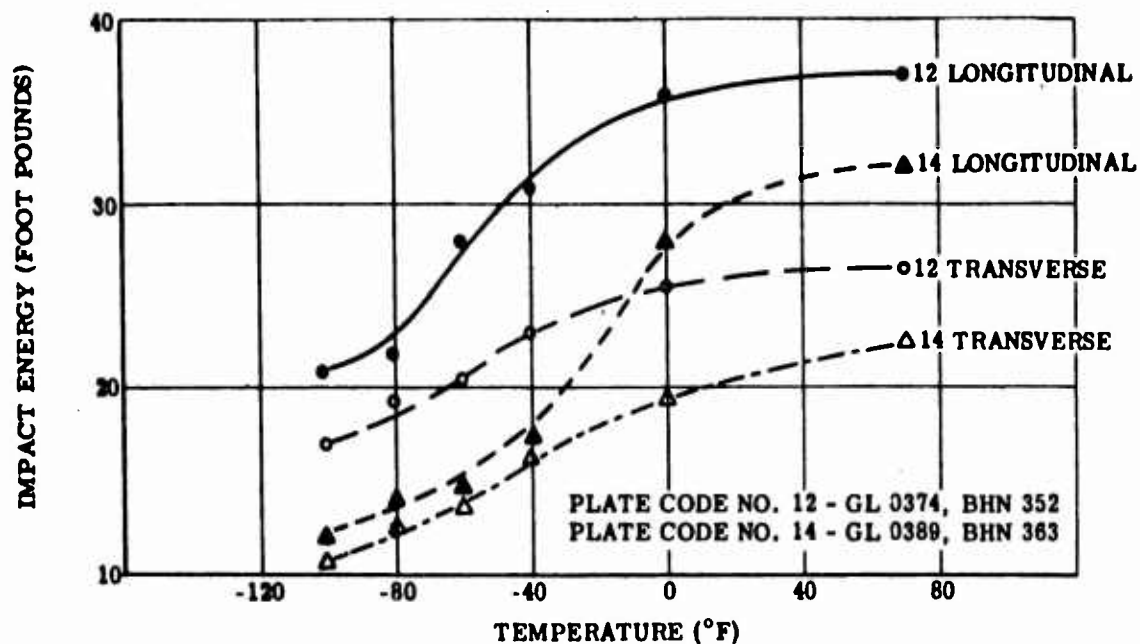


FIGURE 1. CHARPY V-NOTCH ENERGY - TEMPERATURE TRANSITION CURVES FOR STEELS 12 AND 14

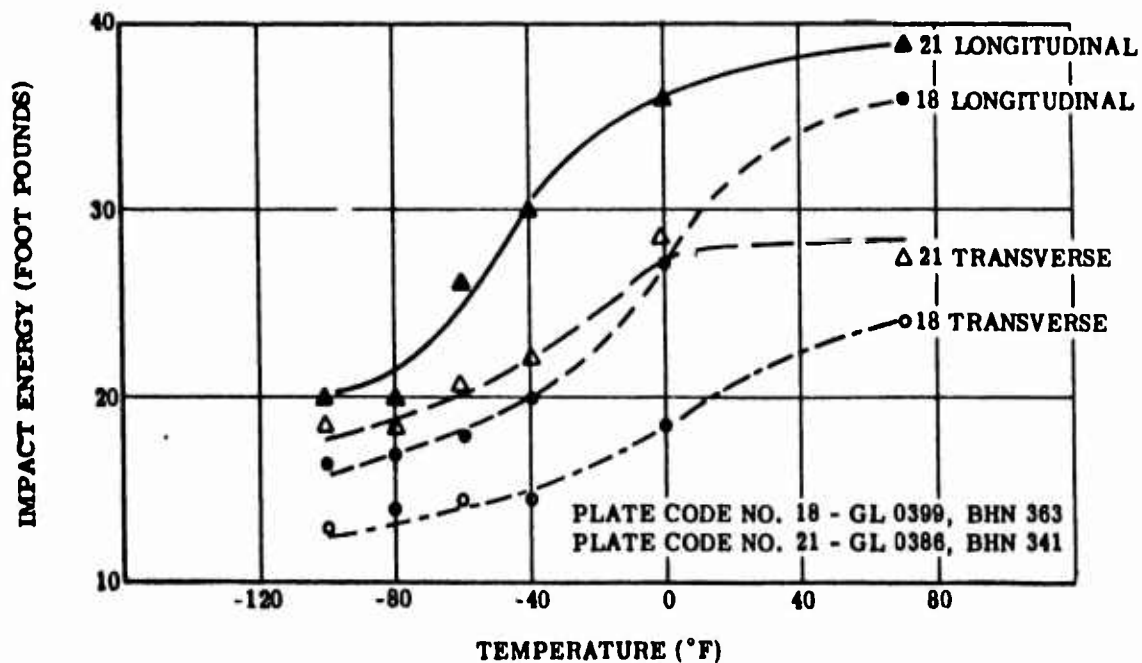


FIGURE 2. CHARPY V-NOTCH ENERGY - TEMPERATURE TRANSITION CURVES FOR STEELS 18 AND 21

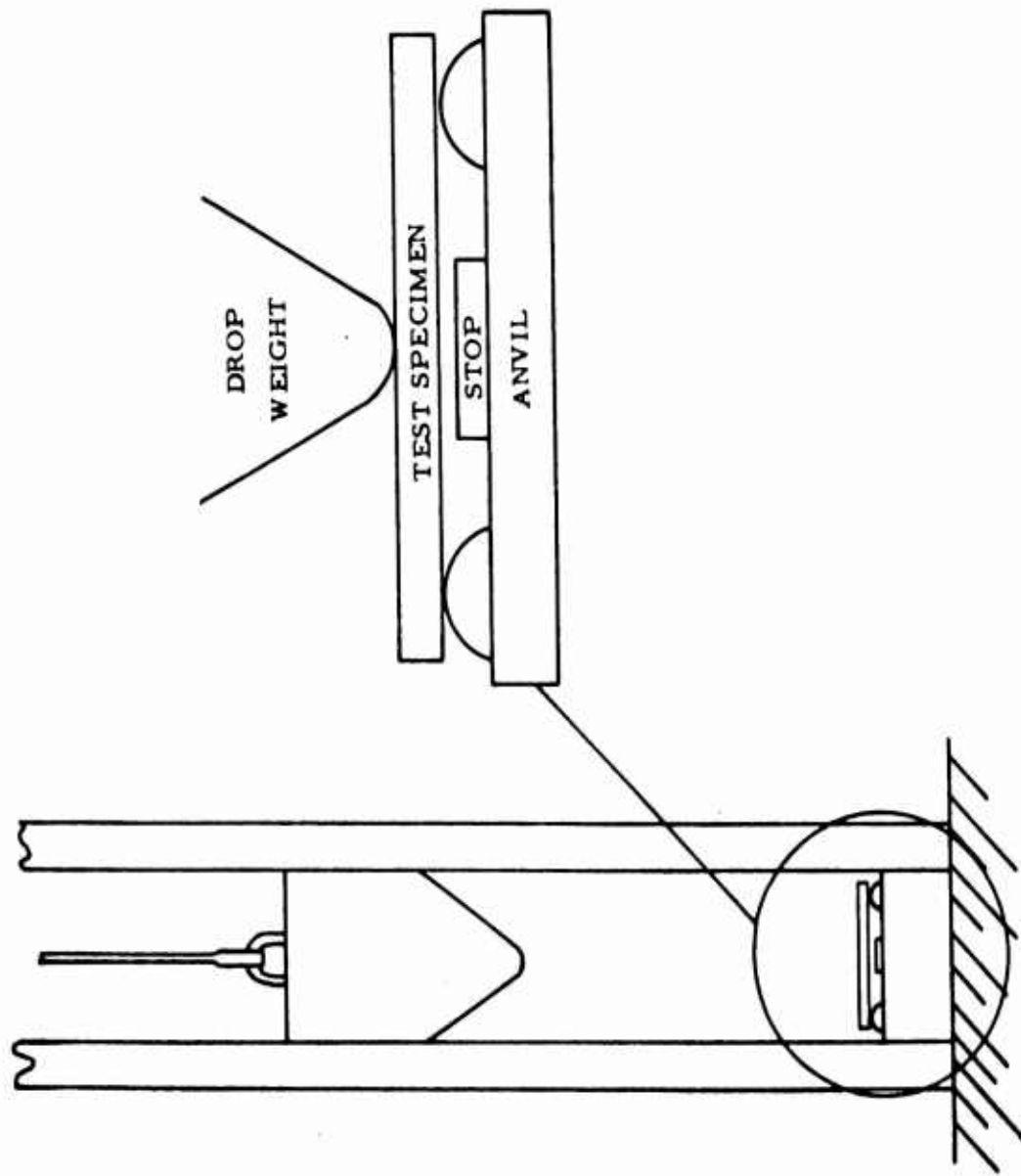


FIG 3. SCHEMATIC OF NAVY CRACK STARTER DROP WEIGHT TEST

stop distance on a specimen size of  $1/2 \times 3-5/8 \times 14$  inches. The crack starter bead used on these specimens was prepared utilizing electrode supplied under "Class A" (48 Rc minimum) Specification MIL-E-13865 (Ord) entitled "Electrodes, Welding, Covered Steel (For Hard Surfacing)". The bead was welded in one continuous pass rather than a split bead made in two passes having overlapping weld craters at the notch center. After welding, the hard-facing beads were notched so that the root of the notch was 0.070 inches above the plate surface.

Based on a later publication<sup>5</sup> by the Naval Research Laboratories and their normalization procedures<sup>9</sup> published in 1959, a standard retest effort was initiated in 1960 specifying both the recommended specimen size and stop distance for  $1/2$  inch plate; 2-inch x 5-inch at an anvil stop distance of 0.090 inches, and the old specimen size of  $3-5/8 \times 14$  inches with an adjusted stop distance of 0.5 inches. Drop weight energies were established by utilizing the hard-facing bead (same specification as above) as a strain gage in the manner outlined by Puzak and Babecki<sup>9</sup> in order to establish a drop weight height which would produce both specimen contact with the anvil stop and a crack opening in the hard-facing bead of 12 to 18 mils. An adequate low temperature range for testing specimens was obtained through the use of liquid nitrogen and alcohol. Temperature was measured by an iron-constantan thermocouple and box potentiometer.

#### Explosion Crack Starter Bulge Tests<sup>1</sup>

Fig. 4 shows the arrangement of equipment for this test. Twelve bulge plate specimens,  $1/2 \times 20 \times 20$  inches were prepared from steels 9, 31 and 32. In the center of each plate a circular crack starter was made by drilling a  $1/2$  inch hole to a depth of one-half the plate thickness and then filling the whole with hard-facing weld-metal. Each explosion bulge plate was impacted with a 3 pound bare pentolite charge detonated at a standoff distance of 24 inches over a 20 inch square die having 12 inch diameter cavity. The charge weight and standoff distance combination was experimentally established by weld-metal crack initiation and a desired plate bulge depth of  $3/4$  to 1 inch. An inverted cardboard box placed over the sample and die was used to support the explosive. Testing temperatures were ambient,  $20^{\circ}$ ,  $0^{\circ}$ ,  $-20^{\circ}$ ,  $-40^{\circ}$  and  $-60^{\circ}\text{F}$ ; two plates being tested at each temperature.

### RESULTS AND DISCUSSION

#### Drop Weight Crack Starter Tests

Nil-ductility transition temperatures obtained by the drop weight test are shown in Table IV; also presented are impact energy values at

TABLE III  
DROP WEIGHT TEST BRITTLE FRACTURE TEMPERATURES (NOT)  
AND CORRESPONDING CHARPY V-NOTCH ENERGY VALUES

STEEL CODE NO.	BRINELL HARDNESS (AVERAGE)	NOT TEMPERATURE ° F	TRANSVERSE IMPACT ENERGY AT NOT TEMPERATURE <sup>2</sup>
1	363	-70	15
2	363	(-70)	13.5
3	363	(-80)	14.5
4	363	(-70)	13.5
5	352	-90	15
6	363	-80	14
7	363	-90	15.5
8	352	-100	14.5
9	352	-110	-
10	363	-90	14
11	363	-50	14
12	352	-	-
13	363	(-100)	15.5
14	363	-90	12.0
15	352	(-100)	-
16	363	-90	-
17	363	-80	14
18	363	-70	14
19	363	-70	15.5
20	341	-110	-
21	341	-110	18.5 •
22	363	-110	-
23	352	(-110)	15.5 •
24	341	(-110)	15.5 •
25	363	(-110)	14.5 •
26	363	(-110)	16 •
27	341	-130	-
28	363	-80	12
29	352	-80	-
30	352	(-80)	12
31	341	-100	-
32	341	-100	13

<sup>1</sup> STANDARD SPECIMEN (1/2" x 2" x 5") TEMPERATURE VALUES CORRECTED FOR INFLUENCE ( 10° F )  
OF HEAT AFFECTED ZONE. VALUES IN PARENTHESES REPRESENT CORRECTED TEMPERATURES OBTAINED  
FROM EARLIER NON-STANDARD TESTS.

<sup>2</sup> ENERGY VALUES (FOOT POUNDS) DIRECTLY OBTAINED OR INTERPOLATED FROM TABLE. ASTERISKED VALUES  
REPRESENT IMPACT ENERGIES AT LOWEST TESTING TEMPERATURE (-100° F) RELATIVE TO NOT VALUES.

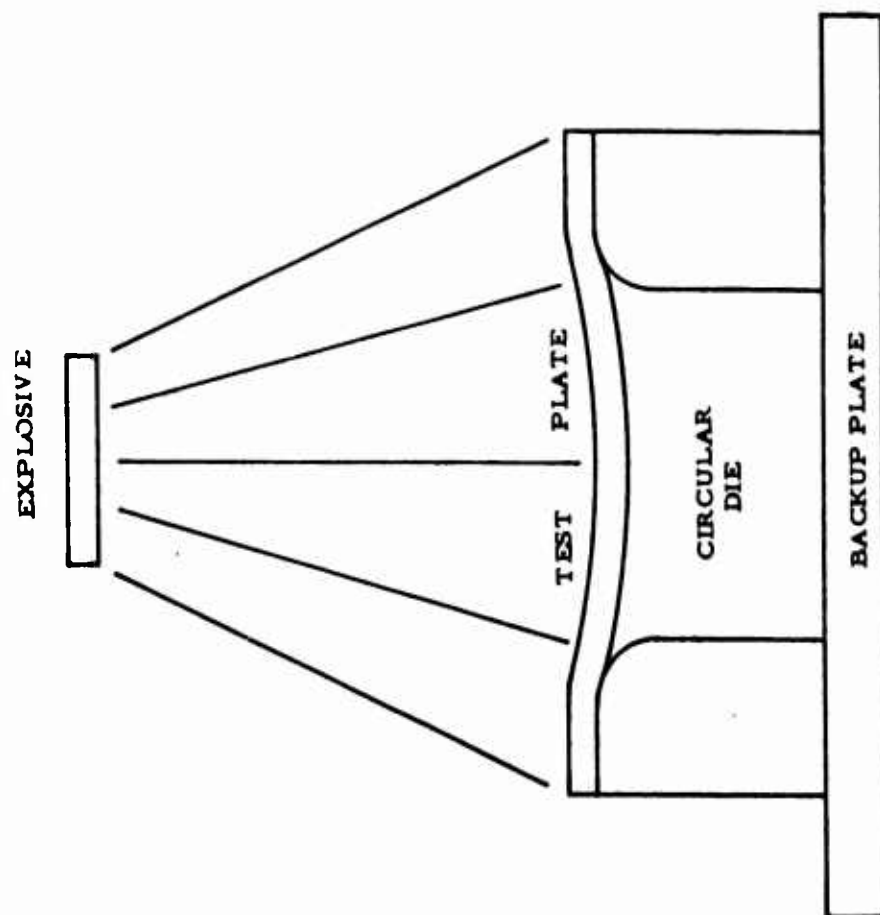


FIG. 4 SCHEMATIC OF EXPLOSION CRACK STARTER BULGE TEST

the various NDT temperatures. NDT temperature values include two corrections. The first is a minus 10°F adjustment for differences in the test procedure used, i. e. non-standard vs. standard procedure. Since all tests were not made by the non-standard method, the correction was necessary for only those steels whose fracture values are shown in parentheses. A second correction of plus 10°F was made for changes in material behavior caused by the heat affected zone from welding of the hard facing crack starter bead. This correction was applied to all NDT temperature results.

The temperature change due to the influence of the heat affected zone was posed as an important test consideration by Murphy, et al<sup>7</sup>; they interject this as a critical element for investigation of the brittle response of a material. Pellini and Puzak<sup>8</sup> recommend the use of reheat treatment for those materials where HAZ hardnesses would be less than the base material; otherwise fictitiously low values for NDT temperature will be obtained. The use of reheat treatment, however, introduces two aspects which may defeat the intended goals of the originally developed drop weight test. First, the use of reheat treatment could very well produce base metal structures significantly different from the original "as-received" material. Second, the development of a suitable tempering cycle to reproduce the original material hardness presents a time consuming "trial and error" process. Since reheat treatment was not employed in the basic test work, it was desired to learn the influence of reheat treatment on the NDT temperature. This was done by reheat treating an entire group of 2 x 5 inch specimens with and without hard-facing weld beads. Afterwards crack starter welds were placed on the beadless specimens. Therefore, the specimens welded prior to heat treatment did not contain a heat-affected zone. This procedure gave positive assurance that an identical base-metal structure and hardness were developed in all specimens. The removal of HAZ was found to raise the NDT temperature by 10°F for the Mn-Cr-Mo steels.

An average NDT temperature of approximately -90°F was found for all Mn-Cr-Mo steels, including those heat treated by a source other than the manufacturers (20-26). A re-average without heats 20 thru 26 gives an average NDT temperature of approximately -80°F. Therefore, the behavior of all Mn-Cr-Mo heats is rather consistent when grouped according to either source of manufacture or by heat treatment. It is interesting to note that the impact energy at NDT temperature is about the same for these steels.

The average NDT temperature for the Mn-Mo steels (discounting hardness variation) is approximately -90°F. The Mn-Mo steel results

were too limited to compare material behavior on basis of manufacturer. The impact energies at NDT temperature for the Mn-Mo steels were found to be lower than the Mn-Cr-Mo steels.

In the drop weight tests most of the specimen fractures obtained at or below the NDT temperature revealed smooth, dull gray surfaces indicative of fine grained, fully heat treated steels.

### Explosion Crack Starter Bulge Tests

Figures 5, 6 and 7 show the results of bulge tests on steels 9, 31 and 32. These tests were conducted in 1956 at Aberdeen Proving Ground, Aberdeen, Maryland coincident with the first drop weight tests. The performance of bulge plates at the same test temperature was not very uniform as evidenced by differences in the extent of cracking. This irregular behavior was attributed to the circular (plug-weld) type of crack starter. The crack initiation and propagation response from such a crack starter would be random in nature and this could create some differences in degree and direction of cracking.

A flat break (complete cracking without bulging) was never attained for the range of temperatures utilized; thus a temperature indicative of NDT was never reached. However, transition temperatures for fracturing under elastic and plastic loading (FTE, FTP) were determinable from the test sequence. The FTE temperature for steel 9 occurs at  $-50^{\circ}\text{F}$ . Below this temperature ( $-60^{\circ}\text{F}$ ) crack propagation is relatively easy, as evidenced by the fact that the cracks are beginning to extend through the elastically-loaded edge regions of the plate supported by the die. At  $-40^{\circ}\text{F}$ , which is just above FTE, crack propagation becomes difficult as indicated by the cracks tending to remain within the central bulge (or plastically-loaded) region. Likewise the examination of the figures will reveal that the FTE for steels 31 and 32 is  $30^{\circ}\text{F}$ .

An estimate of the temperature intervals between both FTP and FTE (from explosion bulge tests) and NDT (from drop weight tests) were made for steels 9, 31 and 32. For making FTP determinations from NDT, an interval of approximately  $185^{\circ}\text{F}$  was evident for all steels. The NDT-FTE interval was  $60^{\circ}\text{F}$  in the case of steel 9 and  $70^{\circ}\text{F}$  for steels 31 and 32. Although higher than the normally acknowledged<sup>4</sup> allowances of  $80^{\circ}$  to  $120^{\circ}\text{F}$  for FTP and  $30^{\circ}$  to  $50^{\circ}\text{F}$  for FTE, the spreads are considered to be reasonably valid since they could be explained by the generally low crack resistance of the basic materials and their broad transition zones i. e. very gradual decrease in impact energy absorption between test temperatures which would be reflected in a broadening of the temperature intervals. For

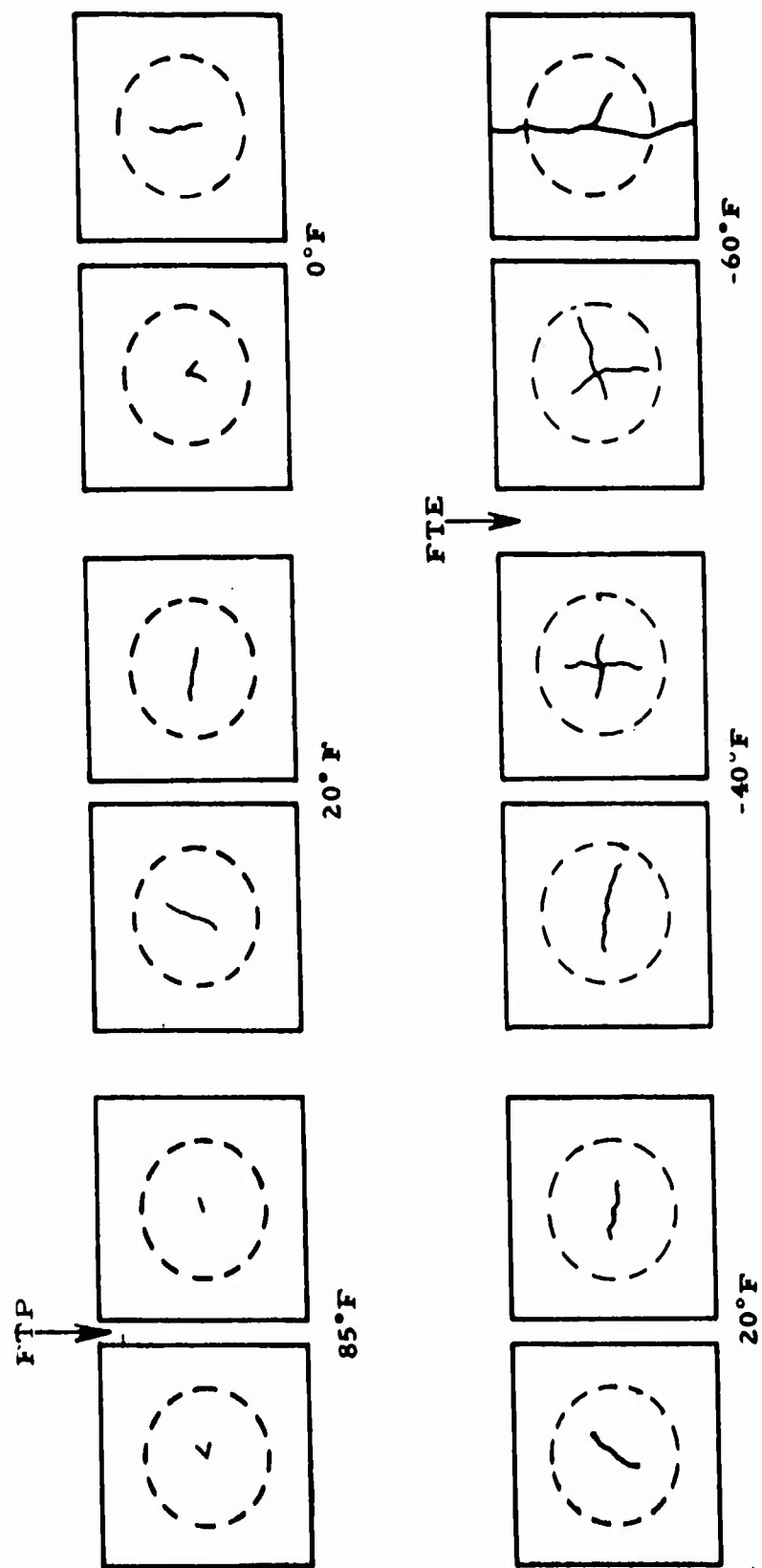
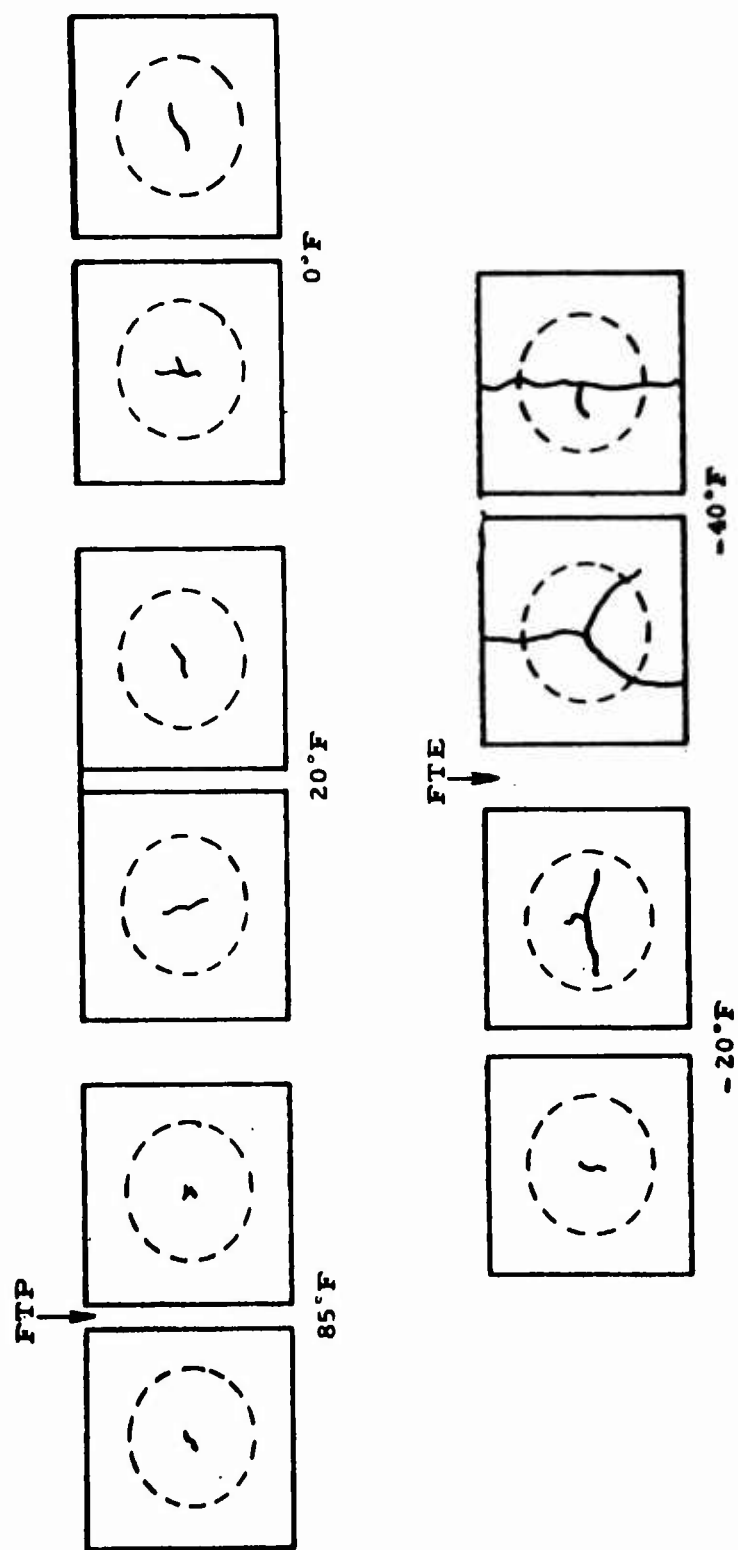


FIG. 5. EXPLOSION CRACK STARTER BULGE TEST RESULTS OF STEEL 9





Page 1.3

FIG. 6 EXPLOSION CRACK STARTER BULGE TEST RESULTS OF STEEL 31

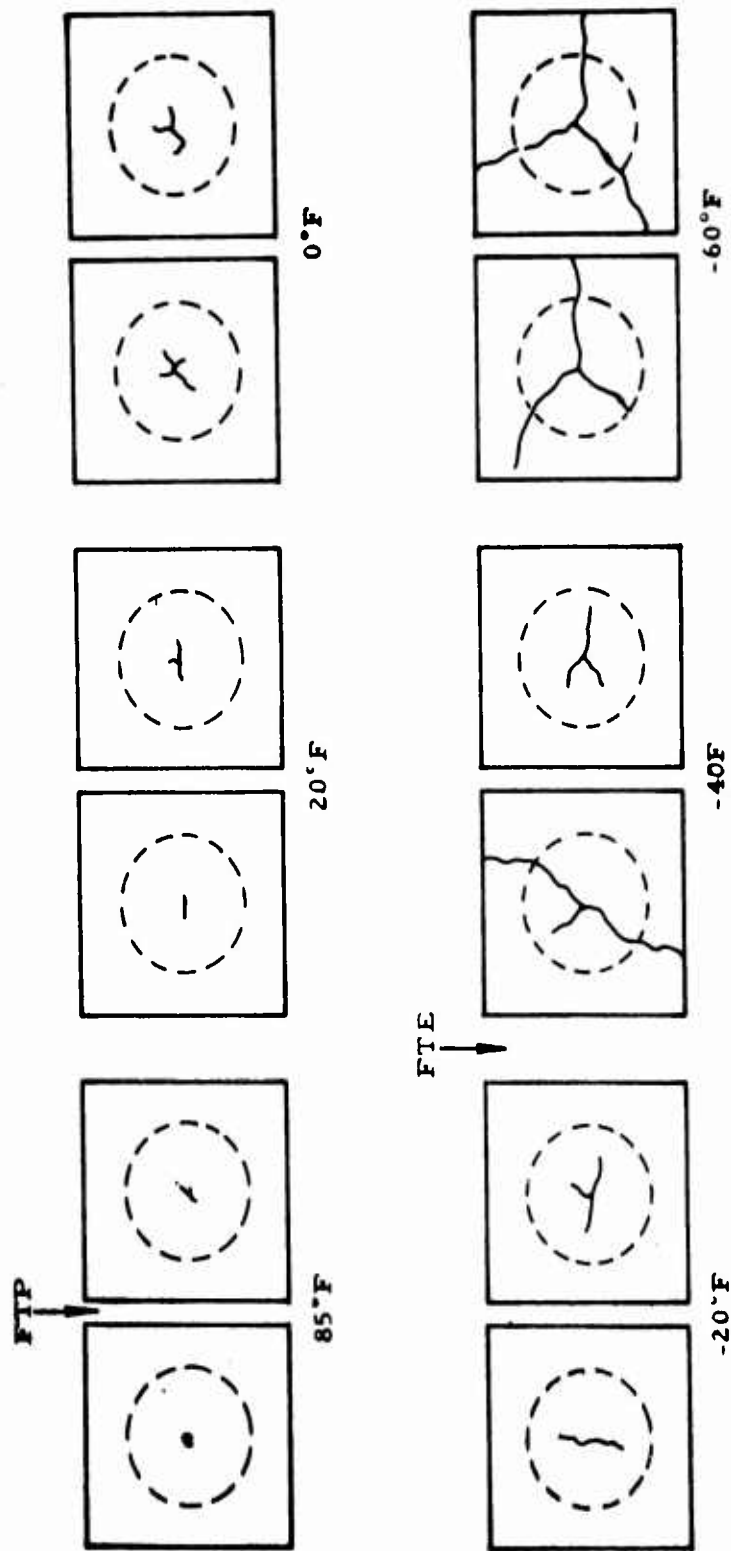


FIG. 7. EXPLOSION CRACK STARTER BULGE TEST RESULTS OF STEEL 32

the interpretations of service performance to follow in this report, an interval of 50° was used in making general estimates of FTE temperatures.

#### SIGNIFICANCE OF NDT TEMPERATURES:

The first question that would be asked by material users or designers after inspection of data similar to that presented here is: "What does it mean in product performance and current design concepts?" This question reflects a natural or universal reaction to any new information, particularly in applications where material behavior is critical and failure by cracking can be catastrophic.

For armored vehicle applications, materials are required to withstand penetration from armor piercing projectiles and to provide structural integrity against normal functional loads down to operating temperatures as low as -40°F. In actual use elastic loads of some stress magnitude do develop during normal operation of armored structures. In addition, the armor structure would be under some level of elastic preload stress stemming from constraint developed during fabrication by welding. Welding also introduces numerous potential crack initiation sites.

To preclude the possibility of brittle fracture under the normal service conditions stated above, an armor steel NDT temperature of just below -40°F would be satisfactory. It is possible, however, that deformation (or accidental) loads at a crack flaw position might be encountered. Under this added circumstance a much lower material NDT temperature is required. If the fracture transition elastic (FTE) temperature of the armor were -40°F, it would allow for the following combination of conditions before fracture occurred:

- (1) a crack flaw,
- (2) -40°F operating temperature,
- (3) accidental loading at the crack position.

Fractures, once initiated, would only propagate through adjacent material that is under nominal elastic loads if the temperature was below -40°F, but would stop at the edge of the deformation region if the temperature was above -40°F. Under the above conditions armor materials should have a maximum NDT temperature of -90°F. In view of the small probability for occurrence of all prerequisite conditions for brittle failure (particularly when compared with normal probabilities of perforation from small arm attack) this NDT provides a substantial margin of safety for crack-free vehicle performance. Since an average NDT temperature of -90°F was

found for the steels evaluated here, a safe temperature of operation by the FTE temperature criteria would be approximately  $-40^{\circ}\text{F}$ .

This generalized situation can be more readily demonstrated by the results tabulated in Table V. The information shown represents the reaction of several of the test materials ( $1/2'' \times 18'' \times 36''$  plates) to a severe form of ballistic shock. Specifically, the source of shock is the 37mm HE projectile which provides the combined effect of kinetic and explosive energies emanating from 0.10 pounds of explosive filler and 1.33 pounds of steel shot. Impacts were directed on the weld-metal crack-starters. Average length of cracking, determined by dividing total length of cracking by the number of cracks, both with respect to deformed and undeformed areas, was used as the basic criteria for determining the inter-relationship of bulge test FTE temperature predictions and actual plate ballistic behavior. Whether or not cracking stayed within bulged region at test temperatures (ambient and  $-40^{\circ}\text{F}$ ) coincided relatively well with predictions based on the FTE temperatures found for these materials by the explosion bulge test.

There are recognized departures in the ability of crack starter test criteria to predict a steel's susceptibility to cracking. This occurs with steels having low Charpy upper shelf characteristics (20 - 25 ft). What seemingly appears as brittle cracking is merely low energy ductile shearing. This form of anomalous behavior in steel has been recognized and reported by Babecki, Puzak, et al<sup>10</sup>. Such "low energy absorption shear" failures in  $1/2''$  armor plate was believed to be found when extensive cracking was observed in the floor plate of the engine compartment of a large number of armored vehicles. The static stress state, developed in this floor plate by various pre-assembly fabrication operations of cold-straightening, cold-forming and full-penetration welding, was bi-axial in nature. In operation, additional stresses were imposed from engine weight and operation. The cracking generally occurred in low-mileage vehicles. Figure 8 is a sketch of floor plate design showing major attachments and plate edges involved in structural welds. The cracks usually started from the vicinity of welds or surface cracks developed from cold forming or straightening. Inspection reports on the cracked plate disclosed Brinell hardness readings of 363 to 388 and Charpy V-notch values in the transverse direction of 12 to 14 foot pounds at  $-40^{\circ}\text{F}$ .

Immediate corrective action consisted of altering the engine mount to redistribute engine weight from the floor to the vehicle side walls, increasing the floor thickness, eliminating full-penetration welding of drain valve and inspection hole ring castings (to reduce some of the restraint from welding), and lowering the hardness of material (to decrease susceptibility to crack initiation and increase resistance to crack propagation).

TABLE V  
SIGNIFICANCE OF BRITTLE FRACTURE  
TEMPERATURES RELATIVE TO CRACK STARTER BALLISTIC BEHAVIOR

STEEL CODE NO.	BRINELL HARDNESS (AVERAGE)	CRACK-STARTER EXPLOSION BULGE TEST FRACTURE TEMPERATURES (°F)		NDT DROP WEIGHT FRACTURE TEMPERATURE (°F)	EXTENT & MODE OF CRACKING* FROM SHOCK-IMPACT OF 37 mm H.E. PROJECTILE	
		FTP	FTE		H.F. Weld	H.F. Weld
					+65° F	-40° F
31	341	85	-30	-100	6 (3) WB	29 (3) TP
32	363	85	>-40	-100	18 (3) EB	26 (4) EB

\* First number indicates total cracking in inches. The parenthesized number represents the number of cracks and the letters reflects area limits of cracking i. e. WB - within bulge region, EB - edge of bulge (outer), and TP - through plate. Bulge diameter produced by projectile impact - approximately 8".

Note: Without a crack starter, material was void of any cracking at test temperature of -40° F.

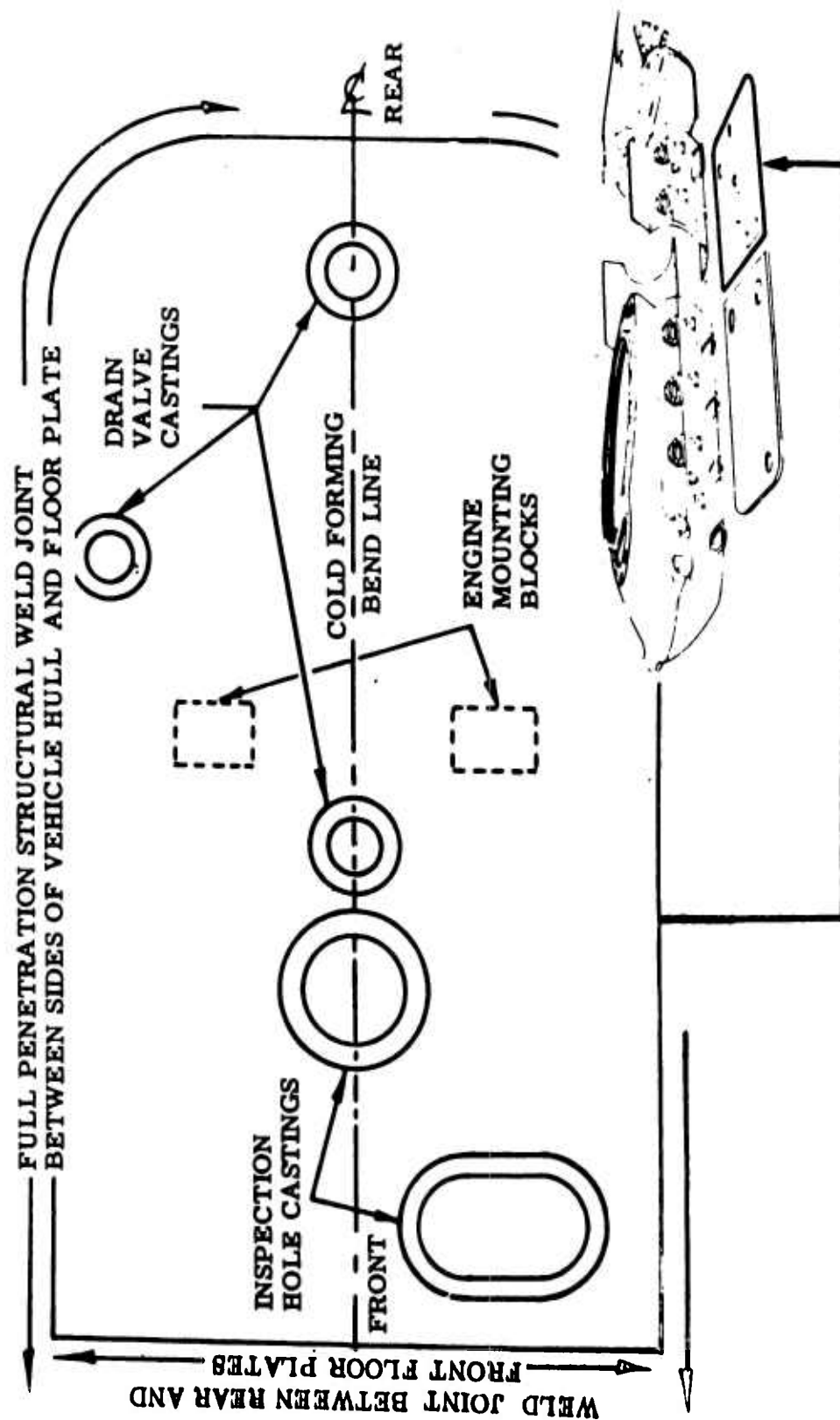


FIGURE 8. BOTTOM PLAN VIEW OF ENGINE COMPARTMENT FLOOR PLATE

Although fracture plate sections were not available to visually ascertain the extent of true brittleness, it may be said with certainty that ambient temperatures never approached values indicative of a likely nil-ductility transition (NDT) temperature, let alone the fracture transition elastic (FTE) temperature for the material; in fact, lowest ambient temperatures would have more closely approached the fracture transition plastic (FTP) temperature. Since no metal deforming loads were involved, the likelihood of serious cracking would not have been expected in terms of previously acknowledged transition temperature interpretations.

In view of this experience, it can only lead one to conclude that 1/2" armor plate in the presence of extreme stress conditions and latent defects is prone to cracking by low energy absorption without reaching temperatures indicative of any of the likely critical transition values expected for this type steel. The probability of cracking is even more likely in plate material tempered to the high end of the specified hardness range. This incident, however, should not detract from the predictive or practical value offered by the crack-starter drop weight test. With a better appreciation of the special limitations found by experience, the test should prove more valuable in making realistic appraisals of the performance of steels in service.

#### CONCLUSIONS:

1. Corrected NDT temperatures varied from  $-50^{\circ}$  to  $-110^{\circ}\text{F}$  for the Mn-Cr-Mo steels and  $-80^{\circ}$  to  $130^{\circ}\text{F}$  for the Mn-Mo steels. The average NDT temperature for both steel analyses was  $-90^{\circ}\text{F}$ . Without reheat treatment of the specimen to eliminate influence of crack-starter bead heat-affected zone, the NDT temperature is fictitiously lowered by approximately  $10^{\circ}\text{F}$ .
2. Limited crack-starter bulge test data generally confirms "rule of thumb" relationships offered by Puzak, et al, in approximating the FTE temperature. The temperature adjustment for determining the FTP temperature was significantly higher than "rule of thumb" allowances i. e.  $180^{\circ}\text{F}$  vs  $120^{\circ}\text{F}$ .
3. Estimates of safe operating temperature by FTE temperature criteria for the steels investigated indicates freedom from excessive cracking to a temperature of approximately  $-30^{\circ}\text{F}$ . Keeping material at low side of specification hardness range can reduce this critical temperature to much safer values as well as decrease the probability of "low energy shear" ruptures.

4. The NDT temperature determined by the Navy crack-starter drop weight test (as interpreted by the explosion bulge test and the Charpy V-notch impact test) provides a rather knowledgeable means by which a steel can be appraised for suitability to a critical operating environment.

#### REFERENCES

1. Pellini, W. S. "Use and Interpretation of the NRL Explosion Bulge Test", Naval Research Laboratory Report 4034, September 1952.
2. Puzak, P. P., Eschbacher, E. W., and Pellini, W. S. "Initiation and Propagation of Brittle Fracture in Structural Steels". The Welding Journal, December 1952.
3. Pellini, W. S., Puzak, P. P., and Eschbacher, E. W. "Procedures for NRL Drop Weight Test" - NRL Memo Report 316, June 1954.
4. Pellini, W. S. "Evaluation of the Significance of Charpy Tests", American Society for Testing Materials, Special Technical Publication No. 158, 1954, pp. 216 - 261.
5. Puzak, P. P. and Pellini, W. S. "Evaluation of the Significance of Charpy Tests for Quenched and Tempered Steels" - The Welding Journal, Research Supplement, June 1956, pp. 275s to 290s.
6. U. S. Army Ord Corps Aberdeen Proving Ground Test Report AD-1245 (Classified) "Investigation of the Shock Resistance of 1/2" Rolled Armor at Various Temperatures". December 1956.
7. Murphy, W. J., McMullen, W. D. and Stout, R. D. "Relative Behavior of Notch-Toughness Tests for Welded Steel" - The Welding Journal, Research Supplement, June 1957, pp. 307s - 311s.
8. Pellini, W. S., Puzak, P. P., Discussion (Reference 6) "Relative Behavior of Notch-Toughness Tests for Welded Steels", The Welding Journal, Research Supplement, November 1957, pp. 511s - 512s.
9. Puzak, P. P., Babecki, A. J. "Normalization Procedures for NRL Drop Weight Tests" - The Welding Journal, Research Supplement - May 1959, pp. 209s - 218s.



10. Babecki, A. J., Puzak, P. P. and Pellini, W. S. "Report of Anomalous Brittle Failures of Heavy Steel Forgings at Elevated Temperatures" ASME Paper No. 59-Met. 6, presented by Metals Engineering Conference, Albany, New York, 29 April - 3 May 1959.
11. Pagano, V. H. and McHugh, C. O. "An Appraisal of Brittle Fracture Temperature of Rolled Armor Steel by the NRL Drop Weight Test" R&E Report No. 42 U. S. Army Tank Automotive Command, April 1961.

#### DISCUSSION

Dr. Hammer: The paper is up for discussion.

Mr. Zaroodny: Could you try something like measuring the length of the cracks?

Mr. Pagano: We have not considered this. We actually haven't made the analysis to this point but we feel that utilizing the basic criteria that has already been established with respect to the bulge may help us in this respect.

Mr. Zaroodny: Well, you have very well brought out that the future will probably bring actual measurements rather than interpolating between temperatures.

Mr. Pagano: I don't know actually; a number of plates were tested at the same temperature, and you get this variation. This is the thing that disturbed us a little bit and we felt that this might be the reaction of the crack started due to the load. It may take off in one direction, more prone to a fracture, or may take off in a longitudinal manner and then change direction to the transverse, following the path of the least resistance. This is some of our reasoning on it.

Mr. Pagano: I don't know how many people are familiar with the low-blow Charpy test by Hartborne and Horner. They use the pre-crack by fatigue rather than low-blow. This particular thing now defines the temperature which they have shown correlates fairly well with the NDT temperature. So there is a direct tie-in, and you can come up with a whole set of design curves correlating critical design stress to critical crack size and NDT temperature.

## DYNAMIC STRESS CONCENTRATION FACTORS

Richard Shea\*

### ABSTRACT

The problem of the response of structural discontinuities to short duration stress pulses is studied experimentally. Employing explosively induced stress pulses in thin plastic plates, containing central circular holes, a dynamic stress concentration factor is determined as a function of pulse frequency. It is concluded for this loading case, that the dynamic stress concentration is significantly lower than the static value.

### NOMENCLATURE

Symbol	Description
$c_1$	= Dilatational wave velocity
$c_2$	= Distortional wave velocity
$d$	= Representative discontinuity dimension, (Hole diameter in this case)
$E$	= Young's modulus
$h$	= Thickness of shear plate
$k$	= Stress concentration factor
$t$	= Time
$v$	= "Primacord" burning rate
$v_o$	= Impact velocity of shear plate
$w$	= Width of model
$\alpha$	= Angle of biased edge of model
$\epsilon_{\max}$	= Maximum (peak pulse) strain
$\epsilon_{\text{nom}}$	= Nominal (peak pulse) strain
$\epsilon_{\text{nom}}$	= Nominal peak pulse strain corrected for attenuation
$\lambda$	= Wave length of dilatational pulse
$\nu$	= Poisson's ratio
$\rho$	= Mass density
$\sigma_{\max}$	= Maximum (peak pulse) stress
$\sigma_{\text{nom}}$	= Nominal (peak pulse) stress
$\tau$	= Period of dilatational pulse

\*Mr. Richard Shea, U. S. Army Materials Research Agency, Watertown Arsenal Laboratories, Watertown, Massachusetts.

## INTRODUCTION

Many studies have been made of stress distribution in the vicinity of discontinuities such as holes and notches. These studies, both theoretical and experimental, have provided a great deal of information on the behavior of many of the more common discontinuities under static loading. The usual design procedure for obtaining the maximum stresses associated with such discontinuities has been primarily a matter of applying the pertinent stress concentration factors to the nominal stresses obtained from the simple strength of materials formulae.

This design method has been adequate generally, and even conservative in many instances, for static loading considerations. When dynamic loads are involved, the usual recourse has been to follow the same procedure, but to increase the margin of safety to allow for the uncertainty of the actual dynamic stress. Obviously, this approach will lead to an efficient design only by pure chance.

The purpose of this study is then to investigate some of the more general aspects of the behavior of discontinuities under dynamic loads. Specifically, the geometry considered here is a thin plate containing a central circular hole; and the loading is of a short duration, discrete pulse nature. The problem is approached experimentally, using explosively induced stress pulses in thin plastic plates.

Single, discrete, compression pulses are propagated longitudinally through plates containing the discontinuities. The emphasis is directed toward stress pulses having durations that are much shorter than the fundamental dilatational period of the plates.

Some previous experimental work in this area has been undertaken by Durelli, et al.<sup>1,2</sup> Employing dynamic photoelastic techniques the same problem was investigated. In these studies the pulse durations were several times longer than the period of the plates; and accordingly, no apparent dynamic effect was noted.

In the early phases of this program an attempt was made to generate short duration stress pulses by the use of a spring-propelled shear plate impacting the edge of a rectangular plate containing a central circular hole (see Figure 1). The alignment in this scheme was a highly critical factor, and the pulse lengths obtained were about five times the diameter of the holes. Again, the stress concentration factor observed was essentially equal to the static value.

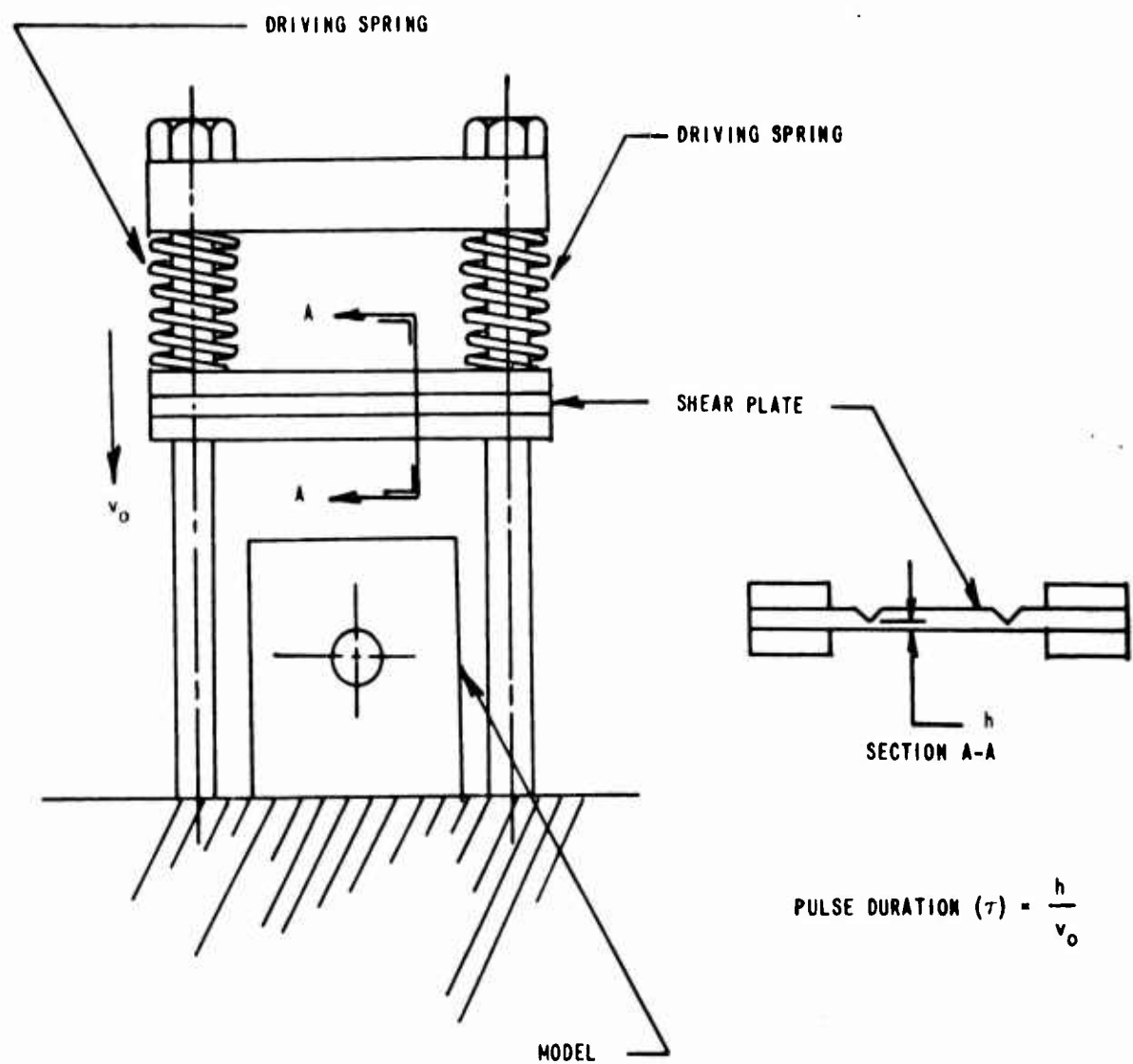


Figure 1. SCHEMATIC OF SPRING-PROPELLED LOADING DEVICE

Pao<sup>3</sup> has studied the problem of the vibratory loading of an infinite plate containing a central circular hole. In this theoretical approach it is noted that, when the wave length of the vibration is of the same order of magnitude as the diameter of the hole, the maximum stress at the hole varies with the forcing frequency.

## FORMULATION

### Dynamic Stress Concentration Factor

In the usual terminology for the case of plane stress, the stress concentration factor is expressed as the ratio of maximum to nominal stresses.\*

$$k = \frac{\sigma_{\max}}{\sigma_{\text{nom}}} \quad (1)$$

While this is based on static reasoning it may be extended to include dynamic considerations with no loss of generality. Assuming the attenuation of the pulse to be insignificant, if  $\sigma_{\text{nom}}$  is defined as the peak pulse stress several wave lengths upstream of the discontinuity, and  $\sigma_{\max}$  is defined as the peak pulse stress at the discontinuity,  $k$  will still portray the effect of the discontinuity.

The configurations considered here are such that at the points where both  $\sigma_{\text{nom}}$  and  $\sigma_{\max}$  occur, a state of uniaxial stress exists. In the nominal stress field, during the time of initial pulse passage, there is only a stress in the direction of the pulse propagation. At the edge of the hole, there can be no radial stress, so that there is an uniaxial stress in the tangential direction.

Therefore, the stress concentration factor can be written in terms of the nominal and maximum strains.

$$k = \frac{\epsilon_{\max}}{\epsilon_{\text{nom}}} \quad (2)$$

---

\*  $\sigma_{\text{nom}}$  is based on the net area at the discontinuity in both the static and dynamic sense, i. e., the effect of the absence of the material at the discontinuity is considered, but the associated non-uniform stress distribution is not.

Here the same restrictions regarding the definitions of the dynamic maximum and minimal stresses must be observed.

### Pulse Frequency Parameter

Since an effect of pulse duration, or conversely pulse frequency, on the response at a discontinuity is suggested, a dependency is implied of the form:

$$k = f\left(\frac{d}{\lambda}\right) \quad (3)$$

Here  $d$  is a representative geometric dimension of the discontinuity, the hole diameter, in this case; and  $\lambda$  is the wave length of the stress pulse. Figure 2 illustrates these dimensions for a plane compression pulse propagating longitudinally along a plate with a central circular hole.

The pulse wave length is a function of both the material of the member and the duration of the applied load.

$$\lambda = c_1 \tau \quad (4)$$

The dilatational wave velocity (which is dependent solely on the material) is represented by  $c_1$ , and the loading duration by  $\tau$ .

This study has been restricted to the effect of the dilatational (compression) pulse. Since there is also a distortional (shear) pulse associated with a dynamic loading, attention must be directed to that portion of the member which is unaffected by the shear pulse (at least during the passage of the initial compression pulse.) This is accomplished by observing only the initial response of the member at locations relatively far removed from the area at which the load is applied. In effect the dilatational pulse is allowed sufficient room to "outrun" the distortional pulse. Inspection of Equations 5, below, will show that the dilatational velocity ( $c_1$ ) is always greater than the distortional velocity ( $c_2$ ).

$$\begin{aligned} c_1 &= \sqrt{\frac{E}{\rho(1-\nu^2)}} \\ c_2 &= \sqrt{\frac{E}{2\rho(1+\nu)}} \end{aligned} \quad (5)$$

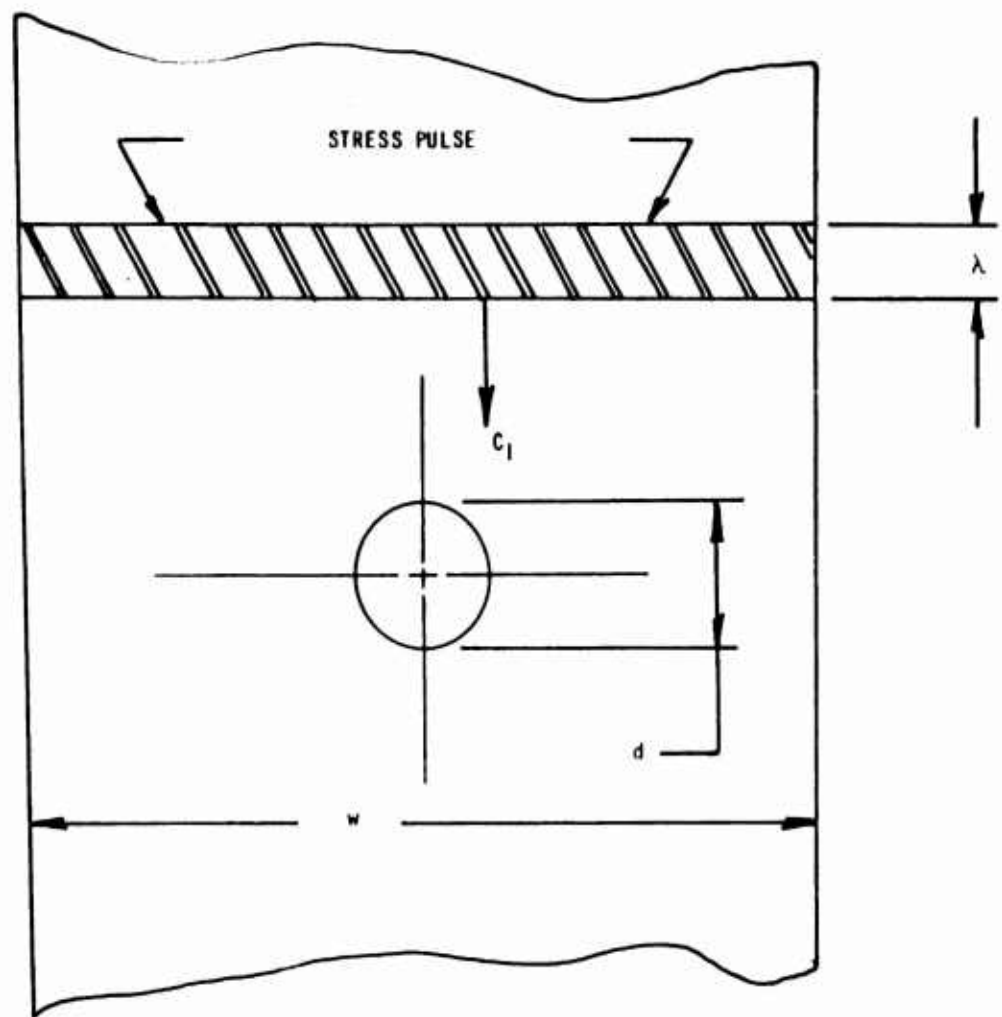


Figure 2. PROPAGATION OF STRESS PULSE IN FINITE PLATE CONTAINING CENTRAL CIRCULAR HOLE

## EXPERIMENTAL TECHNIQUE

### Models

Effort was directed toward obtaining pulse frequency parameters varying from about 1.0 to 5.0. However, since it is impractical to vary the pulse length, the variation of the  $d/\lambda$  parameter was accomplished by changing the physical dimension,  $d$ . The significant geometric parameters were kept constant by scaling other pertinent model dimensions in the same proportion as  $d$ .

The models were fabricated from thin (1/4-inch Plexiglas) plastic plates. The use of plastic is desirable from several precepts. First, the elastic wave velocities in plastics are considerably lower than in most metals. Thus, it is possible to achieve desirable (i.e., relatively large)  $d/\lambda$  values without having to resort to large, and therefore, unwieldy models. Second, plastics possess low elastic moduli so that small loads will produce strains sufficiently large for accurate measurement.

The plates were generally in the form of trapezoids. The over-all dimensions varied from about 4" x 10" to 36" x 60" in order to bracket a sufficient range of the pulse frequency parameter. The discontinuities considered in the initial phase of this study were central circular holes varying from 1.9 to 9.0-inch diameters.

### Loading

Lengths of "Primacord" detonating fuse were placed along the biased edge of the models as shown in Figure 3. Detonation of the fuse was accomplished by initiation of a No. 6 blasting cap at the upper end of the "Primacord." The burning rate of the "Primacord" is approximately 250,000 inches per second; and the burning duration, at a point, about 20 microseconds.

This technique, which is attributed to Christie,<sup>4</sup> imparts sharp, reproducible pulses, of about 20 microseconds duration, to the plate. Referring again to Figure 3, if the angle  $\alpha$ , between the bias and the horizontal, is set such that  $\sin \alpha = \frac{v}{c_1}$ , (where  $v$  is the burning rate of the "Primacord") it is possible to obtain a short duration pulse which propagates longitudinally down the model.

Some initial experimentation was necessary to determine the



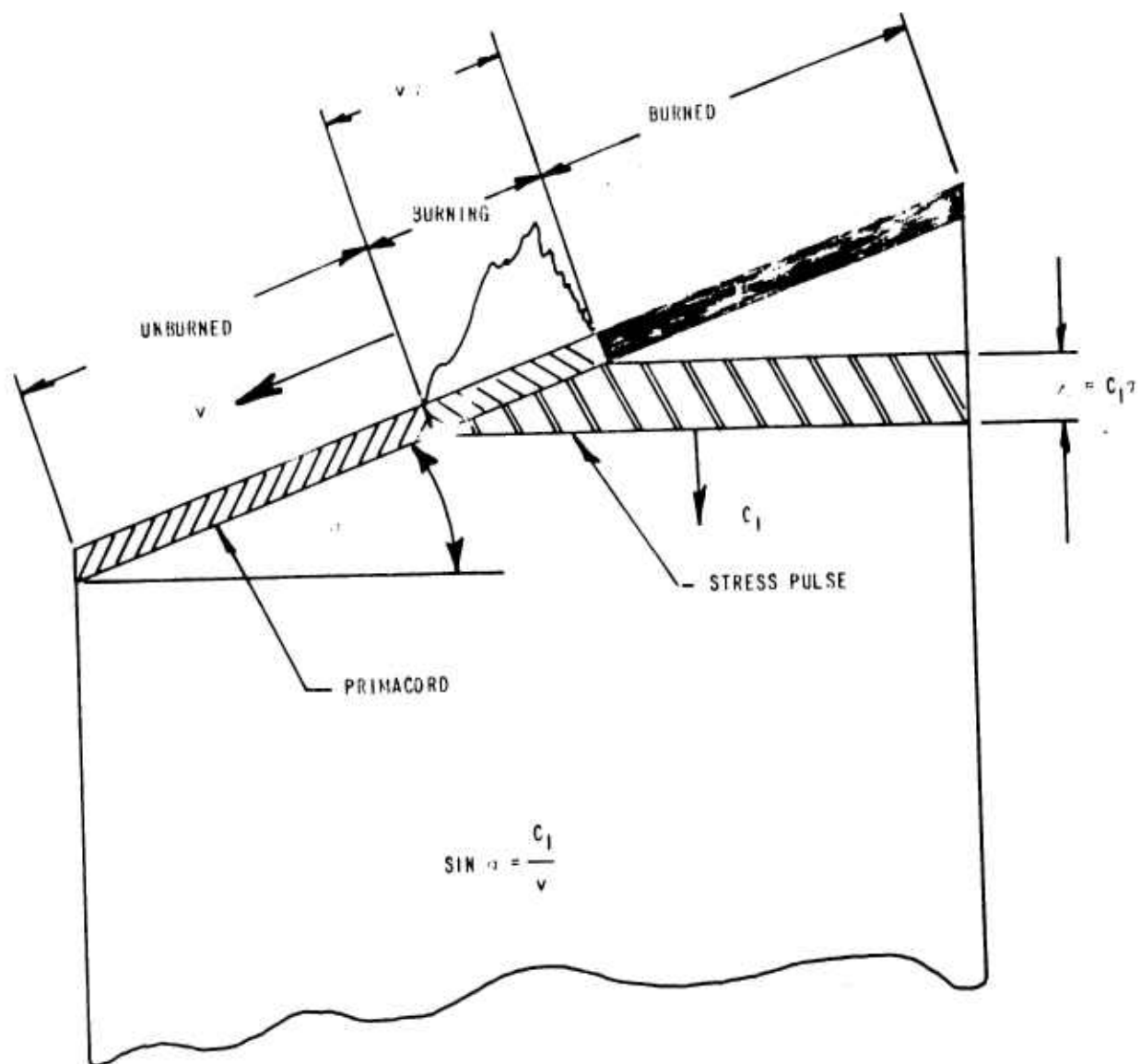


Figure 3. LOADING TECHNIQUE

correct value of  $\alpha$ . This was due to the variability of Young's modulus with strain rate which in turn effects the wave velocities. Essentially, the velocity of the dilatational wave was determined by measuring the time delay of its arrival at two points on a longitudinal line; and the angle,  $\alpha$ , adjusted accordingly. To check the angle, the arrival of the pulse at two points on the same transverse line, but at opposite edges of the plate, was noted.

The pulses generated by this method were quite reproducible, having durations of 20 microseconds, which in "Plexiglas" correspond to a wave length of 1.9". Although the amplitudes of pulses on different models were not identical, (due probably to the variation of the explosive loading in the Primacord) the method faithfully reproduced pulses of the same duration and general shape. Figure 4 is a tracing of a typical oscilloscope record showing the pulse shape obtained by this loading technique.

#### Instrumentation

The instrumentation employed in this study consisted of 1/16-inch foil strain gages, a trigger gage, suitable ballast circuits, and dual beam oscilloscopes. This is shown schematically in Figure 5.

The oscilloscopes were triggered by the strain signal from a gage in the nominal stress field. This signal was delayed sufficiently to insure observance of the entire strain phenomenon. The delay may be seen in Figure 4 at the origin of the trace.

The strain gages were located typically as shown in Figure 5. As may be noted, four gages were located (2 gages back to back, at locations above each of the transverse extremities of the hole) in the nominal stress area. This was done to provide assurance that the pulse was essentially uniform as regards both amplitude and orientation across the width of the model, and to cancel the effect of any pulse variations through the thickness of the model.\* The nominal strain was obtained by averaging the

---

\* For "Plexiglas"  $\alpha$  is approximately 25 degrees. If steel or aluminum were employed as the model material,  $\alpha$  would have to be about 75 degrees, which would have been quite awkward. This, then, is another reason for employing a plastic model.

\*\* No strain differences through the thickness were noted however. The back gages could be properly omitted with no loss of accuracy.

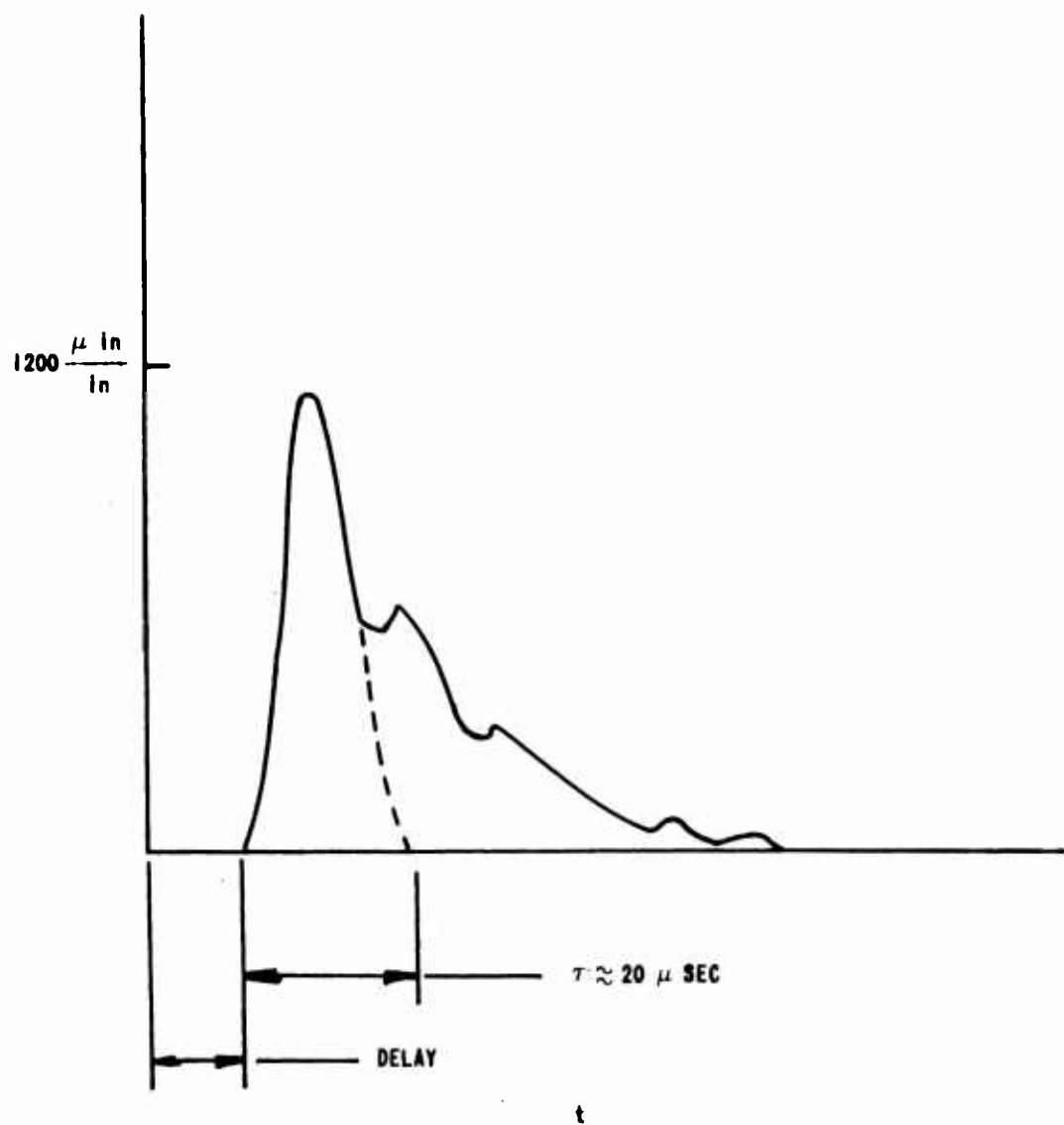


Figure 4. TYPICAL STRAIN PULSE

outputs of the two gage pairs. In all cases the times of pulse arrival at the two transverse locations were generally coincident within 1 or 2 microseconds.

Also as shown in Figure 5, two gages were located at the opposite transverse extremities of the hole. Again this was done to provide assurance of pulse uniformity. The orientation of the pulse passage at this location was essentially horizontal within several microseconds in all cases.

## LIMITATIONS

### a. Response of Strain Gages on Plastics

Clark<sup>5</sup> has noted that wire resistance strain gages mounted on one-half inch square bars of "CR-39" plastic exhibited only about 75% of the strain sensitivity that would be expected. The effect was noted both statically and dynamically in relatively close agreement, and was attributed to the wire of the strain gages stiffening the plastic.

Assuming that this reduction in sensitivity is constant, the stress concentration factor, being simply a ratio of strains, should be unaffected. However, since the stiffness of the models at the regions of nominal and maximum stress differs significantly (at least in the static sense) it was decided to observe this phenomenon for the particular configuration being studied.

A sheet of "HYSOL 6000 OP", a birefringent plastic, having physical properties similar to "Plexiglas" was fabricated into a model with the same geometric parameters as the models used in the primary testing phase. The model was loaded statically in tension; and the maximum and nominal stresses determined photoelastically. After unloading, foil strain gages were applied as on the dynamic models. The model was loaded again and the maximum and nominal stresses determined, this time from the output of the strain gages.

The comparison between these results indicated, for the configurations studied, that the foil strain gages gave results, for both the nominal and maximum strains, which were as close to the photoelastic values as could be reasonably expected.

The fact that the reduced strain sensitivity did not occur in this study may be due to the use of foil type strain gages which are not as stiff

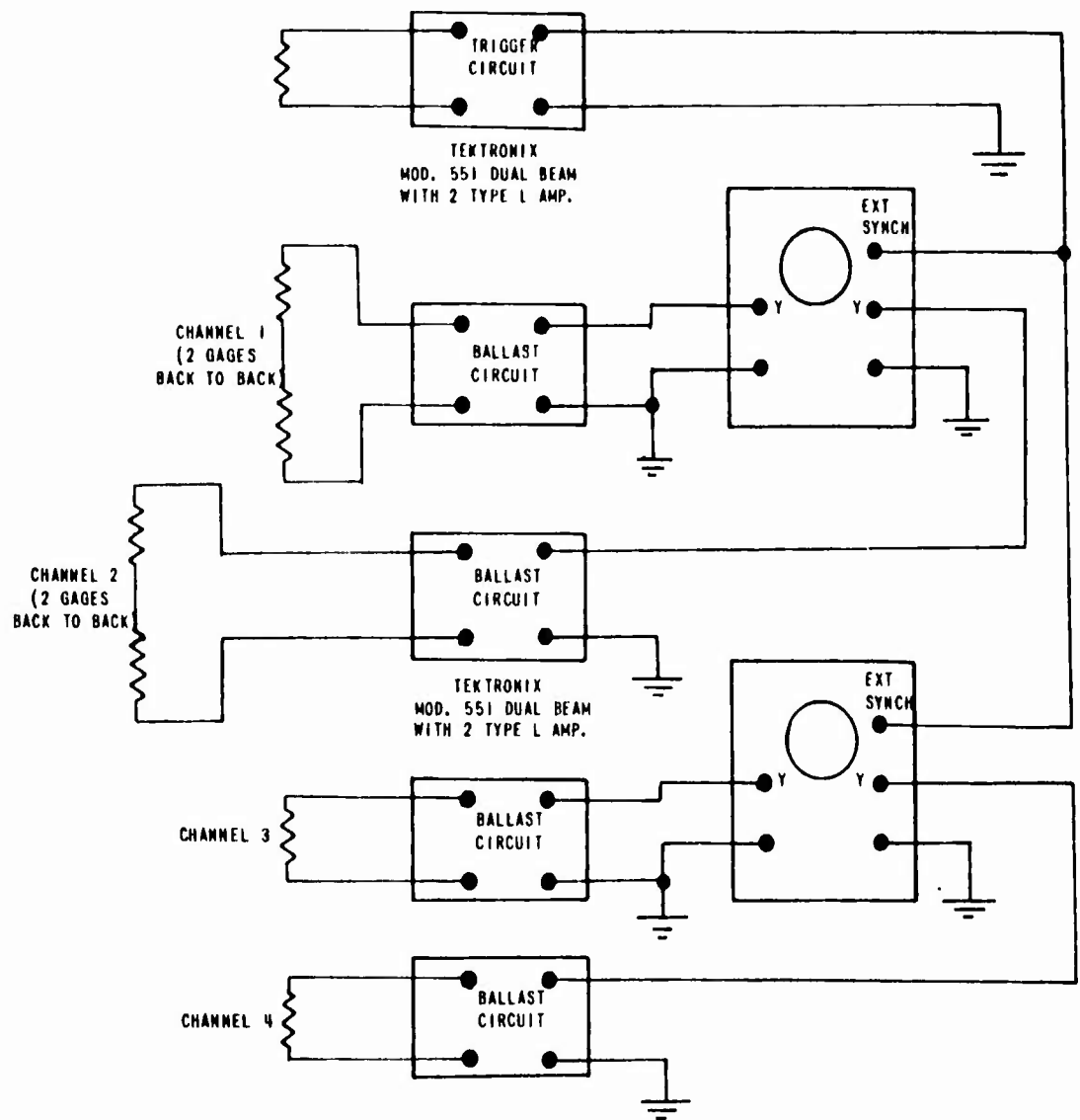


Figure 5. SCHEMATIC OF STRAIN GAGE CIRCUIT

as wire gages. In any event since the static check showed no significant loss of strain sensitivity, it is felt that dynamically any error, which may exist, may be properly neglected.

#### b. Dynamic Response of Strain Gages

There is some tendency to doubt the validity of strain gage response to high frequency excitation. For example, while studying the propagation of plastic waves in soft aluminum, Gillich<sup>6</sup> noted that resistance strain gage measurements deviated significantly from diffraction grating readings at strains above 2%, and at strain rates corresponding, to wave velocities. However, in the present study, the maximum strains recorded were always much lower than 2%, generally in the range of 1200 to 1500 microinches per inch.

On the other hand, while Clark<sup>5</sup> did find a difference in dynamic strains between strain gage measurements and photoelastic techniques, the identical difference was observed statically.

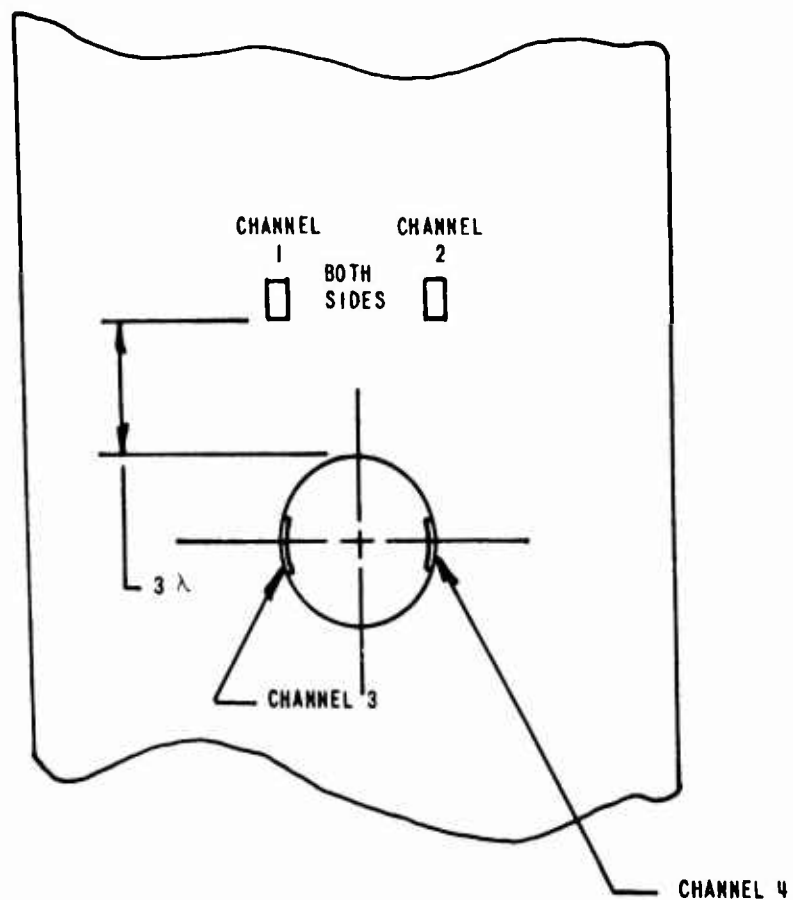
One prevalent criticism of employing strain gages for high frequency measurements, stems from a lack of confidence in the dynamic qualities of adhesives. While this is, no doubt, an area worthy of additional investigation, it was found, in this study, that the adhesive bond was generally excellent. The adhesive employed was Eastman - 910; and in practically all cases, the gages were found to be securely bonded after the test.

#### c. Attenuation of the Stress Pulse

One of the assumptions made in the formulation of the equations for the dynamic stress concentration factor was that the attenuation of the pulse between the locations of the nominal and maximum stresses could be neglected. However, the attenuation is actually significant, and it was therefore necessary to apply correction factors to account for the pulse decay.

A series of tests was conducted on models with no discontinuity, but otherwise identical to the models used in the primary testing phase. A correction factor was determined for each of the model sizes, and applied to the nominal strains. The corrected nominal strains were then employed in the determination of the stress concentrations.

Using this concept, Equation 3 may be rewritten:



CHANNELS 1 & 2 - NOMINAL STRAIN  
CHANNELS 3 & 4 - MAXIMUM STRAIN

Figure 6. LOCATION OF STRAIN GAGES

$$k = \frac{\epsilon_{\max}}{\bar{\epsilon}_{\text{nom}}} \quad (6)$$

Where  $\bar{\epsilon}_{\text{nom}}$  is the attenuated nominal strain.

## RESULTS AND CONCLUSIONS

The results of this study are indicated in Figure 7.\* As may be noted there is a pronounced variation of the stress concentration factor with the pulse frequency. Particularly in the region of pulse durations of the same length as the hole diameter, the stress concentration factor drops off significantly.

This may be explained by a purely physical argument of the stress pulse propagation. Since the band of stressed material is about the same length as the discontinuity, there is not sufficient time, or space, for a secondary pulse to be reflected from the hole boundary and reinforce the main pulse. As the band is diminished relatively to the hole, there is even less opportunity for reinforcement to occur. On the other hand for long duration pulses, the band becomes quite large (approaching a static loading condition) and there is sufficient reinforcement to bring about a high stress concentration factor.

It may be concluded from this study that static criteria are not necessarily valid in the dynamic sense. For the particular case considered the results applied to a design problem would be striking. For not only would the designer use a conservative static stress concentration factor, but would probably compound the inefficiency by resorting to a heavy margin of safety.

## ACKNOWLEDGEMENT

The author wishes to acknowledge Messrs. Joseph I. Bluhm and John J. Hannon of the U. S. Army Materials Research Agency: To Mr. Bluhm for suggesting the problem, and for his advice and encouragement: To Mr. Hannon for designing and setting up the instrumentation, directing the experimental program and assisting in many ways too numerous to elucidate.

---

\* Pao's results for an infinite plate with a circular hole under vibratory loading (Figure 3, Reference 3) are superposed on this figure. While the cases examined are somewhat different, the agreement in the trend is significant.



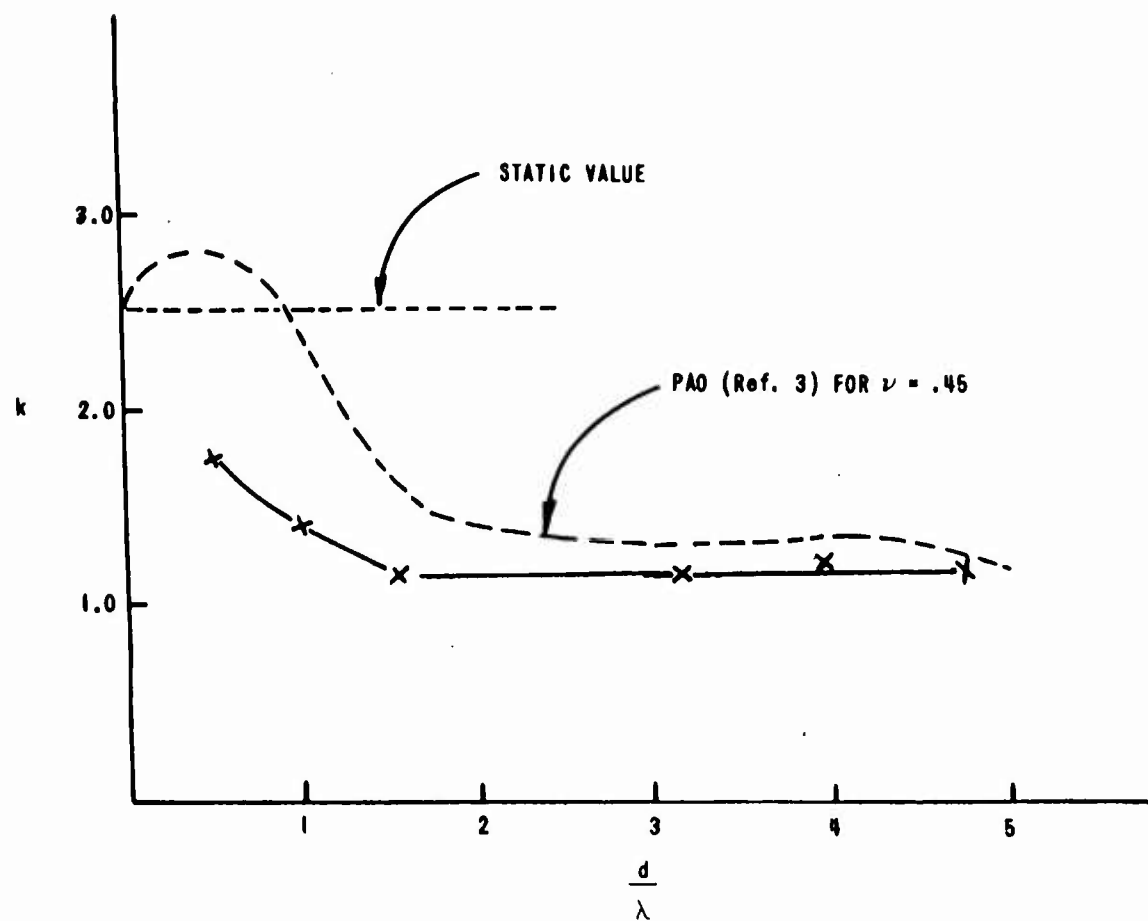


Figure 7. VARIATION OF STRESS CONCENTRATION WITH PULSE FREQUENCY

#### REFERENCES

1. Durelli, A. J., Dally, J. W., and Riley, W. F., Stress Concentration Factors Under Dynamic Loading Conditions, Armour Research Foundation. AFOSR-TN-58 892, 1958
2. Durelli, A. J. and Riley, W. F., Stress Distribution on the Boundary of a Circular Hole in a Large Plate During Passage of a Stress Pulse of Long Duration, ASME Paper No. 61-APM-4, 1961.
3. Yih-Hsing Pao, Dynamical Stress Concentration in an Elastic Plate, ASME Paper No. 61-APMW-17, 1961.
4. Christie, D. G., Reflection of Elastic Waves from a Free Boundary, Philosophical Magazine, vol 46, 1955, pp 527-541.
5. Clark, A. B. J., Static and Dynamic Calibration of a Photoelastic Model Material, CR-39, S.E.S.A. Proceedings, vol XIV, No 1, 1957
6. Gillich, William J., The Response of Bonded Wire Resistance Strain Gages to Large Amplitude Waves in Annealed Aluminum, Master's Essay, The Johns Hopkins University, 1960.

## DISCUSSION

Mr. W. Griffel, Picatinny Arsenal: Did you have a chance to study the effect of discontinuity?

Mr. Shea: No, up to this point we considered only the classical case of the central circular hole in the plate. We would like to extend it to other configurations, though.

Mr. Griffel: That would be really very interesting and useful too.

Mr. Shea: I think other configurations might have some very interesting implications.

Dr. Gay, BRL, APG: Are the springs behaving more elastically than visco-elastically? This is one of the perennial problems with dynamic stress analyses.

Mr. Shea: Well, let me only say that I wouldn't bank on it being completely elastic as opposed to the visco-elastic concept. But just looking at the pulse, etc., I have a feeling that it is a fairly elastic response. I think that this would be a very hard thing to prove anyway.

J. C. Hanson, Rock Island Arsenal: Did you have any trouble separating bending stresses at the surface from the force wave or the waves transmitted through the plastic? Was there any problem there?

Mr. Shea: No, if you remember we talked about the nominal gage field and at least we had two gages back to back. If there had been any bending which there shouldn't be since the bending is a somewhat slower phenomenon than the compression parts, we should have been able to pick it up here, but there was essentially no difference from one surface to the other.

J. C. Hanson: What kind of gages did you use?

Mr. Shea: These were Budd gages - 1/16 of an inch foil - I forget the exact designation right now.

Dr. Kumar: The gages that you used did of course have some kind of averaging effect - even though they were more or less 1/16 of an inch. Was this significant, do you think?

Mr. Shea: I don't think so because as I noted the wave length of the pulse in this material turns out to be almost 2 inches - 1.9 inches, and the gage itself is only 1/16 inch gage length which will integrate somewhat but really relatively little.

## THE DYNAMIC BEHAVIOR OF HYPERCRITICAL-SPEED SHAFTS

John E. Voorhees,\* C. C. Mellor, Jr.,\*\* and R. G. Dubensky\*\*\*

### ABSTRACT

In connection with the need for light weight components in military helicopters and STOL AND VTOL aircraft, a research program has been conducted by Battelle to determine the merits of hypercritical-speed power transmission shafts. For transmitting a given horsepower, torque and consequently shaft size and weight may be reduced as operating speed is increased. However, extremely large deflections and even destruction of the shaft and its bearings can result from operation at shaft critical speeds; for this reason designers of power transmission equipment normally avoid the problem by operating shafts below their first critical speed.

Experiment has shown that power transmission by shafts operating at speeds above their first critical is practical, since one or two dampers strategically located along the shaft have limited vibration very effectively. With just one damper, shafts have been operated at more than sixty times their first critical speed. With two dampers, operation at even higher speeds was observed, in one case reaching 159 times the first critical speed. Generally, best operation occurred with the damper or dampers positioned close to the ends of the transmission shafts.

A systematic procedure for the design of shaft dampers using an electrical analogy has been developed. The initial experimental verification of the design procedure showed excellent performance. Using this procedure in a given power transmission situation it is believed that a system of dampers can be designed to prohibit excessive and dangerous vibration amplitudes at the desired operating speeds.

\*John E. Voorhees, Director of Machine Dynamics Research, Batelle Memorial Institute, Columbus, Ohio.

\*\* C. C. Mellor, Jr., Research Engineer, Machine Dynamics Research, Batelle, Memorial Institute, Columbus, Ohio.

\*\*\* R. G. Dubensky, Research Engineer, Batelle Memorial Institute, Columbus, Ohio.

The design and analysis of high-speed shafting by electrical analogy adds understanding to the experimental program. The analogy shows, for instance, that broad tuning of the shaft system is quite dependent not only upon damping, but also upon the weight ratio of the damper to the shaft. The smaller the ratio, the wider is the acceptable speed range of shaft operation. Description of the mechanical shaft in terms applying to high-frequency electrical transmission lines opens the door to straightforward design of hypercritical-speed shafting, since the electrical theories are so highly developed.

Once a suitable high-speed shaft system has been designed, similar operation can be achieved with shafts of other dimensions and materials by applying modeling equations developed in the research program. Use of these equations can provide dynamically similar operation of dissimilar shafts by adjustment of damper parameters.

Application of torque to high-speed shafting has been studied both theoretically and experimentally. Although theory predicts a lowering of shaft critical speed, experiment has not shown this to be so. The application of torque has shown a tendency, however, to cause a "corkscrew" shape at torsional shear stresses near the yield point of the material. But neither the application of steady-state nor intermittently-applied torque has caused a change in lateral critical speed or vibration amplitude.

Theory and experiment have shown that critical speed varies with axial shaft-end loading. Tension on the shaft ends increases critical speed, and compression decreases it.

Experimental work has been conducted using shafts coated with damping materials in order to reduce vibration amplitude. An improvement was noted in shaft operation at the lower critical speeds. Operation was totally unsatisfactory, however, at higher speeds.

Compared with solid shafts, tubing has the ability to transmit the same degree of power but with higher critical speeds and with decreased shaft weight. The resulting decrease in weight would appear highly desirable in applications to aircraft. All of the research results are equally applicable to the design of solid and tubular shafts.

Research has shown that hypercritical-speed shafting, with its associated advantage in weight, is a very practical and feasible means of transmitting power. With today's high-speed power sources it is especially attractive, since considerable weight could be pared from engines and gearing by transmitting power at the same high speed as it is produced.

## INTRODUCTION

For any rotating shaft there exists a series of discrete speeds, called critical speeds, at which the centrifugal force resulting from unbalance causes progressively greater shaft deflection. The elastic restoring forces developed as the shaft deflects are overcome by the centrifugal force developed by the deflected shaft. Extremely large deflections and even destruction of the shaft and its bearings can result from operation at these speeds, and for this reason designers of power transmission equipment normally avoid the problem by operating shafts below their first critical speed.

There are, of course, disadvantages to restricting operation to below the first critical speed. For transmitting a given horsepower, torque and consequently shaft size must be increased as operating speed is reduced. In case of long shafts, the shaft size may be increased above that size required to transmit the torque simply to raise the first critical speed above the operating speed range. Alternatively, the shaft size may be determined by the torque loading, but additional bearings may be installed to support the shaft and thereby raise its first critical speed. On a relatively stiff shaft with closely spaced bearings, flexible couplings are often required at each bearing. The major disadvantage of these conventional design practices applied to aircraft is the weight penalty.

Recognition of the potential weight reductions achievable through the use of hypercritical-speed power transmission shafting has led the Air Force and the Army Transportation Corps to sponsor a research program at Battelle Institute to determine the feasibility of such shafts. The STOL and VTOL aircraft in which these shafts are ultimately to be applied require the transmission of high horsepower over distances of many feet by mechanical shafting. Significant weight savings in these aircraft will be accompanied by important gains in performance.

This technical paper is a progress report covering the most significant findings of the first year's research on hypercritical-speed shaft performance and design, during which the feasibility of these shafts has been convincingly demonstrated. The equipment used for experiments with reduced-scale power transmission shafts is discussed, along with a condensation of the most pertinent experimental results. Dynamic scaling relationships, by which full-scale shaft performance can be demonstrated through experiments with shaft models, are presented. A new method of hypercritical-speed shaft design based upon an electrical analog is described.

## EXPERIMENTAL PROGRAM

### Experimental High-Speed Shaft Machine

In order to obtain useful information concerning hypercritical-speed power transmission shaft operation it was necessary to design and build a shaft test machine. Since investigation of full-scale power transmission shafts would have involved excessive cost, it was decided at the outset of the program to conduct the research with reduced-scale shafts and to incorporate a modeling procedure to relate the information obtained to full-sized shafts.

Figure 1 is a schematic diagram of the machine. Essentially the machine consists of a straight bed to hold the spindle assemblies and the intermediate shaft support bearings, and an electronically-governed variable-speed drive to rotate the shafts. The bed is capable of accepting commercially available shafts 12 feet in length, and the spindles and intermediate support assemblies accept shaft diameters 1/2 inch and smaller. The support assemblies are designed to provide adjustment of damping and spring rate with the least possible difficulty. Intermediate supports and the brake-head spindle assembly can be moved and clamped to the bed at desired distances from the drive-head spindle assembly. Guards which limit shaft vibration amplitude can also be clamped at desired distances along the bed. The drive-head assembly rotates the shaft at various speeds, and is belt driven from the variable-speed drive mechanism. Also at the drive-head assembly is a stroboscope actuator which permits observation of the shaft by stroboscope either once or twice per shaft revolution.

The drive mechanism consists of two 7-1/2-horsepower motors powering two eddy-current clutches. This double assembly was adapted from a previous research program, and the fact that two motors and two clutches were used is not significant to this machine. The clutches transmit power to a common shaft. Power is transmitted by belt to a speed-change mechanism consisting of two pulley assemblies, and from there to the drive-head assembly. By varying clutch output speed and by changing speed ratio in the two pulley assemblies, drive-head spindle speed may be varied from zero to nearly 50,000 rpm with considerable horsepower available at the drive-head spindle. The highest speed achieved with an experimental shaft is 45,500 rpm.

Speed is regulated by controlling eddy-current clutch excitation. The control box, which mounts a direct-reading tachometer and a potentiometer to change shaft speed, may be carried by the operator to any

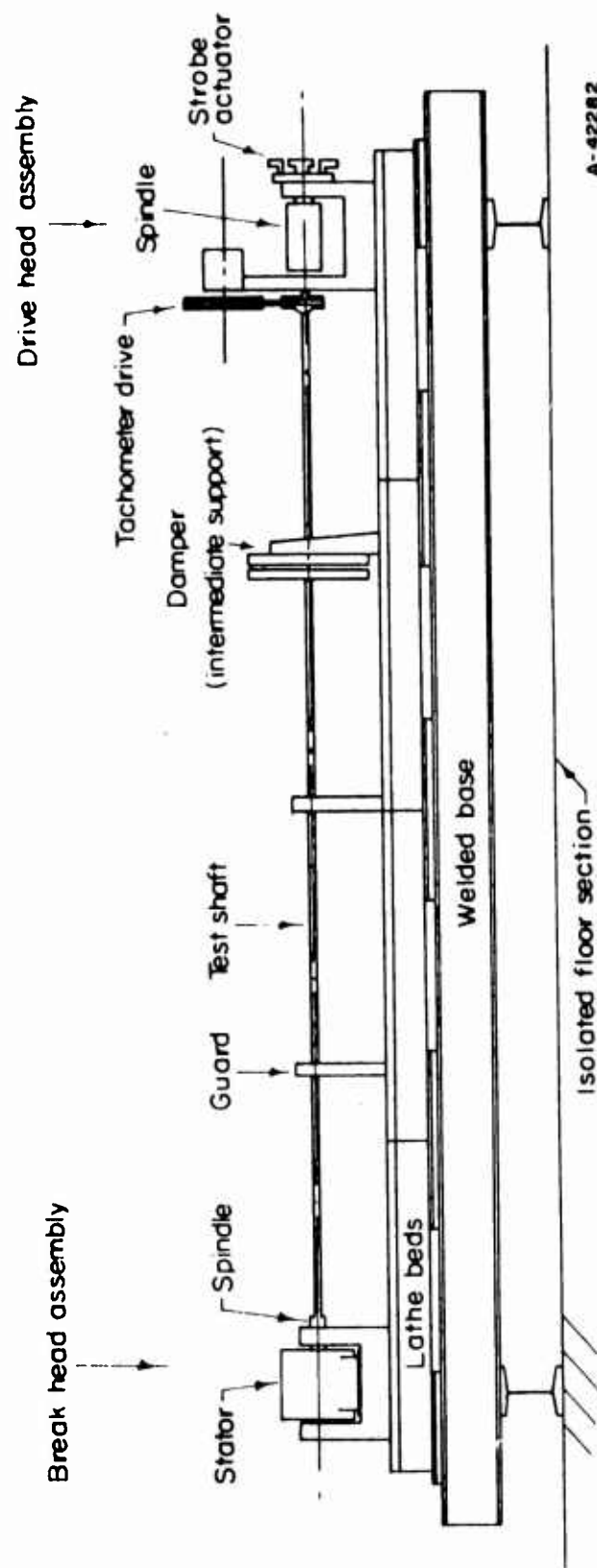


FIGURE 1. SCHEMATIC DIAGRAM OF TEST MACHINE BED AND EQUIPMENT



position along the test bed. Because of the varying power requirements of test shafts as they are brought up through critical speeds, an electronic speed governor is incorporated in the speed control system to maintain selected operating speeds with negligible drift.

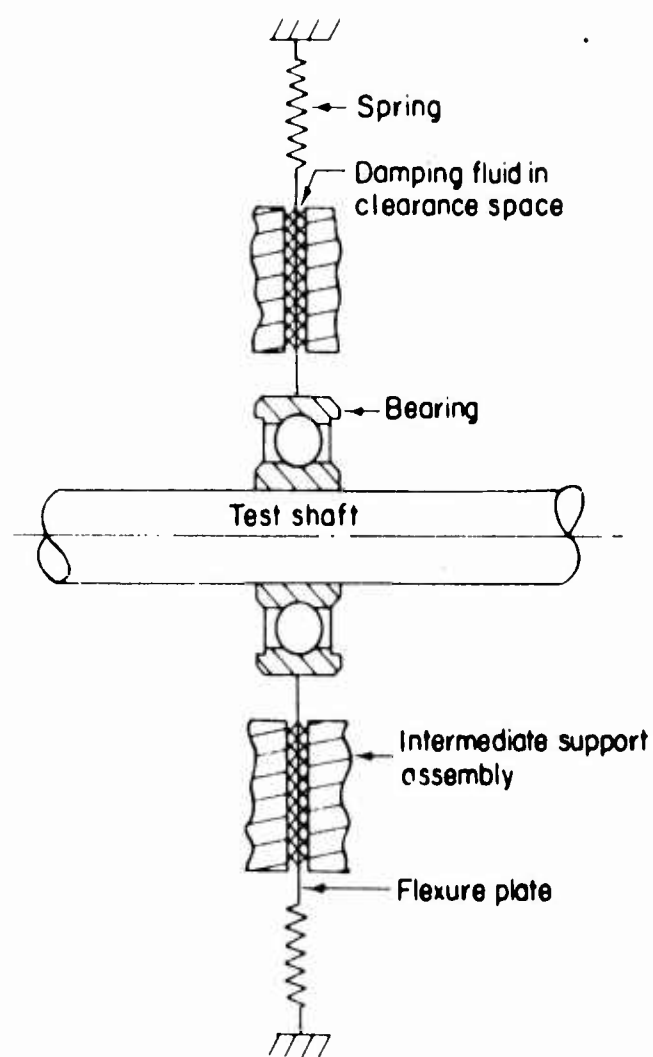
Figure 2 is a schematic diagram of the intermediate support bearing and damper assembly. The intermediate support consists of two heavy square plates, one of which is bolted to a lathe steady-rest. The plates are bolted together parallel to each other with ground spacers between them to provide the necessary oil film thickness for support damping. An 0.018-inch-thick flexure plate, which mounts the support bearing, is sandwiched between the heavy outer plates. By filling the gap between the outer plates and flexure plate with a damping fluid such as oil and clamping the test shaft in the support bearing bore, viscous damping forces are generated when the vibrating shaft causes the damper assembly to move laterally. The damping factor may be changed by inserting spacers of different thickness between the outer plates or by using damping fluid of different viscosity.

The flexure plate to which the support bearing is fastened is laterally supported at its four corners by four springs. Adjusting the lateral flexibility of the support can be done either by changing to springs of a different spring rate or by changing the point at which the springs are clamped.

Four circumferential slots have been cut in the flexure plate at a slightly larger diameter than the support bearing housing. The slots reduce the bending stiffness of the flexure plate to minimize its effect on shaft behavior. Tests show that the intermediate support does not act strictly as a simple support, but has some moment absorbing ability. The initial angular motion of the bearing is practically free from moment restraint due to the built-in radial clearance in the Barden support bearings. After the free motion is taken up in the bearing, moment restraint increases due to bending of the flexure plate.

### Experimental Results

Numerous experiments conducted upon the high-speed shaft test machine have shown that transmission shafts can be operated dependably at and above their first critical speeds. Although most tests were conducted with a standard steel shaft size of 1/4-inch-diameter and 89.3 inches long, the modeling procedure developed during the research program permits similar operation to be obtained with any other shaft diameter and length.



A-42283

FIGURE 2. SCHEMATIC DIAGRAM OF INTERMEDIATE SUPPORT DAMPER

In each test series the intermediate support or supports were adjusted to provide a certain value of lateral spring rate and damping. Then, for each discrete location of the intermediate support, shaft speed was increased through a rather wide range while vibration behavior was noted. The support was repositioned along the shaft in small steps in order to furnish a continuous plot of shaft vibration control with respect to damper location.

Figure 3 is a graph of the most successful single intermediate support test results, with shaft speed plotted against damper location. For each support location an upper and lower limiting speed was observed at which shaft vibration amplitude equaled or exceeded  $3/8$  inch peak-to-peak. Between the two limiting speeds there occurred a speed range in which shaft vibrations were well controlled, with amplitudes less than  $3/8$  inch peak-to-peak. The limiting speeds for each support location form an envelope which describes satisfactory shaft operating speeds with respect to support location along the shaft. All of the single support test series showed the best operating speed range to be obtained with the support located toward a shaft end.

Referring again to Figure 3, with the support located at 5.05 per cent of shaft length from one end, vibration control was satisfactory from zero speed to 22,000 rpm. This corresponds approximately to the twelfth critical speed of an unsupported shaft. Moving the support to 3.36 per cent of shaft length from one end increased the satisfactory top speed to 26,000 rpm, but with diminished low speed vibration control. Support spring constant and damping factor in this test series were  $K = 11.6$  pounds per inch and  $C = 1.736$  pound-second per inch.

In the two-support tests highest speed operation was again attained with supports located toward each shaft end. However, during some tests vibration was so violent that in two cases shafts were bent. More dependable operation was obtained with one support close to a shaft end and the other near mid-span as indicated in Figure 4. A noteworthy feature of this arrangement is that vibration amplitude control is not particularly sensitive to location of the center support. With one support located at 3.36 per cent of shaft length and the other positioned between 42 and 49 per cent from the other shaft end, double amplitudes were limited to less than  $1/4$  inch from approximately 2000 to 25,000 rpm. Damping values and spring rates were the same as used in the best single-support test:  $K = 11.6$  pounds per inch and  $C = 1.736$  pound-second per inch.

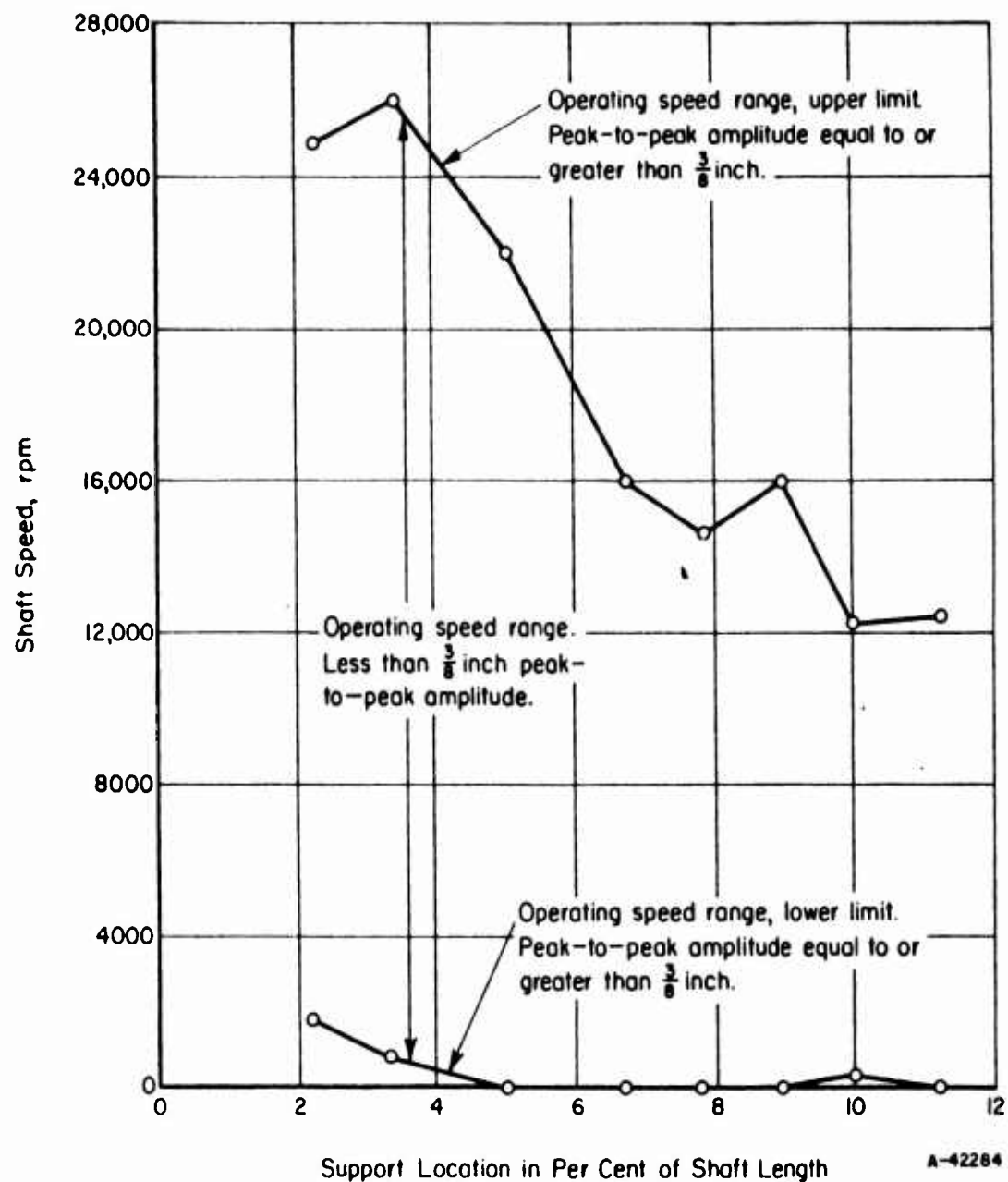


FIGURE 3. SHAFT SPEED VERSUS SINGLE DAMPED SUPPORT LOCATION FOR A 1/4-INCH DIAMETER, 89.3-INCH LONG STEEL SHAFT WITH CLAMPED ENDS

Support Characteristics:  $K = 11.6 \text{ lb/in}$ ;  $C = 1.736 \text{ lb-sec/in}$ .

Another two-support test conducted with the same support flexibility,  $K$ , but with 43 per cent as much damping showed the similar trend of best attainable operating speed range with dampers set close to each end. However, the highest operating speed was just 17,500 rpm. The conclusion to be reached here is that the damping was not sufficiently high to provide best operation.

Tests with three supports showed decreasing ability to control vibration at high speeds. All, however, controlled low-speed amplitudes well enough. In experiments completed to date, much more successful high-speed shaft operation has been achieved with one or two damped supports than with three.

#### DYNAMIC SCALING PROCEDURE

The relationships between shaft and support parameters for similar dynamic behavior were demonstrated during the research program. By applying these relationships to determine the appropriate support characteristics, shafts of dissimilar dimensions and materials will have dynamically similar behavior. For instance, a 1/4-inch-diameter, 89.3-inch-long steel shaft has been run dependably to the twelfth critical speed using a single damped intermediate support. With the proper adjustment of the support, shaft of any other size and material could be run dependably to its twelfth critical speed.

The relations which define dynamically similar shaft behavior are shown below. The numerical subscripts refer to each separate shaft system.

$$\frac{W_1}{W_{s1}} = \frac{W_2}{W_{s2}}$$

$$\frac{K_1}{K_{s1}} = \frac{K_2}{K_{s2}}$$

$$\frac{C_1}{C_{s1}} = \frac{C_2}{C_{s2}}$$

$$X_1 = X_2$$

where

$W$  = support bearing weight, lb.

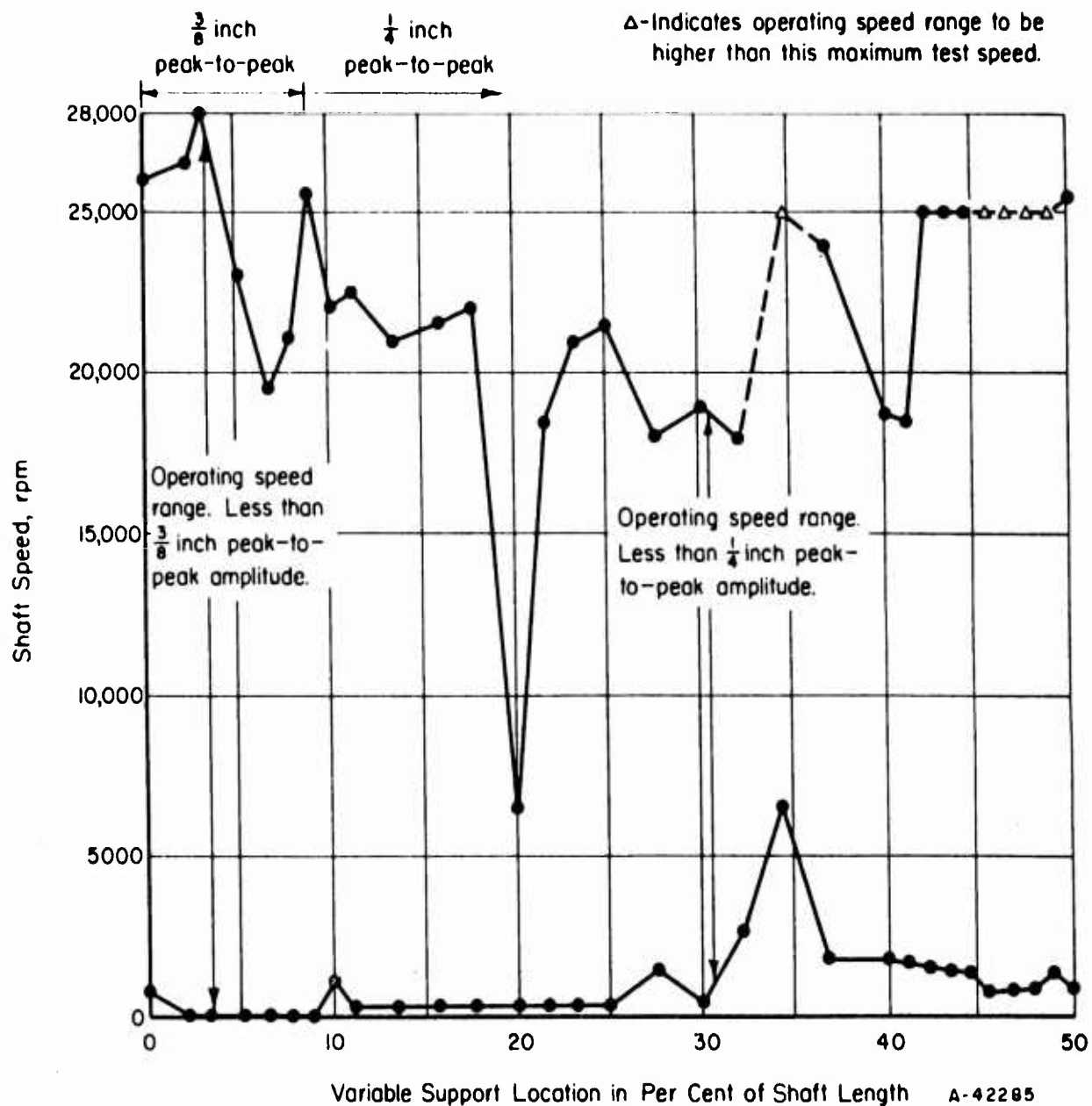


FIGURE 4. SHAFT SPEED VERSUS SUPPORT LOCATION

One support fixed at 3.36 per cent from one end,  
 other support varied from other end toward shaft  
 mid-point. 1/4-inch diameter steel shaft 89.3  
 inches long with clamped ends.  $K = 11.6$  lb/in,  
 $C = 1.736$  lb-sec/in.

K = support spring rate,  $\frac{\text{lb}}{\text{in.}}$

C = support damping coefficient,  $\frac{\text{lb-sec}}{\text{in.}}$

X = location of support from shaft end with respect to over-all shaft length

$W_s$  = shaft weight, lb.

$K_s$  = characteristic shaft lateral stiffness, measured at center of shaft span,  $\frac{\text{lb}}{\text{in.}}$

$C_s$  = characteristic shaft critical damping value,  $\frac{\text{lb-sec}}{\text{in.}}$

$$C_s = 2\sqrt{\frac{W_s K_s}{g}}$$

When the parameters of two high-speed shaft systems are related in the above manner the dynamic behavior of the shafts will be similar. These relationships permit the extrapolation of design data from successful small-scale tests to large-scale shaft applications. The relationships established for scaling purposes are totally compatible with the design by electrical analogy.

#### HIGH-SPEED SHAFTING DESIGN BY ELECTRICAL ANALOGY

Conventional methods of analysis of high-speed shaft behavior have been used with considerable success in the digital computer analyses conducted throughout this research program. Although the conventional analysis procedures permit accurate calculation of critical speeds and shaft deflections, they are somewhat cumbersome as aids to high-speed shafting design. An analytical approach to high-speed shafting design was therefore sought which would provide more insight into the manner in which shaft vibration is related to the dynamic parameters of the shaft and its intermediate support bearings.

The general arrangement of the high-speed shafts and their supports studied in this program is shown in Figure 5-a. As indicated in the figure the ends of the shafts were rigidly supported in the spindles of the testing machine. For the purposes of developing a suitable analogy this shaft configuration was considered equivalent to the configuration shown in Figure 5-b, where the rigidly clamped shaft ends are replaced by a spring-

mass combination. To justify this change the following reasoning was employed: For each critical speed of the fixed-ended shaft a shorter shaft having simply-supported ends can be found which has the same critical speed. The fixed-ended shaft is therefore considered equivalent to a simply-supported shaft joined at each end to a short cantilever beam. The springs and masses shown in Figure 5-b attached to the ends of the shafts are equivalent to the effective masses and spring rates of the short cantilevered ends of the shaft in Figure 5-a.

The mechanical system shown in Figure 5-b is considered equivalent to the electrical system shown in Figure 5-c for the purposes of establishing an analogy to electrical transmission lines. In Figure 5-c the spring-mass combination representing the fixed ends of the shaft has been replaced by a capacitance and inductance combination. At an equivalent distance in vibration wave lengths down the transmission line from the end, a combination of capacitance, resistance, and inductance is placed in series with the line to represent the dynamic characteristics of the shaft support bearing. Each additional shaft support bearing is replaced by its analogous resistance, capacitance, and inductance at the correct distance in wave lengths from the end of the transmission line. It should be noted here that for purposes of wave length measurements along the line, the end of the mechanical shaft is considered to lie at the juncture between the equivalent simple beam and the equivalent cantilever as shown in Figure 5-a.

For efficient energy transfer in high-frequency electrical transmission lines the load on the transmission line is designed to appear purely resistive at the operating frequency, and to have a resistance value equal to the characteristic impedance of the transmission line. In the case of the high-speed shaft the load to which vibratory energy is to be delivered is the damper located at the intermediate support bearing. One, two, or more intermediate support bearings may be used.

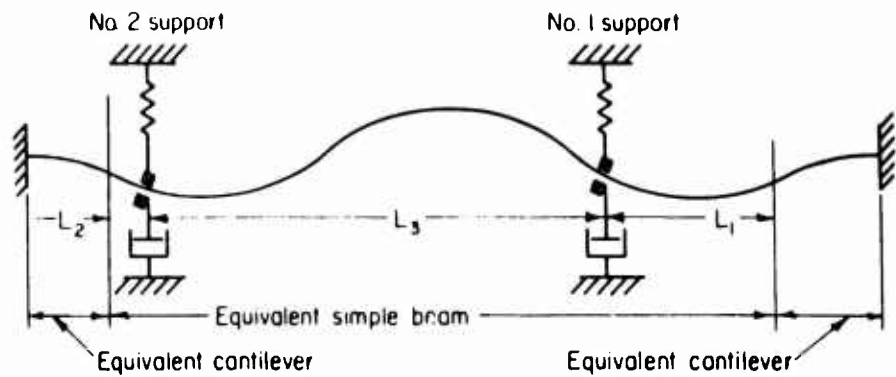
In order to determine the impedance matching ability of intermediate supports on a vibrating shaft, certain relationships between mechanical and electrical quantities were developed. The characteristic impedance of the vibrating shaft at any critical speed has been determined to be:

$$Z_c = D^2 (Df)^{1/2},$$

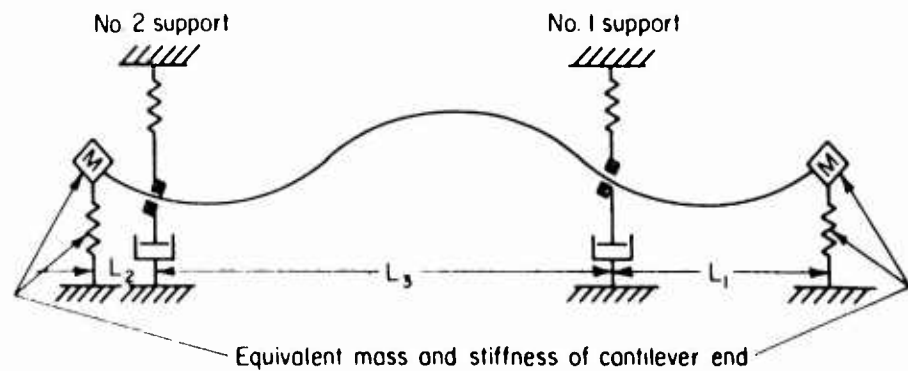
where

D = solid steel transmission shaft diameter, in.

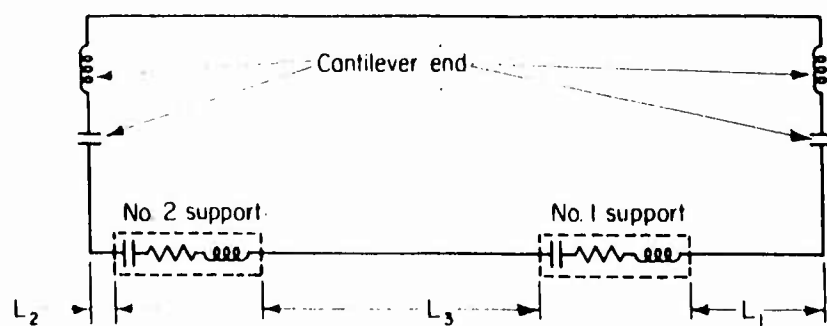




a. General Arrangement of High-Speed Shafts Studied



b. Equivalent Mechanical Representation of High-Speed Shafts



c. Electrical Analogy of High-Speed Shafts

A-42286

FIGURE 5. DEVELOPMENT OF AN ANALOGY BETWEEN A HIGH-SPEED SHAFT AND AN ELECTRICAL TRANSMISSION LINE

$f$  = lateral critical speed,  $\frac{\text{rev}}{\text{sec}}$

$Z_c$  = characteristic impedance,  $\frac{\text{lb-sec}}{\text{in.}}$

The reactance at the shaft end is the sum of the reactive components of the equivalent cantilever mass and spring rate:

$$X_c = \frac{-jK_c}{2\pi f} + j2\pi f M_c$$

where

$X_c$  = reactance at shaft end,  $\frac{\text{lb-sec}}{\text{in.}}$

$K_c$  = spring rate measured at the end of cantilever,  $\frac{\text{lb}}{\text{in.}}$

$M_c$  = concentrated equivalent mass at the end of cantilever,  $\frac{\text{lb-sec}^2}{\text{in.}}$

$f$  = critical speed being examined,  $\frac{\text{rev}}{\text{sec}}$

$j = -1$

The reactance of the intermediate support is given as:

$$X_n = \frac{-jK}{2\pi f} + j2\pi f M$$

where

$X_n$  = reactance at support bearing,  $\frac{\text{lb-sec}}{\text{in.}}$

$K$  = support spring rate,  $\frac{\text{lb}}{\text{in.}}$

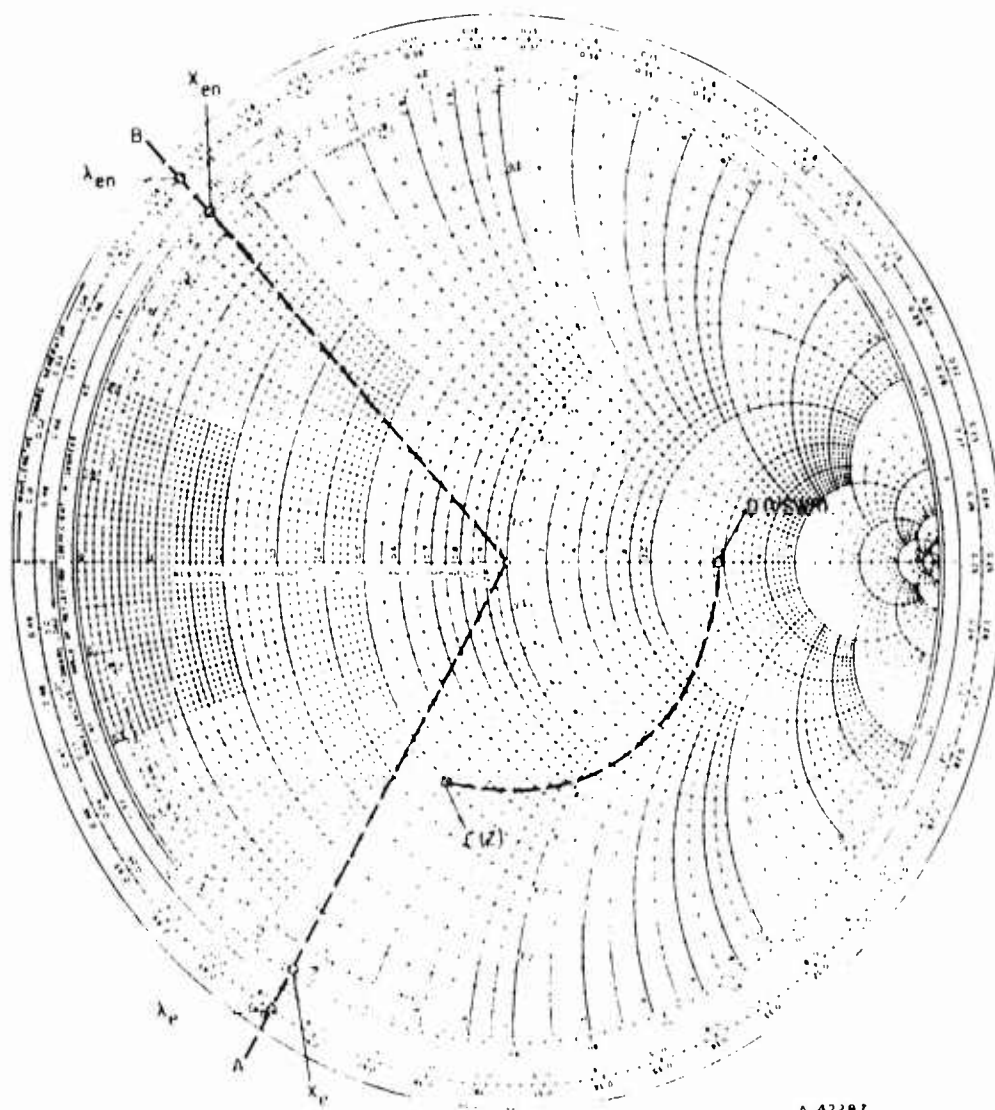
$M$  = support bearing mass,  $\frac{\text{lb-sec}^2}{\text{in.}}$

The reactance,  $X_{en}$ , of the equivalent cantilever viewed from the support is found by a different method; by use of the Smith Chart which is shown in Figure 6. The Smith Chart is a complex plot of load impedance on a transmission line as seen from various points along the line. In addition, the Smith Chart indicates a value of voltage standing wave ratio (VSWR) for each value of load impedance. To make use of the Smith Chart all reactance values, such as  $X_c$  and  $X_n$ , must be "normalized" by dividing by the characteristic shaft impedance  $Z_c$ .

The procedure for using the Smith Chart for calculations of high-speed shaft performance is as follows:

- (1) After the reactance at the shaft end,  $X_e$ , is calculated, it may be located on the Smith Chart. Radial line A in Figure 6 passes through a typical value of  $X_e$  as indicated.
- (2) A reference location on the wave length circle, at  $\lambda_e$ , is also identified by line A.
- (3) The distance in wave lengths from the reactance at the shaft end to the intermediate support bearing is next determined. This number of wave lengths is then added to  $\lambda_e$ , giving  $\lambda_{en}$ , and radial line A is rotated clockwise to the position of radial line B which passes through  $\lambda_{en}$  on Figure 6. It should be noted that one full revolution around the chart corresponds to a distance of one-half wave length along the shaft.
- (4) The value  $X_{en}$  identified by radial line B in Figure 6 is the reactance of the shaft end restraint as seen from the location of the support bearing.
- (5) To the value of  $X_{en}$  is added the previously calculated value of  $X_n$ , plus the normalized resistive component of impedance at the support bearing representing the damper. This total impedance value at the support bearing,  $Z$ , is then located on the Smith Chart, as at point C in Figure 6.
- (6) On the Smith Chart an arc can then be drawn from point C to the righthand section of the horizontal centerline, at point D in Figure 6. Point D gives the value of voltage standing wave ratio (VSWR) for an electrical transmission line. This quantity expresses the relative severity of vibration on the high speed shaft. The optimum value of VSWR is one, indicating no standing waves.

When the above procedure is followed in designing a damped support for a high-speed shaft, it is possible to select values of the support spring rate, mass, damping, and location, so that  $X_{en} + X_n = 0$ , and the resistive component contributed by support damping equals  $Z_c$ , at any one selected critical speed. This produces a VSWR of one at that critical speed, and produces minimum shaft vibration. The VSWR can



A-42287

FIGURE 6. SMITH CHART FOR ELECTRICAL TRANSMISSION LINE CALCULATIONS

then be calculated by the above procedure at other critical speeds to judge the degree of shaft vibration to be expected. The limited work completed to date has not established limiting values of VSWR, although values under ten appear to be satisfactory with the commercial quality shafting being used in experiments.

In the limited time which remained in the research program following development of the electrical analogy an experiment was conducted to demonstrate the validity of the procedure. A steel shaft 1/2 inch in diameter and 138 inches long was equipped with two damped support bearings. One of these damped support bearings was designed by arbitrary choice to provide correct impedance matching at the sixth critical speed. Table 1 lists values calculated for the VSWR at the first nine critical speeds with one damper provided.

TABLE 1. VALUES OF VSWR PREDICTED FOR SHAFT OPERATION WITH ONE DAMPED SUPPORT BEARING AT THE CRITICAL SPEED INDICATED, FOR EXPERIMENTAL SHAFT 138 INCHES LONG AND 1/2 INCH IN DIAMETER

Critical Speed	1st	2nd	3rd	4th	5th	6th	7th	8th	9th
VSWR for support optimized for sixth critical	29.	4.5	2.0	19.	3.8	1.0	2.4	8.5	33.
VSWR for support optimized for fourth critical	3.0	---	---	1.0	--	--	--	5.9	80.

The table shows high values of VSWR at the 1st, 4th, and 9th critical speeds when the support is optimized for the 6th critical. It was therefore decided to add a second damped support bearing designed for optimum performance at the 4th critical speed. Values of VSWR were then calculated for operation with the second bearing alone, at the 1st, 8th, and 9th critical speeds. Obviously the second bearing gives a low VSWR at the speed for which it was designed, but it was also effective in lowering the VSWR at the 1st and the 8th critical speeds. At the ninth, however, a high value of VSWR was obtained.

Experimental operation of the shaft fully confirmed the predictions of performance. Very smooth, vibration-free running was obtained at

speeds up to 11,000 rpm. The predicted 9th critical speed was 11,300 rpm. A noisy vibration developed at the 9th critical speed, but it was possible to operate at and to exceed this speed without damage to the shaft or the machine. As speed was increased noise was detected at several discrete speeds, but successful shaft operation was achieved up to 45,500 rpm, the top speed that the test machine could reach, limited by belt slippage. This speed is between the 18th and 19th critical speeds of the shaft tested.

Work planned for the future in regard to high speed shafting design by electrical analogy includes:

- (1) A more comprehensive experimental verification of the design procedure already established.

- (2) Additional analysis and experimentation regarding the effect of shaft end restraints.

- (3) Establishment of optimum design procedures for one and two damped support bearings for shaft operation over a wide speed range.

- (4) Determination of safe allowable values of VSWR relative to initial shaft crookedness.

With the data obtained from the planned future work it is expected that a straight-forward design procedure will be established which will permit prediction with good accuracy of the satisfactory operating speed range of hypercritical speed power transmission shafts.

#### OTHER RESEARCH AREAS

Application of torque to high-speed shafting has been studied both theoretically and experimentally. Although theory predicts a lowering of shaft critical speed as torque is applied, experiment has not shown this to be so. The application of torque has shown a tendency, however, to cause a "corkscrew" shape in the shaft at torsional shear stresses near the yield point of the material. But neither the application of steady-state nor intermittently applied torque has caused a change in lateral critical speed or vibration amplitude. Additional experimental work is planned to confirm these findings.

Theory and experiment have both shown that critical speed varies with axial shaft-end loading. Tension on the shaft ends increases critical speed, and compression decreases it. Additional work will be conducted to relate axial load and critical speed in a quantitative manner.

Experimental work has been conducted using shafts coated with damping materials. An improvement was noted in shaft operation at the lower critical speeds. Operation was totally unsatisfactory, however, at higher speeds. This behavior results from the fact that the shaft does not flex repeatedly when running at a critical speed, hence little energy is dissipated in the coating.

### CONCLUSIONS

In the past year, research conducted with high-speed power transmission shafts has produced significant results. The major conclusions to be drawn are:

- (1) Power transmission by shafts operating at speeds above their first critical is practical, since one or two dampers strategically located along the shaft have been shown to limit vibration very effectively.
- (2) A systematic procedure for the design of shaft dampers using an electrical analogy has been developed. The initial experimental verification of the design procedure showed excellent performance. Using this procedure in a given power transmission situation it is believed that a system of dampers can be designed to prohibit excessive and dangerous vibration of any shaft at the desired operating speeds. Added experimental verification of this design procedure is planned.
- (3) Once a suitable high-speed shaft system has been designed and demonstrated, similar operation can be achieved with shafts of other dimensions and materials by applying modeling equations developed in this program. Use of these equations can provide dynamically similar operation of dissimilar shafts by adjustment of damper parameters.

In short, hypercritical-speed shafting, with its associated advantage in weight, is a very practical and feasible means of transmitting power. With today's high-speed power sources it is especially attractive, since considerable weight can be pared from shafts, bearings, and gearing by transmitting power at the same speed as it is produced.

## DYNAMIC RESPONSE OF MILITARY BRIDGES

W. G. Corley, 1st Lt., CE \*

### ABSTRACT

This paper presents the results of dynamic loading tests on three full-size bridge structures tested at the U. S. Army Engineer Research and Development Laboratories. These structures include two steel I-beam bridges with 78-ft spans and an aluminum truss bridge with a 105-ft span. Dynamic loads were simulated by vibrating the bridges at their natural frequencies.

Stresses obtained from measured strains and periods of vibration are compared with those computed for each structure. In each case, computed stresses were within 0.5 ksi of those measured. The observed period of vibration for each bridge was in good agreement with the computed value.

The observed fatigue behavior of each of the three structures was compared with that which would be predicted from laboratory tests on small specimens of steel and aluminum. Laboratory tests indicate that the steel I-beam structures should withstand more than two million cycles of the applied stress. Thus, the lack of failure of the test structures is in agreement with the predicted behavior. Although the aluminum truss structure failed at a slightly lower number of cycles than would be predicted by tests on smaller specimens, the difference was within the limits of error of the data obtained from the laboratory tests. In general, the behavior of each of the three structures was in agreement with that predicted.

### 1. INTRODUCTION

#### 1.1 Object

The safety factors normally used in civilian bridge design limit the allowable stresses to a point where fatigue is seldom a controlling factor.

---

\* 1st Lieutenant William Gene Corley, Project Engineer, Bridge Branch, Bridge and Marine Group, USAERDL, Fort Belvoir, Virginia



The development of lightweight transportable bridges to meet the modern Army's demands for increased mobility has necessitated the use of high strength material and high allowable stresses, i.e., 80% of yield strength. Thus the stress range in a military bridge is much larger than the stress range found in a civilian type bridge. Since fatigue is influenced both by the number of load repetitions and the range over which the stress is expected to vary, the possibility of fatigue failures in military bridges is increased and must be investigated during design.

Although a large amount of data is available on the fatigue behavior of structural grade steel and a few of the more common aluminum alloys, relatively little is available on recently developed high strength steels and aluminum alloys. In addition, there are very few tests reported which correlate the behavior of small laboratory specimens with that of actual structures.

In this paper, the results of dynamic loading tests on three full-size structures are reported. Measured strains and periods of vibration are compared with those computed for each structure. In addition, the fatigue life of each bridge is compared with that which would be predicted from laboratory tests on small specimens of steel and aluminum.

## 1.2 Scope

The tests reported in this paper were carried out on two steel I-beam bridges with 78-ft spans and one aluminum truss bridge with a 105-ft span. All tests were carried out at the U. S. Army Engineer Research and Development Laboratories, Fort Belvoir, Virginia. The I-beam bridges consisted of two pair of 40-ft beams connected with bolted joints at the centerline of the span. The aluminum truss span was made up of two parallel trusses each of which contained seven 15-ft panels. The panels were joined by means of removable steel pins. Aluminum alloy 2014-T6 was used to fabricate the truss panels.

## 2. DESCRIPTION OF TESTS

### 2.1 General

Any elastic system can be forced to oscillate at its natural frequency by the application of an external alternating force with the same frequency. In an ideal system with no damping, the amplitude of vibration would increase without limit regardless of the magnitude of the applied force. In a system with damping, the amplitude of vibration will remain a finite

value if the externally applied energy does not exceed that which is dissipated through damping. Thus, in a real system, where damping is always present, any desired amplitude may be obtained by applying the proper amount of input energy.

For computing the natural frequencies of the test structures reported in this paper, each of the three structures has been idealized by assuming that it consists of a uniform elastic beam with a concentrated mass at mid-span. The differential equation for a vibrating beam of uniform stiffness is given by the expression:

$$EI \frac{\partial^4 y}{\partial x^4} + \mu_1 \frac{\partial^2 y}{\partial t^2} \quad (I)$$

where

- E = modulus of elasticity
- I = moment of inertia of the beam
- y = lateral deflection of the beam
- x = horizontal displacement
- t = time
- $\mu_1$  = mass per unit length

A solution to Equation (I) can be obtained by Rayleigh's method (1, 2). If the deflected shape is assumed to be half a sine wave, the fundamental period of vibration is given by the expression:

$$T = \frac{L}{\pi} \sqrt{\frac{2 [0.5w + W]}{3 EIG}} \quad (II)$$

where

- T = period of vibration in seconds per cycle
- L = span in inches
- w = weight of bridge in pounds
- W = weight of concentrated load in pounds
- G = acceleration of gravity in feet per second per second

Although there are some differences between the test structures and the assumptions on which Eq. II is based, these differences are of minor importance. In general, Eq. II can be used to compute the fundamental period of vibration for each of the test structures reported in this paper.

## 2. 2 Test Structures

Tests on three bridge structures are reported in this paper. These include one 105-foot, single-truss span of the Bridge, Fixed, Aluminum,

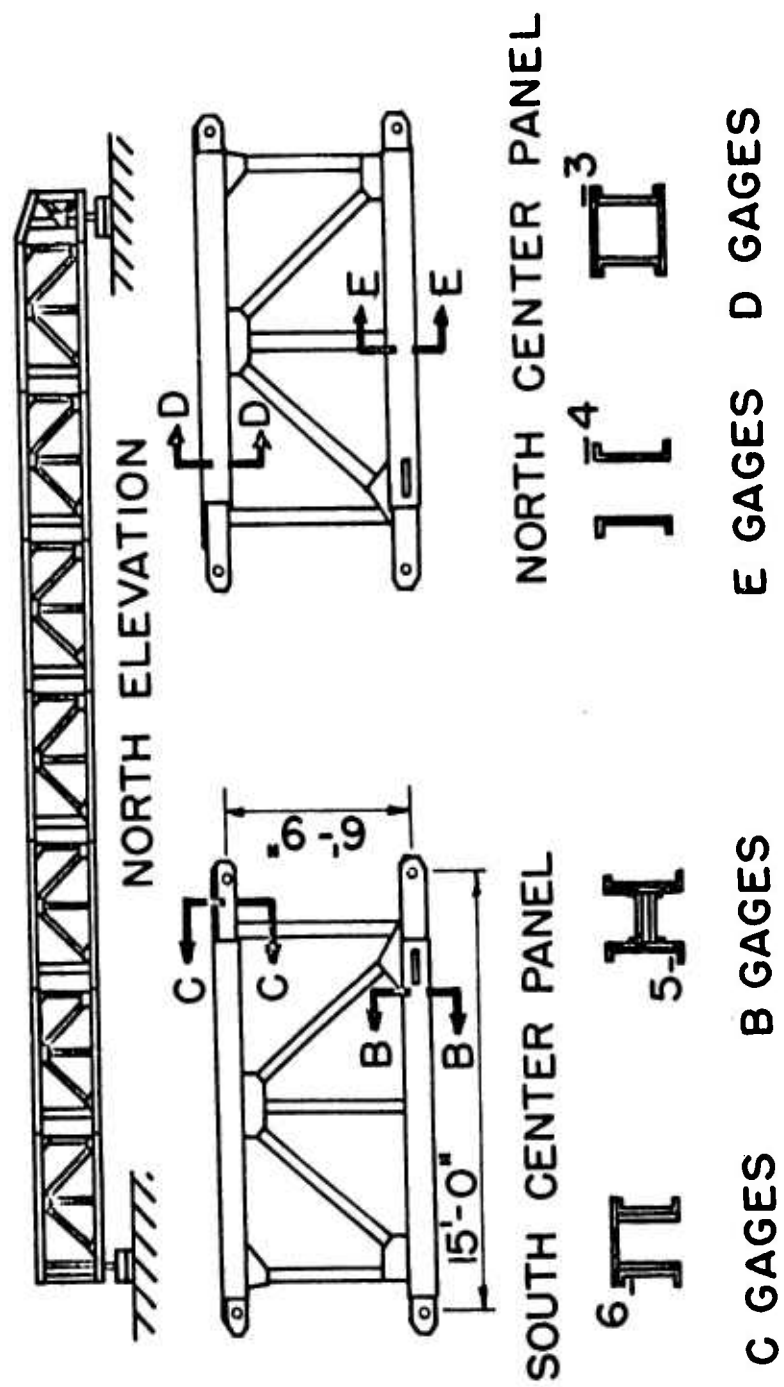
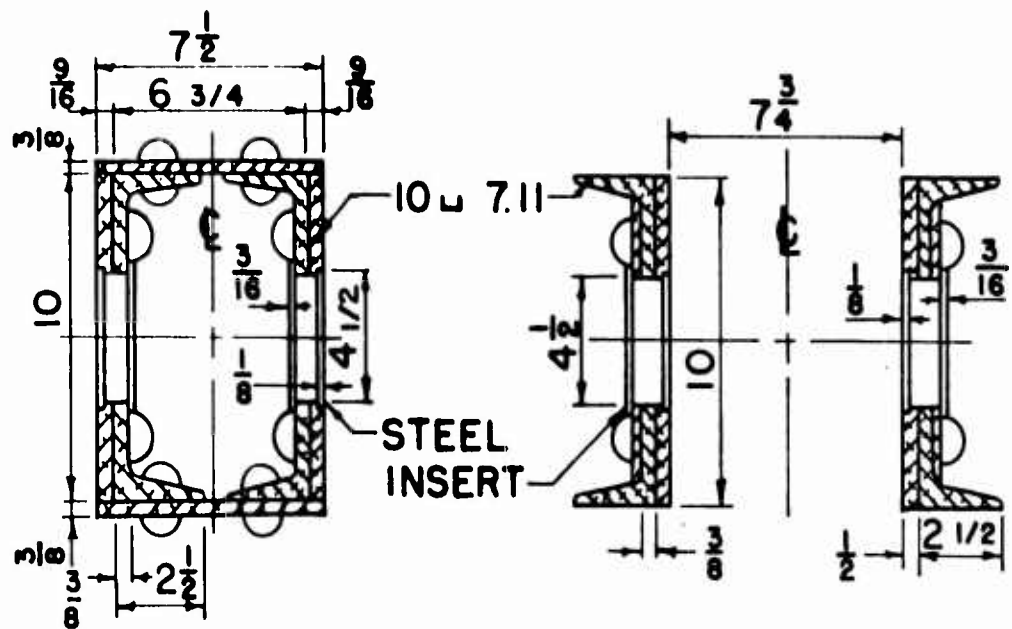
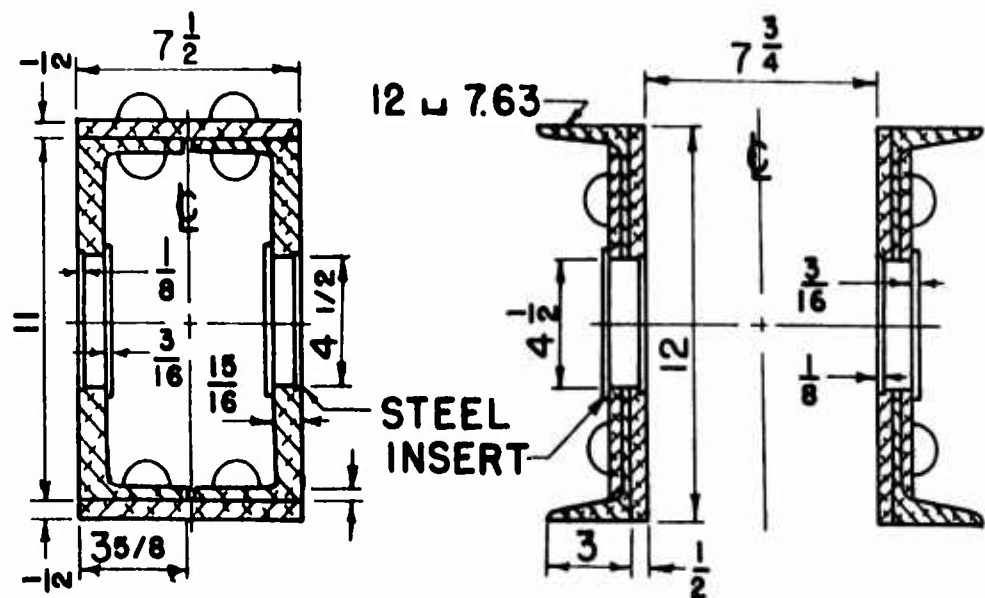


Fig. 1 Layout and Dimensions of T-6 Aluminum Bridge



UPPER MALE JOINT

UPPER FEMALE JOINT



LOWER MALE JOINT

LOWER FEMALE JOINT

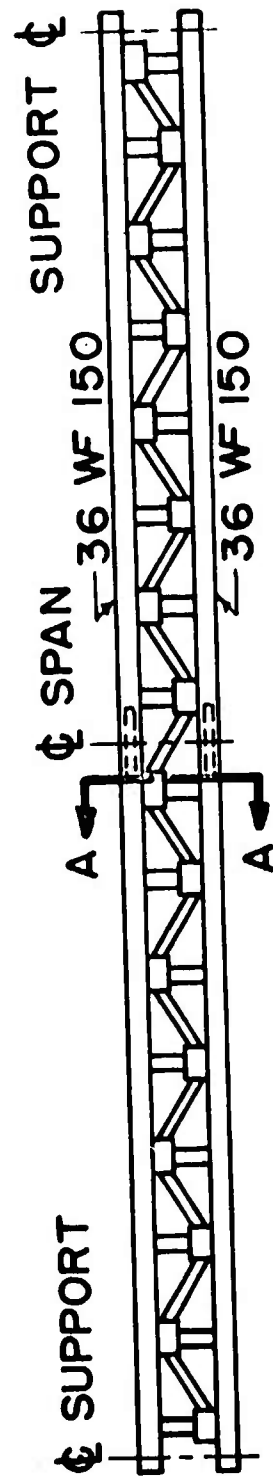
Fig. 2 Details of Joints of T-6 Aluminum Bridge

TABLE I  
TYPICAL MINIMUM SPECIFIED MECHANICAL PROPERTIES OF ALUMINUM ALLOY 2014-T6

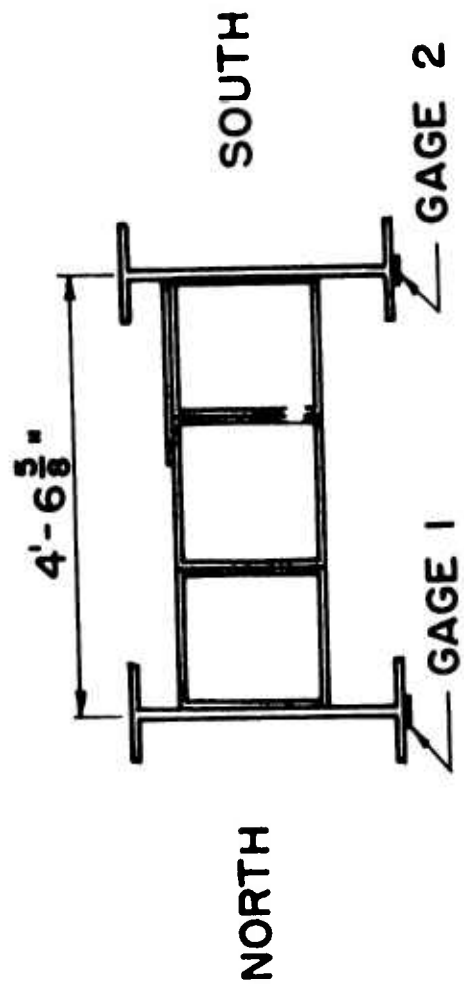
	Tension			Compression		Bearing	
	Ultimate Strength ksi	Yield Strength ksi	Elongation % in 2 in.	Yield Strength ksi	Ultimate Strength ksi	Yield Strength ksi	
Extrusions	60	53	7	55	114	85	
Alclad Plate	64	57	8	58	124	93	

TABLE II  
PHYSICAL CONSTANTS AND DIMENSIONS FOR TEST STRUCTURES

Structure	Length ft	Moment of Inertia (in) <sup>4</sup>	Modulus of Elasticity lb/in <sup>2</sup> x10 <sup>6</sup>	Total Weight of Structure lbs
T-6	105	113,700	10.6	53,600
36 WF 150	78	18,024	30	31,600



PLAN VIEW



SECTION AA

Fig. 3 Layout and Dimensions of 36 WF Structures

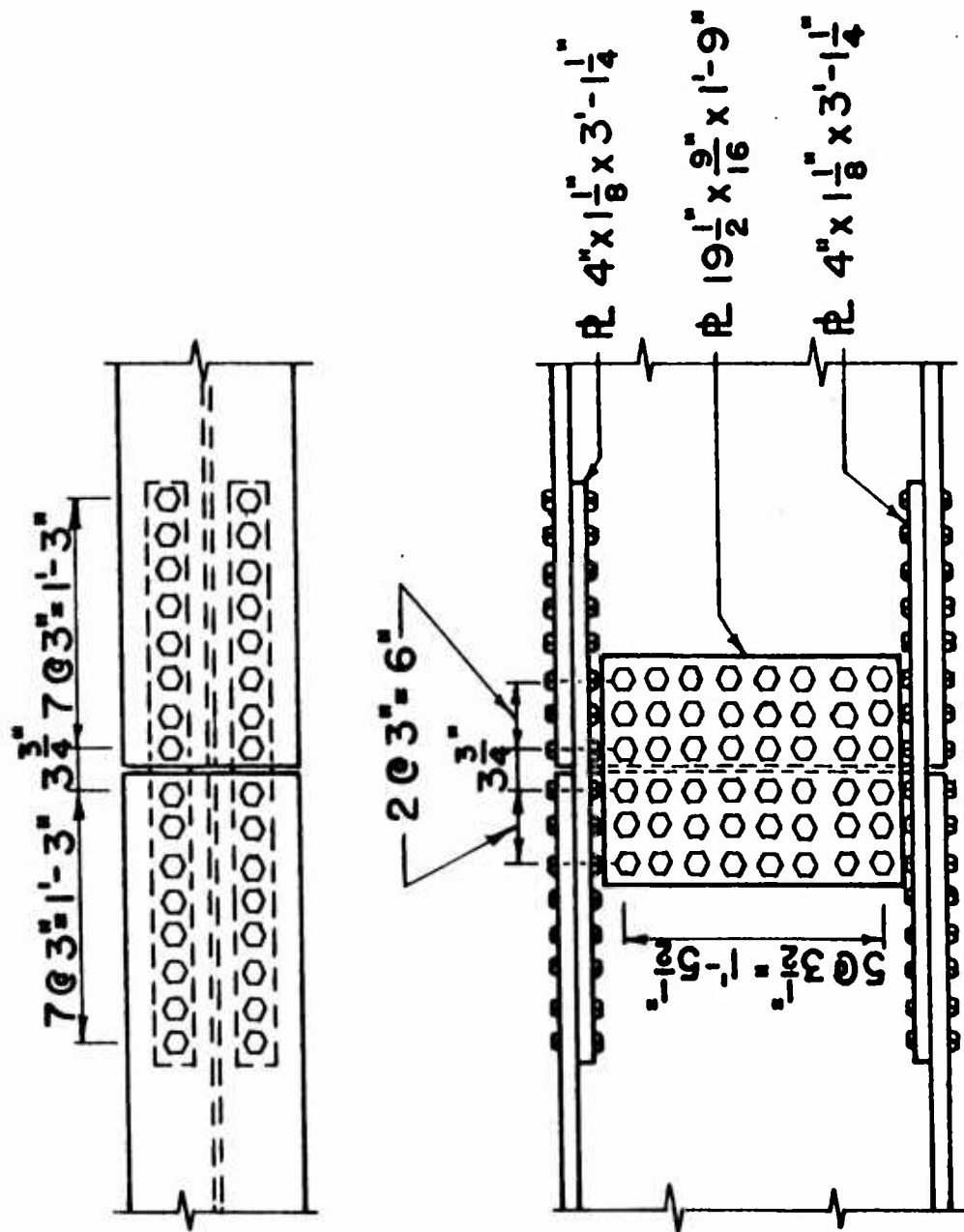


Fig. 4 Details of Bolted Joints



Single-Lane, Highway, Pony Truss Portable Panel (referred to hereafter as the T-6 Bridge) and two 78-foot simple-span bridges fabricated from standard 36 WF 150 structural steel beams with bolted joints at the centerline of the span.

The T-6 bridge is of riveted construction and is designed for rapid field assembly. All field connections are made by means of removable steel pins. Each truss panel is 15 feet long and 6 feet 9 inches high from center to center of pins. In the test bridge, each of the two trusses was made up of seven interior panels and one end panel. The distance between truss centerlines was 16 feet 11 inches and the clear roadway width was 13 feet 6-1/2 inches. Figure 1 shows the layout of the test bridge and the panel dimensions. The joints for connecting the panels consist of built-up aluminum sections with steel inserts in the pin holes. Details of these joints are shown in Fig. 2.

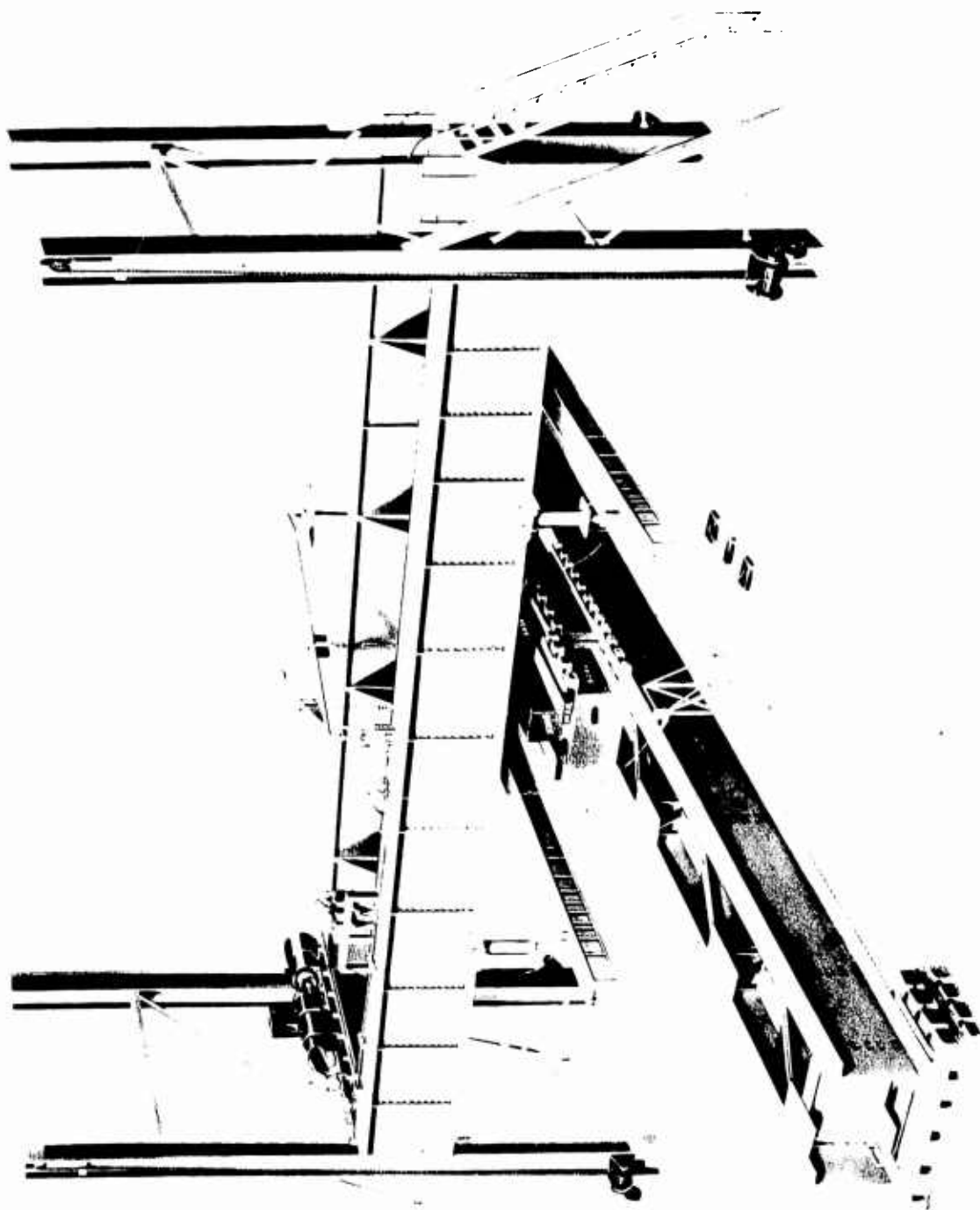
The T-6 bridge is fabricated of aluminum alloy 2014-T6 extrusions and alclad plates. Table I shows typical minimum specified mechanical properties of this material for the sizes used. Pertinent dimensions and physical constants for the test structure are shown in Table II.

Additional mass was added at the centerline of the bridge span by placing large steel and concrete weights on the roadway. Eighty-seven tons of these weights were placed symmetrically with respect to the center of the bridge. The loaded area extended 15 feet on each side of the centerline of the span.

Each of the 36 WF 150 test structures was made up of four 40-ft beams. These beams were fastened together with 1-1/32-inch diameter turned bolts which had a yield strength of about 50 ksi. The bolts were tightened with a standard size ratchet wrench. Bolt tension was not controlled and may be considered to be small. The paint was not removed from the joint surfaces. Figure 3 shows the general layout and dimensions of the two spans tested. Details of the bolted joints are shown in Fig. 4.

The 36 WF 150 beams and all splice plates were of structural grade steel. Pertinent dimensions and physical constants of the two test structures are shown in Table II.

Large steel and concrete weights were placed near the centerline of the span of each test structure in a manner similar to that employed on the T-6 bridge. On the first structure reported, a twenty-ton load was used for the first half of the test and twenty-seven ton load was used for the second half. A twenty-seven ton load was used for the entire test on



the second 36 WF structure. The loaded areas extended 6 feet 9 inches on each side of the centerline of the span.

### 3. INSTRUMENTATION AND TEST EQUIPMENT

#### 3.1 Loading Equipment

All tests were carried out in a 350-ton capacity test frame. Figure 5 shows this frame as it was used to apply repeated loads to the 36 WF structure. Loads were applied by means of a 2-1/2-inch diameter hydraulic cylinder. In order to obtain the loads necessary for the tests reported in this paper, the hydraulic circuit was maintained at a pressure of 1500 psi by means of a hydraulic pump driven by an electric motor. A two-way limit switch was operated by the deflection of the bridge. This switch excited a three-way solenoid valve which controlled the direction of flow to a cylinder located at the ends of the loading beams. A flow valve was used to control the rate of fluid flow to the cylinder.

The loading beams were connected to the test structure by means of two steel cables. In order to keep some tension in the cables. In order to keep some tension in the cables at all times, a spring shock was provided immediately behind the cylinder. Lateral adjustment of the loading beams was provided at their supports. The vertical stroke of the cables was adjusted by sliding the cable hangers along the loading beams.

#### 3.2 Stress and Deflection Measuring Equipment

Strains were measured by means of SR-4 gages placed as shown in Figs. 1 and 3. Two Model BL-32, Brush, Universal analyzers with direct-inking oscillograph attachments were used to record strain measurements. Since only two gages could be read at any time, it was necessary to stop the strain recorder in order to read any other two of the various gages.

During the dynamic loading portion of the test, the amplitude of deflection was measured by means of a pencil trace taken at the centerline of the span. Levels were run to obtain static deflections of the structure before and after loading. For the T-6 bridge, the loaded structure was jacked up until a condition of "zero stress" existed in the top chord; i.e., the panel pins in the center bay could be moved. All strain gage readings were then referenced to this condition. For the 36 WF structures, strain gage readings were referenced to computed dead load strains.

## 4. TEST RESULTS

### 4.1 T-6 Bridge Span

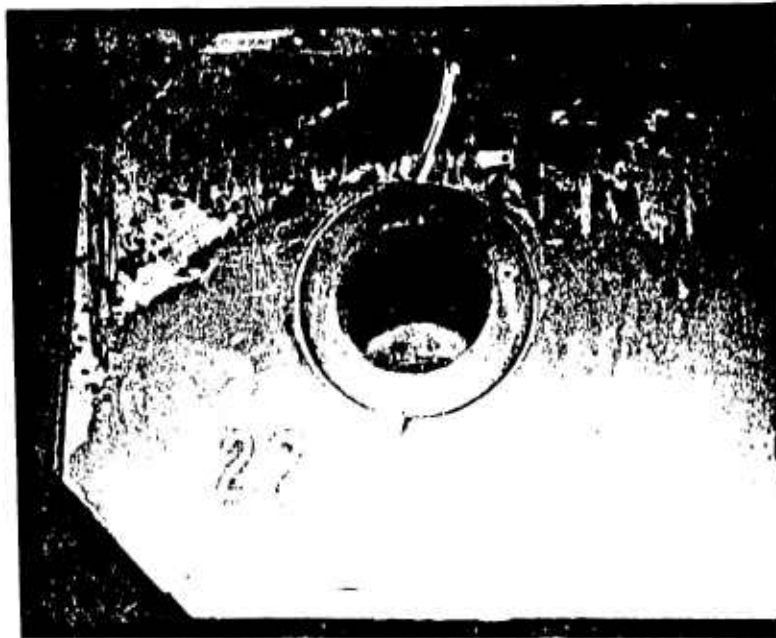
The T-6 bridge equipment used in the fatigue tests had been used previously in field assembly and static tests. The fatigue tests were begun immediately after the completion of the static tests.

With an 87-ton mass at the centerline of the bridge, a 2-inch amplitude of deflection would produce stresses equivalent to the design stresses of Class 50 and Class 78 (Class loadings are approximately the ton equivalent of tracked military vehicles) military loads at the top and bottom of the vibration node, respectively (3). The amplitude was varied slightly during the test in order to obtain measured strains corresponding to those computed for the Class 50 and Class 78 loads.

After the beginning of the dynamic testing phase, periodic observations were made of the strain amplitude, deflection amplitude, and period of vibration. Table III shows typical values observed during the tests.

The test was halted four times to adjust the cable tension. At approximately 16,000 cycles, a loud noise, originating in the vicinity of the north truss, was heard. The test was immediately halted and a detailed visual inspection of the bridge was made. This inspection failed to reveal the source of the noise. The test was then continued to 18,300 cycles at which time a second report was heard. The test was again halted in order to facilitate a visual inspection. This inspection revealed a failure in the lower chord male joint of the 3rd north truss. Figure 6 shows close-ups of the failure after the male joint had been removed from the panel. The steel insert which was removed from this hole is shown in Fig. 8.

During disassembly of the bridge, local damage was discovered at three other locations. The failure of the lower chord male joint of the north truss permitted the northeast corner of the bridge to lift out of the male end post base plate. This permitted a steel pintle to punch a hole in the base plate. Bearing failures occurred in the top chord male joints of panels 4 and 5 of the south truss. This permitted the rivets in the vicinity of the pin hole to work loose. It was also observed that general yielding had occurred in the lower chord of the sixth south truss panel. Close inspection revealed the presence of a crack in the top flange of the channel. This crack passed through one of the cover plate rivet holes. A close-up of this damage is shown in Fig. 9. Oxide coatings on the crushed aluminum of the south top chords and on the faces of the crack in the bottom south chord indicate that this damage may have occurred during the static load tests.



Exterior View

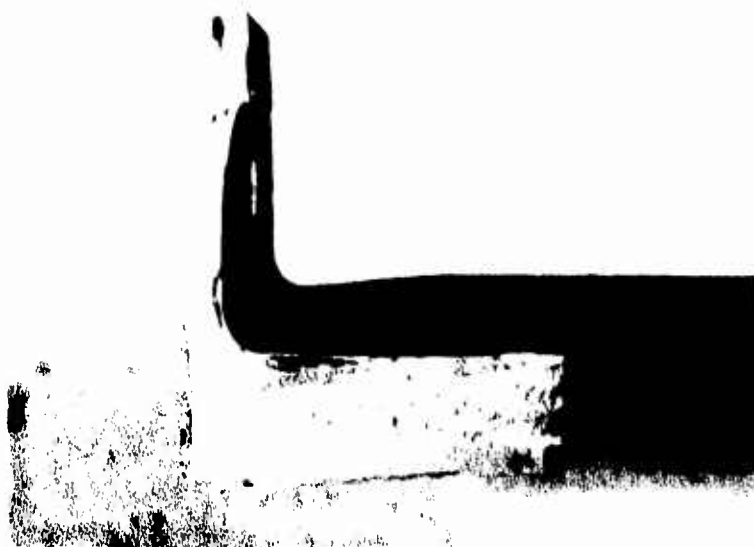


Interior View

Fig. 6 Lower Joint After Development of  
Fatigue Crack



Top



Bottom

Fig. 7 Close-up of Ruptured Joint



Showing Local Yielding

Fig. 8 Steel Insert Removed from Ruptured Joint



Fig. 9 Lower Chord of Sixth South Truss Panel  
Showing Local Yielding



TABLE III

## TYPICAL TEST RESULTS

Structure	Added Load Tons	Frequency Cycles/min	Deflection Amplitude in.	Gage No.	Measured Stress	
					Maximum ksi	Minimum ksi
T-6	87	70	$2\frac{1}{2}$	3	23.7	15.5
				4	23.7	18.9
				5	26.5	17.9
				6	15.0	9.0
36 WF	20	145	$2\frac{1}{2}$	1	8.0	21.0
				2	8.0	21.0
36 WF	27	134	$2\frac{1}{2}$	1	13.0	27.0
				2	13.0	27.0

TABLE IV  
COMPARISON OF MEASURED AND COMPUTED PERIODS OF VIBRATION

Structure	Weight Added Tons	Natural Period Computed Seconds	Natural Period Measured Seconds
T-6	87	0.870	0.857
36 WF	20	0.420	0.413
36 WF	27	0.469	0.448

#### 4.2 36 WF 150 Spans

The first of the two 36 WF spans was initially loaded with 20 tons of weights and oscillated at an amplitude which would give a measured strain corresponding to a stress variation of 5.4 ksi in the extreme fibers of the gross section. This corresponded to a nominal maximum stress on the net section of 8 ksi at the bottom of the vibration node and 21 ksi at the top of the node. After 300,000 cycles of this stress variation had been applied, the load was increased to 27 tons. The test was then continued using the same nominal deflection amplitude. This resulted in a stress variation between the limits of 13 and 27 ksi. Table III shows typical values of quantities measured during this test. After 3,000,000 cycles of the 13 to 27 ksi stress, the bolted joints were disassembled and inspected visually. This inspection failed to indicate any signs of fatigue damage.

A second span was assembled from previously unused beams and was loaded with 27 tons of dead weight. This span was also subjected to vibrational loads between the limits of 13 and 27 ksi. After 300,000 cycles, this joint was disassembled and found to be undamaged.

### 5. DISCUSSION OF RESULTS

#### 5.1 Dynamic Behavior

In Section 2, it was shown that Eq. II could be used to find the natural period of vibration of an elastic beam with a mass concentrated at its centerline. Since, in a real system, it is not physically possible to concentrate a mass of this magnitude at the center of a span, it would be expected that Eq. II would be slightly in error. If Eq. II had been developed for an applied mass which was distributed over a finite distance about the center of the span, the computed period of vibration would be smaller than that for an equal concentrated mass. For this reason, it would be expected that Eq. II would over-estimate the value for the period of vibration of the three test structures reported in this paper.

Table IV shows a comparison of measured and computed period of vibration for each of the three test structures. As expected, Eq. II gives a period of vibration which is slightly higher than that measured. In general however, the error is small and Eq. II is sufficiently accurate for practical application.

## 5.2 Fatigue Behavior of the T-6 Bridge Span

Since the T-6 bridge failed in the joint where no strain gages were present, stresses computed from measured strains are not available at the section of failure. Consequently, computed stresses were used to compare the behavior of the test structure with that of small specimens in the laboratory.

During the test the nominal stress on the net section of the joint that failed had a lower limit of about 18.6 ksi tension and an upper limit of about 24.0 ksi tension. Thus, the stress ratio (ratio of minimum stress to maximum stress) based on the nominal stress at the section was about 0.8. Reference 4 indicates that the stress concentration factor for this joint would be about 2.8.

In reference 5, Holt, Eaton, and Matthiesen have presented the results of a number of tests on aluminum alloy joints. The stress concentration factors of these joints were in the range of 2.4 to 2.8 and a number of the joints were fabricated of aluminum alloy 2014-T6. Consequently, it is possible to compare the behavior of the T-6 bridge with test results presented in reference 5. Figure 10 shows three S-n diagrams for aluminum alloy 2014-T6. These curves are extrapolated from the data in reference 5 and include stress ratios of 0, 0.5, and 0.75.

By plotting the point corresponding to the failure of the T-6 bridge on Fig. 10, it can be seen that this point lies below the curve corresponding to a stress ratio of 0.75. Thus, this comparison indicates that there is relatively good correlation between the behavior of the laboratory specimens and that of the full-size structure.

## 5.2 Fatigue Behavior of the 36 WF 150 Spans

Since neither of the two 36 WF spans was tested to failure, it is not possible to make a direct comparison between the behavior of the test spans and that of small laboratory specimens. However, it is possible to extrapolate the results in order to determine if the lack of failure is in line with laboratory tests.

Laboratory tests have shown that bolted connections will exhibit higher fatigue strengths than riveted joints if the bolts are tightened enough to prevent slip in the joint (6, 7, 8). If slip does occur, the bolted joint will have about the same fatigue strength as a similar riveted joint. Figure 11 shows a static load versus deflection curve for a 36 WF span similar to the two tested in fatigue. It can be seen that some slip occurs under the dead weight of the beam and that the slip continues as the load increases. Thus, it would be expected that the fatigue strength

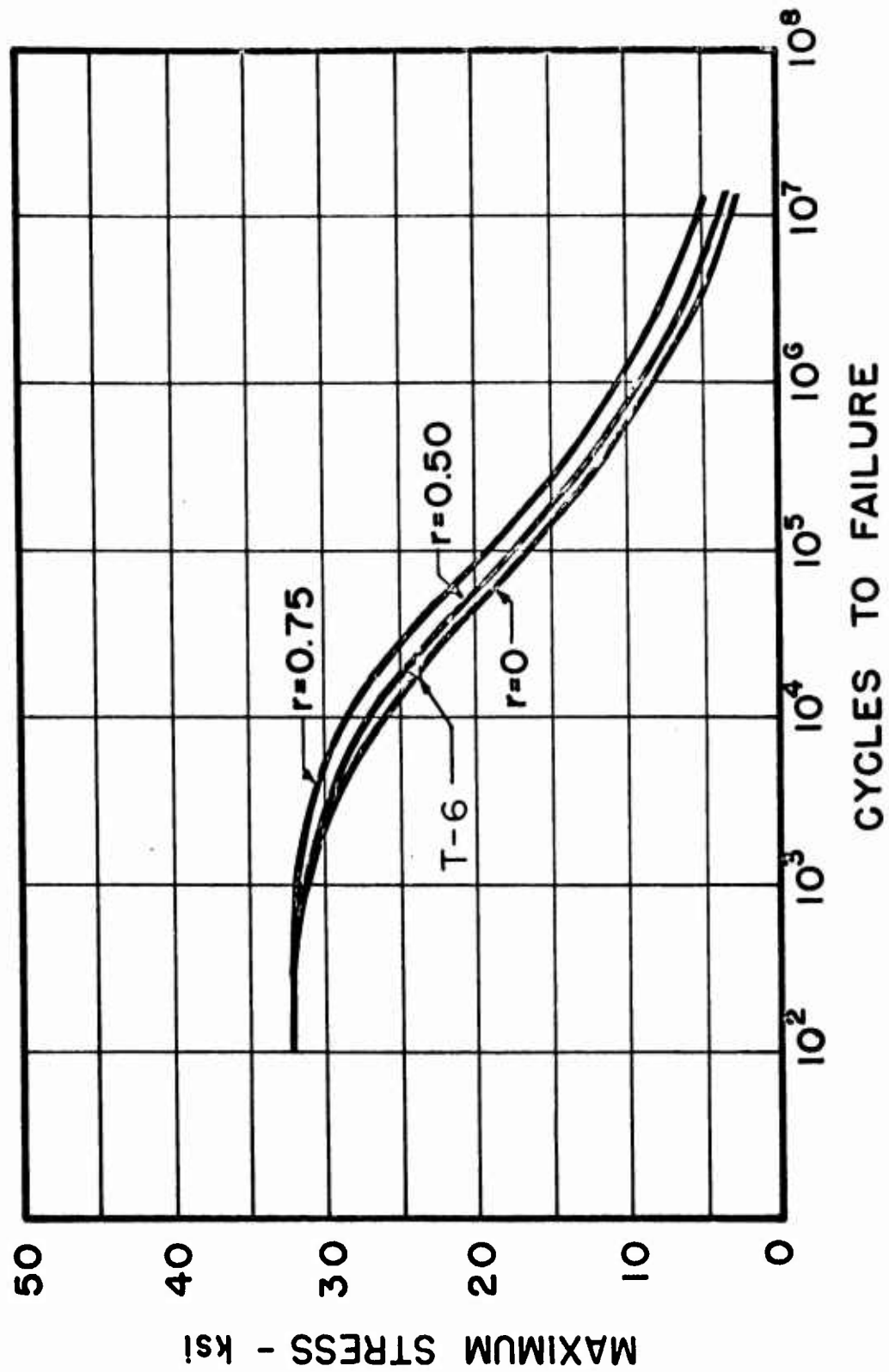


Fig. 10 Comparison of S-n Curve Obtained from Laboratory Tests on Small Specimens of Aluminum with Conditions in T-6 Aluminum Bridge at time of Rupture

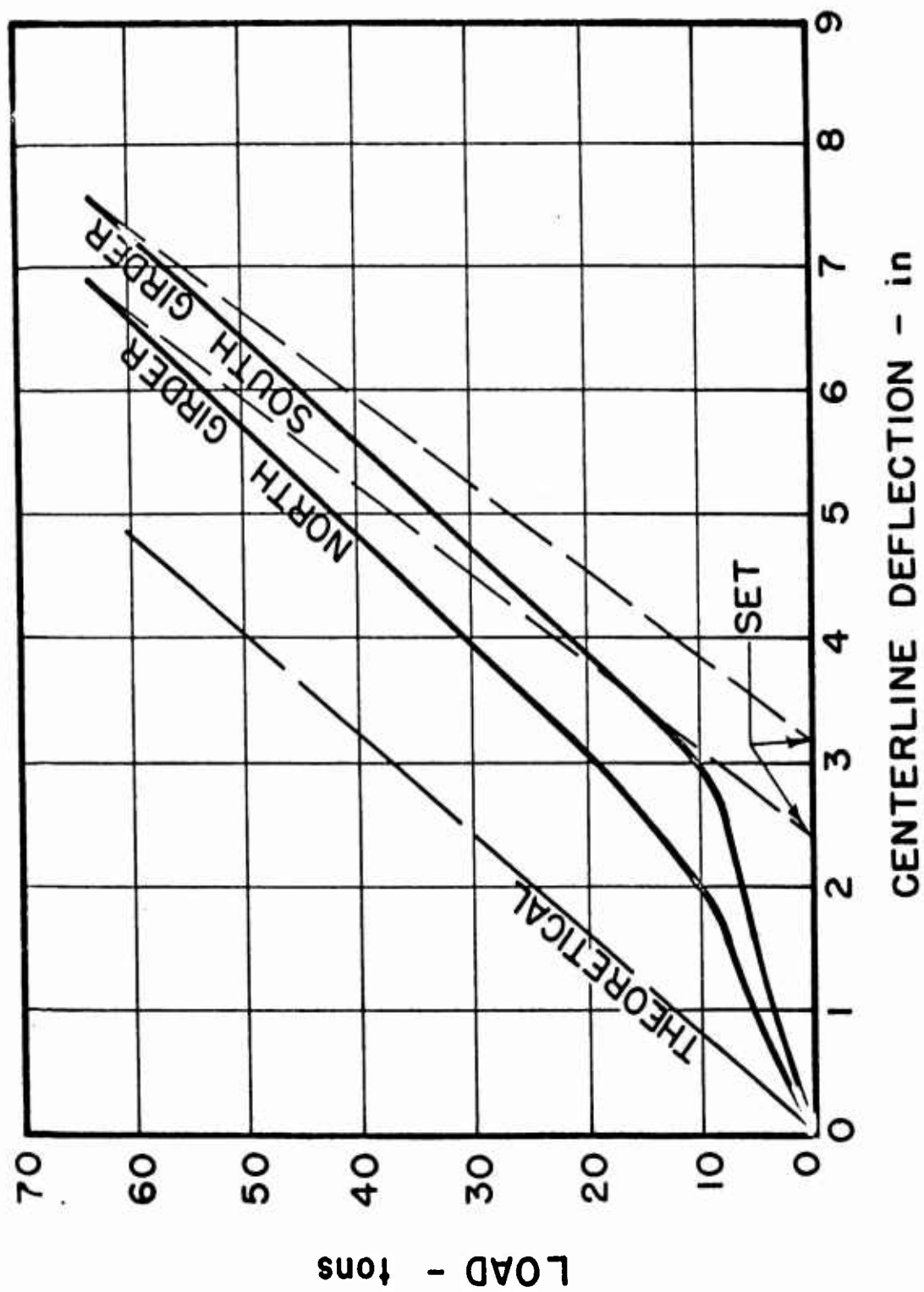


Fig. 11 Static Load Versus Deflection Curve Obtained from 36 WF Structure Similar to those tested in Fatigue

of the two beams reported in this paper would be comparable to that of similar spans fabricated with riveted joints.

Wilson has shown that, for steel, the stress which will cause failure at a given number of cycles can be found from the following relation (6):

$$S_n = F \left( \frac{2,000,000}{N} \right)^{0.10} \quad (III)$$

$S_n$  = maximum stress in the stress cycle, psi

$F$  = fatigue strength for failure at 2,000,000 cycles, psi

$N$  = number of cycles to failure

Equation III is valid only if the ratio of maximum stress to minimum stress is constant. If it is necessary to determine the maximum stress to cause failure for a different stress ratio, the following expression may be used (9):

$$F' = \left( \frac{3 F_1}{2 - r} \right) \quad (IV)$$

where

$F'$  = maximum stress for any particular value of  $r$

$F_1$  = fatigue life for complete reversal

$r$  = ratio of minimum stress to maximum stress

In reference 6, it was reported that, for riveted joints of structural grade steel, the fatigue strength for a cycle of 0 to maximum tension is about 26,000 psi. Using this value with Eq. III and IV, it is found that, for the stresses used in these tests, both 36 WF spans should have been able to sustain more than 2,000,000 cycles. Consequently, neither of the I-beam structures would have been expected to fail under the conditions imposed.

## 6. SUMMARY

This paper presents the results of dynamic loading tests on three full-size bridge structures tested at the U. S. Army Engineer Research and Development Laboratories. These structures include two steel I-beam bridges with 78-ft spans and an aluminum truss bridge with a 105-ft span. Dynamic loads were simulated by vibrating the bridges at their natural frequencies.

Stresses obtained from measured strains and periods of vibration are compared with those computed for each structure. In each case, computed stresses were within 0.5 ksi of those measured. The observed period of vibration for each bridge was in good agreement with the computed value.

The observed fatigue behavior of each of the three structures was compared with that which would be predicted from laboratory tests on small specimens of steel and aluminum. Laboratory tests indicate that the steel I-beam structures should withstand more than two million cycles of the applied stress. Thus, the lack of failure of the test structures is in agreement with the predicted behavior. Although the aluminum truss structure failed at a slightly lower number of cycles than would be predicted by tests on smaller specimens, the difference was within the limits of error of the data obtained from the laboratory tests. In general, the behavior of each of the three structures was in agreement with that predicted.



## REFERENCES

1. Den Hartog, J. P. "Mechanical Vibrations" McGraw-Hill New York, 1947
2. Tong, K. N., "Theory of Mechanical Vibration", John Wiley and Sons Inc., New York, 1960
3. "Principles of Bridging", Department of the Army Technical Manual, U. S. Government Printing Office, January, 1955
4. Frocht, M. M., and H. N. Hill, "Stress Concentration Factors Around a Circular Hole in a Plate Loaded Through Pin in the Hole", Journal of Applied Mechanics ASME, V. 7 No. 1 March 1940
5. Holt, M., J. D. Eaton, and R. B. Matthiesen, "Fatigue Tests of Riveted or Bolted Aluminum Alloy Joints" Journal of the Structural Division, ASCE V. 83, No. ST1, January, 1957
6. Wilson, W. M., and F. P. Thomas, "Fatigue Tests of Riveted Joints", University of Illinois Engineer Experiment Station Bulletin No. 302, May 1938
7. Lenzen, K. H., "The Effect of Various Fasteners on the Fatigue Strength of a Structural Joint", Proceedings, American Railway Engineering Association, V. 51, 1950
8. Munse, W. H., D. T. Wright, and N. M. Newmark, "Laboratory Tests of High Tensile Bolted Structural Joints", Transactions ASCE, V. 120, 1955
9. Moore, H. F., "Materials of Engineering", 8th Edition, McGraw-Hill, New York, 1953

## DISCUSSION

Dr. Beeuwkes: Did you ever correlate the developed stress and the rotating beam stress?

Lt. Corley: No, these were tests on riveted lap joints, single lap joints. It was direct tension fatigue test.

Dr. Beeuwkes: Could you compare the failures you got in the two cases, that is, compare characteristics of the failure that you got in the bridge and in the small specimen. Did they appear to be the same?

Lt. Corley: Yes, they did.

Dr. Beeuwkes: The failures, or the initial cracks?

Lt. Corley: We did not conduct these tests, they were conducted by ALCOA. They involve a large series of tests on riveted joints. The types of failure were the same, however, they were complete fracture. They initiated as small cracks around the pin hole and as soon as they had propagated far enough, then, of course the rest of the cord failed in a more or less ductile manner - ductile as 24T6 can be.

Dr. Kumar: I had a question along the same lines as Dr. Beeuwkes did. This was about the surprising closeness of the curves of fatigue that you have plotted, i. e., the SN curves for the bridge and specimen. When you said the SN curve for the bridge, what did you really mean?

Lt. Corley: If I said from the bridge, I didn't mean for the bridge. The SN curves were for the small laboratory specimens. The point at which the bridge failed was plotted on the same curve.

Dr. Kumar: Well, usually as we are all aware, the fatigue curve, SN curve, has such a tremendous scatter that to call it a curve is misleading. If the bridge failed as the curve indicated it would, this may really be accidental, because even laboratory specimens will have discrepancies of several million cycles.

Lt. Corley: This is very true, and I agree with you 100%. Of course, if we could we would like very much to test many more bridges but naturally this runs into too much money. We were very happy though with the fact that this point was so close to the curve. Concerning the validity of saying that we've proven that the small specimens can or do predict exactly what the forthright structure is going to do, I don't intend to get this impression across at all. This is simply one bridge that we tested. The results on this bridge did agree with the curve.

J. N. Crenshaw, Army Missile Command - Redstone Arsenal: Clarify for me one point; namely, the application of the additional load - was this done by hydraulic cylinder?

Lt. Corley: No, sir, the additional load, in fact I should say more precisely, the additional mass was applied by means of concrete and steel which were simply set on the bridge.

J. N. Crenshaw: This essentially answers my question.

John F. Ward (NASA, Langley Research Center): Could you, by any chance, repair the joint and continue the tests. You have a lot of joints on this bridge and you consider only one joint in the bridge failure.

Lt. Corley: Is the question, do we consider going on and getting more?

No. In fact this was done quite a while ago and the tests on this particular bridge have been stopped, so there will be no additional tests. We would like to make additional tests but it is something that is not contemplated right now.

## STRUCTURAL DESIGN CRITERIA FOR MILITARY VEHICLES

C. H. Winfree\*

### ABSTRACT

The objective of this paper is to outline primary problem areas of vehicle design and to define design criteria applicable to military vehicles. Vehicle structural requirements are presented from the design engineers view point. Loads imposed upon a wide range of military vehicles are defined and assigned numerical values. When applicable, the load direction and magnitude is expressed as formulae or curves. As an aid to reducing weight and cost, design procedures are presented with methods for evaluating and controlling safety factors, symbols, weight and structural reports. This paper will provide some guidance to those companies entering into military vehicle design and construction. For more experienced companies it should be of some help as a check of present design procedures.

### INTRODUCTION AND PRIMARY PROBLEMS

Since graduation the author has been engaged in the design and analysis of military vehicles. During this time a serious lack of factual information pertaining to vehicle design has become obvious. It appears that most structural design has been based upon a cut and try procedure, to wit, "if it fails beef it up". This method may be satisfactory for a manufacturer producing a single type and weight of vehicle year after year, but is inadequate for organizations designing many types of vehicles.

The objective of this paper is to outline and define design criteria applicable to military vehicles and to present some of the problems facing vehicle designers. Particular emphasis is given to the hull structure of light weight track laying vehicles and components affecting hull construction.

The lack of established automotive design criteria results in entirely too much verbal information based on personal desire, whims and "guestimation". Using questionable data leads to disagreements between

---

\* Mr. Clarence H. Winfree, Chief, Hull & Turret Section, Design Branch, Army Tank Automotive Center, Warren, Michigan

individuals and results in an excessive amount of "cut and try" type of designing. With personal whims and data changing each day, the design engineer inevitably develops a philosophy of over designing. This system has never been satisfactory and in view of the rapid growth and complexity of military vehicles it represents a futile attempt to achieve the desired end results.

If any authoritative design criteria can be established, confirmed and compiled into a design manual the problem of piece-meal distribution of information would be settled.

A useful design manual should meet the following requirements:

- a. Adequately indexed and readily available to the designer. Designers do not have the time, and management will not tolerate a system that requires extensive searching for information.
- b. Methods for efficiently coordinating design procedures.
- c. Standard forms for load factors, weight, stress, etc., together with an explanation of the form.
- d. A simple system whereby engineers could request correction or revision to the manual.
- e. An indication regarding the accuracy of information contained in each section.
- f. References to other sources of information, and where the information can be obtained (ASTIA numbers)

There are two primary problem areas in attempting to establish a design manual; determining the magnitude of loads imposed on military vehicles and arranging the design manual in a usable form.

A good manual containing data required for military vehicle design would reduce lead time at least 25% and cost per vehicle 5% or more.

This paper is an elementary approach to the problem. The following suggestions are offered regarding manual preparation.

- a. A decision has to be made regarding the need for a manual.
- b. Turn the problem over to a private company not engaged in the design or manufacture of automotive products. Anyone engaged in automotive work is too biased with personal opinion to perform the task of compiling facts.
- c. A formal search through the libraries and files of this country and others should be conducted to determine if a vehicle design manual has already been published. If none is found in the search, a system of locating and retrieving information pertaining to vehicles should be initiated.

Design criteria presented herein is the result of structural analysis and test data on several vehicles. It is believed to be reasonably accurate, but additional confirmation is needed on load factors. Load factors used are open to question, but once they have been selected or established the remaining structural analysis should be rigorous and definite. Considerable information is based on past vehicle performance and history.

#### FUNDAMENTALS OF VEHICLE DESIGN

1. Non-armored hull weight is 6 to 10% of gross vehicle weight.
2. Design the hull to accommodate components; don't expect much change in components to accommodate the hull.
3. Avoid undue complexity. Monocoque structures should be employed when possible with a minimum amount of internal reinforcements.
4. Avoid ridiculous tolerances in hulls.
5. Design door and hatch torsion bars from 80,000 psi, to 100,000 psi. Cover and protect all bars from damage.
6. Use stacked torsion leafs when length is at a premium. (Do not use on suspension.)
7. Provide water drain holes for all enclosed areas. Standard MS drain valves may be satisfactory for hull drains.
8. Consider the number of vehicles to be manufactured. Is the number large enough to justify expensive forging dies?

9. Reasonable notches in ductile material, subject to few repeated loads, are not valid stress concentration points.
10. The driver location relative to the C. G. effects vehicle load factor.
11. Muzzle brakes look good on paper; but they create severe blast problems.
12. Vehicles get covered with dirt and mud; enclose or protect delicate systems.
13. Track laying suspension weight is 18 to 24% of gross vehicle weight.
14. Track strength requirements depend upon vehicle weight, not sprocket torque output. Band tracks require a tensile strength of 3 to 5 times vehicle gross weight.
15. Allow 4 to 8 inches of wheel travel from static to bump position.
16. Provide bump stops for all wheels.
17. Shock absorbers are required only on front and rear wheels.
18. A stiff suspension gives better side slope performance.
19. Road wheel strength is determined by bump-stop requirements.
20. Stress suspension torsion bars to 140,000 psi. Design and manufacture them in accordance with Detroit Arsenal torsion bar specifications. (Too much study has gone into bars for anyone to start over.)
21. Vehicles without idlers tend to throw tracks due to dirt and rock wedging at rear wheels.
22. Avoid screws and bolts under 5/16" diameter in the hull structure. Mechanics twist them off.
23. Fine threads have less tendency to loosen up than course threads.
24. Provide positive locks for critical bolts subject to continuous vibration.
25. Avoid requiring two wrenches for items which must be serviced or removed frequently.

26. All design is a compromise; don't sacrifice an entire vehicle to appease organizations or individuals who over emphasize one particular segment of vehicle design.

### DESIGN CRITERIA

Establishing structural design criteria involves the formulation of detailed information on:

- |                         |                          |
|-------------------------|--------------------------|
| (a) Basic road load.    | (e) Safety factors.      |
| (b) Gun recoil load.    | (f) Material properties. |
| (c) Handling load.      | (g) Symbols.             |
| (d) Weight and balance. | (h) Structural report.   |

Due to radically different conditions to which military vehicles are subjected it does not appear feasible to establish one set of design criteria applicable to all types.

This paper makes no pretense of answering all problems involved in military vehicle design, even portions of the criteria probably are in error. If the design data is used with caution, a reasonably satisfactory vehicle performance may be expected.

The following pages present a typical load factor outline. (This particular outline is from the XM 104 self-propelled howitzer.)

### LOAD FACTORS

The hull structure shall be capable of supporting the following accelerations (applied loads) without suffering detrimental permanent deformation, or design loads without structural failure, (+ indicates force acting upward on part)

- a. For road loads.

Vertical (Applied loads):

Positive:  $\pm 26$  at front to 0 at rear; or  $+26$  at front to  $+13$  at C.G.; whichever is greater. Flat cut off at  $+13$ .



For design  $\pm 40$  at front to 0 at rear; or  $\pm 40$  at front to  $\pm 20$  at C. G.; whichever is greater. Flat cut-off at  $\pm 20$ .

Negative: -13 at front to -10 at C. G. with flat cut-off at -11.

Longitudinal:  $\pm 20$

- 10

Transverse:  $\pm 10$

b. For rail transportation.

Vertical:  $\pm 2$

Longitudinal:  $\pm 12$

Transverse:  $\pm 3$

c. For air transportation Spec. MIL-A-8421.

Vertical:  $\pm 3$

Longitudinal:  $\pm 3$

Transverse:  $\pm 3$

The following ultimate accelerations (design loads) are required.

Vertical:  $\pm 4.5$

Longitudinal:  $\pm 8$

Transverse:  $\pm$

d. For air drop.

Vertical:  $\pm 15$

(HIGED-B-6-10 requires 40 to 100g)

## BASIC ROAD LOADS

All basic road loads result from extremely complicated dynamic motions of complex structures operating over undefined highway and cross-country terrain. It is probably the most hopeless analytic problem on earth, yet a problem as old as the wheel. Such problems are far beyond engineering and we can only hope that some dynamist will eventually solve this problem. If this one problem could be answered, I believe military vehicle design could turn into a true analytical science, rather than relying so much on past experience and "guestimation".

Requirements of combat vehicles are determined by cross-country acceleration factors which are typically five to ten times greater than highway requirements. Approximately half of the load imposed upon combat vehicles results from rotational accelerations and the remainder from linear accelerations.

The determination of basic road loads requires the application of experimental methods. At present there exists no completely satisfactory methods of calculating road loads for ordnance vehicles. Present methods require information to be estimated from strain gages, oil pressure, accelerometer readings, broken parts and past performance of similar vehicles under tactical or simulated tactical conditions.

In addition to the basic load factors, a shock factor is required for small items. A "small item" for this purpose is defined as an item having a weight less than 3% of empty vehicle weight.

Four terms which are frequently used without well defined meanings are applied load, design load, safety factor and margin of safety. The first two are explained in the following paragraphs, the difference between safety factor and margin of safety factor and margin of safety is covered later in this paper.

### A. APPLIED LOAD:

This term is also known as the limit load, or simply as the load. Applied load for military vehicles is the maximum load the vehicle is expected to sustain and continue operation with no appreciable loss of characteristics. Applied loads should not cause detrimental permanent deformation of the vehicle structure. Please note that detrimental has been underlined, this point should be emphasized. Many parts of vehicles produce no detrimental results when permanently deformed and should not be

designed on the basis of deformation. Examples are small brackets, lifting eyes, bump stops, air extraction and drop systems, spades and joints. Generally, items associated with armament and suspension are more sensitive to deformation than hull structures. Items usually sensitive to slight deformations should be considered for re-design to reduce sensitivity.

Obtaining values for effective applied loads is complicated by the lack of any definite criteria of what is expected of the vehicle.

## **B. DESIGN LOAD:**

This term is also known as ultimate or ultimate design load. Design load represents the value at which complete structural failure is expected. For 1st or 2nd line combat vehicles, personnel incapacitation occurs near this point. Loads of this magnitude approach accidents and result from striking large boulders, walls, trees, nosing over high walls onto concrete pavements and bad air drops. In combat vehicles the required design loads are so high that fatigue should present no problem in hull structure. For non-combat wheel vehicles, fatigue may play a predominant role in failures. Values of design load can frequently be determined from broken parts. If a test vehicle is available, structural fuses may be incorporated and varied in strength to determine the magnitude of design loads.

Presented in figure 1, are curves of basic vehicle load applicable to typical military vehicles. Figure 2 is a shock factor curve for mounting small items.

The following outline gives a procedure for the use of these curves.

1. Select vehicle class and estimated weight.
2. Enter load factor curve, figure 1, and obtain basic load factor (n).

This is the design load for the front end of rigid hull vehicles such as tanks, self-propelled howitzers, armored personnel carriers, etc. The maximum load factor near the C. G. will be approximately 1/2 of this value. For trailers, this represents a general design load factor.

For typical track layers, calculate design loads for sprockets and wheels by the following equations.

# PROPOSED LOAD FACTORS

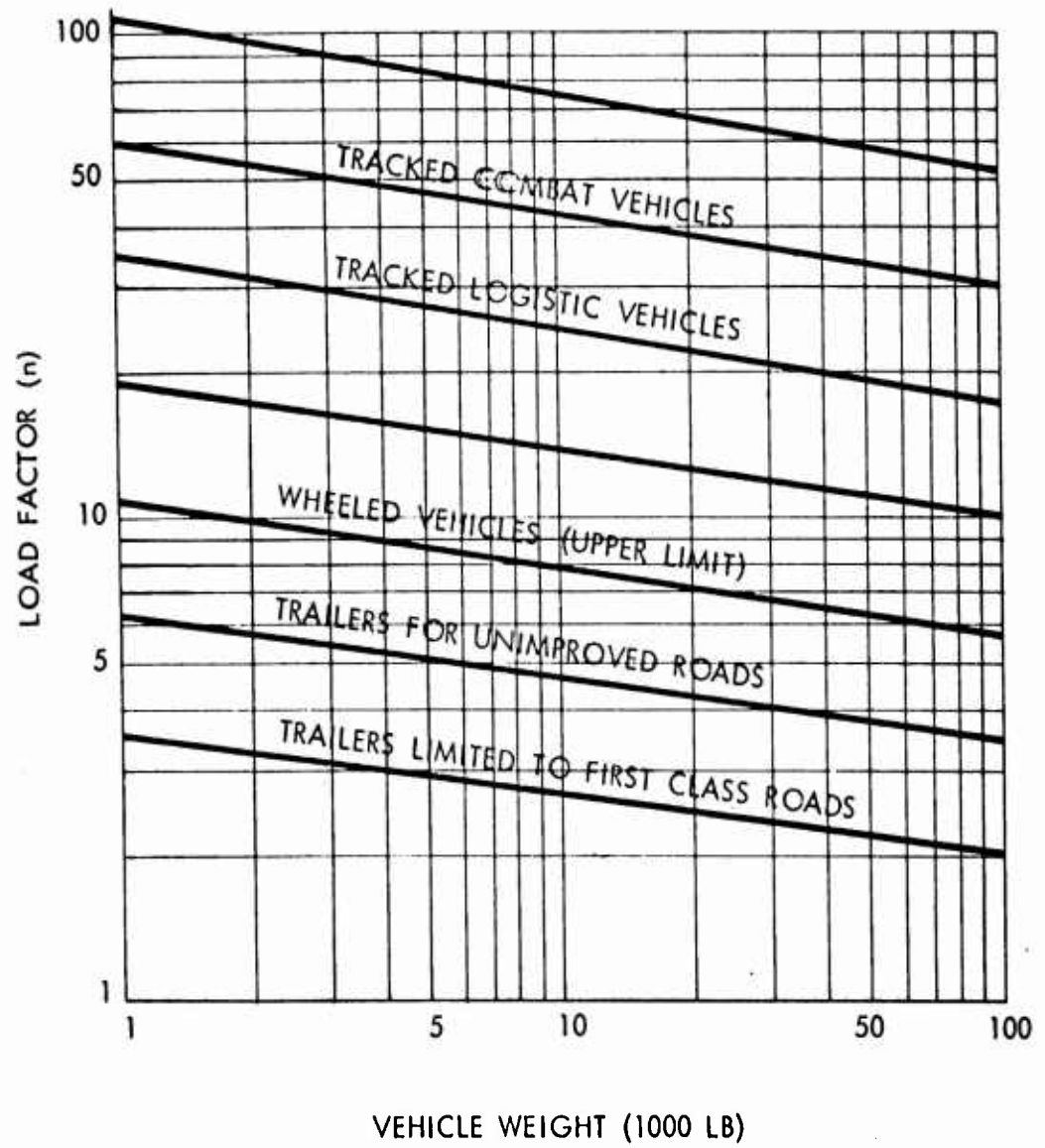
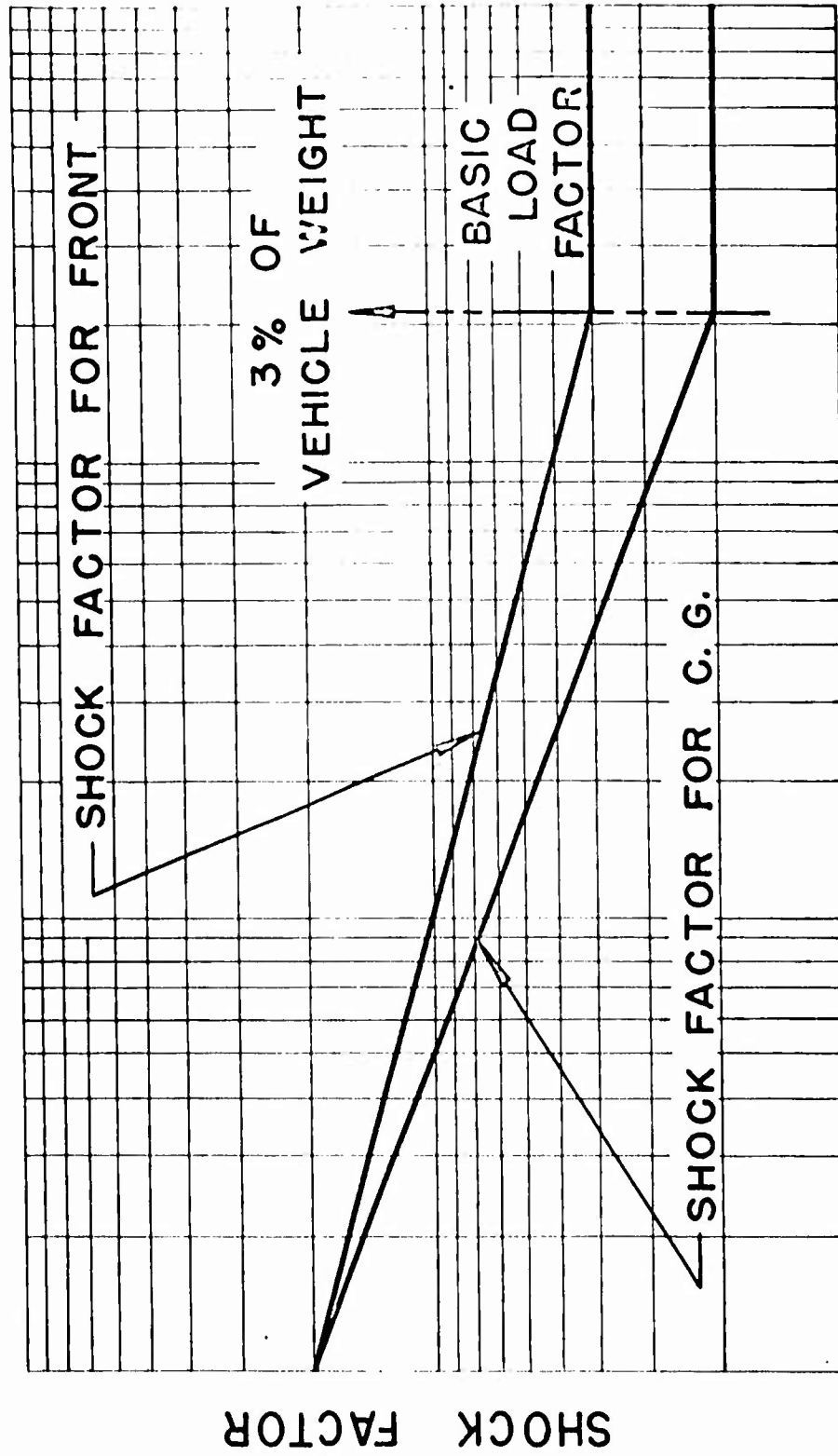


(Figure 1)



WEIGHT OF MOUNTED ITEM

Figure 2

Design load at centerline of track on forward sprocket

=  $n(.15)$  vehicle weight

Design load for No. 1 road wheel

=  $n(.1)$  vehicle weight

Design loads for other wheels

=  $n(.05)$  vehicle weight

In no case should suspension design loads be taken as less than 1.4 (vehicle weight).

3. To obtain the required mounting strength for small items, construct a shock factor curve similar to figure 2.

#### GUN RECOIL LOADS

Gun recoil loads are obtained by established methods of calculation and confirmed by test firing. Calculations can be made according to ORDP 20-342 "Recoil Systems" or Detroit Arsenal publication "Design of Hydraulic Orifice for Recoil Control." Both methods give results having a reasonable degree of accuracy, gun recoil loads are known more accurate than any other loads in combat vehicles. One question frequently asked is what effect short peaks or spikes in hydraulic recoil systems have upon hull and spade structures. Spikes of less than 3 milliseconds duration have no appreciable effect upon vehicles structure or spade load.

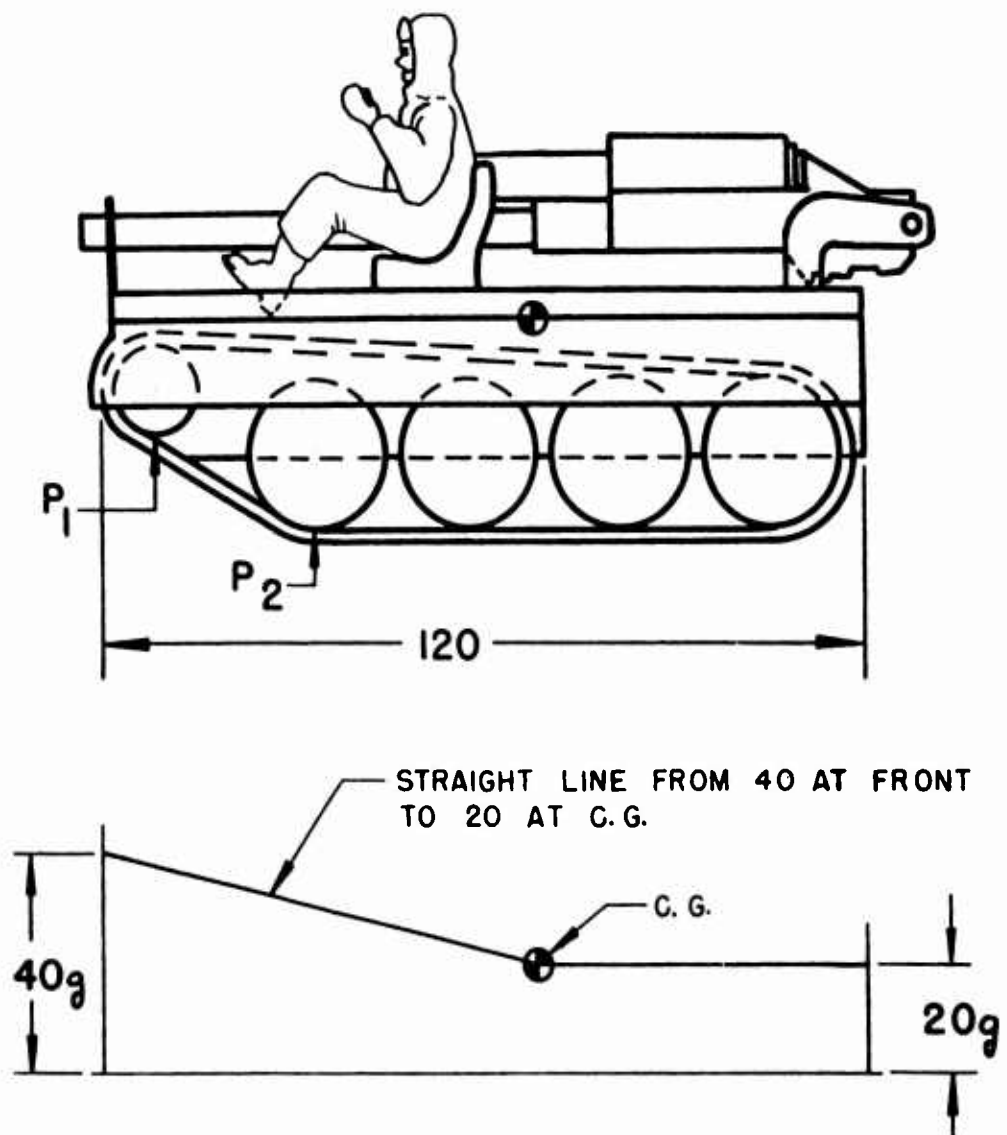
Recoil loads are transmitted through the gun mount, vehicle structure and spade into the earth. Reactions from the earth may be distributed uniformly over the spade or concentrated due to large rocks. Concentrated load from rock presents the primary spade problem, distributed loading generally presents no problem. Investigation should be conducted for different angles of elevation and azimuth considering ledge rock in the earth. Ordinary dynamic and static equations provide satisfactory answers to spade loads.

Figure 4 presents a typical calculated spade strut load curves resulting from gun recoil. The abrupt change around  $50^{\circ}$  results from a change in recoil length.

ARDCM 80-1, Volume 1, Part E, gives recoil loads for 50 caliber and 20-mm guns.

# XM 104

## BASIC ROAD LOAD FACTORS



$P_1 = 7$  TIMES GROSS VEHICLE WEIGHT  
APPLIED AT  $\phi$  OF TRACK

$P_2 = 4$  TIMES GROSS VEHICLE WEIGHT

Figure 3

# XM 104 PILOTS CALCULATED SPADE STRUT LOADS

200

180

160

140

120

100

80

60

40

20

0

NO. 1- NO LARGE ROCKS 0° AZIMUTH

NO. 2- NO LARGE ROCKS  $22\frac{1}{2}^\circ$  AZIMUTH

NO. 3- LARGE ROCKS

APPROXIMATELY 9 INCHES OUTBOARD  
OF SPAR  $22\frac{1}{2}^\circ$  AZIMUTH

ROD PULL- 23,000 & 36,000 LBS.

ASSUMPTION: SPADE ROTATION TAKES  
PLACE ABOUT CENTROID OF  
ENCLOSED EARTH

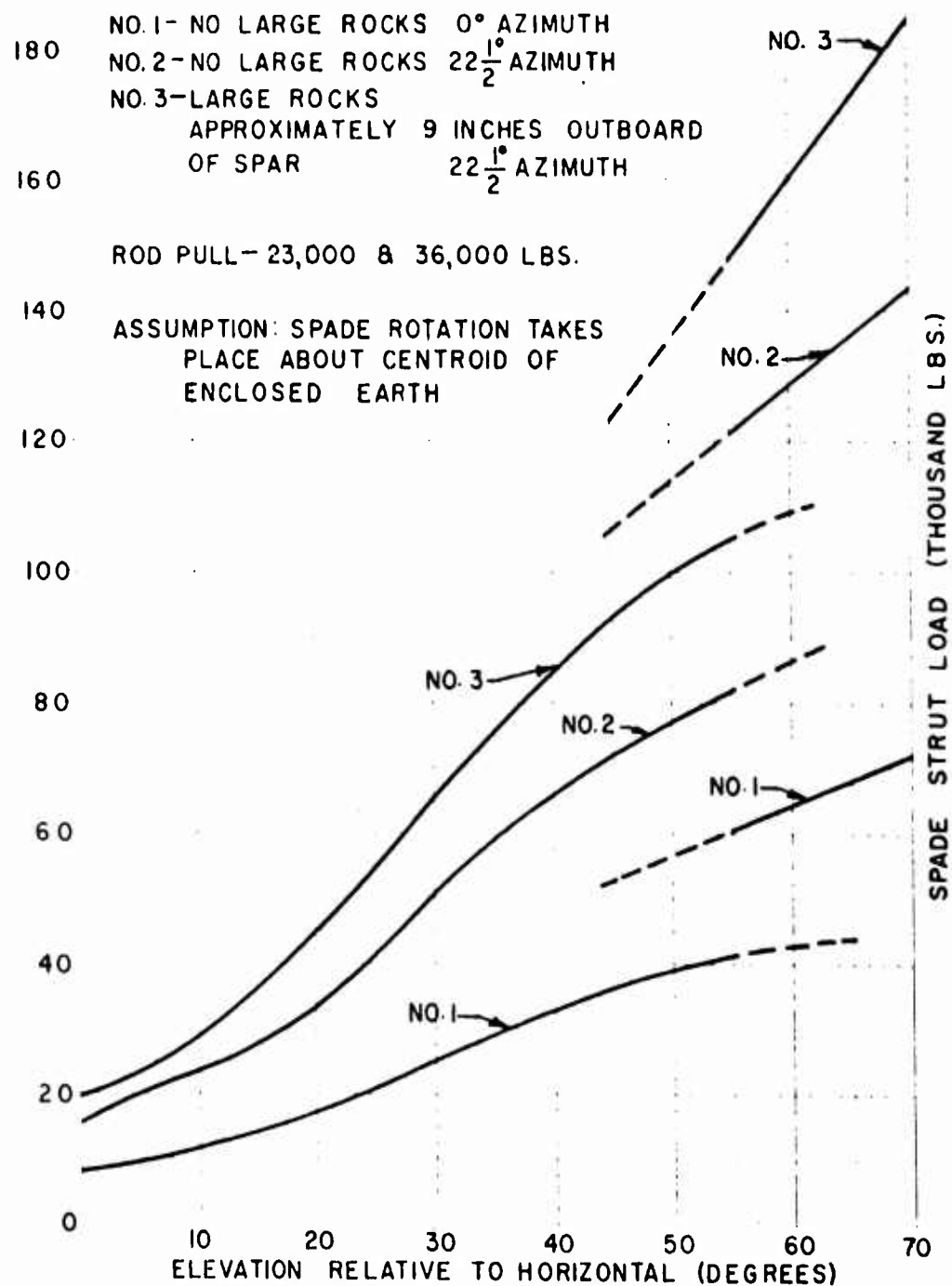


Figure 4



## HANDLING LOADS

Handling loads are determined by methods of transportation, and a minimum strength factor dependent upon the abuse to which the vehicle is subjected. Small parts which a man can step on should withstand a load of 300 pounds.

With the exception of air transportation requirements, design loads for transportation systems are not well defined by any military specification.

The following specification may be of some help.

- a. For rail transportation.

Vertical:  $\pm 2g$

Longitudinal:  $\pm 12g$

Transverse:  $\pm 3g$

- b. For marine shipment a load factor of 2g is adequate.

- c. For air transportation.

Spec. MIL-A-8421, General Specification for Air Transportability Requirements.

- d. For parachute delivery.

Mil-STD-669 "Air Delivery Loading Environment and Related Requirements For Military Material"

MIL-STD-814 "Requirements for Tiedown, Suspension and Extraction Provisions on Military Materiel For Air Delivery"

Loads imposed upon equipment during drop, depend upon the vehicle attitude at time of contact and shock absorbing equipment incorporated in the delivery platform.

Vertical: 15g, with shock absorbing equipment.

HIGED-B-6-10, 40 to 100g with no shock absorbing system.

e. Slings eyes should conform to MIL-STD-209. The standard should read "Without detrimental deformation" in place of yield. In addition to the requirements of MIL-209, any one eye should have an ultimate strength sufficient to support the vehicle weight.

#### WEIGHT AND BALANCE

Controlling weight and center of gravity requires continuous maintenance of weight and balance forms. MIL-STD-254 presents an elaborate weight control system for aircraft, which could be adapted to automotive use with major modifications. A relatively simple weight control form may consist of part weight tabulated relative to the zero reference line and summations made for vehicle C.G. By custom, the turret center line is the zero reference line, this practice leads to confusion if the turret moves relative to the hull. For vehicles without turrets, zero reference is taken a few inches forward of the hull with the final drive output located on a station number divisible by 10. If the final drive location moves, no change is made in vehicle station lines. Locating the zero reference forward of the vehicle avoids negative stations. Normal ship building and aircraft practice should be followed relative to station lines, water lines, and buttock lines.

Structural weight has a large influence on initial cost and a secondary effect on recurring or maintenance type cost. In making a decision on whether to change weight and in allocating weight targets, it is important to consider at least the following factors:

1. Design functions - difference between essential primary and desirable secondary functions. Can the vehicle be operated without the part; can the part be eliminated?
2. Structural integrity and degree of analysis required.
3. Vehicle performance.
4. Cost.
5. Producibility.
6. Schedule.
7. Growth factor.
8. Effect on other components.

9. The maximum weight that is permitted for air delivery.
10. Cost of shipping additional weight, this critical if air shipment is probable.

As an aid to controlling or guiding weight reduction programs, the following check list is presented.

1. The mental attitude of personnel working on the project; has any desire been created to design light structures? Is management willing to pay for weight control? Are people working on weight control, or just talking about it?
2. Check the equipment on the vehicle, what part is really required? How many items are only someones desire? It will take a battle to remove anything, but there is a lot of useless equipment on vehicles.
3. Use the shortest, most efficient path for load transmission.
4. Use existing material and avoid adding additional parts.
5. Do not complicate interior stowage with necessary reinforcements.
6. Use alloy steel heat treated to 125,000 psi for brackets and irregular shapes; use 160,000 to 180,000 psi for symmetrical items under known loading conditions.
7. Use aluminum where it is worth while, thin sections, buckling problems, spacer filler, etc. Avoid aluminum castings in primary structures.
8. Avoid joints, especially in highly loaded parts.
9. Use care in joint selection, tension joints, or shear joints.
10. Use sheet metal stampings with integral beads and reinforcements.
11. Avoid overdesign.
12. Use simple bushings in place of anti-friction bearings.

## SAFETY FACTORS

Concurrent with the establishment of basic loads and load distribution are the problems of selecting and applying factors of safety, consideration of stress concentrations, detailed environmental and life requirements, and the balancing of all against "optimized" weight.

The more exact the knowledge of the basic loads, the more it is possible to design structures with the minimum safety factors compatible with reasonable reliability. Design analysis should indicate the accuracy to which load factors are known and "factors of ignorance" should not be confused with safety factors.

Safety factors are used for the following reasons:

1. Safety factors provide a standard difference between applied load and structural failure. This is the classical meaning generally expressed as,  $\text{APPLIED LOAD (SAFETY FACTOR) = DESIGN LOAD}$ .
2. For structures where deformation is unimportant it provides a uniform criteria for failure.
3. To account for unknowns in loading, analysis, material and fatigue. These are truly "factors of ignorance", which are generally called safety factors.

Safety factors should not be confused by being indiscriminately placed on both the load and on the allowable stress level. Extreme care must be exercised to avoid multiplication of safety factors. Investigation has revealed many cases where safety factors were 5 to 10 times the quoted value. Common methods of "slipping in safety factors" while determining strength of structural components are:

- a. Working to yield stress when ultimate is critical.
- b. Failure to account for plasticity.
- c. Use of curved beam equation when they are not applicable.
- d. Incorrect use of allowable stress.
- e. Overlooking a primary loadpath.

f. Undue simplification of analysis.

g. And the fatal remark of the boss "it looks skimpy, better beef it up."

There is only one thing certain about a structure, if no failure ever occurs, it is overdesigned. To avoid multiple safety factors, select a value before starting and apply it to the load, do not enter safety factors during stress calculations.

The relation comparing the allowable load with the design load is termed the margin of safety and is defined as:

$$MS = \frac{\text{allowable load}}{\text{design load}} - 1$$

$$\text{or } MS = \frac{\text{allowable stress}}{\text{design stress}} - 1$$

The allowable load is usually determined by the shape of the part and material properties, it must not be confused with design load. In case of a redundant structure, where failure of an individual element would result in the load being carried by other members, a negative margin of safety may be acceptable. In a well design structure, the margin of safety should be zero or a slight positive value. The positive margin of safety is that overdesigned portion of a structure which cannot practically be eliminated.

#### CASTINGS:

The allowable stresses for castings as specified in MIL-HDBK-5 are obtained from test specimens. The actual cast members often contain hidden imperfections which do not occur in the test specimens. Ductility of castings is often a small fraction of wrought material. It is therefore necessary to use an additional factor of safety, usually 2.00. For castings subject to x-ray inspection, close quality control and controlled ductility this factor may be reduced to a minimum of 1.25.

#### FITTING FACTOR:

Failures are more likely to occur at the end connections of members than in the members themselves, because of local stress concentrations, eccentricities of the connections, or severe vibration conditions. For this reason an additional safety factor (fitting factor) of 1.2 will be used in the

design of connections and fittings.

#### BEARING FACTOR:

Where bolts must resist shock or vibration loading, as in suspension and engine mounts, the bolts tend to hammer back and forth in the holes. This hammering action may enlarge the bolt holes and eventually cause failure of the member if the bearing stress is high. For such conditions a bearing factor of 2.0 will be required.

#### SCREWS IN SHEAR AND TENSION:

Screw threads in shear shall not exceed 30% of full shank rated strength, and the joint will be classified as a friction joint. Due allowance for fatigue in screw and bolt threads shall be made. In structures subject to fatigue, only rolled threads should be allowed on screws and bolts.

Load factors are usually established by estimations from past vehicle performance, and must be approved by the section chief and vehicle manager. As a result of this limitation of authority, design engineers exercise very little control over load factors. The design engineer's greatest contribution to weight reduction is through judicious selection of load transmission path and careful strength analysis. Failure to recognize that design criteria is structural strength (not stress level), will produce inconsistent margins of safety.

Examples of parts which fail at stress levels other than yield or ultimate

1. Structures which may fail at low stress level.
  - a. Plate buckling.
  - b. Columns.
  - c. Flange crimping.
  - d. Twisting.
  - e. Shear buckling.
  - f. Fatigue.
2. Structures which fail at high stress levels.
  - a. Redundant structures.
  - b. Plastic bending (Modulus of rupture).
  - c. Short compression blocks.
  - d. Curved beams of solid section.

The above examples should point out the futility of a specification giving "working stress" for vehicle design. Proper criteria for stress level can only be selected from consideration of part function, shape and mode of failure. Such statements as "working stress 50% of yield" are absurd for vehicle design. In general, hull or frame design should be based on structural strength and not directly on material characteristics.

#### FACTORS OF SAFETY

Suggested safety factors used to obtain design loads from applied loads:

- |                                     |     |
|-------------------------------------|-----|
| 1. Structures in general.           | 1.5 |
| 2. Handling load per specification. |     |
| 3. Bearings. MIL-HDBK-5             |     |
| 4. Joints. MIL-HDBK-5               |     |

The following should be applied in addition to the general structural factor of 1.5.

- |  |      |
|--|------|
| 5. Casting   | 2.00 |
| (With X-Ray, close quality control and<br>minimum elongation of 7%.) | 1.2  |
| 6. Fittings  | 1.2  |
| 7. Gun recoil loads that offer a hazard<br>to personnel              | 1.6  |
| 8. Gun travel lock when loss results in a<br>hazard to personnel     | 1.5  |

#### MATERIAL PROPERTIES

For design purposes it is suggested that material properties be taken from MIL-HDBK-5. Values specified are minimum aircraft material properties and should be considered as probable properties for automotive materials. This publication was compiled for design use and is recommended in lieu of specifications. Several specifications contain elaborate information on grain size, legal requirements, etc., and fail to give tensile strength. Entirely too many specifications are being written without any consideration of the designer, and have become so complex that they are impracticable for design work.

Questions regarding critical material should be answered by the Department of the Army Supply Manual TB-754-1 "Conservation of Material."

Within reasonable limits the cost of material has little effect upon part cost. End product cost depends primarily upon the design engineers efforts to avoid unnecessary complications and expensive manufacturing processes.

### SYMBOLS

Unless otherwise indicated structural symbols and methods of analysis should be in accordance with Military Handbook 5. (MIL-HDBK-5) This handbook presents the best set of structural symbols in existence, and yet many engineers and authors refuse to accept any standard. Each writer flounders through life, dreaming up his own symbols for each problem, and often changes the meaning from one page to the next. This absurd refusal of engineers and authors to accept standard symbols is equivalent to each person dreaming up a new language and spelling system every time the mood strikes. Effective engineering communication can never be achieved unless standard symbols are accepted.

The aluminum and aircraft companies have accepted MIL-5, and found it very satisfactory, and yet military organizations make little effort to abide by their own standards. Authors of ORDP publications, and other military work should be required to comply with MIL-5. This simple step would greatly increase the readability and value of many publications.

### STRUCTURAL REPORTS

Reports establishing and documenting the results of structural analysis usually must include the following:

1. Introduction - to outline what the report is intended to cover or its objective. In many structural reports no introduction is included, and readers waste time looking for information the analyst had no intention of covering.
2. Load Report - in which is presented the basic load on all important elements. Special design methods on which the design is based should be included.
3. Weight Report - to reduce complexity of reports, calculations of weight and center of gravity may be included with the structural report.
4. Structural Analysis - which includes shear and moment diagrams based on loading condition presented in the load report, design criteria, detailed stress analysis and margin of safety.



Structural reports that cannot be retrieved or understood are useless for future reference. The following may help in maintaining reports.

Using an outline drawing of the vehicle, apply vectors for all known external loads. Several outlines may be required to present different loading conditions. Certain loads are obviously not critical and can be eliminated by inspection. At this point load distribution and path must be selected and approximate size of parts calculated. From here on, calculations and revisions constitute design work. For each part the final structural report should contain:

- a. Statement of problem and part number.
- b. Information given pertaining to the problem, and a sketch of the part (if applicable).
- c. Objective of analysis. This can save considerable time for readers.
- d. Solution.
- e. Results, including the margin of safety.
- f. Recommendations: Here the designer should include remarks regarding the part, comments on other approaches which were tried and discarded, and methods which might be applicable to future design.

When the vehicle is complete, arrange the book into a logical order, remove extraneous information, and rework the index.

## REFERENCES

1. Seely and Smith, Advanced Mechanics of Materials, Wiley Pub.
2. Roark, Formulas for Stress and Strain, McGraw-Hill
3. Timoshenko, Strength of Materials, McGraw-Hill
4. Timoshenko, Theory of Plates and Shells, McGraw-Hill
5. ASME Handbook, Metal Engineering Design
6. Alum. Company of America, Alcoa Structural Handbook
7. Gerard, Minimum Weight Analysis of Compression Structures, Interscience
8. F. R. Shanley, Weight Strength Analysis of Aircraft Structures, Dover Publications, Inc., New York, N. Y.
9. M. Hetenyi, Handbook of Experimental Stress Analysis, John Wiley and Sons
10. Summerill Tubing Co., Aircraft Tubing Data
11. Bleich, Buckling Strength of Metal Structures, McGraw-Hill
12. Associated Spring Corporation, Handbook of Mechanical Spring Design
13. McGraw-Hill, Shock and Vibration Handbook
14. Strength of Metal Aircraft Elements, MIL-HDBK-5
15. NACA Index of Aircraft Structures Research Reports June 1947, NACA Index No. 7E29
16. NACA Index of NACA Technical Publications 1915 1949 US 92 A 25, Later Index by years
17. HIAD - Handbook of Instruction for Aircraft Designers
18. HIGED - Handbook of Instructions for Ground Equipment Designers

19. HIAGSED - Handbook of Instructions for Aircraft Ground Support Equipment Designers
20. Ordnance Corps Pamphlet (ORDP)
21. Military Handbooks
22. Mobility Requirements, Ground Support Equipment, General Specification for MIL-M-8090
23. ARDC TR-59-1 Production Design Handbook

# THE EFFECT OF HIGH RATE LOADING ON THE MECHANICAL PROPERTIES OF ORDNANCE MATERIALS

Alexander Hammer\* and Hubert Cadle\*\*

## ABSTRACT

It is a well-known fact that Cr -Mo -V Steel, presently the best available barrel material because of its high strength and erosion resisting properties, has a yield strength of 15,000 psi at a temperature of 1200°F. It is equally well known that Cal .30 barrels made from this material and fired seven 125-round bursts become hotter than 1200°F in the area in front of the liner. The most advanced but static theories indicate 75,000 psi total equivalent stress in this area; i.e., a value about five times larger than the statically determined yield stress. These barrels were gaged after firing and no plastic deformation could be detected, eliminating any possible tie-in with plastic design theories. Now, either the stresses are actually less than those calculated, or the mechanical properties of the metals at high rate loading are well above those values which are presently considered by design engineers.

Primary purpose of the investigation, results of which are reported in the paper, is to prove the latter. The investigation was conducted with a gas system testing fixture in which gas, emitted while firing a gun, is used to initiate pressures in test specimens. In this fixture, Cal .30 barrels were modified to allow the gas to escape through an orifice into a gas cylinder. The size of this orifice, its location along the barrel, the initial volume of the gas cylinder, the movement of piston in the gas cylinder so as to allow its volume to be changed, and the weight of the moving piston are parameters which can be changed to vary the characteristics of the gas pressure in the cylinder.

The parameters of the test vehicle were changed and three distinctly different reproducible families of pressure-time curves were obtained in the gas cylinder, each one having the same peak pressure, but

---

\* Dr. Alexander Hammer, Chief, Mechanical Research Branch, Springfield Armory, Springfield, Massachusetts

\*\* Mr. Hubert H. Cadle, Mechanical Engineer, Research & Development, Springfield Armory, Springfield, Massachusetts

the time to obtain same varied from .5 to 1.5 ms. Through differential areas the pressure in the cylinder was increased ninefold, and through a fluid medium was applied against the internal walls of cylindrical test specimens. Pressures, measured in the fluid, were correlated to stresses and strains established on the surfaces of the specimens, and it was found that specimens which yielded, when loaded statically, at 100,000 psi stress, remained elastic under dynamic conditions even at 120,000 psi stress, indicating a clear 20 per cent gain for the material tested at existing conditions.

A very important area directly affected by the investigation is light-weight design. It can be proven that the mechanical properties of Ordnance materials at actual working conditions are in excess of those which are used at present as design criteria and it is evident that large numbers of weapon components were overdesigned, that they are too big and too heavy.

One appreciates that maintaining the present high stresses, but reducing weight will be preferred to reducing stresses in unchanged over-designed components.

---

It is a well-established fact that Cr-Mo-V steel, presently the best available barrel material because of its high strength and erosion-resisting properties, has a yield strength of approximately 15,000 psi at a temperature of 1200°F. It is equally well-established that Cal .30 barrels made from this material when fired seven 125-round bursts became hotter than 1200°F in the area forward of the liner. The most advanced static theories indicate 75,000 psi total equivalent stress in this area; i.e., a value about five times larger than the basic static theory suggests. These barrels were gaged before and after firing, and no plastic deformation could be detected, thereby eliminating any possible tie-in with plastic design theories. Now, either the stresses are actually less than those calculated, or the mechanical properties of the metals at high rate loading are well above those values which are presently considered by design engineers. In either case the result is overdesign of components and in consequence waste of materials, manufacturing time, storage place and transportation cost and sometimes the difference between optimum and not feasible design.

The first step in the investigation, with which we are concerned here, was to establish the relationship between static and dynamic yield stresses in a material at ambient temperature. Since barrel design falls in a particular problem area, Cr-Mo-V steel in the form of thick-wall tubes was chosen for testing.

In small arms barrel design, rifling and friction forces are present, but they are small in magnitude and are neglected. The force with which we are concerned, then, is the internal pressure which acts so as to produce tangential and radial strains in the tube. The test specimen was designed in such a manner as to minimize longitudinal forces and end effects.

Figure 1 shows the test specimen in the form of a thick-wall tube. The length of the test specimen was so established that the effect of the reinforced ends would not be reflected in the center section. Available theory was used to determine the spacing of reinforcing bands on a tube in such a manner that the effect of one would not influence the effect of the band adjacent to it. This length was doubled and the necessary length to provide a portion which should respond like an infinitely long tube was added.

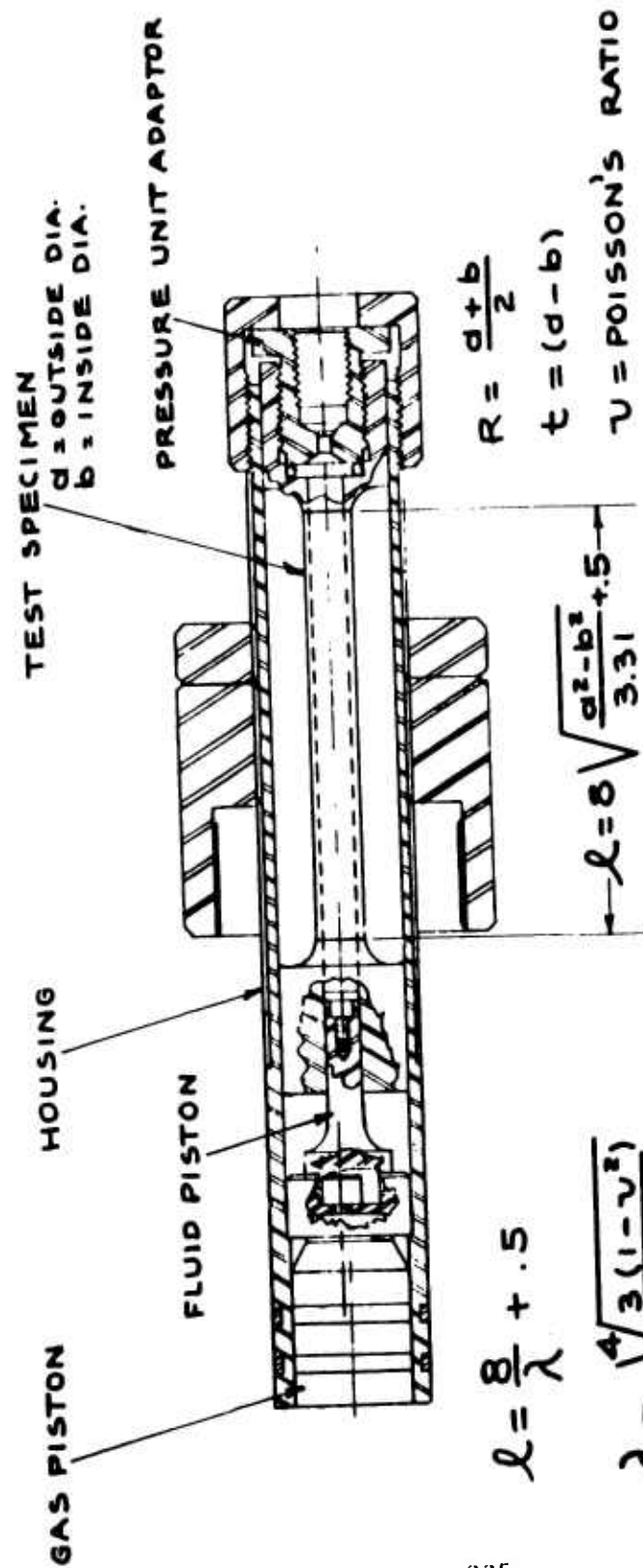
A piston at one end, and an adapter for a pressure transducer at the other entraps a fluid medium. The test specimen is encased in such a manner that the reaction of the force applied to the piston is absorbed at one end while the other is permitted to float free. Force is applied to the piston in the casing and is transmitted to the fluid by the piston in the test specimen. The resultant pressure of the fluid acts upon the pressure transducer and also upon the walls of the specimen.

In the center of the specimen, one foil strain gage is mounted in the tangential direction and another is mounted in the longitudinal direction. Unilateral applied strain in the tangential direction on the outside surface of an infinitely long thick-wall tube is the result of an application of internal pressure. The longitudinal gage, then, should monitor that strain reflecting Poisson's Ratio.

Figure 2 is a picture of the test specimen, adaptor, and component parts. An "O" ring with a teflon spiral back-up washer seals the small piston. A glass-fibre-impregnated teflon washer seals the pressure adapter. A Kistler 601 pressure transducer is used to monitor the internal pressure. Incidentally, the area ratio of the piston in the adapter to that in the specimen is nearly 9/1.

In a variety of small arms, the chamber pressure resulting from the burning of the charge is in the neighborhood of 50,000 psi. The time required to reach this pressure is usually about .5 milliseconds.

Figure 3 shows a characteristic pressure-time curve taken in the chamber of a Cal .50 gun. The pressure reaches approximately 50,000 psi and the rise time is about .6 milliseconds.



225

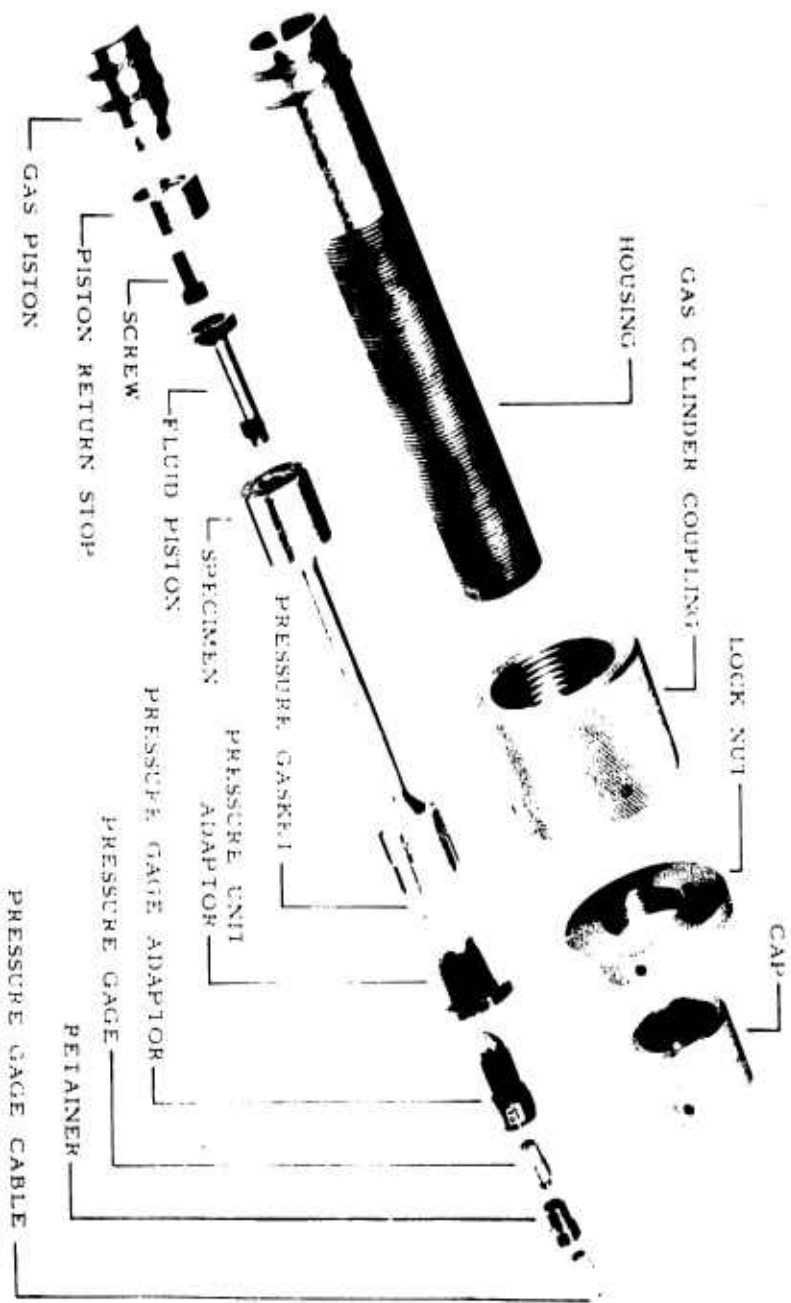
$$L = \frac{8}{\lambda} + .5$$

$$\lambda = \sqrt[4]{\frac{3(1-\nu^2)}{R^2 t^2}}$$

$$\lambda = \sqrt{\frac{3.31}{(d^2 - b^2)}}$$

# INTERNAL PRESSURE TEST SPECIMEN

Fig. 1



19-058-1035/ORD-60

SPRINGFIELD ARMORY - ORDNANCE CORPS

20 Sept 1950

PRESSURE SPECIMEN WITH COMPONENT PARTS

Fig. 2



PRESSURE - TIME FOR CAL 50 GUN CHAMBER

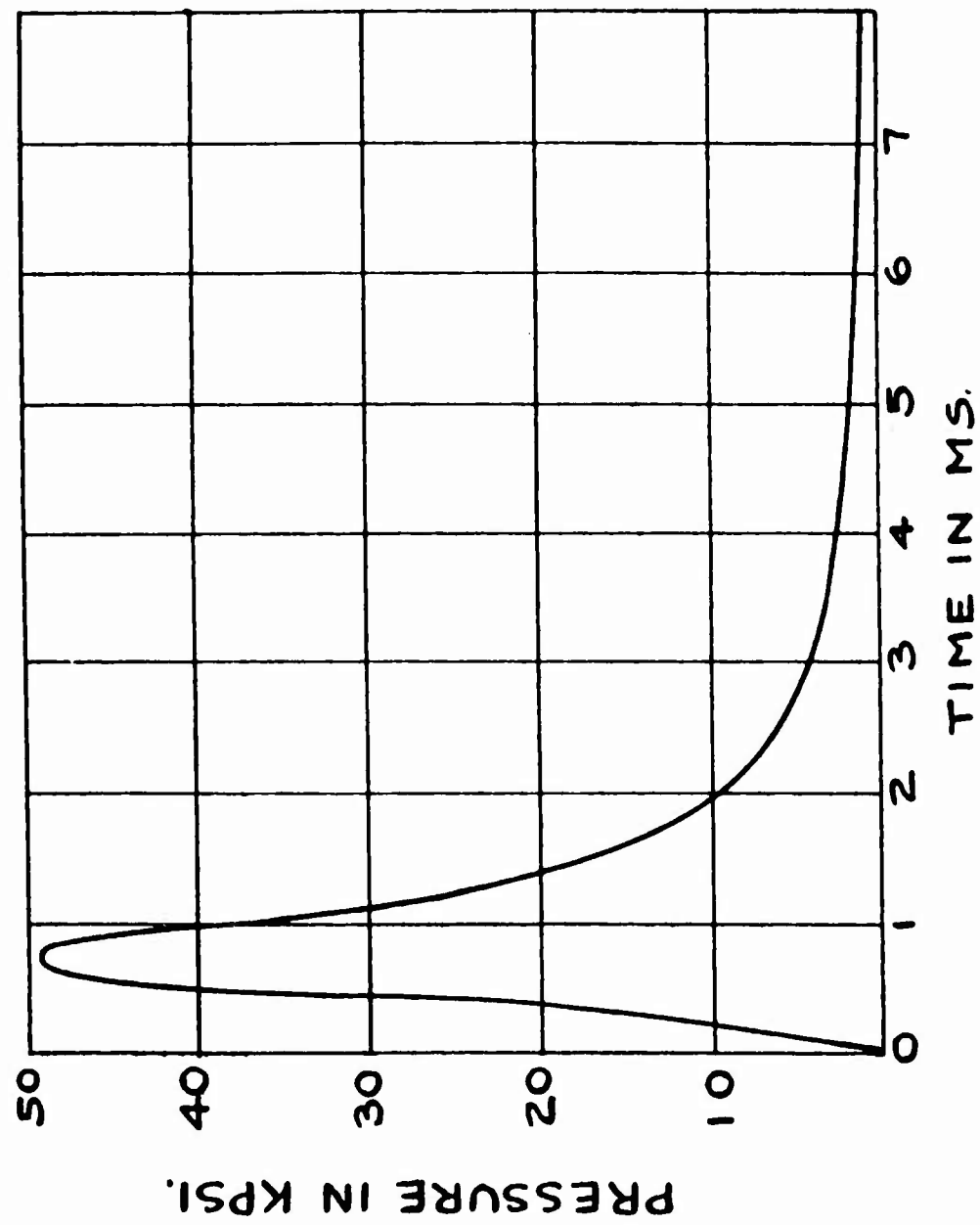


Fig. 3

A gas system testing fixture (Figure 4) was modified by the addition of the specimen adapter which was shown in the first and second figures. Through the use of this fixture it is possible to apply dynamic loads similar to those obtained in the firing of a gun. The propellant gas from a Cal .30 rifle is bled from a port in the side of the barrel into a gas cylinder. This gas pressure is impinged on the piston located in the specimen adapter which in turn forces the piston in the test specimen against the fluid medium. The pressure in the gas cylinder is magnified in the specimen by the differential areas of the two pistons. The compressed fluid applies the resulting pressure against the walls of the test specimen. In the gas system testing fixture, various parameters, such as the size and position of the gas port in the gun barrel, and the initial volume of the gas cylinder can be changed so as to obtain the necessary pressure-time relationships.

Figure 5 depicts a pressure-time curve obtained through the use of the gas system testing fixture. The pressure is approximately 48,000 psi and the rise time is about .5 milliseconds. The useful portion of the curve is not unlike the actual chamber pressure-curve shown previously. The pressure fluctuations which appear after the main peak are of no consequence, providing that the pressure there is lower than that which would cause the material to yield in a static test.

The instrumentation used to monitor pressure, time, and strain is shown in Figure 6. A Kistler amplifier delivers the pressure pulse to a Tektronix 551 Dual Beam oscilloscope and a 536 X-Y scope. In static tests, the tangential and longitudinal strain are monitored separately through transducer plug-in units powered by a Tektronix 127. Dynamic strains are monitored through a DC balancing and calibrating unit. These signals are delivered to both scopes through choppers so as to provide the extra trace of each scope. Through this system, the dual beam scope produces the three variables vs. time, while the X-Y scope shows pressure vs. tangential strain and pressure vs. longitudinal strain.

Polaroid camera photographs were taken of the test data delivered to the oscilloscopes. Pressure, tangential strain, and longitudinal strain plotted against time is shown in Figure 7. These curves tell us little more than to assure that the rise time is that in which we are interested. Looking at the pressure curve, the rise time is about .5 milliseconds. A rough comparison between the pressure and tangential strain curves leads us to expect that these variables are proportional to each other.

It is apparent from the shape of the pressure-strain curve (Figure 8) that this test specimen did not yield on the outside surface. The specimen is one of a series designed to bracket the yield point of the material. Furthermore, we now see the longitudinal strain as compression according

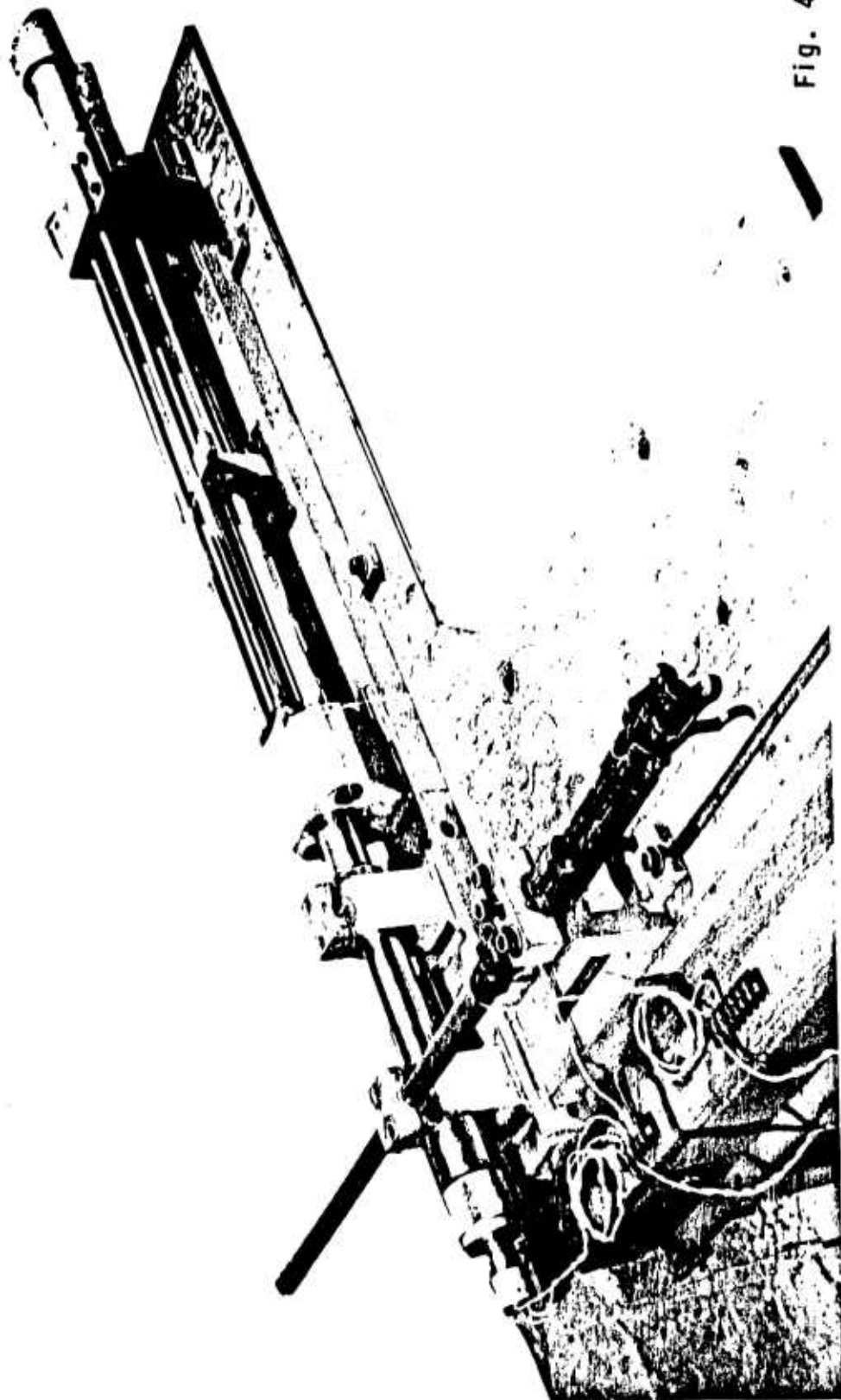


Fig. 4

SPRINGFIELD ARMORY- ORDNANCE CORPS

Proj:

Date: 19 Sept 1960

Neg: 19-058-1009/ORD-60

GAS SYSTEM TESTING-FIXTURE MODIFIED TO APPLY PRESSURE TO TEST SPECIMENS

PRESSURE CHARACTERISTICS IN TEST SPECIMEN

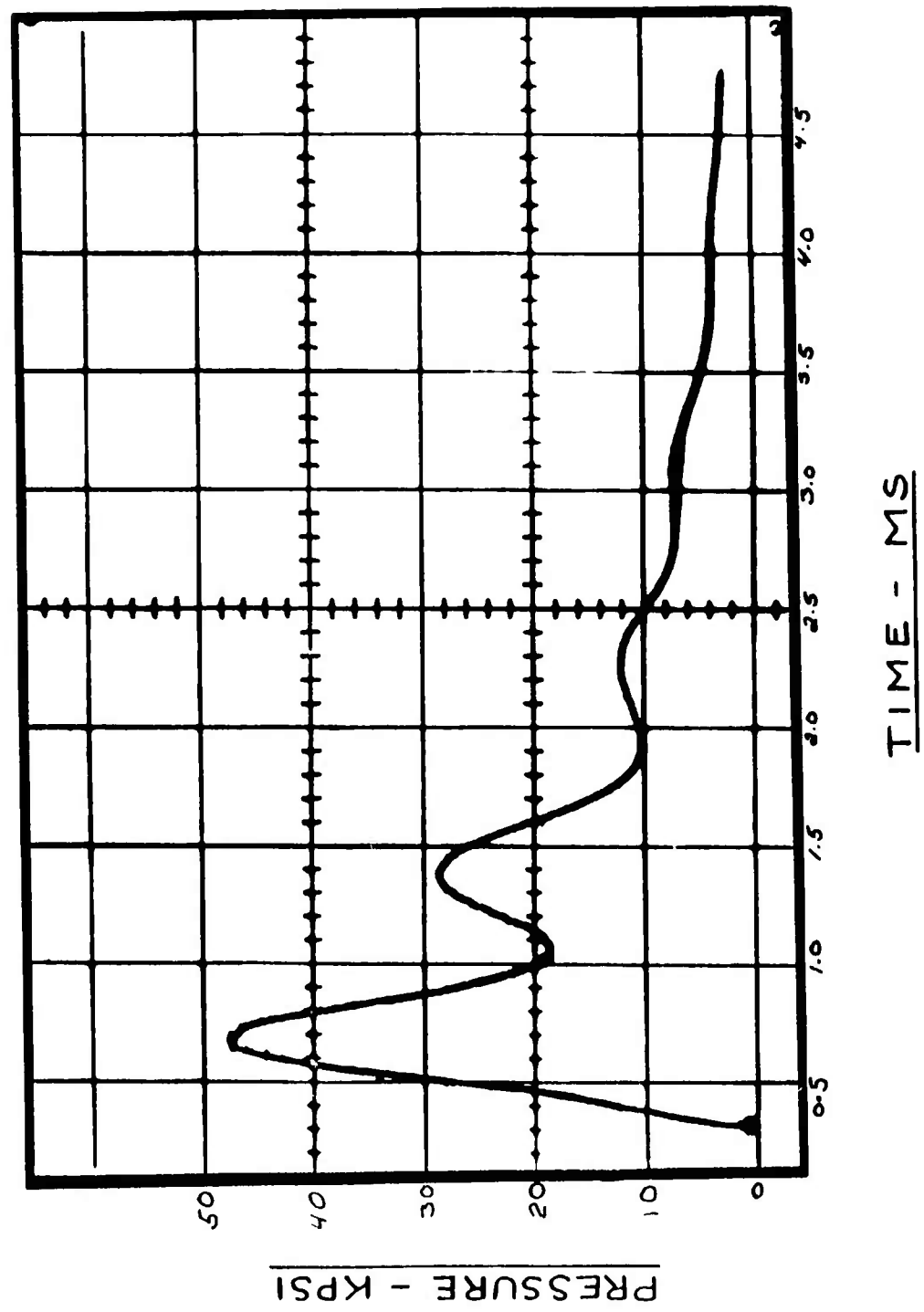


Fig. 5

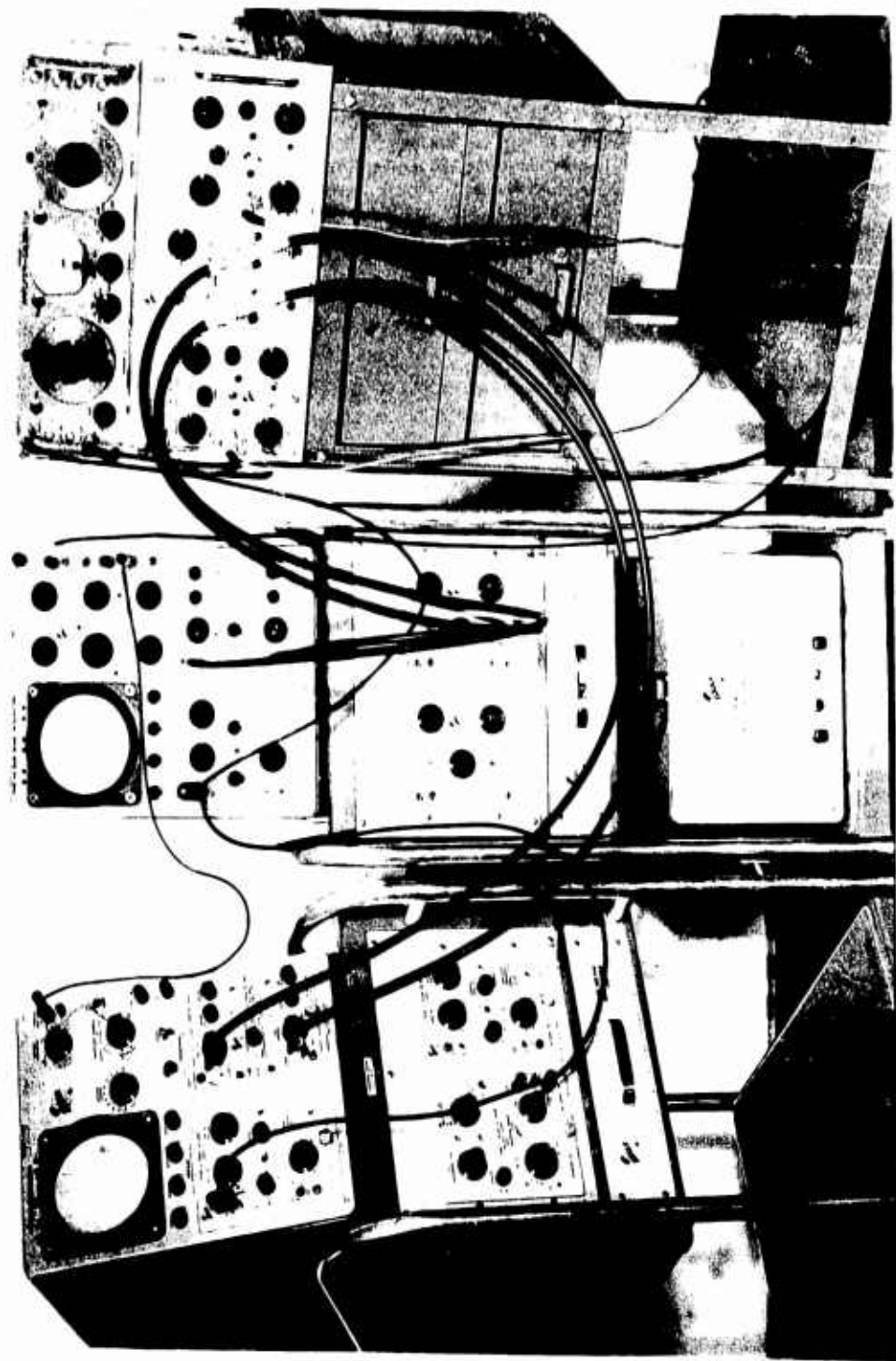


Fig. 6

TIME PRESSURE, AND STRAIN RECORDING EQUIPMENT

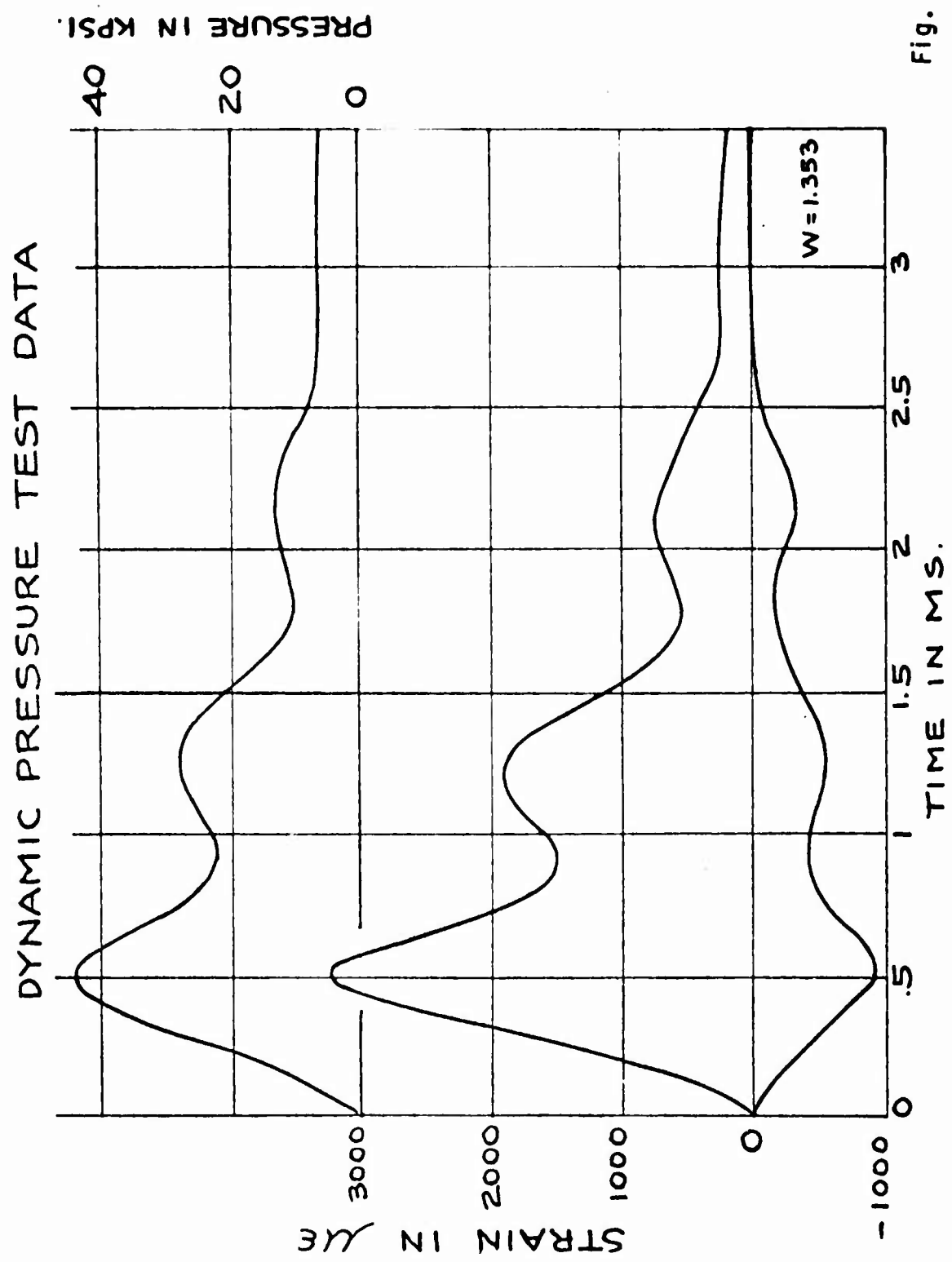


Fig. 7

# DYNAMIC PRESSURE TEST DATA

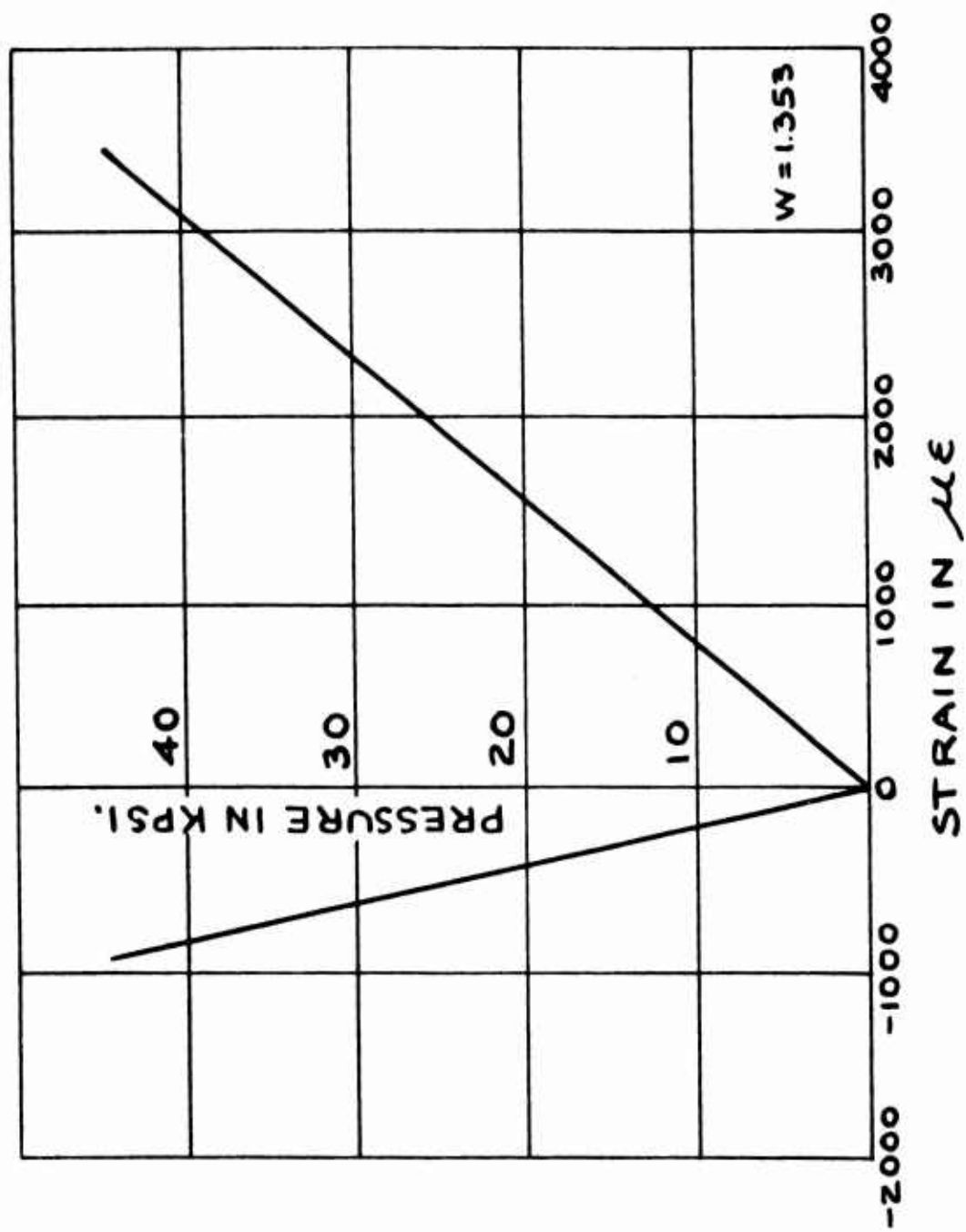


Fig. 8

to our predictions. If a negligible amount of friction from the bearing of the piston "O" ring on the inside wall of the specimen results in a negligible compressive force, the longitudinal strain should reflect a value which is no greater than that expected by Poisson's Ratio. In other words, the slope of the longitudinal strain curve should be 25% to 30% that of the tangential strain curve.

Using another test specimen, static force is applied through the same adapter used in the dynamic test. It was not necessary to record a plot of the three variables vs. time.

These static data (Figure 9) of pressure vs. tangential strain and longitudinal strain are like the dynamic curves except that the specimen is allowed to yield. Again we have obtained the compressive strain which should reflect Poisson's Ratio.

To check the basic validity of the data; however, it is necessary to compare the ratio of longitudinal to tangential strain obtained in the dynamic test to that obtained in the static test. If the two ratios are the same, it is reasonable to assume that the forces transmitted to the walls of each test specimen are of the same type, and that Poisson's Ratio in the dynamic application did not differ from that established in the static situation. We may now arrange the data so that the dynamic stresses can be compared to the static stresses.

We have established that the ratio of longitudinal strain to tangential strain is the same for both cases. The Lamé relationships (Figure 10) may be used to transform the pressure-strain curves to stress-strain curves. The wall ratio of each test specimen was obtained by measuring the inside diameter with an air gage and the outside diameter with special micrometers each sensitive to the nearest 50 millionths of an inch. The concentricity was checked by actually measuring the variation in thickness of the tube wall at the section where the strain gages are mounted.

Considering the outside surface of the tube where the strain measurements are taken, we observe that this boundary condition precludes radial stress. Conveniently, then, the equivalent pressure stress is the unilateral tangential stress,

$$\sigma_c = \frac{2P}{W^2 - 1}$$

where the pressure is the measured quantity at the measured tangential strain.



# STATIC PRESSURE TEST DATA

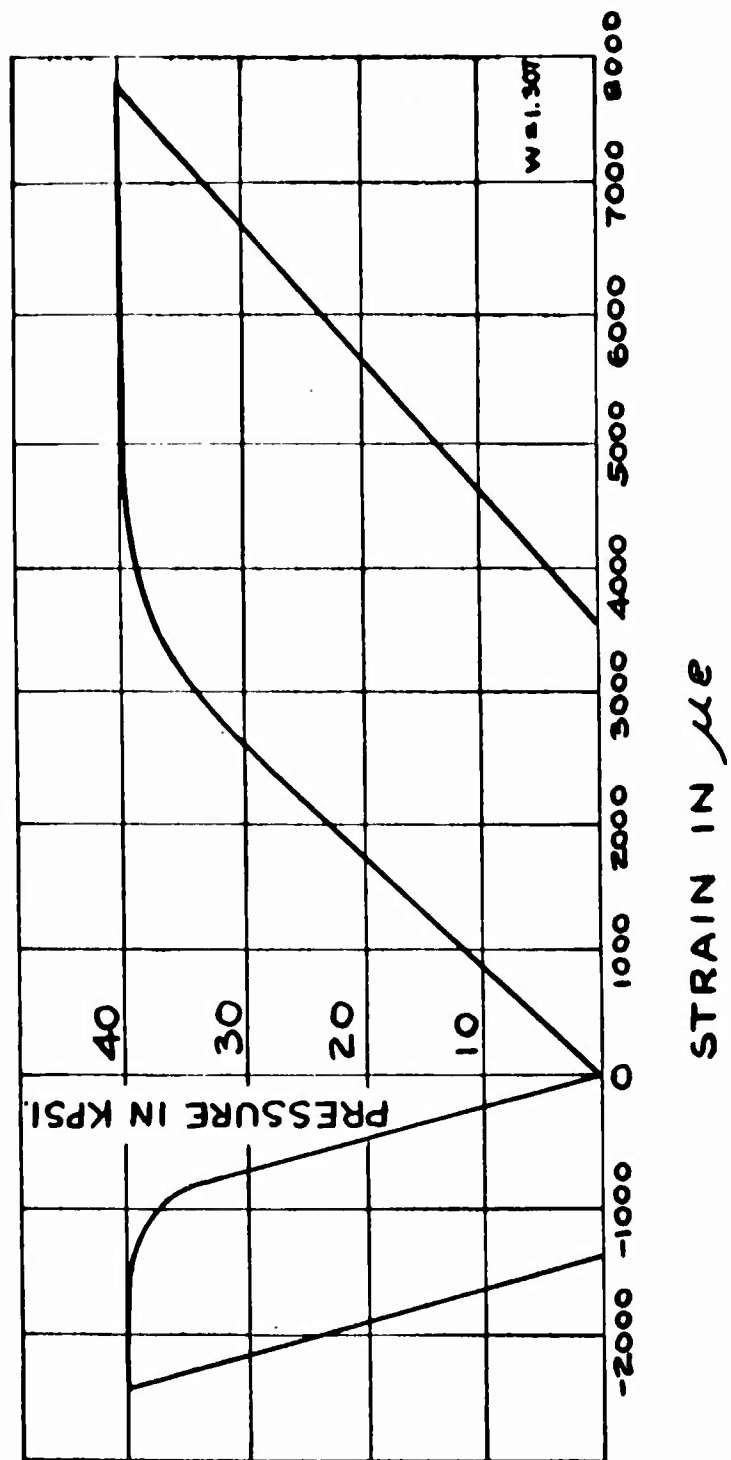
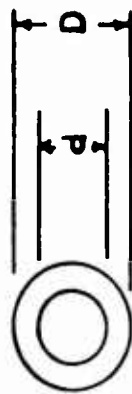


Fig. 9

LAME' RELATIONSHIPS FOR THICK WALL TUBES  
AND  
TOTAL EQUIVALENT STRESS BASED ON von MISES-HENCKY THEORY



Internal Pressure Only

Inside Surface Conditions

$$\sigma_e = P \frac{W^2 + 1}{W^2 - 1}$$

$$\sigma_r = -P$$

$$\sigma_e = (\sigma_e^2 + \sigma_r^2 - \sigma_e \sigma_r)^{1/2} \\ = P \frac{(3W^2 + 1)^{1/2}}{W^2 - 1}$$

$$W = \left[ \frac{\sigma_e^2 + P(4\sigma_e^2 - 3P^2)^{1/2}}{\sigma_e^2 - 3P^2} \right]^{1/2}$$

Outside Surface Conditions

$$\sigma_e = \frac{2P}{W^2 - 1}$$

$$\sigma_r = 0$$

$$\sigma_e = \frac{2P}{W^2 - 1}$$

$W$	Wall Ratio	$= \frac{D}{d}$
$\sigma_e$	Tangential Stress	
$\sigma_r$	Radial Stress	
$\sigma_e$	Equivalent Pressure Stress	
$P$	Internal Pressure	

Fig. 10

Figure 11 shows the characteristic stress-strain curves reflecting the dynamic and static data. We first observe that Young's Modulus of proportionality stress to strain is the same in both the static and dynamic situations. And the answer to our problem appears in the fact that the dynamic stress is greater than the static stress at the yield point of the material in each case. Here the ratio of dynamic yield stress to static yield stress is about 1.15.

Now, since we are concerned with the soundness of the entire tube when faced with a design problem, we may resort to the Lamé relationships for the inside surface (Figure 10). Here the stresses are tangential and radial. Combining these stresses according to the von Mises-Hencky theory of failure,

$$\sigma_e = P \frac{\sqrt{3W^4 + 1}}{W^2 - 1}$$

and solving for the design wall ratio, we have this expression:

$$W^2 = \frac{\sigma_e^2 + P\sqrt{4\sigma_e^2 - 3P^2}}{\sigma_e^2 - 3P^2}$$

In order to obtain practical values for W, limitations put on the interrelation of pressure and equivalent pressure stress are obvious.

Test results indicate that for the selected wall ratios of 1.35 - 1.38, for the described load application, and for internal pressures which peak in approximately .5 milliseconds, the equivalent pressure stress increased by a factor K = 1.15. However, in actual design of Cr-Mo-V tubes which must withstand internal pressures alone, this factor K is assumed to be 1.30.

It is possible that the assumed 30% increase of yield strength results in some slight but surely not detrimental permanent deformation of the inside surface of the tube and further experimentation will be needed to correlate laboratory results to practically proven empirical design criteria.

In reference to the phenomenon experienced with the Cal .30 barrel, the statically determined yield strength, at the proper elevated temperature, will have to be increased many times in dynamic application, if the presently used factor K = 5, applied to obtain the permissible total equivalent stress, should be proven to be correct in laboratory application.

Future investigation will include tests similar to this one, but performed on different materials; test specimens will be subjected to constant high and low temperature; and finally, transient temperature and repeated high rate loading will be induced, thereby simulating the effects of automatic firing with small arms weapons.

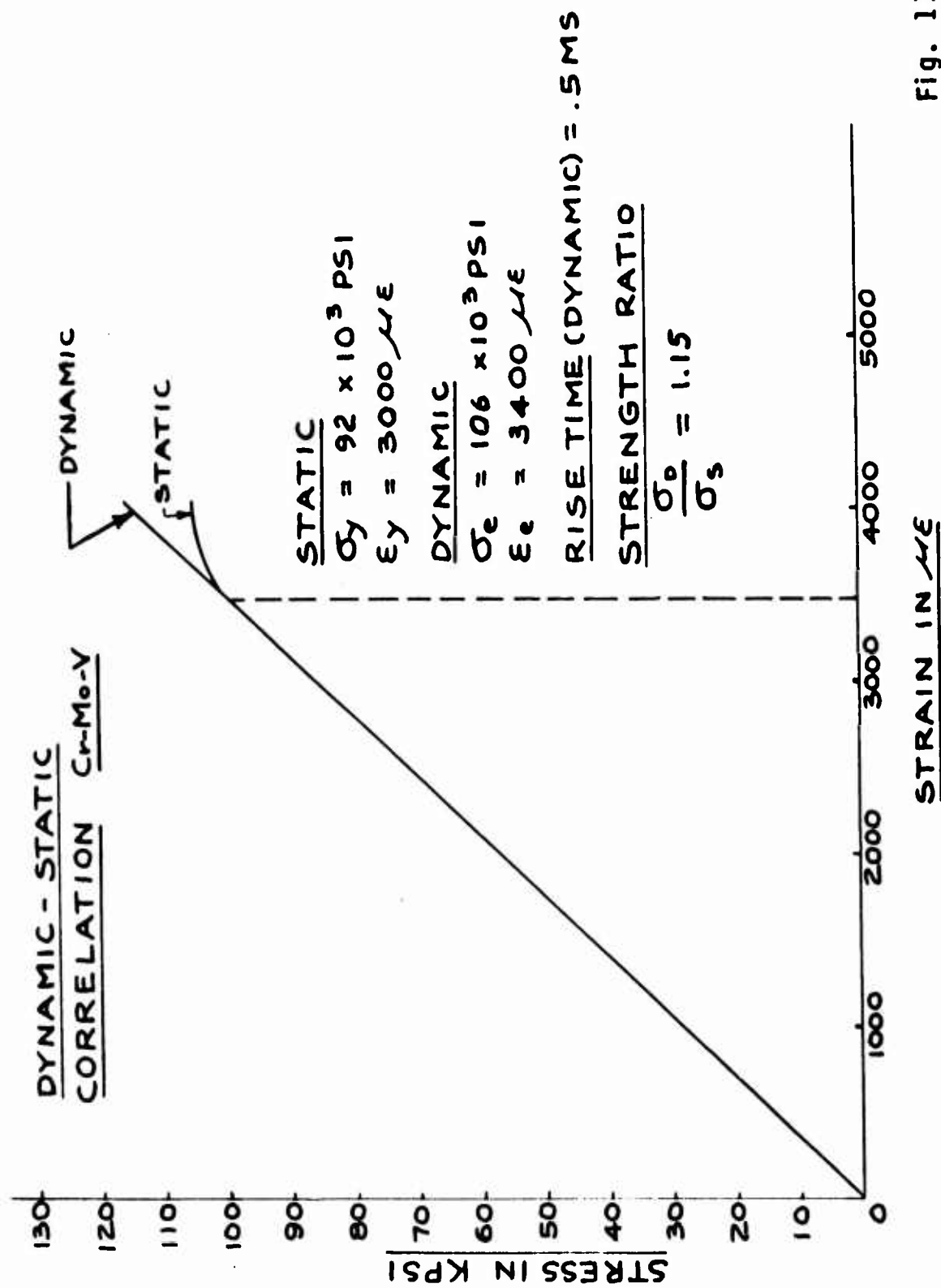


**Fig. 11**

#### INTRODUCTORY COMMENTS BY DR. ALEXANDER HAMMER:

When Design Criteria was selected as subject for Sessions III and IV, it was hoped that papers would be presented which would help the designer of Army materiel in his task to achieve optimum design. We held Conferences in the past when the scientists spoke to scientists. This time, we were fortunate enough to secure the participation of a large number of designers, and we intend to help them by proving or disproving the validity of certain empirical postulates concerning the increase of yield strength of materials, when the time necessary to reach peak loading is only half to one millisecond, which characterizes small arms barrel design.

As a sort of introduction to the two papers to be presented by Springfield Armory at this Session, I would like to mention the fact that if the Cal .30 all purpose machine gun barrel is fired seven 125-round bursts, needing each time 14 seconds for firing and 46 seconds for cooling, the outside surface of the barrel about 2 inches in front of the liner, i. e., about 12 inches from the breech end, becomes 1400°F hot. The temperature at the inside surface, of course, is much higher. Even if we assume an average temperature of 1400°F, the yield strength of the barrel material, Cr-Mo-V steel, equals about 10,000 psi. The total equivalent stress in this barrel at the above mentioned position, considering the pressure and temperature stresses, equals 70,000 psi, which is seven times higher than the yield stress of the material at 1400°F.

There is no interrelation with plastic theories, because careful checking of the outside surface dimensions proves no changes. At the inside surface, permanent deformation may have taken place, but not sufficient to be detrimental to the life of the barrel which is determined by the criteria of 200 fps muzzle velocity drop or 20% keyholing.

If the barrel designer would accept the 10,000 psi yield stress as design criteria, he would end up with an extremely heavy barrel. And this barrel, design-wise, would be worse than a light one because the thermal stresses in it would be excessive, being directly proportional to the temperature difference which is much larger in a heavy barrel than in a light one. The lighter, thinner barrel will be hotter, but the thermal stresses in it will be reduced considerably.

I fully agree with the statement that one picture is worth thousands of words and to help you visualize above statements I will show you a colored motion picture about firing a Cal .30 tank machine gun barrel three thousand rounds without interruption. This barrel is covered by a jacket. In order to give you a better view, some of the holes in the jacket were eliminated.

The showing-time is short and I do not want to interrupt it, so I tell you now that the barrel is gaged before firing, it becomes cherry-hot during firing and is gaged after firing. From the colors, judge for yourself the temperatures, and the gaging results will indicate the status of the barrel before and after firing.

Three Government laboratories, located in Watertown, Watervliet and Springfield are engaged at present in activities covering the dynamic behavior of materials. It would be beneficial to correlate these activities which use different methods to induce impact loading peaking in from half a millisecond to ten milliseconds time. The test specimens used are of different designs, sizes and materials.

Only after we do test identical specimens and induce loadings of the same peaking time, will we be permitted to correlate our results. If the application of gas-hydraulic-or steam pressures will not result in appreciable differences, we may divide the field and cover only that portion of the time band which is closest to our particular area of load application.

#### DISCUSSION:

Mr. Zaroodny: I want to express my admiration for this paper which perhaps we didn't applaud loud enough. And would you allow me to make a recollection: In the early years of the war Mr. Kent's development of the theory of piezo electric gages was still something of fairly novel and it was a great disappointment to us at APG that the actual establishment of the powder charge had been done with the help of copper crush gages. However, there was a 15 to 20% discrepancy between pressure measurements made with piezo electric or copper crush gages. The story goes that Mr. Kent had brought this fact to the attention of the Chief of Ordnance, General Barns, who allegedly said: This war will be won with copper pressures. Well it has been and now after some time after the war, I am extremely happy to see another explanation of the factor 1.2.

Dr. Kumar: I would like to commend the fine presentation that we heard just now and the fine movie by Dr. Hammer and Mr. Cadle. I have only a couple of questions about the design theory. It is very beautiful to see how the whole thing has been demonstrated experimentally. The analytical explanation of it may reveal even more. I see that you are using von Mises-Hencky theory of failure and considering only the pressure stresses. If you would consider the thermal stresses also you could improve the theory still more.

Dr. Hammer: In our first series of tests we did not consider temperature effects because only single shots were fired with the testing fixture. Consequently the used analytical equations were correct. However, if and when

temperature will be considered, we will have to prove much larger differences between dynamic and static yielding than the 15% found at ambient temperature. Designers today, and this is proven by practical experience, permit total equivalent stresses manyfold of that of yield at various elevated temperatures. Even for pressure stresses alone and for the barrel material mentioned the intuitively accepted increase is 30 to 40%. So you see, there is still a discrepancy between laboratory results and those observed or proven by actual experience.

Glenn Taylor - APG, BRL: Would you care to comment on the deformation, if any, on the bore of Cal .30 tubes after prolonged tests at elevated temperatures?

Mr. Cadle: I think perhaps Dr. Hammer would want to talk about this.

Dr. Hammer: It depends what do you consider "prolonged test at elevated temperatures". I witnessed erosion tests with 85-round bursts the barrel lasting at least 5,000 shots, or with 125-round bursts firing at least 3,000 shots. There were no dimensional changes at the outside surface. What happened at the inside was hard to determine because of the simultaneous happening of yield and erosion. However, as long as the criteria for barrel life was met, the barrel was considered sound. No matter how hot the barrel got, up to temperatures mentioned before, if opportunity was given to periodical cooling, it could and actually did last 25,000 shots. Now, to answer your specific question concerning the deformation of the bore of the barrel which fired without interruption 3,000 shots and was shown to you on the colored motion picture, no doubt, it could not be considered serviceable any more. Its rifling was lost completely. Again, I must mention, the mechanical and chemical effects were present simultaneously.

## DETERMINATION OF YIELD STRENGTHS OF ENGINEERING MATERIALS AT HIGH LOADING RATES

Earl H. Abbe\*

### ABSTRACT

Several years ago a small project was initiated at Springfield Armory to investigate the effect of Loading Rate on the Yield Strength of Face Centered Cubic, Body Centered Cubic, and Close Packed Hexagonal Materials. This investigation was sponsored by Office of Ordnance Research.

An attempt was made to devise a simple dynamic test. To this end a fixture designed and fabricated by Westinghouse Electric Co. was used. This fixture contained a short hollow cylindrical fluid filled specimen between two parallel circular plates, held together by three equally spaced bolts. The upper plate contained a piston, which when struck by a falling weight, transmitted the force to the fluid filled specimen. The lower plate contained an instrumented plunger which recorded the force and time. A major disadvantage of the system was the development of end clamping effects which were not measurable because of lack of adequate instrumentation.

The approximate ratios of static to dynamic yield strength at a strain rate of approximately 300 inches/inch/sec. are reported.

A new fixture was designed which eliminated the end effects. It consists of a circular plate mounted on three short columns and a piston in the center. The specimen, a hollow cylinder approximately 4 inches long is threaded into the bottom of the circular plate in line with the piston. The lower end of the specimen is threaded into a thick hollow cylinder with a plunger inserted into its lower end. The end of this plunger rests on the base plate which supports the fixture.

Data on 4340 steel quenched and tempered to 140,000 psi tensile strength tested on this fixture together with tensile specimens of the same material and heat treated to the same physical properties and tested by Watertown Arsenal at a lower strain rate are reported.

---

Increasing demands upon the engineer to design and develop stronger, lighter structures has led him to seek new design criteria. The area in which we are particularly concerned in this investigation, is the dynamic behavior of metals. It has been found that many materials appear to behave elastically, when dynamically loaded, at stresses greater than

---

\*Mr. Earl H. Abbe, Supervisory Physical Metallurgist, Springfield Armory, Springfield, Massachusetts



those necessary to induce plastic deformation when statically loaded.

Our ultimate objective is to obtain sufficient data to produce a family of curves for several engineering materials, such as is schematically represented in Figure 1. The ordinates represent the yield strength and the strain rate is progressively increasing on the abscissa. This is a purely idealistic concept where A, B, and C represent the static yield strength of three materials and the curves originating at these points might illustrate the dynamic behavior of these materials at various strain rates. The dynamic yield strengths at strain rate 2 would be G, H, and I respectively. Let us now suppose that whereas the loading may approach strain rate 2, the minimum strain rate is 1. The designer must use the minimum strain rate in order to avoid plastic deformation, therefore, he could use the values D, E, and F less, of course, the selected factor of safety.

Figure 2 illustrates a series of load vs time traces for some material. Load A represents the static yield strength. Curves X, Y, and Z represent three different loading cycles. By construction curves X and Y have the same maximum load C. The strain rate of X  $\left(\frac{D}{T} \text{ or } \tan \alpha\right)$  is somewhat greater than  $\frac{D}{K}$  or  $\tan \beta$  and if the material is sensitive, or perhaps I should say, less sensitive, then the material loaded in accordance with curve Y should be more liable to plastically deform than the same material loaded in accordance with curve X. Will the material behave in this manner? Before we investigate this subject further let us look at curve Z. It was so constructed that the loading rate is exactly the same as Y, however, it peaks at load B and the load is maintained for a considerably longer period of time. Z only reaches a maximum of B, which is much lower than C, although both of these are greater than the static yield strength A. With the same loading rate, will material loaded in accordance with trace Y be more liable to plastically deform than the same material loaded in accordance with Z due to the greater load level?

Another criteria is based on rise time and OP, QQ, and OR would represent the rise time for X, Y, and Z respectively. Based on this criteria Y would be more liable to plastically deform than X but I am not sure how to estimate the relative behavior of Z in relation to X and Y. Under this concept, due to the lack of symmetry of the loading and unloading, pulse duration OL, OM, and ON may be reported with  $\frac{OL}{2}$ ,  $\frac{OM}{2}$ , and  $\frac{ON}{2}$  as loading time.

No plastic deformation would be expected for any of these cycles if the static yield strength on this diagram were at C instead of A, if the material in general is insensitive to load rate below static yield point, then only that portion of the curve above level A is significant and the only criteria should be S, T, U, AB, and AC. Now S and T are equal but U is much greater; will Z, therefore, plastically yield before X and Y or since AC is much greater than AB will these yield before Z? Perhaps it is the area of the curve above the static yield strength which will determine

the order of plastic deformation of the material. If this be the case all three should behave in the same manner since these areas are all approximately equal. Probably the behavior is related to overstress, rate of loading above yield strength, and duration of the overstress.

Based on the above discussion we feel that the structure must be designed, using a dynamic criteria representing all the conditions, selecting the least dynamic influence with the probability that more instantaneous loads will have less effect on the material. Of course, high explosives with rise time in the order of microseconds or less may result in an entirely different behavior of the material, this is why the curves in Figure 1 dropped off at the right hand side of the diagram.

A few years ago we were engaged in a modest investigation of "Effect of Crystalline Structure of Metals on Ratio of Static to Dynamic Yield Strength" sponsored by the then Office of Ordnance Research. We employed a cylindrical specimen and drop weight machines to induce an impulse load. Figures 3 & 4 illustrate the drop testers. The Tinius Olsen Impact Tester employs a 10 and a 20 pound hammer which can be dropped from any height up to 10 feet. The Westinghouse machine has a carriage weighing 26 pounds which can be loaded with weights up to 321 pounds. The drop height can be varied continuously to 3 - 1/2 feet by presetting hoist limit and drop limit microswitches. A table, weighing approximately 1600 pounds, on which the fixture is mounted, rests on a large coil spring and is free to slide between the rails.

The fixture is illustrated in Figure 5. The specimen, a ring one half inch high, one half inch bore, and having a maximum outside diameter of one inch, is clamped between the upper and lower heads. A piston fits into a hole in the upper head and an instrumented plunger extends through the lower head. The space inside the specimen between the piston and the instrumented bar is filled with a fluid (glycerine). A blow on the piston causes an internal pressure to induce a circumferential strain in the specimen. In this system it was difficult to prevent leakage and eliminate the effect of axial compressive stresses.

At a recent meeting of engineers and scientists of Watervliet Arsenal and Springfield Armory it was proposed that several of the approaches to the dynamic yield strength be explored using a common material and similar conditions of loading rates and pressures in an attempt to determine what degree of correlation exists.

We were invited to participate and in June of this year initiated the present investigation. Our objectives were to cooperate in the above program and to endeavor to develop data on the dynamic yield strength of materials at different loading rates. The testing method should be relatively simple and economical and above all, able to reproduce results consistently. The approach selected was to use hollow cylindrical test specimens hydrostatically loaded, Figure 6. A fixture was designed and fabricated, consisting of a top plate supported by three equally spaced columns mounted on a

base plate. A hole through the top plate accommodates a piston and a specimen screws in at the bottom side. Screwed onto the other end of the specimen is a short hollow cylinder (a sealing chamber) having a plunger inserted into it from the opposite side with one end resting on the base plate. The sealing chamber has an opening for a pressure gage while the top plate has an orifice with a ball check valve through which fluid is introduced into the specimen. The specimen is stressed by transmitting, through the fluid, a force applied to the top plate piston, developed by dropping a weight from some height. The instrumentation consists of two oscilloscopes, a piezo electric pressure gage and amplifier, two strain gages with their associated D. C. bridges.

The specimens are instrumented with strain gages and a pressure pickup to determine the tangential and transverse strain on the surface of the specimen and internal pressure which induced that strain. One oscilloscope records tangential and transverse and pressure v. s. time while the other oscilloscope records tangential and transverse strain v. s. pressure.

It was decided that since Dr. Hammer's group were developing pressures in excess of 50,000 p. s. i. with a rise time of approximately 1/2 millisecond that we should initially strive to operate within these parameters. These values are in line with the pressure time curves for much of the ammunition currently being used in small arms. We set up our equipment in the Westinghouse Drop Tester, slide 7 and, using a 76# weight developed peak pressures of 31,200 p. s. i. with rise time of 4 milliseconds at 2 foot drop height. This was unexpected so we transferred the fixture to the Tinius Olsen Tester with the results shown. In our prior investigation we had experienced no difficulty in developing the pressures and rise times desired but now our results were way out of line. The differences found with the two machines we attributed to the variation in rigidity of the two bases. The slow rise time must be due to the much larger volume of fluid in our present system. In order to check this we inserted a loose steel plug inside the specimen which would substantially reduce the volume of liquid. As you can see rise time and pulse width are reduced and the peak pressure substantially increased. Figure 8 shows the effect of further reduction in the volume of fluid and the influence of the mass of the hammer. The introduction of a rubber pad between the plunger and the hammer reduced the shock waves and "hash" on the oscillograms. It is our belief that the relative compressibility of the fluid used will further affect the rise time and we intend to investigate this variable in our future work. This study has been quite valuable as it produced a simple method for obtaining quite a wide range of rise times for subsequent investigations.

Many investigators in the past have been content to work with annealed low strength materials. Such materials would not be used in structures where the increase in dynamic over static yield strength would be important. Most annealed structures have an entirely different crystalline structure from those found in hardened materials, and they may behave in a different manner and degree. We selected 4340 steel

from a single heat and heat treated it to 140, 200, and 280 thousand p. s. i. tensile strength and made specimens for this investigation together with specimens for Dr. Andersen of Watertown Arsenal Laboratory, and material for Dr. Hammer of Springfield Armory.

Figure 9 is a table of the preliminary results on quarter inch tensile test specimens. Static tests were conducted with the results shown. The dynamic tests were conducted by Dr. Andersen of Watertown Arsenal using his "Medium-Speed Tensile Testing Machine". Notched tensile bars with the same diameter at the bottom of the notch were also tested as indicated. A total of 24 tensile bars and 15 notched bars were submitted. One half will be tested at room temperature and the other half at  $-65^{\circ}$  F. Due to the capacity limit of this equipment it will probably be necessary to reduce the section size of the specimens in order to complete the investigation.

Figure 10 is a table of static and dynamic tests run on the specimens designed for this investigation.

### CONCLUSIONS

Based on the complexity of the problem we have, of course, not been able to develop any useful engineering data in this short time, but we believe that our investigation has been beneficial in the following respects:

1. High strength materials are being tested by several methods with many variables removed in order to determine reliability of these techniques.
2. Dynamic yield strength values of engineering materials at various strain rates are being developed.
3. Methods of producing various strain rates have been discovered.

### RECOMMENDATIONS

1. Unless serious fault can be found in this investigation, that it be continued.
2. Concentrated effort be applied to determine most realistic parameter or parameters for describing high rate loading, including:
  - a. Rise time
  - b. Strain rate
  - c. Slope of curve
  - d. Duration of load above static yield strength level
  - e. Area of curve above SYS line
  - f. Slope of curve above SYS
  - g. Others

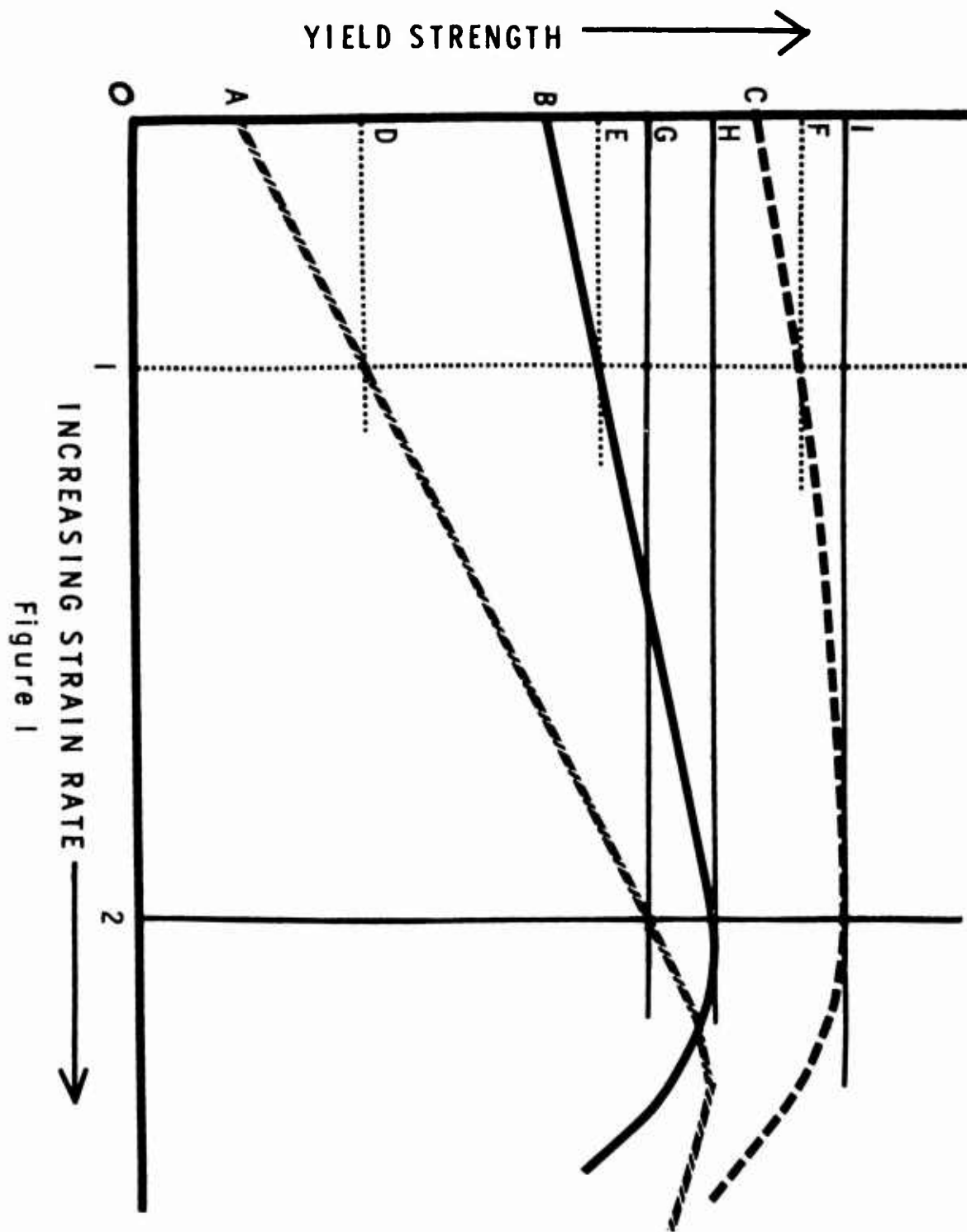


Figure 1

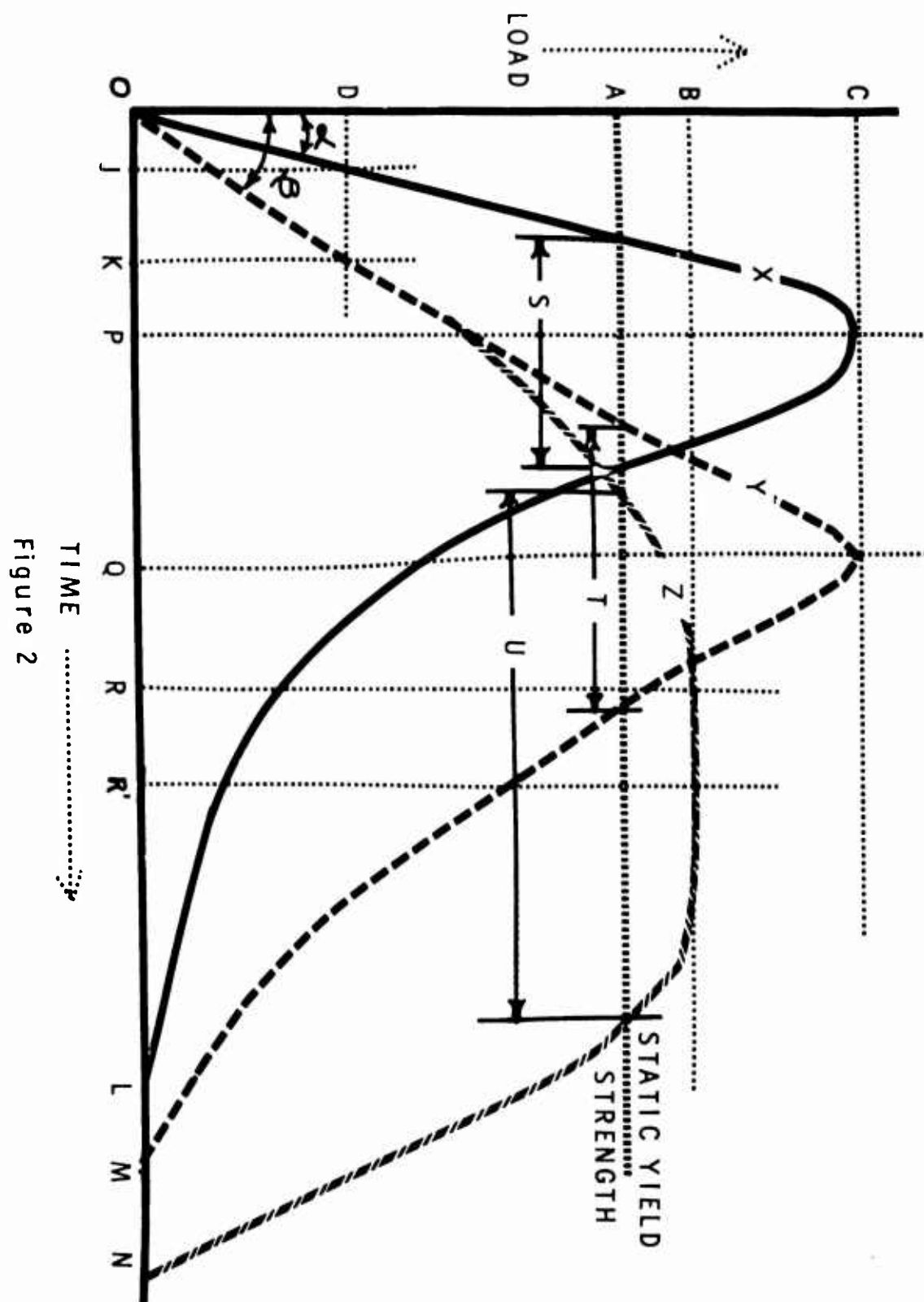
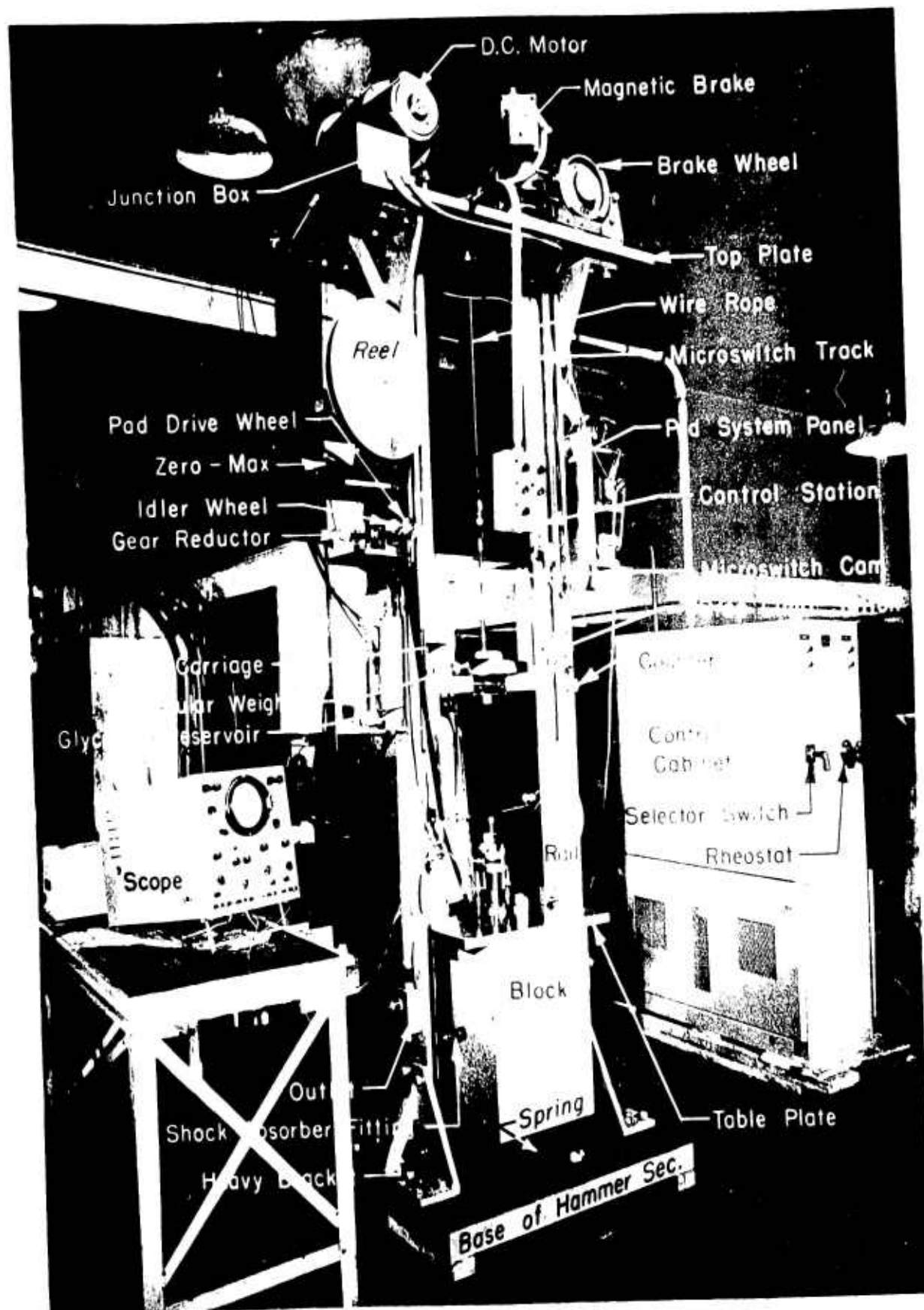
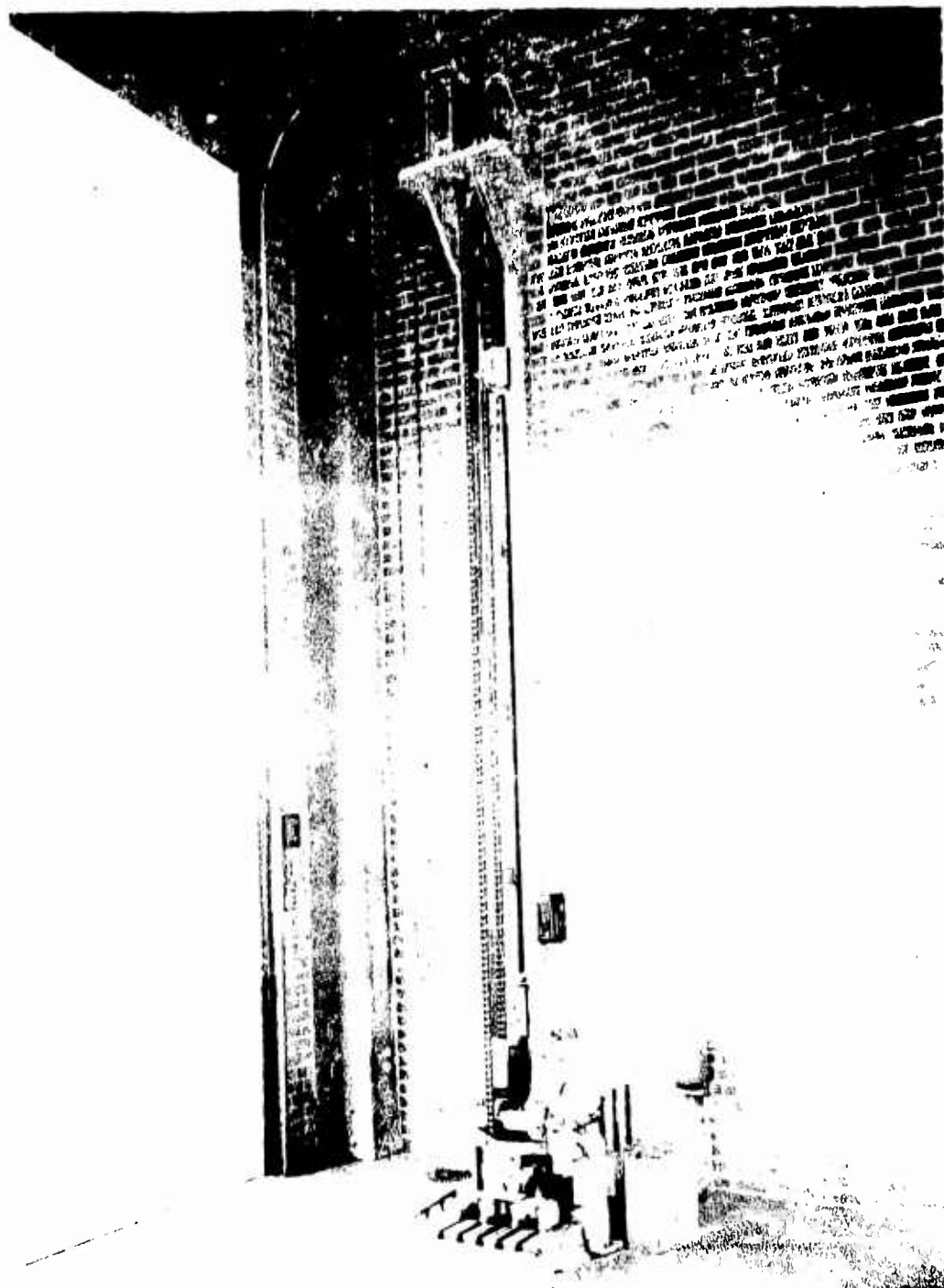


Figure 2



"CODE WE-1"



13181-SA SPRINGFIELD ARMORY - ORDNANCE CORPS 12 Nov 1957  
TINIUS OLSEN IMPACT TESTING MACHINE



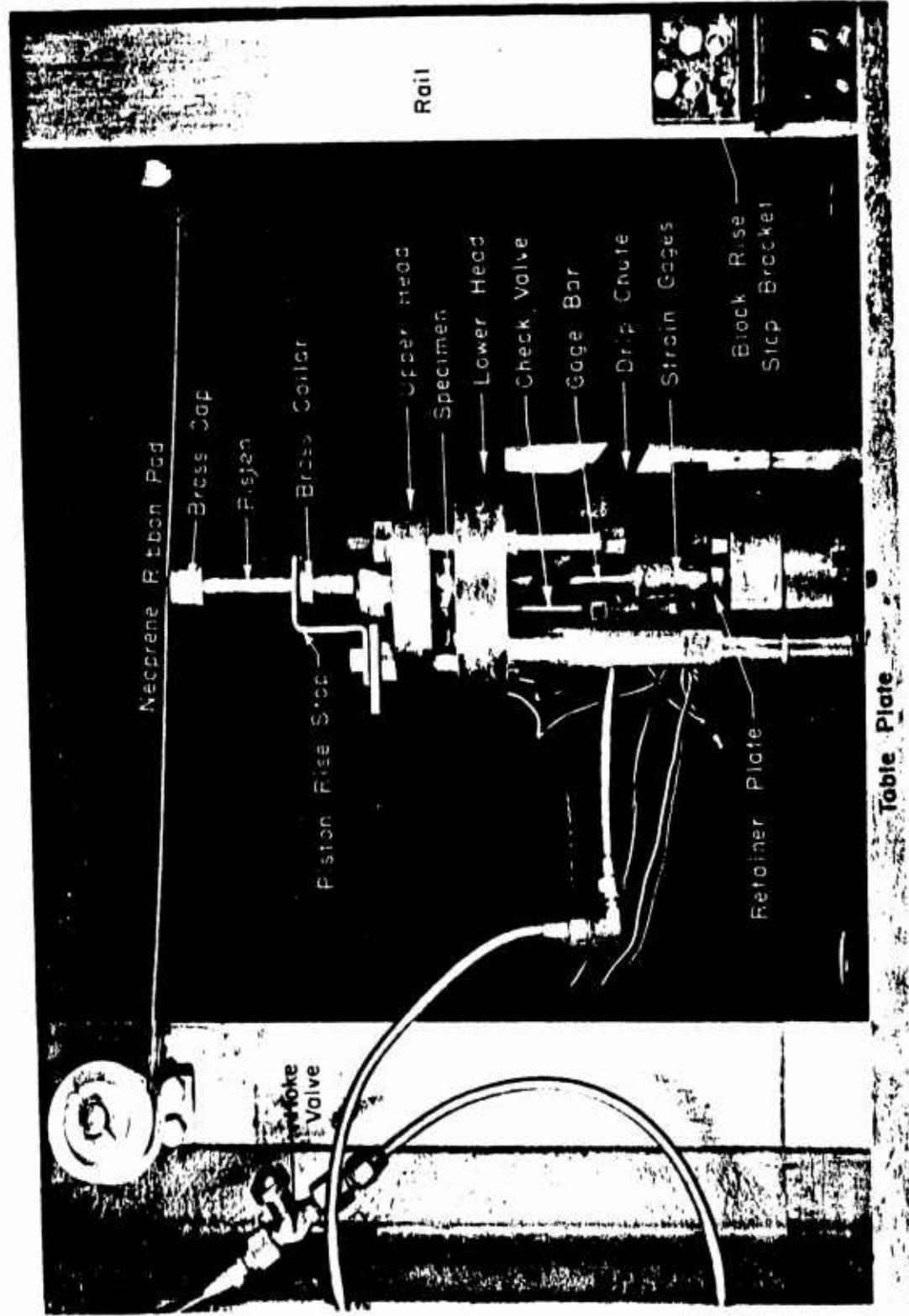
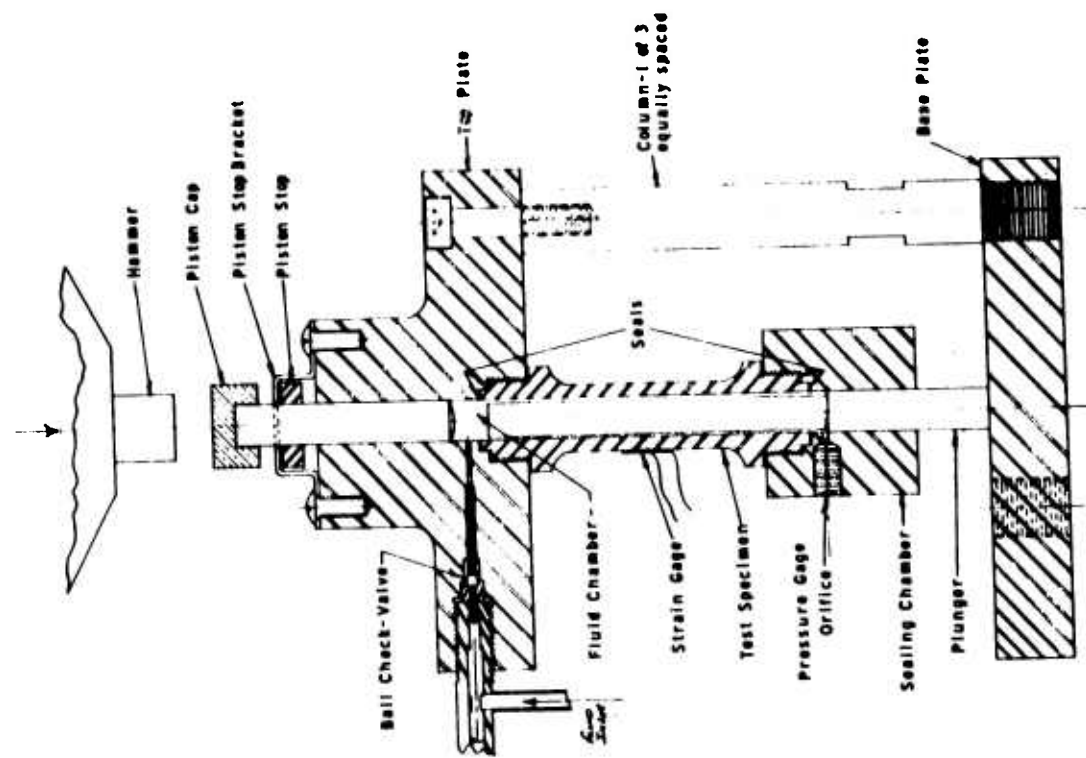


Fig. 5 SPECIMEN HOLDING ASSEMBLY OR ANVIL



High Rate of Loading Test Set-up

PRELIMINARY RESULTS OF DROP TESTS

HEIGHT (ft)   PULSE WIDTH (ms)   RISE TIME (ms)   PEAK PRESSURE (psi)

Westinghouse Tester 76# Weight Fluid Glycerine

2	8.4	4.	31,200
---	-----	----	--------

Tinius Olsen 20# Weight Fluid Glycerine

2	4.6	2.0	15,000
3	4.6	2.0	20,500
4	4.6	2.04	25,000
5	4.66	2.0	29,000
6	4.8	2.14	32,500
7	4.66	2.0	36,500
8	4.6	2.01	40,000
9	4.72	2.0	43,300
10	4.5	1.94	45,600

Westinghouse Tester 76# Weight Fluid Glycerine 1/4" Plug in Specimen

2'2"	8.7	3.84	32,500
------	-----	------	--------

Tinius Olsen 20# Weight Fluid Glycerine 7/16" dia. Plug 4" long

4	3.4	1.4	34,000
5	3.4	1.32	40,000
7	3.4	1.21	49,300
8	3.45	1.39	52,000

FIGURE 7

PRELIMINARY TESTS RESULTS OF VARIABLES

<u>HEIGHT (ft)</u>	<u>PULSE WIDTH (ms)</u>	<u>RISE TIME (ms)</u>	<u>PEAK PRESSURE (psi)</u>
Tinius Olsen Tester Fluid Glycerine .435" dia. x 4.35" Plug in Specimen			
	20# Weight		
2	2.8	1.3	29,800
4	2.95	1.1	37,000
	10# Weight		
2	1.98	.95	17,000
4	2.12	.85	26,000
8	2.25	.95	36,000
10	2.17	.91	41,000
	10# Weight Rubber pad on Piston		
10	2.33	1.09	38,000
	20# Weight Rubber pad on Piston		
4	3.22	1.7	35,300
6	3.19	1.5	48,800

FIGURE 8

FIGURE 9

<u>Static Test</u>		<u>4340 Steel</u>		<u>1" Gage Length</u>			<u>Rise Time ms</u>	<u>Fract. Time ms</u>
No.	Dia. inch	Temper OF	UTS KSI	Elong. %	R.A. %	Y.S. KSI		
21	.252	1200	129	23	66.9	114		
25	"	1200	127.5	23	66.9	114		
10	"	850	202	12.7	55.6	192		
11	"	850	202	12.5	55.6	192		
28	"	400	293	10	46.8	243		
30	"	400	292	11	46.8	243		
<u>Dynamic Test</u>		<u>Smooth Specimens</u>						
3	.252	1200	140	22	65.6	126	2	6
4	"	1200	146	22	62.8	132	2	7
2	"	850	205				4	1/2 sec
		<u>Notched Specimens</u>						
45	.252	1200	200				3-1/2	4
32	"	1200	196				4	5
38	"	850	240 )	Did not break			7	
"	"	"	260 )				5	
34	"	850	284				4-1/4	4-1/4
46	"	400	260 )	Did not break			5	
"	"	"	280 )				4-3/4	
"	"	"	340 )				4	
"	.160	"	367				2	4
42	"	400	350				5	5
43	"	400	365				7	7
31	"	850	265				6	6

FIGURE 10

Test Results

Specimen	Rc Hardness	Test Condition	Rise Time ms	$\sigma_{y,p}$ Combined Stress at Yield Point psi
A	40	Dynamic	1.18	259,000
B	40	Static		247,000
C	25	Dynamic	0.9	152,000
D	25	Dynamic	1.15	152,000
E	25	Static		144,400

Formulae for Y.P. Calculations Based on Lamé's Equations &  
Distortion Energy Formula for Inside Wall Surfaces

$P_i$  = Internal Pressure

$\sigma_t$  = Tangential Stress

$\sigma_r$  = Radial Stress

$\sigma_{y,p}$  = Combined Stress at Yield Point

$a$  = Inside Radius

$b$  = Outside Radius

$$\sigma_t = P_i \left[ \frac{a^2 + b^2}{b^2 - a^2} \right]$$

$$\sigma_r = -P_i$$

$$\sigma_{y,p} = \left[ \sigma_t^2 + \sigma_r^2 - \sigma_t \sigma_r \right]^{\frac{1}{2}}$$

The primary factors concerned by utilization, in design, of stresses higher than the static yield strength, are the magnitude of the loads and the relations between loads and time.

Once we have applied loads at rates high enough to exceed the static yield strength, the material is in an unstable state and it is only a matter of time before gross yielding and fracture occur, as shown by Clark and Wood and others. I believe Mr. Abbe does very well in reiterating this fact by way of his quest; from this fact limbs the benefit of strain rate effects in design to very special situations.

A. G. H. Andersen

W. A. L.

## EXPLOSIVE DEFORMATION OF BEAMS

E. N. Clark\*, F. H. Schmitt\*\*, D. G. Ellington\*\*\*

### ABSTRACT

This paper is an abstract of work being done at Picatinny Arsenal as part of the Air Force Aeronautical Systems Division program on structural response to impulsive loading.

To date experiments which determine the central deflection versus time of rigidly clamped and free rectangular beams of constant cross section have been performed.

Beams of 6061 T6 Al, 20240 Al and a soft 1010 steel were placed on supports approximately ten inches apart and centrally loaded with a sheet of high explosive. The central deflection of these beams was observed with a framing and streak camera. Representative graphs are included.

The high explosive (trade name EL 506 D) was calibrated by measuring the velocity imparted to a known mass of aluminum which was covered by an effectively "infinite" but known amount of HE. It was determined that the HE delivered 18.60 ( $10^4$ ) dyne per gm of HE through a .055 inch thick sheet of polyethylene.

### INTRODUCTION

This paper is an abstract of work being done at Picatinny Arsenal studying the plastic deformation of various structural elements of air frames. To date the major effort has centered on the calibration of the impulse imparted by the explosive and the deformation of rectangular beams of constant cross section, both free and clamped. This work is supported by the Air Force and complete details and results of the work may be obtained by referring to progress reports (1). This report will

---

\* E. N. Clark, Chief Dynamics Unit, Engineering Sciences Laboratory, Feltman Research Laboratories, Picatinny Arsenal, Dover, New Jersey.

\*\* F. H. Schmitt, Physicist, Dynamics Unit, Engineering Sciences Laboratory, Feltman Research Laboratories, Picatinny Arsenal, Dover, New Jersey.

\*\*\* D. G. Ellington, Chemical Engineer, Dynamics Laboratory, Engineer Engineering Sciences Laboratory, Feltman Research Laboratories, Picatinny Arsenal, Dover, New Jersey.



describe the experimental techniques and give some of the results. A complete description of all results may be found in the cited reference. We shall discuss first the calibration of the impulse and then the beam measurements.

## CALIBRATION OF EXPLOSIVE

### Preparation of Explosive

The high explosive used was a composition of approximately 80% PETN and 20% latex rubber. The HE (trade name EL 506 D) was purchased from DuPont and came in sheet-form 16" x 10" x .050". It was rolled at the Arsenal in a roll mill to smaller thicknesses of 0.010", 0.015", 0.020", 0.030" and 0.045". Each thickness of HE was used in the calibration to determine the impulse/unit weight it would produce.

From each thickness of HE available, a rectangular section of approximately 2" x 1.75" was cut with a "cookie cutter". The dimensions of each sample area were measured with a traveling microscope to one-thousandth of a millimeter and each sample was weighed to one-tenthousandth of a gram. The thickness of each sample was measured at twelve different locations and only samples that showed less than 0.0007" variation in thickness were used. Thus, the weight per unit area of explosive was determined and the requirement of uniformity of thickness assured that its variation across the sample was small.

### Experimental Setup

In order to measure the impulse that the HE would deliver to aluminum, the following basic experiment was performed: A rectangular piece of aluminum (called time piece or pellet), 1.5" x 1.2" x 0.25", was surrounded by baffles, set loose enough to permit the time piece to fall freely under the influence of gravity. See Figures 1 and 2.

This grouping of metal was supported approximately 3 feet off the ground. A piece of low density ( $1.09 \text{ gm/cm}^3$ ) polyethylene was placed over the time piece to reduce the possibility of spall. The sample of HE was then centered over the polyethylene and time piece, and taped in place. A fan shaped piece of the same HE was taped to the 2" wide side of the sample to act as a lead and was detonated by an electric blasting cap. A streak camera, focused on an edge of the time piece and at 90 degrees to the direction of detonation, and a Fastax framing camera, focused on the time piece edge facing the detonation front, were used to observe the motion of the time piece.

Reference markers, 0.030" steel drills, were mounted under the steel plate and just in front of the vertical plane of the edges of the time piece, in view of the camera. The drills were placed about one inch apart; however, exact measurements to one-thousandth of a millimeter were taken.

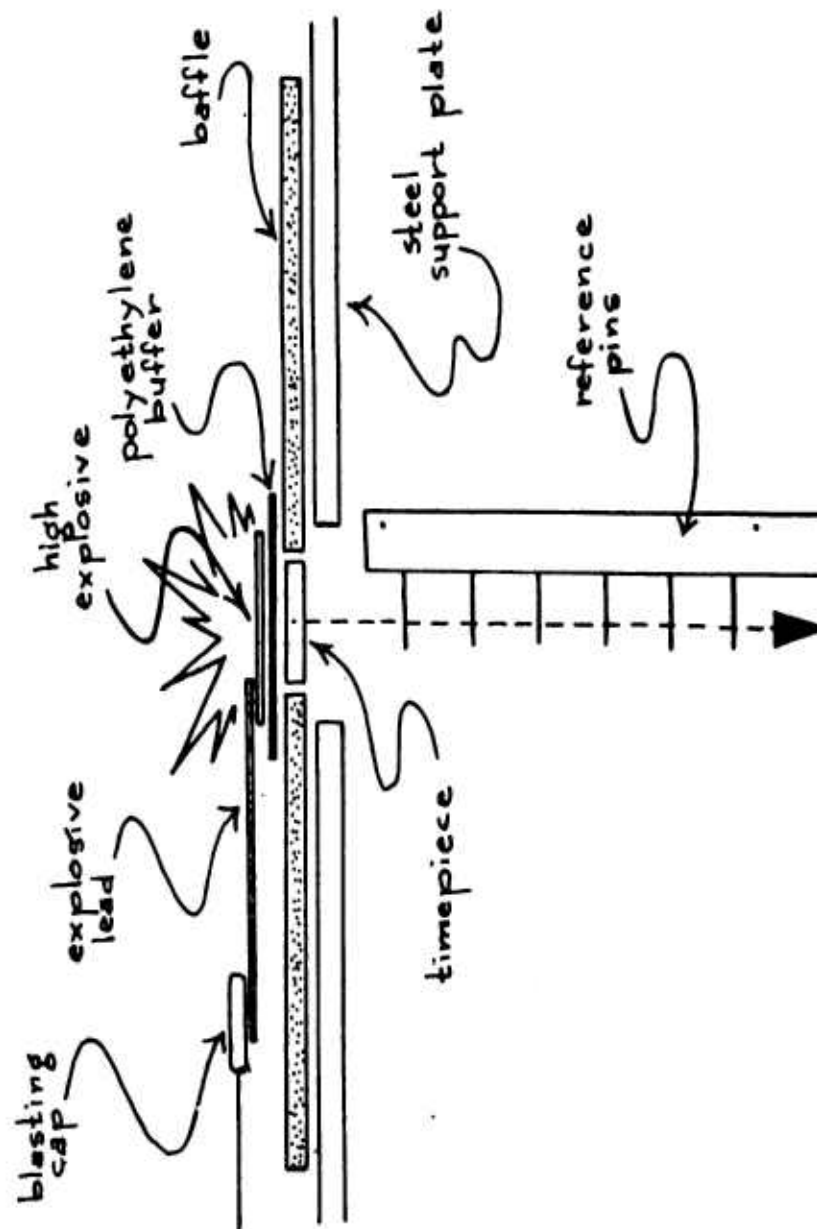


FIG. 1: CROSS SECTIONAL VIEW OF  
EXPLOSIVE - TIMEPIECE ARRANGEMENT

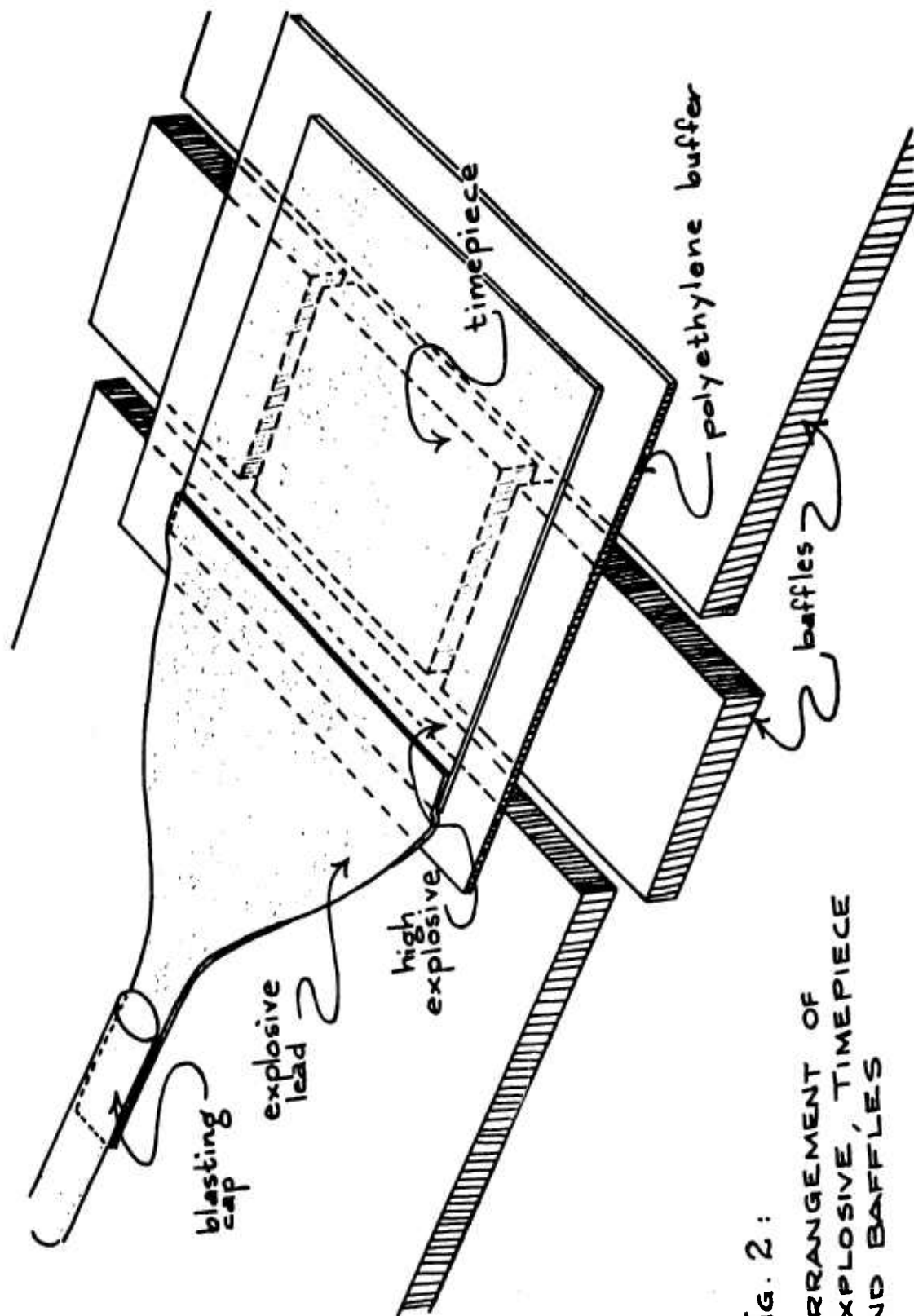


FIG. 2 :  
ARRANGEMENT OF  
EXPLOSIVE, TIMEPIECE  
AND BAFFLES

A time scale for the streak camera was placed on the film by photographing a 10 kc signal on an oscilloscope which came from a secondary frequency standard. The framing camera used the time calibration pips from a 1 kc frequency standard. Both oscillators were checked periodically and were found to have negligible error.

The streak camera consisted of a 30" focal length lens focusing the image of the event on a slit. A General Radio 35mm oscilloscope camera, which can transport film at the rate of 150' per second, was focused on the back of the same slit. This camera gave extremely sharp and well defined traces and it was possible to determine the velocity of the time piece to better than 0.2% by this method.

Thus, with the known mass of the time piece, the impulse imparted to the time piece could be determined. The explosive was cut so that it overlapped all edges of the time piece sufficiently so that no edge effects of the explosive were felt by the time piece. The amount of effective explosive was determined by multiplying the area of the time piece by the weight per unit area of the explosive.

### Results

Figure 3 gives a plot of the results of specific impulse  $\frac{(\text{dyne-sec})}{\text{gm}}$  as a function of  $w/c$ , the ratio of weight per unit area of pellet to weight per unit area of explosive. Each point is the average of at least 3 shots and the numbers next to the point indicate from top to bottom, the thickness of the explosive in thousandths, the length of the time piece in inches (it always had a width of 1.2") and the thickness of the time piece in inches. The vertical line represents plus or minus 1 standard deviation.

The point 45, 1, 1/4 represents a point where all the time pieces spalled, although the spall did not separate. The point is shown on the graph; however, the fact that spall occurred is considered sufficient justification to neglect this point and it has not been considered in the analysis. The point 10, 1, 1/4 represents 10 shots, only 5 of which actually detonated, but there is no apparent reason why this point has such a high specific impulse.

At least square fit of the data gives a slightly positive slope; however, it has no statistical significance and we therefore conclude that the impulse is independent of  $w/c$  throughout the range that we have studied. The fact that the impulse is independent of  $w/c$  is further verified by independent measurements (2 and 3) taken by flash radiography. These experiments establish that the impulse is independent of  $w/c$  beyond a value of  $w/c \approx 3$ .

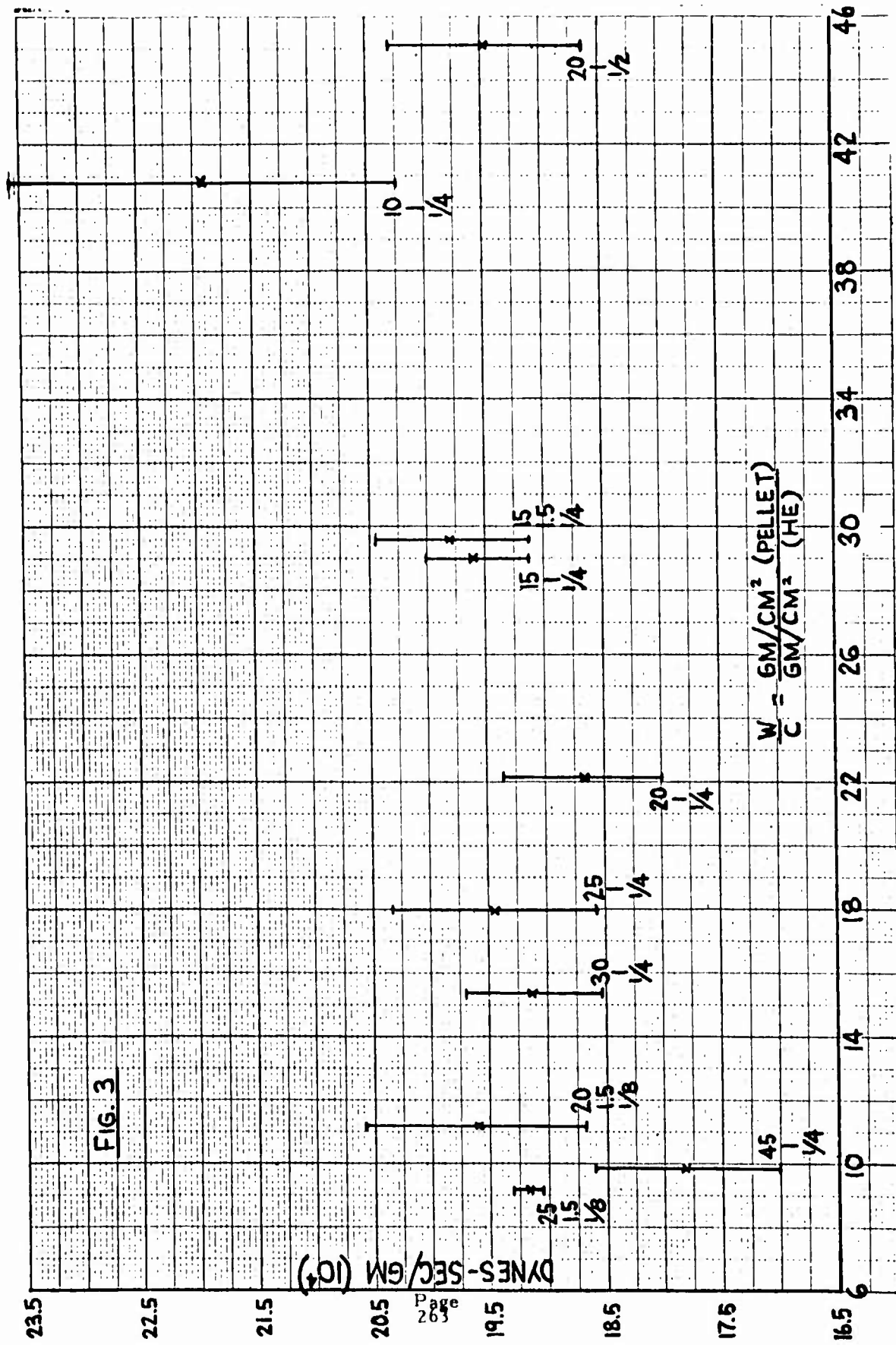


TABLE I  
Edge Effect on Impulse (1)

Pellet Position	Test 1	Test 2	Test 3	Test 4	Test 5	Test 6	Test 7	Test 8	Avg Impulse dyne sec x 10 <sup>3</sup>	5
1	.970	.908	.635	.991	.922	.152		.756	.152	.385
2	3.745	4.126	3.512	3.794	3.590	.212		1.833	.484	.342
3	15.969	18.169	17.945	17.319	18.784	1.117		3.221	1.061	.2775
4	22.531	23.931	23.395	23.785	24.712	3.645	19.156	18.355	3.662	1.077
5	"	"	"	"	"		21.781	23.311	17.757	.937
6	"	"	"	"	"		23.795	24.751	23.364	.746
7	"	"	"	"	"		24.114	23.640	23.849	.681
8	"	"	"	"	"		23.986	22.141	23.786	.723
9	"	"	"	"	"		22.734	22.101	23.512	.835
10	"	"	"	"	"		22.164	21.612	23.176	1.089
11	16.917	18.752	17.848	19.523	16.752			16.577	17.729	1.203
12	3.716	3.605	3.496	4.233	3.352	2.668		2.269	3.384	.6321
13						.694		1.308	1.001	.4342
14						.466		.432	.775	.2824
15	.742		.915	.965	1.132	.285				
16										

Note 1: Explosive covered pellet positions 5 through 8

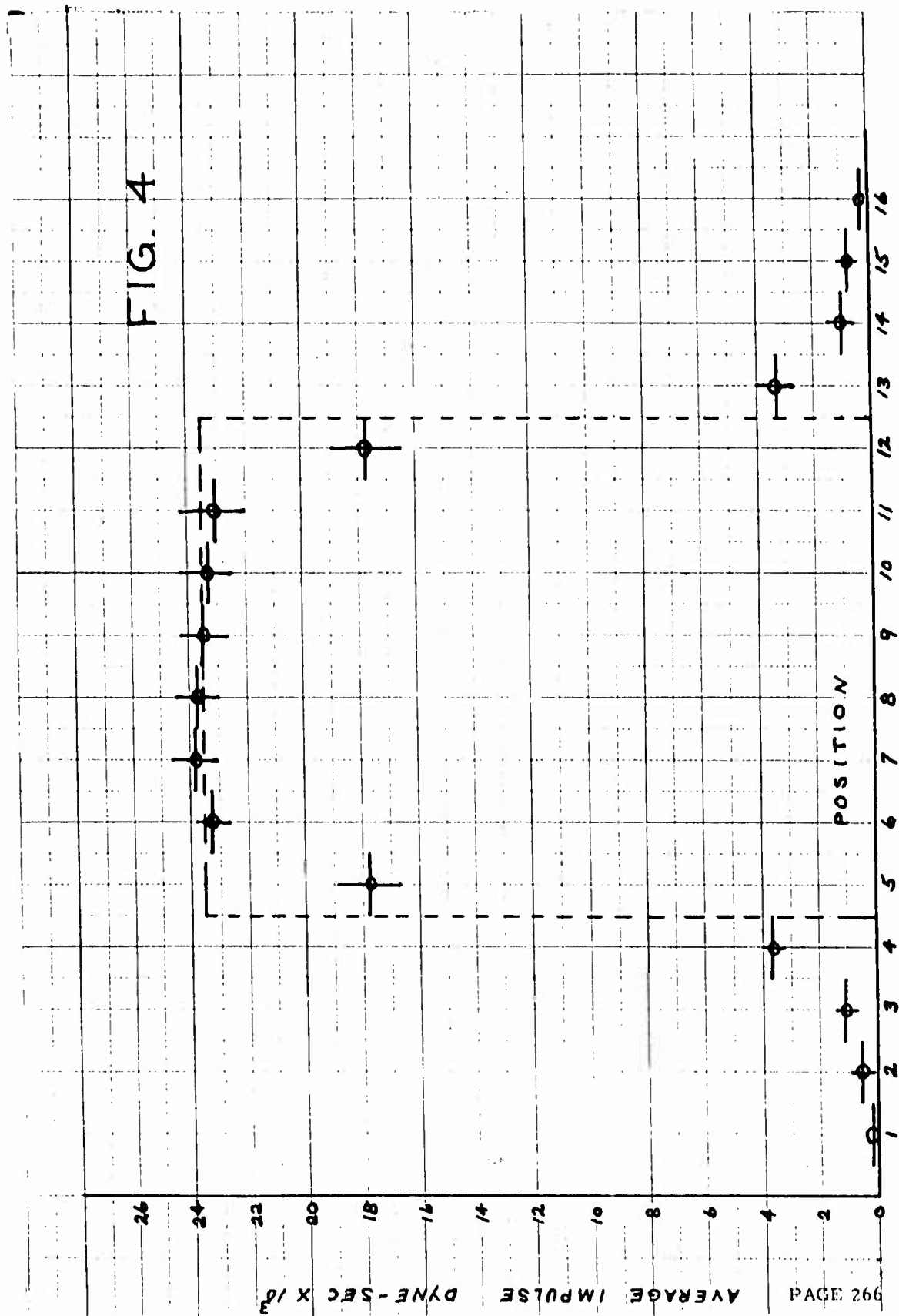
TABLE II

## EFFECT OF BLAST LOADING AND RELEASE WAVE LOSS ON COMPUTED IMPULSE

Particle Position ( Not Covered With HE )	Avg Impulse dyne sec x 10 <sup>3</sup>	Avg Impulse	Impulse Gain Due to Blast	Difference
1	0.152	5.359	10.804	-0.730
2	0.484			
3	1.061			
4	3.662			
13	3.384	5.445		
14	1.001			
15	0.775			
16	0.285			
Particle Position (Covered with HE)	Avg Impulse dyne sec x 10 <sup>3</sup>	*	Impulse Loss Due to Release Wave	
5	17.757	5.753	11.534	
12	17.729	5.781		

\* = (Avg Impulse for positions 6-11) - (avg impulse of  
Specific particle 5 or 12)

FIG. 4





### Edge Effects

The experiment to measure the specific impulse of the explosive was designed to avoid any effects resulting from exposed edges of explosives. Since the method of loading the beams was that of laying a strip of explosive across the beam, there were two edges exposed. Thus, it was necessary that experiments be conducted to determine the size of this effect. This was accomplished by arranging 16 time pieces  $1/4$ " thick and  $1/4$ " long and the usual 1.2" wide, in the manner of a single time piece  $4" \times 1.2" \times 1/4"$ . The arrangement was loaded with a 2" wide piece of explosive centrally located. The velocities of the pieces were determined by streak and framing camera. A variation of this experiment was to make the central 6 pieces one single time piece since it was found that the central six had the same velocity and we thus lessened the amount of smoke as seen by the camera.

The framing camera was used to get the velocity of the center of mass by making successive measurements on a diagonal thus locating the coordinates of the center of mass. It was assumed that there was only motion parallel to the plane of the film, that is, the velocity had no horizontal component normal to the film plane. This assumption tends to be verified, since the horizontal velocity that can be measured in the plane of the film is negligibly small.

The results of 7 sets of these measurements are given in Figure 4 and Table I. These results are taken from the framing camera only, since the measurement of the slower fragments with the streak camera were difficult to measure accurately. However, the streak camera measurements of the experiments, where the 1.5" wide central time piece was used, did provide an opportunity to compare the streak and framing camera results, as will be discussed later.

Referring to Figure 4, the sum of the ordinates under the dotted rectangle represents the total impulse, assuming the specific impulse quoted and neglecting all edge effects. The edge effects are made up of two phenomena. The first is an expansion of the detonation products from the edge, faster than if confined by more explosive, which results in a loss of impulse. The second is blast loading of the structure beyond the region in contact with the explosive. Unless the moment of the impulse is critical, the two effects cancel out to well within experimental error as can be seen from Table II. These particular tests were done for 0.015" thick explosives. (For the expansion of the detonation products the effect scales according to the thickness.) The scaling laws for blast effects are not particularly adaptable to these circumstances since the distance to where the pressure is sensed is smaller than the width of the explosive and the explosive may approximate a semi-infinite sheet. However, since the thickness of explosive used, at worst, was twice this thickness and the effect rather small, no appreciable error should result in applying the same results found for 0.015" up to a thickness of 0.030".

### Comparison of Streak and Framing Camera Data

As mentioned earlier, most of the impulse calibration was performed with streak camera coverage only, or at any rate, this was the only data reduced. However, framing camera observations did indicate that the spin was small and observations of how the time piece hit the armor plate floor confirmed these conclusions.

Since the framing camera was relied upon primarily for the edge effects, this provided the opportunity for a comparison of the streak and framing camera data. The framing camera always permitted measurements to be made on a number of corners of the time piece so that by measuring the coordinates of the ends of a diagonal the coordinates and velocity of the center of mass could be determined. The results of 14 different measurements taken with the 1.5" pellets in the edge effect experiment and some taken with 2 1/2" long pellets are given in Table III.

The differences in the impulses for any given film number consist of the experimental errors of the two camera measurements and any effect due to spinning of the pellet. Any correlation which would exist between the framing and streak camera results would represent either a detectable variation in the explosive or possibly some interference due to the baffles which would result in a changed specific impulse. At a 95% confidence level there was no significant correlation; however, there was at a 90% level. It appears, therefore, that approximately 1/3 of the spread in results is due to variation in the explosive, and probably 1/2 of the spread to the spinning of the pellet.

The Puolter Laboratories of the Stanford Research Institute have performed similar measurements with this explosive (3). In their experiment they measured the velocity of a time piece 2" x 3" with the explosive flush on all sides except where the explosive lead was connected. Since the explosive lead covered the 2" side, a correction for the edge effect of 8" must be applied to their results to make them compatible with our own.

The result quoted by the Stanford Research Institute for their experiment is  $2.2 \times 10^5 \frac{\text{dyne sec}}{\text{cm}^3}$  for aluminum and a buffer of 1/16" polyurethane with a density of  $0.63 \text{ gm/cm}^3$ . This value is their impulse constant for aluminum and is obtained by dividing the impulse/unit area by the thickness of HE rather than by the weight of the explosive as we have done. Our comparable figure is  $2.593 \times 10^5 \text{ dyne sec/cm}^3$  with a buffer of 0.055" and  $1.09 \text{ gm/cm}^3$  density polyethylene. However, from Table II we see that for our 2.4" of edge for 0.015" thick explosive, the impulse lost was  $11.53 \text{ dyne sec} \times 10^3$ . Using these figures, a correction can be calculated which will raise the SRI value to  $2.46 \times 10^5 \text{ dyne sec/cm}^3$ , thus giving an agreement within 5.2% which is entirely satisfactory in view of experimental errors and differences associated with the experiments.

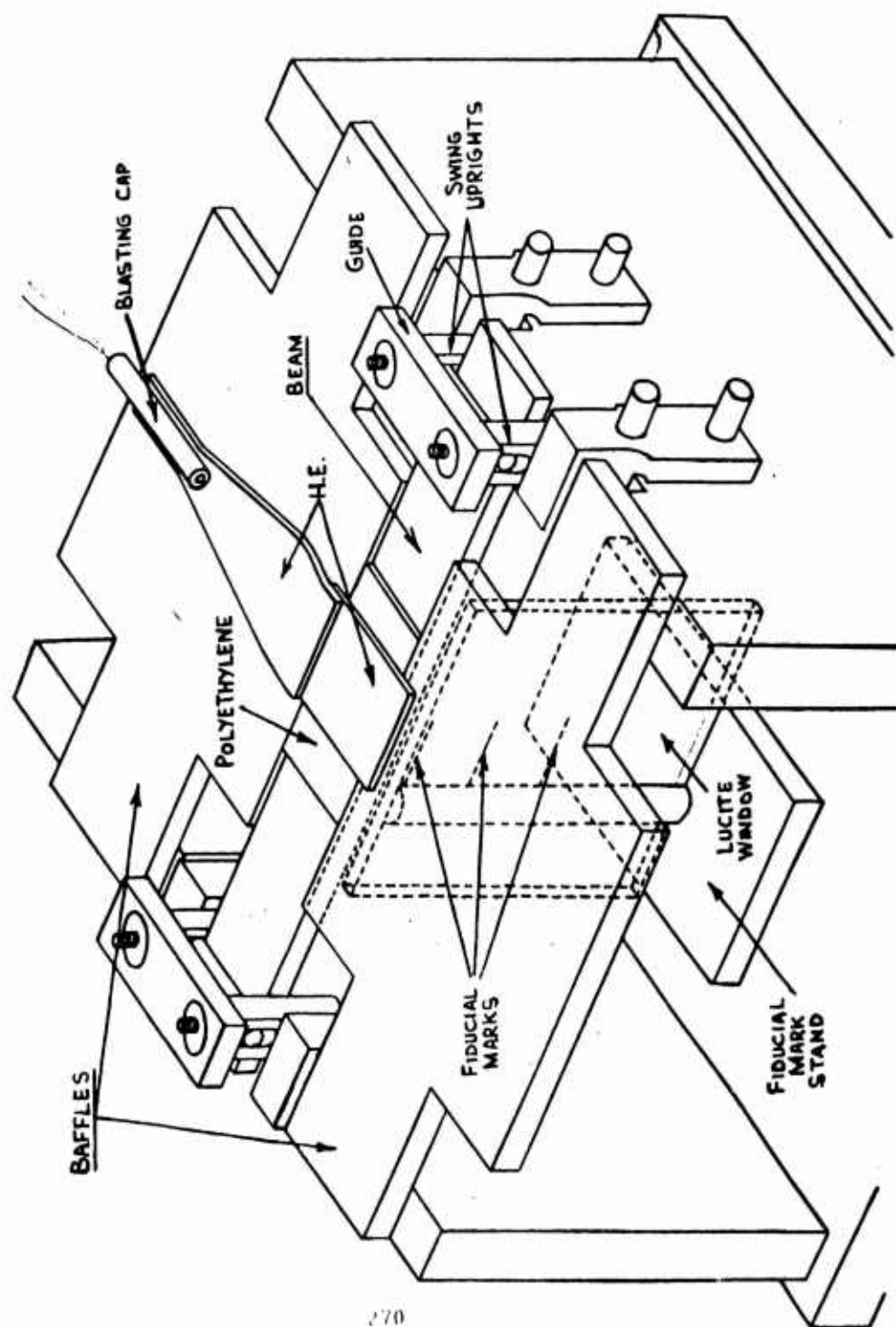
TABLE II  
SPECIFIC IMPULSE AS DETERMINED BY FASTAX (FRAMING) AND G. R. (STREAK) CAMERAS

Shot No.	Fastax $\frac{\text{dyne sec} \times 10^4}{\text{gm}}$	G. R. $\frac{\text{dyne sec} \times 10^4}{\text{gm}}$
135	17.974	19.187
136	18.404	19.392
139	17.996	-
140	18.720	-
141	18.149	18.412
143	19.632	-
144	18.338	18.703
146	17.171	-
147	19.355	18.105
150	17.562	-
151	18.010	19.377
152	18.547	18.918
153	17.874	18.417
154	19.387	18.976
Avg 18.366		Avg 18.831
$\sigma = 0.711$ coef var = 3.87%		$\sigma = 0.456$ coef var = 2.42%

\* Grand Average of  $18.599 \frac{\text{dyne sec}}{\text{gm}}$

\* This value is used in beam calculations for this lot of explosive

FIG. V     STAND FOR FREE BEAMS



### Free Beams

The experimental set up used in the free beam experiments is shown in Figure 5. The beams had nominal dimensions of 12 inches length, 1.2 inches width, and either 1/4 or 1/8 inch thickness. Three types of beam material were studied - 6061 T6 Al, 20240 Al and a soft 1010 steel.

The beams were supported on a 0.3 inch diameter fixed steel rod, 10.068 inches apart. A similar rod was used on top of beam and was fashioned into a roller assembly which pivoted about the fixed rod. This arrangement permitted the beam to deform without introducing tension at the support ends and yet prevented vertical motion of the beam (rebound). This roller assembly was made from aluminum, wherever possible, in order to keep the mass and moment of inertia as low as possible. The roller assembly as used with 1/4" Al and steel beam had a mass of 82.8 gm and a moment of inertia of 517.61 gm-cm<sup>2</sup>. With the 1/8" Al beams the figures were 48.0 gm and 257.23 gm-cm<sup>2</sup>. (The guides were removed with the thinner beams.) These figures are 3.6% and 3.3% of the moment of inertia of the 1/4" Al and 1/8" Al beams respectively.

In order to prevent any binding between the beam and roller a .005 inch gap was introduced at set up, between the beam and the roller. This gap was sufficient to permit the beam to move through a relatively large angle before the roller was forced to move. Framing camera pictures showed that the rollers did not start to move until the beam had undergone almost maximum deflection; therefore, the roller had little effect on the motion of the beam up to the first maximum.

Baffles the same thickness as the beam were placed in front of and to the rear of the beam and held in close contact by tape. These baffles were generally sufficient to keep the smoke of the explosive from obscuring the motion of the beam. However, if difficulty with smoke was encountered, the beam was then raised 1/8" so that the baffle would be effectively thicker and thus act for a longer time. A second method which was sometimes used was that of placing a thin sheet of lucite under the front baffle very close to the front edge of the beam so that the light reflected from the beam would have to go through only a thin layer of smoke. With these techniques it was possible to photograph the motion of any explosive beam combination attempted.

Whenever it was possible, the bottom of the beam was placed slightly below the bottom of the baffle so that the rest position of the beam could be accurately determined. In cases where this was not possible the bottom of the beam was measured in reference to a fiducial marker which was visible in the film, thus determining the rest position of the beam. Zero time was determined by observing the flash across the film at the detonation time. The time for the detonation to sweep across the beam (approximately 5 microseconds) verges on the time resolution of the camera and is small compared to the time of motion of the beam.

Fiducial markers placed approximately 1 inch apart are placed as close to the plane of motion of the front of the beam as possible, in most instances

TABLE IV

Film No.	Beam Material	Beam** Thickness Inches	Effective Impulse dyne-sec x 10	Deflection				HE COVERED Central Inches of Beam
				Max Inches	Time to Max micro sec	Permanent		
						Front Inches	Back Inches	
(1)								
P 20-25-86	2024-0 Al	1/4	20.1	.710	678	.588	-	1.988
87	"	"	20.2	.701	640	.588	-	1.988
88	"	"	19.7	.702	648	.572	-	1.988
(2)								
B 15-25-118	2024-0 Al	1/4	15.1	1.65	2230	1.12	-	1.988
119	"	"	15.5	1.60	2060	1.06	-	1.988
120	"	"	15.3	1.51	2110	.934	-	1.988
122	"	"	15.6	1.53	2230	1.08	-	1.988
P 24-25-110	6061-T6 Al	"	30.8	.837	492	.590	.634	1.988
111	"	"	28.8	.737	491	.494	.522	1.988
112	"	"	28.9	.788	535	.550	.564	1.988
113	"	"	26.5	.718	488	.487	.514	1.988
B 20-25 121	6061-T6 Al	1/4	21.6	1.54	1890	.781	-	1.988
123	"	"	20.1	1.45	1830	.553	-	1.988
124	"	"	22.0	1.64	1870	.834	-	1.988
P 15-125-100	2024-0-Al	1/8	15.6	*.873	*555	.921	.945	1.731
101	"	"	15.4	.894	4660	.893	.949	1.731
104	"	"	13.6	*.892	*602	.879	.879	1.731
				.903	1217	.795		
				*.766	*585			
				.809	2512			
B 15-125-134	2024-0-Al	1/8	6.71	*2.63	*4015	1.93	.7952	.7952
136	"	"	6.92	2.73	6000	1.74	-	.8140
				*2.24	*3082			
				2.26	3929			
				*2.64	4313	1.85	-	.8040
				2.68	5356	1.85	-	.8040
P 15-125-92	6061-T6 Al	1/8	16.4	.690	677	.580	.705	1.932
93	"	"	14.7	.663	661	.563	.635	1.932
95	"	"	16.2	.720	671	.581	.700	1.932

Film No.	Beam Material	Beam** Thickness Inches	Effective Impulse dyne-sec x 10 <sup>4</sup>	Deflection			HE Covered Central Inches of Beam
				Max Inches	Time to Max micro sec	Permanent Front Back Inches	
B 15-125-128	6061-T6 Al	1/8	7.94	2.19	2700	.978	1.009
130	"	"	7.55	1.97	2510	.925	.9945
131	"	"	7.50	1.98	2460	.995	.9973
P 20-125-89	(3) 1010 steel	1/8	19.4	.620	884	.549	1.932
90	"	"	19.3	.617	979	.561	1.932
114	"	"	22.5	.789	761	.616	1.988
B 15-125-127	(3) 1010 steel	"	13.3	* 2.17	*5130	1.65	1.731
129	"	"	14.7	2.18	5471	1.84	1.731
132	"	"	14.8	* 2.30	*4939	-	-
				2.31	5451	-	-
				* 2.25	*4916	1.78	1.731
				227	5185	-	-

Nominal dimensions of beams as follows:

Clamped beams  
22 inches long  
1.2 inches wide  
thickness as given in table

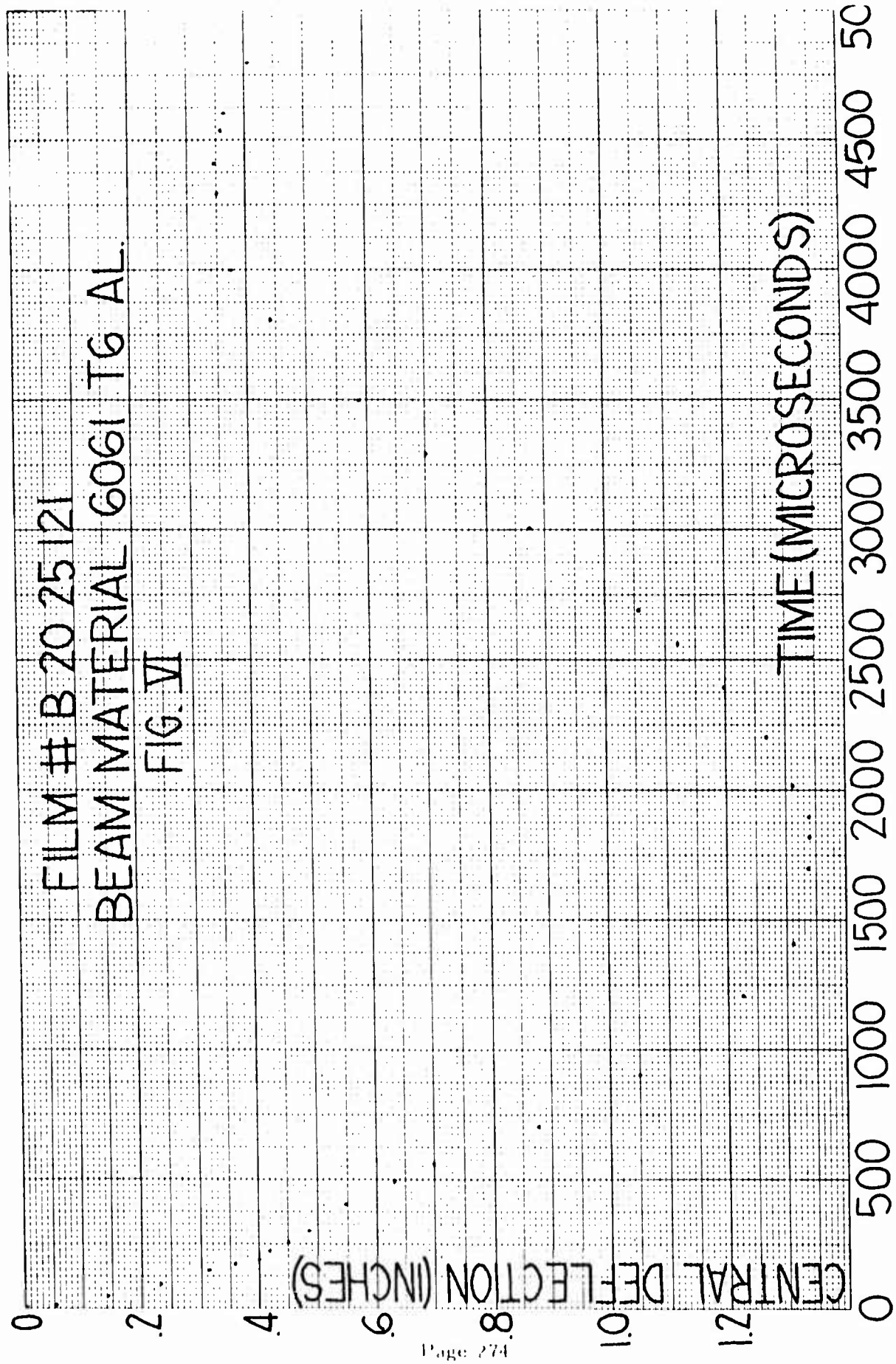
Free beams  
12 inches long  
1.2 inches wide  
thickness as given in table

Distance between supports  
Clamped beams - 10.010 inches  
Free beams - 10.068 inches

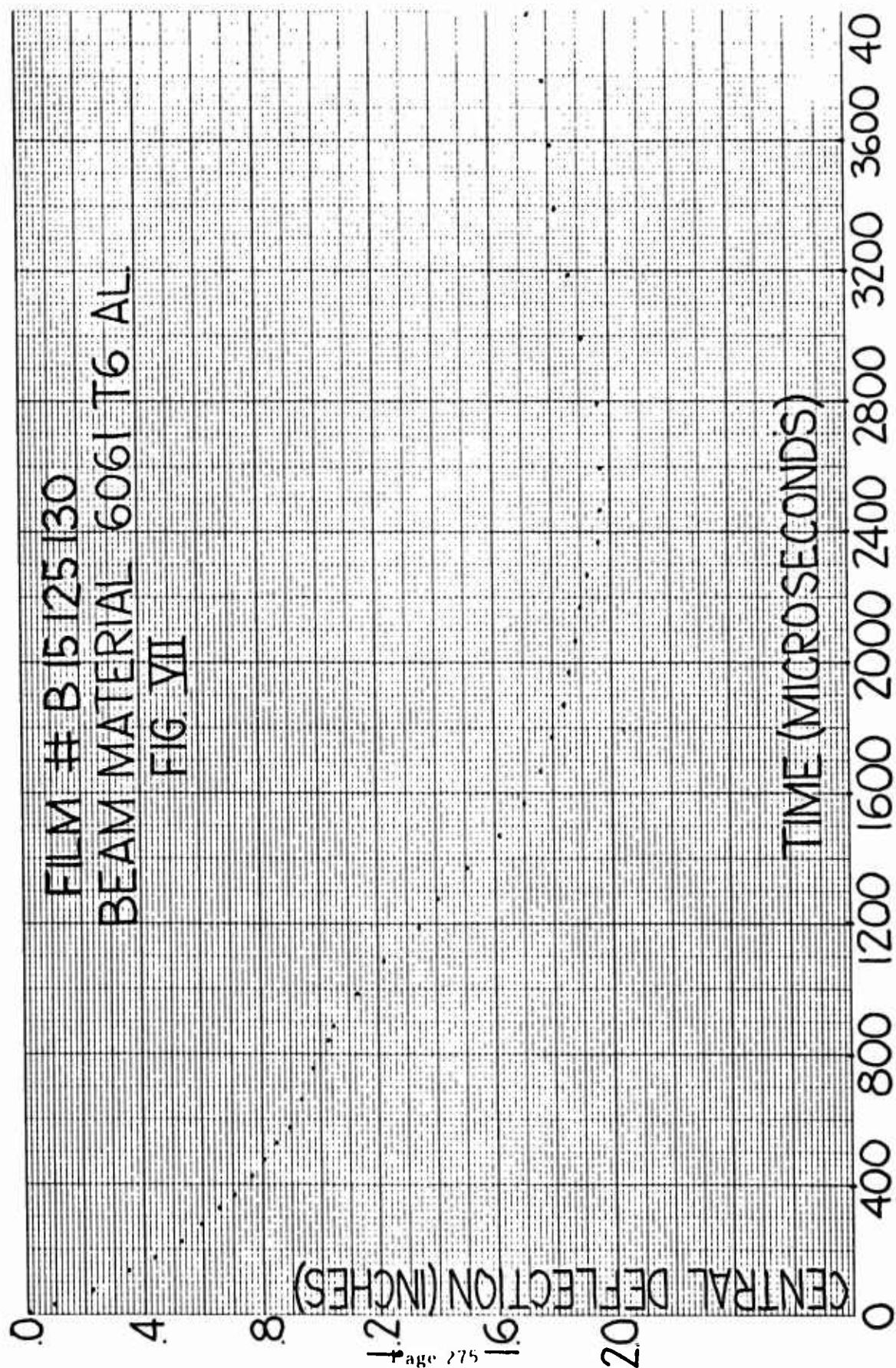
- (1) The "P" prefix indicates clamped beam  
(2) The "B" prefix indicates free beam  
(3) 1010 steel beams heat-treated as follows:

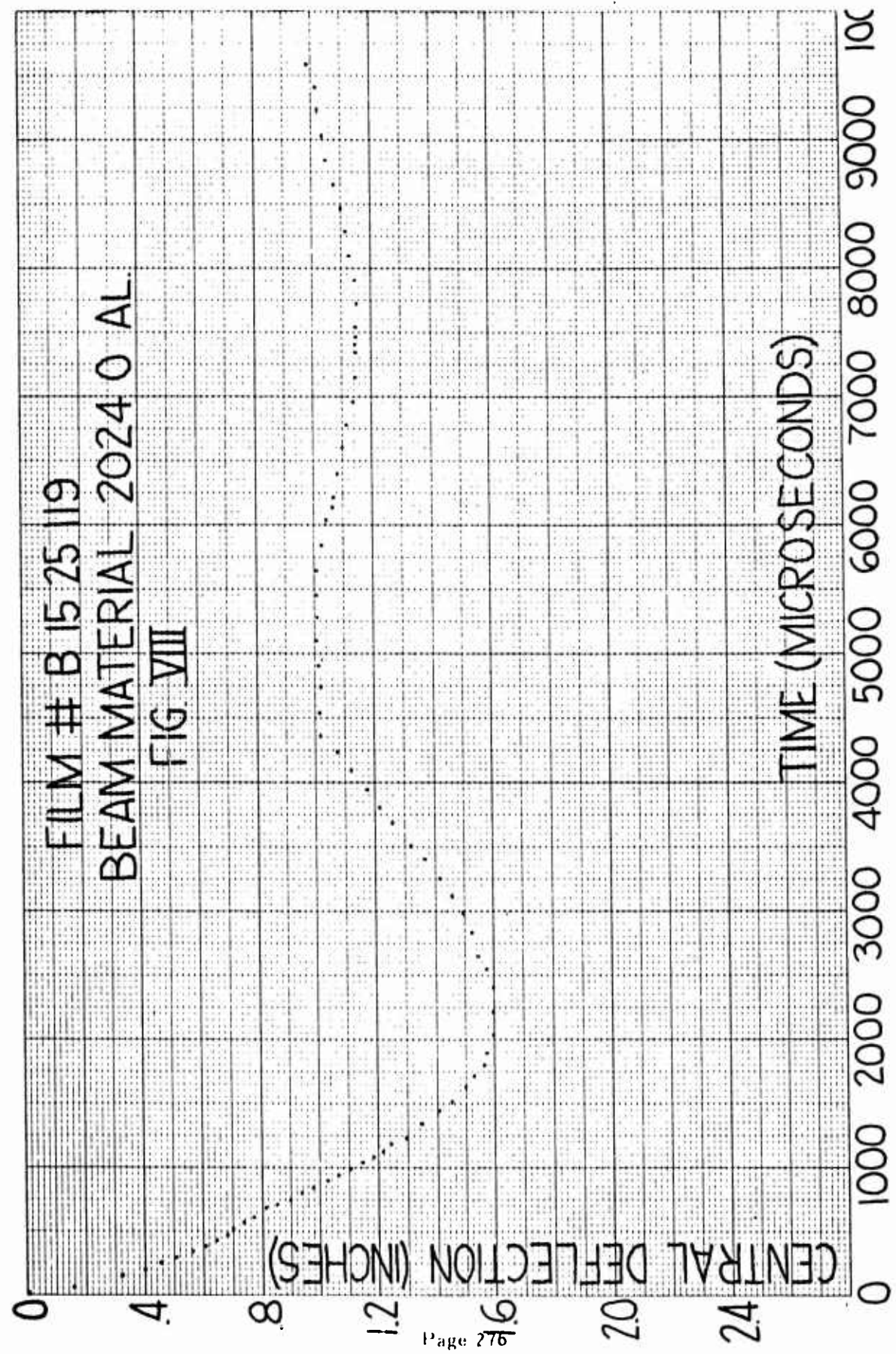
Normalized @ 1650° F for one hour - air cooled  
Annealed @ 1600° F for one hour - furnace cooled  
@ 250° F per hour in hydrogen atmosphere

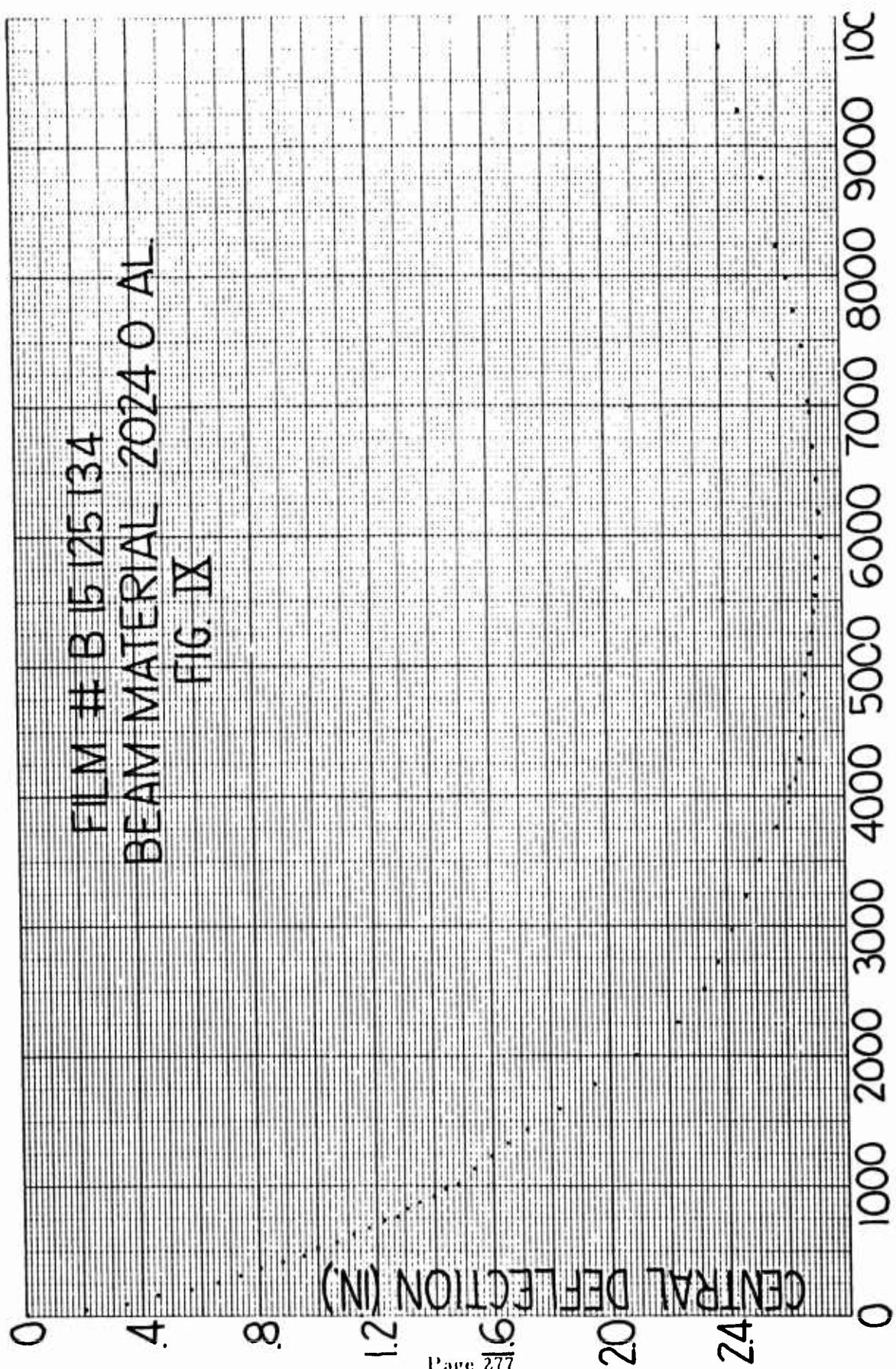
\* First observed maximum  
Yield  
\*\*2024-8 Al 11,000 psi  
6061-T6 Al 40,000 psi  
1010 Steel 12,000 psi



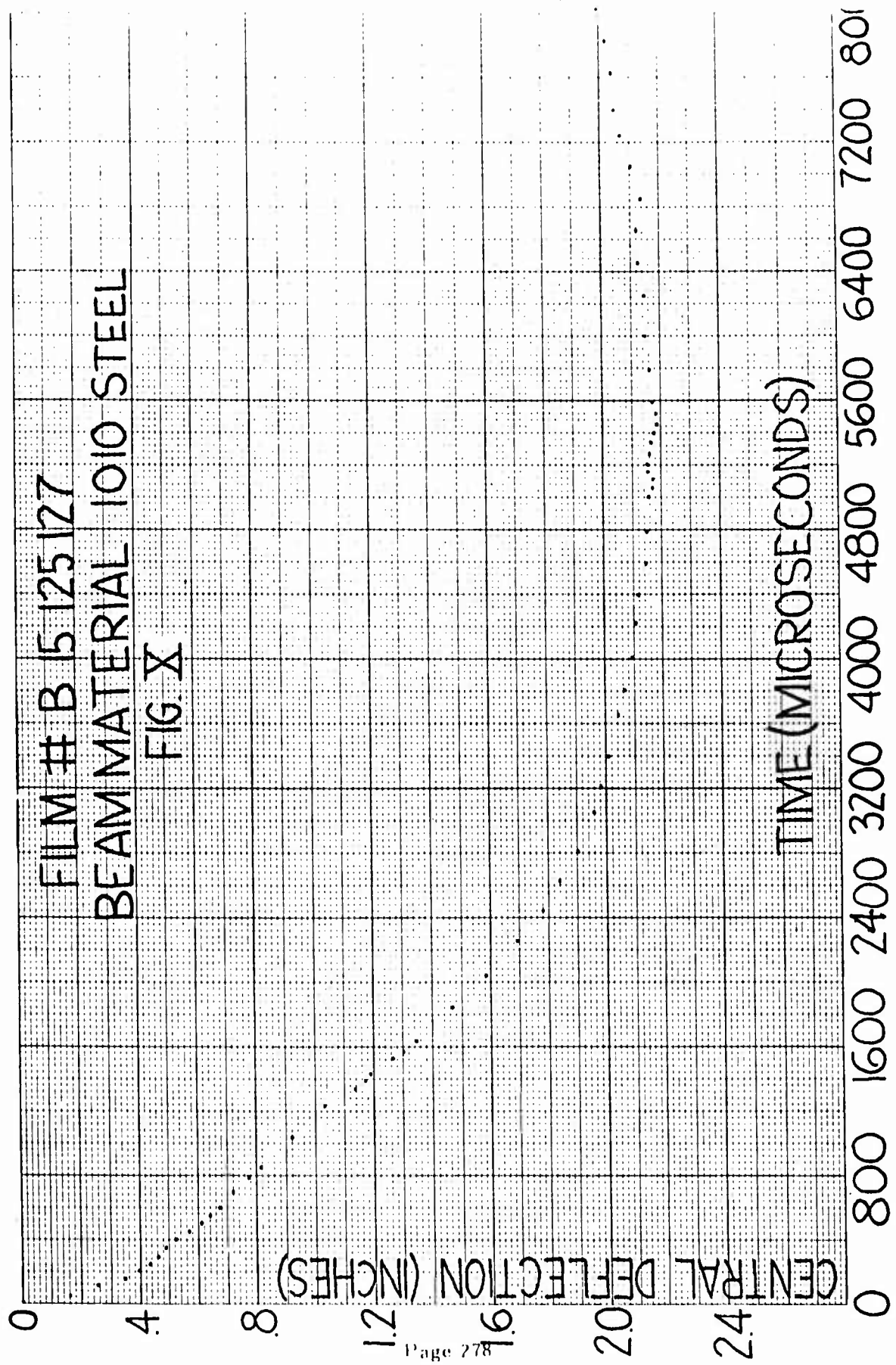












within  $1/16$ ", although in the case where it was necessary to use a lucite sheet, this distance was increased to  $1/4$  inch. Since the distance from the beam to the lens of the streak camera was generally 8 feet, the maximum error introduced by parallax was 0.25% although in most cases it was considerably less, therefore, the error introduced in this manner was neglected.

All free beams were 12" long, and were supported on uprights 10.068" apart, resulting in an approximate 1" overhang at each end of the beam. The beams were loaded with sheet explosive initiated in an identical manner to that used in the impulse calibration work and a sheet of .055" polyethylene was placed between the explosive and the beam. Three shots, each of five different types of free beams, have been fired to date. The results are given in Table IV for each shot. The position-time history for a typical shot for each type of beam are given in Figures VI to X. The B prefix in film numbers on graphs denotes a free beam test.

#### Clamped Beams

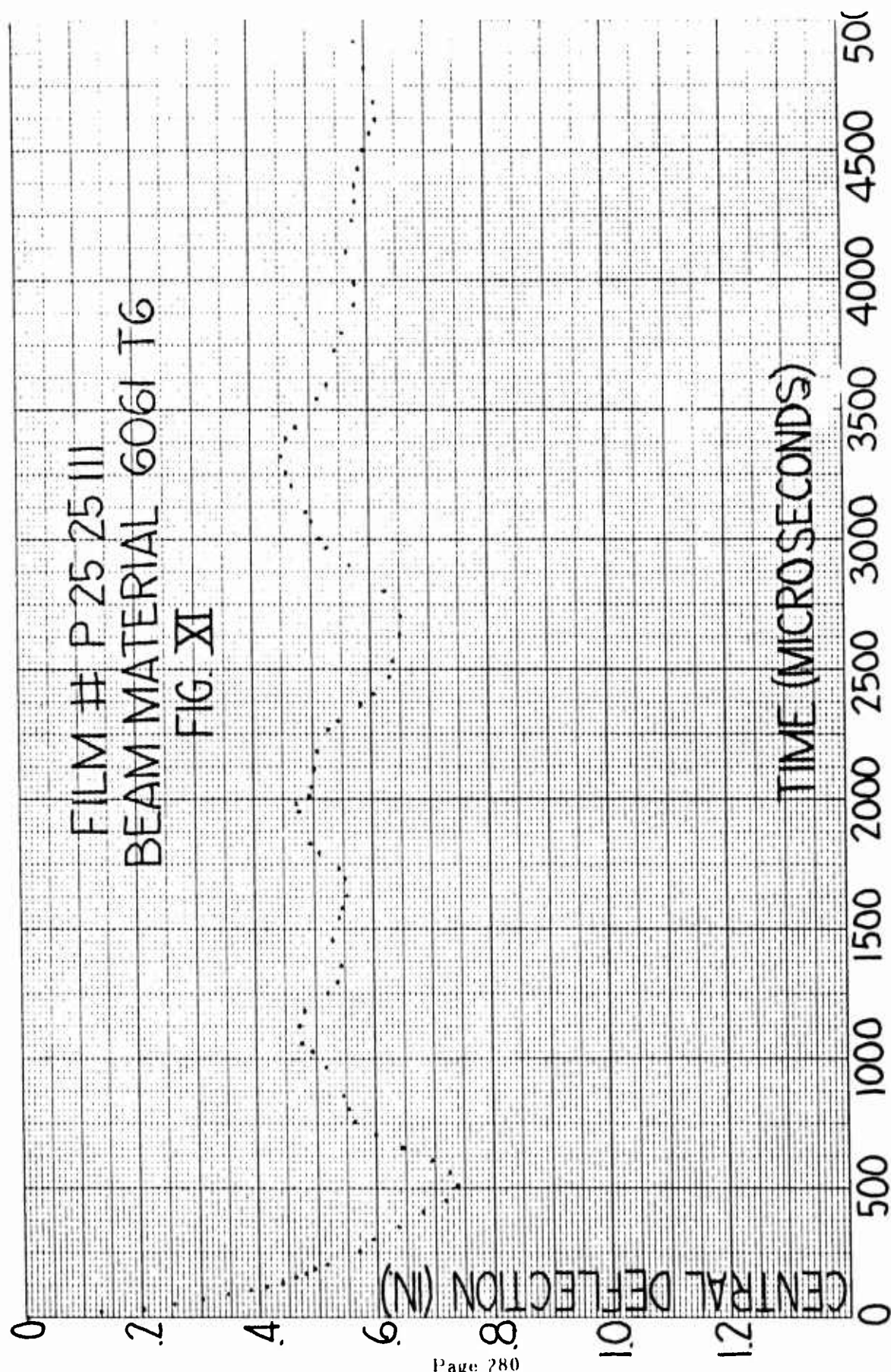
For the observation of the clamped beam motion, essentially the same experimental conditions existed, with the exception of the stand. (The stand was constructed with 4" thick steel uprights which were welded to a 1" steel base plate and held apart at the top by a 2" x 2" steel spacer). The supports could withstand considerably more force than the tested beams could apply and still undergo only negligible deflection. The beam was clamped at each end to the upright by a 1" knurled steel plate held down by four 1" steel bolts torqued up to 200 ft-lbs. After firing, the beams were examined at the knurled marks for signs of slipping and none were found.

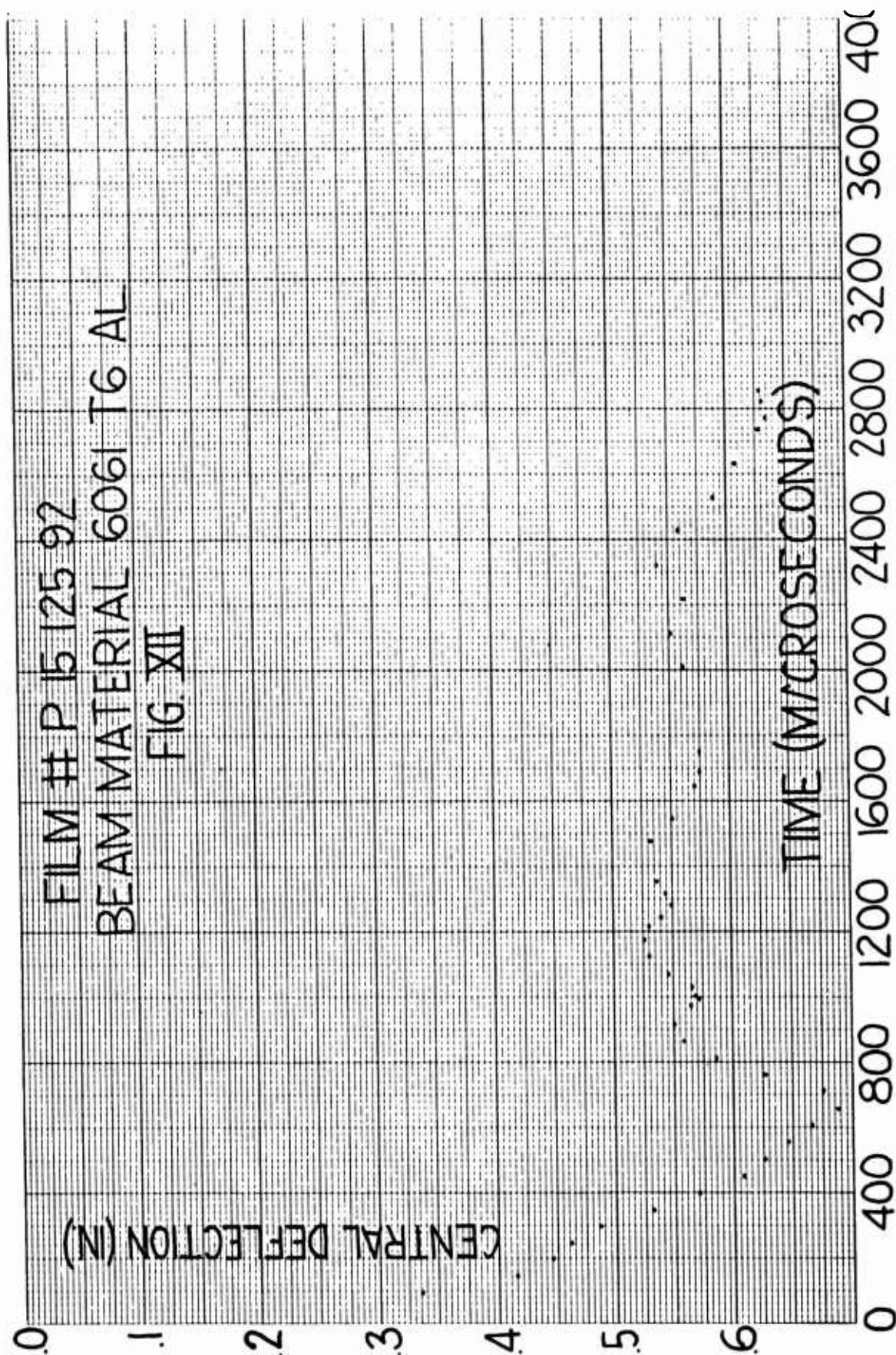
Table IV gives the results of the series of clamped beams tested, and the position time histories of typical beams of each type are given in Figures XI to XV. P prefix in film number on graph denotes clamped beam tests.

Referring to the results of the edge effect experiment it can be seen that the blast effect has a significant range. Therefore, since an explosive lead was only on one side of the beam, the loading was somewhat asymmetrical due to this blast effect. It will be noted, however, that the experiment did measure the total impulse acting on the time pieces and, since the beam had similar geometry, also the total impulse acting on the beam. However, the impulse acting across the width of the beam was (due to this blast) not completely uniform. This non-uniformity was not observable on any of the beams except some of the weaker clamped beams. Where this is the case the deflection is given for both the front and back edge of the beam, the back edge always being that with the larger deflection.

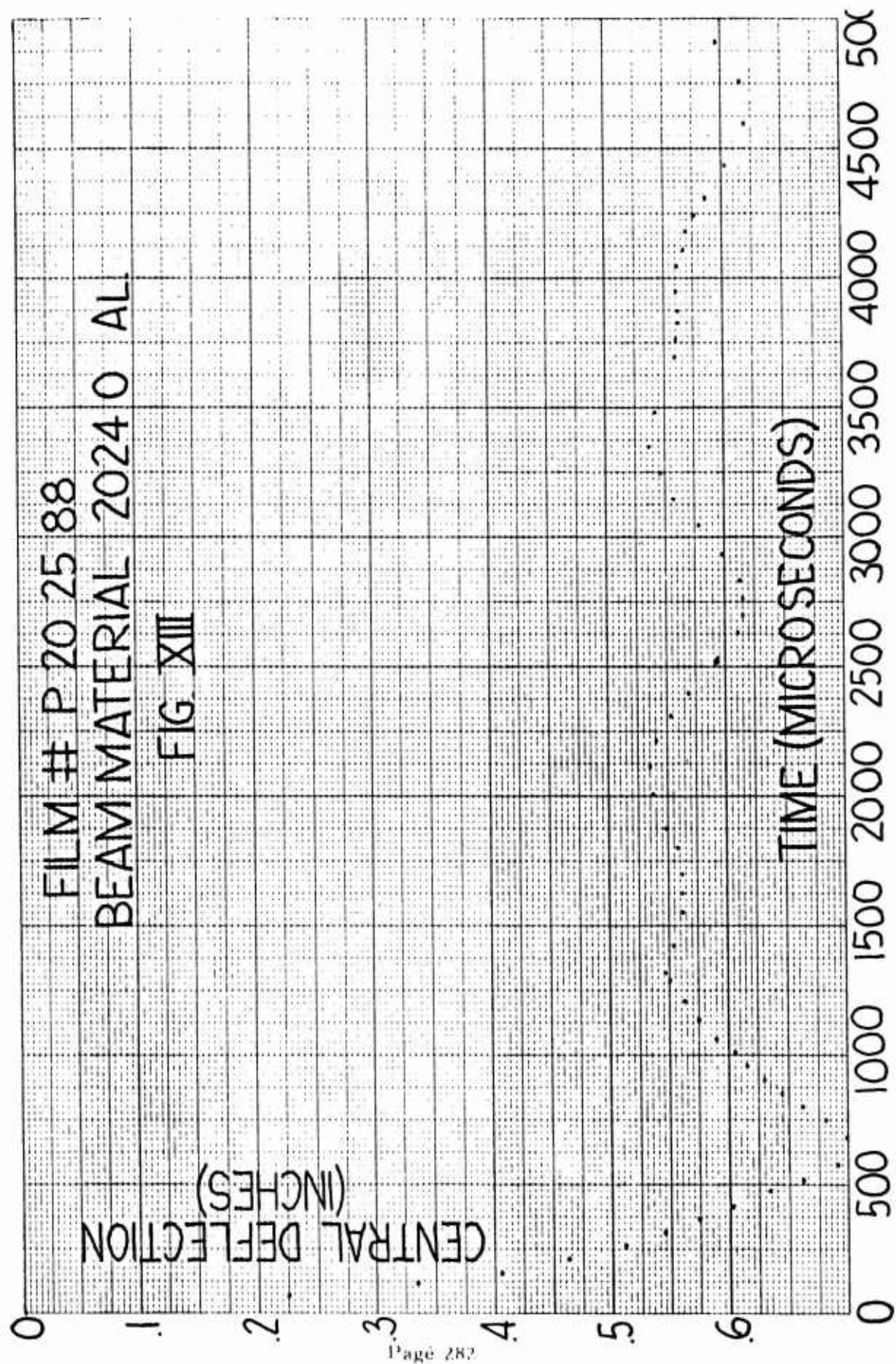
#### Metallurgy of the Beams

Care was taken to assure that the beam remained physically undamaged in the sense that there was neither spalling nor corner cracking. Considerably less explosive than that needed to produce spall was used and the

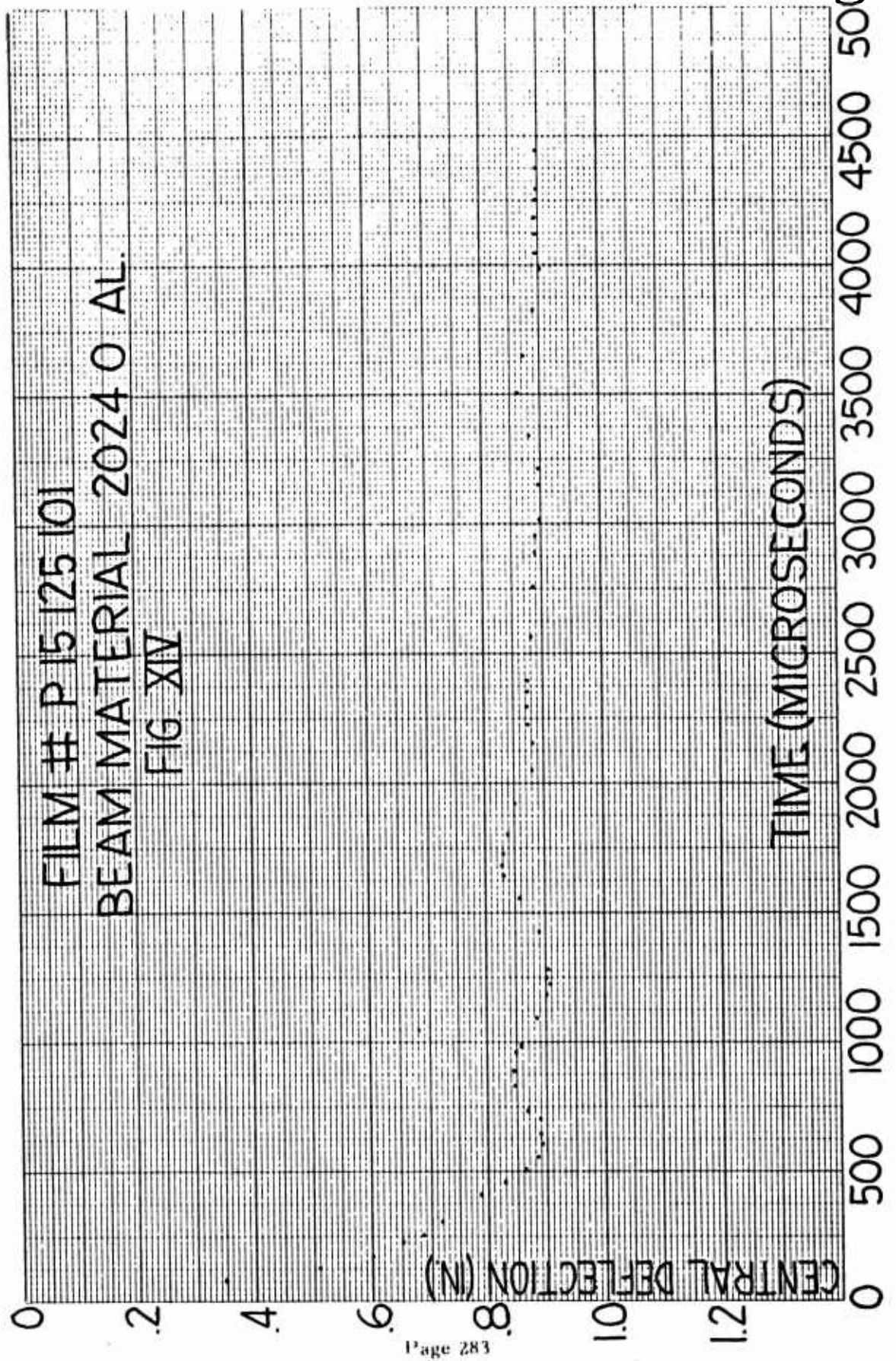


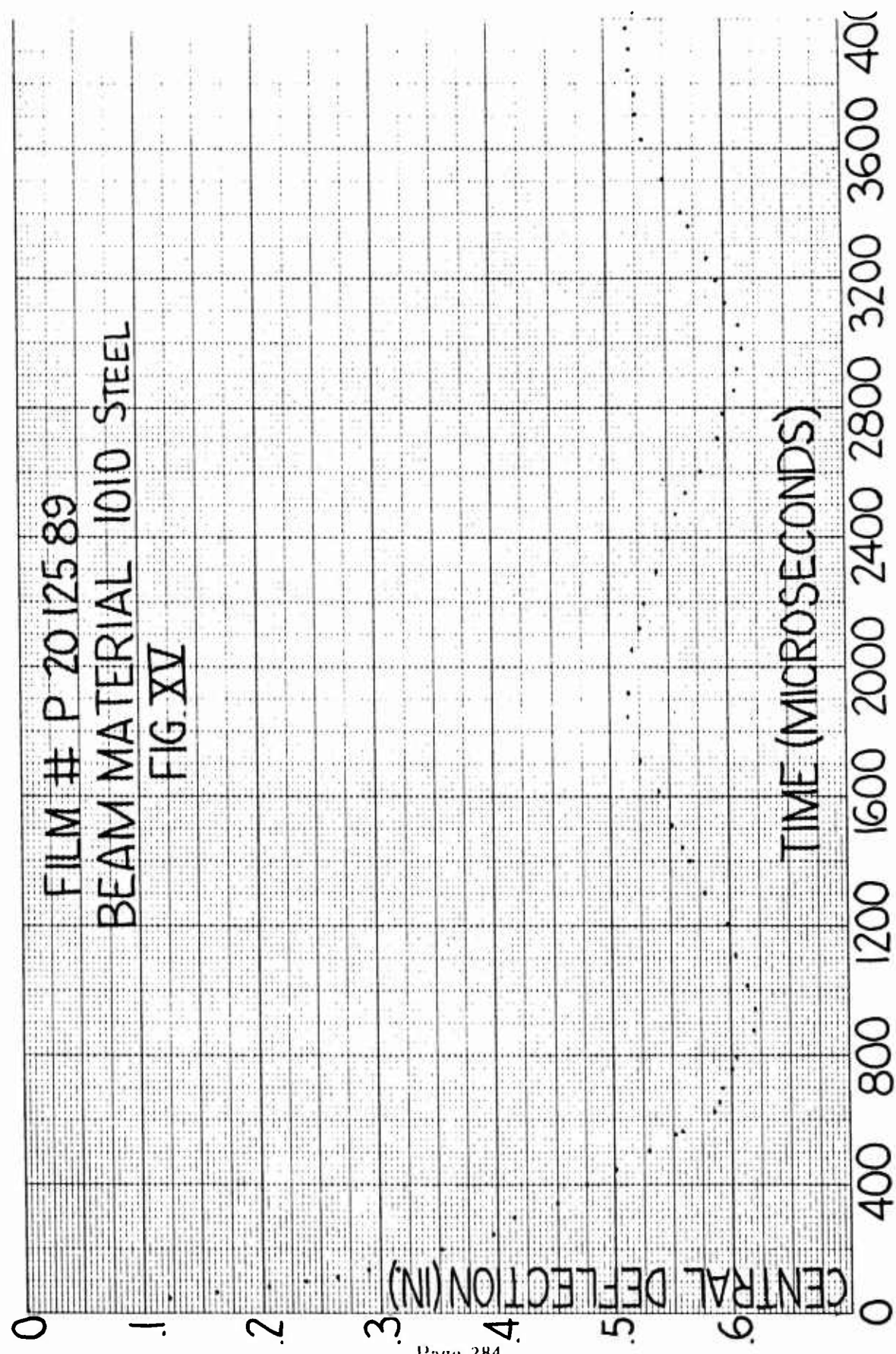












front baffle was of the same material as the beam to prevent shock reflection from the front of the beam with the possible resultant corner cracking. As a result, it is believed that in no case was the beam damaged in this sense, although it is planned to section various parts of the beam samples to assure that this is true.

When each set of beams were made, test coupons were prepared for testing in both static stress strain machines and the Picatinny High Rate Machine to be described by Mr. Roach later in these proceedings. However, since the high rate data is relatively recent, insufficient analysis has been given to the data and only the static values are presented here.

#### Comparison of Results with Theory

Most of the beam results of this work are relatively recent and have therefore not been compared extensively with theory. However, the first series of beams, the free 1/4" 6061 T6 aluminum results, have been studied to a limited extent. Professor Borg (4) of Stevens Institute of Technology has developed a theory which essentially partitions energy among various modes of vibration. Professor Borg has made calculations for this experiment and the results are given below:

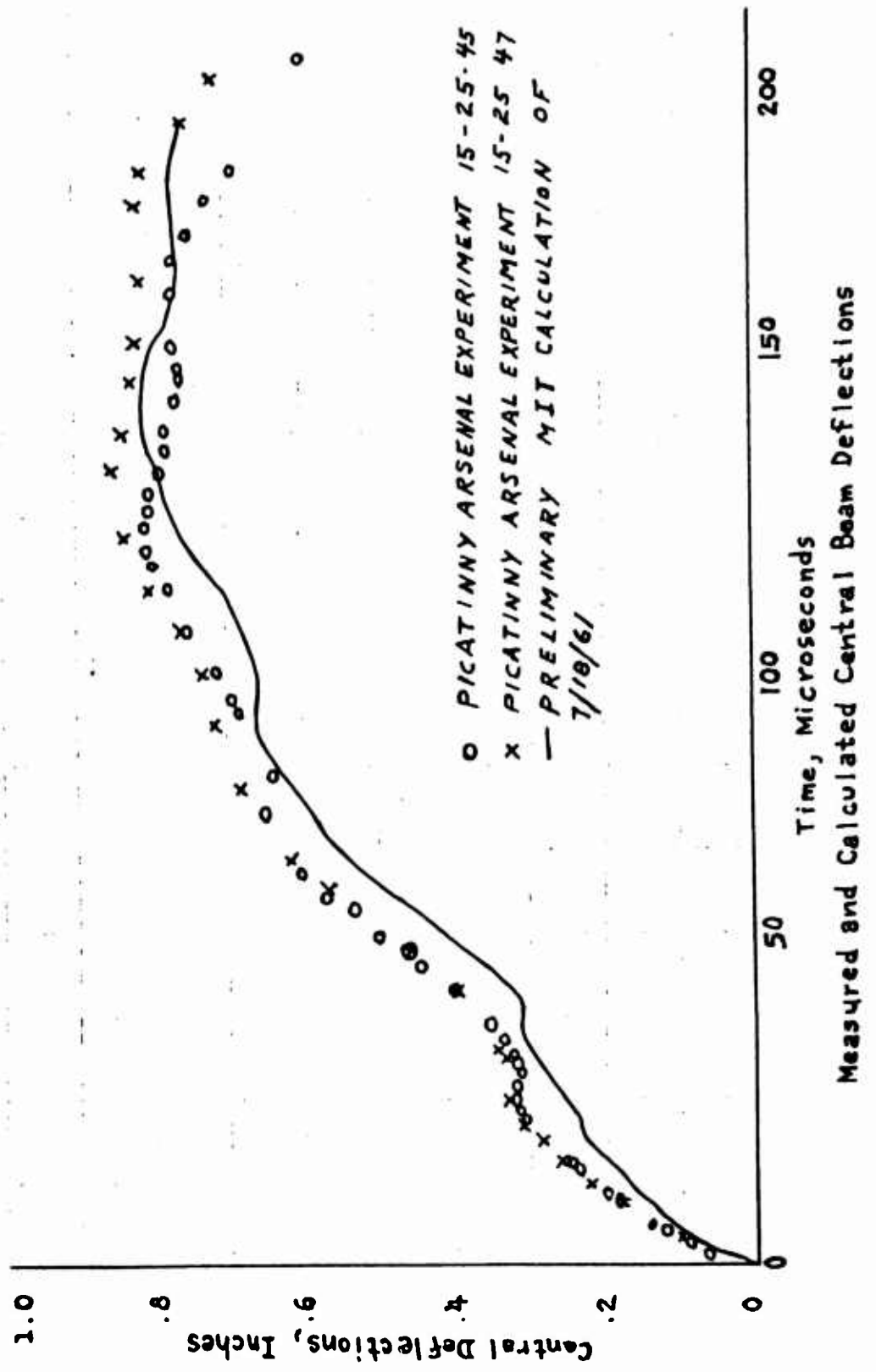
	Theory Assumed Simply Supported	Experiment (avg)
Max Deflection	1.38"	1.35"
Time to Max Def, sec	2210	1790
Permanent Def	0.85"	0.547"

It will be noted that agreement for the maximum deflection is quite satisfactory while that for the permanent deflection is much less so. (However, it might well be expected that the roller assembly which oscillates many times with large amplitude before the permanent deflection occurs might take up considerable energy which would thus result in an experimentally smaller permanent deflection). Further, the time to maximum deflection is rather insensitive since that part of the deflection time curve is rather flat and the actual time of maximum is normally determined by some higher order component of the oscillation. Thus, for this particular experiment the agreement appears satisfactory within the limits of the experimental conditions.

Professor Symonds (5) of Brown University has made calculations for this same beam. However, this theory assumed a rigid-perfectly plastic model and the condition which determines the applicability of this theory, that the plastic deformation must be much larger than any possible elastic vibration, is violated. Also, this theory only predicts the permanent deflection and we have already seen that the experimental conditions of the experiment need improvement in this regard, therefore the agreement was unsatisfactory. It is interesting to note that the average deflection for the three beam deflections, according to Professor Symonds, was 0.88" while

that of Professor Borg's was 0.85". This value is in good agreement with results we have obtained with firings of the same type beams which were resting only on the bottom support cylinder and the rest of the end constraint removed.

The Massachusetts Institute of Technology, as part of this same Air Force project, is conducting a theoretical study of this problem. Figure XVI, taken from an early progress report indicates the agreement obtained for this same 1/4 aluminum beam. The calculations were made by dividing the beam into 60 mass points, each point connected to its neighbor by two non-linear springs. The conditions on the spring in this case were for an elastic, perfectly plastic model, and the calculations were made on their IBM 7090.



#### REFERENCES

1. Progress Reports to Flight Dynamics Laboratory, Aeronautical Research Division, Wright Air Development Division, MIPR (33-657)-2-R&D 182
2. Unpublished Data, Courtesy Dr. P. O. Hoffman of these laboratories
3. "Techniques for Simulating Impulses on Re-entry Vehicles",  
G. R. Abrahamson, Stanford Research Institute, 3 March 1961
4. "The Analysis of Ship Structures Subjected to Slamming Loads",  
S. F. Borg, Journal of Ship Research, Vol. 4, No. 3, December 1960
5. "Large Plastic Deformations of Beams under Transverse Impact",  
E. H. Lee and P. S. Symonds, Journal of Applied Mech. Vol. 19, pp  
308-315, 1952

## ACKNOWLEDGEMENTS

The authors wish to acknowledge with sincerest thanks the assistance of Messrs. Louis Toscano, Charles Coles and Spero Nicolaides for assistance in performing the experiments reducing the data. Professor Emmett Witmer of Massachusetts Institute of Technology who made suggestions with regard to the edge effect experiments; Mr. Lauro d' A. Menezes who performed the metallurgical examination of the beam and Mrs. Margaret O'Neill who did a fine job of typing the report under pressure of limited time.

## DISCUSSION

Dr. Kumar: I would like to remark that this was a very fine paper. I commend you especially for the very quick to the point manner in which you presented so much material, Dr. Clark. May I just ask one question? Was this primarily a basic study or was there any specific purpose for considering explosive loading of this type? In reality would the beams be exposed to this type of load?

Dr. Clark: We are studying impulsive motion. We want the loading to be short with regard to the response time of the beam. Actually this is simulating another effect that we are interested in. The purpose of the work is to generate experimental information on impulsive motion of this type of structure. In correlation with MIT we are doing an analytical and theoretical study of the same problem.

## THERMAL STRESSES ARISING IN GUN TUBES DURING REPETITIVE FIRING

Lt. L. G. Mielke\* and T. F. MacLaughlin\*\*

The stress field in a smooth-bore gun tube due to thermal shocks resulting from repetitive firing has been determined analytically by Pascual and Zweig<sup>1</sup>. An experimental program for determining these stresses was formulated because there are two limitations which exist in the mathematical analysis. These limitations are (1) difficulty in obtaining stresses at the bore surface and (2) difficulty in extending the analysis to include rifled gun tubes. Two experimental approaches are being employed concurrently. One of these is known as photothermoelasticity, a photoelastic method developed by Gerard and associates<sup>2, 3, 4</sup> for evaluating thermal stresses. The other technique utilizes an electrical analog model.

This paper reports the preliminary study that has been done, outlines the experimental program which has just begun and discusses the expected scope of the project.

### PROBLEM

The complete stress field in a gun tube is composed of two separate stresses, pressure and thermal. The pressure stresses within the wall of the tube are caused by rapidly expanding gas and also by the radial deformation of the tube due to the interference fit between the projectile and bore. The thermal stresses are caused by the hot gases giving up heat to their cooler surroundings and also heat which is generated at the interface between the projectile and bore. This paper will deal with only the latter classification of stresses.

The problem is as follows - Determine the thermal stress distribution in a hollow tube with a variable temperature on the bore surface and a convective boundary condition to constant temperature surroundings at the external surface.

One of the most difficult tasks connected with either of the experimental techniques to be discussed later is the generation of a temperature or voltage

---

Lt. L. G. Mielke, Experimental Mechanics Laboratory, Watervliet Arsenal, Watervliet, New York.

\*\* T. F. MacLaughlin, Experimental Mechanics Laboratory, Watervliet Arsenal, Watervliet, New York.



which duplicates the actual temperatures that exist on the internal surface of the tube. Figure 1 approximates very closely an actual set of experimental data and was used by Pascual and Zweig<sup>1</sup> in their mathematical analysis. This data was chosen for initial studies as it provided a theoretical solution with which a portion of our results could be correlated.

### TEMPERATURE DISTRIBUTION ON BORE OF GUN TUBE

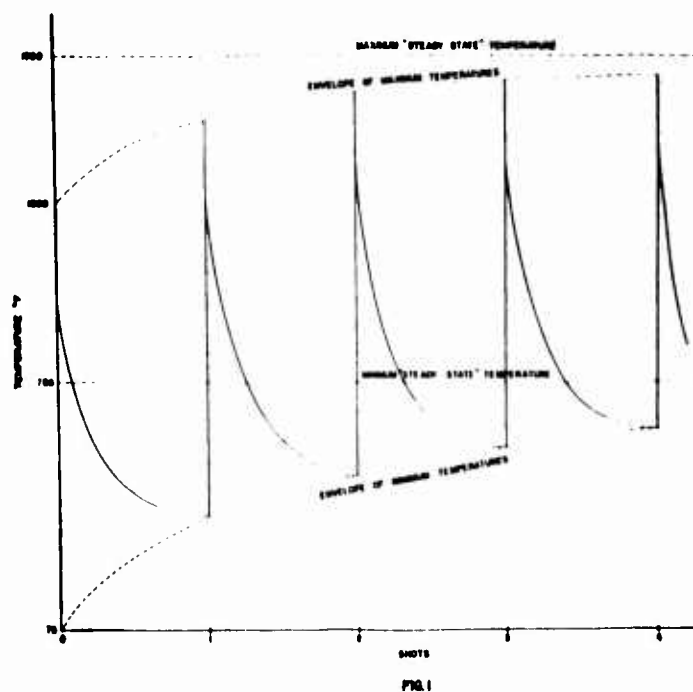


FIG. 1

### PHOTOTHERMOELASTIC APPROACH

The basic heat conduction equation in cylindrical coordinates is

$$\frac{\partial^2 t}{\partial r^2} + \frac{1}{r} \frac{\partial t}{\partial r} = \frac{1}{\alpha} \frac{\partial t}{\partial \tau} \quad (1)$$

where  $t$  is temperature,  $r$  is radial position,  $\alpha$  is thermal diffusivity and  $\tau$  represents time. The boundary conditions which must be satisfied are

$$\begin{array}{lll} a \leq r \leq b & t = t_0 & \tau < 0 \\ r = a & t = f(\tau) & \tau \geq 0 \end{array} \quad (2)$$

$$r = b \quad \frac{\partial t}{\partial r} = - \frac{h}{k} (t - t_0) \quad \tau \geq 0$$

where  $a$  is the inner radius,  $b$  is the outer radius,  $t_0$  is the external surroundings temperature and  $h$  is the convective heat transfer coefficient. The expressions may be nondimensionalized by introducing

$$\vartheta = \frac{t - t_0}{t_r - t_0}, \quad r' = \frac{r}{a}, \quad \beta = \frac{b}{a}, \quad \tau' = \frac{\tau}{\tau_0} \quad (3)$$

where  $t_r$  is a reference temperature and  $\tau_0$  is the time for one complete cycle (shot). The results are

$$\frac{\partial^2 \vartheta}{\partial r'^2} + \frac{1}{r'} \frac{\partial \vartheta}{\partial r'} = \frac{a^2}{\alpha \tau_0} \frac{\partial \vartheta}{\partial \tau'} \quad (4)$$

$$\begin{aligned} 1 \leq r' \leq \beta & \quad \vartheta = 0 & \quad \tau' < 0 \\ r' = 1 & \quad \vartheta = g(\tau') & \quad \tau' \geq 0 \\ r' = \beta & \quad \frac{\partial \vartheta}{\partial r'} = -\frac{ha}{k} \vartheta & \quad \tau' \geq 0 \end{aligned} \quad (5)$$

Therefore, a solution for the temperature distribution must be of the form

$$\vartheta = f \left[ r', \tau', \frac{a^2}{\alpha \tau_0} \right] \quad (6)$$

To insure the same relative temperature distribution in the gun as exists within the photoelastic model the following conditions must be fulfilled

$$r'_m = r'_p, \quad \tau'_m = \tau'_p, \quad \left. \frac{a^2}{\alpha \tau_0} \right|_m = \left. \frac{a^2}{\alpha \tau_0} \right|_p \quad (7)$$

where the subscripts  $m$  and  $p$  denote model and prototype.

To evaluate the thermal stresses in a smooth bore tube from the temperature distribution the equations taken from Timoshenko<sup>5</sup> may be applied

$$\sigma_r = \frac{\gamma E}{1 - \nu} \left[ \frac{1}{r^2} \left[ \frac{r^2 - a^2}{b^2 - a^2} \int_a^b tr \, dr - \int_a^r tr \, dr \right] \right]$$

$$\begin{aligned}\sigma_{\theta} &= \frac{\gamma E}{1-\nu} \frac{1}{r^2} \left[ \frac{r^2 + a^2}{b^2 - a^2} \int_a^b tr \, dr + \int_a^r tr \, dr - tr^2 \right] \\ \sigma_z &= \frac{\gamma E}{1-\nu} \left[ \frac{2}{b^2 - a^2} \int_a^b tr \, dr - t \right]\end{aligned}\quad (8)$$

where  $\sigma_r$ ,  $\sigma_{\theta}$  and  $\sigma_z$  are the stresses in the radial, tangential and axial directions,  $\gamma$  is the coefficient of linear expansion,  $E$  is Young's modulus and  $\nu$  is Poisson's ratio. These relations may be nondimensionalized by utilizing the appropriate expressions from equation set (3). The results are

$$\begin{aligned}\frac{\sigma_r}{\frac{\gamma E}{1-\nu} (t_r - t_0)} &= \frac{1}{r^2} \left[ \frac{r^2 + 1}{\beta^2 - 1} \int_1^{\beta} \vartheta r' \, dr' - \int_1^r r' \, dr' \right] \\ \frac{\sigma_{\theta}}{\frac{\gamma E}{1-\nu} (t_r - t_0)} &= \frac{1}{r^2} \left[ \frac{r^2 + 1}{\beta^2 - 1} \int_1^{\beta} \vartheta r' \, dr' + \int_1^r \vartheta r' \, dr' - \vartheta r'^2 \right] \\ \frac{\sigma_z}{\frac{\gamma E}{1-\nu} (t_r - t_0)} &= \frac{2}{\beta^2 - 1} \int_1^{\beta} \vartheta r' \, dr' - \vartheta\end{aligned}\quad (9)$$

Equation set (9) applies to both model and prototype since the relative temperature distributions are identical in both cases. It is then apparent that

$$\begin{aligned}\left. \frac{\sigma_r}{\frac{\gamma E}{1-\nu} (t_r - t_0)} \right|_m &= \left. \frac{\sigma_r}{\frac{\gamma E}{1-\nu} (t_r - t_0)} \right|_p \\ \left. \frac{\sigma_{\theta}}{\frac{\gamma E}{1-\nu} (t_r - t_0)} \right|_m &= \left. \frac{\sigma_{\theta}}{\frac{\gamma E}{1-\nu} (t_r - t_0)} \right|_p \\ \left. \frac{\sigma_z}{\frac{\gamma E}{1-\nu} (t_r - t_0)} \right|_m &= \left. \frac{\sigma_z}{\frac{\gamma E}{1-\nu} (t_r - t_0)} \right|_p\end{aligned}\quad (10)$$

Evaluation of the photoelastic fringe pattern provides a means for calculating the stresses within the model. The stress-optic law,

$$\sigma_1 - \sigma_2 = \frac{C}{t} N \quad (11)$$

where  $\sigma_1$  and  $\sigma_2$  are principal stresses,  $t$  is the model thickness,  $C$  is the material stress-optic coefficient and  $N$  is the fringe order, can be rewritten, because of rotational symmetry, as

$$\sigma_r - \sigma_\theta = \frac{C}{t} N \quad (12)$$

The equilibrium equation for a cylindrical element under stress may be expressed as

$$\frac{\partial \sigma_r}{\partial r} + \frac{1}{r} \frac{\partial \tau_{r\theta}}{\partial \theta} + \frac{\partial \tau_{rz}}{\partial z} + \frac{\sigma_r - \sigma_\theta}{r} = 0 \quad (13)$$

Because of rotational symmetry and axial uniformity of the thermal load which will be applied the two terms  $\frac{\partial \tau_{r\theta}}{\partial \theta}$  and  $\frac{\partial \tau_{rz}}{\partial z}$  are zero and equation (13) reduces to

$$\frac{\partial \sigma_r}{\partial r} + \frac{\sigma_r - \sigma_\theta}{r} = 0 \quad (14)$$

Equation (14) can be combined with equation (12) and the result integrated between the internal radius  $a$  and some point  $r$ . The final form is

$$\sigma_r \Big|_a^r = -\frac{1}{t} \int_a^r \pm \frac{CN}{r} dr \quad (15)$$

Once the radial stress at some point  $r$  is known the stress in the tangential direction can be obtained by equation (12) and the stress in the axial direction may be obtained by a similar equation written for the radial and axial stresses. Therefore, the complete stress pattern in the model can be evaluated. These results can be introduced into equation set (10) which will yield the corresponding stresses which exist within the gun.

#### EXPERIMENTAL APPARATUS

Figure 2 shows the general apparatus set up for the photoelastic study of the problem. From Fig. 1 it can be observed that the data shows an instantaneous bore temperature rise upon firing and a very rapid decline in

# APPARATUS SET UP FOR STUDYING THERMAL STRESSES ARISING IN GUN TUBES DURING FIRING

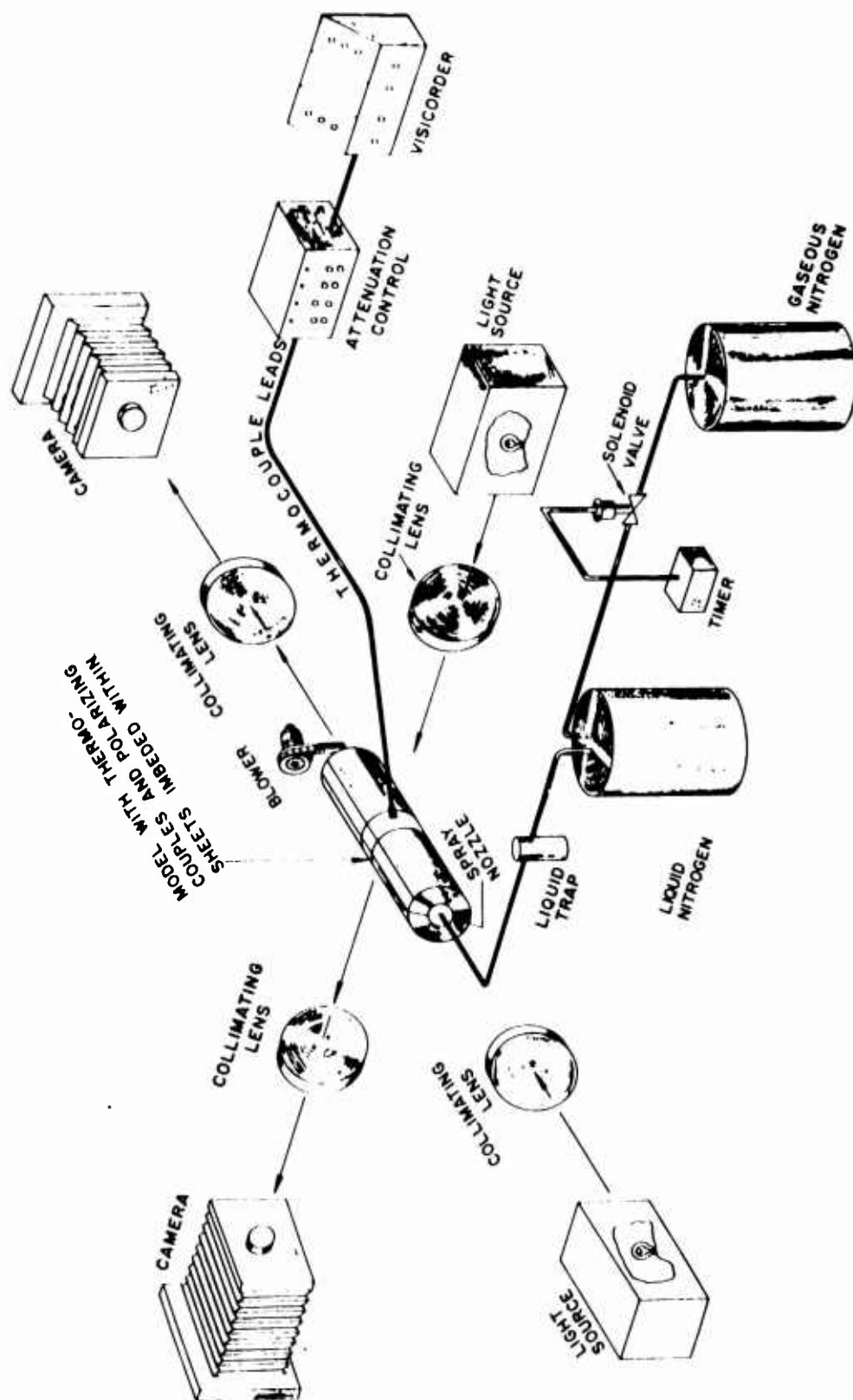


FIG. 2

temperature immediately after combustion of the propellant. Since the photoelastic material from which the model is constructed will not tolerate high temperatures, it was decided that cold thermal shock would more easily simulate the chosen data. Another factor in favor of the low temperatures is that the stress optic coefficient for the photoelastic material is almost constant in this region<sup>3</sup> whereas at higher temperatures it exhibits a definite temperature dependency. Cold gaseous nitrogen will be used to provide a time-temperature relation which duplicates as nearly as possible the curve of Fig. 1. The bore temperatures will be scaled down such that the entire temperature variation will take place from 75°F to approximately 0°F. The scaling process will have no effect on the relative magnitude of the stresses produced. However, due to the reversal in direction of the thermal shock simulating firing conditions, the algebraic sign of the stresses in the model will be opposite from those in the gun.

The flow of cold gas will be regulated by a timer. At some preset time the timer will trip a micro switch energizing a solenoid valve allowing gaseous nitrogen to flow into the liquid nitrogen container. The gas pressure is sufficient to force the liquid out of the container and into the line leading to the model. As the liquid proceeds along the tube, it will absorb heat from the surroundings causing it to boil and vaporize. Just prior to entering the model the two phase flow of gas and liquid will flow through a trap which retains the liquid. The cold gas will continue on into a spray nozzle inside the model which will discharge the gas out against the bore surface of the tube producing a rapid decrease in temperature. Free convection will not be sufficient to warm the tube as quickly as is necessary so a small blower will be used to speed up the process.

Two polariscopes are required for this experiment, one of which will be in line with the axis of the model. With this polariscope, fringe patterns will be obtained which can be used to evaluate the stress differences in the radial and tangential directions. The second polariscope positioned with its axis 90° from the first will be used to obtain stress differences in the radial and axial directions.

Figure 3 shows the details of the model. Hysol 4290, an epoxy resin, was selected for fabrication of the model since its stress optic coefficient is nearly constant within the temperature range under consideration and also it possesses a high figure of merit (fringe/inch °F). The lower cylindrical section shown in Fig. 3 consists of a 0.375" test specimen which is sandwiched between two plane polarizing sheets which act as polarizer and analyzer for the polariscope. On either side of this unit is placed a larger cylindrical piece made of the same material as the test specimen. The temperature on the internal surface of the tube is not a function of location

PLANE POLARIZING-  
SHEETS, AXES  
CROSSED WITH 45°  
ORIENTATION TO  
EDGES

PHOTOELASTIC  
PLASTIC



**VIEWING  
DIRECTION**

**FIG. 3**

for a particular time, nevertheless, the heat flow will be two dimensional near the ends of the tube. The cylindrical end sections then provide a means of eliminating any axial heat flow in the test specimen located in the center.

The stresses in the axial direction will be obtained by interpretation of the fringe pattern in the material between the two long polarizing sheets in the upper section of the model. The polarizing sheets have been cut with their axes at  $45^\circ$  to the axis of the tube to allow maximum light transmission. Step shaped pieces which approximate the outside surface of the tube were used to allow the light beam to pass through the model without being deflected. To check the effect that this break in geometric boundary has on the stress distribution two small polarizing sheets were placed around a piece of photoelastic material and imbedded in the center of the tube wall as shown on Fig. 3. After thermal loading, the fringe pattern in the small test specimen and in the larger circular test specimen could be observed by viewing the model along its axis. Good correlation of the two fringe patterns would indicate relatively little change in the stress distribution due to altering the boundary. The stress distribution obtained from viewing the model at  $90^\circ$  to the axis of the tube could then be considered to be the same as that which exists in the unaltered region of the model.

#### THERMAL-ELECTRICAL ANALOGY

##### Theory

Consider the one dimensional unsteady conduction equation written in rectangular coordinates

$$\frac{\partial^2 t}{\partial x^2} = \frac{1}{\alpha} \frac{\partial t}{\partial \tau} \quad (16)$$

where  $x$  is the distance along the heat flow path. If we consider an electrical current carrying cable of negligible inductance which has its properties of resistance and capacitance uniformly distributed along its length, the expression which relates the voltage to various points along the cable is given by

$$\frac{\partial^2 V}{\partial x^2} = RC \frac{\partial V}{\partial \tau} \quad (17)$$

where  $V$  is voltage,  $R$  is resistance,  $C$  is capacitance and  $x$  is the distance along the current flow path. From the similarity between equations (16) and (17) it is apparent that a solution for the temperature would



be identical to a solution for the voltage if  $\frac{1}{\alpha} = RC$ . Therefore, the heat transfer system can be imitated by an electrical cable. In practice, the electrical cable is replaced by series resistors and parallel capacitors which is equivalent to lumping the resistance and capacitance of a section of the cable at one point. A known voltage or current is impressed upon this circuit and the resultant voltages are measured at the various nodal points. The theory of the method is extensively discussed in references 6 and 7.

The geometrical configuration under study and the corresponding electrical circuit are shown in Fig. 4. A thermal resistance may be

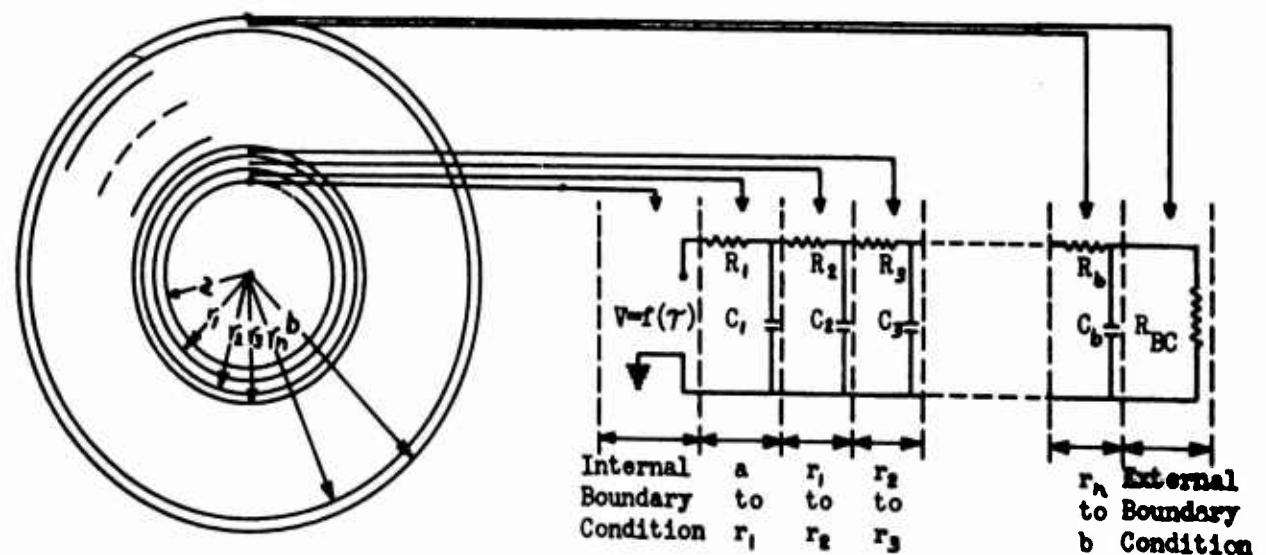


Fig. 4. Electrical analogy to heat flow through hollow cylinder.

defined as

$$R_t = \frac{1}{k A} \quad (18)$$

where  $k$  is the thermal conductivity and  $A$  the area through which the heat is flowing. This can be interpreted as a resistance to heat flow just as an electrical resistor is a resistance to electrical current flow. Similarly, a thermal capacitance can be defined as

$$C_t = \rho A c_p \quad (19)$$

where  $\rho$  is density and  $c_p$  is specific heat.  $C_t$  is analogous to an electrical capacitor. With these definitions, equation (16) can be written

$$\frac{\partial^2 t}{\partial x^2} = \frac{\rho A c_p}{kA} \frac{\partial t}{\partial \tau} = R_t C_t \frac{\partial t}{\partial \tau} \quad (20)$$

using the definition for thermal diffusivity,  $\alpha = \frac{k}{\rho c_p}$ . The necessary

condition for analogy may be expressed as  $R_t C_t = RC$ . It is often convenient to change the scale of some of the physical quantities. Equation (17) may be rewritten as

$$\frac{\partial^2 V}{\partial x^2} = (mnR) \left(\frac{C}{m}\right) \frac{\partial V}{\partial (n\tau)} \quad (21)$$

The scale factor  $n$  enables scale changes in the time base. The scale factor  $m$  is employed to allow the use of standard circuit elements. Without its use, values of resistance would be relatively small (order of magnitude 500 ohms) and the values of capacitance would be very large (0.5 farad). The resistors and capacitors in the circuit in Fig. 4 are given by

$$R = \frac{mn}{kA} \quad (22)$$

$$C = \frac{\rho A c_p}{m} \quad (23)$$

From the resultant voltage field, the thermal stresses can be obtained from equation set (8).

#### Experimental Procedure

A 90mm gun tube has been chosen for study. The tube is subdivided into ten concentric tubes of equal wall thickness as Paschkis and Heisler<sup>8</sup> reported very good correlation for more than 8-1/2 segments. Since the heat propagation through a steel gun tube is quite rapid, there have been no changes made in the time base between gun and model. The scale factor  $m$  is chosen as  $4.4 \times 10^5$ . The internal segment has a resistance and capacitance of 343K ohms and 2.79  $\mu f$  respectively. The values of the external tubular segment are 202K ohms and 4.73  $\mu f$ . All other segments have values of resistance and capacitance between these limits. Careful selection of resistors and capacitors enables trimming of the circuit elements to  $\pm 0.1\%$  of their calculated values. The external convective boundary

condition is simulated by a resistance of 79.5 megohms.

The voltage input must duplicate in shape the temperature-time curve of Fig. 1. The technique shown in Fig. 5 is used to accomplish this.

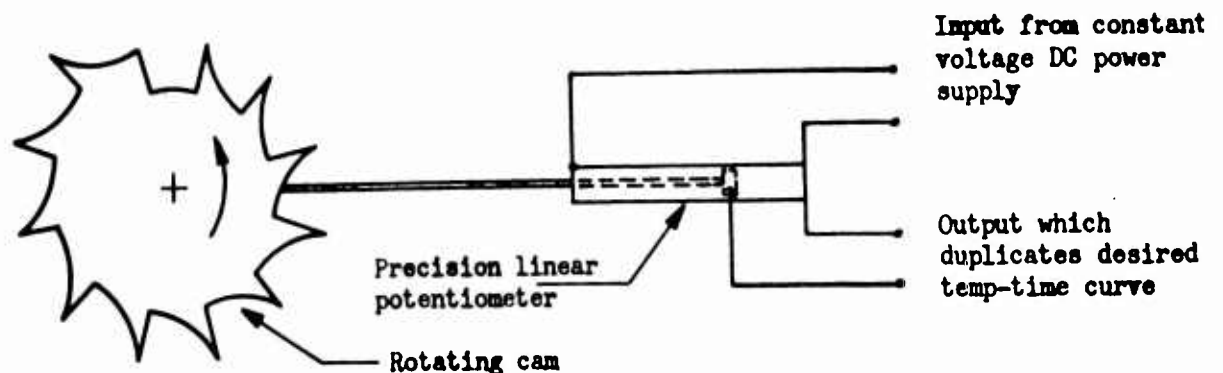


Fig. 5. Technique for generating non repetitive voltage pulses.

An oscillograph is used to determine the voltages. High sensitivity galvanometers are inserted into the circuit immediately after each resistor. Each galvanometer is calibrated in  $\mu\text{a/inch}$  deflection. The voltage drop in each section is obtained by multiplying the resistance of the section by the current flowing through it.

#### PROGRESS THUS FAR

##### Photoelastic Approach

At present one smooth bore model has been constructed with a radius ratio equal to 1.8. No reportable data has yet been obtained, but preliminary investigations indicate data taken from the model will correlate fairly well with the theoretical work. Difficulty is experienced in controlling the bore temperature according to Fig. 1 for more than three shots. It is hoped that satisfactory results could be obtained for ten shots.

##### Thermal Electrical Analog

The circuit for a smooth bore tube has been designed and constructed. Standard carbon resistors and paper capacitors were used as circuit elements. The reliability of the circuit has been checked with a constant

voltage input, corresponding to a constant bore temperature, and the results are within 1% of the calculated values for the major portion of the wall thickness and not exceeding 3% at any point. The function generator shown schematically in Fig. 5 is being constructed and no serious problems are anticipated in completion of this phase of the project.

#### SCOPE OF ANTICIPATED EXPERIMENTS

The photoelastic investigation will encompass construction and testing of at least two models. One has already been fabricated and the other would have the same overall dimensions but would differ from the first in that it would be rifled. Correlation between smooth bore tube and theoretical solution will provide confidence that the photothermoelastic technique will yield accurate results for the rifled tube, which will be studied during the second phase of the experimental program, and for which case other methods are unavailable. If time permits, other rifled tubes with a variety of radius ratios will be investigated.

It is expected to employ the thermal-electrical analog to smooth bore tubes only, as considerable difficulty is experienced in deducing the stresses in a rifled tube from the temperature field.

## REFERENCES

1. Pascual and Zweig, "Transient Thermal Stresses in Gun Tubes - Part II," Watervliet Arsenal Technical Report.
2. Gerard and Gilbert, "Photothermoelasticity: An Exploratory Study," Journal of Applied Mechanics, Vol. 24, Trans. ASME, Vol. 79, 1957, pp. 355-360.
3. Trampusch and Gerard, "Physical Properties of Plastics for Photothermoelastic Investigations," Journal of Applied Mechanics, Vol. 25, Trans. ASME, Vol. 80, 1958, pp. 525-528.
4. Trampusch and Gerard, "An Exploratory Study of Three-Dimensional Photoelasticity," Journal of Applied Mechanics, Trans. ASME, 1960.
5. Timoshenko, "Strength of Materials, Part II," D. Van Nostrand Co., Inc., Third Edition, 1956, pp. 228-234.
6. Lawson and McGuire, "The Solution of Transient Heat Flow Problems by Analogous Electrical Networks," Institution of Mechanical Engineers, Vol. 167, No. 3, 1953, pp. 275-287.
7. Paschkis and Baker, "A Method for Determining Unsteady-State Heat Transfer by Means of an Electrical Analogy," Trans. ASME, 64, 1942, pp. 105-112.
8. Paschkis and Heisler, "The Accuracy of Lumping in an Electrical Circuit Representing Heat Flow in Cylindrical and Spherical Bodies," Journal of Applied Physics, Vol. 17, No. 4, April 1946, pp. 246-254.

## DISCUSSION

Dr. Kumar: I just wanted to comment on the fine work that Lt. Mielke has done. One of the project investigators in our Office, Dr. Frocht, has been working on photoelasticity and I am sure you are familiar with his work. The interesting thing is that he is considering plastic deformation at the same time. As the presentation was made today, this was strictly thermoelastic study of the gun tube. It will be very interesting to see how possible thermoplasticity could be introduced into it. Maybe just ideally plastic assumptions may be made. If you can find a suitable material that will fit the gun material that you have used as far as the photoelastic analog is concerned, that would be extremely remarkable. I enjoyed your presentation; it was very fine.

## COMPARATIVE FORMING TECHNIQUES FOR TITANIUM HELMETS

Helen E. Agen\*

### ABSTRACT

Titanium alloys, on a strength-to-weight basis, offer the best resistance to ballistic penetration of all known metallic armor materials. Difficulty experienced in cold deep-drawing of titanium helmet shells, led to the investigation of three methods of forming: hot deep draw, spinning and high-energy forming. As a result of this work, the feasibility of hot deep-drawing helmet shells from titanium sheet material at a temperature of 1300°F was established. The spinning process was not successfully brought to final forming. Six helmets were successfully fabricated from 3 percent Mn complex + 4 Al titanium alloy sheet of .075 and .100 gages. Forming was accomplished at elevated temperatures using sand as the transfer medium and pistol powder for the explosive. Ballistic capabilities of the finished helmet shells were evaluated using the GE fragment simulator test. The translation of the results of this investigation into a feasible technique adaptable to production fabrication will require additional work.

---

A review of the personnel armor protective requirements for future warfare conditions determined the need for new and improved materials and forming techniques in the production of the combat helmet.

Materials studies revealed that titanium and titanium alloys exhibited better strength-to-weight ratios than the more common armor materials. Ballistic testing of the heavier gage titanium plate materials showed excellent resistance to penetration by both fragment simulating and armor piercing projectiles; however, the investigation also revealed that the ballistic performance of titanium materials could not be extrapolated with any degree of accuracy. Therefore, lower gauge sheet material of the more promising alloys were evaluated at Battelle Memorial Institute by the

---

\*Helen E. Agen, Mechanical Engineer, Quartermaster Research and Engineering Command, U. S. Army, Natick, Massachusetts.

Quartermaster Corps. The ballistic results showed the same marked superiority as was witnessed in the armor plate studies. It was determined that further work should be conducted on experimental helmet shapes fabricated from titanium alloys.

Concurrently with the materials study, an investigation was conducted on new and improved methods of forming helmets. It was observed that the standard helmet shell varied in thickness as much as 30 per cent between the rim and crown. The ballistic protective capability decreased proportionally as the thickness of the corresponding helmet areas. It is believed, however, that this variation in shell thickness can be overcome by the utilization of new and improved forming techniques.

An early attempt in FY55 to cold draw titanium alloy helmets was not successful; however, by 1959 the advancements in the state of the art of forming warranted another attempt. Three methods of forming were investigated---hot deep draw, spinning and high energy forming.

For the hot deep draw process, commercially available 6 AL-4V titanium alloy was selected and procured in sheet form 0.076 inch thick. During the forming operation, the dies were heated to a temperature of approximately 1300 degrees Fahrenheit. The completed shell was formed in three steps. The crown was deep drawn the entire depth of six inches in a single draw. Then the brim was shaped to the proper contour. Finally, the outer edge of the brim was handtrimmed. The finished shell was comparable in weight to the M-1 helmet.

Seven shapes were successfully drawn. Most of the shapes formed had wrinkled brims. It was believed that this wrinkling at the brim could be eliminated by improving the method of securing the blank so that equal pressure would be applied in the brim area during the deep draw process.

A check of the thickness variation throughout the crown area of the shell showed thinning in the order of 10 per cent as compared to the 30 per cent thinning witnessed in the fabrication of the Standard, Hadfield Steel M-1 Helmet.

The result of this experiment determined the feasibility of hot deep drawing titanium helmet shells.

The spinning process is one of the simplest methods of metal working. Basically, it is the pressure forming of sheet metal or light plate on a rotating chuck or die. The shaping being performed on a lathe, the form is of necessity concentric about an axis. The adaption of the spinning

technique to the preforming of titanium helmets was attempted. Two titanium alloys, 6AL-4V and 5AL-2.5N, were procured in 0.125 inch thick sheets.

Forming was accomplished by placing titanium alloy discs, in a lathe, against a hemispherical mandrel of the same concavity as the M-1 helmet. As the lathe rotated, an external pressure was applied to the disc. The disc was heated to 1200 degrees Fahrenheit throughout the spinning process. Six hemispherical shapes of each of the two alloys were fabricated. The spun shapes were 0.075 inch thick.

Final shaping, using Government furnished dies, could not be accomplished because the dies were designed for Hadfield steel helmet fabrication using sheet material 0.043 inch thick. The space between the ring die and the punch die would not permit insertion of the 0.075 inch thick spun hemispheres. In addition, any attempt to bring the existing dies up to the forming temperature of 1200 degrees Fahrenheit required for forming would have annealed the dies, making them useless. Since this method showed no promise of adoption to mass production, further development was abandoned.

The materials investigation showed the 3 per cent Mn complex 4-4AL titanium alloy had the best ballistic characteristics of all the alloys tested; therefore, it was decided to use this material for the high energy forming experiments. Titanium sheet material was procured in two thicknesses; the 0.075 gauge, which is comparable in weight to the 0.044 gauge Hadfield used in the fabrication of the M-1 helmet shell, and the 0.100 gauge, which is comparable in weight to the one-piece helmets of the European countries.

The microstructure of the basic annealed material was typical of an alpha and beta stabilized alloy with a Rockwell C 36.5 hardness. Material testing predicted a low rate of formability at room temperature due to the small spread space between yield (135,000-145,000 PSI) and ultimate (150,000-160,000 PSI) strength. Elevated temperature bend tests indicated a forming temperature above 1050 degrees Fahrenheit and hot dimpling tests set 1200 degrees Fahrenheit as the most desirable forming temperature. Solutionizing did not occur at forming temperatures nor was there any evidence of aging when the material was exposed to temperatures between 950 degrees and 1200 degrees Fahrenheit.

An experimental Kirksite die shaped to the contour of the M-1 helmet was fabricated to develop suitable forming techniques and to ascertain such requirements as size, shape, and type of explosive charge. Early tests conducted with this die confirmed the previous assumption that this



material could not be cold formed. In addition, the necessity for a two stage forming procedure requiring two sets of dies was established.

A hemispherical die, of the same diameter as the helmet, was designed to preform the blank to the width and depth of the shell. The second die, identical in shape to the M-1 helmet, was designed for the final forming of the finished shell. Sim-Ply-Trol temperature control units were used to control the temperatures of the upper and lower sections of the forming equipment. Sand contained in a closed hopper was used as the energy transfer medium and pistol powder was the explosive.

The equipment developed is depicted in Figure 1. The procedure in forming the titanium helmets consisted primarily of pre-heating the dies, positioning the prepared blank, putting a limited amount of sand in the hopper for heat retention, pulling a vacuum between the blank and the die, positioning of a prepared charge, filling the hopper with sand and firing the charge. Six helmets, three from the 0.075 gauge and three from the 0.100 gauge material were successfully fabricated. An average of ten detonations was required to form each helmet, (Figure 2). The thickness variation in the crown area was greater than that evidenced in the M-1 helmet, (Figure 3).

Although the process of high energy forming investigated proved impractical and costly, it is significant inasmuch as it established the feasibility of forming helmets from titanium.

Evaluation of the finished helmets showed no adverse ballistic characteristics resulting from forming. Approximately 50 per cent increase in protection was offered by the titanium shells formed from the 0.075 gauge material and those formed from the 0.100 gauge offered up to 80 per cent increase over the standard M-1 shell.

Because of the superior ballistic performance of the titanium helmets as compared to the standard Hadfield steel shell, further work will be directed to the development of an adequate titanium helmet forming technique. Attention is being directed to a fabrication procedure using a combination of deep drawing and high energy forming at elevated temperatures. The deep draw method is suggested for the preforming to maintain a closer tolerance in the crown area of the helmet. Final forming is to be accomplished by an explosive gas method. The substitution of the explosive gas technique is proposed in order to eliminate the detrimental aspects of gun powder detonation. It is expected that the combined techniques will provide a production method of fabricating helmets with more rigid thickness tolerances.

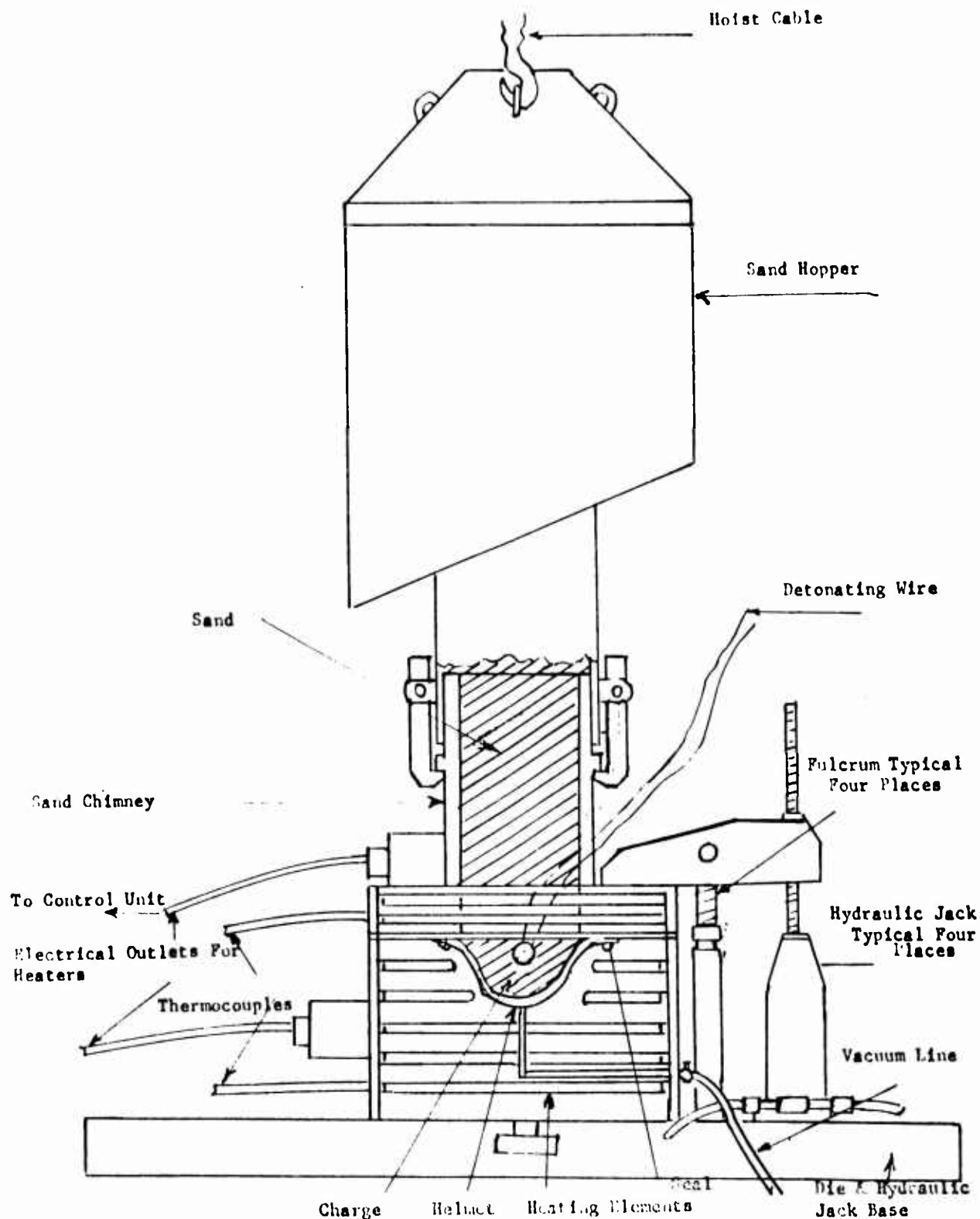


Figure 1 Cross Section of Explosive Forming Set-up Used in Helmet Forming



FIGURE 2

TITANIUM HELMET SHELL FORMING DATA

Helmet No.	Sheet Gage	Rc Hard	Wt. (oz)	Thick Variation (Crown Area)
1	.075	43	32-5/8	.063-.076
2	.075	43	30-1/2	.057-.075
3	.100	36.5	39 1/2	.071-.087
4	.100	37	38-3/4	.071-.083
5	.100	39.5	39-1/2	.071-.090

HADFIELD STEEL HELMET SHELL DATA - AVERAGE

Helmet	Sheet Gage	Rc Hard	Wt. (oz)	Thick Variation (Crown Area)
M-1	.044	28-50	29-3/4-33	.031-.041

FIGURE 3

Mr. Charles J. Kropf - ATAC, Detroit Arsenal: To what extent can this same technique you have been describing be applied to other military items that you might visualize?

Dr. Kumar: I was wondering about the comment you made concerning the thinness of the helmet in a particular area. Can this be possible controlled by choosing an initial plate which is of variable thickness instead of taking a plate which is of uniform thickness. I realize that this will not be probably very economical but would insure that the end produce would have more thickness in the area where it is needed.

311

#### INTRODUCTORY COMMENTS BY THE CHAIRMAN, SESSION IV

R. Beeuwkes\*

Properties of materials are determined in tension tests. In the upper yield point region we have obvious over shooting of stress which for most applications is not very significant. Emphasis has therefore been laid in this meeting on the lower yield point stress. But if you observe stress-strain increases as the temperatures lowered very considerably, so that what we are ascribing to a rate of strain effect is really an effect of work hardening in very many applications. Many years ago, Srohmayer observed that the effected yield point in the material was much closer to the yield point under fatigue conditions, namely, what he observed was the endurance limit. Concerning this I am thinking especially of body centered cubic materials. There are complications with materials like lead, aluminum, and copper which I am not discussing at all. I think then in many cases in design we should be concerned more with the limit that is nearer the fatigue limit. Now in the tension tests we do a lot of work; we develop a lot of heat to get a lot of temperature. The temperature rise is markedly dependent upon the temperature itself at which we are making the test, the ambient temperature, if we are going to low temperature testing, because the specific heat is way down there. It is very difficult to make an isothermal test under low temperature conditions. Once we get past the tensile stress our specimen begins to neck. When it necks, it not only develops its stress concentration which is very large in general before breaking, but the strain rate goes up, too. If you thought you had isothermal conditions in general while you were getting up to the tensile point, you'll hardly have them once you've gotten well past the tensile point. A very small proportion of your entire gage length will actually be strained. You use a specimen several inches long and you may find that something like five hundredths of an inch of it is actually being stretched. You would have to slow the machine way down if you wanted to preserve isothermal conditions, and on the other hand what you are really getting as you approach breaking is a very high rate of strain test under static conditions. To add to these complexities, very often people will put a little taper in the specimen to begin with. This will give you somewhat erratic stress strain curve but you will have even worse results at very low temperatures. You'll get brittle fracture and much lower stresses than you would normally expect. Perhaps what I am saying is rather obvious to you all. I read in a little book by Max Borne - that greatness of Einstein's work was that he based all his theory on fact - fact was obvious to all but noticed by none. I hope that we all try to do a little Einstein here this afternoon.

---

\* Dr. Reinier Beeuwkes, Watertown Arsenal Laboratories, Watertown, Mass.

## EXPERIMENTAL DYNAMICS OF MATERIALS

George Gerard\*

The general objectives of this presentation are concerned with various experimental techniques used to obtain dynamic stress-strain data in the yield region for various materials. A general review and critique of one-dimensional experimental techniques utilized by various investigators is presented from the viewpoint of plastic wave propagation. Specific experiments concerned with plastic wave propagation are then considered and conclusions drawn from such experiments concerning the dynamic stress-strain properties of materials are presented.

An experimental technique for two dimensional structural elements is then presented and results on the dynamic stress-strain characteristics of several materials are presented.

### REFERENCES

1. Gerard, G., "The Impact Tube - A New Experimental Technique for Applying Impulse Loads," American Society for Testing Materials, Symposium on Impact Testing, STP 176, pp. 94-109, 1955.
2. Gerard, G., and Papirno, R., "Dynamic Biaxial Stress-Strain Characteristics of Aluminum and Mild Steel," Transactions, American Society for Metals, Vol. 49, pp. 132-148, 1957.
3. Papirno, R., and Gerard, G., "Dynamic Stress-Strain Phenomena and Plastic Wave Propagation in Metals," Transactions, American Society for Metals, Vol. 53, pp. 381-406, 1961.

---

\* George Gerard, Director of Engineering Sciences, Allied Research Associates, Inc., Concord, Massachusetts.

## DISCUSSION

R. C. Geldmacher, New York University: Did you include bending stresses when you calculated your stresses from displacements? One would have to take the derivatives to include the stresses due to bending.

Dr. Gerard: This I presume refers to the diaphragm that we showed.

Mr. Geldmacher: Right.

Dr. Gerard: The diaphragms were extremely thin; they were something in the order .010 inches and had about a 12 inch span and when we calculated the bending stresses in there they were extremely small, particularly if we got out into the large deflection region.

Mr. Geldmacher: You could ignore the bending stresses?

Dr. Gerard: Yes, that's right. Incidentally, we found out also that we could ignore any dynamic effects of the diaphragm because from the deflection measurements we found there was a constant velocity process after the first motion.

Mr. Geldmacher: The reason I ask is that anyone who has tried to get bending stresses from deflection measurements is probably running into the same difficulty that we have because it is almost impossible to make that extra differentiation to get the stress. So your results are very far off. I thought you might have had a new technique here that would let us get stresses from the deflection curve.

Dr. Gerard: We are strictly concerned with the membrane situation.

Mr. Geldmacher: Right.

Dr. Eugene A. Ripperger, University of Texas: I would like to ask two questions. In that slide in which you compared the theoretical and the measured velocities, the theoretical velocities were computed simply as the square root of  $E/\rho$ ?

Dr. Gerard: Yes, the square root of  $E/\rho$  and  $E$  was the static value obtained with this loading cycle and particular material.

Dr. Ripperger: Well, then the question that I really wanted to ask was: The curve for the theoretical results had some curvature along that leading step, so to speak, and I would think that this would be a straight vertical line. Was not the static modulus constant up to the point of preloading?

Dr. Gerard: Yes, but the reason that the theoretical line was curved and was not a straight vertical line was because of the fact that we were using the three dimensional theory which includes a dispersion effect.

Dr. Ripperger: You have answered my question satisfactorily; now, let me ask you the second one. In comparison with the velocities where you were superimposing the small pulse on the pre-stressed specimens, it wasn't clear to me whether the plastic strain that you were showing was the strain due to the small pulse or it was the strain which you had in the specimen before you sent the pulse through it.

Dr. Gerard: Those were strains which resulted from the pulse.



## A METHOD FOR RAPID DYNAMIC EVALUATION OF LARGE WEAPON COMPONENTS

T. F. MacLaughlin\* and J. P. Purtell\*\*

### ABSTRACT

A description is given of a high energy impact machine which closely simulates the firing of large weapons, and is used to dynamically evaluate a variety of weapon components. Dynamic stress analyses and fatigue life data are obtained by simulated firings at a rate of 100 per minute, making economically possible realistic life estimates. Problems in simulation and instrumentation are also discussed.

### INTRODUCTION

During the late 1800's many design features of heavy artillery weapons with which we are familiar today came into being. The principles of breech loading, rifled gun tubes, fragmentation projectiles and the first recoil mechanisms were developed prior to the turn of the century. From 1900 to the present time, in spite of many design improvements and modifications, the fundamental principles of many of our artillery weapons have remained relatively unchanged.

In recent years, however, much effort has gone into reducing the weight of large weapons, thereby increasing mobility without reducing effectiveness. Watervliet Arsenal engineers have achieved weight reductions up to 50% in weapons using kinetic energy ammunition, while still increasing range and rate of fire. To accomplish this, new types of ammunition fired at greatly increased chamber pressures have been employed. In addition, the introduction of still a different type of ammunition has made possible phenomenal weight reductions; for example, six to one in one particular system with even greater lethality being obtained.

These factors naturally have resulted in a departure from traditional design concepts, especially with regard to breech components, necessitating more sophisticated stress analysis and closer evaluation of component fatigue characteristics.

---

\* T. F. MacLaughlin, Research Mechanical Engineer, Experimental Mechanics Laboratory, Watervliet Arsenal, Watervliet, New York.

\*\* J. P. Purtell, Chief, Experimental Mechanics Laboratory, Watervliet Arsenal, Watervliet, New York.

## DESCRIPTION OF IMPACT MACHINE

For the past ten years a series of high energy impact machines have been developed at Watervliet Arsenal for dynamically evaluating the breech components of various heavy weapons. These machines have been designed to repetitively simulate actual firing load pulses at a rate such that rapid evaluation is possible.

Two steam-driven single-acting pile hammers act as energy sources for the machine currently in operation. The smaller of these hammers may be equipped with either a 1000- or a 5000-pound weight which can be dropped from a maximum height of 42 inches, and is capable of a maximum striking energy of 17,500 foot-pounds. The larger hammer contains a 10,000-pound weight which can be dropped from heights up to 39 inches, producing a maximum striking energy of 32,500 foot-pounds. Both hammers deliver 50 to 100 blows per minute, depending on the drop height.

The impulse delivered by the hammer is transmitted to the test specimen through a piston arrangement and a pulse-shaper, the configuration of which depends upon the particular weapon component being tested. The pulse-shaper is needed in order to simulate the load pulse rise time and maximum force experienced in actual firing. In general, it consists of a fluid chamber acting as a liquid spring whose spring constant may be adjusted by varying the fluid volume.

The specimen holders consist of simulated shortened gun tubes, known as tube adapters, to which the breech components are attached as in the actual gun. The adapters are shrink-assembled or screwed into the test machine, and can be readily changed for different specimens.

The entire machine rests on an eight foot cube of concrete which is set into a concrete shell located on bed rock beneath the laboratory floor. Fabrica insulating material is located between the cube and the shell.

A new impact machine, which will be capable of producing a maximum striking energy of 60,000 foot-pounds, is currently being designed at Watervliet Arsenal. This new machine will be used for dynamic evaluation of breech components for future weapons having higher performance characteristics than today's weapons.

## FATIGUE TEST CONFIGURATIONS

The high energy impact machine has been used to evaluate fatigue and stress distribution characteristics of breech components for a number

of different weapons. The first type of component to undergo testing was the breech ring of a sliding block type breech mechanism. Figure 1 shows schematically the test assembly for this specimen. It can be seen that the fluid chamber provided force magnification as well as pulse shaping. The strain gaged load cell was calibrated in the machine by applying known amounts of static fluid pressure to the fluid chamber and correlating strain with load. The bottom of this cell was cartridge-shaped so that the load would be distributed to the test specimen in approximately the same manner as in actual firing.

Another component to be impact fatigue tested was the coupling of a split chamber breech, illustrated in figure 2. The significant difference in this specimen from that of the previously described test was that the coupling was of much lighter construction and was sensitive to lateral pressure as well as axial thrust due to firing. This prompted a relocation of the fluid chamber such that this lateral pressure would be simulated. The fluid chamber between the upper and lower pistons was removed in order to obtain the proper pulse duration. The correct peak load was obtained in spite of the loss of the force magnification feature, by improving the bearing surfaces on the pistons and increasing the drop height to nearly its maximum value. Load pulse monitoring was accomplished by strain gages which were mounted on the piston and breech chamber and were calibrated in the machine by static fluid pressure measurements as before.

Figure 3 shows the impact machine configuration for the screw block type breech mechanism, which was very similar to that of figure 2, except that a single piston was used, providing a more efficient force transfer from falling weight to specimen.

Finally, a comparison of the fatigue lives of various types of mortar baseplates has been made, using the 1000-pound weight with the smaller hammer (figure 4). This test differed from the breech component tests in that (1) relatively low thrust levels were required (approximately one-twentieth that of the breech component tests), and (2) no fluid chamber was needed to obtain the proper force-time pulse due to the springiness of the baseplate itself. Also, it should be pointed out that although the firing pulse was simulated, other field conditions were not; namely, angle of firing and means of supporting the baseplate. These factors were not considered significant due to the comparative nature of the test.

#### ANALYSIS OF IMPACT MACHINE

A vibrational analysis was performed on the impact machine in order that fluid chambers and pistons could be readily redesigned for different

of different weapons. The first type of component to undergo testing was the breech ring of a sliding block type breech mechanism. Figure 1 shows schematically the test assembly for this specimen. It can be seen that the fluid chamber provided force magnification as well as pulse shaping. The strain gaged load cell was calibrated in the machine by applying known amounts of static fluid pressure to the fluid chamber and correlating strain with load. The bottom of this cell was cartridge-shaped so that the load would be distributed to the test specimen in approximately the same manner as in actual firing.

Another component to be impact fatigue tested was the coupling of a split chamber breech, illustrated in figure 2. The significant difference in this specimen from that of the previously described test was that the coupling was of much lighter construction and was sensitive to lateral pressure as well as axial thrust due to firing. This prompted a relocation of the fluid chamber such that this lateral pressure would be simulated. The fluid chamber between the upper and lower pistons was removed in order to obtain the proper pulse duration. The correct peak load was obtained in spite of the loss of the force magnification feature, by improving the bearing surfaces on the pistons and increasing the drop height to nearly its maximum value. Load pulse monitoring was accomplished by strain gages which were mounted on the piston and breech chamber and were calibrated in the machine by static fluid pressure measurements as before.

Figure 3 shows the impact machine configuration for the screw block type breech mechanism, which was very similar to that of figure 2, except that a single piston was used, providing a more efficient force transfer from falling weight to specimen.

Finally, a comparison of the fatigue lives of various types of mortar baseplates has been made, using the 1000-pound weight with the smaller hammer (figure 4). This test differed from the breech component tests in that (1) relatively low thrust levels were required (approximately one-twentieth that of the breech component tests), and (2) no fluid chamber was needed to obtain the proper force-time pulse due to the springiness of the baseplate itself. Also, it should be pointed out that although the firing pulse was simulated, other field conditions were not; namely, angle of firing and means of supporting the baseplate. These factors were not considered significant due to the comparative nature of the test.

#### ANALYSIS OF IMPACT MACHINE

A vibrational analysis was performed on the impact machine in order that fluid chambers and pistons could be readily redesigned for different

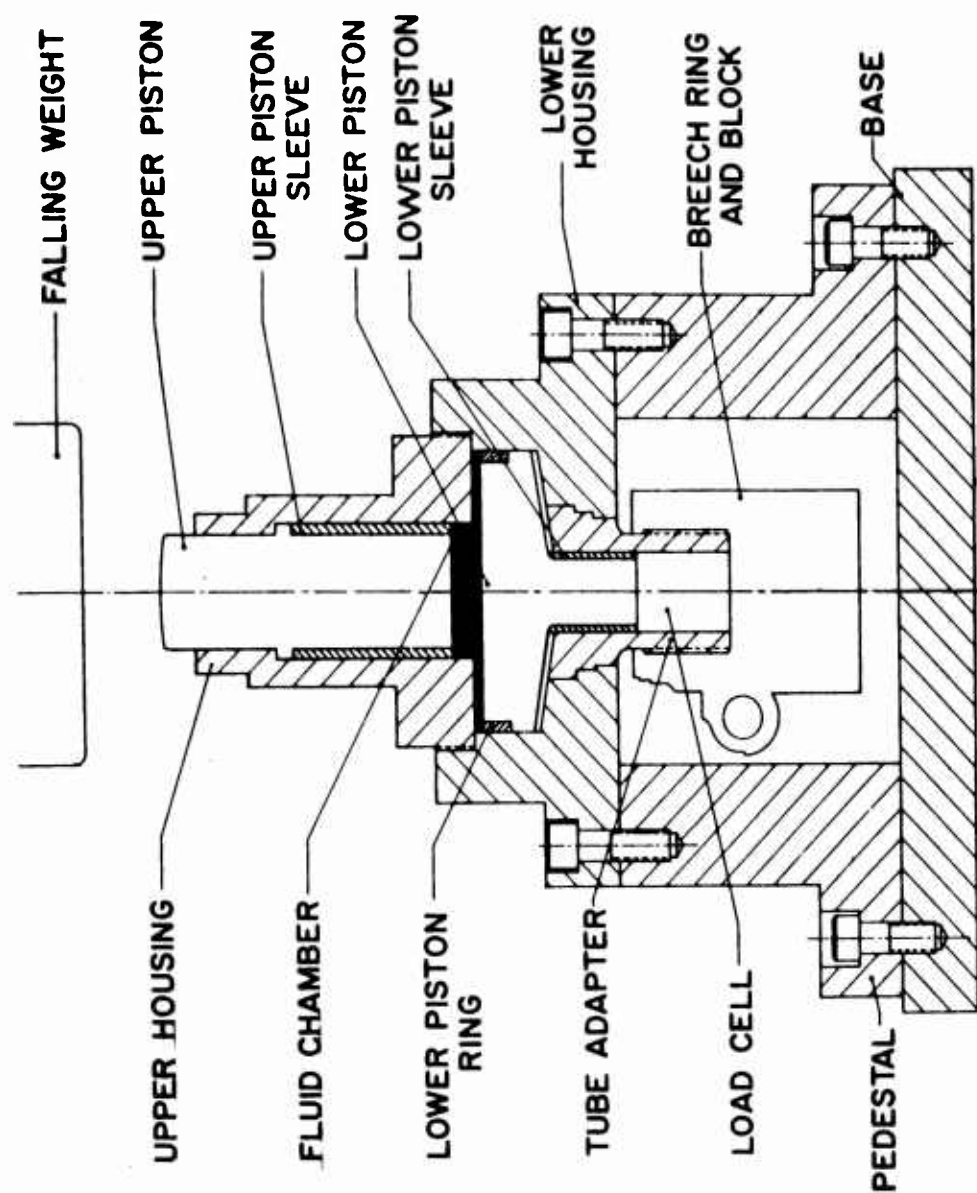


FIG. 1  
FATIGUE TEST CONFIGURATION  
SLIDING BLOCK TYPE BREECH MECHANISM

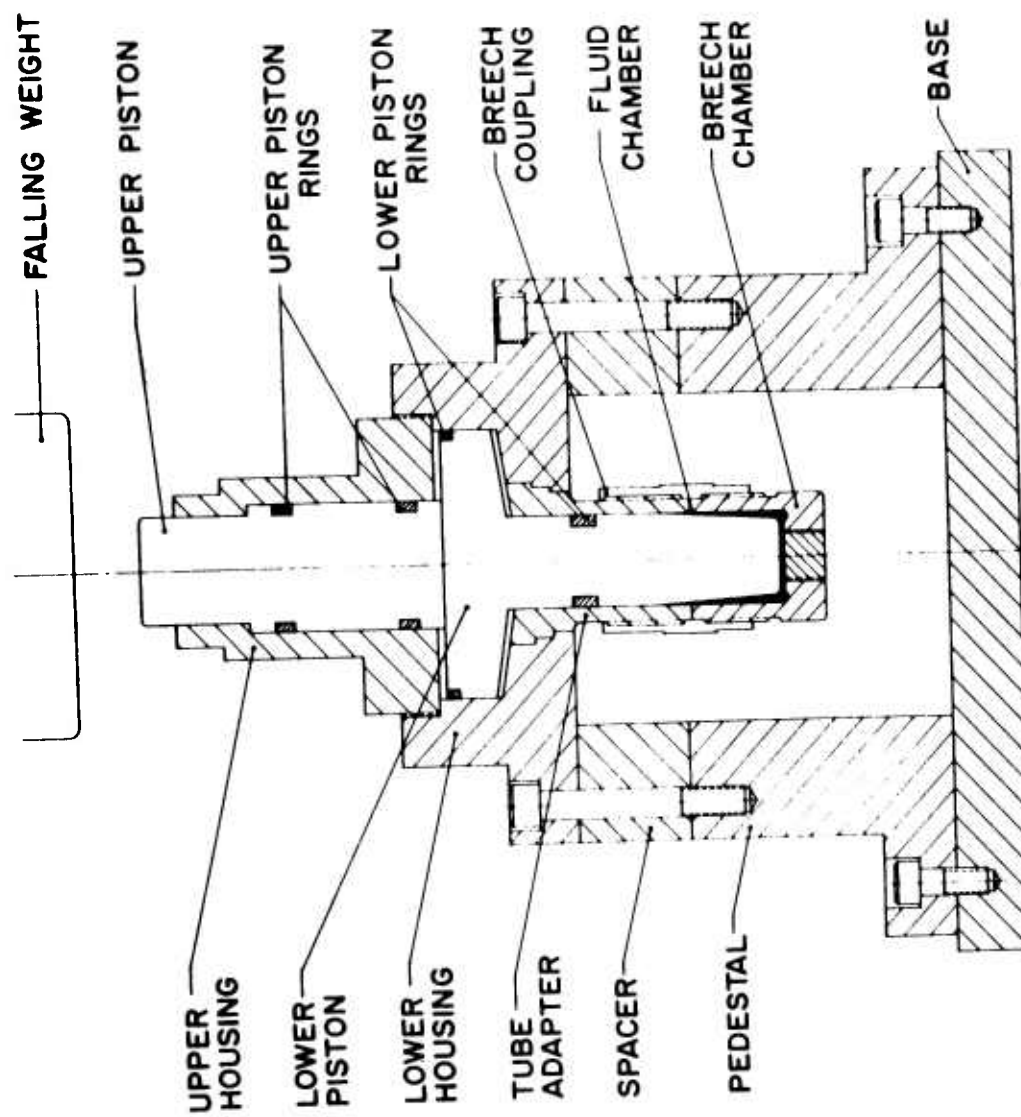


FIG. 2  
FATIGUE TEST CONFIGURATION  
SPLIT CHAMBER BREECH MECHANISM

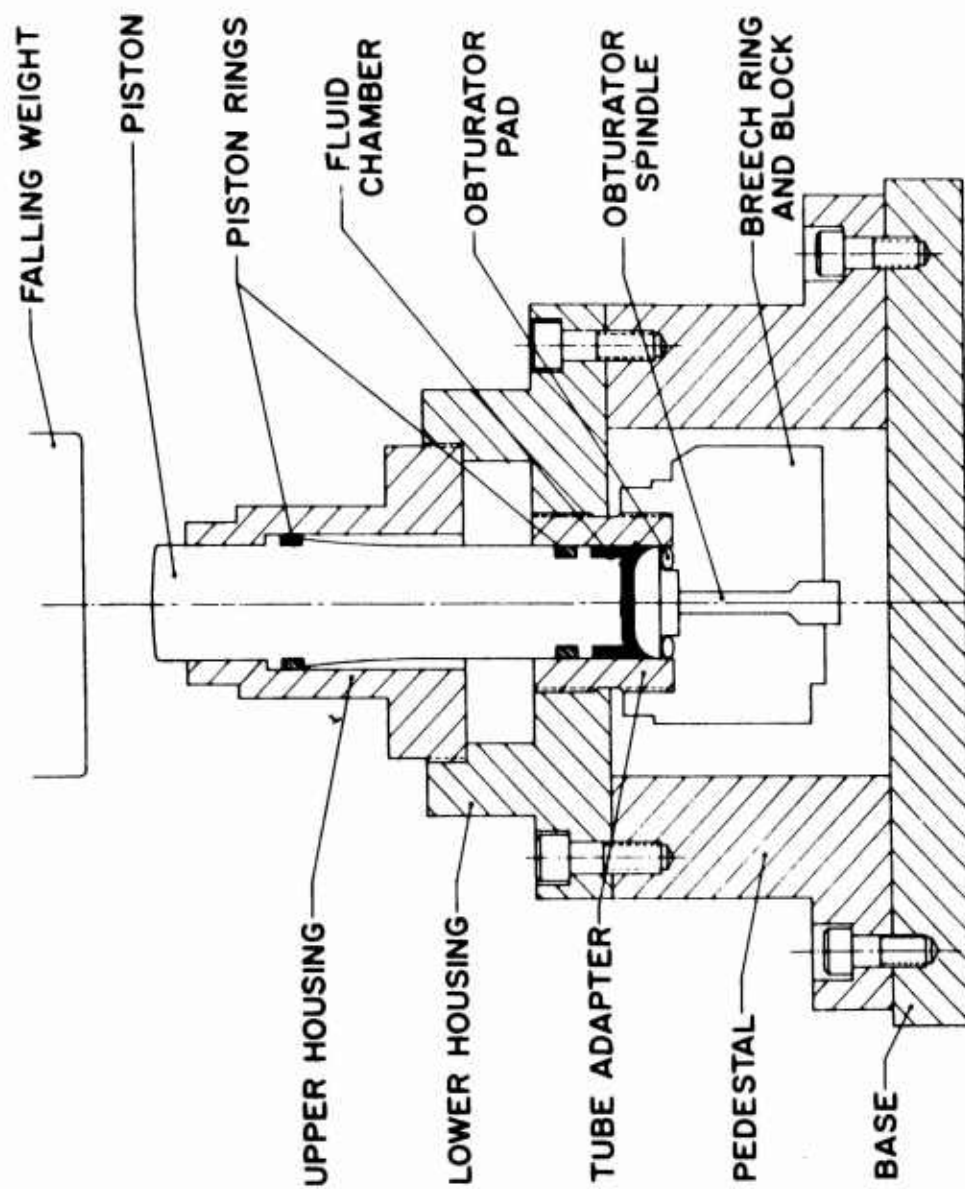


FIG. 3  
FATIGUE TEST CONFIGURATION  
SCREW BLOCK TYPE BREECH MECHANISM

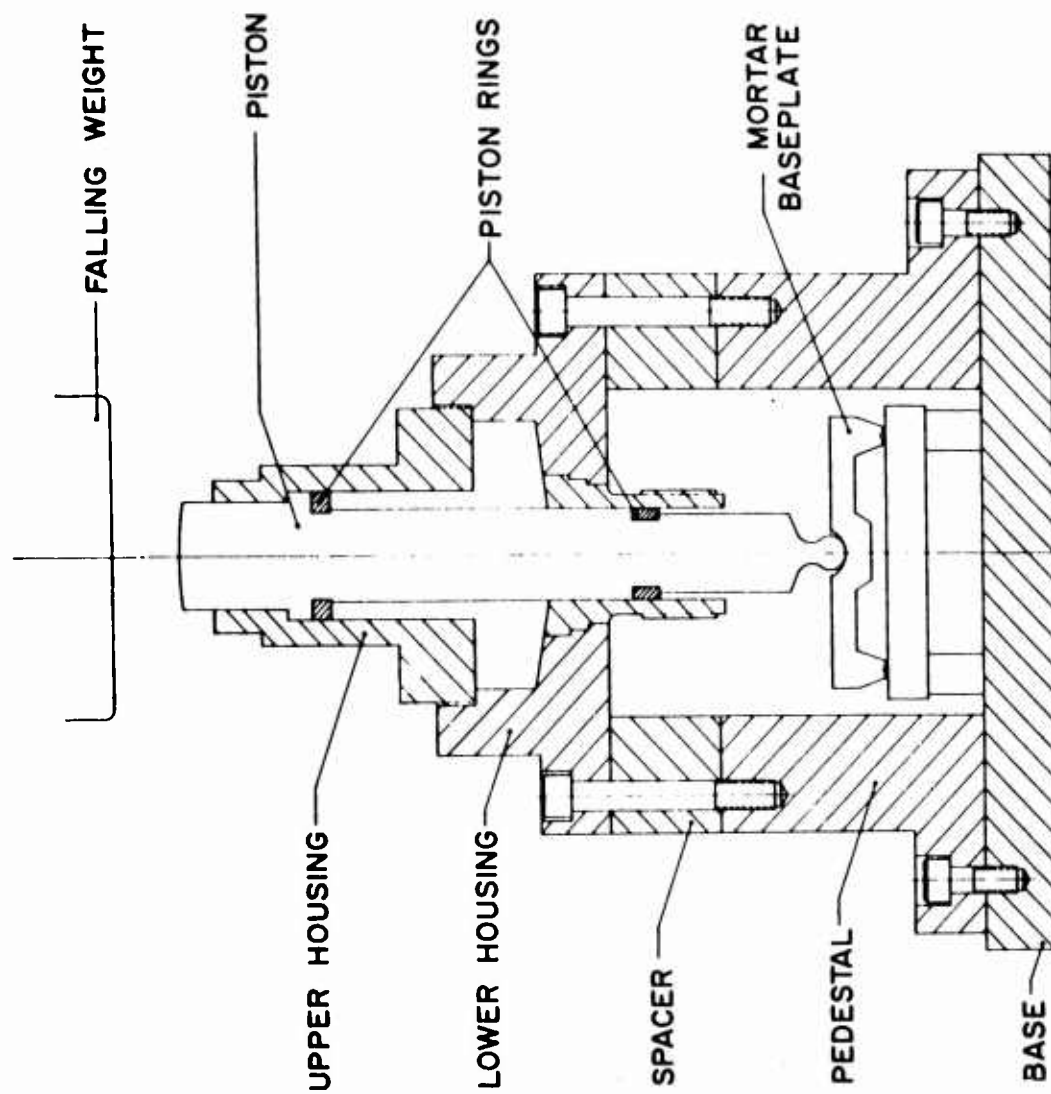


FIG. 4  
FATIGUE TEST CONFIGURATION  
MORTAR BASEPLATE



tests. The machine and the specimen were represented by a series of springs and masses which reduced to three or four degrees of freedom, depending on the test. Figure 5 illustrates the spring-mass representation for the test arrangement shown in figure 1. The analysis was accomplished by the use of well-known vibrational methods<sup>1</sup>, and a solution was obtained for the force-time pulse experienced by the specimen.

The results of applying this analysis to the mortar baseplate test, which reduced to a three-degree-of-freedom system, are represented in figure 6. It is seen that good correlation was achieved with regard to pulse duration and maximum force.

### EXPERIMENTAL PROCEDURES AND RESULTS

A typical test procedure for dynamic evaluation of a breech mechanism consists of the following phases.

1. Selection of a series of breech components. This may involve a comparison of alternate design features, or repetitive tests on several identical components in order to determine more accurately the fatigue life.
2. Static Test. This phase consists of pressurizing the fluid chamber, locating the critically stressed regions, and determining a static stress-strain analysis in these regions. Brittle coating and photoelastic coating techniques are employed along with strain gages and the appropriate switching and balancing units and strain indicator.
3. Dynamic Test. The impact machine is used to subject the test specimen to repetitive simulated firing pulses. Strain gages mounted in critically stressed regions are monitored by oscilloscopes or oscillographs. Cathode followers and oscilloscopes are used to record traces from pressure gages and accelerometers. The falling weight interrupts a light beam entering a photocell, triggering the oscilloscopes and activating a counter. At certain intervals during the fatigue test the machine is disassembled and the specimens undergo magnetic particle inspection for fatigue cracks.

The degree of simulation achieved by the impact machine is demonstrated by figure 7, which shows a typical comparison of traces obtained from a strain gage mounted on the breech block of the screw block type breech

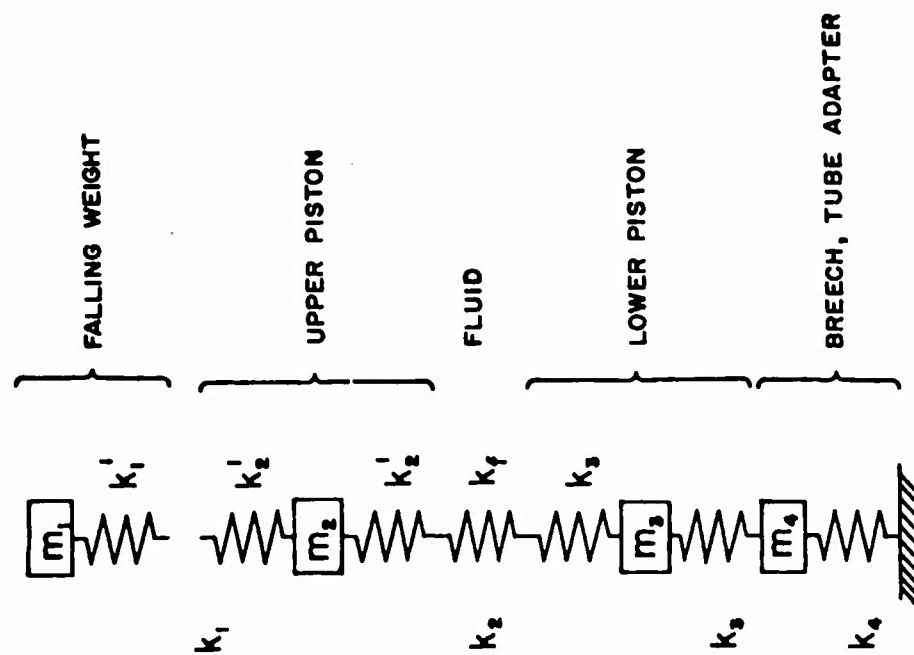


FIG. 5  
 SPRING-MASS REPRESENTATION—SLIDING BLOCK TYPE  
 BREECH MECHANISM FATIGUE TEST.

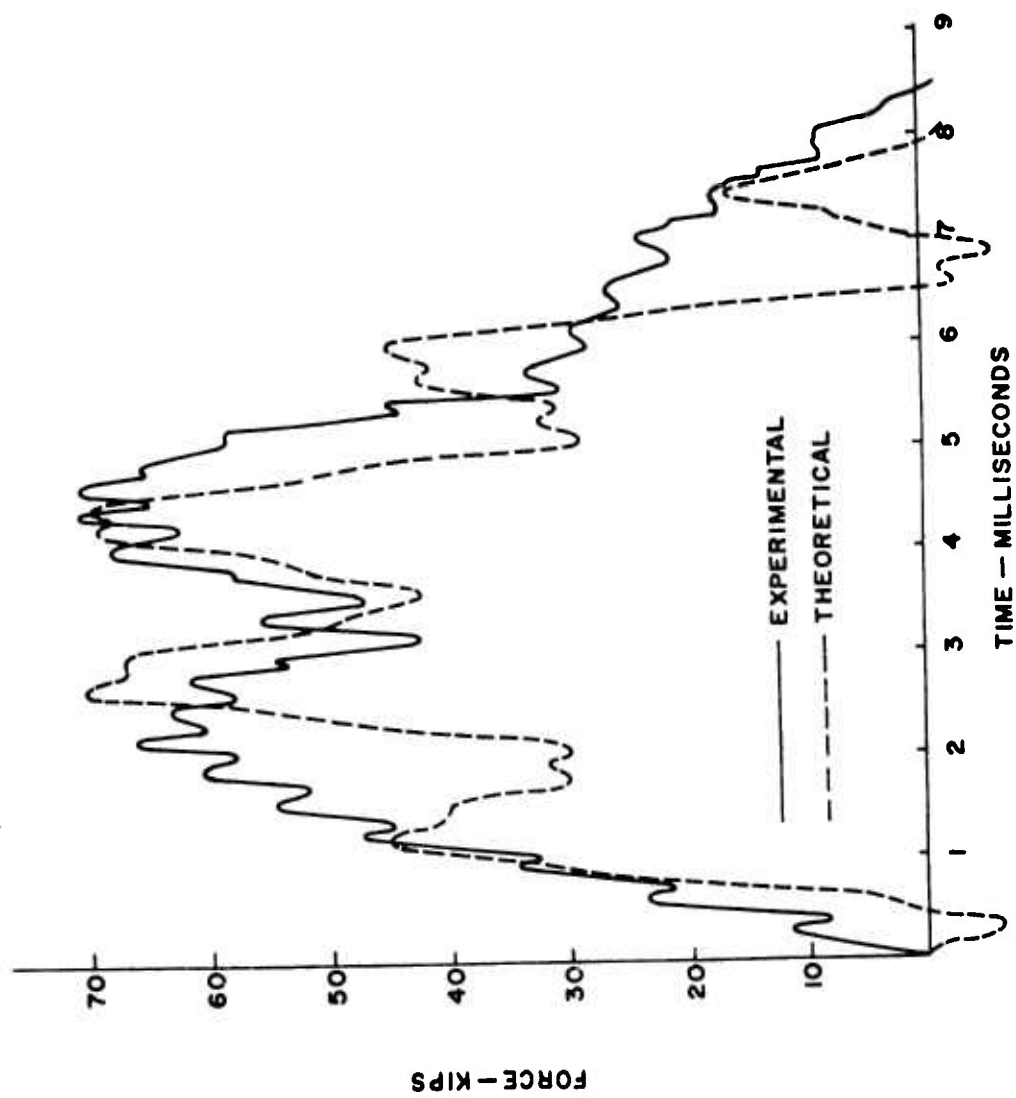


FIG. 6  
 FORCE - TIME - PULSE  
 MORTAR BASEPLATE FATIGUE TEST

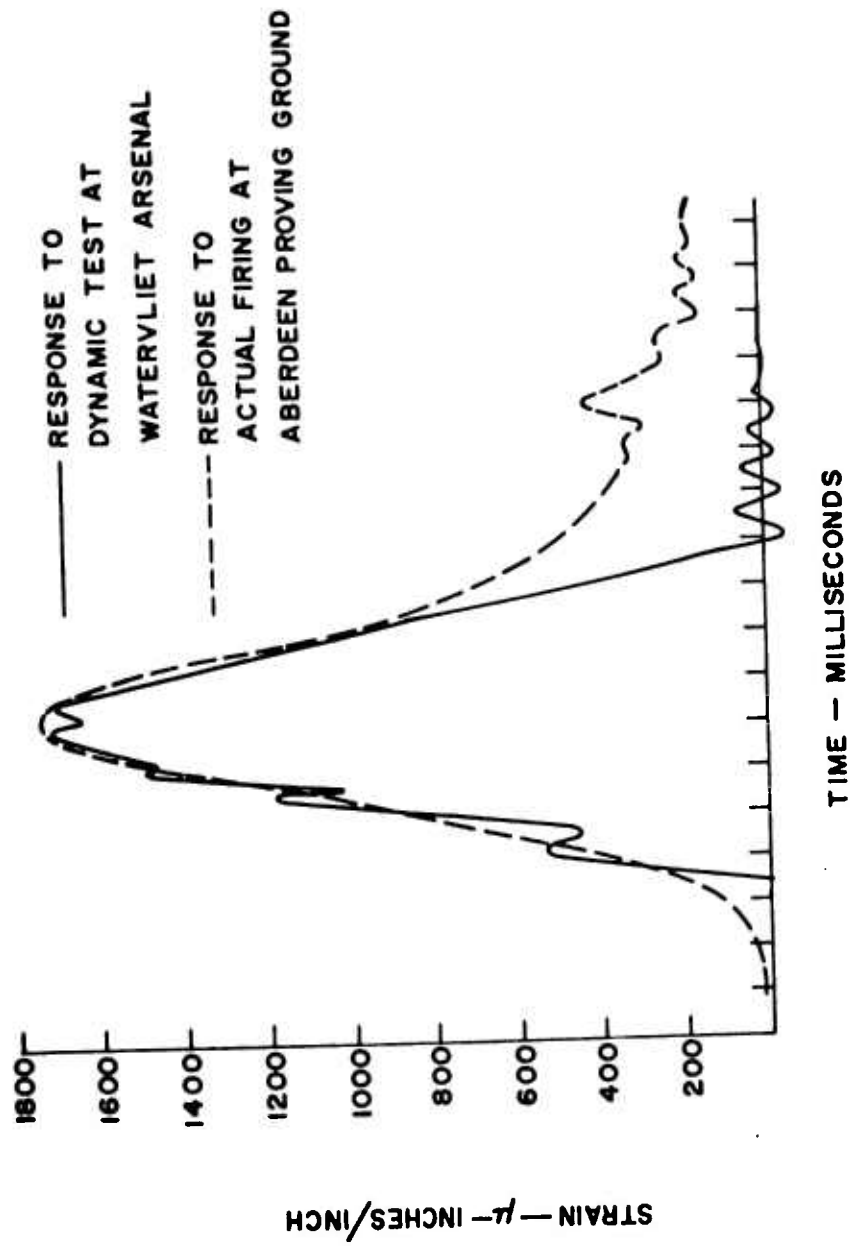


FIG. 7  
STRAIN-TIME PULSE — STRAIN GAGE LOCATED  
TANGENTIALLY ON REAR FACE OF SCREW TYPE  
BREECH BLOCK

mechanism (figure 3). To obtain this data, a gaged breech mechanism which had been tested on the impact machine was taken to Aberdeen Proving Ground and strain recordings were made during actual firing.

In order to obtain a realistic life estimate of a given component, a statistical technique for the analysis of small sample sizes is employed<sup>2, 3</sup>, since fatigue testing many identical specimens is economically unfeasible. Using fatigue life data obtained from relatively few specimens, this technique provides a means of estimating the safe life for various values of reliability and statistical confidence. For example, it may be desired that a component be .9999 reliable (i.e., no more than one failure out of 10,000 specimens is tolerated). By conservatively estimating the failure distribution from the available experimental data, it is possible to select a rated life corresponding to a given statistical confidence level. The statistical confidence is defined as the probability that the predictions are on the conservative side.

#### CONCLUSION

A dynamic stress-strain analysis of a given breech mechanism is obtained, along with fatigue information which is used to estimate condemnation limits for the various components. The accumulation of information from various tests provides a valuable guide to the future design of heavy weapons. To obtain dynamic evaluation by means of field testing with live ammunition would be prohibitive due to both economic and time limitations. At a time when lighter and higher performance weapons are under development, therefore, the usefulness of the high energy impact machine has been well established.

#### ACKNOWLEDGEMENTS

Many people have contributed significantly to the development of the high energy impact machines. Much of the original development work was done by C. W. Egan, formerly Chief of the Experimental Mechanics Laboratory. A. Doty has been responsible for most of the mechanical work, and instrumentation has been accomplished through the efforts of G. Ingram and J. Barrett. R. Lasselle, as project engineer on many of the experimental programs, has made many significant design contributions.

## REFERENCES

1. Den Hartog, J. P., "Mechanical Vibrations," McGraw-Hill Book Company, Inc., 1956 (Fourth edition), pp. 79-83, 122-126.
2. Pope, J. A. (Editor), "Metal Fatigue," Chapman and Hall, Ltd., 1959, pp. 123-130
3. Egar, C. W., Purtell, J. P., MacLaughlin, T. F., "Dynamic Simulated Firing of Heavy Weapon Components," Institute of Environmental Sciences, 1962 Proceedings.

## DISCUSSION

Mr. Zaroodny, APG-BRL: I am very happy to see that this type of work is being taken up seriously and so much of it is being done. However, there are lots of items in which our experience gained at the proving grounds does not support your results. In particular I would like to mention mortars. You said that the pulse on a mortar base plate, although very short in duration, is more or less simulating the thing by virtue of flexibility of the base plate.

Mr. MacLaughlin: I believe that it was simulating the actual response that the base plate received.

Mr. Zaroodny: We have measured the response of the base plate and I am sorry to say that it was nothing like what you infer. There was only one similarity in that the curves were extremely hashy. What happens is that the ground behaves first as though it were a rigid system. Then this rigid system suddenly breaks down and offers only a small amount of resistance. Then around the time when the mortar effects the shell there occurs a very sudden growth of resistance. At any rate the phenomenon is not so simple as it was indicated by you.

Mr. MacLaughlin: Thank you very much for your comments. I realize that we are greatly simplifying the situation of the mortar base plate. I think that I can only reiterate what I said before in that we are trying to compare different base plates only. If we were to make a complete analysis on the mortar base plates as we do try to do on most of our breech components, we would go into much more detail on simulation. This I readily admit.

## TENSILE IMPACT ON RUBBER AND NYLON

Malcolm N. Pilsworth, Jr.\*

### ABSTRACT

The program under which this work is being done is called "The properties of materials at high rate of strain." So far the attention has been mainly on the tensile impact of polymeric materials at rates where the response is of a wave nature. This is where the ratio of the impact velocity to the velocity of propagation in the material is an appreciable fraction of the breaking strain.

The immediate objective has been to find a means of describing or characterizing the response under these conditions. For example, to what extent is a dynamic stress-strain curve useful here?

An apparatus is described capable of delivering a tensile impact at velocities of about 150 ft/sec. Several methods of observing the response were used including a photographic technique with a high-speed stroboscope.

Possible dynamic stress-strain curves may be deduced from the measurements. If we assume that such a curve completely defines the response of the material we may use the equations and method of von Karman to construct the wave pattern of the response. On doing this we find that the constructed response always has more distinct waves and sharper wave fronts than the observed response. In visco-elastic terms this means that an appreciable fraction of the relaxation time spectrum is included in the range between the total time of the test (a few milliseconds) and the time required for a constructed wave front to pass a point in the sample (several hundred microseconds).

For rubber it was assumed that this delayed response (that is, delayed in relation to the wave front) could be expressed by a creep function. A graphical analysis was made in which the increase in strain due to such a creep function was added to the strain constructed from a stress-strain curve. The resulting strain wave pattern agrees with the observed pattern much better than does that constructed from a stress-strain curve alone.

---

\* Malcolm N. Pilsworth, Jr., Quartermaster Research & Engineering Center, Pioneering Research Division, Natick, Massachusetts.

At low rates of strain the determination of the variation in the properties of materials with the speed of testing is a straightforward matter. However, when the response of the sample is dominated by inertial effects, the observation of material properties is more of a problem. For tensile impact this situation arises when the ratio of the velocity of impact to the velocity of propagation of a strain pulse in the material is an appreciable fraction of the breaking strain, since this ratio determines the pulse height. The object of the present work on two representative polymeric materials, a rubber strip and a high-tenacity nylon yarn, is to determine a method of characterizing the response of such materials to tensile impact. Much of this work appears in a recent report<sup>1</sup>.

It is convenient to describe the response of materials with a stress-strain curve. If the stress can be applied uniformly throughout the sample this is correct. If inertial effects prevent uniform stressing there are limitations. If we use a stress-strain curve in such a case we are assuming that the initial response of the material is so rapid as to be considered instantaneous compared to the time scale of the experiment and that any subsequent creep is so slow that it may be ignored for the time of the experiment. Experimental techniques designed to check this assumption were used. Also there are other ways to examine the likelihood of materials responding in this way. Even if it is indicated that a dynamic stress-strain curve is not completely correct, it may still be useful.

If we assume that the material obeys a dynamic stress-strain curve, the response to a tensile impact may be calculated by a method of characteristics as given by von Karman<sup>2</sup>. The procedure described in this report is to obtain enough information to estimate such a dynamic stress-strain curve and also to get some measure of the response. The calculated and measured responses may then be compared.

An apparatus was constructed, as sketched in Figure 1, that uses heavy rubber bands to accelerate a slider along tracks. The sample is placed between the tracks and fastened to a T-shaped head mass. Projections on the bottom of the slider strike this head mass at about 150 ft/sec. Several methods have been used for observing the response. In one method, the sample is fastened between the head mass and a lighter tail mass. The motion of the tail mass is a measure of the force at the tail end of the sample, and the distance between the masses is a measure of the average strain. The force at the tail end may also be observed by means of a calibrated weak link.

At present we are using high-speed photography to observe the local strain. The sample is illuminated with an Edgerton, Germeshausen and



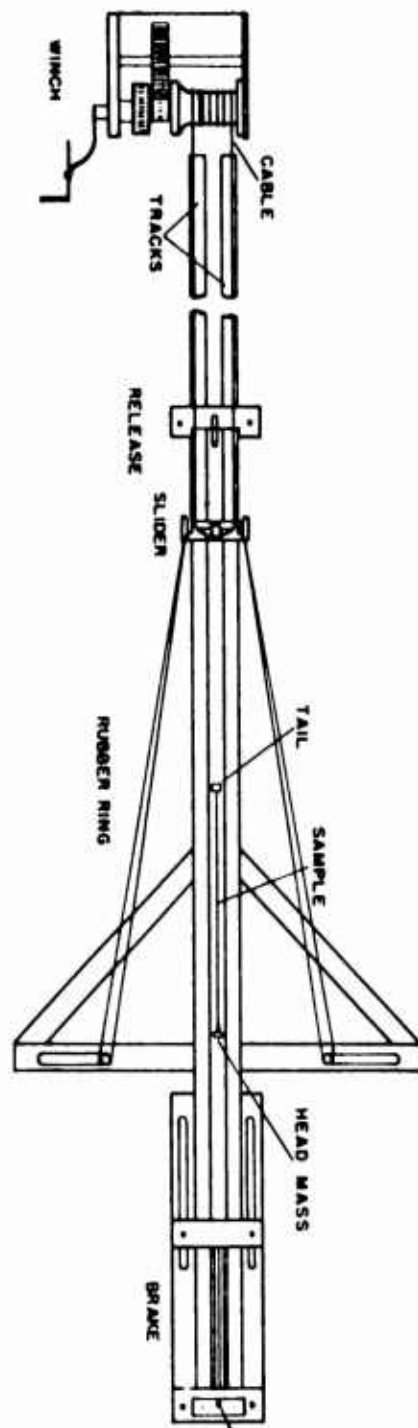


Figure 1. Rapid-impact machine.

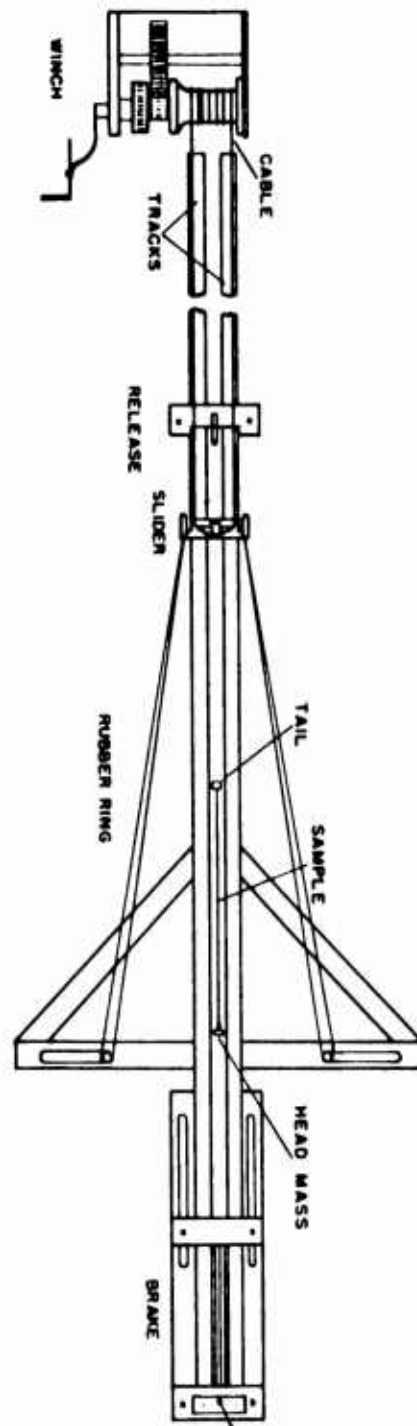


Figure 1. Rapid-impact machine.

Grier No. 501 High-Speed Stroboscope. The event is pictured in a still camera, the images being separated with a moving mirror. Regularly spaced, contrasting marks are made on the sample.

The best pictures so far have been made with the rubber strip. This was white natural rubber with a 0.080 inch square cross section. Figure 2 is a picture of an impact on a sample 10 cm long with marks every centimeter. The impact was at 138 ft/sec. The picture was taken at a strobe rate of 2000/sec at f/11 on Polaroid 3000 film. At the upper left the sample before impact may be seen. The path of the slider is from upper left to lower right. Near the middle of the picture it passes out of the region illuminated by the strobe into a region with steady light. Down the left side may be seen the successive images of the rubber sample as it is stretched. The sample failed at the moving end in about 10 millisec. It is interesting to note how rapidly it retracted after failure. This velocity was measured at 525 ft/sec. Fixed targets drew the white lines at the ends of the picture which serve as calibration marks to correct for the distortion introduced by the motion of the plane mirror.

Measurements were made from this picture to get strain-time-position data. The results are shown in Figure 3 with time and position as coordinates and strain as a parameter. (Position is defined as numerically equal to distance on the unstrained sample, measured from the fixed end.)

The initial pulse and the first reflection from the fixed end are well defined but after this the strain hardly seems to proceed as a pulse at all. From values of the propagation velocity, from the value of the strain on the plateaus after a pulse, and by comparison with a slow-speed stress-strain curve, a possible dynamic stress-strain curve may be deduced. Assuming that the material obeys this curve we may calculate the response as mentioned above. This is shown in Figure 4.

The calculated values for the initial pulse and the first reflection agree well with the measurements. Also the general level of strains and the times required to reach them agree reasonably well. But after the first pulse and reflection the wave shapes are markedly different. The calculations give curves of increasing sharpness until finally they become shock waves. No such sharp pulses were observed.

This could mean either that we have not used the correct stress-strain curve or that it is not correct to assume the material obeys a fixed dynamic stress-strain curve. Even if a curve had been assumed without the steep portion that accounts for the calculated shock fronts, the calculated pulses would still be well defined. This means that although the larger portion of

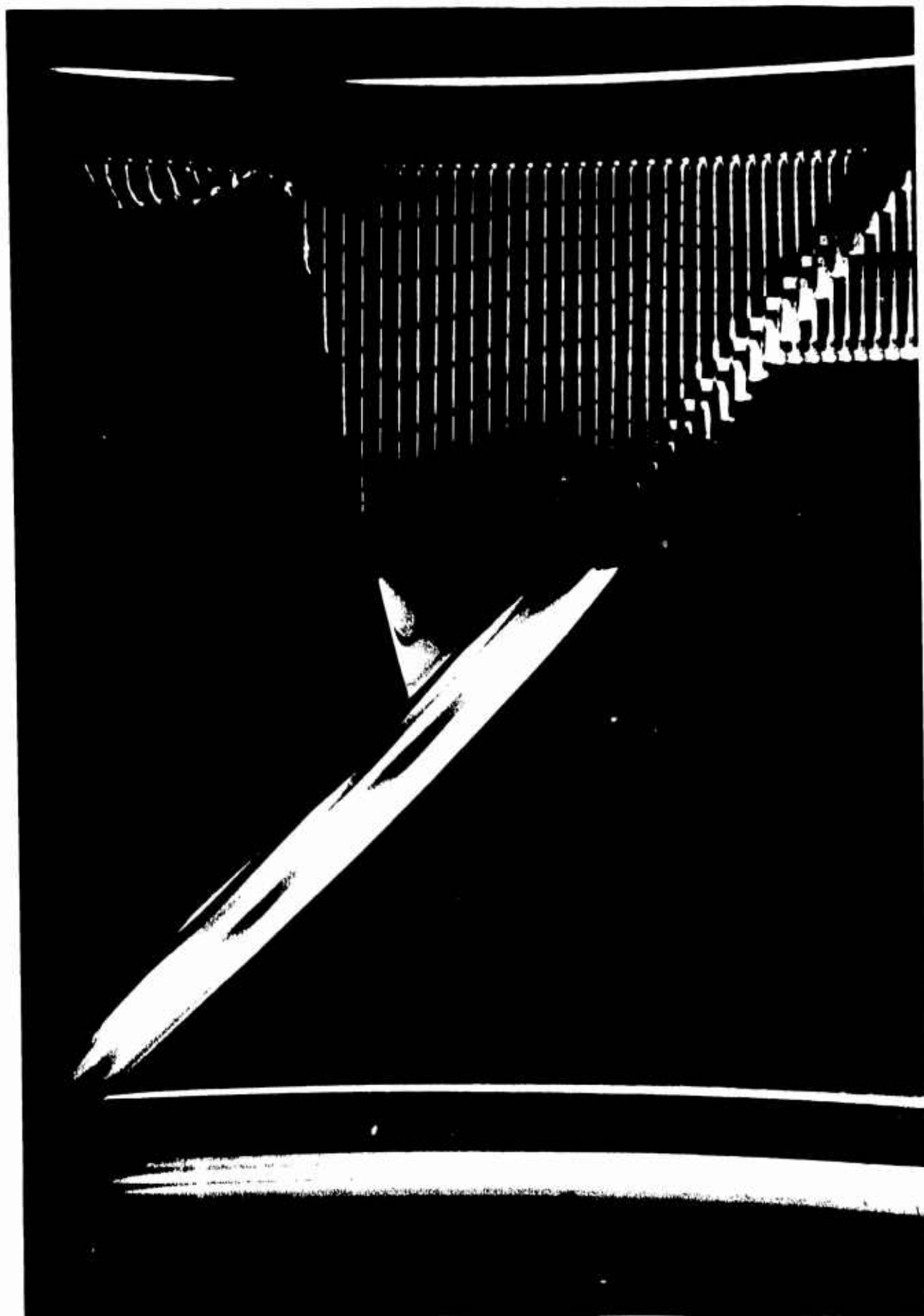


Fig. 5

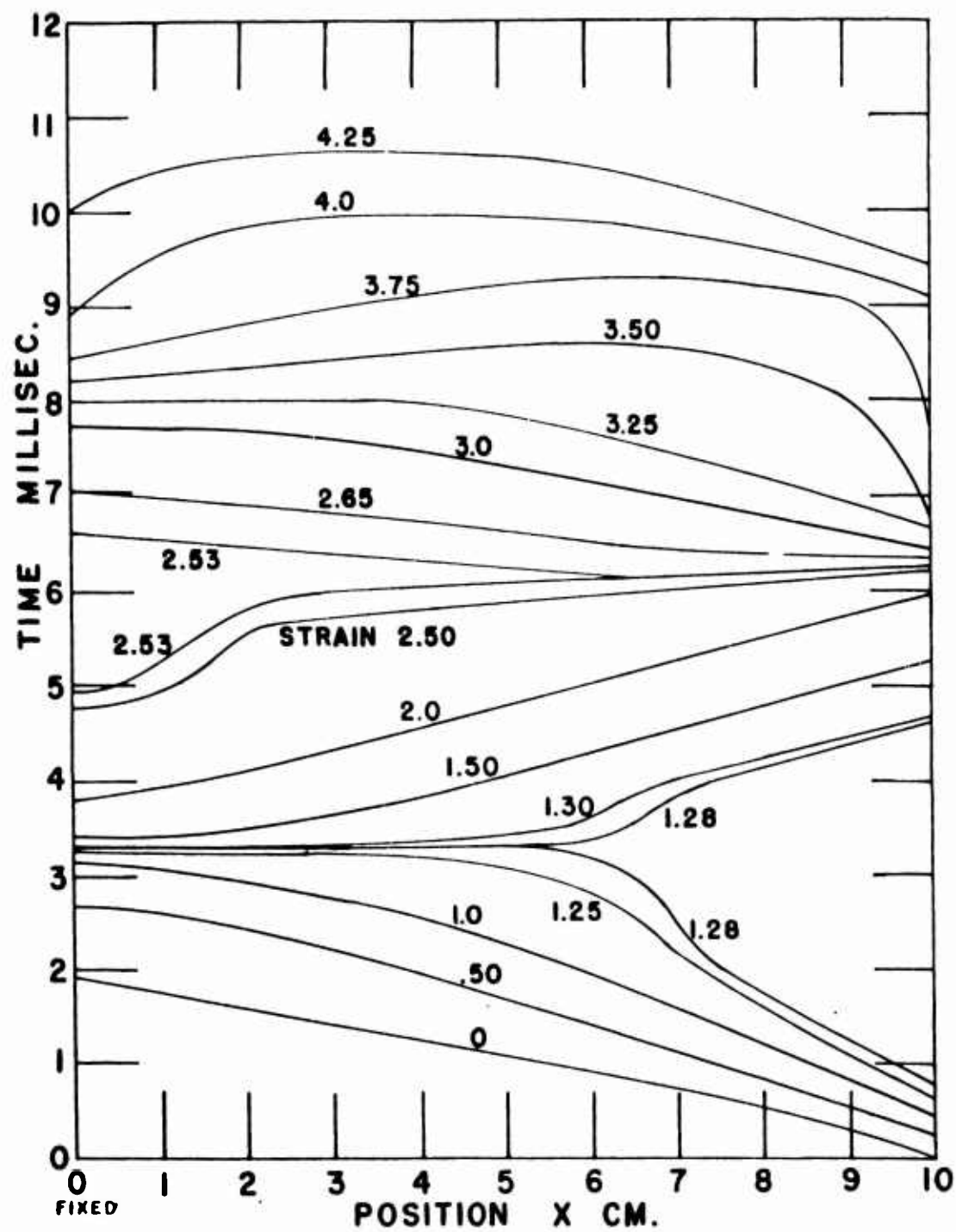


Figure 3. Rubber impact. Position vs. Time, showing lines of constant strain.

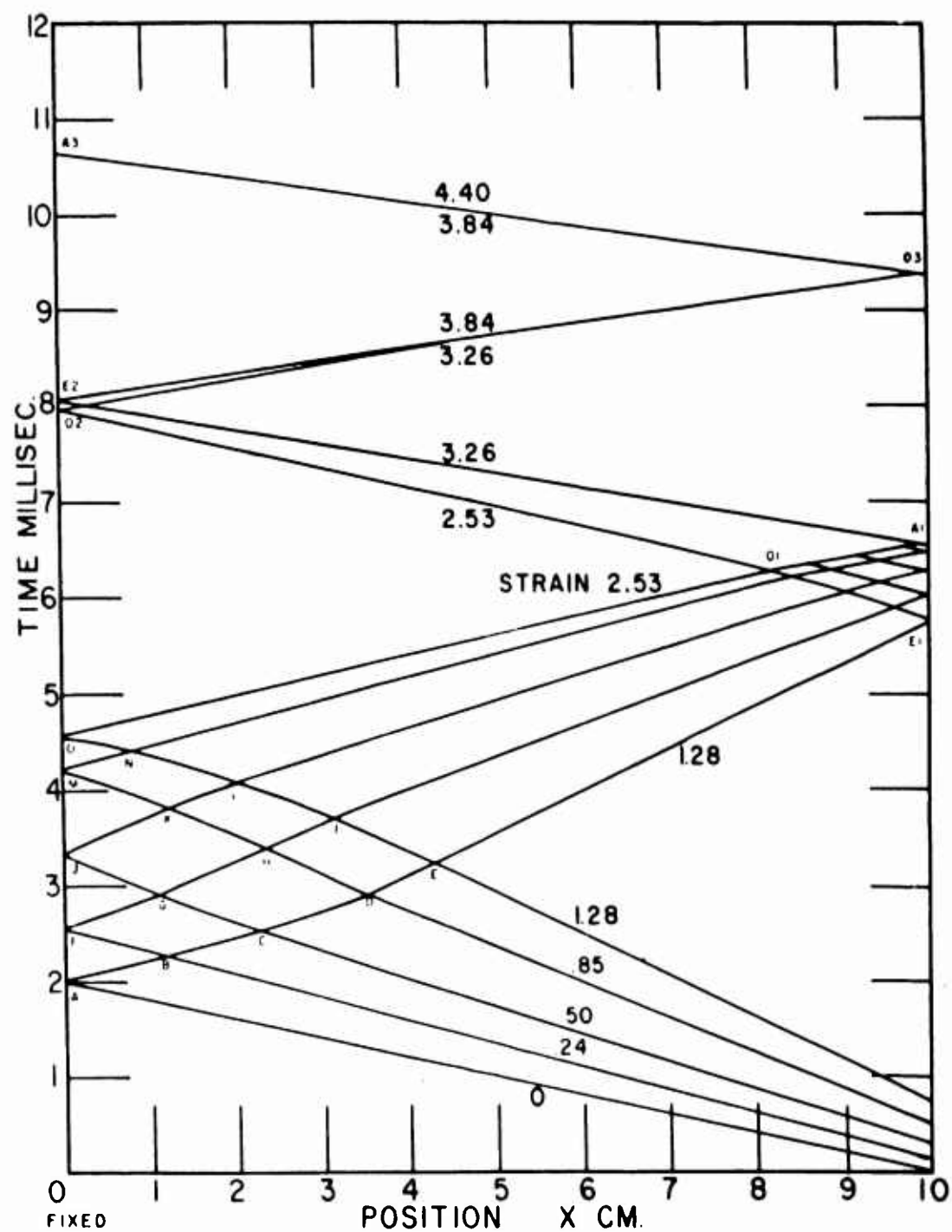


Figure 4. Position-time diagram for a rubber impact calculated from characteristics.

the change in strain may be occurring in times too short to observe here, there is still an appreciable change of strain in the millisecond region.

A modified calculation was made to see if we could get better agreement with the observed strain pattern. For this, pulses from a stress-strain curve were combined with the creep occurring after the passage of each pulse. The rate of this creep was estimated from the difference between the data and the calculated pulse values. This calculation (Figure 5) gives considerably better agreement with the data than results calculated from a stress-strain curve alone.

So our experiments indicate that the initial response of rubber does not all occur in times shorter than a millisecond. There are some considerations that confirm this conclusion. In viscoelastic terms our requirement of an instantaneous response in times shorter than we can observe and with no measurable change in the time scale of the experiment means a relaxation-time distribution curve with a peak in the microsecond region, almost zero in the millisecond region and a rise again for longer times. Most viscoelastic materials have more continuous relaxation-time spectra than this.

For some materials, of which rubber is one, the principle of time-temperature equivalence allows us to construct a curve of the time response of the material<sup>3,4</sup>. To do this the creep is measured over a wide range of temperatures. The response at low temperatures and in moderate times is similar to that at higher temperatures and much shorter times. With the proper procedure a curve may be constructed to represent the response at a single temperature (Figure 6). Since the time scale extends from  $10^{-9}$  to  $10^4$  seconds, a log scale must be used. The curve is sigmoid in shape, rising very rapidly in the microsecond region and having a very gentle rise, linear with log-time, above a second or so.

In order for an impact-response calculation based solely on a stress-strain curve to be correct, the rapid rise in this sigmoid curve must occur in a few microseconds and the linear region must extend below a millisecond. This would correspond to a relaxation-time spectrum with an isolated peak in the microsecond region. This does not seem to be the case. Although temperature-creep tests were not made on the present sample, published curves (Figure 6) for similar rubbers<sup>3</sup> show that the strain is still increasing fairly rapidly in the millisecond region. Since there is appreciable change of strain with time within the time scale of the impact, we cannot expect to see well-defined pulses throughout the test and, as noted above, we did not.

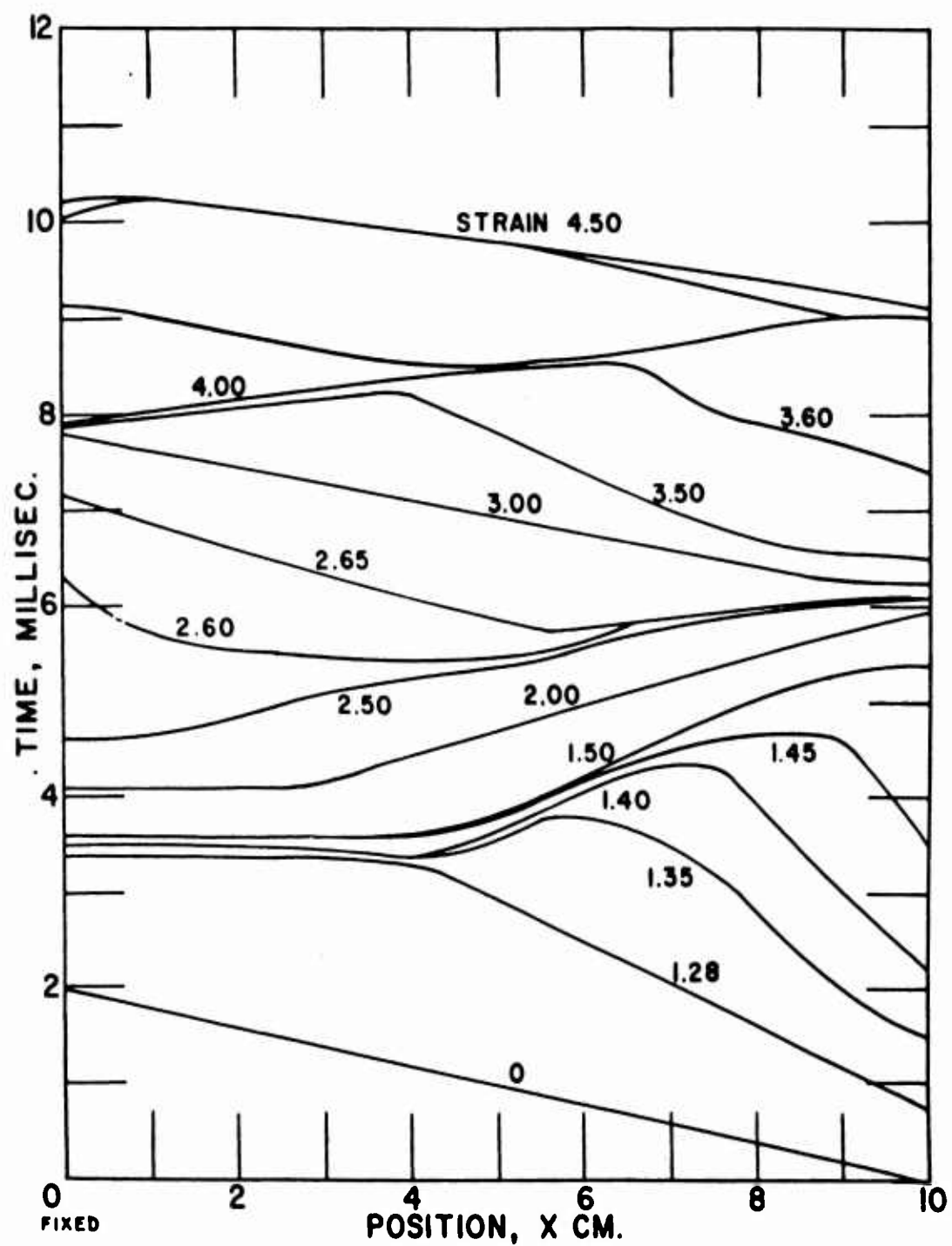


Figure 5. Position-time diagram for a rubber impact obtained by combining characteristic calculation and creep.



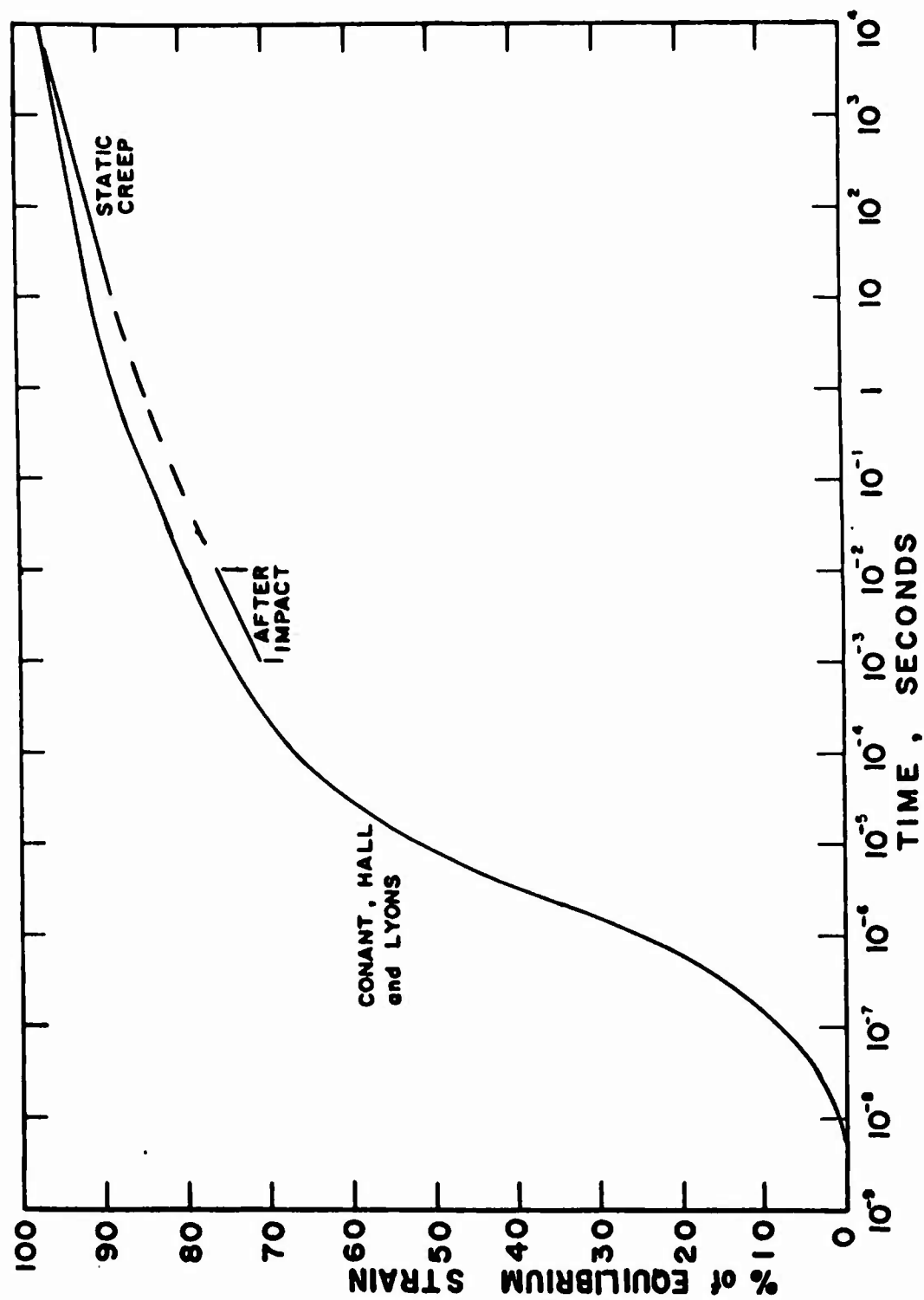


Figure 6. Creep of natural rubber at room temperature determined by time-temperature equivalence. Creep measured after impact for a similar sample is also shown.

Another experimental technique was used to measure how much the strain changes in the time scale of an impact experiment. For this a long rubber sample was used so that there would be no reflection from the fixed end in the time that the sample was observed (about 10 millisecc). The initial pulse was the same as with a short sample but once the observed portion has reached the velocity of the head it moves with constant strain except for the small amount of creep which we want to measure. This creep was about at the limit of our accuracy, and fairly-elaborate smoothing techniques were required to get a reasonably-accurate determination.

The rate of creep measured was reasonable in comparison with time-temperature determined curves (see Figure 6) but was somewhat less than that used in the above calculation combining stress-strain determined pulses with creep. This must mean that creep or observable change in strain is not the only thing that is preventing the occurrence of sharp pulses. After the initial pulse passes, the material continues to relax slowly. Some of this relaxation will appear as creep but some will appear as a temporary decrease in stress. The actual stress level will of course be always increasing but the relaxation tendency will have to distribute itself along the sample at propagation velocities and so should have a smoothing effect on the strain-wave pattern.

So far it has not been possible to get pictures with the nylon yarn good enough for an analysis as with the rubber, because the smaller cross section of the yarn makes it a poorer photographic subject, and the much-smaller strains make accuracy more difficult. However, tests were made that should help us to decide whether nylon yarn as well as rubber has appreciable creep during the time of an impact test. The yarn was 1066-denier high-tenacity nylon. It was impacted at 160 ft/sec.

These tests enable us to compare the shape of the first pulse in the nylon with that calculated from a stress-strain curve. The stress-strain curve for this purpose was obtained from the motion of a tail mass. Strictly, this will not give a stress-strain curve since it measures strain averaged over the whole sample and stress at just one end. However, if the pulses in the nylon tend to smooth out as they do in the rubber (and the photographs obtained indicate that they do smooth out), a stress-strain curve determined in this fashion should not be much in error. In any case only the lower part of the curve is used here and it differs little from a static curve. Assuming that this curve determines the response of the material, the strain-wave pattern may be calculated. From this the stress at the fixed end may be determined as a function of time.

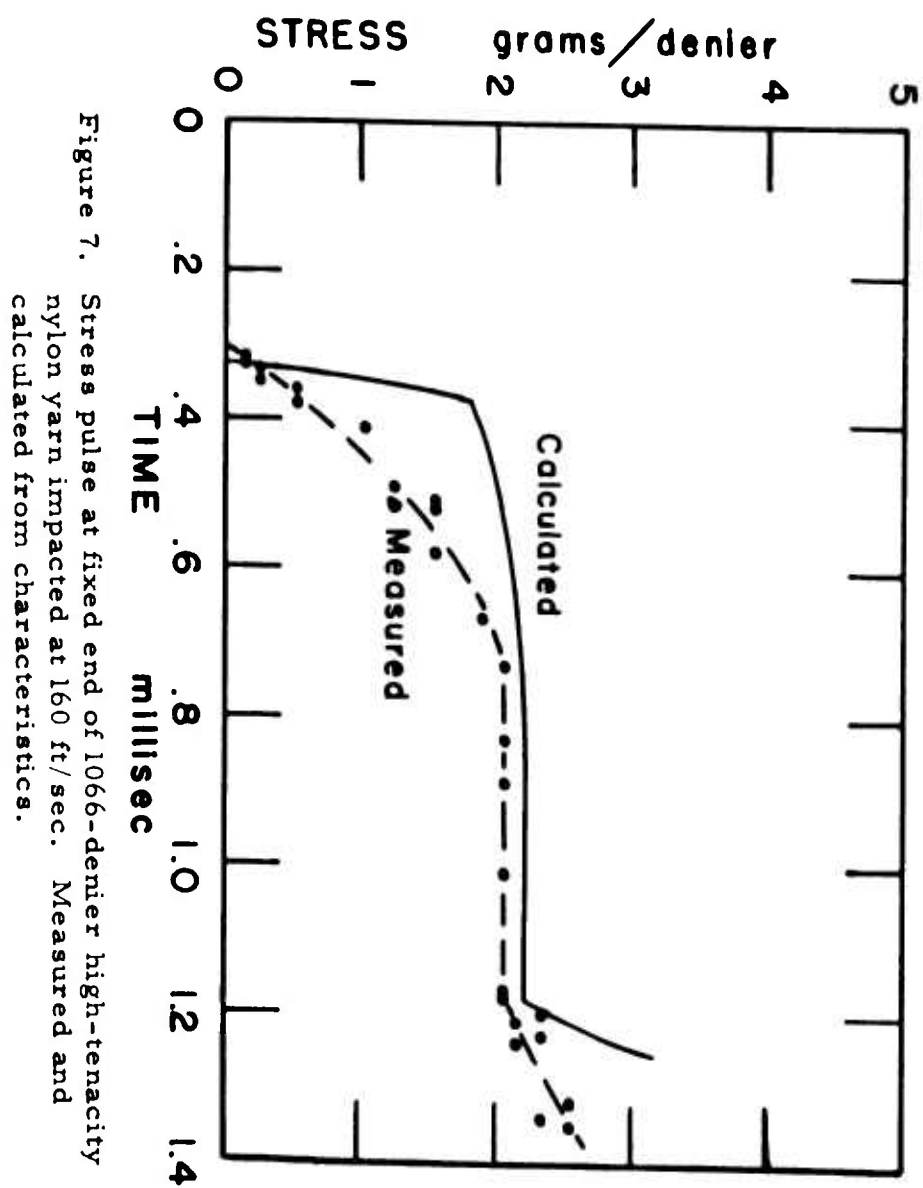


Figure 7. Stress pulse at fixed end of 1066-denier high-tenacity nylon yarn impacted at 160 ft/sec. Measured and calculated from characteristics.

This stress was measured by means of "weak links". The sample was held at the fixed end by a weak link formed by one or more strands of fine copper wire. The force to break one strand was known. From a series of tests with various numbers of strands in which the time to break after the initial impact was measured, the stress-time curve at the tail was determined. This seemed to work well for the initial pulse but at greater stresses there was excessive scatter. This measured curve was corrected for the estimated time it took the weak link to break after it was loaded. The calculated curve was corrected for the small but finite time it took the head mass to reach full velocity, and the two curves are compared in Figure 7.

The level of stress after the passage of the initial pulse agrees very well for the measured and calculated cases. However the calculated stress rises more sharply than that measured. So the material does not respond as rapidly as the calculation from a stress-strain curve indicates.

To summarize we may say that a stress-strain curve may be used to determine the over-all impact response of both materials studied, rubber and high-tenacity nylon yarn. Such an analysis, however, indicates steep wave fronts that would require more rapid response than the materials exhibit. So for a complete picture of the response we must include some slower-acting mechanisms.

#### REFERENCES

1. Pilsworth, M. N. Jr., Tensile impact on rubber and nylon. Quarter-master Research and Engineering Center, Pioneering Research Division, Technical Report PR-3 (1962).
2. von Karman, T., P. Duwez, The propagation of plastic deformation in solids, J. Appl. Phys., 21, 987 (1950).
3. Conant, F. S., G. L. Hall, W. J. Lyons, Equivalent effects of time and temperature in the shear creep and recovery of elastomers, J. Appl. Phys., 21, 499 (1950).
4. Wood, L. A., The elasticity of rubber, J. Wash. Acad. of Sci., 47, 281 (1957).

## HIGH LOADING RATE TESTING MACHINE, DEVELOPMENT AND TYPICAL MATERIALS TESTING APPLICATIONS

T. M. Roach, Jr.\*

### ABSTRACT

The Ordnance Design Engineer is often faced with problems for which it would be advantageous to have dynamic strength data available for use in designs where the maximum load is applied to the design item on a scale measurable in milliseconds. This paper covers the design, development and testing applications of a high loading rate tensile testing machine that was constructed and delivered to this Arsenal by the Hesse-Eastern Division of Flightex Fabrics, Inc., in order that this dynamic strength data could be obtained. The testing machine to be discussed is capable of making tension or compression tests in which the time to reach a desired stress level may be varied from one second down to five milliseconds. It is possible to apply a preset value of stress and maintain this stress at a constant level until yielding of the specimen occurs. Tests to fracture may also be performed and stresses up to 300,000 psi may be applied to a .250 inch diameter specimen. Provisions are provided for testing specimens at various temperatures from -65°F to 300°F. A number of special carburized steel specimens were taken to fracture in the low millisecond time range, in order that the effects of carburization depth could be assessed. The results of this series of tests are reported. Also discussed are the dynamic tests performed on two component items, shot-start and shock screw, and several pearlitic malleable iron specimens.

### INTRODUCTION

Scientists have recognized for some time that a difference exists between the mechanical properties of metals under dynamic and static conditions of loading. Investigations of this relationship have shown that in most cases an increase in the loading rate raises both the yield and ultimate strength of the material.

A phenomenon which should be considered important to the Ordnance design engineer whose item is loaded to peak stress in the low millisecond

---

\*T. M. Roach, Jr. Physicist, U. S. Army Munitions Command, Picatinny Arsenal, Dover, New Jersey.

range is "delayed yielding." When certain metals, particularly mild steel, are loaded rapidly to a constant stress level above the yield stress, a time delay for initiation of plastic flow is exhibited.<sup>1</sup> It was after a review of this work, reported by Drs. Clark and Wood, that the Metallurgical Coordination Committee of Picatinny Arsenal recommended that arrangements be made to have a typical shell steel tested in their machine at the California Institute of Technology. Dr. Rolf Weil of the Arsenal's Engineering Research Section, visited Drs. Clark and Wood in 1956 and used this machine to perform a series of tests on a typical shell steel which had a static yield strength of 85,000 psi. Yield delays of 7 milliseconds were obtained with loads of about 94,000 psi at  $10^7$  psi/sec loading rates.<sup>2</sup> After these encouraging results were obtained it was decided to obtain a high-loading rate testing machine for use at Picatinny Arsenal.

#### MACHINE REQUIREMENTS:

The following machine requirements were established by the Arsenal's Metallurgical Coordinating Committee:

- a. The machine shall be capable of making tension or compression tests in which a stress is rapidly applied to a specimen.
- b. The range of time to reach a desired stress level shall be from one second down to five milliseconds. If the capability to apply the load faster can be incorporated without unduly complicating the design, this would be desirable.
- c. It shall be possible to apply a pre-set value of stress and maintain this stress at a constant value until yielding of the specimen occurs. The applied stress shall be able to cause fracture, but it shall be possible to apply a stress which does not.
- d. The load system, including the specimen, must be critically damped and should remain so at the various elongations in the specimen to be tested.
- e. The specimen dimensions and the load system shall permit applications of a stress up to 300,000 psi.
- f. The specimen shall be short enough so that up to necking down, the stress is approximately uniform over the gage length at any instant.
- g. There shall be provisions for testing specimens at various temperatures from  $-65^{\circ}\text{F}$  to  $300^{\circ}\text{F}$ .

h. A permanent test record shall be made as part of the testing procedure.

i. No components of the machine shall be damaged when the specimen fractures.

j. The machine shall allow the stress to be applied in two steps above an initial value, applied in the manner required in "c" above, and shall be able to re-apply a second stress within 50 milliseconds after the stress has been removed.

A basic machine design that appeared to be capable of meeting the above specifications was conceived by the Hesse-Eastern Division of Flightex Fabrics, Inc. Everett, Mass. and submitted to Picatinny Arsenal. The proposed machine included a loading system that depended on a balanced pneumatic-hydraulic pressure arrangement; it was planned to introduce compressed gas on one side of the system, which would be held in equilibrium by a volume of fluid at equal pressure on the opposite side. With this system linked to a test specimen, rapid loading was to be accomplished by quickly venting some of the fluid out of the operating cylinder. In the basic proposal, loading time was to be controlled by the variable restrictions and quick operating electrically controlled valves. Sequencing of valve actions were to be initiated and timed by electrically operated, adjustable time delay relays. The maximum loading rates requested in the specifications indicated a need for very high speed valve actions.

The operating cylinder and piston was designed with sufficient stroke length to allow application of successive rapid loads, and also to accommodate elongation of ductile specimens. Two accumulator tanks were to be included, with a system of manifolding and valving to allow two step or two pulse load patterns.<sup>3</sup>

#### MACHINE CONSTRUCTION:

After the machine design was formalized to a point where all major dimensions and operating parameters were established; sketches of the various detail parts and sub-systems were prepared. This design was submitted for Arsenal approval and at this time it was decided to build a bread board version of the test machine. After assembly of the machine had progressed to a point where it could be considered operational, preliminary tests were conducted to determine the spring constant of the machine and damping requirements. Some design deficiencies were revealed in these tests and changes were introduced which served to correct these problems. The instrumentation system for read-out of load and strain data was also

selected at this time. The transducers selected were a Baldwin-Lima-Hamilton-SR4 resistance strain gage separable extensometer to measure strain, and a Cox and Stephens resistance strain gage load cell to measure load. A Tektronix dual beam oscilloscope was selected for signal display. The original instrumentation system for displaying the transducer outputs on the oscilloscope proved to be troublesome and was discarded. Two Tektronix, type Q plug-in units, which provide excitation voltages for the strain gages or transducers, were substituted. A stainless steel cylindrical enclosure was fabricated to surround the specimen and provide a heat shield. This unit is fitted with a 750 W calrod heating element that was shaped to surround the gage length portion of a standard tensile specimen. A copper constantin thermocouple operating a millivoltmeter pyrometer was provided for sensing specimen temperature. Low temperatures may be achieved by placing an acetone and dry ice bath, or other type of coolant in the specimen chamber.

Figure 1 shows the testing machine and associated recording equipment and Figure 2 the piping and valve layout.

#### EVALUATION TESTS:

Machine evaluation tests were performed prior to acceptance and all the required operational tests were performed satisfactorily except the capability to apply the desired load to a specimen in five milliseconds. It was suggested at this time that a burst or rupture disk technique be tried. The disk would be designed to fail at a predetermined pressure level, and provide the required fast rise times. A burst disk holding fixture was designed to hold the burst disk, and loading times of less than five milliseconds were obtained using this system. At the present time a new technique is being investigated that will permit a single thickness rupture disk to be used through the entire pressure range.

Illustrations of the various loading modes are shown in Figure 3. These are reproductions of the Polaroid test records. Record (a) was obtained with the machine selector switches set for the "load and hold" condition of loading, (b) was obtained with the selector switches set for the "load and unload" condition, (c) is the result of a "two step" loading selection and (d) shows the "load, unload and reload" condition.

#### EXPERIMENTAL RESULTS:

1. After machine installation was completed in the Engineering Sciences Laboratory at Picatinny Arsenal, tests were made to check machine performance. Two typical load to fracture records that were obtained



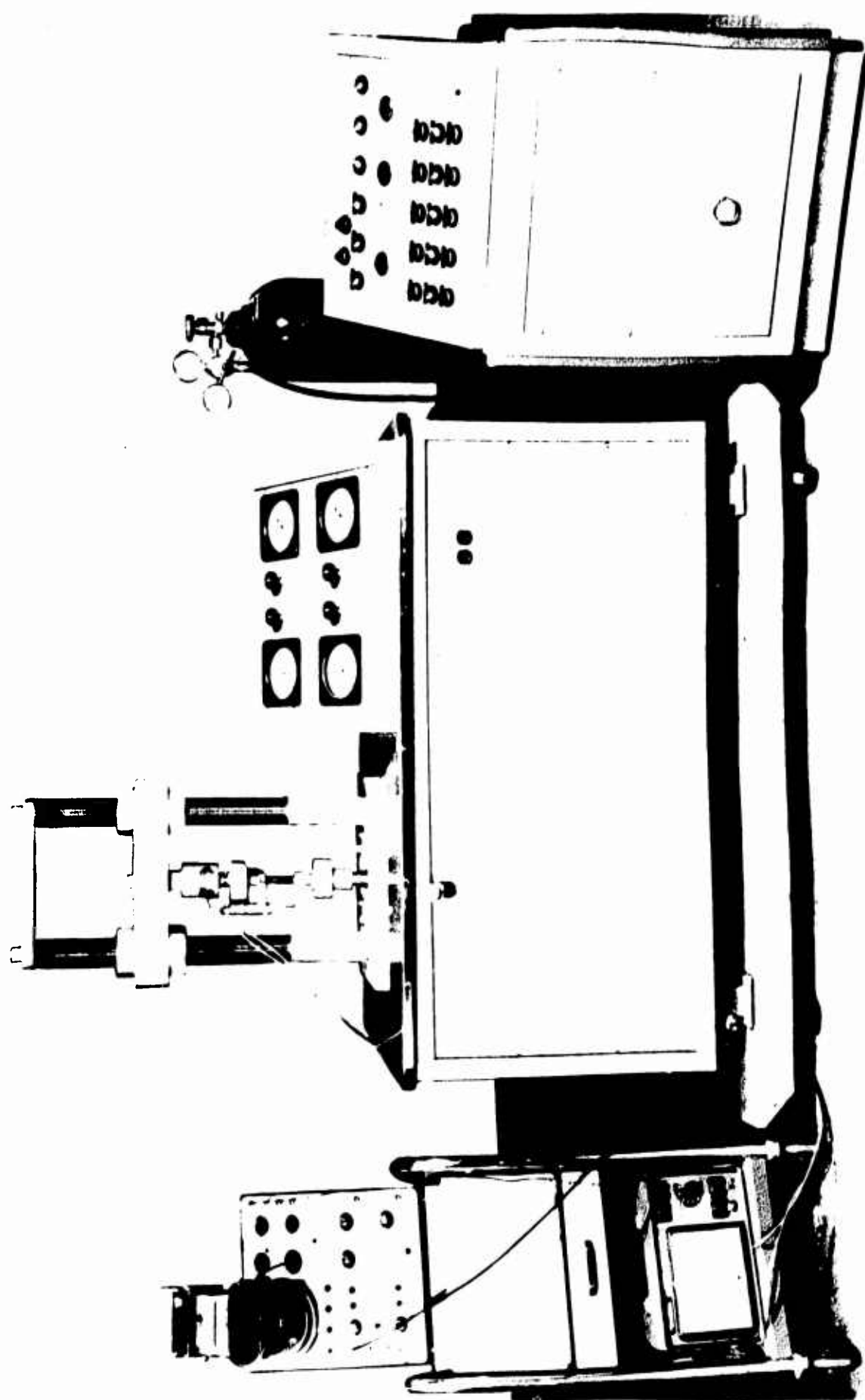
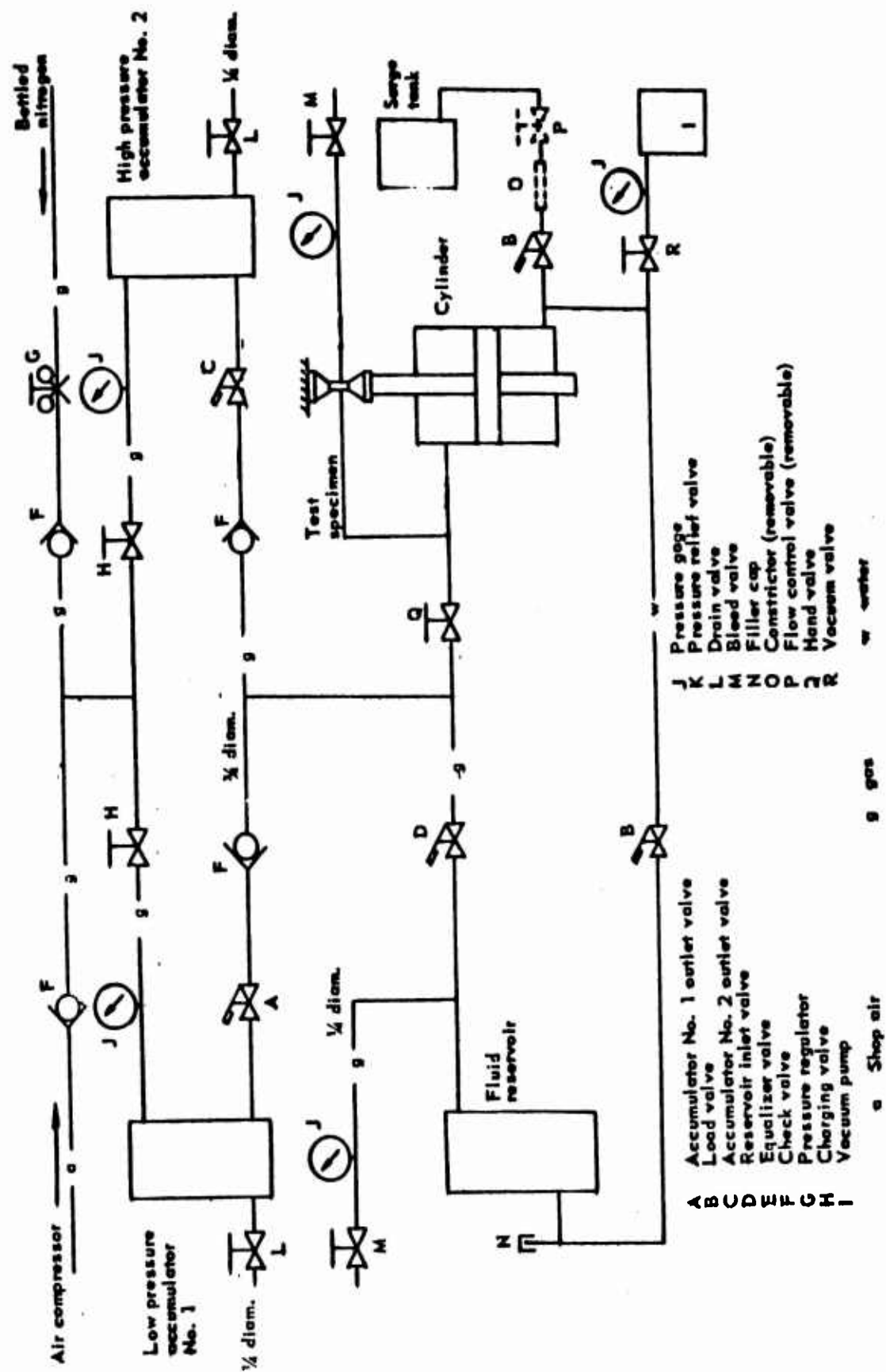


Fig 2 Schematic of high loading rate testing machine



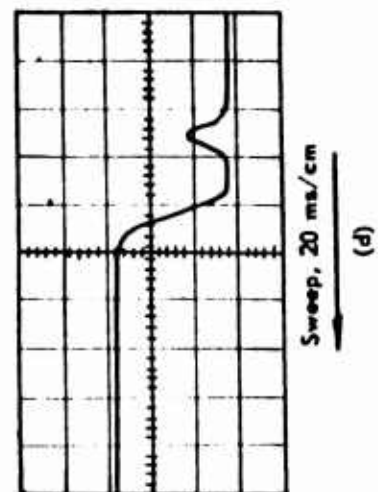
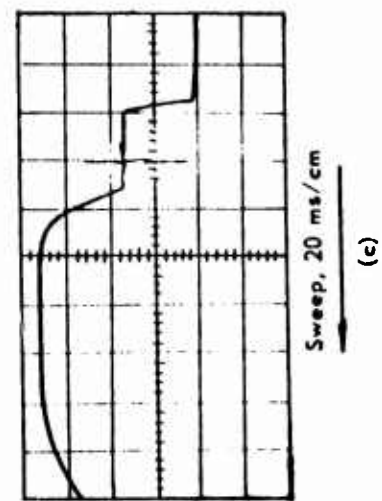
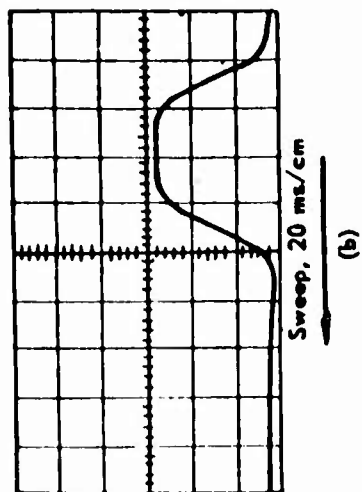
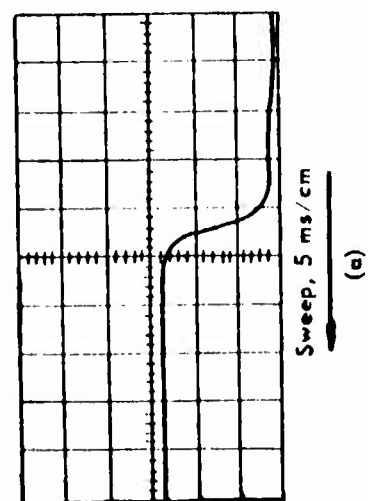


Fig 3 Machine loading modes

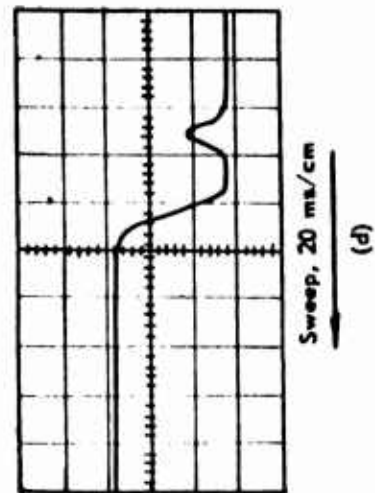
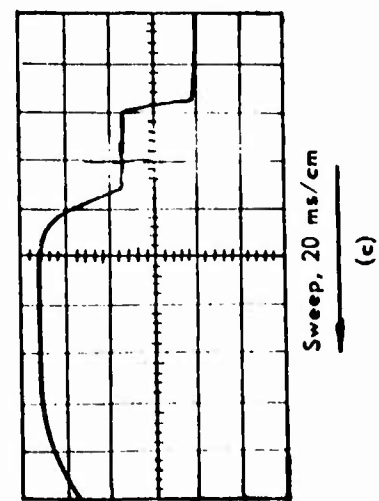
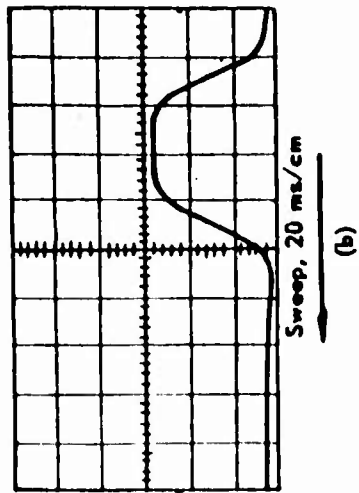
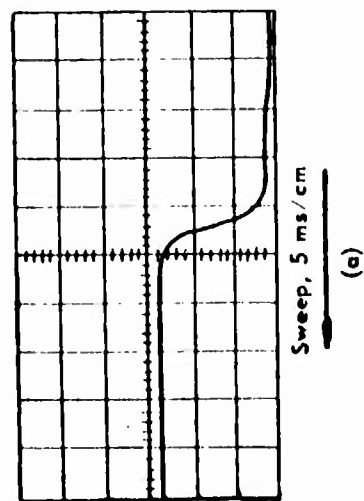


Fig 3 Machine loading modes

during these tests are shown in Figure 4. Record (a) shows failure of a medium carbon steel specimen with an applied piston pressure of 375 psi. The peak load in this case was 4,500 pounds, equivalent to a maximum stress level of 91,000 psi. Record (b) shows failure of an aluminum alloy with the same machine loading of 375 psi. The peak load in the case was 3,450 pounds, equivalent to a maximum stress load of 70,400 psi. The specimens used to check initial machine performance were supplied by the manufacturer. Static strength data was not made available.

2. It was requested by Dr. Rolf Weil, of Stevens Institute of technology, soon after machine installation, that a series of special carburized steel specimens be taken to fracture in the low millisecond time range. Figure 5 (a) shows the load and strain record for an SAE 1045 steel specimen that had been carburized for a six-hour period. The peak load for this specimen was 7700 pounds, which is equivalent to a maximum stress level of 157,000 psi. Record (b) shows the load and strain traces for a specimen that had been carburized for a nine hour period. The peak load in this case was 6400 pounds, equivalent to a maximum stress level of 130,000 psi. Figure 6 (b) shows the type of test specimen used in this series of tests. Type C-7 wire strain gages were bonded to all carburized specimens. The records obtained in this series of tests clearly showed the effects of the depth of carburization on fracture strength. Dr. Weil has evaluated this work and has incorporated it in a detailed report (Confidential).

3. Several pearlitic malleable iron specimens (this material used in the 105mm, M442 shell) were taken to fracture in the low millisecond range. In the test record shown in Figure 7 the peak load is 4000 pounds, equivalent to a maximum stress level of 81,600 psi. This work was requested after the question had been raised as to whether this material could possibly have a variant dynamic fracture strength or even be stronger under static loading conditions. At the present time a program is under way to test 40 specimens of this material both statically and dynamically. Test specimens are being taken from four different projectiles and both tensile and compressive tests will be performed.

4. It was requested that a number of shock-screws be taken to fracture in the low millisecond time range. Figure 8 shows a particular type of failure that was encountered in these tests and Figure 9(b) shows a typical test record for this item. The drawing of the shock-screw in Figure 8 was made six times actual size as the screws overall length is only 11/16 inches. This item is part of the fin assembly on an artillery round and its function is to prevent the fins from opening prematurely. As both Watertown Arsenal and Picatinny Arsenal manufacture these screws, samples from each installation were included in the test group. Of the twelve screws tested only

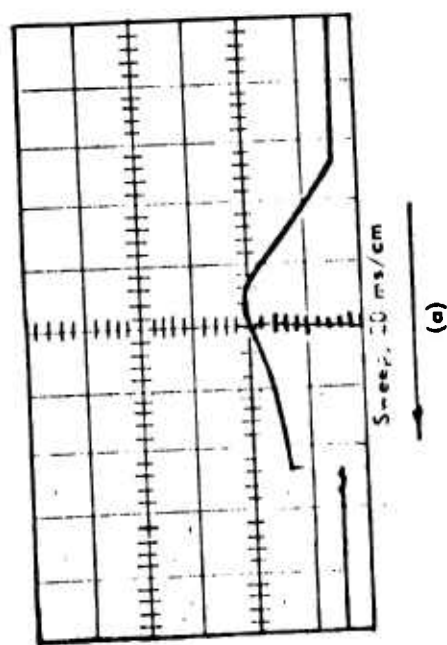
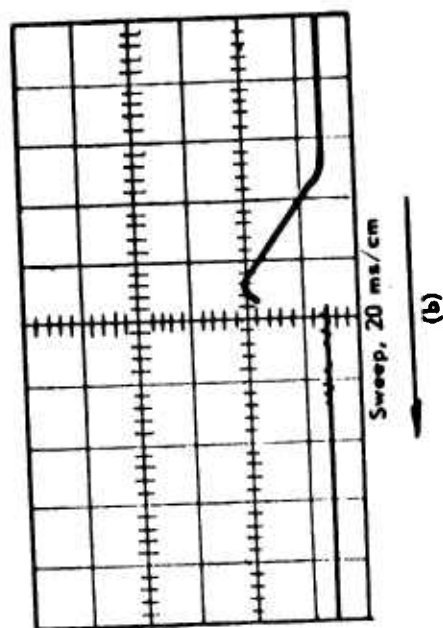


Fig 4 Fracture records

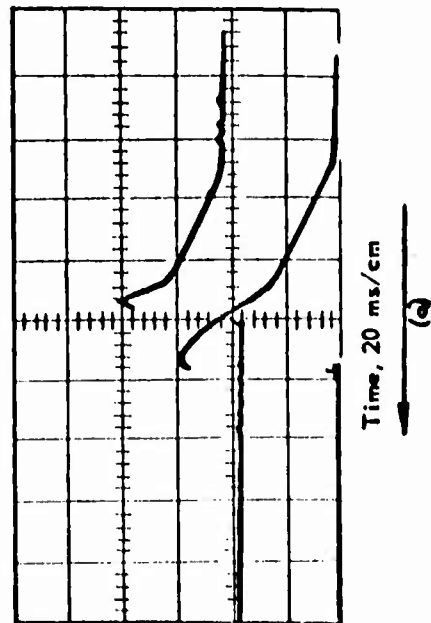
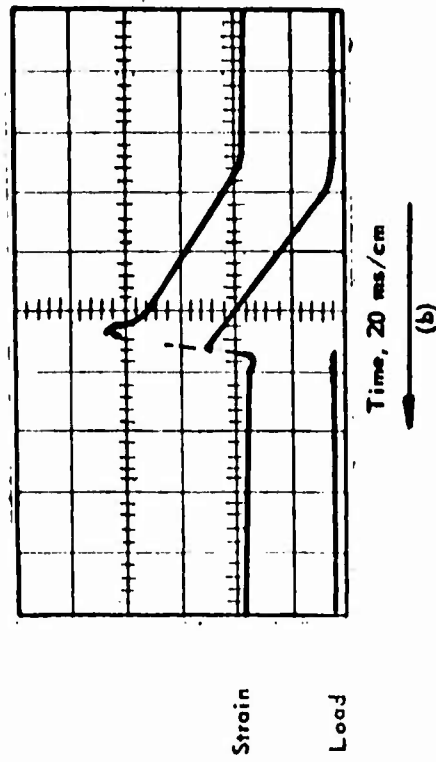
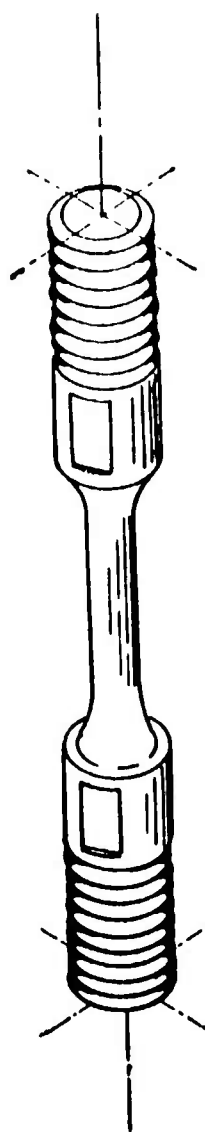


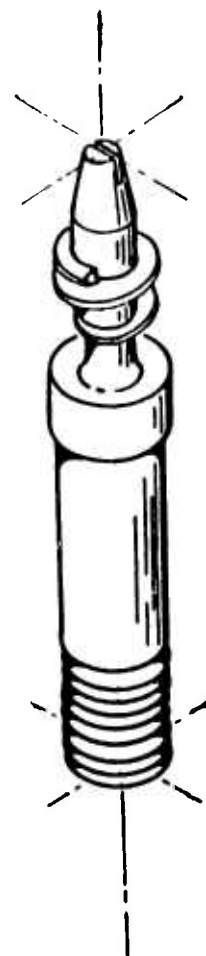
Fig 5 Load and strain records of carburized steel specimens



(a)



(b)



(c)

**Fig 6 Test specimens**



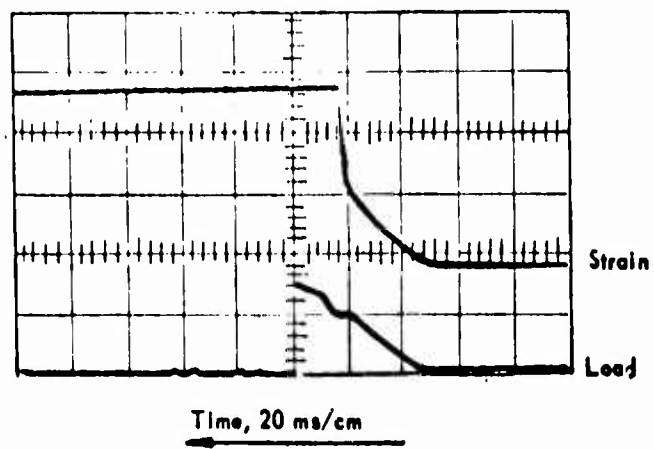


Fig 7 Pearlitic malleable iron specimen

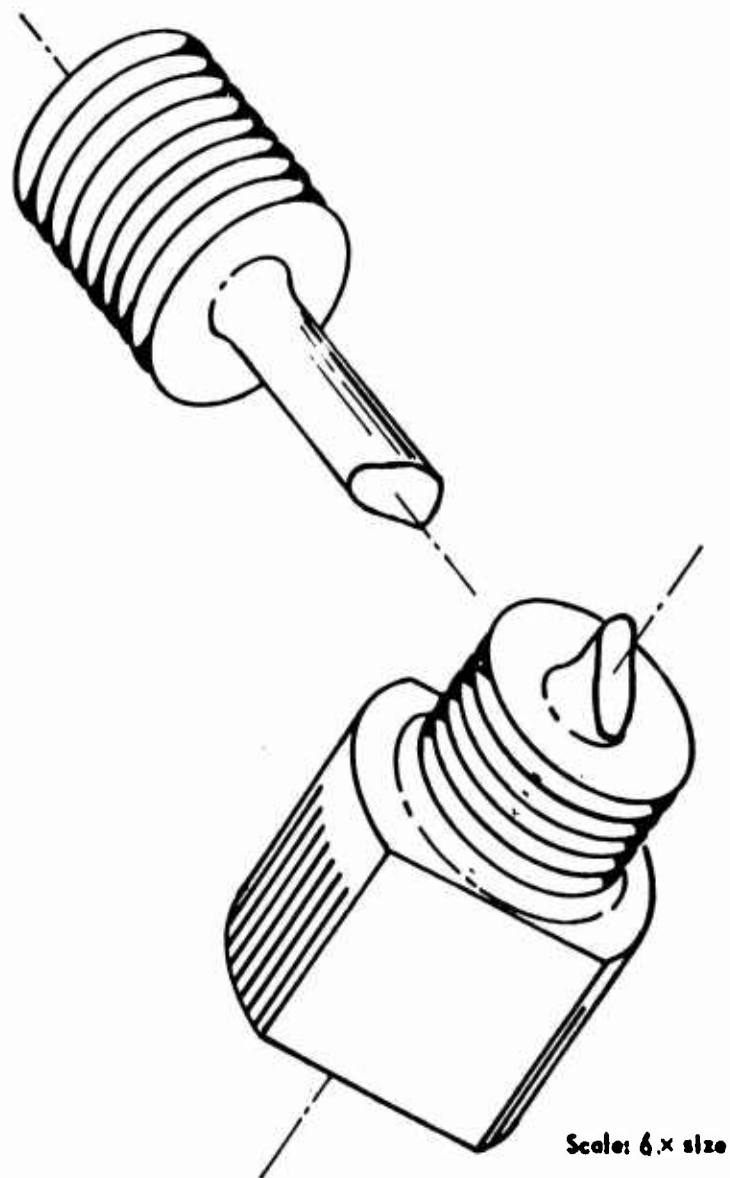
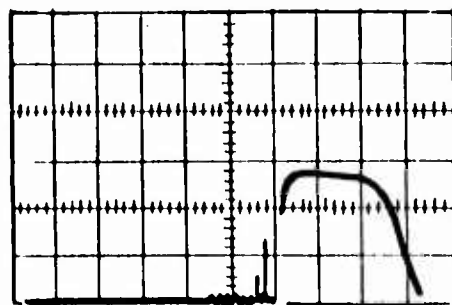
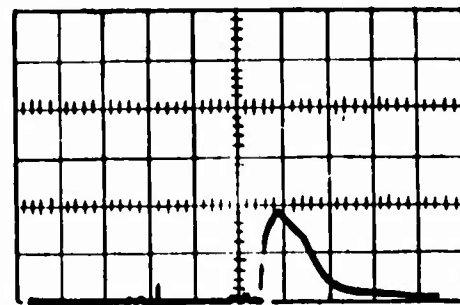


Fig 8 Shock screw (failure)



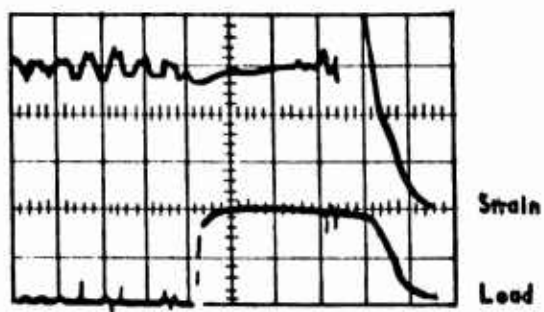
Time, 10 ms/cm

(a) Shot-Start



Time, 20 ms/cm

(b) Shock screw



Time, 5 ms/cm

(c) Aluminum alloy 6061-T6

Fig 9 Typical test records

one failed to neck down before fracture, and it is felt that the screw could have cocked in the holding device and permitted a bending condition to exist. The maximum stress level in this case was 195,000 psi and was the highest stress measured for the group. The average maximum stress for the Watertown Arsenal screws was 179,300 psi and the average for the Picatinny Arsenal screws turned out to be 179,000 psi.

5. A number of shot-start components were fractured in the low millisecond range. The function of the shot-start, shown in Figure 6 (c), is to retain the projectile in the cartridge case until the propellant gas pressures reach a relatively high value, at which point the shot-start fractures and the projectile takes off. A load to fracture record for one of these components is shown in Figure 9 (a). The peak load was 8,300 pounds, equivalent to a maximum stress of 170,000 psi. The rise time to this stress level was eight milliseconds. A static fracture test was performed and the peak stress was found to be 171,500 psi. These items are manufactured from SAE 4140 steel. A second group of these components, made by a different manufacturer, are being evaluated, and preliminary results indicate they are stronger. One shot-start was loaded to 8800 pounds (load and hold) with no fracture or apparent elongation. A second item fractured at a load of 10,000 pounds, equivalent to a maximum stress of 204,000 psi.

6. An experimental investigation which involves the dynamic loading of small aluminum and steel beams is being conducted by the Dynamics Unit at Picatinny Arsenal. This work is being sponsored by the Air Force, with the analytical work on this program being assigned to a group at the Massachusetts Institute of Technology. The M.I.T. analysts have requested that coupons of the three materials used in the explosive loading tests be fractured statically and at various loading rates. Figure 6 (a) shows a typical coupon specimen with a foil type strain gage bonded at the midpoint of the gage section. The three metals to be tested were (a) SAE 1100 steel (b) 6061-T6 aluminum (c) 2024-0 aluminum. Ten coupons of each type of alloy were prepared and instrumented with foil type strain gages. Figure 9 (c) shows a load and strain record for one of the 6061-T6 aluminum specimens. The peak load, which was reached in approximately five milliseconds, is 3,100 pounds, which is equivalent to a maximum stress of 49,700 psi. As only four 6061-T6 aluminum specimens have been fractured, all in the 5-8 millisecond time range, no data is available at this time for noting rate effects.

## CONCLUSIONS

The high loading rate testing machine described in this paper has proven to be a very useful tool in research tasks and in the investigations of parts, components and subassemblies of various small Ordnance structures. This machine has proven it can meet the specific performance specifications. It has been shown, using the rupture disk technique, that the time required to reach a desired stress level can be less than the required five milliseconds. In one of the shock screw fracture tests the peak stress was reached in three milliseconds.

## REFERENCES

1. D. S. Clark, Trans. ASM, Vol. 46, p 34, 1954.
2. Mechanical Properties of Shell Steel at Rapid Loading Rates, Rolf Weil, Picatinny Arsenal Technical Memorandum No. 35, August 1956.
3. Development of High Loading Rate Testing Machine, Robert E. Sebring, Final Summary Report, Hesse-Eastern Division, Flightex Fabrics, Inc. September 1961.

## DISCUSSION

Dr. A. G. H. Andersen, Watertown Arsenal: I would like to ask what is the actual fastest speed that you have?

Mr. Roach: Dr. Andersen, two milliseconds is the best and we hit that once and we have hit three milliseconds several times.

Dr. Andersen: You do expect eventually to get down to the millisecond range.

Mr. Roach: It is two millisecond I am talking about.

Dr. Andersen: I should say microsecond range.

Mr. Roach: No, this machine will not go to the microsecond range. We ask in the specs that it go down to five; we hope for better and with the burst disc we are down to 2 and 3 milliseconds.

Dr. Andersen: You don't expect anything better than that?

Mr. Roach: I think that is all they are going to get out of this machine.

Dr. Andersen: There seems to be a stopping point for most of these machines that we have heard about lately.

Mr. Roach: Right.

Mr. Robert Schwartz, Munitions Command, Dover, N. J.: Many years ago we conducted a great deal of dynamic loading tests, perhaps not on machines but I recall that we had an artillery shell pretty well instrumented where we got the actual dynamic stress under loading conditions, so we

had pretty realistic conditions as to what is happening during the maximum stress conditions when firing in a gun. How do these latest static machines compare with the realistic gun firing conditions that we are trying to simulate to get some data for?

Mr. Roach: Well, the shell is so designed that it is assumed that the stresses are of a certain magnitude. In the gun firing the idea is to check the calculated values. You instrument the shell in the critical region under the rotating band and you measure your deflections and the corresponding stresses. We have found close agreement for the rotating band but back under the band you have a definite yielding in most cases and at the present time we are studying the filler supporting effect. In other words we have slimmed down the artillery shell; thinned the walls down by a factor of three, and waited for the filler to start supporting it. The idea was to introduce the filler into the theory by letting the filler support the walls that are starting to deflect and even if they go a little plastic, it won't hurt anything. It is a one shot item. I don't know if this answers your question exactly, Bob, but what we are trying to do is to measure these things under actual firing conditions, check the designer out this way, hoping that we are helping him.

C. Kropf, U. S. Army Tank-Auto Cnd, Centerline: It was interesting to note the effect of the increased case depth on the deterioration of the dynamic yield strength. I am wondering if any evaluation had been made regarding the quality of case depth.

Mr. Roach: Was this in the work done by Dr. Wald?

C. Kropf: Yes.

Mr. Roach: He has done a pretty thorough job of analyzing these records. He was going to speak here today but his report was confidential and that knocked it out but he would have probably included some remarks on this because I know he has done a thorough analysis.

H. Cadle, Springfield Armory: I would just like to comment on the Q units that are used in the dynamic loading at times. We found that you have to be a little bit careful as you get down to frequencies lower than what you have been having so far. At 6 KC the Q unit has a 3 DB shift and we found that in a half a millisecond rise time we did not get good response.

Mr. Roach: It is interesting that you mention this. We were fortunate in having three Q units and we found one of them was not performing satisfactorily so we pushed it aside and we checked the other two out completely, and we were satisfied with them.

Abraham L. Dorfman, Picatinny Arsenal: In response to Bob Schwartz's question, I think, Tom, correct me if I am wrong, in setting the specifications for that piece of equipment the 5 milliseconds or better was based upon the actual results of firing bursts.

Mr. Roach: That was the idea.

Mr. Dorfman: I think that answers your question, Bob. This is the order of time that we are experiencing in firing.

Mr. Roach: Right, that was it.

## A MEDIUM-SPEED TENSILE TESTING MACHINE AND ITS PERFORMANCE IN TESTING OF SOME ORDNANCE MATERIALS

Dr. A. G. H. Andersen\*

### ABSTRACT

A pneumatic tensile tester, recently designed and built at Watertown Arsenal Laboratories, has a load capacity of 12,000 pounds and an idling speed of about 300 in./sec. over a 3-inch stroke, at 500 psi nitrogen or less than half the allowable maximum pressure.

Loads and strains may be recorded by oscillographs or oscilloscopes. The scope can be triggered through an electric circuit by an internal, automatic poppet valve in the main gasport. External, auxiliary diaphragm valves are actuated by solenoids. Excess energy of piston assembly, after a tensile rupture, is absorbed through rapidly damped oscillations between two air cushions at opposite ends of the cylinder.

The machine is mounted on a carriage resting on springs and Barry-mounts so that operation at full load transmits negligible vibrations to the floor. Weight of machine and carriage is 700 pounds; base, 600 pounds; and steel safety cabinet 400 pounds.

Short descriptions and a number of illustrations are presented which show typical actions of the machine and results of various tests recently performed on ordnance materials.

### INTRODUCTION

Dynamic testing of mechanical properties of materials began in the early years of this century and has, in recent years, become of increasing interest to the U. S. Army Ordnance Corps. It is interesting to note that in 1936 Watertown Arsenal constructed and applied one of the early dynamic testing machines.

Since the advent of electric resistance strain gages and oscilloscopes in the materials testing field the techniques of high-speed testing have advanced rapidly. This development has continued at a fast pace since the early days of World War II.

Dynamic testing includes a large variety of testing techniques depending mainly upon speed, cycling, temperature and motive power. Dynamic testing

---

\*Dr. A. G. H. Andersen, Materials Engineering Laboratory, Watertown Arsenal, Watertown, Massachusetts.



equipment, according to its objectives, tends to be highly specialized. Although a number of machines of different designs have been developed, for medium-speed testing, few of these are commercially available. Probably no generally preferred type of medium-speed machine exists today, although piston-type machines actuated by inert gas, seem to predominate in current usage in the loading rate range pertaining to much ordnance materials testing.

Characteristic features of dynamic testing apparatus generally, are the ranges of rates of loading and straining. With reference to rates of straining, three distinctive groups of equipment are recognized:

1. The Hopkinson bar type of testing for studying the truly high-speed dynamic reactions of metals - the elastic and plastic wave phenomena.
2. The high-speed tensile testing machines, operating at strain rates from roughly 10 per second to 1000 per second and higher.
3. The medium-speed tensile testing machines, operating in the range of 0.01 per second to 100 per second.

While it is customary to state the strain rate ranges obtainable with specific dynamic tensile testing equipment, the strain rates themselves are not characteristics solely of the equipment.

With dynamic testing equipment that transforms a negligible proportion of the applied kinetic energy into strain energy, the strain rates are definite characteristics. This is not usually the case with piston driven machines arranged to start the straining of specimens from rest. In these machines, the rates of strain attainable, depend upon properties of the specimens as well as on the loading rates. Maximum load and loading rate rather than strain rate characterize any of these machines.

Various means are used for driving the tensile testing machines. The fastest machines are piston-type machines driven by explosive charges, imparting strain rates claimed to reach 25,000 per second.<sup>2</sup> Rotary drum-type machines have produced strain rates up to 1000 per second. Pendulum impact machines have been reported to operate at 150 per second. Piston-driven, pneumatic and hydraulic machines usually are limited to ranges below 100 per second.

#### GENERAL CHARACTERISTICS OF THE TESTING MACHINE

The Fast-Acting Tensile Tester, designed and built at Watertown Arsenal, has components arranged essentially similar to those of the ordinary hydraulic tensile testing machines by which a piston, connected to the

upper crosshead, is made to strain the specimen. However, this machine utilizes high-pressure gas for driving power. A diagram of the machine is shown in Figure 1.

Power is supplied according to a principle commonly used for dynamic piston-driven testing machines in that the piston is held stationary by balanced pressures on its two sides and made to move by unbalancing the pressures. The load capacity of the machine is 12,000 pounds in tension between crossheads. With specimens secured tightly in the grips, loading rates of 5KLb per millisecond have been achieved during rise times of 2 m sec. more commonly, rise times of 3 to 8 milliseconds at loading rates of 1 to 2 KLb per milliseconds have been employed. The strain rates obtained on high strength, low modulus alloys with these loading rates were between 2 and 7 in./in. per second. These rates can be considerably increased when slack is allowed to occur between the crosshead and the specimen grips, thereby causing the moving components to acquire kinetic energy before engaging the specimen.

Load, strain and crosshead travel data can be photographically recorded on an oscilloscope, triggered through an electric circuit by an internal automatic poppet valve in the main gasport. External valves actuated by solenoids provide convenient control of the gas flow through the machine. The machine is mounted on a carriage flexibly supported by springs on a heavy base resting on Barrymounts so that operation at full load transmits negligible vibrations to the floor. Surplus energy of the moving components is absorbed by rapidly damped oscillations of the piston assembly between two air cushions forming at the extreme ends of the cylinder.

## DESCRIPTION OF THE MACHINE

### Assembly

The machine consists of a cylindrical stanchion containing all mobile components excepting supports, a base, a mounting platform, tie rods, and a beam for securing the stanchion to the platform (Figure 2) and electric controls.

The stanchion assembly (Figure 3), consists of a cylinder with a piston in its lower end, a frame terminating in a cap in its upper end, (2, Figure 3) and near its middle the lower platen (x-5, Figure 3). The cylinder has eight gasports interconnected by four vertical passages shown in (Figure 3, F-1, F-2, F-3).

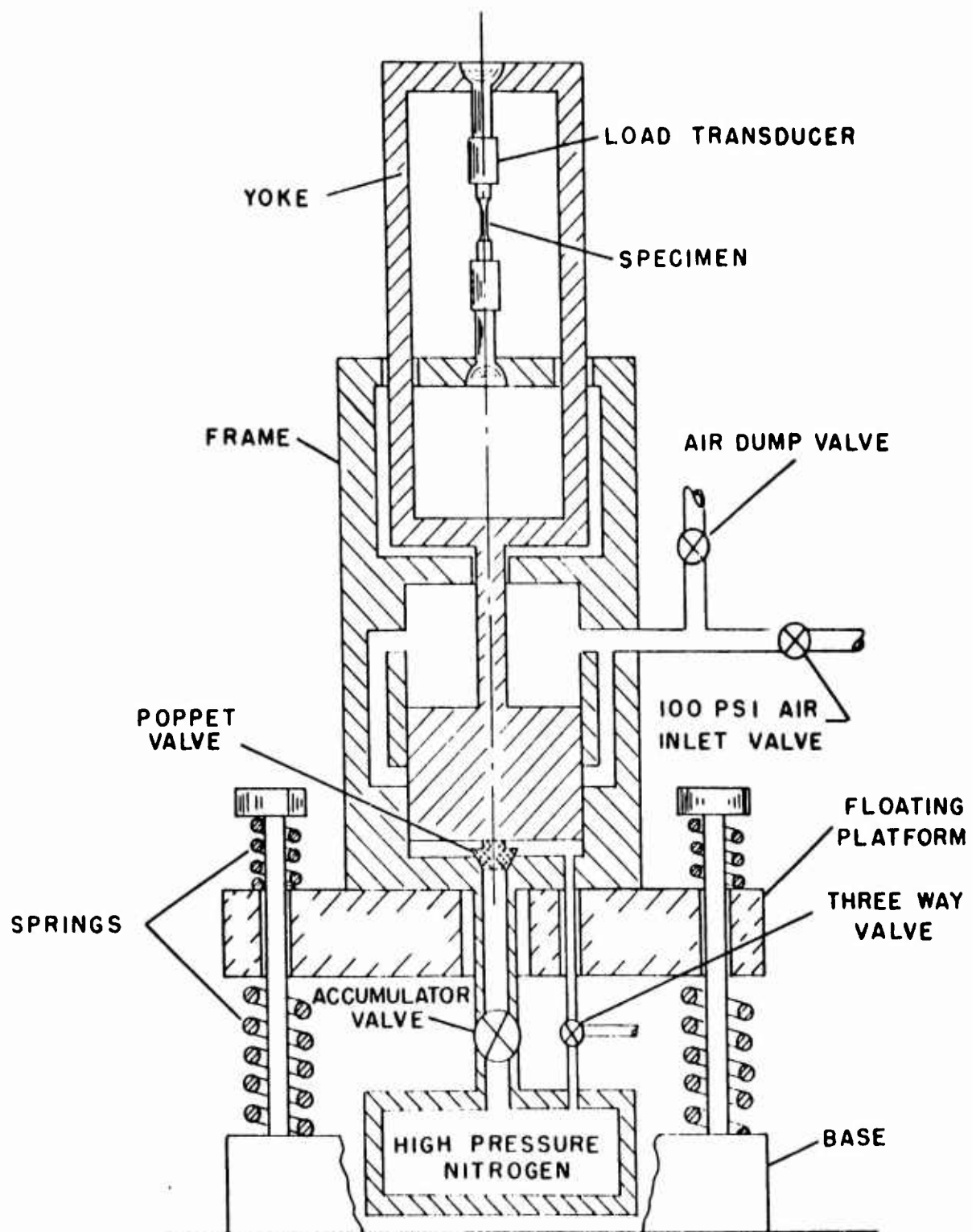


Figure 1. DIAGRAM OF THE FAST-ACTING TENSILE TESTER

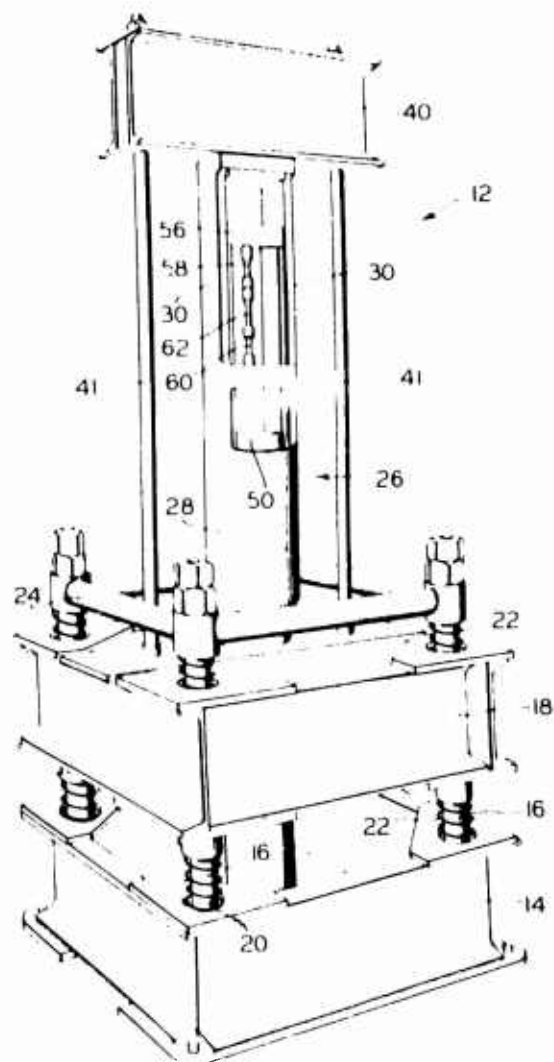


Figure 2. ORTHOGRAPHIC REPRESENTATION OF MACHINE

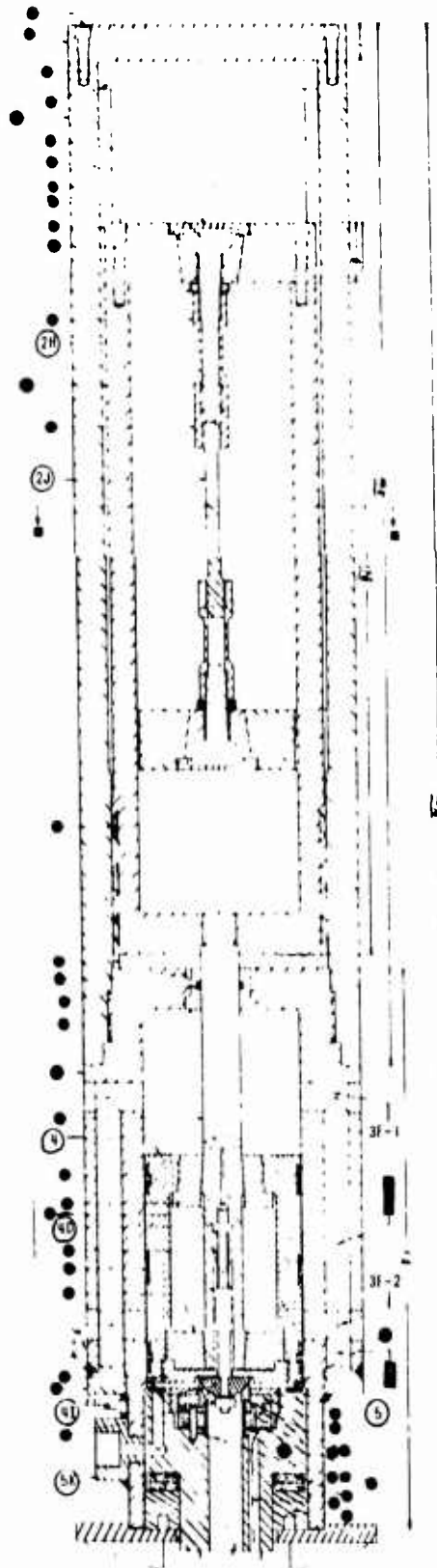


Figure 3. FAST-ACTING TENSILE TESTER

The piston is provided with a connecting rod (4A, Figure 3) having a bore into which is fitted a spring with guide rod (4D, Figure 3.) This bore also contains, slidingly, the stem of the poppet valve head (4E, Figure 3). The piston rod passes through a bushing in the cylinder head and is connected to a circular table carrying two posts (2, Figure 3) terminating in the upper platen, (2-E, Figure 3). The posts pass freely through slots in the lower platen. The platens carry accurately aligned ball and socket joints (2B, Figure 3) with stems to receive the specimen holders, (2I, Figure 3).

At the lower end of the stanchion, the cylinder is closed by a block and sealing rings shown in (5, Figure 3). Through the block runs a 1-inch diameter bore terminating in the electrically insulated valve seat (5c, Figure 3).

The stanchion rests on a platform of structural steel (18, Figure 2) and is secured thereto by two tie rods and a girder (4I and 40, Figure 2). The platform rests on springs carried by the base (14, Figure 2) and guided by four posts (16, Figure 2) which extend from the base through holes in the platform. Springs are similarly provided above the platform, and are held in place, by the railing (24, Figure 2) attached to the posts.

As a safety measure, the cylinder is covered by a 1/4-inch steel shell. All parts of the machine below the top level of the cylinder are located within a steel plate cabinet whose topside deck forms the work table of the machine. The plates are of various gages, from 1/8 to 1/4 inches, according to safety considerations. The base and carriage are welded structures of steel plate and channels, as can be seen in Figure 2. The railing and spring stops, visible above the carriage, are welded aluminum tubes.

The piston, shown in Figure 3, is aluminum alloy 7075-T6 except for the steel bushing in its topside. The yoke is of titanium alloy 6Al-4V (120,000 psi Y.S.) and weighs 25 pounds. If it were made of steel of the same strength, its weight would amount to 42 pounds. However, the higher rigidity of steel could possibly be beneficial.

#### Specimen Holders

Grips are provided for round specimens and for two types of flat test pieces, viz., with and without pin holes, respectively. An adjustable compression head and pressure transducer are available. When used, these are mounted between the lower platen and the movable table. Buffers tipped with rubber are provided for use with the pressure-head, in order to stop the table and piston assembly from appreciable motion in case a specimen should collapse.

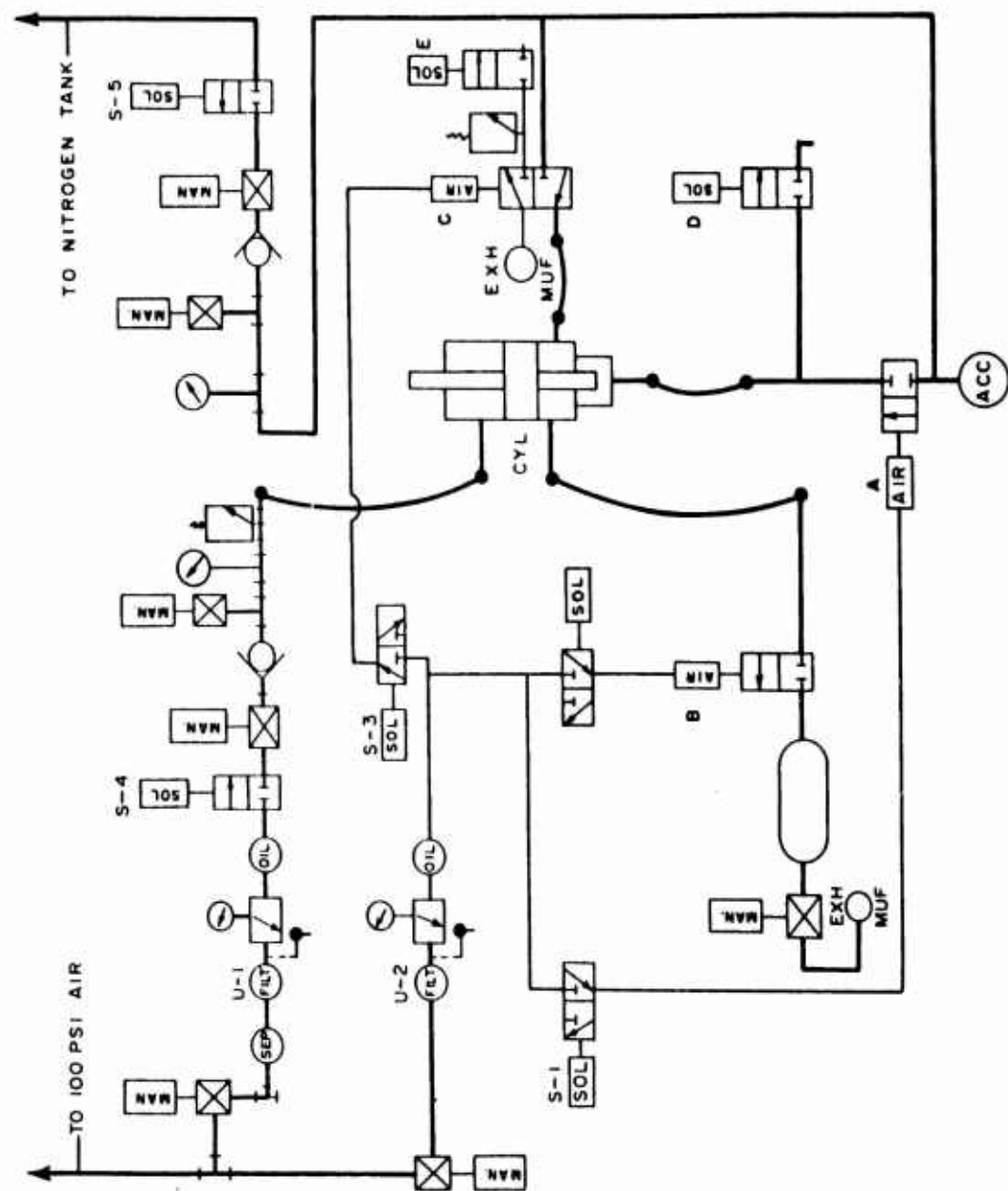


Figure 4. FUNCTIONAL DIAGRAM

Provision has also been made for hydrodynamic testing; intensifiers, with pressure manifolds for pressure gages and tubular specimens are available, but have not yet been put to use.

#### Dimensions and Weights

The net floor space required is 45.3 x 47.5 inches, not including the space required by the 9-inch diameter nitrogen cylinders. The height to the work table is 41 inches and the over-all height of the machine is 75.5 inches.

	<u>Weight of Components</u>	<u>Pounds</u>
(1) Piston and Yoke Assembly with Transducers		36
(2) Testing Machine, less (1)		262
(3) Testing Machine Proper (net)		298
(4) Carriage, including Overhead Girder and Tie Rods		402
(5) "Floating Unit (3) and (4)		700
(6) Base with Attached Accessories		600
(7) Net Weight, without Steel Cabinet		1300
(8) Steel Cabinet		400
(9) Total Floor Weight		1700

#### OPERATION OF THE TESTING MACHINE

Activated by high-pressure gas, the piston complex (Item 1 above listed) will be impelled upwards and the cylinder will recoil. In order to take this downward thrust, the cylinder is attached to a carriage which rests on springs fixed to a heavy base. The piston complex may, after the specimen is broken, possess high kinetic energy. Its motion can be stopped and reversed by a cushion of trapped gas in the cylinder head and this action impels the machine and carriage upwards. Hence, springs are provided above the carriage to take its upward thrust. The carriage thus "floats" between two sets of springs held in position by sturdy rods that pass with loose fit through holes in the carriage. Therefore, these are secured in position between the carriage and an overhead girder by means of two tie rods. This arrangement is illustrated by Figure 2.

A sectional view is shown by Figure 3 from which the functioning of the machine may be understood. Dry nitrogen gas is lead into the cylindrical space beneath the poppet valve head, designated as 4I in Figure 3. This chamber is connected through a valve to an accumulator, shown in Figures 4 and 5, which can be safely charged with nitrogen up to 1200 psi.

Ordinarily, only a small pressure under the valve head would be required to lift the piston assembly enough to let the high-pressure gas escape past the valve into the space under the cylinder and thereby impel the



piston upward. However, the slight motion of the poppet valve head required to initiate this event, is prevented by the admittance of low-pressure air through channels (3F1 in Figure 3) into the space between the cylinder head and the piston's upper face. The ratio of the areas of the piston face and the valve opening is 20:1, so that an air pressure 1/20 the nitrogen pressure is needed to balance the forces on the valve and piston. With a somewhat higher ratio of air pressure to nitrogen pressure, say 1/15, the valve will remain securely seated. The 1:15 force seating the valve may be augmented by putting the specimen under more or less initial tension.

In time, however, wear and tear will cause gas to leak past the poppet valve. Therefore, arrangement has been made to vent the space under the piston, above the valve, to the atmosphere through the fitting 5K, Figure 3, and a three-way valve connected thereto.

Upon "striking," the accumulator valve (A, Figure 4; D-998, Figure 5) opens, the air pressure above the piston is dumped through the dump valve (B, Figure 4; C-1945, Figure 5).

Thus, with the dump valve and the accumulator valves open, the force under the poppet valve increases and the force on the cylinder top decreases until the former exceeds the latter. With a tight specimen, the resisting force of the specimen may prevent the poppet valve from opening. Positive action is nevertheless assured, for now the vent of the three-way valve is automatically closed and a small stream of high pressure gas is let in under the piston, through this valve. The entrance of this gas causes the piston to move up slightly. The poppet valve stem which slides in the piston rod is depressed by a slight spring pressure (see Figure 3), but pressed upwards by the difference in pressure acting on the upper and lower faces of the poppet valve head. The latter pressure exceeds the former and the poppet valve head moves up in unison with the cylinder, thus initiating admission of the main stream of high pressure gas through the poppet valve opening.

Now, the piston assembly with the poppet valve assembly retracted as shown in Figure 6 moves upward impelled by the gas pressure, until it reaches the portholes 3F1 and 3F2, Figure 3, and moves toward their upper edges. Communication is thereby established between the accumulator and the surge tank (shown in Figures 4 and 5) so that their pressures tend to equalize. Moving past the portholes, the piston traps and compresses the gas in the upper portion of the cylinder forming thus a spring cushion that reverses the direction of motion of the piston. The entrapped gas reaches a higher pressure than that in the system generally and, through a channel in the piston rod, (104, Figure 6) it transmits pressure to the top surface

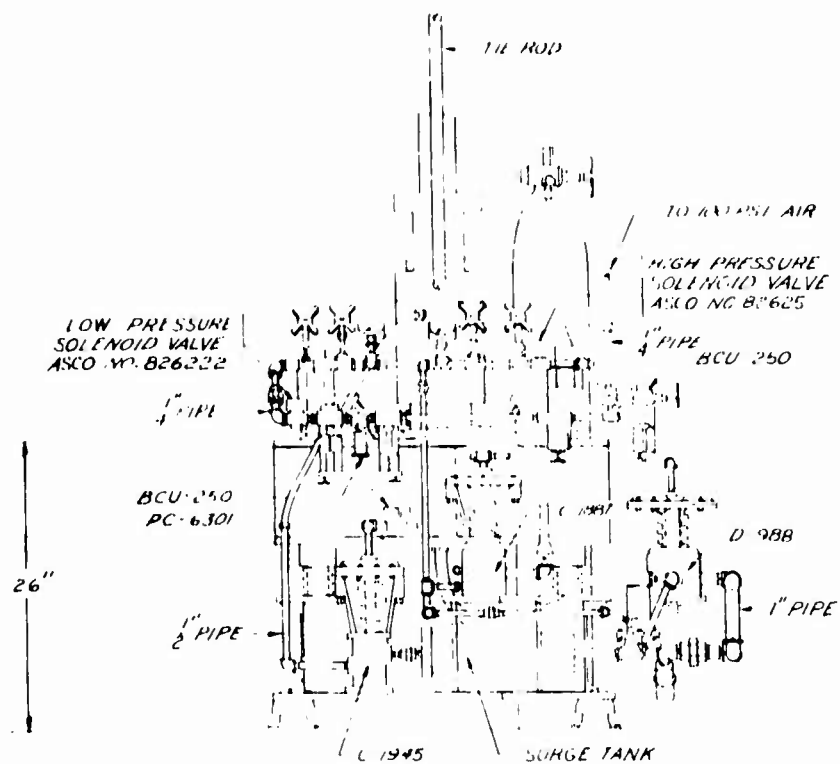


Figure 5a. ASSEMBLY, VALVES AND PIPING

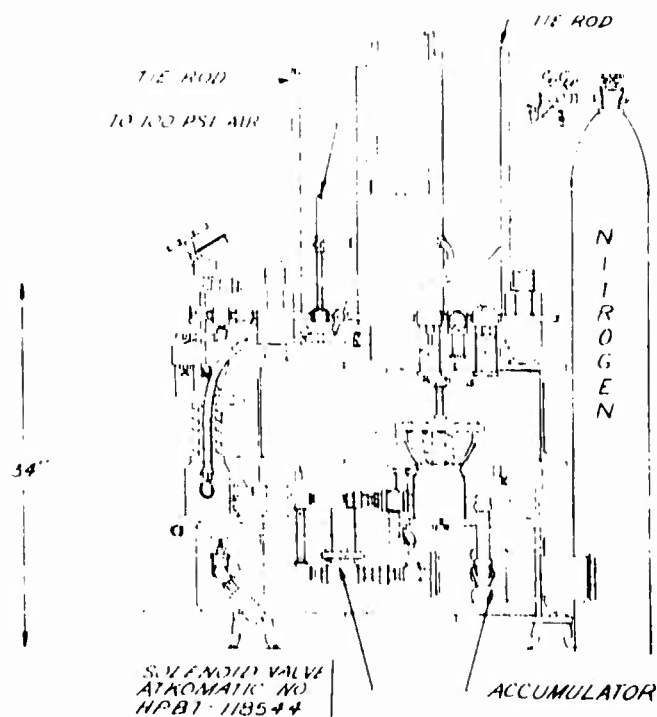


Figure 5b. ASSEMBLY, VALVES AND PIPING



of the poppet valve stem. This pressure, aided somewhat by the spring (4D of Figure 3), overcomes the inertial force between the poppet valve head and the piston, causing the poppet valve assembly to move downward to its extended position ahead of the piston as shown in Figure 7. The parts are proportioned so that the valve head becomes seated when the piston's lower face passes the portholes (3F2 of Figure 3). The gas entrapped between the piston and the closure (5 of Figure 3) aided by the spring (4D of Figure 3) keeps the valve closed and the compressed gas, acting as a spring cushion, finally reverses the motion of the piston, completing the first cycle during the upstroke of which the specimen 2J was ruptured.

A second cycle commences without active pressure in the accumulator and is followed by additional cycling until the energy of the system is reduced to zero. The damping process may be influenced by releasing more or less gas through the surge tank valve to the atmosphere.

#### LOAD AND STRAIN GAGES

The specimen to be tested (2J, Figure 3) is attached through tubular adapters (2H, Figure 3) to ball and socket joints in the crossheads. One adapter also serves as load transducer and is supplied with four SR-4 gages connected to form a complete bridge circuit. Small strains are measured by SR-4 gages attached to the specimen. Crosshead travel can be measured by means of a linear potentiometer gage or a differential transformer gage, attached to the frame, and actuated through a wiper and rod attached to the upper crosshead.

The outputs of the gages are fed into an oscilloscope triggered by a battery current through the poppet valve head and the electrically insulated valve seat. When the valve head raises from the seat, it acts as a switch, breaking the circuit, thereby energizing a thyatron which triggers the scope.

#### THE PNEUMATIC SYSTEM

A functional diagram is shown schematically in Figure 4 and a layout of the high pressure lines in Figure 5. All pressure lines, leading to and from the cylinder mounted on the floating carriage, are flexible, extra-strong braid tubing. All other high-pressure lines are extra-strong steel pipe and fittings. The high-pressure valves are rated at 6000 psi hydraulic pressure but it is recommended that their use be limited to 1500 psi gas pressure. The positions of the valves can be seen in Figure 5. For the sake of convenience, the operating valves are electrically actuated from a central switchboard.

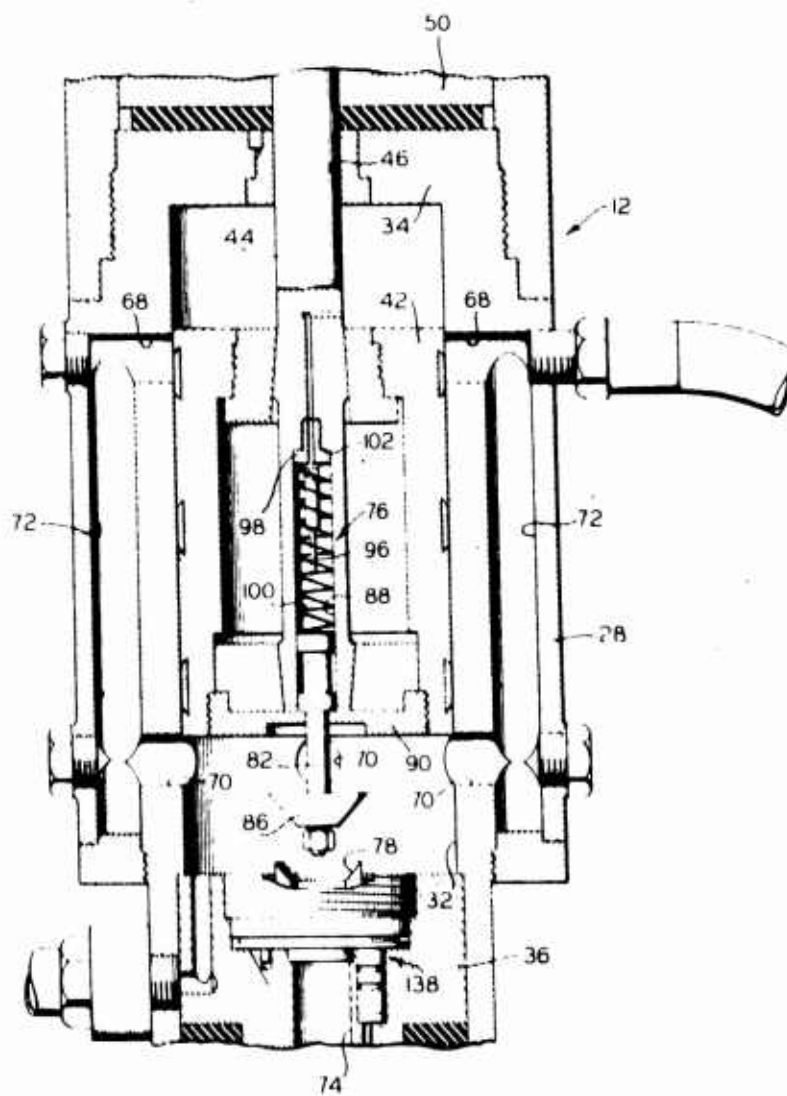


Figure 7. CYLINDER AND PISTON WITH VALVE ASSEMBLY EXTENDED

Referring to Figure 4, low-pressure air is charged into the cylinder head from a 100 psi air main. The air passes through a cleaner-pressure regulator unit before it is admitted to the cylinder through a 1/4-inch pipe and solenoid valve. This air line contains a check valve, a blow-off valve and a pressure gage (shown in Figure 4).

The nitrogen gas is supplied from a commercial tank provided with a gage and regulator. It is charged into the accumulator through a 1/4-inch pipe by means of high-pressure solenoid valve and this line also contains a check valve, blow-off valve and pressure gage. When charging, the accumulator valve A may be kept open and gas at any pressure up to about 900 psi introduced in the space under the poppet valve head. Valve A is then closed while the accumulator is being charged to any desired higher pressure, up to 1200 psi. The 900 psi limit, stated above, is determined from experience as the pressure at which the poppet valve might open prematurely.

The quantity of gas thus charged remains in the accumulator until released through the diaphragm valve A and the 1-inch flexible tubing leading to the space under the poppet valve.

At the instant of striking, the air above the piston in the cylinder head is dumped through the 1/2-inch valve B into the surge tank and then through a throttling valve and exhaust muffler to the atmosphere. The three-way valve, already referred to, which, before striking, vents the space in the cylinder under the piston and, during striking, injects high-pressure gas into this space, is a 1/2-inch diaphragm valve designated C, in Figure 4. The vent line from valve C contains a safety valve and also a 1/8-inch solenoid valve E used only when prestressing a specimen. The valve D is a 1/2-inch valve which is used mainly for quick pressure release when called for. All valves are normally closed and will open and remain open only when energized. The three diaphragm valves are actuated by low-pressure air from the main. The auxiliary air line leads through a cleaner-regulator unit into three 1/4-inch branch lines. Each branch contains a solenoid pilot valve which, upon opening, supplies air at 35 psi to activate its master diaphragm valve. It should be noted that valves A, B and C are comparatively slow acting. The fast action of the machine depends upon the poppet valve which functions suddenly, only after the slower valves have passed gases enough to create excess pressure under the piston. Thereafter, these valves sustain the pressure difference. Adequate functioning of the machine requires that all joints in the pneumatic system are tight.

Figure 8 illustrates the main seal arranged according to P. W. Bridgman's principle of the unsupported area. The figure also shows the seals required

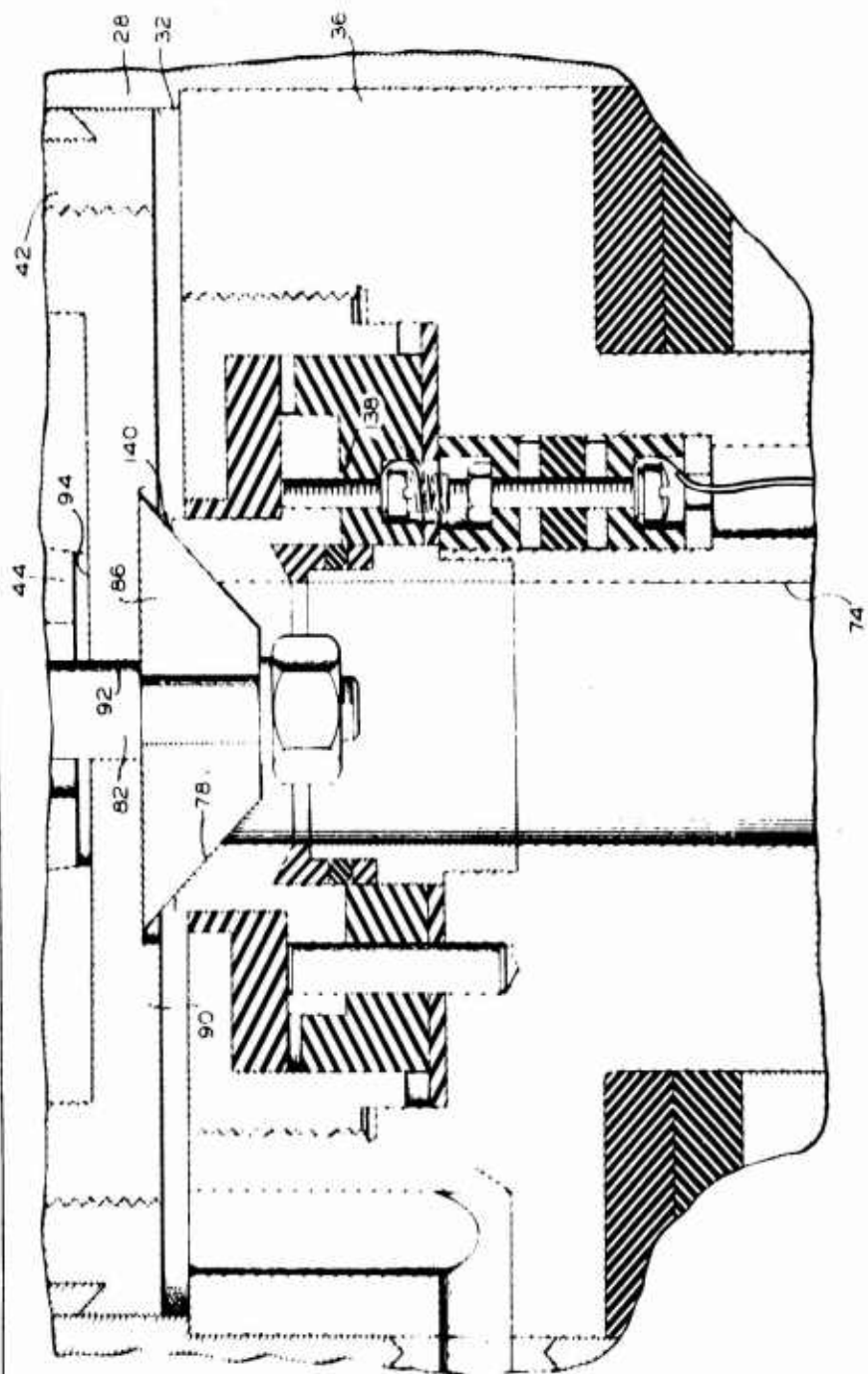


Figure 8. HIGH PRESSURE SEALS

for the insulated valve seat and its electric lead wire, likewise according to Bridgman. The bushing for the piston rod is provided with a rod seal and the piston contains two piston seals as shown in Figure 3.

### SWITCHING SEQUENCES

The electric wires from the solenoids are brought into a switch box situated on the deck of the machine. The solenoids on the charging valves, S-4 and S-5, are connected to individual switches on the panel of the switch box. All three solenoids, S-1, S-2, and S-3, in the auxiliary air lines that operate the diaphragm valves are wired to a compound, rotary switch as well as to push buttons on the switch box panel. There is also a main power push button switch.

By turning the knob, with the power supply off, the rotary switch may be set at position II at which all solenoid circuits, except D, are closed. Closing the power supply switch thereupon energizes the solenoids and opens the valves. The switching schedule is shown in Figure 9.

Valve A opens and admits high-pressure nitrogen under the poppet valve. Simultaneously, both the valves B and C open. With these valves open, as already described, the air in the cylinder head is vented, the gas vent from the cylinder bottom closes and high-pressure gas enters under the piston driving it, and the yoke to which it is attached, upward. A pre-load can be put on a specimen by tightening the grip adapter and by pre-charging gas directly under the piston by manipulating the auxiliary switch Ia which controls valves C and E. When it is desired to dump the pressure above the Valve A in order to limit the duration of a pressure impulse, the rotary switch setting will proceed as from position II to III, thereby closing A and C while opening D. Experience shows that for short impulses this operation requires an electronic timing device, which presently is under study.

Various loading rates may be obtained by varying the pressures and judiciously operating the switches. More direct means for control of speed are, however, being studied.

### TESTS ON DAMPING AND ON VIBRATIONS OF THE MACHINE

By use of the machine for tensile and for compressive testing, the lower platen is struck by a force reacting to the load on the specimen.

When a specimen is to be struck without being fractured as is often the case in compression and in multiple blow tensile testing, the piston complex immediately comes to a stop while the energy employed is dissipated



LEVER SWITCH

1 2 3

	1	2	3
C		V	
E	V	V	

FAST ACTING TENSILE TESTER ROTARY SWITCH				
	O	I	II	III
ON OFF A			V	
ON OFF B			V	
C		I <sub>a</sub>	V	
ON OFF D				V
E		V	I <sub>a</sub>	V

V — DENOTES CLOSED CIRCUIT

NO V — DENOTES OPEN CIRCUIT

Figure 9. SWITCHING SEQUENCES

through the specimen and machine.

But, when rupture occurs in tension of specimens having high strength and low ductility, the piston may travel an additional 3/4-inch or so under high gas pressure and thus acquire say, 250 Ft. Lb. of kinetic energy. This energy could deliver a disturbingly severe blow to vital components, if it were not dissipated gradually. This is done, as already explained, by rapidly damped oscillations of the piston complex. Figure 10 illustrates this by photographic oscilloscope traces of piston travel versus time; these were obtained while running the machine without a specimen in the grips. The maximum speed shown here is 25 Ft. per second corresponding to a kinetic energy,  $\frac{1}{2} m v^2 = 250 \text{ Ft Lb.}$

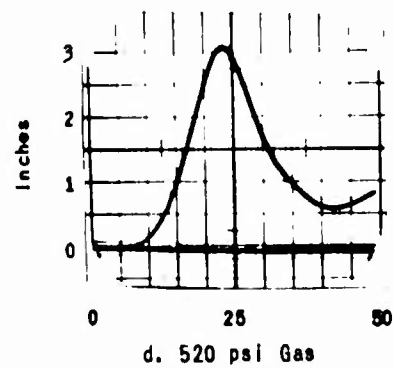
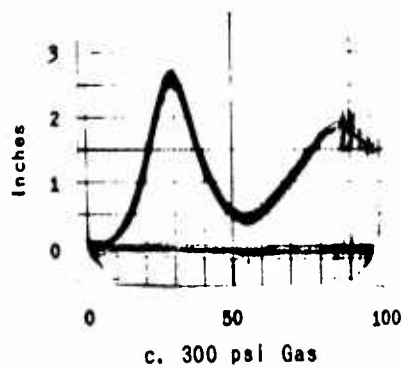
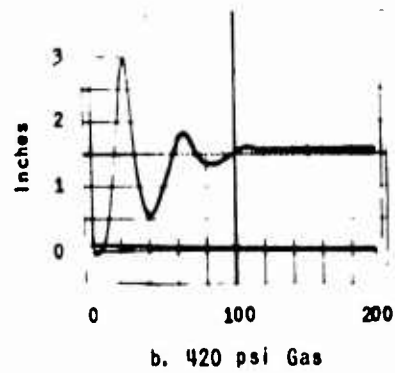
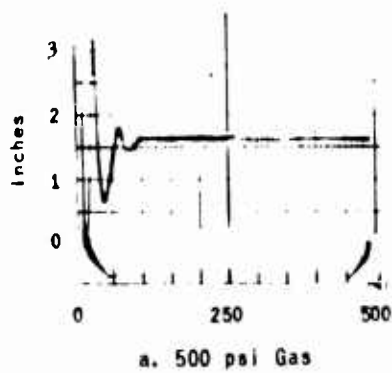
The vibrations which occurred under similar circumstances were registered by an accelerometer attached to the stanchion and recorded as oscilloscope traces of acceleration versus time. These are illustrated by Figure 11. The recorded maximum is 5G's.

In Figure 12 are shown the traces of vibrations occurring during compression testing of a plastic specimen. In this case the accelerometer was affixed to the frame well above the lower platen. The maximum acceleration shown here is 6 G's.

Some materials will collapse during compression; in such an event, the piston complex must immediately be prevented from proceeding under pressure and gaining excessive momentum. This is done by placing suitable buffers adjacent to the pressure head. These, in suddenly stopping the motion transmit the force acting on the piston through the lower platen to the frame. Severe vibrations in the machine may arise therefrom. Some oscilloscope traces of such vibrations may be seen in Figure 13 to reach 18G's. Such, rather excessive, accelerations are preventable by use of suitable buffers and careful avoidance of higher loads than necessary for the purpose at hand.

#### SOME DYNAMIC TESTING OF MATERIALS AT WATERTOWN ARSENAL LABORATORIES

The Fast-Acting Tensile Tester has been used on Research and development projects for tensile testing of alloys at temperatures ranging from -65°F to +170°F; multiple blow tests have been made on notched specimens at room temperature; compression tests on metallic and on plastic specimens at room temperature have also been done.



NOTE: The units of the abscissas are milliseconds

Figure 10. OSCILLOSCOPE TRACES OF CROSSHEAD TRAVEL

FAST ACTING TENSILE TESTER  
WATERTOWN ARSENAL LABORATORIES

19-066-1159/ORD-61

SPECIMEN: NONE. FREE RUN BETWEEN AIR PILLOWS; ACCELEROMETER  
CLAMPED TO LOWER PLATEN

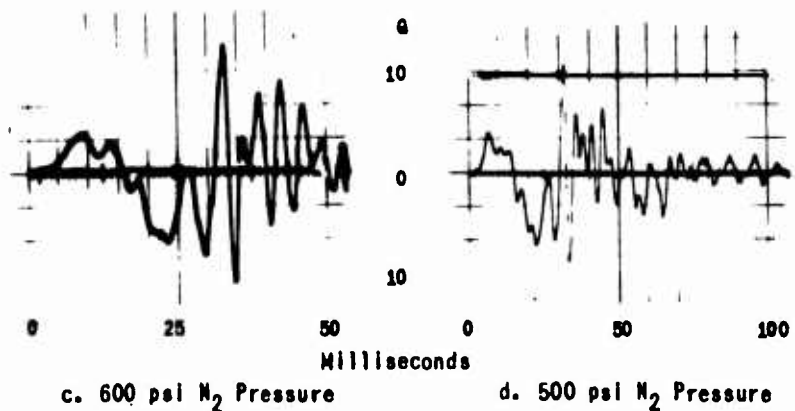
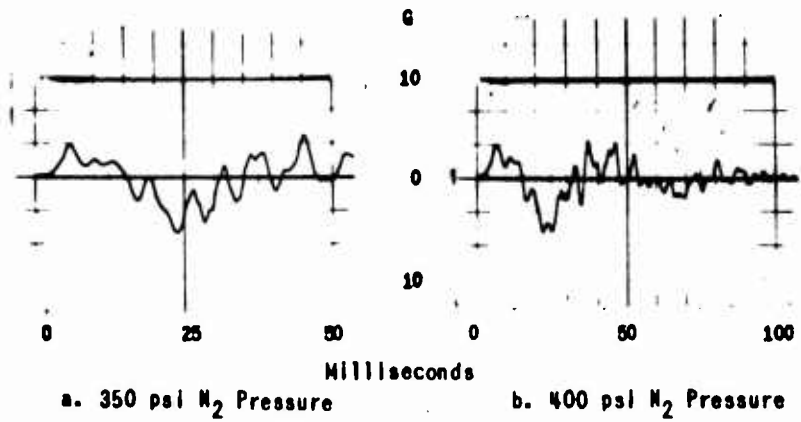
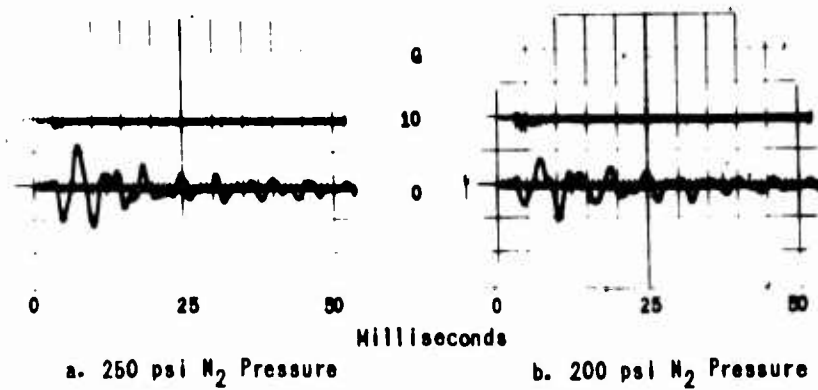


Figure 11. OSCILLOSCOPE TRACES OF VIBRATIONS

FAST ACTING TENSILE TESTER  
WATERTOWN ARSENAL LABORATORIES

19-088-1307/ORD-82

SPECIMEN: EPOXY, NEMA GR.10, REINFORCED GLASS (E-7).  
ACCELEROMETER ON FRAME; CLAMPED ON TOP OF LDT FIXTURE



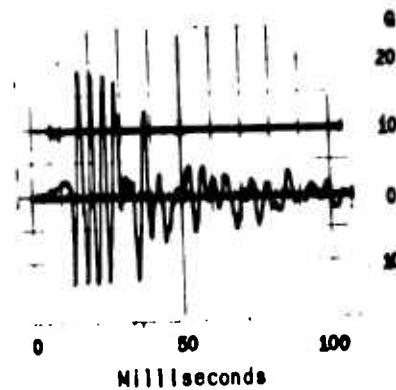
Specimens disintegrated after about one second

Figure 12. OSCILLOSCOPE TRACES OF VIBRATIONS

FAST ACTING TENSILE TESTER  
WATERTOWN ARSENAL LABORATORIES

19-086-1308/ORD-62

SPECIMEN: NONE. STOPS ON TABLE, UNDER LOWER PLATEN.  
ACCELEROMETER ON FRAME CLAMPED TO TOP OF LTD FIXTURE

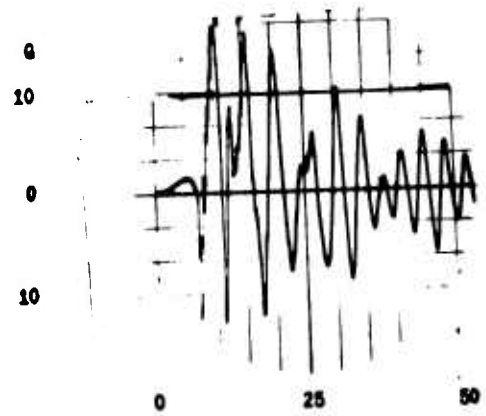


a. 250 psi  $N_2$  Pressure

SPECIMEN: NONE. STOPS ON TABLE, UNDER LOWER PLATEN.  
ACCELEROMETER CLAMPED ON LOWER PLATEN



b. 200 psi  $N_2$  Pressure



c. 250 psi  $N_2$  Pressure

Figure 13. OSCILLOSCOPE TRACES OF VIBRATIONS

FAST ACTING TENSILE TESTER  
WATERTOWN ARSENAL LABORATORIES

19-066-1309/ORD-62

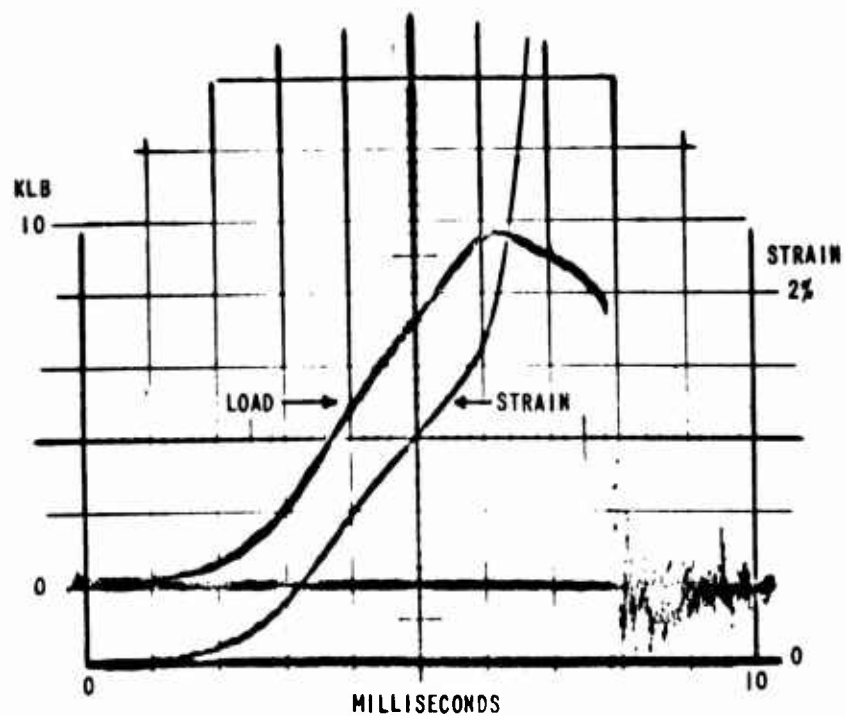
Typical traces of tensile load and strain versus time in a uranium alloy can be seen in Figure 14; a shows strain as in/in, while b shows cross-head distance; two scopes were used in tandem. This distance can often be used to calculate an approximate strain before maximum load is reached, taking into consideration that the total extension of the whole specimen is involved. This, of course, contrasts with the strain measured over a 0.25-inch length at the middle of the specimen as shown in a. It is noted in b that the crosshead speed is nearly uniform until after maximum load has been reached; this indicates that the speed is virtually unchanged during general and local extension of the specimen. Consequently, the true strain takes off at the very high rate observable in a during localized extension. It is not until the specimen, in breaking, releases its load, that the cross-head speeds up; this is quite apparent in b. Sometimes a specimen will break while the load is on the increase; this is shown for a notched specimen in Figure 15. The hash seen on the load baselines indicates shaking of the transducer as its load is abruptly released during fracture of the specimen.

Figure 16 is another instance of using two scopes in tandem. The picture at the left shows that the strain gage failed at 0.85% strain. To the right the LDT trace shows how the piston complex is momentarily retarded near the maximum load and accelerates at fracture. The gap in the trace indicates merely that the active core went beyond the cylinder of the LDT. The low load trace after fracture indicates that the base line was set at a small preload.

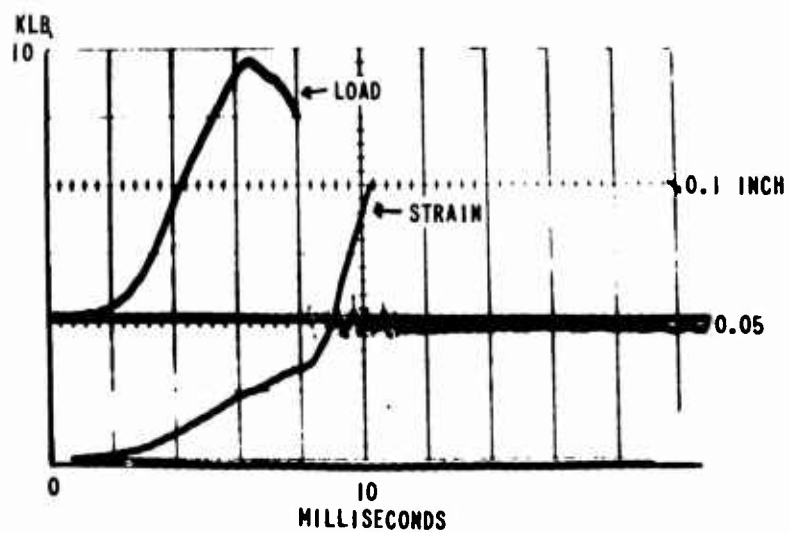
In order to obtain stress-strain curves from the load-strain-time diagrams, the films were put into a photoenlarger and the traces projected onto suitable coordinate paper so that they could be traced off in pencil. The coordinates were supplied with scalars representing stress and strain. From these diagrams crossplots of stress versus strain were finally made. An example of this from the trace in Figure 14a is given in Figure 17. This process is rather cumbersome.

When no especial interest is attached to individual variations of stress and strain with time, x-y records of stress versus strain can be made. A comparison of the two types of records are shown in Figure 18a and b, which were obtained on a uranium alloy, at  $-65^{\circ}\text{F}$ , using two scopes in tandem. Figure 18c and d show stress-strain traces supplied with timing indications; the specimens were cut from the uranium alloy and were tested at  $72^{\circ}\text{F}$  and  $-20^{\circ}\text{F}$ , respectively.

Examples of repeated tensile loading tests are shown in Figure 19 which gives traces of load versus time taken on notched specimens of titanium alloy.



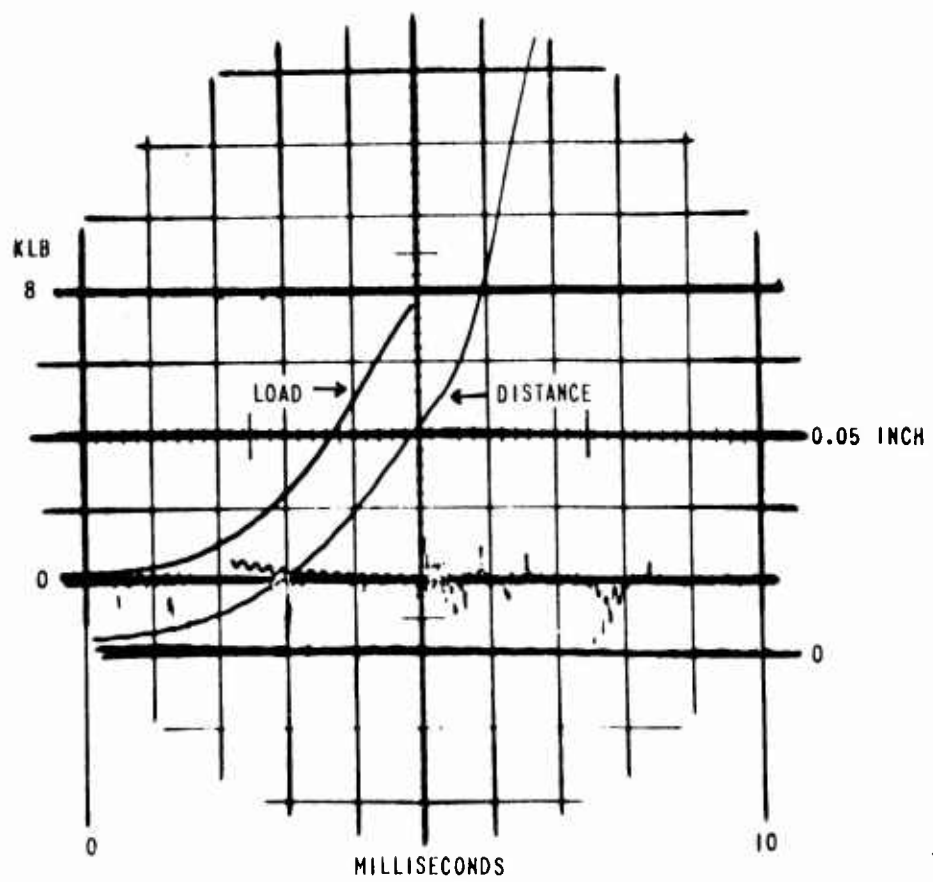
a. LOAD AND STRAIN VERSUS TIME



b. LOAD AND HEAD TRAVEL VERSUS TIME

Figure 14. OSCILLOSCOPE TRACES

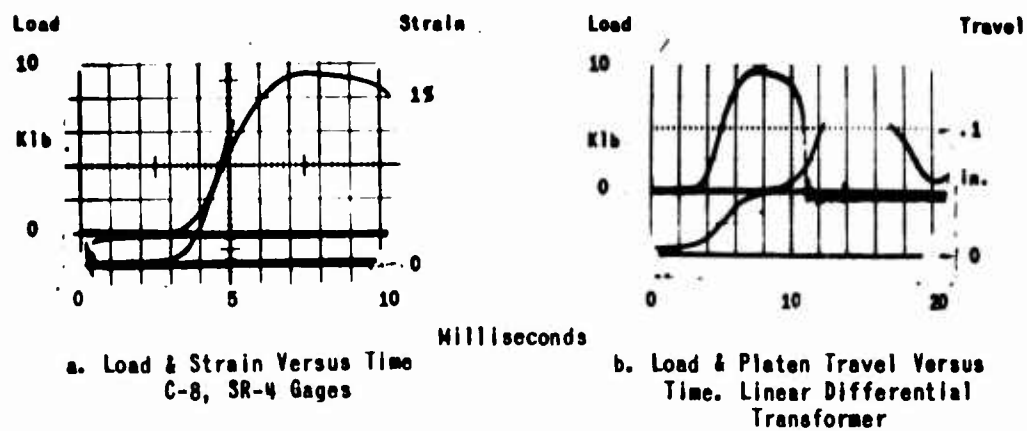




NOTCHED SPECIMEN

Figure 15. OSCILLOSCOPE TRACES OF LOAD AND HEAD TRAVEL  
VERSUS TIME

SPECIMEN: 3E, T-7; 72°F



Dumont Dual Beam & Tektronix Dual Beam Scopes in Tandem

Figure 16. OSCILLOSCOPE TRACES

FAST ACTING TENSILE TESTER  
WATERTOWN ARSENAL LABORATORIES

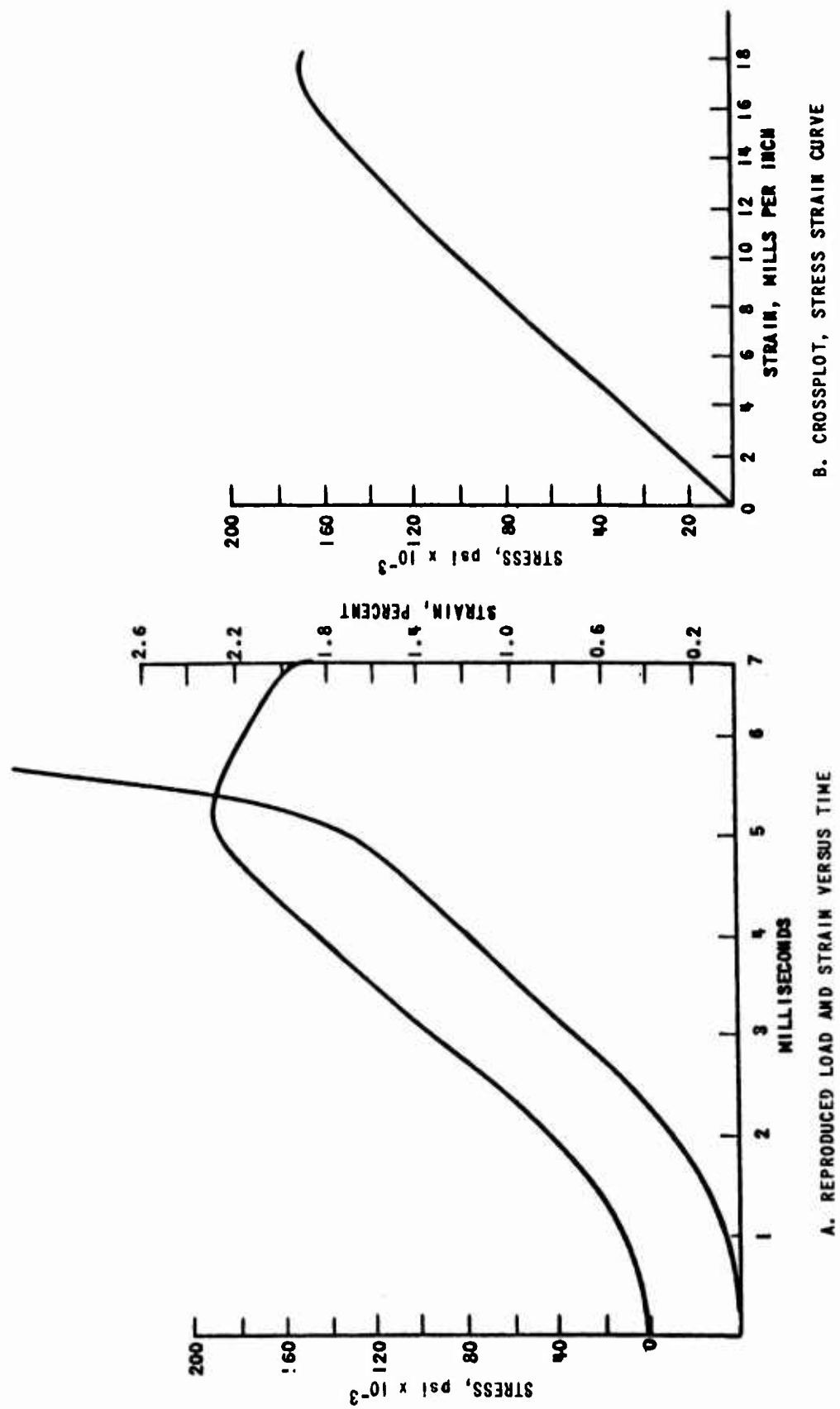
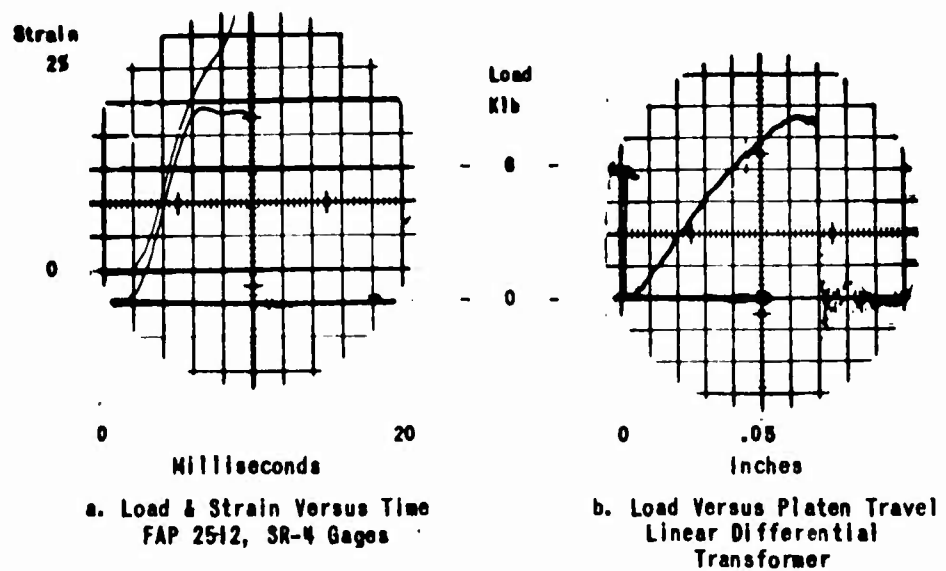
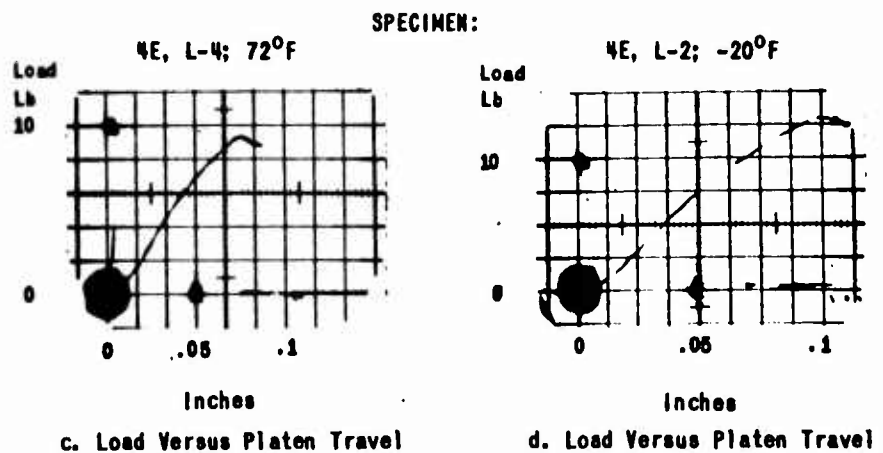


Figure 17. STRESS STRAIN TIME DIAGRAM

SPECIMEN: E3, L-11; -65°F



Dumont Dual Beam & Tektronix Dual Beam Scopes in Tandem

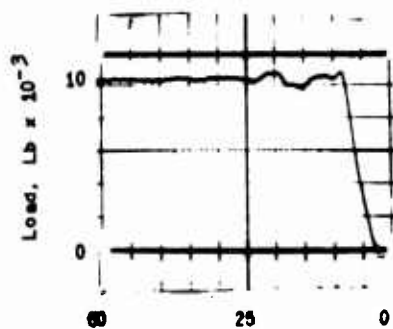


Linear Differential Transformer, Dumont Scope

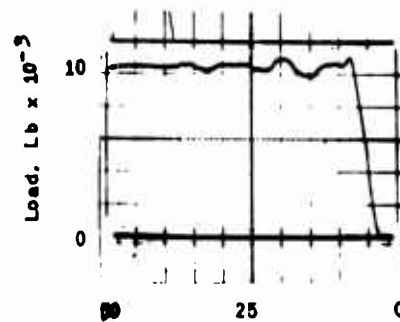
Timing: 1 millisecond per dash

Figure 18. OSCILLOSCOPE TRACES

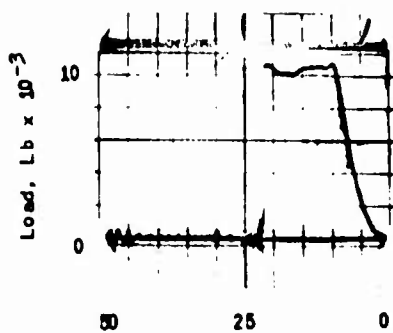
FAST ACTING TENSILE TESTER  
WATERTOWN ARSENAL LABORATORIES



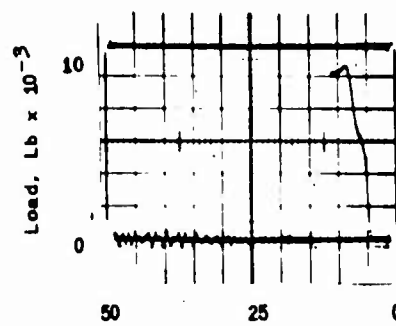
a. Spec. 13, 5th Cycle



b. Spec. 13, 6th Cycle



c. Spec. 11, 35th Cycle  
Fracture



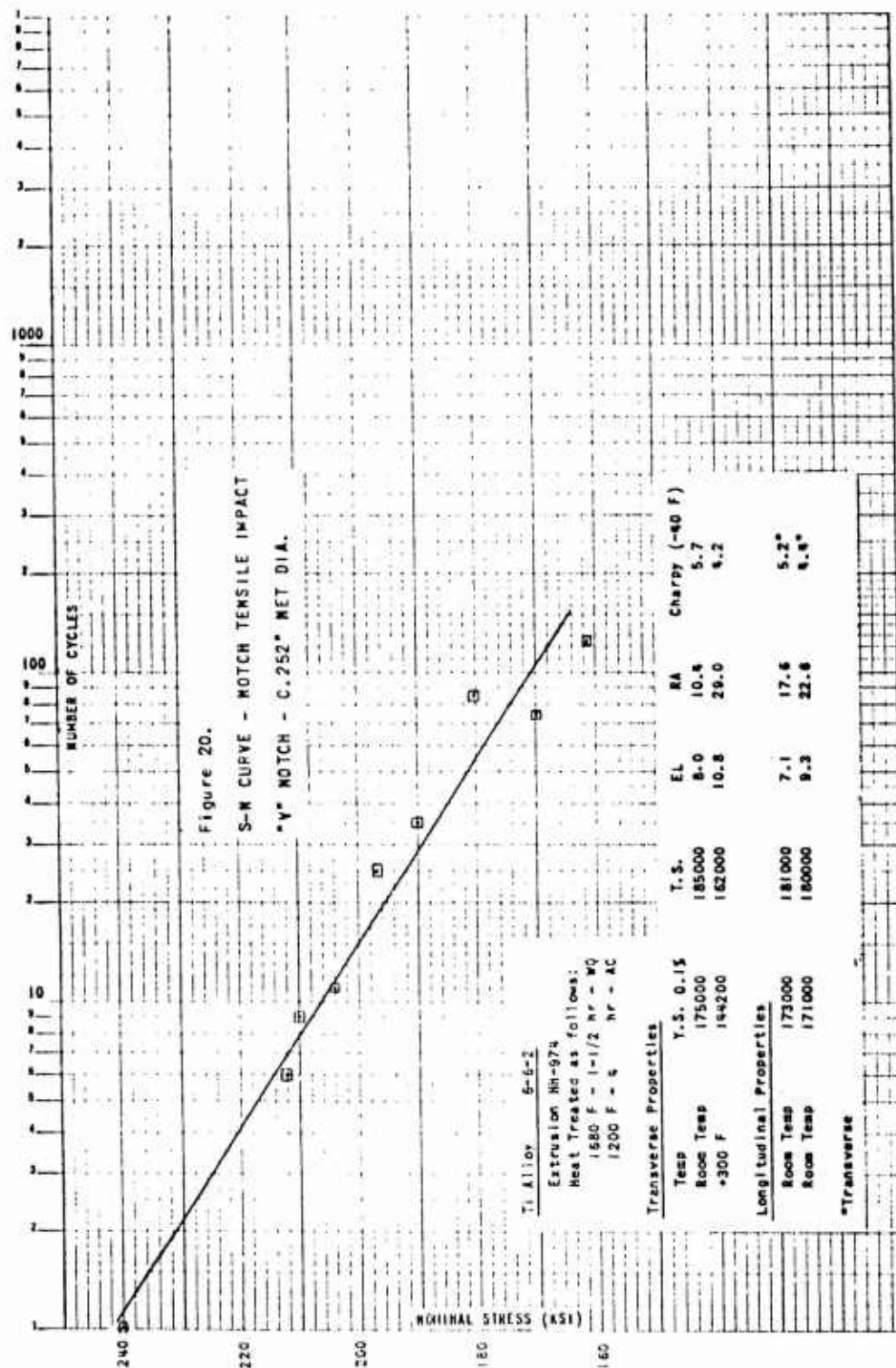
d. Spec. 16, 9th Cycle  
Fracture

NOTE: The units of abscissas are milliseconds

Figure 19. OSCILLOSCOPE TRACES OF REPEATED LOADING TESTS

FAST ACTING TENSILE TESTER  
WATERTOWN ARSENAL LABORATORIES

19-066-1159/ORD-61



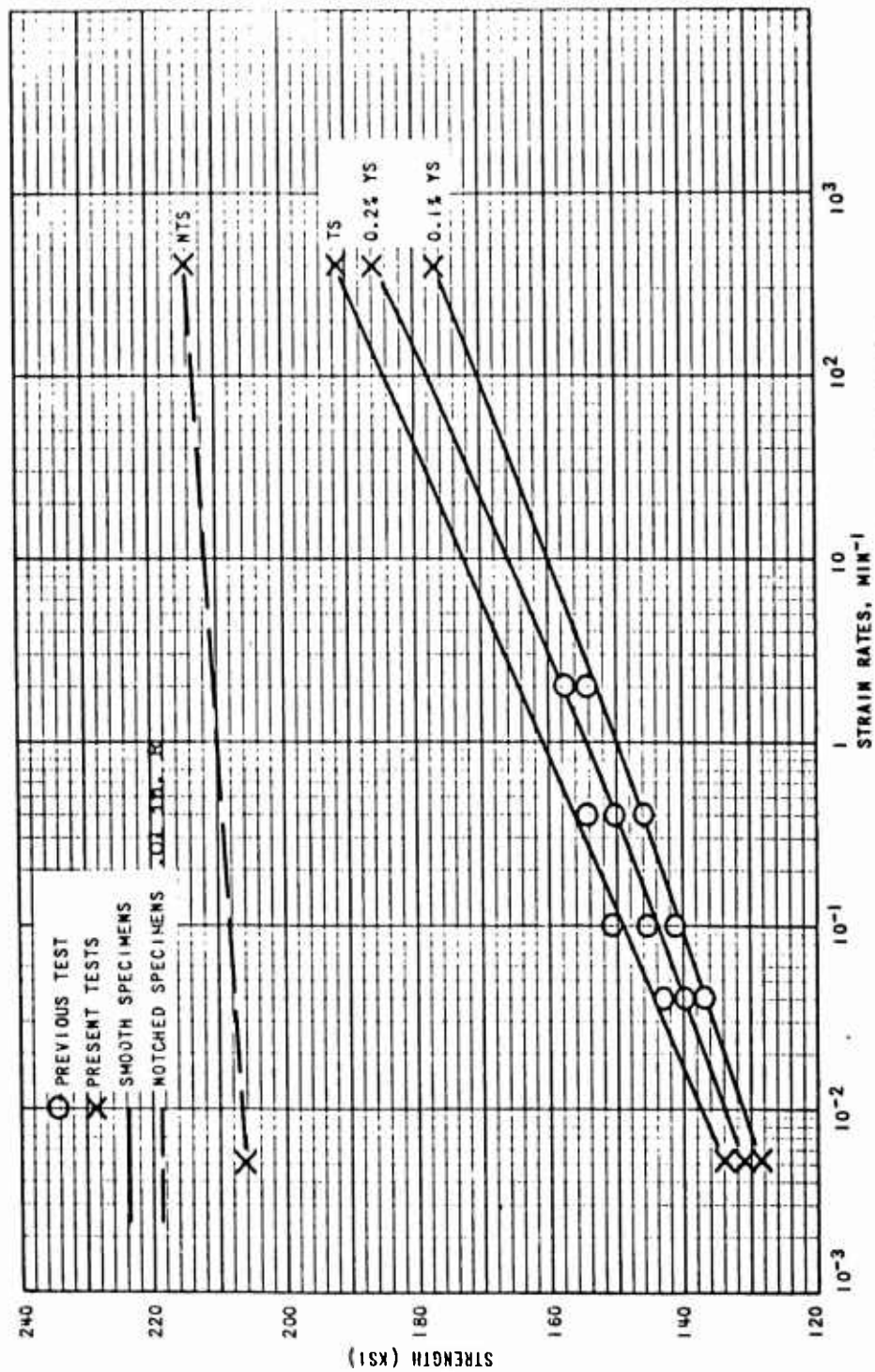
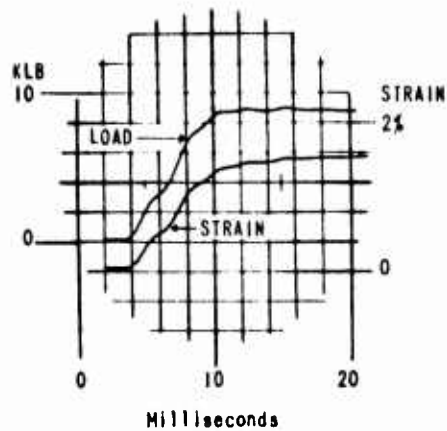
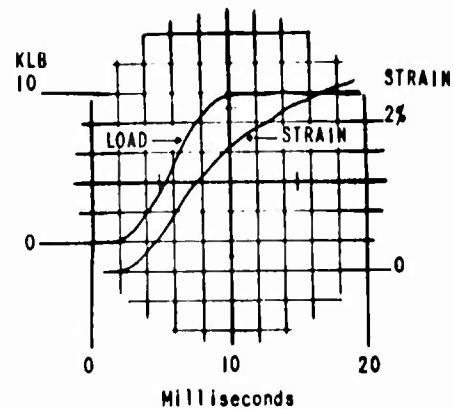


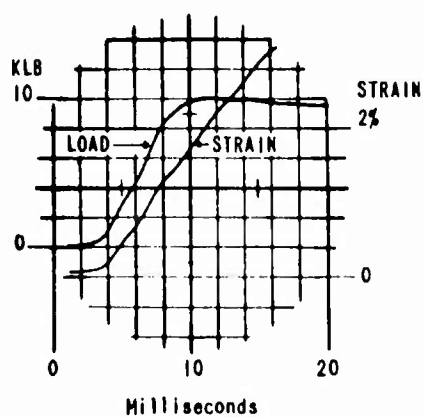
Figure 21. STRENGTHS VERSUS STRAIN RATES, 70 F



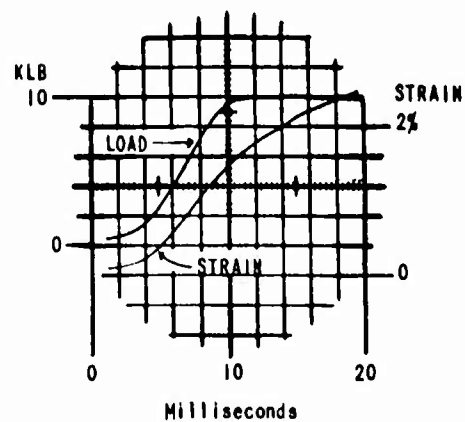
a. SPECIMEN CL-3



b. SPECIMEN CL-4



c. SPECIMEN CL-5



d. SPECIMEN CL-6

Figure 22. OSCILLOGRAMS. LOAD AND STRAIN  
VERSUS TIME, COMPRESSION.

FAST ACTING TENSILE TESTER  
WATERTOWN ARSENAL LABORATORIES



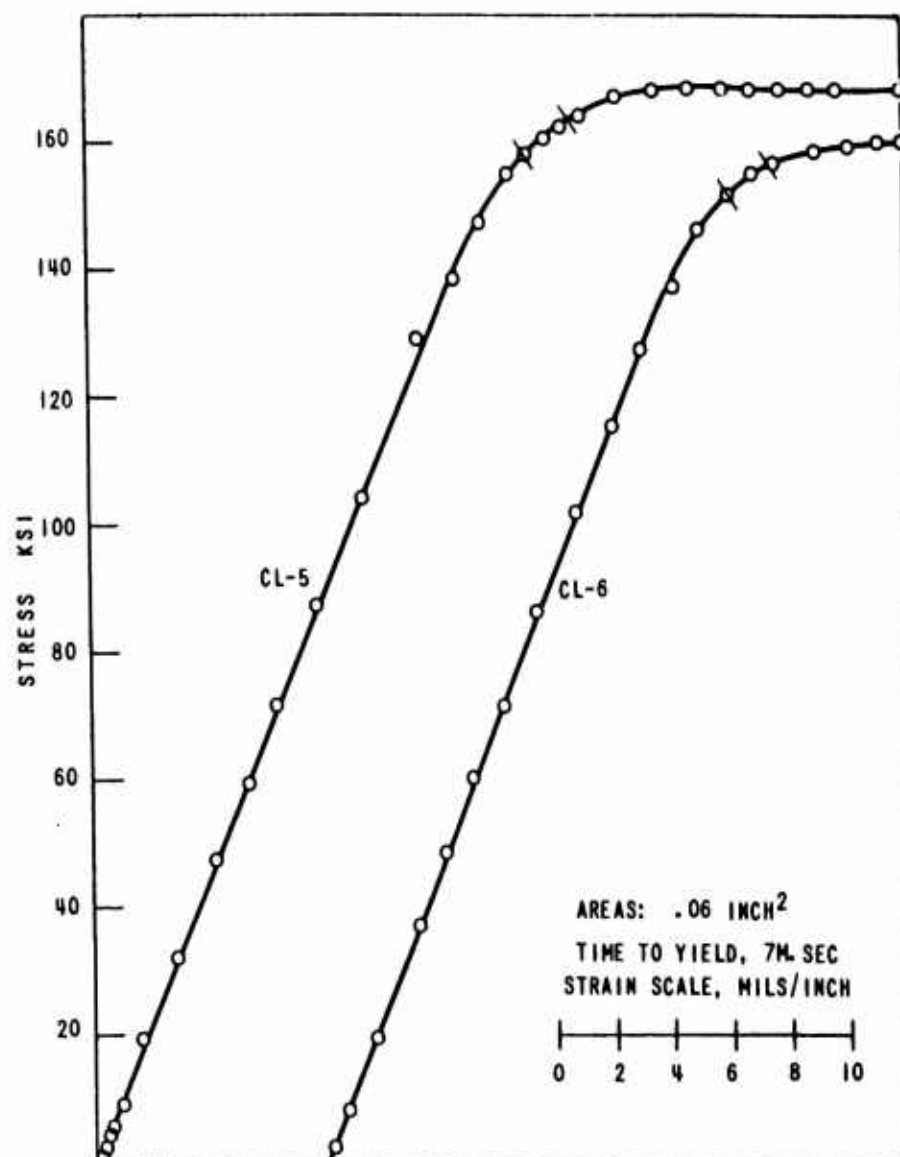


Figure 23. STRESS STRAIN CURVES, COMPRESSION, DYNAMIC

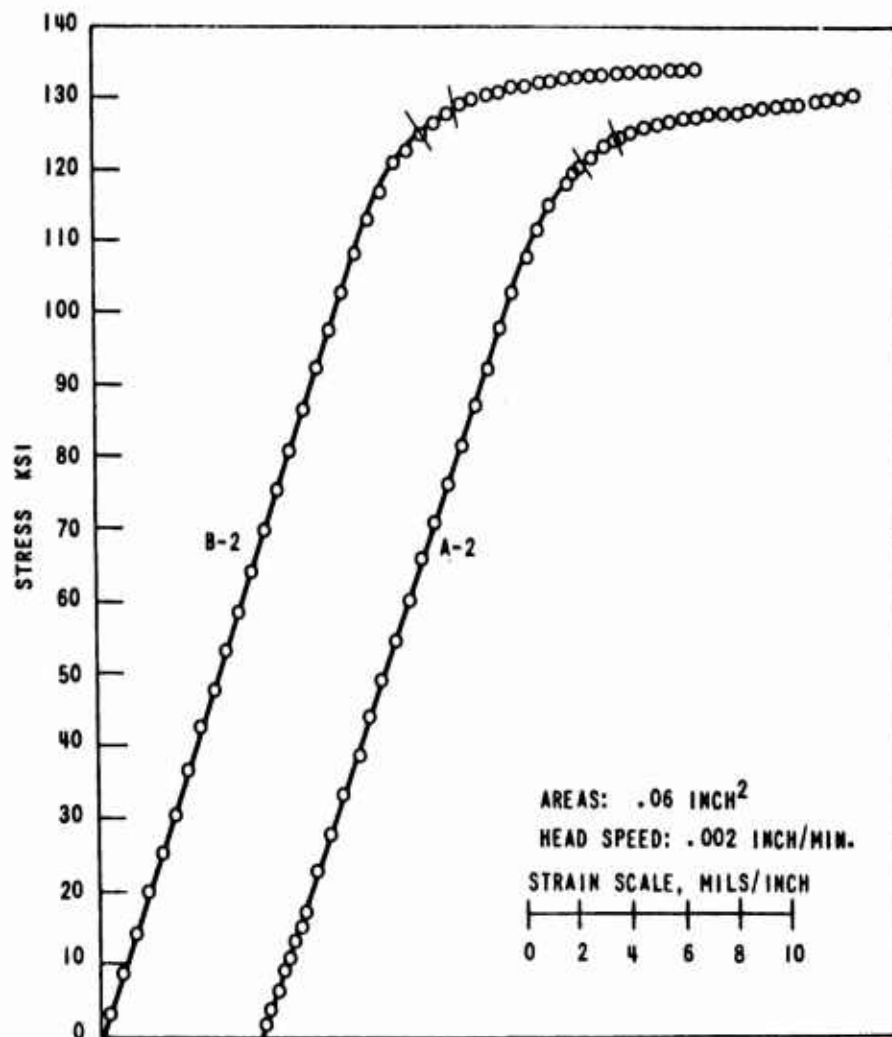


Figure 24. STRESS STRAIN CURVES, COMPRESSION, STATIC

It can be seen from Figure 20 that the number of strikes (cycles) required to break the specimens increased from 1 at 240 KSI to 126 at 161 KSI.

Another example of the kind of information obtained is given in Figure 21. This shows how the strength of a uranium alloy at room temperature increased as the strain rates were increased, both on smooth and on notched specimens. Similar graphs for  $-20^{\circ}\text{F}$  and  $-65^{\circ}\text{F}$  show quite different variations and taken together these graphs give important information of the effect of notches and stress concentration on the over-all load carrying ability of alloys. Lack of space permits no further discussion of this, but reference is made to (T-5096 Aft Joint, Sections III, V, VIII, WAL June 1962.) A number of compression tests have been made on the uranium alloy and on various plastics materials. Examples of the traces obtained are given in Figure 22 which represents the alloy. The dynamic stress-strain diagrams obtained from Figure 22c and d are shown in Figure 23, and the corresponding quasi-static stress-strain curve is shown in Figure 24.

The examples with illustrations, given above will indicate the working and capability of our Fast-Acting Tensile Tester to accomplish one phase of the investigation of dynamic properties of materials at Watertown Arsenal Laboratories.

#### ACKNOWLEDGEMENT

The building of this machine is, of course, a cooperative undertaking and the author wishes to express his sincere appreciation to all the Watertown Arsenal Laboratories' employees who contributed or assisted in its design and manufacture and the preparation of this paper. For some of the drawings we are indebted to Springfield Armory.

#### REFERENCES

1. Mann, H. C., High Velocity Tension Impact Tests, ASTM Proceedings, v. 36, 1936 p. 85.
2. Austin, A. Leroy, and Steidel, Robert F., A Method for Determining the Tensile Properties of Metals at High Rates of Strain, the Society of Experimental Stress Analysis. Paper No. 514.

## DISCUSSION

Questioner: How much does this machine cost?

Dr. Andersen: That is an engineering question. As you know, an engineer is a person who can produce a machine at lower cost than his competitors. I should say that this machine has been used for many purposes. It is not only the building of the machine that figures in the cost but all the little side issues we have been able to do and frankly, they have never shown me the cost of these items. I don't think they would be excessive but to answer your question, I do believe you could build this machine for \$20,000.

# A NEW CONCEPT FOR STUDYING PRESSURE VESSEL CONFIGURATIONS UNDER HIGH PRESSURES AND LOADING RATES

T. E. Davidson\* and D. P. Kendall\*\*

## ABSTRACT

This paper discusses the design and operation of a newly developed testing system for hydrodynamically producing pressures up to 50,000 psi in full scale pressure vessel configurations. Rise times of 3 milliseconds can be obtained in large vessels and considerably shorter rise times are possible in smaller vessels.

Two existing systems are described and an analytical method of determining the pressure-time response for any similar system is presented. Several experimental pressure-time curves are shown and compared with the computed curves.

The possibility of using such a system as a basis for a high strain rate tensile testing machine is discussed.

## LIST OF SYMBOLS

$M$  = mass of fluid, lb mass  
 $V$  = volume, cu in.  
 $L$  = length of each feed pipe, in.  
 $A$  = cross sectional area, sq in.  
 $P$  = pressure, psi  
 $d$  = average weight density of fluid, lb per cu in.  
 $\rho$  = mass density of fluid, lb mass per cu in.  
 $\rho_0$  = mass density at zero pressure  
 $f$  = friction factor

---

\* T. E. Davidson, Chief of Physical and Mechanical Metallurgy Laboratory, Watervliet Arsenal, Watervliet, New York.

\*\* D. P. Kendall, Project Engineer in Physical and Mechanical Metallurgy Laboratory, Watervliet Arsenal, Watervliet, New York.

$v$  = velocity of fluid in pipe, in. per sec  
 $D$  = inside diameter of pipe, in.  
 $C$  = constant, cu in. per psi  
 $F$  = velocity loss coefficient, psi sec<sup>2</sup> per in.<sup>2</sup>  
 $g$  = acceleration due to gravity, in. per sec<sup>2</sup>  
 $t$  = time from opening of feed valve, sec  
 $k$  = compressibility of fluid, sq in. per lb  
 $( )s$  = specimen  
 $( )v$  = valve  
 $( )a$  = accumulator  
 $( )p$  = pipes  
 $( )o$  = initial condition

## INTRODUCTION

It is often desirable, and in some cases necessary, to evaluate design parameters, study materials, and determine the operational characteristics of components in the laboratory under simulated service conditions. The desirability of such a procedure increases with the complexity of the component and/or the extremeness of the service conditions where accurate theoretical solutions are impractical. This report discusses the design and functioning of a hydrodynamic pressure system capable of producing internal pressures in a wide variety of pressure vessels. Pressures up to 50,000 psi can be produced in less than 3 milliseconds. The original intent of this system was to simulate the pressure and pressure rise time in cannon type weapons, thus permitting the laboratory evaluation of the dynamic stress conditions, strength, and low cycle fatigue life characteristics of components and materials associated with new weapon concepts without the high expense of actual firing. This type of system, however, lends itself to a wide variety of studies into the dynamic stress-strain conditions and fatigue characteristics of pressure vessel type configurations subjected to high loading rates and high pressure.

A system for producing high loading rates in pressure vessels must consist of two basic segments; a means for storing the required amount of energy and a means for rapidly releasing this energy and transferring it to the interior of the specimen. The following three basic methods for the storing of energy were considered:

1. a moving mass, accelerated by a prime mover and/or gravity, which has the advantage of being capable of high cyclic loading rates;
2. gas charged accumulator which has the advantage that an accumulator of moderate volume need only be pressurized to slightly more than that required in the specimen;
3. liquid charged accumulator.

The latter approach, consisting of a liquid charged accumulator with a high velocity release and fluid transfer system, was chosen based on the following considerations.

#### 1. Flexibility

Since it is a purely hydraulic system, it can be used to test virtually any component under hydrodynamic loading conditions by simple piping modifications. The peak pressure can be varied over a wide range of values by simply changing the accumulator charging pressure. The rate of loading can be varied by changing orifice or pipe sizes. High or low temperature capabilities can easily be added by heating or cooling the specimen without greatly affecting the remainder of the system.

#### 2. Control

Very accurate control and reproducibility of peak pressure is inherent in this type of system since the peak pressure is directly a function of the compressibility of the liquid and the charging pressure. The former is very nearly a constant at any given pressure and the latter involves measuring and controlling a constant hydrostatic pressure; a rather simple instrumentation problem.

#### 3. Delay Time Capability

As opposed to the moving mass, impact type system, the hydraulic system produces the desired pressure and maintains this pressure for any desired time interval. This permits the study of delay time phenomena.

#### 4. Safety

The hydraulic system offers the advantages over the gas system of much greater safety, due to lower stored energy and fewer seal leakage problems.

#### Fluid Transfer Analysis

Prior to discussing the design and functioning of the individual components of the system, it is important to consider the controlling parameter--the fluid transfer from the feed accumulator to the specimen. The following is an approximate solution to the fluid transfer problem.

The following assumptions were made in the solution of the problem:

1. The compressibility of the fluid (water) is a constant between 0 and the maximum pressure to be used and is given by:

$$\frac{\Delta V/V_0}{P} = k \quad (1)$$

2. Any volume changes due to dilation of the accumulator and the piping are neglected.

3. The Reynold's number for the pipe flow exceeds  $4 \times 10^5$ . Therefore, the friction factor may be considered a constant.

4. The pressure in the pipe is equal to the pressure in the specimen.

The change in mass of fluid in the accumulator during fluid transfer is given by

$$\Delta M_a = \rho_0 k (P_{a0} - P_a) V_a \quad (2)$$

The change in mass in the pipe is

$$\Delta M_p = \rho_0 k P_s V_p \quad (3)$$

The change in mass in the specimen due to compression is

$$\Delta M_{sc} = \rho_0 k P_s V_{so} \quad (4)$$

and that due to dilation is

$$\Delta M_{sd} = \rho_0 (1 + k P_s) k_s P_s V_{so} \quad (5)$$

where  $k_s$  is defined as the change in volume of the specimen due to dilation divided by the initial volume.

The total change in mass in the specimen thus becomes

$$\Delta M_s = \rho_0 P_s V_{so} [k + (1 + k P_s) k_s] \quad (6)$$

Since the change in mass in the accumulator must equal the change in mass in the pipes and specimen

$$k (P_{a0} - P_a) V_a = P_s [k (V_p + V_s) + k_s V_s (1 + k P_s)] \quad (7)$$

For the conditions of this test we may neglect the  $k P_s$  of the  $(1 + k P_s)$  term in eq. 7. This will result in an error of less than five percent and will



thus allow the following constants to be defined:

$$C_a = k V_a \quad (8)$$

$$C_s = k(V_p + V_s) + k_s V_s \quad (9)$$

Equation 7, therefore, becomes

$$C_a (P_{ao} - P_a) = C_s P_s \quad (10)$$

or

$$P_a - P_s = P_{ao} - (1 + \frac{C_s}{C_a}) P_s \quad (11)$$

The pressure difference between the accumulator and the specimen may be considered to be composed of three factors, namely: (1) velocity head loss in the feed valve, (2) a frictional head loss in the pipe, and (3) a velocity head loss on entry into the specimen. These are given by the following equation

$$P_a - P_s = \frac{d}{2g} \left[ \frac{fL}{D} v_p^2 + v_p^2 + F_v v_v^2 \right] \quad (12)$$

where  $F_v$  is a velocity loss coefficient for the valve.

From continuity of flow requirements

$$v_v^2 = (v_p \frac{A_p}{A_v})^2 = v_p^2 \left( \frac{D_p}{D_v} \right)^4 \quad (13)$$

Therefore

$$P_a - P_s = \frac{d}{2g} \left[ \frac{fL}{D} + 1 + F_v \left( \frac{D_p}{D_v} \right)^4 \right] v_p^2 \quad (14)$$

Letting

$$\frac{d}{2g} \left[ \frac{fL}{D} + 1 + F_v \left( \frac{D_p}{D_v} \right)^4 \right] = F \quad (15)$$

in eq. 14 yields

$$P_a - P_s = F v_p^2 \quad (16)$$

From continuity of flow entering the pipes

$$\frac{1}{\rho} \frac{dM}{dt} = A_p v_p \quad (17)$$

Combining eqs. 16 and 17 yields

$$P_a - P_s = \frac{F}{\rho^2 A_p^2} \left( \frac{dM}{dt} \right)^2 \quad (18)$$

and combining eqs. 11 and 18 yields

$$\frac{dM}{dt} = \frac{\rho A_p}{\sqrt{F}} \sqrt{P_{ao} - \left(1 + \frac{C_s}{C_a}\right) P_s} \quad (19)$$

From eqs. 3, 6 and 9, the mass of fluid entering the pipes is given by

$$M = \rho_o C_s P_s \quad (20)$$

therefore, since  $\rho = \rho_o (1 + kP_s)$

$$\frac{dP_s}{dt} = \frac{A_p (1 + kP_s)}{C_s \sqrt{F}} \sqrt{P_{ao} - \left(1 + \frac{C_s}{C_a}\right) P_s} \quad (21)$$

Again neglecting the  $kP_s$  term, separating variables and integrating from 0 to  $P_s$  and 0 to  $t$  gives the following equation for the pressure time curve in the specimen.

$$t = \frac{\sqrt{P_{ao}} - \sqrt{P_{ao} - \left(1 + \frac{C_s}{C_a}\right) P_s}}{\frac{A_p}{2C_s \sqrt{F}} \left(1 + \frac{C_s}{C_a}\right)} \quad (22)$$

## DESCRIPTION OF APPARATUS

### High Speed Valve

In order to release the energy stored in the accumulator into the test specimen in the required loading time, a valve which has the following operating characteristics is required: (1) opening time must be less than one millisecond, (2) time of opening must be controllable within one-half millisecond, (3) must be capable of withstanding the maximum accumulator pressure used both in the closed and open position, and (4) must have a volumetric flow capacity of in excess of 2,000 gallons per minute.

In order to obtain these requirements, a pilot operated valve utilizing the differential area principle was designed. A schematic diagram of this valve is shown in Fig. 1. The operation of the valve is as follows. A pilot pressure of about 8 percent of the accumulator pressure is introduced into the area under the plunger which is sufficient to hold the valve closed. The valve may now be opened by either of two methods. The pressure under the plunger may be released or a pressure equal to or greater than the pilot pressure may be introduced above the plunger through the trigger port. Either of these actions will cause the net force on the plunger to

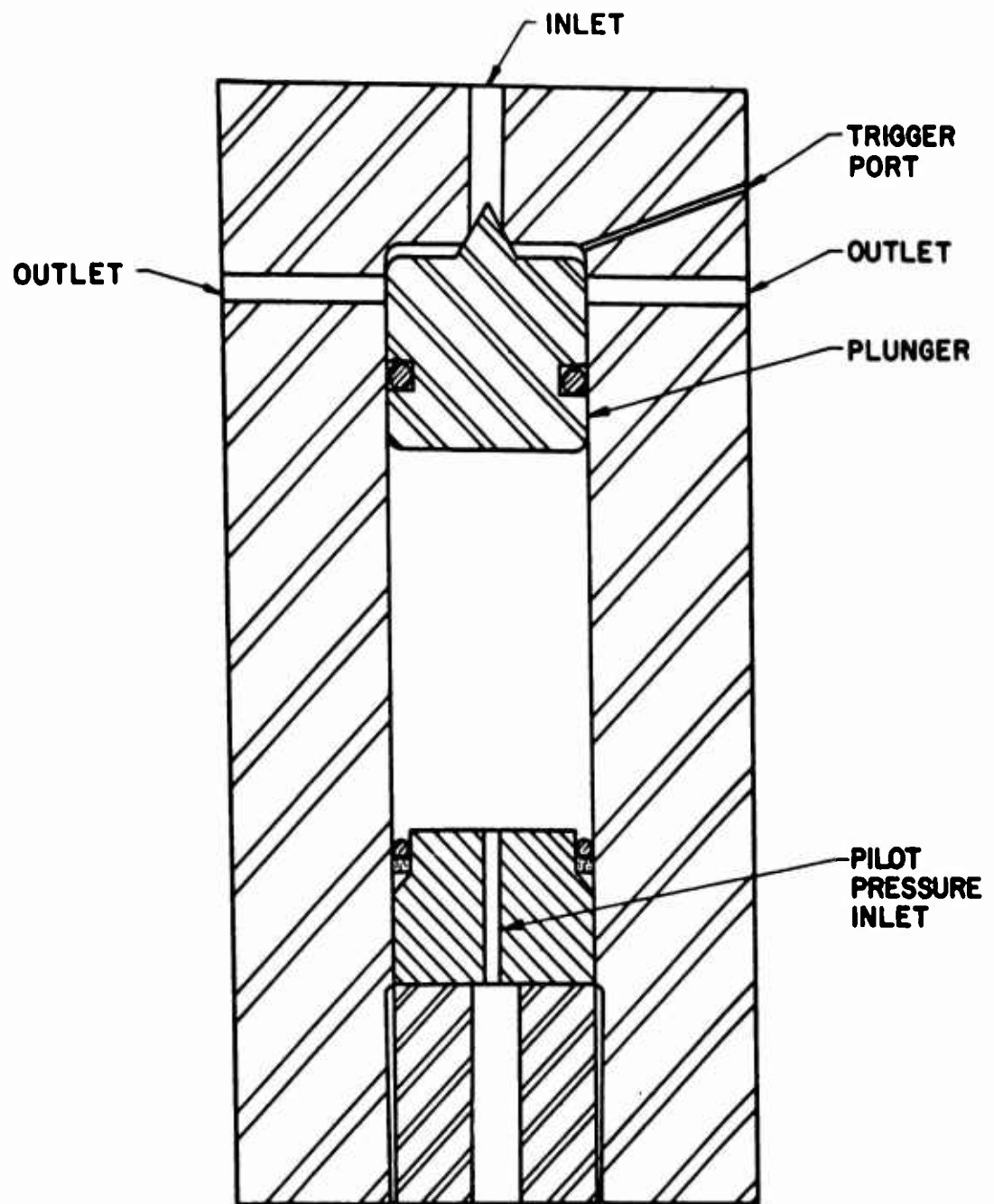


FIG. 1 SCHEMATIC OF HIGH SPEED VALVE

become downward. As the plunger begins to move, the high pressure fluid at the seat will move into the area above the plunger, which will accelerate rapidly downward, compressing the fluid beneath it. The volume of fluid under the plunger is enough so that the compression of this fluid will allow the plunger to move far enough to uncover the outlet ports. Either liquid or gas may be used as a pilot pressure fluid depending on the pressures involved and the compressibility requirements. This means that a high flow rate out of the bottom of the valve is not required, allowing the use of small orifice tubing and valves in the pilot pressure system. In order to prevent premature firing of the valve in case of leakage at the seat, the trigger port is vented to atmosphere through an air operated dump valve which is closed just before the valve is fired.

#### Pressure Release Valve

Along with the requirement for building up a maximum pressure in a given period of time, it is also necessary to relieve this pressure after a specified time and at a given rate. For the particular test described herein, the time at pressure and decay rate should closely approximate that associated with the actual firing of the weapon involved near the maximum pressure.

The pressure release valve is identical in principle and operation to the feed valve. It is opened by a hydraulic "feed back" circuit connecting its trigger port to the feed valve trigger port. The required delay time for the opening of the release valve may be obtained by either of two methods. For short delay times, an adjustable orifice in the feed-back line may be used to throttle the flow to the release valve trigger port and produce the desired delay time. A solenoid operated valve in the feed-back line controlled by an electronic time delay circuit can be used to produce any desired delay time.

#### Description of Operation

The system consists of three primary segments, (1) an accumulator with a high speed valve, (2) piping for controlled fluid transfer to the specimen, and (3) a high speed pressure release valve. A schematic of these components assembled into the final system, along with the test specimen, is shown in Fig. 2.

It may be helpful now to consider the sequence of functions that occur when an attempt is made to produce a desired pressure-time curve. Initially the accumulator is charged to the required pressure using an external, high pressure pumping system. The exact accumulator pressure, of course, is

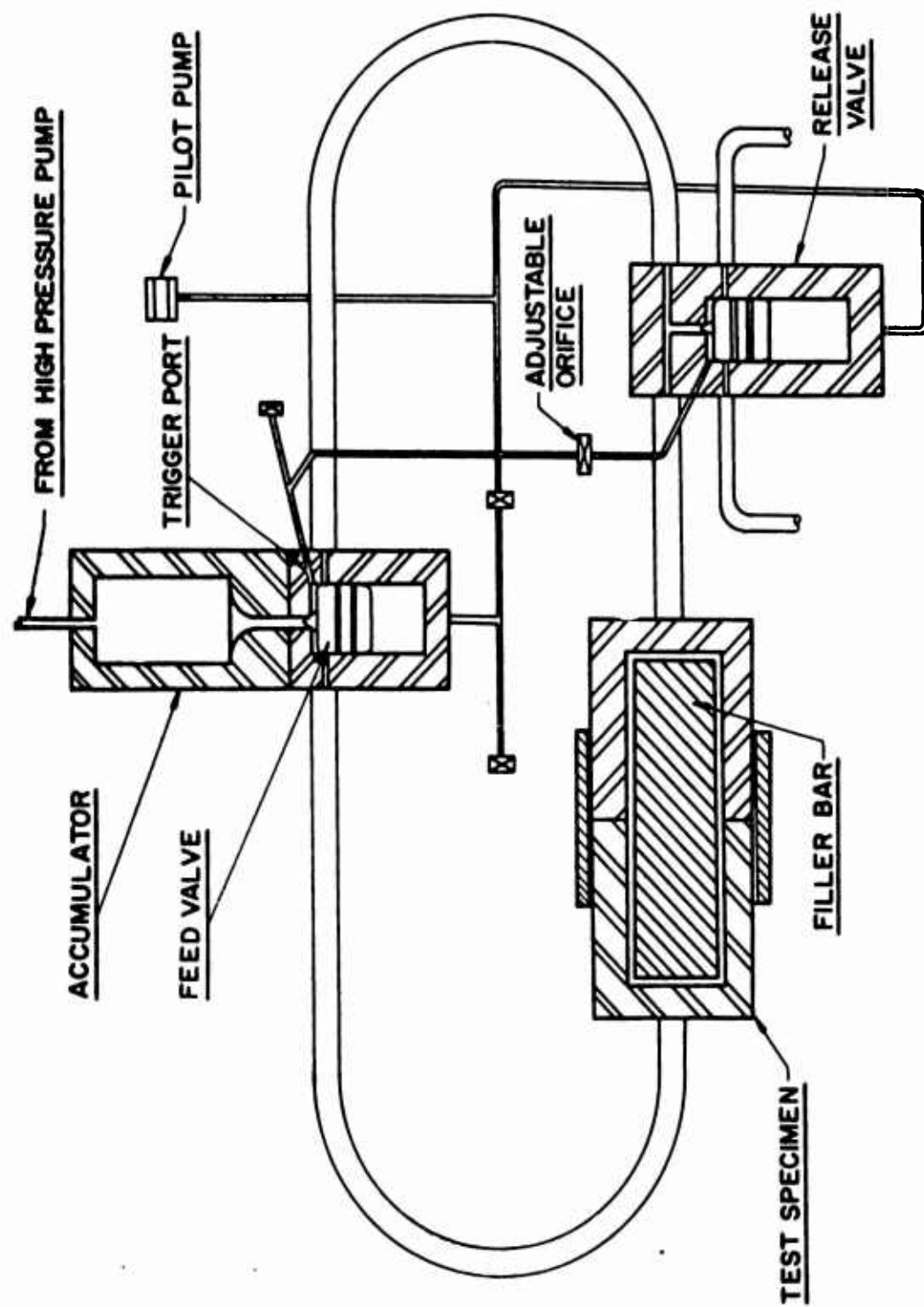


FIG. 2 SCHEMATIC OF TEST SYSTEM

controlled by the desired maximum pressure in the specimen. The high speed feed valve, which is located just below the accumulator and built integral with it, is fired by either of the two methods previously discussed. Fluid now flows out of the feed valve and into the test specimen until an equilibrium pressure is attained. The volume of fluid transferred during this process is kept to a minimum by steel filler bars which occupy most of the volume of the test specimen. The remaining volume is pre-filled with fluid at atmospheric pressure. The fluid is generally piped into both ends of the specimen to assure uniform pressure distribution and to reduce external reaction forces produced by the acceleration of the fluid.

When the test pressure is reached in the specimen and after the desired delay time, the high-speed release valve is opened by the flow of fluid through the line connecting the trigger port of the feed valve with the trigger port of the release valve.

## RESULTS AND DISCUSSION

There are currently two hydrodynamic testing systems in operation at Watervliet Arsenal. The first of these systems has a rated accumulator pressure of 60,000 psi and an accumulator volume of 522 cubic inches. It is currently being used to perform a dynamic analysis on the chamber section of a new type, large caliber cannon. It was designed to simulate the pressure-time response encountered in actual firing. The experimentally obtained and the actual firing pressure-time curves are shown in Fig. 3. Good agreement is shown in the pressure rise and initial part of the pressure decay portions of the curve. Due to reclosing of the release valve, the complete pressure decay portion of the firing curve is not duplicated. If desired, minor system modifications could be made to reproduce this portion of the curve.

Also shown in Fig. 3 is the calculated pressure rise curve as given by eq. 22 using the following constants:

$$k^* = 2.22 \times 10^{-6} \text{ (psi)}^{-1}$$

$$V_p = 50 \text{ cu. in.}$$

$$V_s = 22 \text{ cu. in.}$$

$$V_a = 522 \text{ cu. in.}$$

---

\*Linear approximation of the compression curve for water between 0 and 50,000 psi<sup>(1)</sup>.

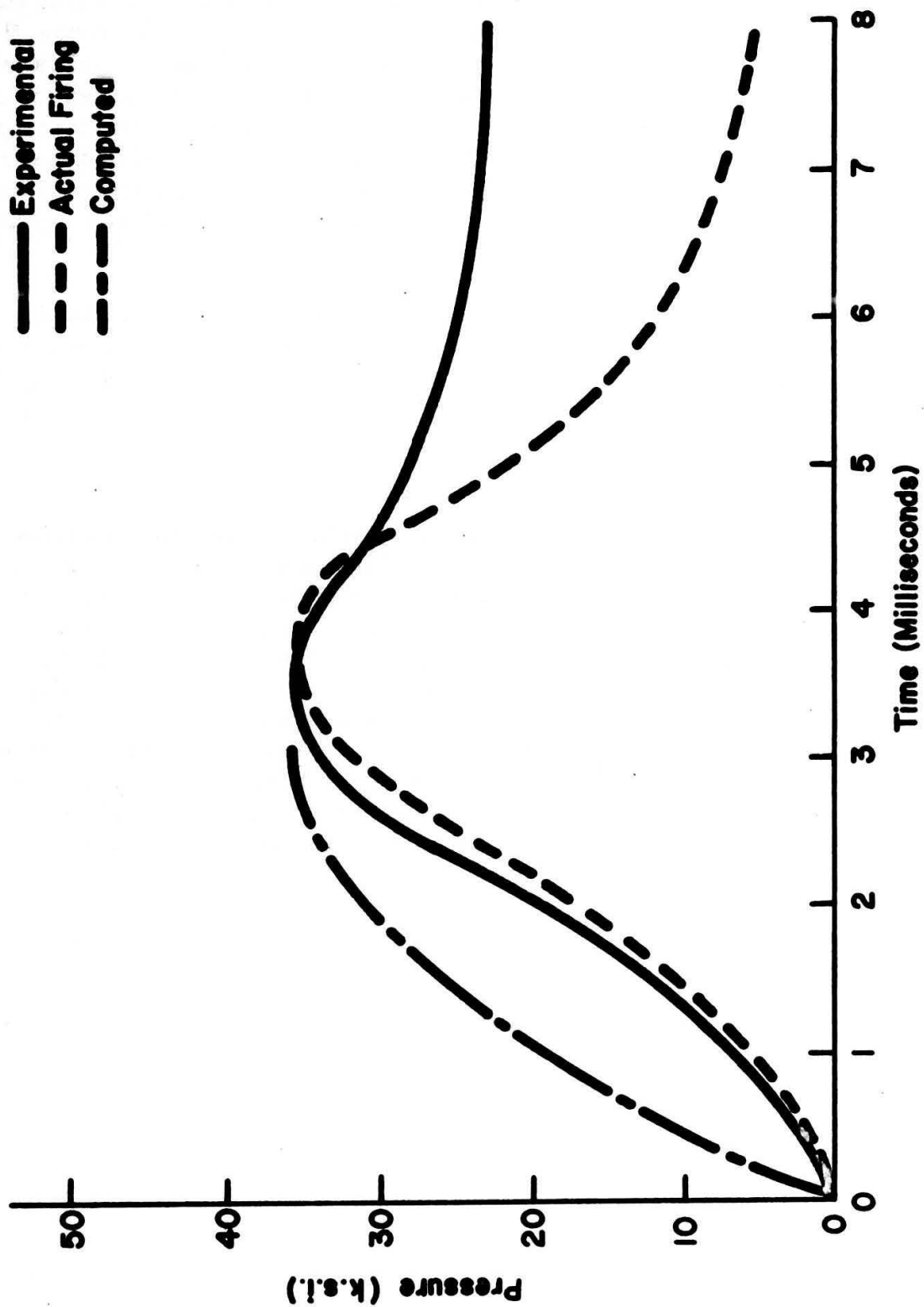


FIG. 3 EXPERIMENTAL, ACTUAL FIRING AND COMPUTED PRESSURE TIME CURVES FOR 60,000 PSI SYSTEM

$$k_s = 5.36 \times 10^{-6} \text{ (psi)}^{-1} \text{ (3)}$$

$$D_p = 0.75 \text{ in.}$$

$$D_v = 0.50 \text{ in.}$$

$$f = 0.024 \text{ (2)}$$

$$P_{ao} = 44,000 \text{ psi}$$

$$L = 56 \text{ in.}$$

The computed and experimental curves are in good agreement with respect to total rise time and peak pressure. The difference in shape of the curves is probably due to the inertial forces involved with accelerating and decelerating the fluid which were neglected in the theoretical analysis.

The second system has an accumulator pressure rating of 30,000 psi and an accumulator volume of 675 cu. in. It is designed for general purpose testing of thin-walled pressure vessels at pressures up to 25,000 psi and strain rates up to 10 in/in/sec. It utilizes compressed nitrogen gas as a pilot pressure fluid and an electronically controlled solenoid valve in the feed-back line to produce delay times variable from one millisecond to one second.

The actual application of this system to date has been restricted primarily to simulated service testing of thin-walled recoilless rifles and mortars. The pressure time response obtained in one such test is shown in Fig. 4 along with the calculated pressure rise curve from eq. 22. The following constants were used in this calculation:

$$k^* = 2.85 \times 10^{-6} \text{ (psi)}^{-1}$$

$$V_p = 3.0 \text{ cu. in.}$$

$$V_s = 17.5 \text{ cu. in.}$$

$$V_a = 675 \text{ cu. in.}$$

$$k_s = 21.3 \times 10^{-6} \text{ (psi)}^{-1} \text{ (3)}$$

---

\*Linear approximation of the compression curve for water between 0 and 20,000 psi(1).



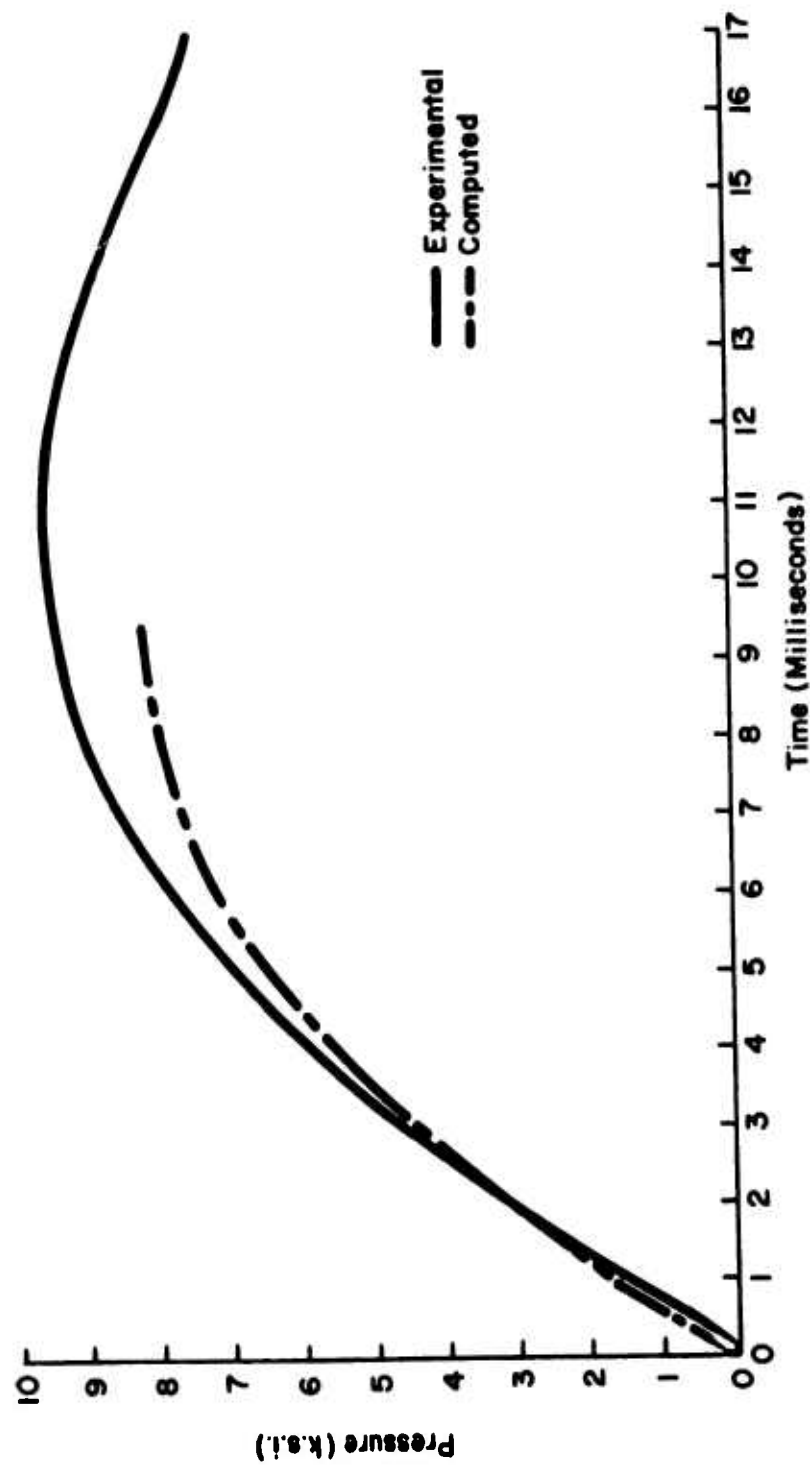


FIG. 4 EXPERIMENTAL AND COMPUTED PRESSURE-TIME CURVES FOR 30,000 PSI SYSTEM

$$D_p = .313 \text{ in.}$$

$$D_v = .375 \text{ in.}$$

$$f = .028(2)$$

$$P_{ao} = 10,000 \text{ psi}$$

$$L = 10 \text{ in.}$$

Good agreement is seen with respect to the pressure rise time. The peak specimen pressure exceeds the calculated equilibrium pressure due to the fact that the inertia of the fluid causes the flow from the accumulator to the specimen to continue momentarily after equilibrium is reached.

One special specimen was tested to determine the feasibility of obtaining very short rise times. This specimen had a 1 in. inside diameter and 9 in. length.  $V_g$  was 2.04 and  $k_g$  was  $4.63 \times 10^{-6}$ . The calculated rise time, using these constants and all other values from the previous example, is 0.62 millisecc. The actual rise time was about 1 millisecc.

#### SUMMARY

A hydrodynamic testing system has been developed for studying a wide variety of pressure vessel configurations at a wide variety of pressures and rise times. This system is adaptable to testing vessels ranging from sections of large caliber cannon to specimens of thin-walled tubing. Pressure rise times can be as short as 3 milliseconds on large, thick-walled vessels or less than 1 millisecond on smaller specimens.

This type of system offers the possibility of developing a high strain rate tensile testing machine by replacing the pressure vessel with a hydraulic piston and cylinder. Such a system is currently being constructed for use with the existing 30,000 psi system. The expected maximum strain rate for this system will be between 10 and 20 in/in/sec at 60,000 lbs. force. The use of the 60,000 psi system with a small diameter piston can theoretically produce strain rates as high as 500 in/in/sec at 60,000 lbs. force.

#### ACKNOWLEDGEMENT

Appreciation is expressed to Messrs. J. Zweig, J. Purtell and D. Sutherland of the Research Branch, Watervliet Arsenal for their assistance in the solution of the fluid transfer analysis problem contained in this paper.

#### REFERENCES

1. Bridgman, P. W., "The Physics of High Pressure",  
G. Bell and Sons Ltd, 1949
2. Shaw, G. V. and Loomis, A. W., "Cameron Hydraulic Data"  
Ingersoll-Rand Company, 1951
3. Timoshenko, S., "Strength of Materials, Part II",  
D. Van Nostrand, Inc., 1942

Barquet Address  
MATERIALS RESEARCH

The Honorable Finn J. Larsen

Assistant Secretary of the Army (R & D)  
Department of the Army  
Washington 25 D. C.

It is interesting to note from the program of your Conference, primarily concerned with the dynamic behavior of materials, that work in this field has been increasing in complexity and sophistication quite rapidly during the last few years. This is rather natural since demands made of materials and requirements in the structures we build from these materials, have been increasingly severe. These severe demands have in turn led to considerable progress in two different areas--the area of improved materials and the field of work in which you are engaged i.e., a better understanding of the dynamic behavior of materials and the structures we build from them.

It would be completely inappropriate for me to address you in the field in which you gentlemen are expert. Therefore, I should like to discuss a number of experiments in the materials research field, and I hope that the majority of you will not have read written accounts of them.

You will recall that some of the first experimental evidence of materials with improved strength were the "whiskers" which formed inside some telephone equipment. When these whiskers were tested it was found they had tensile strengths many times greater than the materials from which they had grown. They were single crystals of high purity. At about that same time, metallurgists and solid state physicists began to have a better understanding of dislocation theory and realized that the number of dislocations found in a piece of material could be correlated to the strength of that material. They also realized that the presence of impurities found in most materials made it impossible to achieve an extremely low number of dislocations per cubic centimeter.

This was also about the time that germanium of high purity was first being produced for transistors. The normal limit of chemical purity at the time meant that we could reduce impurities to about one part per million in a typical material. Refining techniques applied to transistors easily brought this to one part in 100 million, and with some care brought it to one part in a billion.

These various factors made possible an interesting experiment. A thin slice of germanium about the diameter of a quarter was placed across two parallel rods separated so the germanium disc rested on the rods. A third rod, parallel to and between the other two, was placed on top of the disc and pressed down, bending the germanium disc until it broke. Measuring the amount of bending the disc could withstand without breaking was an indication of its strength. Despite the use of high-purity germanium the strength was not appreciably different from normal germanium. As with most materials the experimental strength was about one percent of the theoretical strength. Then one of the metallurgists conducting the experiment realized that under stress dislocations migrate. It was theorized that these were migrating to the surface and that concentrations of the dislocations were leading to minute surface cracks which propagated through the disc and caused failure. All this happened more than 5 or 6 years ago when dislocation theory was not as well known as it now is.

The experiment was then modified so that the disc was stressed in the same fashion as before but the stress was applied while the disc was gently heated--this was done to facilitate migration of the dislocations to the surface--and was placed in a solution which would slowly etch away the surface of the germanium disc. The strength was again measured by the angle to which the disc could be bent before breaking. This time, strength was increased by a factor of 30--in other words the strength was changed from 1/100 of the theoretical strength to 1/3 of the theoretical strength. This was accomplished by forcing the dislocations to migrate to the surface and then etching that surface layer away more rapidly than the dislocations could accumulate and lead to crack failure.

Experiments of this type have increased our knowledge and understanding concerning the strength of materials. We at least have shown that very pure materials with few dislocations will have many times their original strength, if we can keep the dislocations from piling up at stress concentration points. At present, I still have not seen automobile fenders of great strength which are as thin as tissue paper, nor have I seen the steel framework of a skyscraper reduced to soda-straw size. We do, however, have indications that these kinds of things are possible. Undoubtedly someday they will be achieved.

During most of the known history of the human race, ceramics played a significant role. They have been used for simple containers, such as dishes, and, of course, made possible some of the art forms we see around us. It has been only during the last ten years that the understanding of ceramics has progressed to the point that significant engineering of the material could be achieved. It is today possible to take samples of ceramics,

and you are well aware that they are ordinarily extremely brittle, and bend these samples at right angles. I have seen many pieces with about the same cross-section area as that of a pencil and only two or three inches long bent to more than right angles. This too is related to the concentration of dislocations on the surface to a point where they become significant imperfections. It is possible to surface treat sample pieces of ceramics of the type I have mentioned bend them, then either deliberately introduce surface imperfections or simply letting normal handling do so. After this has occurred, the piece will again be quite brittle and will snap if moderate pressure is applied. The surface treatment can be repeated and the piece can again be readily deformed without breaking. In this case, it seems that we are dealing with surface imperfections that lead to crack failure and that the surface cracks rapidly propagate through the ceramic. It is rather interesting to note that the significant work which led to a better understanding of ceramics such as magnesium oxide was performed primarily on silver chloride crystals. It has the happy facility of behaving very much like the magnesium oxide and some other ceramics, at the same time being transparent except at the points where dislocations are introduced. These dislocations can then be photographed even deep inside the crystal, and their migration studied as stress heat, or other environmental conditions are changed.

The implications of ductile ceramics as a regularly used engineering material are tremendous. It would mean that ceramics, in addition to great compressive strength and ability to withstand high temperatures which they already possess, could be formed in the same manner as the metals we regularly use. Machineable ceramics would make possible new engineering concepts of major significance. In addition, ceramic raw materials sell for only a few dollars a ton. If we can obtain ductility without appreciable additional cost, we will accomplish one of the most revolutionary steps possible in the material field.

Another area in which materials knowledge has advanced appreciably in recent years is that of corrosion. In this case, we are ordinarily concerned with improving the resistance of a material to corrosion or improving the oxidation characteristics of the piece of material. We are all acquainted with the fact that aluminum oxide forms rapidly adheres to the surface and effectively prevents continued oxidation of the aluminum under the oxidized layer. It is important to recognize that the layer of aluminum oxide is effectively sealing the surface so that fresh aluminum atoms do not migrate through the oxide layer to the surface, nor do the oxygen atoms from the atmosphere migrate through the oxide layer into the aluminum structure which lies below. What is there about the molecular arrangement of this aluminum oxide layer that effectively prevents the migration

of both aluminum and oxygen through it? As you know, this is most unusual. Rusting of iron proceeds at a rapid rate whether the oxide film spalls off or not, since the oxide film can be readily penetrated by oxygen. For some years studies of a number of different materials have been made by placing a small piece of noble metal, such as gold, on the surface of a fresh piece of material--then exposing the sample to an oxidizing atmosphere and learning which of the two possible migrations predominates; i.e., whether oxygen moves readily through the surface and into the material, or whether fresh atoms from the material move to the surface. The gold wire remains as a marker which indicates the original surface. These studies have advanced our understanding to the point where metallurgists are today working with surface additives with the idea of creating a molecular pattern across the surface which behaves in the same fashion as aluminum oxide. When this is accomplished, it should give us greater flexibility in our designs. We could then select materials according to our structural design needs without being concerned with the corrosion process and give them a coating of much more durability and permanence than the paints we often are required to employ.

We should also recognize that a great deal of progress is being made in the fields we ordinarily think of as more purely the domain of the chemist. Today chemists can at will, produce long-chain plastic molecules and then can cross-link these long chains to a point where plastics have vastly increased ability to withstand high temperatures. You will recall that some of the early experiments which resulted in this capability were accomplished by exposure of plastics to radiation from an atomic pile. I believe that cross-linking of long chain molecules is being routinely done with many plastics today in the laboratory without the necessity of using the radiation. It is, of course, quite obvious that when we allow ablation to occur, plastics can withstand conditions that metals cannot. In fact, some of our reentry vehicles would be destroyed if it were not for the development of successful plastics.

It has been of some interest to note that these sessions have dealt with the problems which arise when explosives are used, as well as the utilization of explosives in deliberately deforming materials. I am sure the studies at Picatinny Arsenal which have already been presented to you in regard to explosive deformation will make even more useful the processes which today are carried on to explosively form shapes as complex as the ogive surfaces of missiles.

I believe that explosive formation, whether performed by primacord explosion or an electrically exploded wire is one of the fine examples of

the kind of work you are doing which has very quickly reached commercial application. In fact, many manufacturers are using these processes for mass production and achieve tolerances which are better than they could have achieved with spinning or similar techniques previously used.

It has been a very great pleasure to participate to a minor degree in this program. I am confident that the exchange of information you are achieving will be extremely worthwhile for every one of you, and will enable you to return to your laboratory with ideas that will eventually benefit the Army in a great variety of ways.

Thank you.



## DYNAMIC BEHAVIOR OF ROCKS UNDER CONFINING PRESSURE

Fred A. Donath\*

### ABSTRACT

Permanent deformation in rock results from the action of differential stress and may be expressed as fracture, flow, or a combination of the two. The strength and ductility of rock change markedly under the influence of confining pressure. As all rocks at some depth below the earth's surface are in effect subjected to confining pressure, experimental data on the failure characteristics of rocks that ignore this variable may be misleading, perhaps meaningless, if applied to below-surface situations.

The ultimate strength of a rock may increase several hundred to several thousand per cent with increasing confining pressure; for many rocks, this increase appears to be nearly linear. Similarly, the ductility increases appreciably with increased confining pressure for most common rocks. The increase in ductility is commonly accompanied by a change in mode of deformation from fracture to flow.

Temperature and strain rate also greatly influence the strength and ductility of rock. The strength of many common rocks is markedly decreased and the ductility is strongly affected by changes in temperature or strain rate. The ductility is normally increased with increase of temperature or lowered strain rate.

The presence of planar anisotropy may have a marked effect on both the breaking strength and the angle of shear fracture in rock. Curves of breaking strength versus inclination of anisotropy are commonly concave upward and parabolic in form. Shear fracture tends to develop parallel to well-developed planar anisotropy for inclinations up to  $45^{\circ}$  -  $60^{\circ}$  to the direction of maximum compression.

### INTRODUCTION

Broadly defined, strength is the resistance offered by a material to failure. A rock is said to be strong if it can sustain great stress without

---

\*Fred A. Donath, Associate Professor of Geology, Columbia University, New York, New York.

fracturing or yielding. "Strength" used without a qualifying adjective or without specifying the conditions under which a rock has been deformed has no precise meaning, however, as the maximum stress it can withstand is strongly dependent on the conditions of deformation. The resistance that a rock offers to deformation may be satisfactorily discussed in terms of its yield strength and its ultimate strength. Large permanent deformation results from the action of differential stress, the difference between the maximum and least principal stresses; hydrostatic stress reduces pore space and produces volume change only. The yield stress of a material is the stress difference at the onset of permanent strain. It is usually indefinite in rocks owing to the lack of a marked break in the stress-strain curve, and it is often preferable to specify the stress at a given small strain. The ultimate strength is the maximum ordinate of the stress-strain curve. It is the greatest stress difference the material can withstand under the conditions of deformation.

For many applications, an equally important property by which the behavior of rocks can be judged is ductility, a measure of the ability of a rock to sustain large permanent deformation without faulting. The ductility of an experimentally deformed rock is determined from the stress-strain curve for a particular test. This curve, load per unit area applied to a specimen versus ensuing strain, is normally plotted with per cent shortening (dimensionless) as the abscissa and true differential stress as the ordinate. True stress is based on actual cross-sectional area of a specimen at a given strain, not on original cross-section. The ductility for a particular test is the per cent strain before faulting. The behavior of a given rock under certain imposed conditions can be described as: very brittle, behaves elastically to the point of rupture, strain before rupture less than 1 per cent; brittle, rupture preceded by negligible flow, 1 to 5 per cent strain; moderately brittle or transitional, faulting follows minor flow, 2 to 8 per cent strain; moderately ductile, significant flow precedes faulting, 5 to 10 per cent strain; ductile, flow is continuous with time and exceeds 10 per cent, perhaps several hundred per cent (cf. Griggs and Handin, 1960, p. 349; see also, Handin and Hager, 1957, 1958, Heard, 1960, Paterson, 1958).

A third property useful in describing the behavior of deformed rocks is the mode of deformation. The two basic modes are fracture and flow. Fracture is deformation with complete loss of cohesion; flow is any deformation, not instantly recoverable, without permanent loss of cohesion (Handin and Hager, 1957, p. 3). All fractures are either extension or shear fractures, depending on whether initial movement is perpendicular or parallel to the fracture surface, respectively (Griggs and Handin, 1960, p. 348). The mode of deformation is a reflection of the ductility of the deformed material.

The maximum compressive stress that a rock can sustain before faulting or losing cohesion is strongly dependent on the magnitude of minimum compressive stress. In ordinary engineering compression tests the minimum stress is atmospheric pressure, in experimental rock deformation the minimum stress during a compression test is confining pressure induced by means of a pressure vessel. A cylindrical rock specimen is placed between a piston and anvil, suitably jacketed, and inserted in a pressure vessel. Radial stresses are exerted on the rock cylinder by liquid surrounding the specimen within the vessel; these stresses are referred to as confining pressure. Axial stresses are induced by the movement of the piston into the vessel to compress the specimen between piston and anvil. Differential stress acts on the specimen when the axial stress exceeds or is exceeded by the radial stresses (confining pressure), and specimen strain is reflected during the course of the experiment by the displacement of the piston with respect to the body of the vessel.

Two basic types of test are common in experimental rock deformation: the compression test, in which the axial stress exceeds the confining pressure; and the extension test, in which the confining pressure exceeds the axial stress. A compression test is made by increasing the axial load while maintaining a constant confining pressure. An extension test is made by subjecting the specimen to a given confining pressure, then reducing the axial load while holding the confining pressure constant.

#### EFFECT OF CONFINING PRESSURE

Increased confining pressure commonly increases the ultimate strength of rocks several hundred to several thousand per cent. Figure 1 illustrates the increase in ultimate strength as a function of confining pressure for several common rock types; data are from Handin and Hager (1957). The Mettawee slate and Oil Creek sandstone are both brittle rocks and though the sandstone sustained better than 10,000 bars<sup>1</sup> differential stress under 2000 bars confining pressure, the slate showed an ultimate strength very similar to many shales, about 3300 bars. Both have high crushing strengths at atmospheric pressure. At 2000 bars confining pressure the Hasmark dolomite has an ultimate strength of about 5400 bars, a 400 per cent increase over its crushing strength. In general, dolomites tend to be strong at all pressures, many have crushing strengths of the order of 1500 bars and ultimate strengths exceeding 7000 bars under confining pressure of 2000 bars. The Muddy shale, Barns sandstone, and Fusselman limestone

---

<sup>1</sup> 1 bar equals 14.5 lbs/in<sup>2</sup>

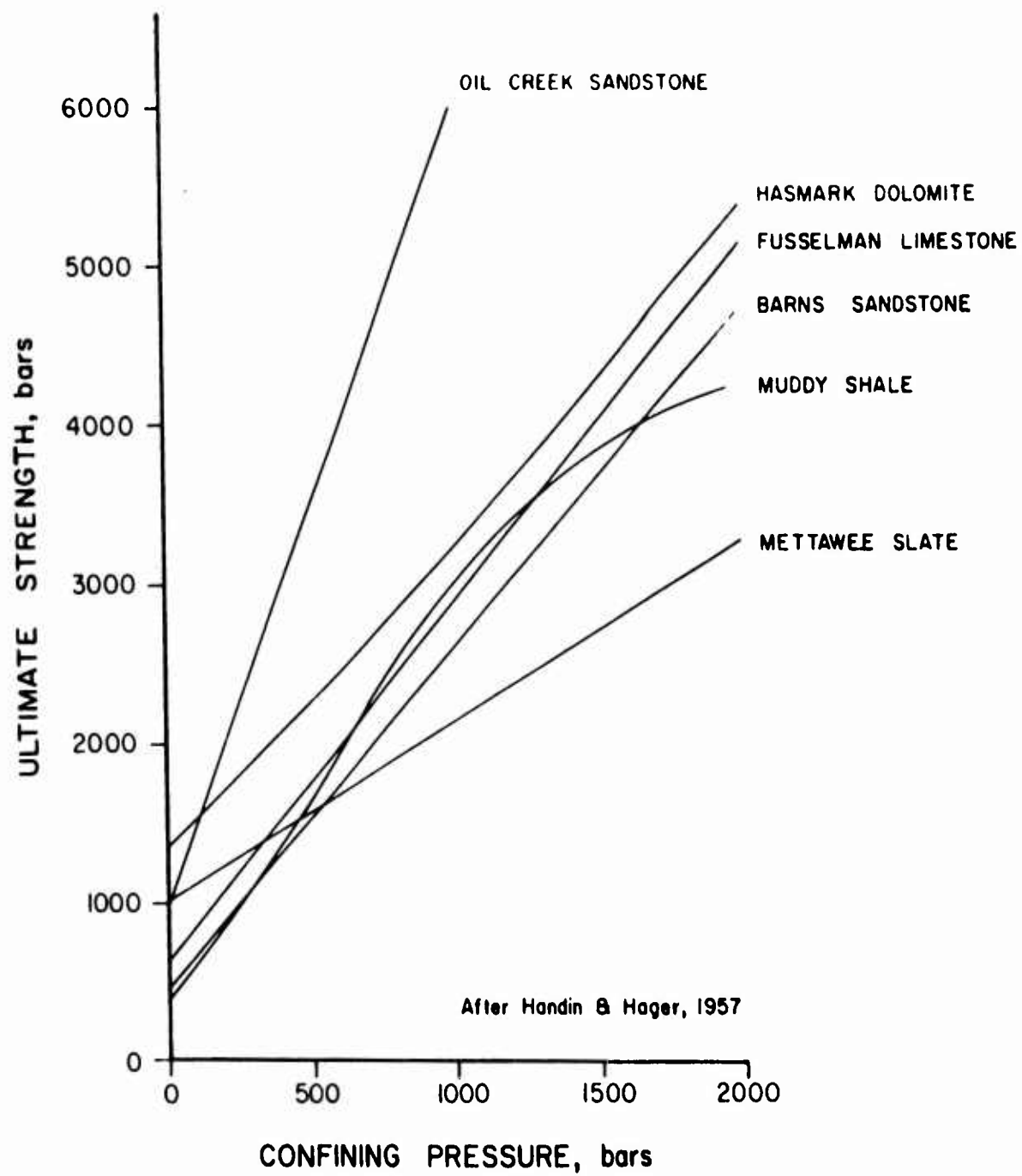


Figure 1

are brittle at atmospheric pressure and have crushing strengths from weak to moderately strong. All show increases in ultimate strength of several hundred per cent. With the exception of the Muddy shale, the increase in ultimate strength of each of these rocks appears to be a nearly linear function of confining pressure.

Similarly, the ductility of many rocks increases markedly with increasing confining pressure. For some rocks, ductility increases only moderate amounts; for a few, it increases but slightly. The increase in ductility as a function of confining pressure is shown in Figure 2 for several common rock types; data are from Handin and Hager (1957). The Mettawee slate and Oil Creek sandstone are brittle at all confining pressures to 2000 bars. Hasmark dolomite is brittle at atmospheric pressure, but shows transitional behavior at higher confining pressures. Blaine anhydrite shows moderately ductile behavior at higher confining pressures, though it also is brittle at atmospheric pressure. The Barns sandstone is brittle under confining pressures to 1000 bars, but becomes very ductile at 2000 bars confining pressure. Like most rocks, the shale and limestone are brittle at atmospheric pressure; however, in sharp contrast to the more brittle rocks, they show increasing ductile behavior with higher confining pressures. The limestone is very ductile even at a confining pressure of 1000 bars. Shear fractures in dolomite typically develop at angles of  $20^{\circ}$  -  $30^{\circ}$  to the direction of maximum compression; shear fractures in the more ductile rocks typically develop at angles of  $30^{\circ}$  -  $40^{\circ}$ .

Under atmospheric confining pressure most rocks are brittle and fail by either extension or shear fracture; under increasingly higher confining pressures, the same rocks may fail by distributed shear and, ultimately, by uniform flow. This transition from brittle to ductile deformation as a function of confining pressure has been nicely demonstrated by Paterson (1958) for a coarse-grained, very pure marble. Longitudinal extension fractures and simple shear fractures developed in specimens of the marble deformed at confining pressures below 100 bars; conjugate shear zones were favored at pressures from 200-300 bars, and distributed shear and uniform flow prevailed for confining pressures above 450 bars. Paterson concluded that for this rock one mile of overburden, the equivalent of about 400 bars pressure, would be sufficient to induce distributed shear or flow rather than a simple shear or shear zone.

#### EFFECT OF TEMPERATURE

Griggs and others (1960) have investigated the strengths of granite, basalt, dolomite, marble, and several other rocks under 5000 bars confining pressure and temperatures from  $25^{\circ}$  to  $800^{\circ}$  C. Some of the results

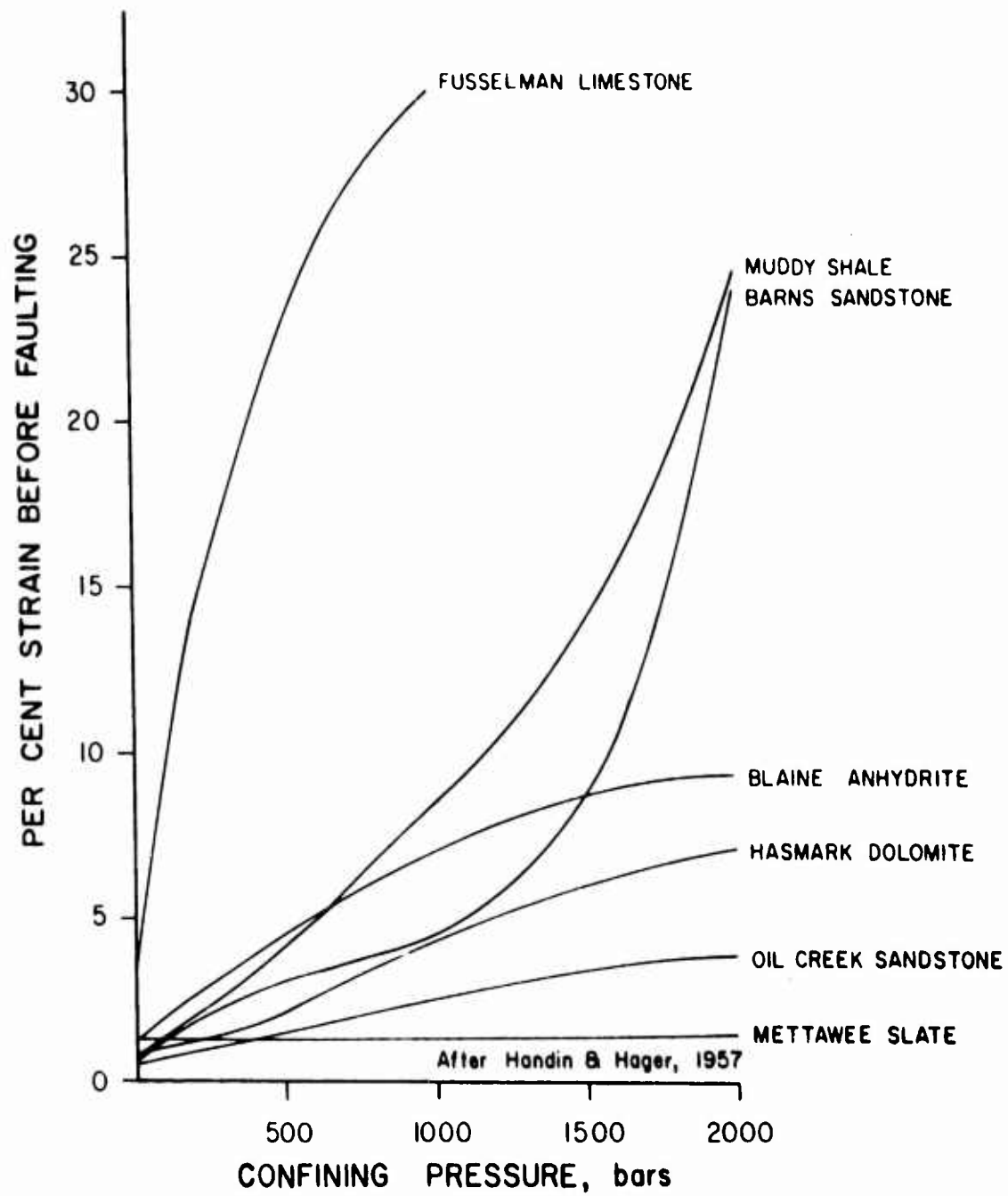


Figure 2

are shown in Figure 3 which is a plot of ultimate strength versus temperature. The ultimate strength of marble is affected most and decreases by about 800 per cent. The strengths of granite and basalt both decrease markedly, basalt is especially affected at temperatures above 600° C. The ultimate strength of dolomite decreases by less than 200 per cent from room temperature to 800° C.

The variation of ultimate strength and ductility with temperature for several rocks tested at 2000 bars confining pressure are shown in Figures 4 and 5; data are from Handin and Hager (1958). According to Handin and Hager, heating may reduce the ultimate strength by lowering the yield stress without affecting the shape of the stress-strain curve. An example of this is Yule marble. Heating may also lower the ultimate strength by reducing or eliminating the work-hardening effect\*. This is the case for Wolfcamp limestone at 2000 bars and 300° C. In contrast, increased temperature may raise the ultimate strength by increasing the ductility in work-hardening rocks, thus permitting greater strains and hence greater differential stresses. This behavior is restricted to rocks whose increased ductility is not accompanied by annealing; it is observed in certain dolomites. Paradoxically, the ultimate strength may also be augmented by introducing work-hardening, owing to a change of the deformation mechanism. Deformation in certain rocks at low temperatures may be cataclastic and therefore involve internal friction. At elevated temperatures intragranular flow predominates over intergranular, but the temperature may not be high enough to allow annealing. Hence, the material work-hardens and raises the ultimate strength above its low-temperature value. Blaine anhydrite provides an example of this type of behavior. The effect of temperature on the ultimate strength of shale is very large, but the flow mechanisms, other than macroscopic shearing, are unknown.

Increased temperature generally increases ductility. Apparently, however, increased temperature can lower the ductility of certain rocks, or lower it slightly before increasing it. Both the Muddy shale and Luning dolomite show slight decreases in ductility with temperature increase to 300° C. The explanation for the Muddy shale is possibly that high temperatures allow more compaction under the hydrostatic pressure imposed on the specimen during "set-up" procedures. The specimen would then presumably compact less under subsequent application of differential stress. The limestone and anhydrite show typically large increases in ductility with increased temperature.

---

\* Work-hardening refers to the observed effect that each increment of permanent strain requires an additional increment of stress difference.

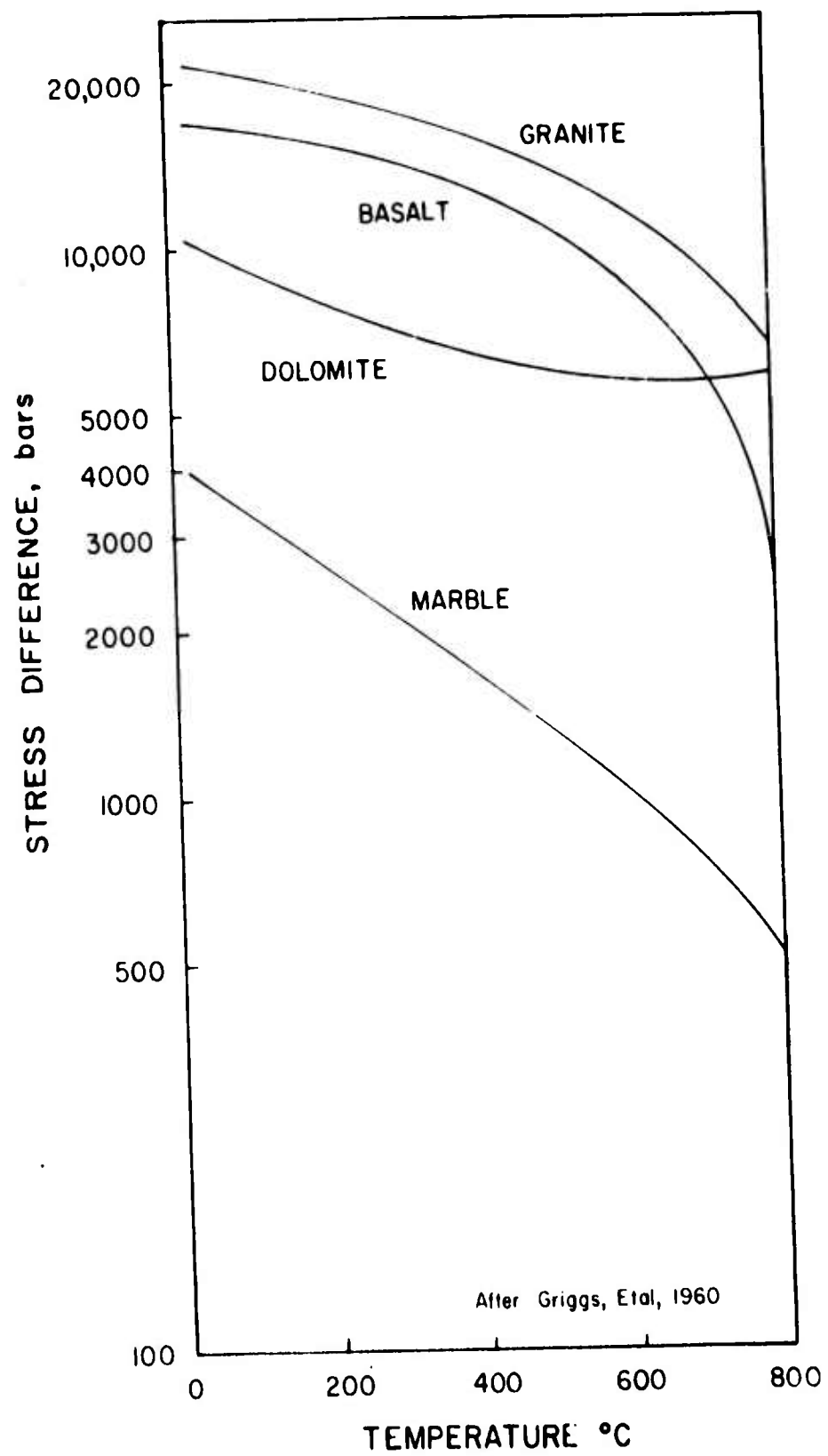


Figure 3



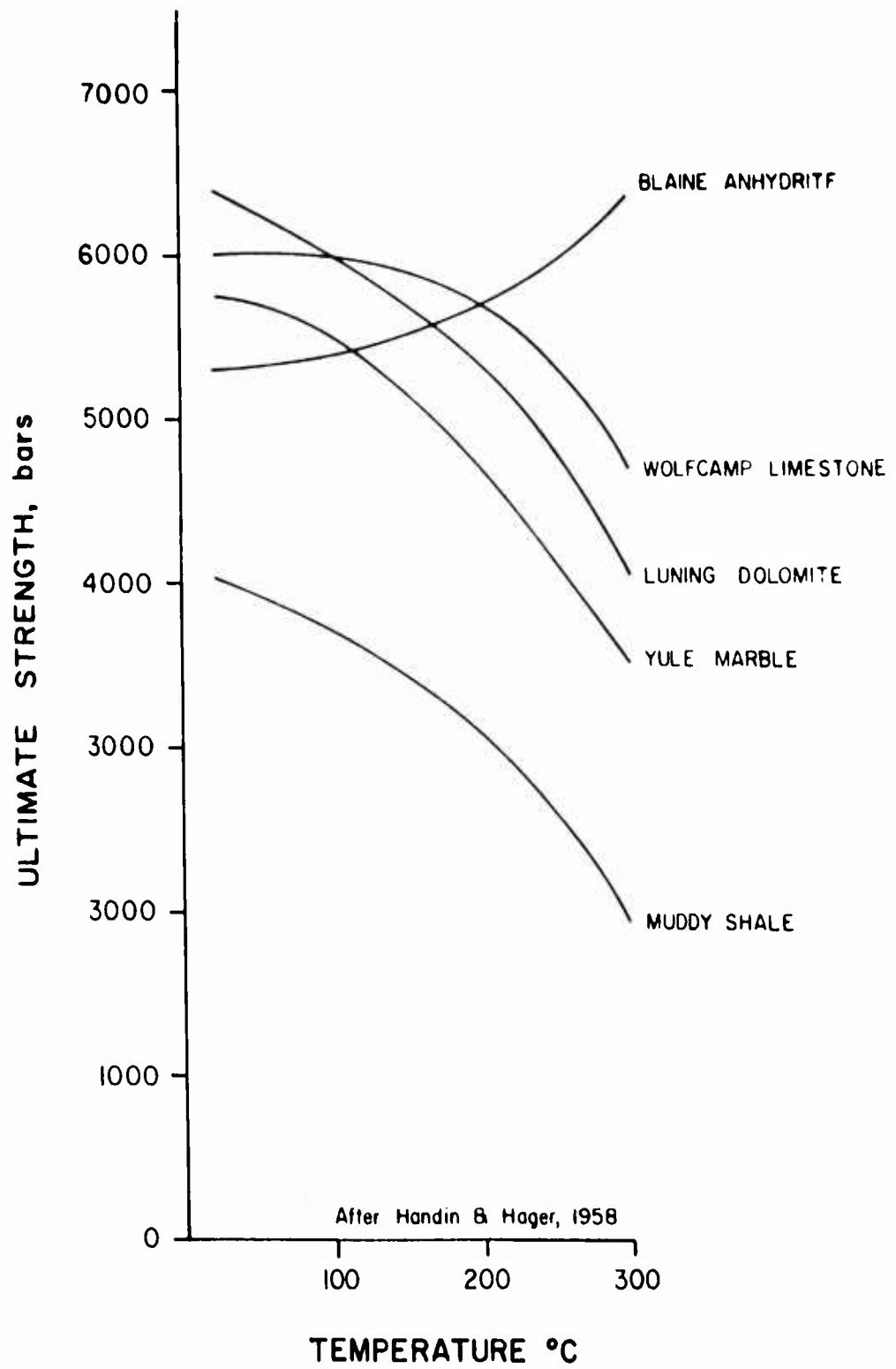


Figure 4

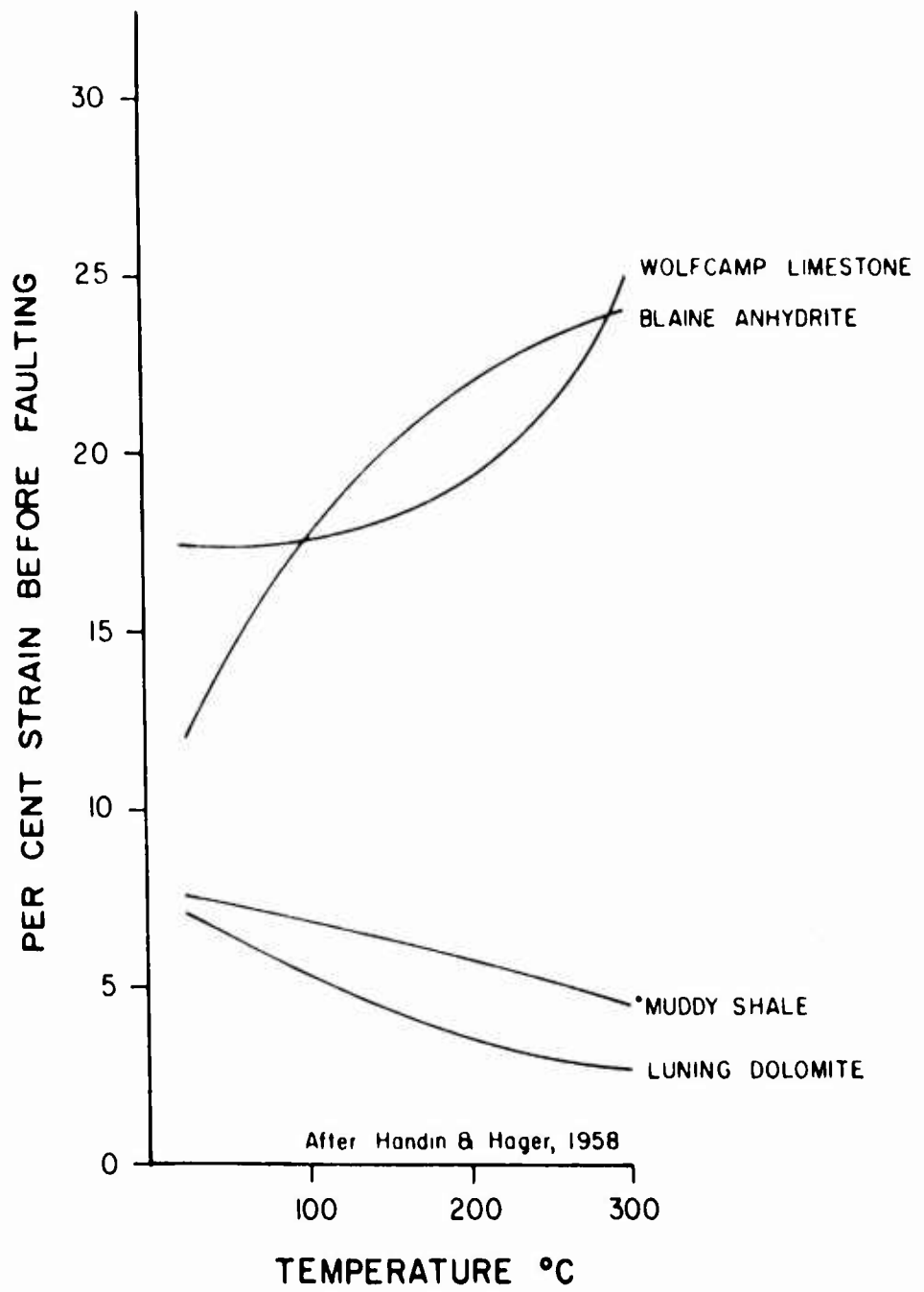


Figure 5

The effect of heating was found by Handin and Hager (1958) to consistently reduce the yield stress (arbitrarily defined as the differential stress at 2% strain) of the rocks tested, though the effect differs from one rock to another and differs with confining pressure for any one rock. The effect of temperature on the yield stress of several rocks is summarized in Figure 6. In certain materials, yielding is associated with intracrystalline gliding; the critical resolved shear stress on glide planes decreases with increasing temperature and it is thus not surprising to observe a reduction of yield stress in materials for which this is an important mechanism of deformation. The lowered yield stresses for dolomite, limestone, and marble possibly reflect in part the effects of temperature on intracrystalline gliding. In sandstone, flow is cataclastic and the yield stress is scarcely influenced by heating. Although the temperature effect on the ultimate strength of shale and siltstone is very large, its effect on the yield strength is small. The flow mechanisms are unknown.

Heard (1960) has investigated the transition from brittle to ductile behavior in Solenhofen limestone as a function of pressure and temperature. Figure 7 shows the boundary between brittle and ductile behavior of jacketed specimens in compression and extension from room temperature to 700° C. Interestingly, the limestone becomes ductile in compression even at atmospheric confining pressure at high temperatures. The brittle-ductile transition is defined by Heard as that point at which 3-5 per cent strain can be induced without notable loss of cohesion. Also of interest is the fact that Solenhofen limestone is brittle in extension at a considerably higher confining pressure than that required to make it ductile in compression.

#### EFFECT OF STRAIN RATE

Less is known about the effect of strain rate on the strength and ductility of rocks than about the other common variables, until recently, practically nothing was known. Robertson (1955) observed that sharply increased strain rate greatly increased the yield strength of rock. Thus, the effect of higher strain rates is to raise the stress-strain curve, as illustrated in Figure 8 (from Serdengecti and Boozer, 1961). An excellent study by Heard (in press) provides the most complete body of data on the effects of strain rate and temperature on the deformational behavior of rock. Heard studied the effects of strain rates from 10 per cent per second to  $10^{-6}$  per cent per second and temperatures from 25° C. to 500° C. on Yule marble. Two of his sets of curves are reproduced as Figures 9 and 10. Although the effect of strain rate is very noticeable even at room temperature (Fig. 9), it becomes remarkably influential at high temperatures (Fig. 10). The greatest differential stress that Yule marble can sustain when deformed at 500° C.,

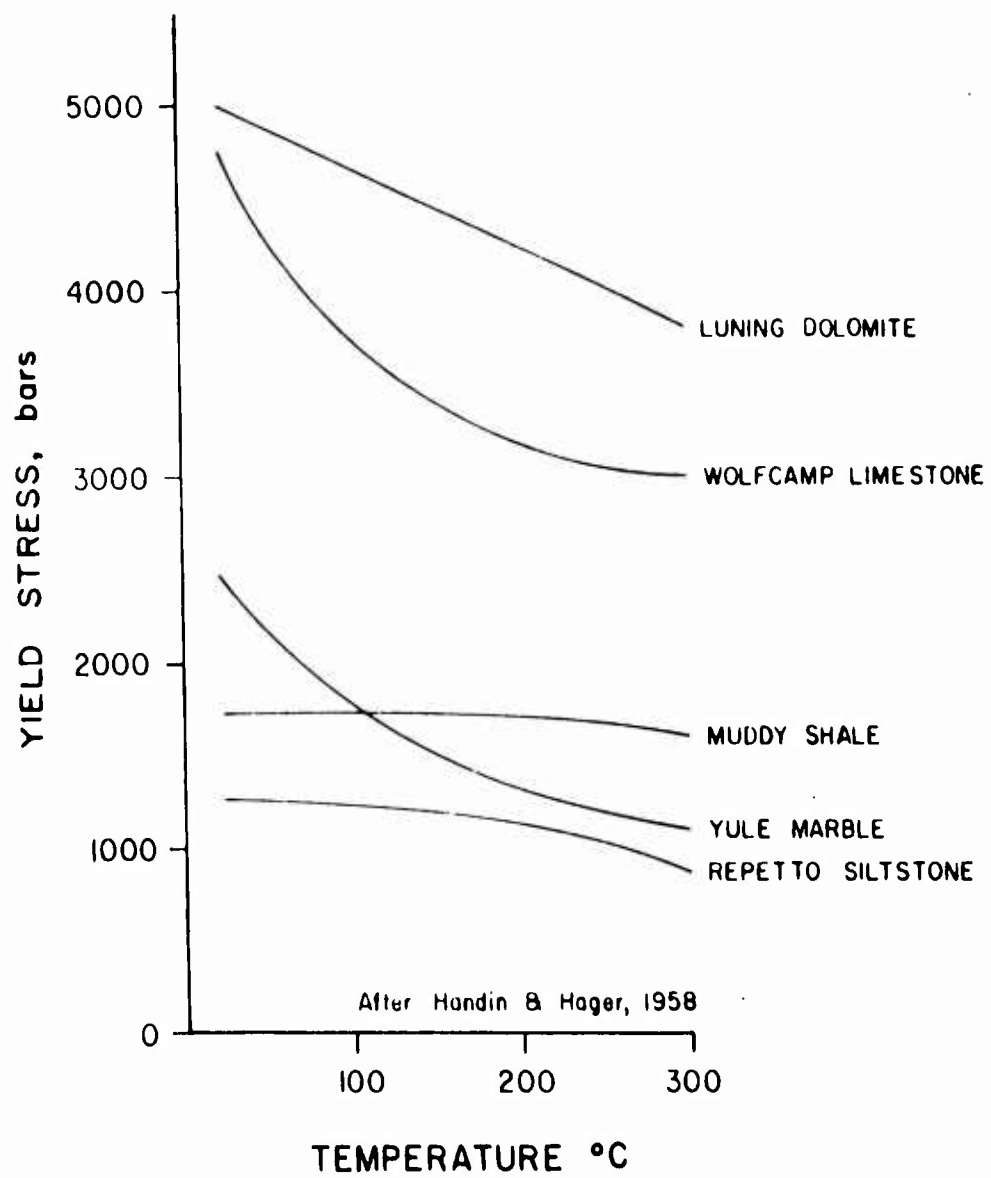


Figure 6

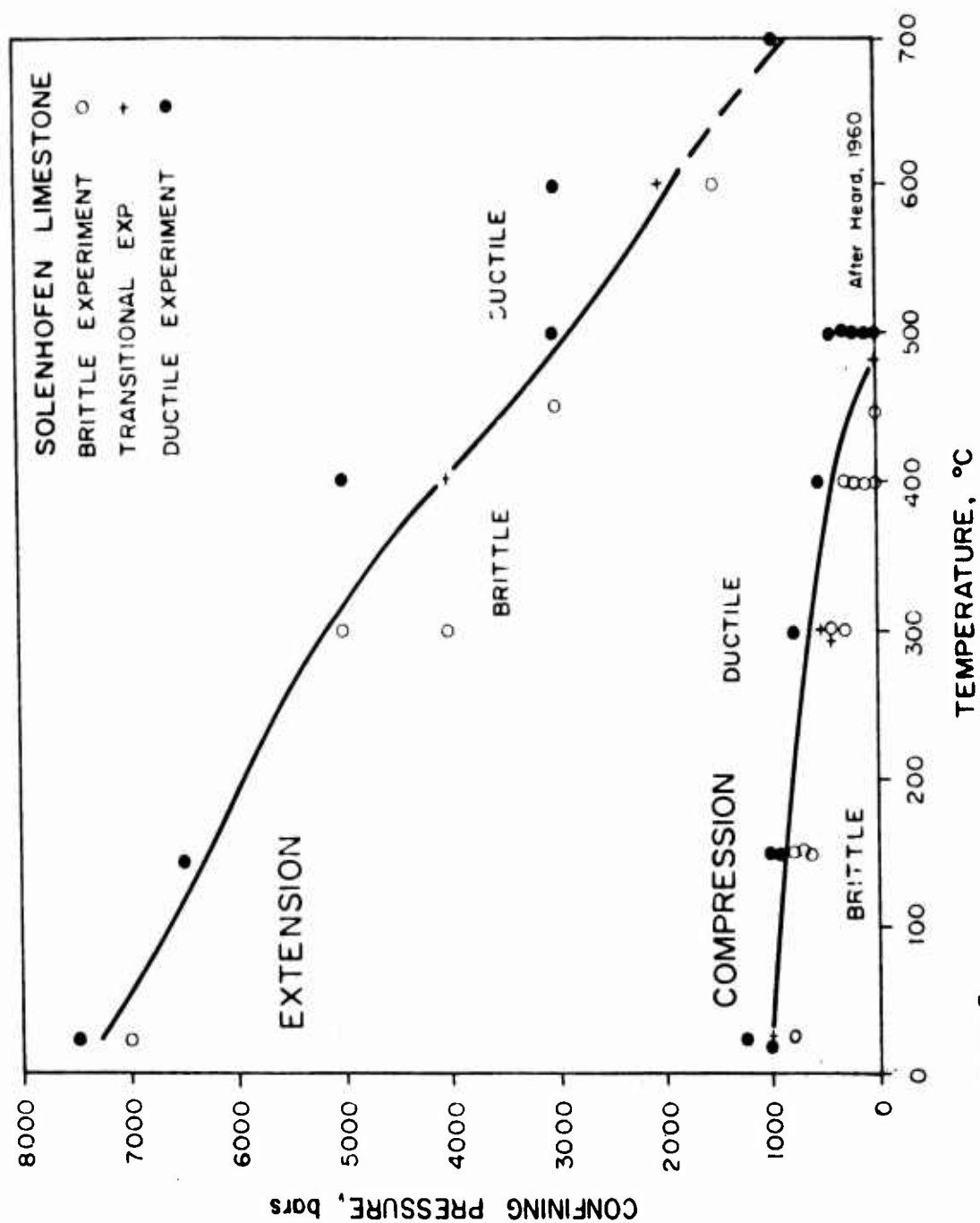


Figure 7

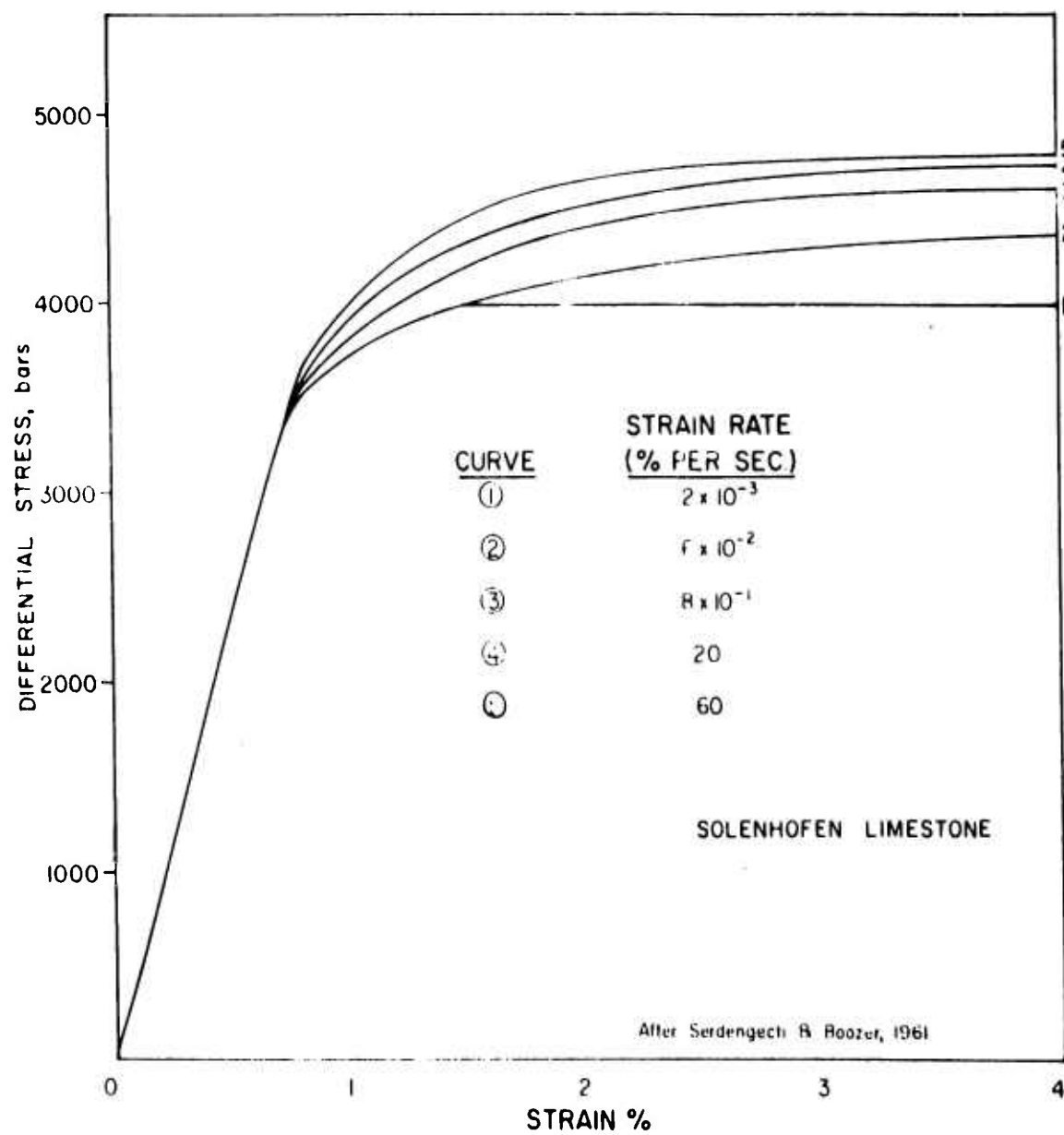


Figure 8

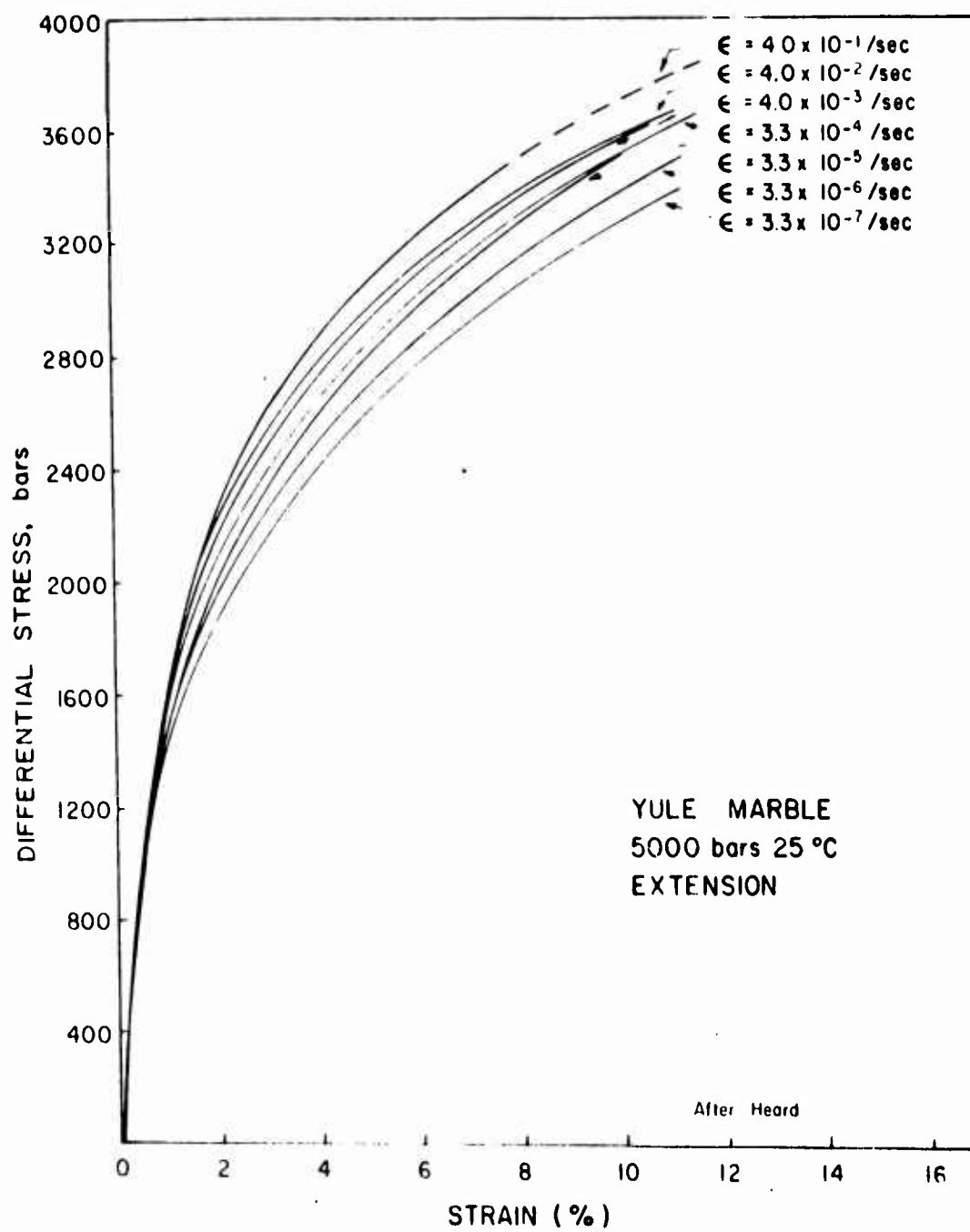


Figure 9

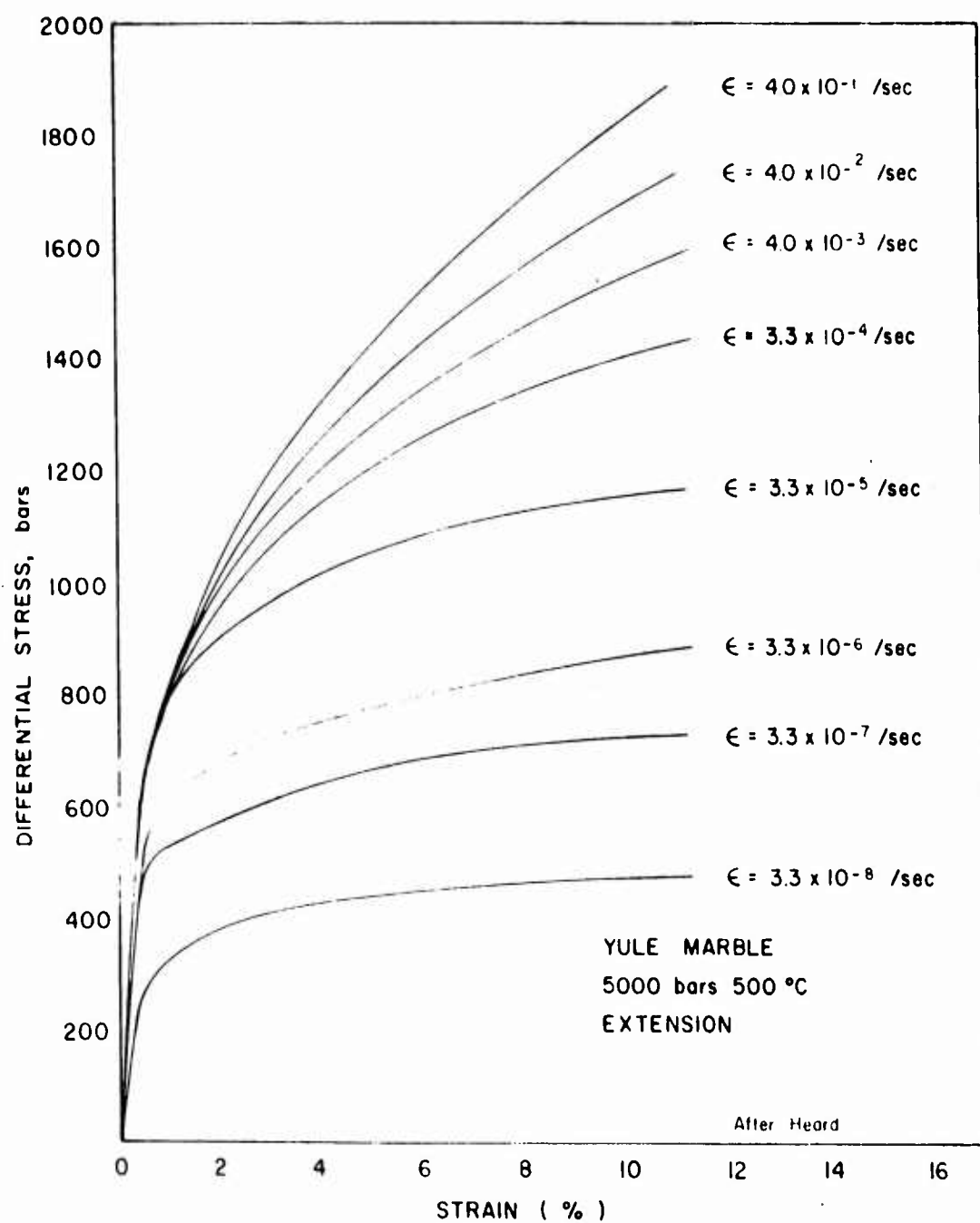


Figure 10



5000 bars confining pressure, and at a strain rate of  $10^{-6}$  per cent per second is, in fact, almost as low as what it can sustain in ordinary tests at room temperature and pressure. The crushing strength of Yule marble is approximately 400 bars.

#### EFFECT OF ANISOTROPY

It is apparent from comparison of the ultimate strengths and ductilities of different rock types that the mineral and rock composition is a most important factor in the deformational characteristics of rock. One of the more influential physical aspects of rock that affects its deformation behavior is planar anisotropy--the presence in the rock of stratification, cleavage, schistosity, or layering of some type.

Planar anisotropy can have a pronounced affect on the strength of certain rocks as demonstrated in a recent study by Donath (1961). One-inch diameter cores of slate, shale, limestone, and several other rocks were cut at angles of  $0^{\circ}$ ,  $15^{\circ}$ ,  $30^{\circ}$ ,  $45^{\circ}$ ,  $60^{\circ}$ ,  $75^{\circ}$ , and  $90^{\circ}$  to the plane of anisotropy for each rock. The cores were trimmed to 2-1/2 inch lengths, and subjected to ordinary compression tests under several different confining pressures. Results for the slate are shown in Figure 11. Curves of differential stress at rupture versus inclination of anisotropy are concave upward and parabolic in form. In slate, cores cut at  $90^{\circ}$  to the cleavage show the greatest breaking strength; cores cut at  $30^{\circ}$  show the lowest breaking strength. The breaking strength for the  $90^{\circ}$  orientation, for compression perpendicular to cleavage, is nearly ten times as large as the breaking strength for maximum compression inclined at  $30^{\circ}$  to cleavage. As would be expected, increased confining pressure produces a noticeable upward shift of the curves.

Figure 12 shows the effect of cleavage on the angle of shear fracture in slate deformed at three different confining pressures. Data points along the line indicate that shear fracture developed parallel to cleavage; this is the case for the 15-, 30-, and several 45-degree orientations. The predicted 30-degree angle for isotropic material is lowered appreciably by cleavage oriented parallel to the specimen axis. Some effect of cleavage appears to be present even in the 60- and 75-degree orientations, but for cleavage oriented at  $90^{\circ}$  the fractures are inclined at about  $30^{\circ}$  to the direction of maximum compression. Results from tests on other rocks indicate that increased ductility reduces the effect of anisotropy on shear fracture.

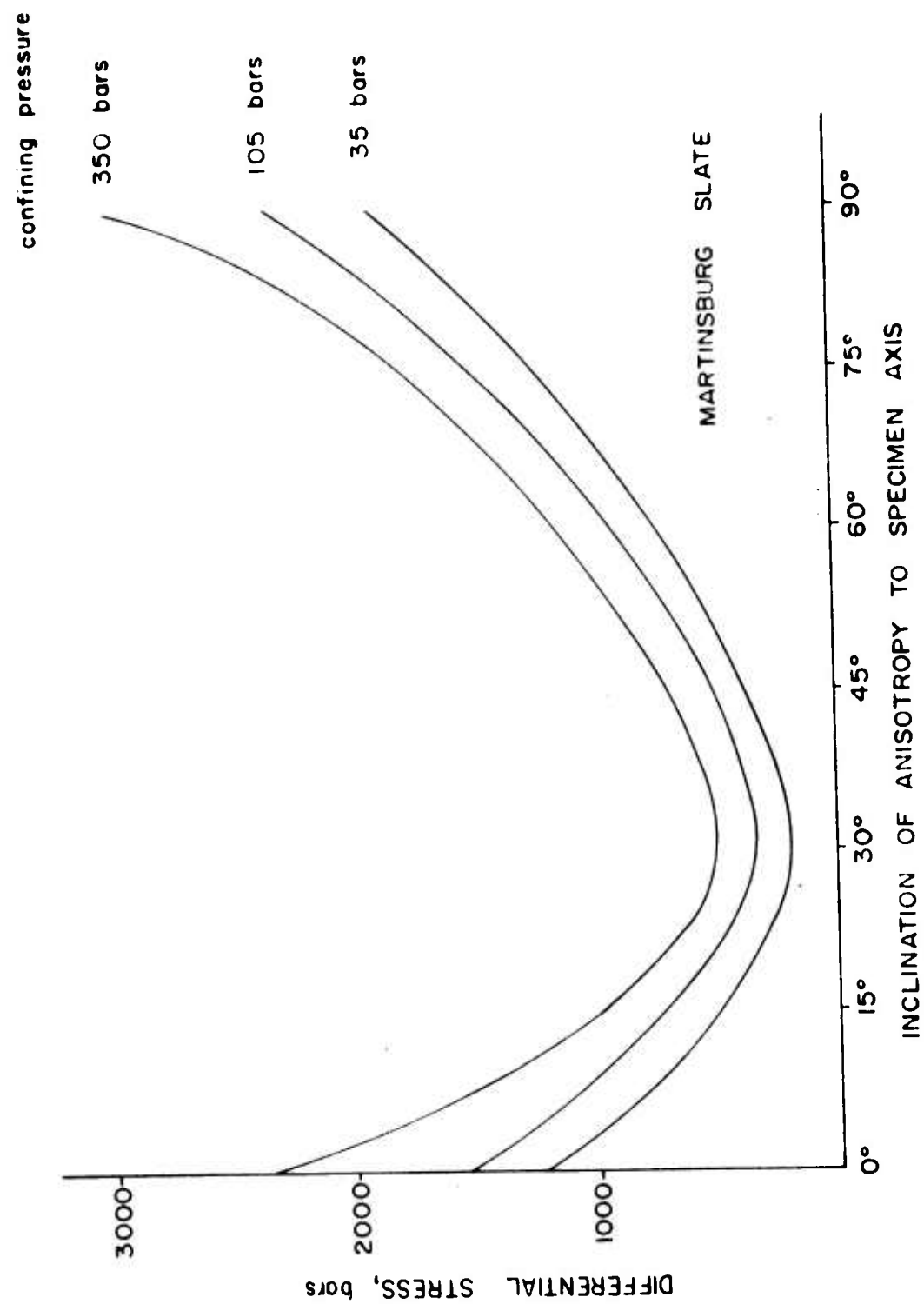


Figure 11

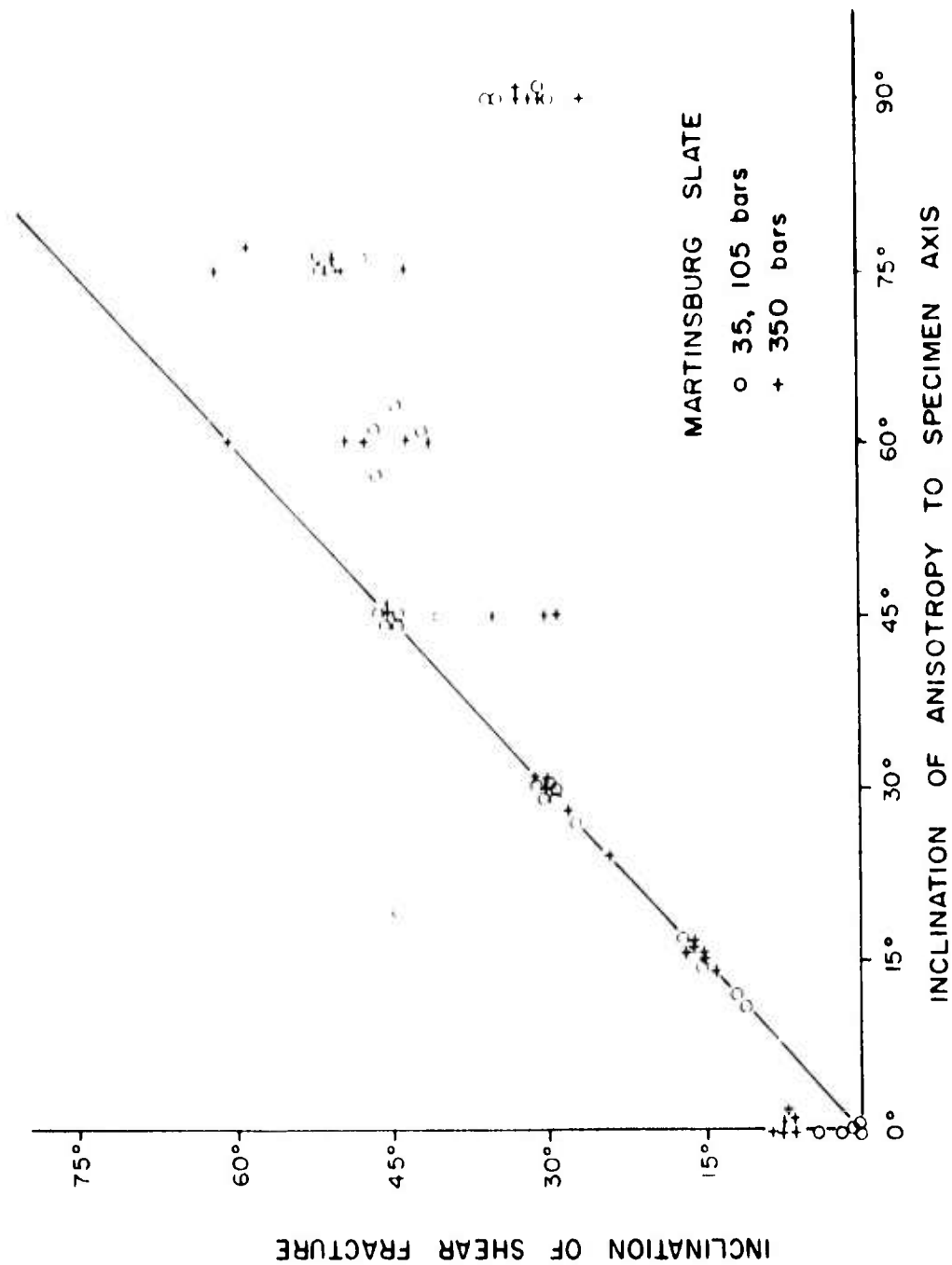


Figure 12

## REFERENCES

1. Donath, F. A., 1961, Experimental study of shear failure in anisotropic rocks: *Geol. Soc. Am. Bull.*, v. 72, p. 985-990
2. Griggs, D. and Handin, J., 1960, Observations on fracture and a hypothesis of earthquakes: *Geol. Soc. Am. Mem.* 79, p. 347-373
3. Griggs, D., Turner, F. J., and Heard, H. C., 1960, Deformation of rocks at 500° to 800° C.: *Geol. Soc. Am. Mem.* 79, p. 39-104.
4. Handin, J. and Hager, R. V., Jr., 1957, Experimental deformation of sedimentary rocks under confining pressure: tests at room temperature on dry samples: *Am. Assoc. Petrol. Geologists Bull.*, v. 41, p. 1-50
5. Handin, J. and Hager, R. V., Jr., 1958, Experimental deformation of sedimentary rocks under confining pressure: tests at high temperatures: *Am. Assoc. Petrol. Geologists Bull.*, v. 42, p. 2892-2934
6. Heard, H. C., 1960, Transition from brittle fracture to ductile flow in Solenhofen limestone as a function of temperature, confining pressure, and interstitial fluid pressure: *Geol. Soc. Am. Mem.* 79, p. 193-226
7. Heard, H. C., In press, Effect of strain rate and temperature on the deformational behavior of Yule marble: *Jour. Geol.*
8. Paterson, M. C., 1958, Experimental deformation and faulting in Wombeyan marble: *Geol. Soc. Am. Bull.*, v. 69, p. 465-475
9. Robertson, E. C., 1955, Experimental study of the strength of rocks: *Geol. Soc. Am. Bull.*, v. 66, p. 1275-1314
10. Serdengecti, S. and Boozer, G. D., 1961, The effects of strain rate and temperature on the behavior of rocks subjected to triaxial compression: *Proc. 4th Symposium Rock Mechanics*, Bull. Min. Industries, Nov. 1961, Penn. State University

## DISCUSSION

James H. Flanagan, QM, R&E Command, Natick: Can you tell us something about the jacketing materials that were used in confining the pressure stress; and can you say something about the reproducibility of rock data? Can you repeat the data on different samples?

Prof Donath: Well, to answer your first question the jacketing material commonly used at the higher confining pressures is thin walled copper tubing of the order of nine thousandths inch thickness. This has a very negligible strength endurance for the rock and often does not affect the results when plotted as a stress-strain curve. To answer your second question - This is pretty much a function of the individual apparatus, the method of preparation of specimens. I can speak for our own work which showed very good reproducibility and we do take considerable care in preparation of specimens. We grind off the ends and the end surface is perfectly normal to the axis of the specimen so that there are no bending moments present. I would say that reproducibility for rocks which are fairly consistent in their general properties is good. We try to pour all the specimens from the same block for a given test series. The reproducibility variation is probably less than 1%.

Mr. Zaroodny, APG-BRL: Very fascinating subject filled with fascinating information. My interest is directed not so much toward the problem of the homogeneous structure as toward the nature of propagation of cracks. Is there something known about what causes the cracks?

Prof Donath: Well, the fracture occurs, of course, only when the material is behaving in rather a brittle fashion and we do find a transition from very brittle behavior to a very ductile one. We don't know very much about the propagation of fractures. There is an experimental study being carried out at this time under confining pressure, on the propagation of fractures by Prof Grace who has been working at Dunbar Laboratories at Harvard the past year. He machined the dumbbell shaped specimens to get away from the end effects and he has found a very close correlation between the orientation and propagation of fracture and grain boundaries. Grain boundaries seem to influence very strongly the direction of propagation of the fracture. In theory, of course, one can predict the orientation on the basis of stress distribution, but when you look at the rock itself you expect to find the properties of the material and the properties of individual grains and their relationship to one another.

George Kaye, Picatinny Arsenal: Where does the application of these rocks lead as compared to the material of concrete which is being used throughout the construction industry?

Prof Donath: You mean what are the engineering applications of studies like this?

George Kaye: Right.

Prof Donath: A very obvious application, perhaps not so obvious to this group, is the effect on drilling rates. A great deal of research has been put into the technology of drilling itself, but just the slightest increase of the efficiency of drilling would save millions of dollars for oil field operations. As you can see from the results I presented here, even the slightest increase of confining pressure causes tremendous increase of strength. This is something that may not be anticipated during drilling or for that matter during excavation at shallower depths where drills are not being used. These are some of the applications you inquired about.

### ERRATA

Paper entitled "Correlation of High Loading Rate Reactions with Low Rate Tests in Metals" by Coy M. Glass.

Please read Fig. 1 in place of Fig. 3 on page

Please read Fig. 2 in place of Fig. 5 on page

Please read Fig. 3 in place of Fig. 7 on page

## CORRELATION OF HIGH LOADING RATE REACTIONS WITH LOW RATE TESTS IN METALS

Coy M. Glass\*

### ABSTRACT

Changes in a tensile specimen during neck-down, when the load is above the ultimate tensile stress, are found to be functions of the rate of application of load. The neck remains volume constant, and the rate of change of dimensions within this volume may be measured from photographs taken during the test.

Analysis of the neck region provides a basis for calculating energy-volume relations as a function of strain rate. Using these relations, and a high velocity stress-strain curve (described in previous papers), a prediction may be made of metal reaction under explosive loading.

In this paper, annealed polycrystalline copper, and single crystal copper specimens are compared, using the above analysis. In an experimental arrangement using explosives, specimens are necked-down and fractured, and the energy distribution in the stress pulse, during necking and fracture, are compared to the process occurring during slow rate deformation.

### INTRODUCTION

In the field of high velocity loading of metals, the concepts currently in use to describe the reaction of metals to explosive loading are insufficient in scope or case of solution for predicting a number of reactions. For instance, equations of state derived from hydrodynamic considerations do not take into account heavy preferred orientation in a metal, because of experimental and theoretical difficulties. The approach taken by some investigators has shown that, under the conditions of measurement, Hugoniot curves (for compression) for single crystals and polycrystalline specimens of the same metal (eg: copper, aluminum, etc.) are identical. No method is available for predicting, for instance, the shear or release wave dependency on crystalline properties, and, in the case of high pressures, the reflected tensile waves are still considered in the hydrodynamic method.

---

\*Coy M. Glass, Ballistic Research Laboratories, Aberdeen Proving Ground, Aberdeen, Maryland.



Solid mechanics has been reasonably successful in describing a number of one dimensional problems in the area of dynamic loading. However, as the problem deviates from one dimensionality, the difficulty of solving the equations becomes insurmountable, particularly if material properties are related to the stress tensors in an effort to describe the metal reaction. In some areas of impact deformation, Bell has been very successful in describing metal reactions and relating them to G. I. Taylor's stress-strain parabola.

However, in general the area of metal reaction under high rate loading is virgin territory, where the imperical experimental approach is still more rewarding than the theoretical one.

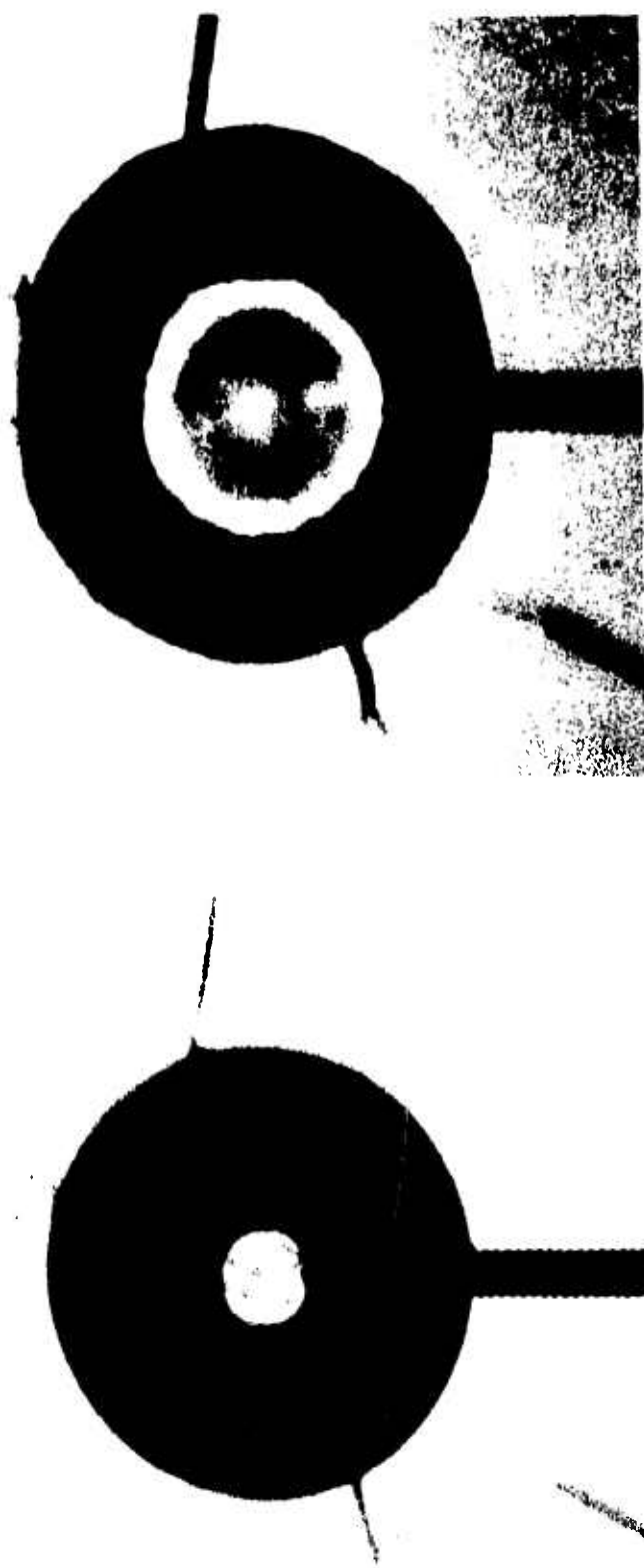
The work reported here describes some results from a long range program designed to obtain basic information on the affect of metal properties on high velocity deformation. It is the aim of this work to define parameters important in the high velocity area, and to relate these parameters to easily measurable, and predictable, low rate properties. The following sections contain brief descriptions of the various aspects of the work. Detailed analyses may be obtained from various open literature publications, BRL reports, and contract progress reports. Several of the latter are currently in process of publication, or are being prepared for publication.

#### CRYSTALLOGRAPHIC INFLUENCES

In low rate testing of metals, slip systems and fracture modes have been defined for various crystal structures. For instance, in face centered cubic materials deformation takes place on  $\{111\}$  type planes, in  $[100]$  type directions in these planes. Cleavage of these crystals occurs on  $\{100\}$  planes. In polycrystalline specimens, heavy preferred orientation will alter strength properties, depending on the direction of stress application compared to the direction of preferred orientation.

##### A. Expanding Cylinders of Aluminum

The analysis of low rate tests has led to a prediction of the results of high rate testing, if one assumes that metals do not act as fluids. Figures 1 through 4 show the results. Single crystal cylinders of aluminum (3 8" I. D. - variable O. D. ) are loaded internally with explosive, and framing camera pictures (at the rate of  $10^6$  frames per second) are made of the cylinders as they expand. Figure 1 shows a single crystal expanding, and it is easy to see the non uniform deformation.



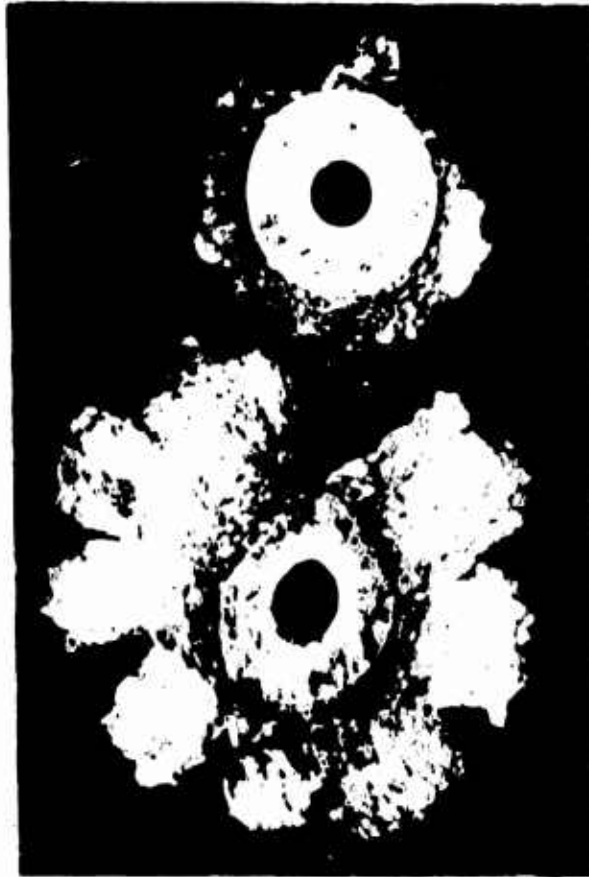
A

B

FIG. 3 - FRAMING CAMERA PICTURES OF AN EXPANDING ALUMINUM SINGLE CRYSTAL SHOWING NON-SYMMETRICAL DEFORMATION



A



B

FIG. 5 - ALUMINUM SINGLE CRYSTAL (A), AND POLYCRYSTALLINE (B)  
SPECIMEN AFTER INTERNAL LOADING

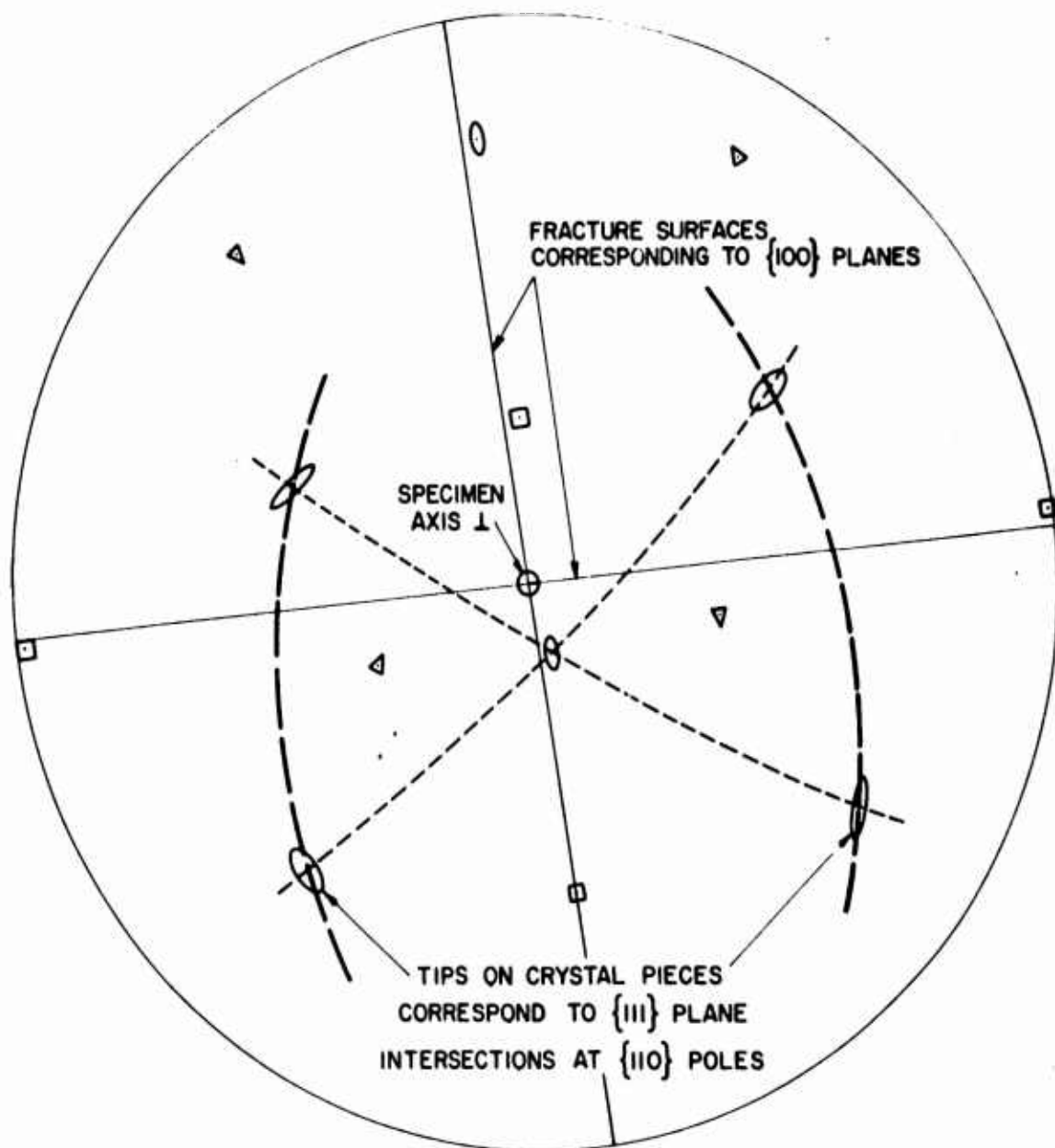


FIGURE 7. FRACTURE SURFACE AND INTERSECTION OF DEFORMATION PLANES SHOWN ON A STEREOGRAPHIC NET FOR CRYSTAL NO. 17.

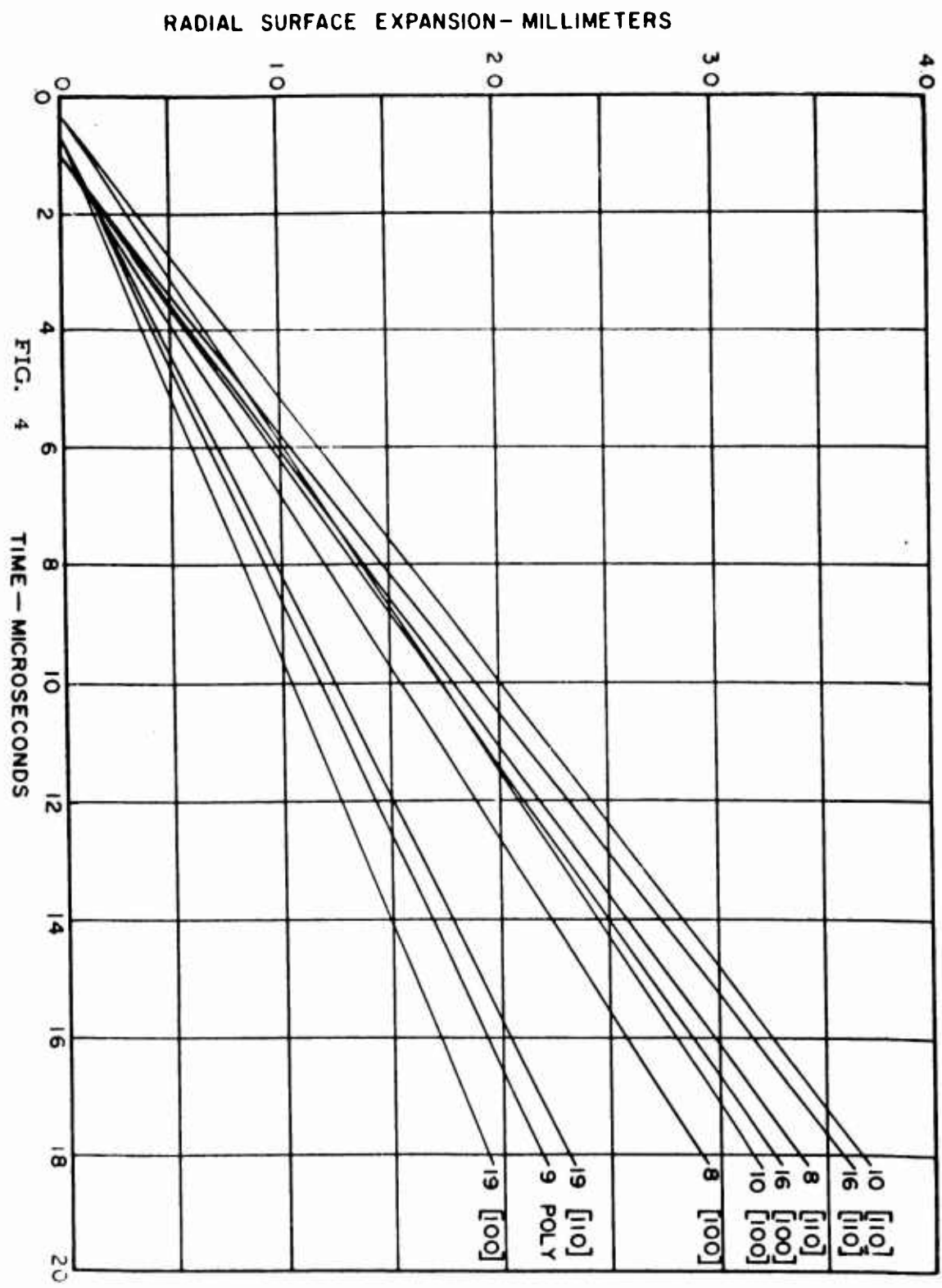


Figure 2 shows a fractured single crystal and a fractured polycrystalline specimen, of the same dimensions. Note the symmetry of fracture in the case of the single crystal, and the generalized deformation in the polycrystalline sample. Crystallographic analysis, using X-rays and metallographic observations, are seen in Figure 3. The single crystals deform on  $\{111\} [110]$  slip systems, and fracture on  $\{100\}$  planes, exactly as in slow rate tests. Figure 4 shows the results of analysis of the expansion of the cylinders along two radii,  $45^\circ$  apart. The single crystals are deforming anisotropically on the first tensile reflection of the shock wave.

The important point to note is that the pressure on the outside surface of these cylinders is approximately  $1.5 \times 10^5$  psi, while the strength of the metal is only approximately  $4 \times 10^3$  psi. At stresses two orders of magnitude greater than the strength of the metal, it still deforms crystallographically.

#### B. X-Ray Analysis

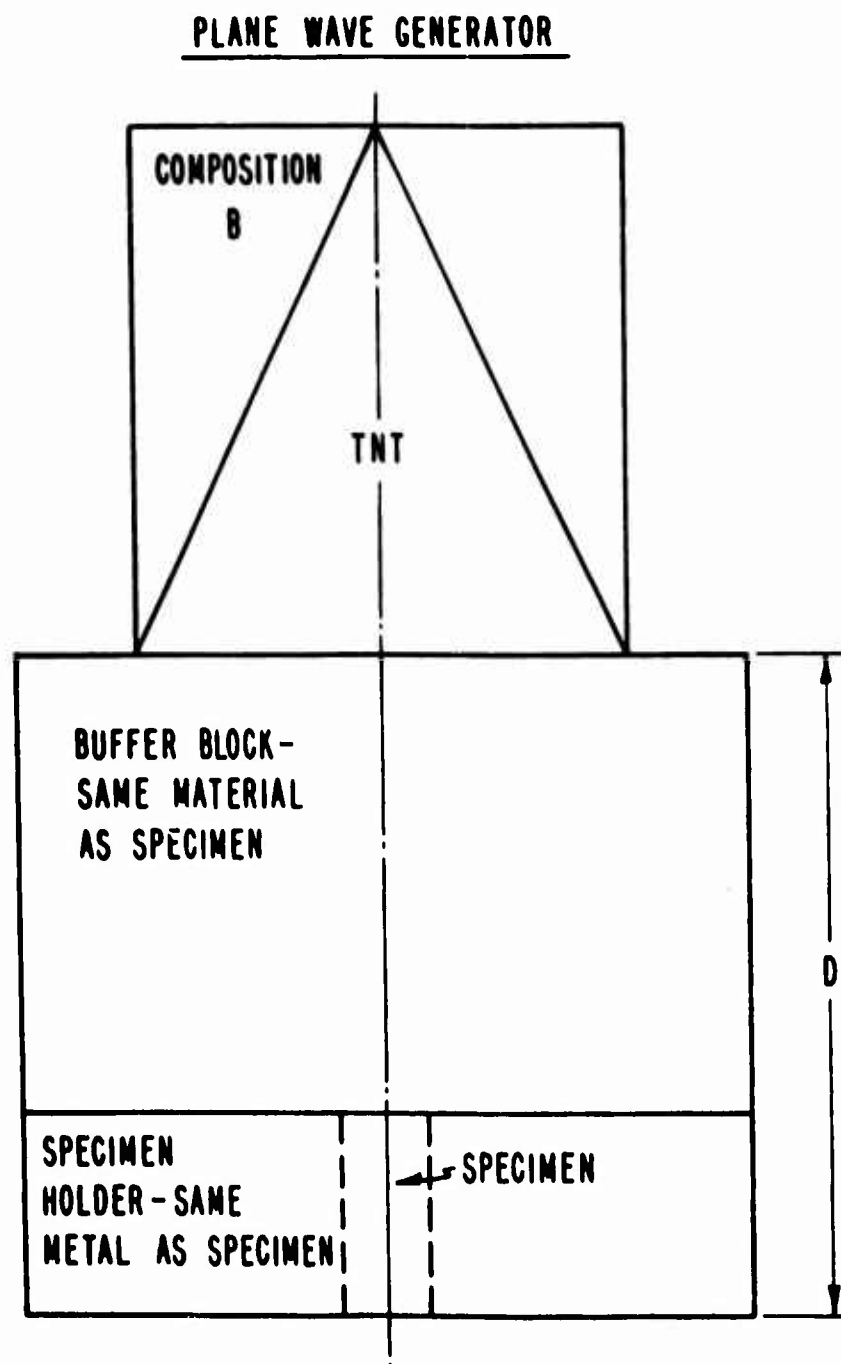
If the analogy is carried further, into polycrystalline specimens containing preferred orientation, analysis shows that in pressure ranges above 200 kilobars (or  $3 \times 10^6$  psi), the preferred orientation alters the deformation and fracture just as in the single crystal tests.

By making use of recrystallization experiments, where stress-grain distributions are correlated with strain analysis from X-ray studies, it has been possible to show that annealed and hardened copper reacts differently under high velocity shear deformation. Annealed materials deform according to a parabolic stress strain relation, while hardened materials deform linearly.

#### FRACTURE STRENGTHS

A second type of correlation is the strength of fracture of metals under high velocity loading. Figure 5 shows an experimental arrangement for fracturing specimens. The buffer thickness may be varied to give different stresses in the specimens. The reproducibility of the system has been determined as excellent. Figure 6 shows the remaining section of a single crystal that has been fractured by the reflected tensile wave. Note that it is necked down at the end where fracture and spall occurred. Single crystals neck down with a non-uniform cross-section. Polycrystalline metals neck down uniformly.

Analysis of the strain distribution has been made, and the ratio of cross-sectional area to original area is taken at the main fracture point and plotted vs. distance from the explosive. Figure 7 shows this plot.



SCHEMATIC OF THE EXPERIMENTAL ARRANGEMENT USED  
FOR SPALL AND FRACTURE STUDIES. DIMENSIONS OF  
THE PIECES ARE VARIABLE

FIG. 5



CROSS SECTION OF COPPER  
SINGLE CRYSTAL C-3



A/A<sub>0</sub> AT MAIN SPALL OR NECK VS. DISTANCE FROM H.E. TO FREE SURFACE

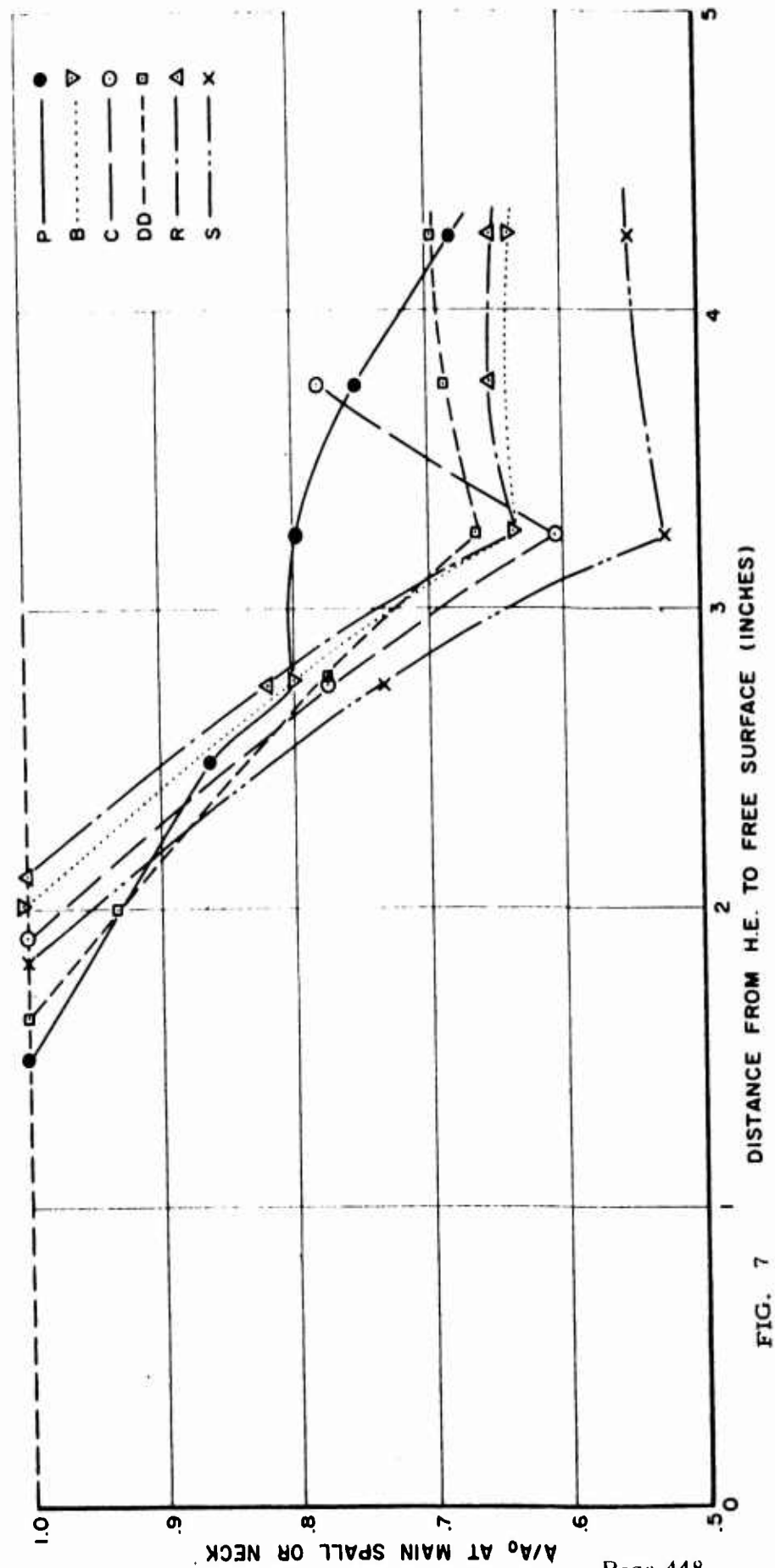


FIG. 7 DISTANCE FROM H.E. TO FREE SURFACE (INCHES)

By correlating distance with pressure in the reflected tensile pulse, the maximum stress at fracture may be obtained. Now, if the point where the curves in Figure 7 intersect the line  $\frac{\Lambda}{\Lambda_0} = 1$ , a theoretical strength

is obtained for the metal in the following manner:

Ignoring the initial specimen compression (which only adds a small correction) it is seen that, at  $\frac{\Lambda}{\Lambda_0} = 1$ , the specimen fractures without neck-down. In other words, no shear flow from the sides has occurred. Therefore, the metal has fractured in tension by separating metal bonds. The strength value for polycrystalline copper is  $2.11 \times 10^6$  psi. This may be compared to the original Frenkel value calculated from the modulus obtained at low rates: i. e.,  $\frac{E}{n}$  where  $n = 10$ . (His value was precisely,  $\frac{G}{2}$ ). The theoretical value is  $1.7 \times 10^6$  psi, a rather good correlation.

A surprising implication in this work is that, at high loading rates, high velocity dislocations do not play a role in the deformation. Mackenzies calculation of a theoretical strength of  $\frac{G}{30}$  (or  $\frac{E}{60}$ ), taking into account dislocations, does not appear to hold up at these loading rates.

## CONCLUSIONS

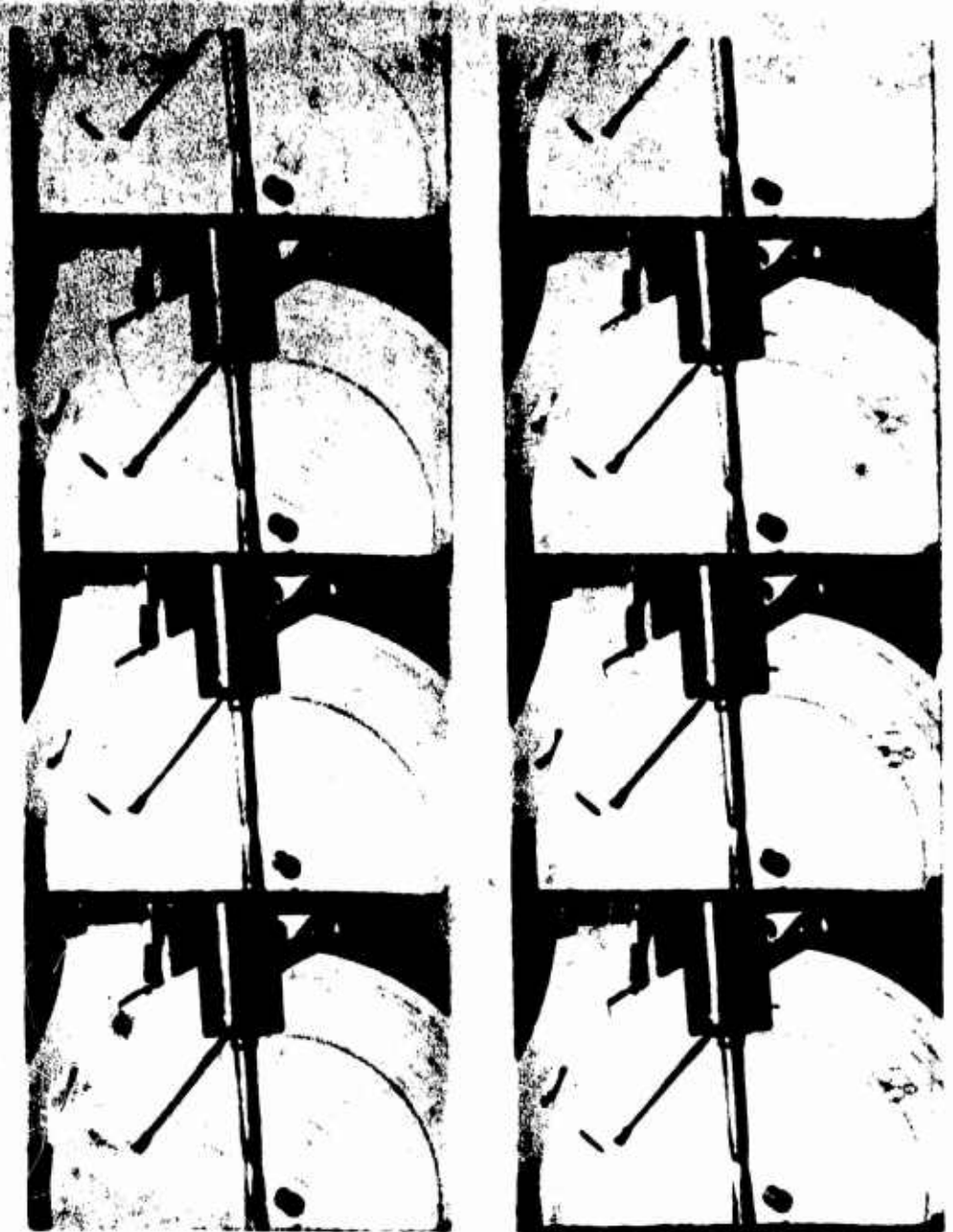
Numerous other correlations have been made, but time does not permit their discussion. A brief listing is made.

1. Using concepts from the theoretical analysis of Truesdale's concerning the velocity of small stress waves in a pre-stressed metal (as used by Bell for plastic waves) fracture times have been calculated at  $10^{-4}$  to  $10^{-5}$  seconds in the copper specimens just discussed.
2. Results from low strain rate tests, where motion pictures have been taken of the necked section, (seen in Figure 8), show the necked region to be volume consistent during deformation. The neck region is analyzed for strain changes during deformation, and a high velocity stress-strain curve, seen in Figure 9, is used to analyze the energy required for fracture of the necked down specimens subjected to explosive loading (previous section). Preliminary results have shown that spall and fracture are stress-time dependent, and not a function of stress only.
3. The last point that will be mentioned concerns hypervelocity impact. Curve A in Figure 9 is a high rate curve, generated from normal slow rate data shown in Figure 9, Curve B. In hypervelocity impact,

metal is deformed in a region around the crater. (See Figure 10). By using the curves in Figure 9, and analyzing the targets for strain distributions in the affected regions and the remainder of the block, an energy balance has been obtained, between incoming energy in the pellet and energy used in the target. The balance is within experimental error; 3%. Therefore, not only has a method been derived for analyzing metal target reaction to hypervelocity impact, but we are now in a position to predict reactions in untested targets.

In conclusion, it appears that the problem of high velocity metal deformation may be attacked in a fairly confident manner through examination of low velocity data. A few simple correlations have been derived from theoretical and experimental considerations.

It remains to carry the data further in obtaining more exact quantitative correlations, and to derive rules that may be used to make general predictions concerning high velocity metal reactions. At the same time, methods will have to be found to incorporate the type of results and analyses discussed here into formal non-linear mechanics theory.



STANDARD TENSILE TEST SHOWING SPECIMEN NECK DOWN

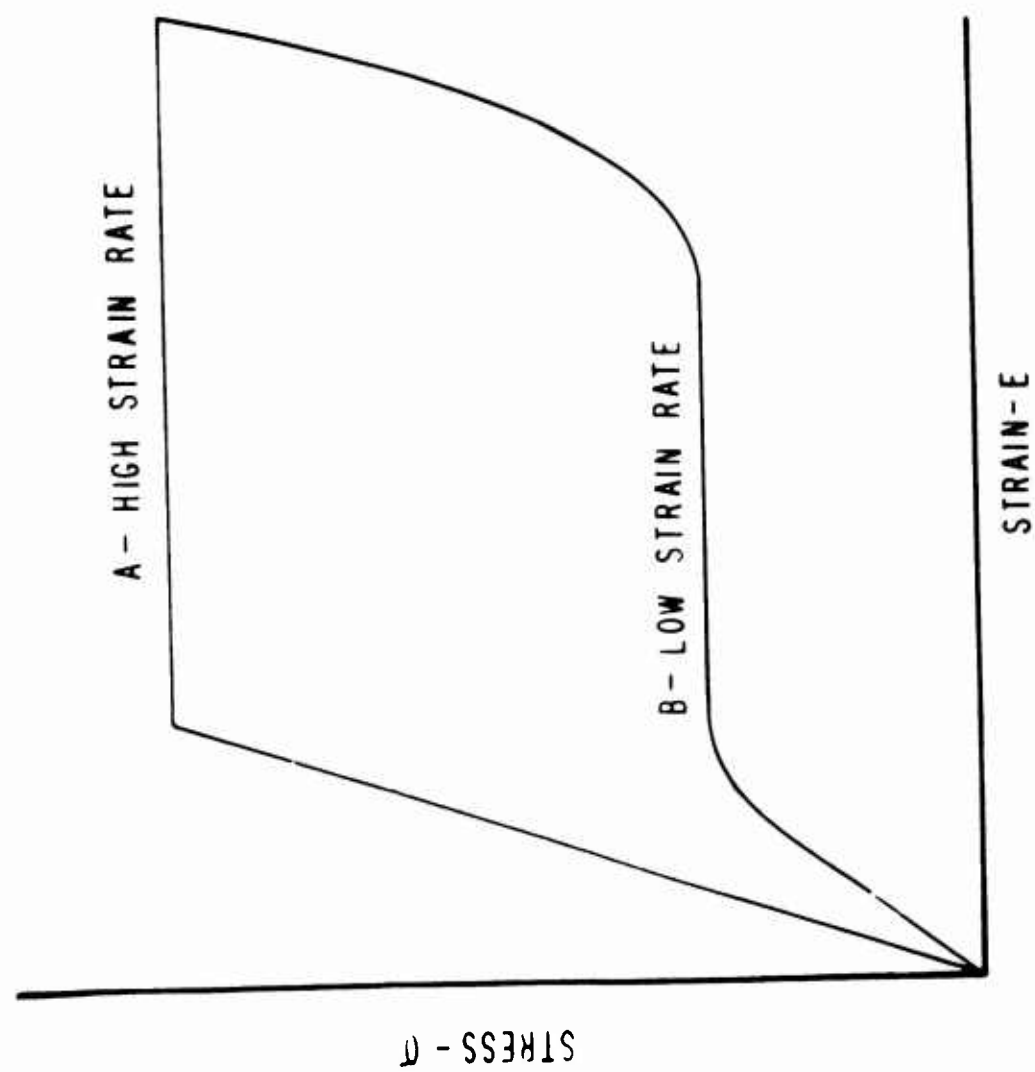
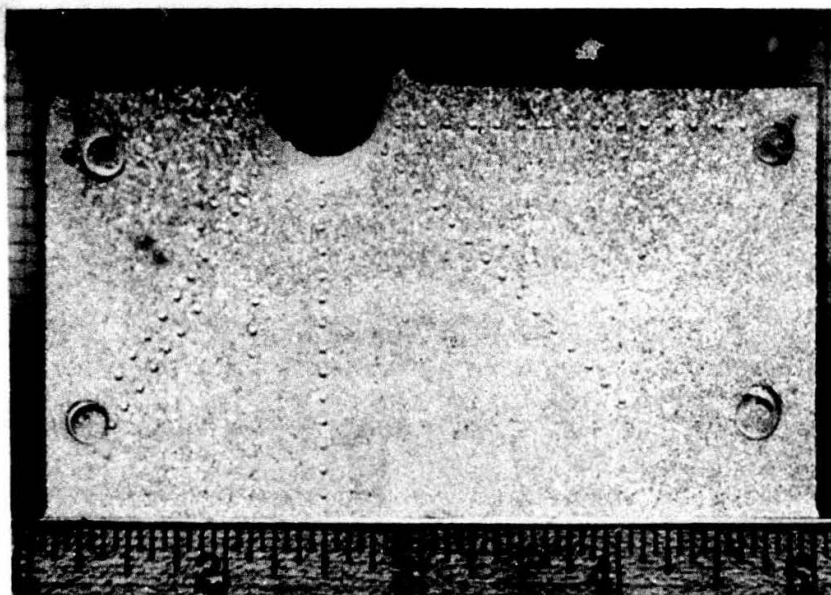


FIG. 9 RATE SENSITIVITY OF STRESS-STRAIN CURVES



CROSS-SECTION OF A COPPER CYLINDER IMPACTED BY A  
0.18 GRAM PELLET AT 5 KM/SECOND

## RESPONSE OF CYLINDRICAL SHELLS EXPOSED TO EXTERNAL BLAST LOADING

William J. Schuman, Jr.\*

### ABSTRACT

A method of predicting permanent deformation of thin-walled unstiffened cylindrical shells exposed to external blast loading from charges of high explosive is presented. Empirical relations are derived from a series of firings conducted primarily at the Aberdeen Proving Ground, against scaled shells. The average deviation between predicted and actual pressures is 3%.

### INTRODUCTION

The Terminal Ballistics Laboratory of the USA Ballistic Research Laboratories has as part of its mission the determination of the response of structures to blast loading. An investigation of the response of thin-walled cylinders to external blast loading was initiated as a basic study of simple structures that have many practical applications.

A survey of previous work indicated that some analytical studies had been made by Brooklyn Polytechnic Institute<sup>1</sup> and Columbia University.<sup>2</sup> However, the loading and boundary conditions were not those of interest and there was no experimental correlation. The Space Technology Laboratories<sup>3</sup> have conducted tests on Mylar cylinders, but their loadings were uniform and the rise times were much slower than those obtained from blast. AVCO Corporation<sup>4</sup> has used sheet explosive applied to segments of the surface of a cylinder to obtain deformation. Southwest Research Institute<sup>5</sup> has also looked at this problem but the experimental work was conducted with one model. Suffield Experimental Station<sup>6</sup> is investigating the details of blast loading of various simple structures including cylinders.

It was determined that the first part of this investigation be concerned with the development of an empirical method of predicting the required pressure necessary to cause permanent deformation to a spectrum of cylindrical configurations and materials. This paper presents the first results of this phase of the investigation.

---

\* William J. Schuman, Jr., Aeronautical Research Engineer, Terminal Ballistics Laboratory, Ballistic Research Laboratories, Aberdeen Proving Ground, Maryland.

## TEST ARRANGEMENT AND PROCEDURE

The cylindrical shells are fabricated from 1040 hot-rolled steel sheet and 2SO and 5052-H38 aluminum foil. The steel shells are formed and butt-welded while the aluminum shells are soldered or taped depending on thickness. The shells are clamped over heavy end caps with a heavy rod through the center of these caps to minimize bending. A typical shell specimen is shown in Figure 1. The diameters vary from 3 to 34 inches, the lengths from 2 to 47.25 inches, the thicknesses from 0.003 to 0.136 inches; giving diameter-to-thickness ratios of 60 to 2000 and length-to-diameter ratios of 0.67 to 10. Many of the shells are geometrically scaled. The dimensions of the shells are listed in Table I.

The shells are mounted at a height of 8 feet to minimize ground effects as shown in Figure 2. They are oriented so that the blast loading impinges on the shells either along a line perpendicular to the longitudinal axis-lateral loading or along an extension of the longitudinal axis-longitudinal loading. A nose cone is added to the shell for the longitudinal loading orientation to minimize disturbance of the flow.

The blast loading is provided by charges of high explosive ranging in weight from one pound to 79,000 pounds. The smaller weights are bare spherical Pentolite while the larger charge weights are bare blocks of TNT. The smaller charges are suspended as shown in Figure 2 while the larger charges are placed on the ground.

The free air blast parameters; overpressure, impulse and duration are determined by use of tabulated data and measured by piezoelectric gages for the larger charges.

A number of shells are positioned about a charge at pressure levels that will not cause permanent deformation. The distances between the shells and the charge are decreased until optimum permanent deformation, approximately 10% of the diameter is obtained.

## RESULTS

The values of pressure and impulse were determined at those distances for which optimum deformation was obtained. The values for lateral loading are listed in Table I along with the shell dimensions and are plotted in Figure 3. Iso-damage curves are drawn through those points that represent various combinations of pressure and impulse for equivalent deformation of a given material and shell configuration. (See points 2-3-4-5, 14-15-16, 38-39-40, etc.) These curves are the boundaries between the damage and no-damage regions. The relationship between pressure and



RESPONSE OF CYLINDERS EXPOSED TO EXTERNAL BLAST LOADING

TABLE I. PRESSURE-IMPULSE DATA FOR LATERAL LOADING

Cyl. No.	Dia. D (in)	Length L (in)	Thickness t (in)	Charge Weight w (lb)	Charge Dist. d (ft)	D/t	L/D	Material	Incident Pressure P <sub>i</sub> (psi)	Incident Impulse I <sub>i</sub> (psi-msec)
1	3	6.0	0.019	389	29.0	158	2.0	Steel	48.5	86.0
2	3	8.62	0.019	1.1	2.5	158	2.87	1040	159	15.5
3	3	8.62	0.019	8.4	7.0	158	2.87		82.4	26.9
4	3	8.62	0.019	64	16.0	158	2.87		58.0	48.8
5	3	8.62	0.019	389	33.8	158	2.87		41.0	85.5
6	3	11.62	0.019	1.1	3.0	158	3.87		118	14.5
7	3	11.62	0.019	8.4	8.0	158	3.87		60.3	25.4
8	3	14.62	0.019	1.1	3.5	158	4.87		82.4	13.4
9	3	14.62	0.019	8.3	9.0	158	4.87		44.8	21.6
10	3	18.0	0.019	389	46.0	158	6.0		17.4	65.0
11	3	8.62	0.035	8.4	4.5	86	2.87		213	32.6
12	3	9.00	0.035	389	23.9	86	3.0		94.0	101
13	6	18.0	0.019	389	44.0	79	3.0		21.8	67.0
14	6	17.50	0.035	8.4	5.8	172	2.91		130	29.6
15	6	17.50	0.035	64	14.0	172	2.91		79.2	52.0
16	6	18.0	0.035	389	28.0	172	3.0		63.0	92.0
17	6	17.50	0.076	8.4	3.0	79	2.91		463	35.5
18	6	17.50	0.076	64	9.0	79	2.91		209	64.0
19	6	18.0	0.076	389	18.0	79	3.0		147	110
20	12	35.38	0.076	389	25.0	158	2.94		83.8	98.8
21	12	35.38	0.136	389	15.0	88	2.94		257	118
22	24	47.25	0.136	389	25.0	176	1.98		83.8	98.8
23	2.5	4.5	0.008	54.5	23.1	313	1.8	Tin/Steel	19.7	33.2
24	6	24.0	0.018	79,000	-	333	4.0	Aluminum*	11.3	290
25	7.5	7.5	0.063	389	25.0	119	1.0	Aluminum*	83.8	93.8
26	7.5	7.5	0.125	389	16.0	60	1.0	Aluminum*	242	117
27	3	6.0	0.003	389	178	1000	2.0	Aluminum	1.87	17.5
28	3	9.0	0.003	389	200	1000	3.0	5052 H-38	1.76	15.7
29	3	9.0	0.006	389	106	500	3.0		4.26	29.2
30	3	30.0	0.006	389	172	500	10.0		1.94	18.2
31	6	18.0	0.003	389	350	2000	3.0		0.82	9.60
32	6	18.0	0.006	389	150	1000	3.0		2.47	21.2
33	3	9.0	0.006	1.1	16.0	500	3.0	Aluminum	3.53	3.90
34	3	9.0	0.006	15.0	60.0	500	3.0	250	1.91	5.93
35	3	9.0	0.006	389	275	500	3.0		1.07	11.7
36	3	12.0	0.006	1.0	20.0	500	4.0		2.57	3.06
37	3	9.0	0.010	15.0	40.7	300	3.0		3.24	8.58
38	3	9.0	0.012	1.1	10.0	250	3.0		7.94	6.02
39	3	9.0	0.012	15.0	15.0	250	3.0		3.97	10.1
40	3	9.0	0.012	389	160	250	3.0		2.07	19.7
41	6	6.0	0.012	389	160	500	1.0		2.07	19.7
42	6	11.0	0.012	389	200	500	1.8		1.76	15.7

\* Type of Aluminum unknown

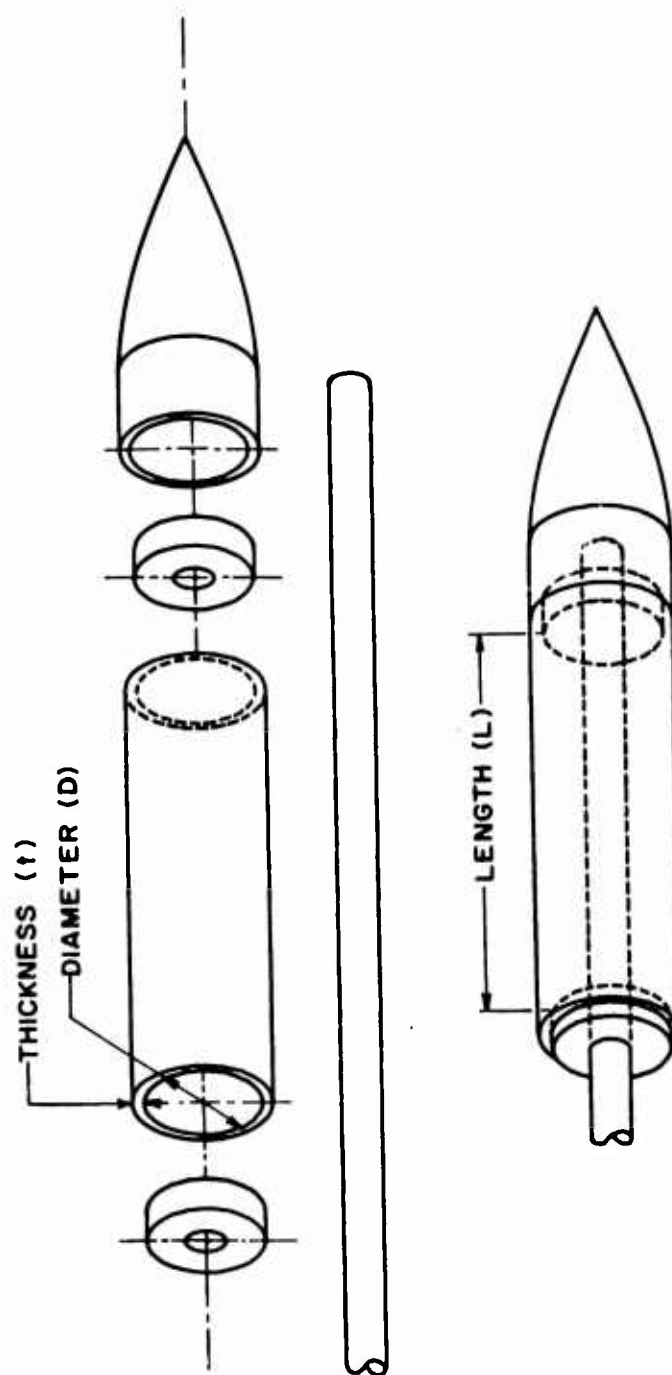


FIG. 1 - TYPICAL SHELL SPECIMEN

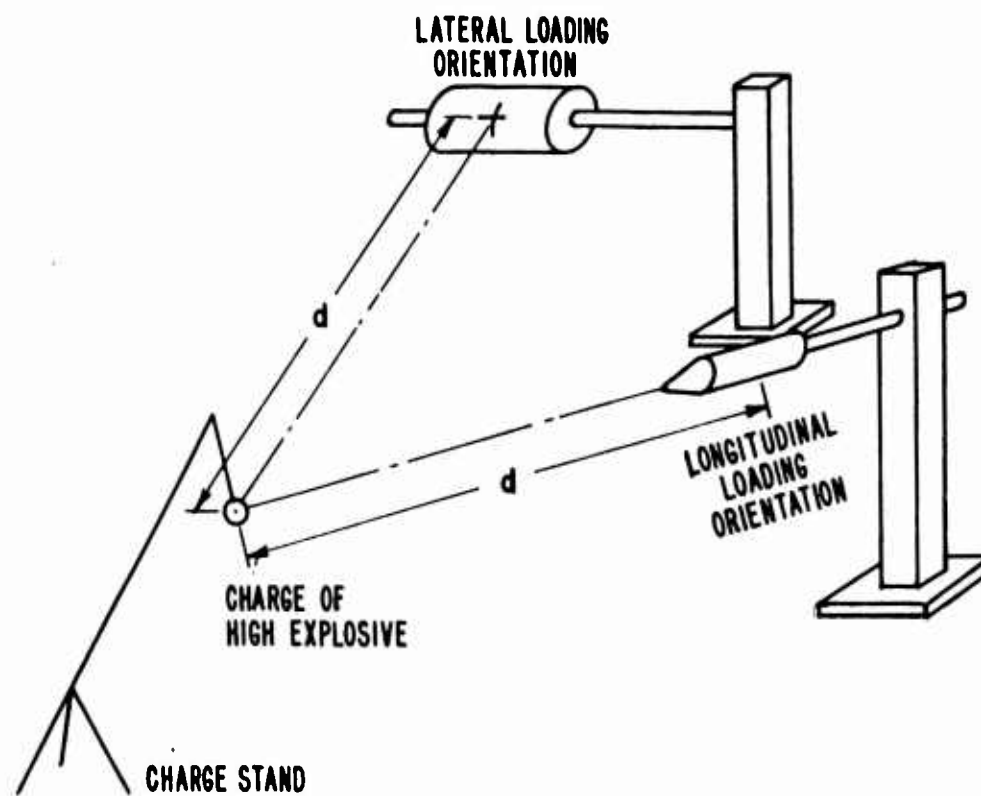


FIG. 2 - TYPICAL FIELD ARRANGEMENT

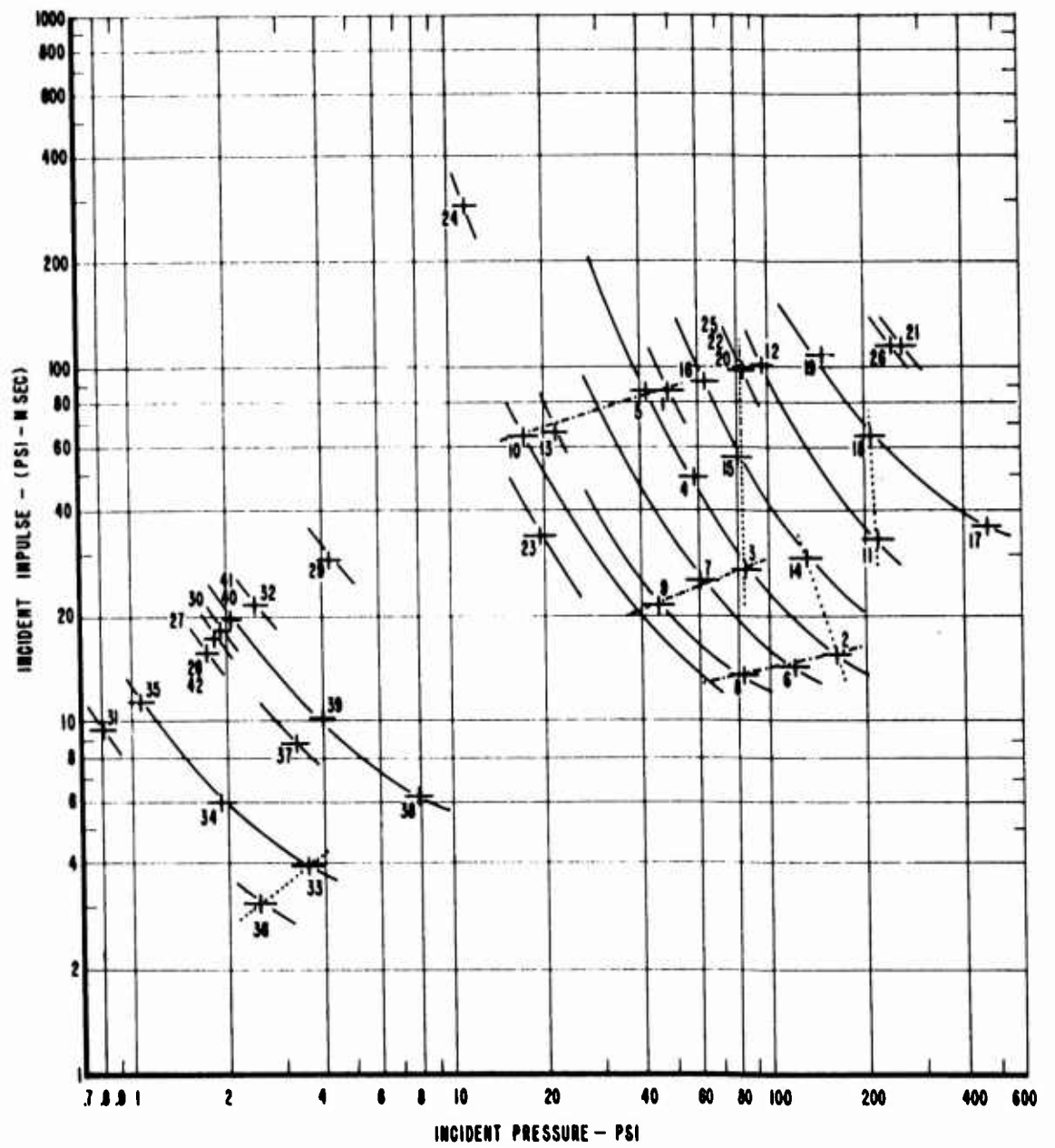


FIG. 3 - ISO-DAMAGE CURVES FOR LATERALLY-LOADED CYLINDERS

charge weight can be determined from these curves.

The dash-dot lines connect points representing only a change of shell length. (See points 2-6-8, 3-7-9, etc.). The relationship between pressure and length or pressure and length-to-diameter ratio can be determined from these curves. The relationships between pressure and diameter, thickness and material can also be determined.

There are two basic types of deformation patterns from lateral loading. The thicker shells deform in one lateral-type pattern as shown in Figure 4. This pattern becomes deeper and spreads toward the end caps as the pressure is increased. The thinner shells deform in a number of longitudinal lobes which increase in length and number with the pressure. The first lobe is shown in Figure 5.

The near vertical dotted lines shown in Figure 3 indicate that the "geometrical" modeling laws apparently hold for these large deformations. Referring to Figure 3, Figure 6 and Table I: point 3 represents a cylinder of given geometry (3" dia., 8.62" length, 0.019" thickness) with a charge weight of 8.4 lb. positioned at a distance of seven feet. Using a model or scale factor of 2 we would expect equivalent deformation of a cylinder whose dimensions have been multiplied by the scale factor 2 (point 15: 6" dia., 17.50" length, 0.035" thickness) with a charge weight of 64 lbs. (that is:  $W \propto d_w^3$  or  $d_w \propto \sqrt[3]{W}$  and  $d_w \propto \sqrt[3]{8.4} \propto 2$  and therefore  $W_2 \propto K^3 \times d_w^3 \propto 2^3 \times 2^3 \propto 64$ ) located at a distance of  $7 \times 2 = 14$  feet. These two points do represent equivalent deformation as does point 20 on the same curve and as do points 2-14 and 11-18 on their respective dotted curves.

There are only two data points for longitudinal loading. These indicate that the critical pressures for lateral loading must be multiplied by a factor of  $\lambda$  where  $3.1 \leq \lambda \leq 5.6$ .

The relationships between the critical pressure and the various parameters have been determined empirically and a graphical presentation made so that the critical pressure may be determined if the material and geometry of the shell and the charge weight are known. The necessary curves are shown in Figures 7 and 8.

The three curves of Figure 7 are plots of the length-to-diameter ratio- $L/D$  vs. critical incident pressure- $p_i$  for the three materials tested: steel and the two aluminums. Each of the three curves is based on a change of  $L/D$  for a constant charge weight of one pound, a diameter of three inches and a constant thickness: steel = 0.019 in. and aluminum = 0.006 in.

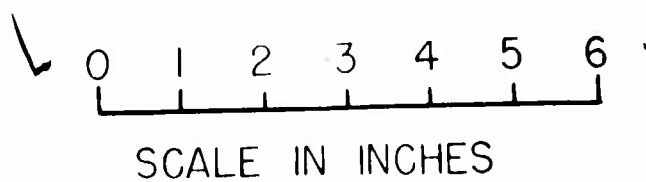
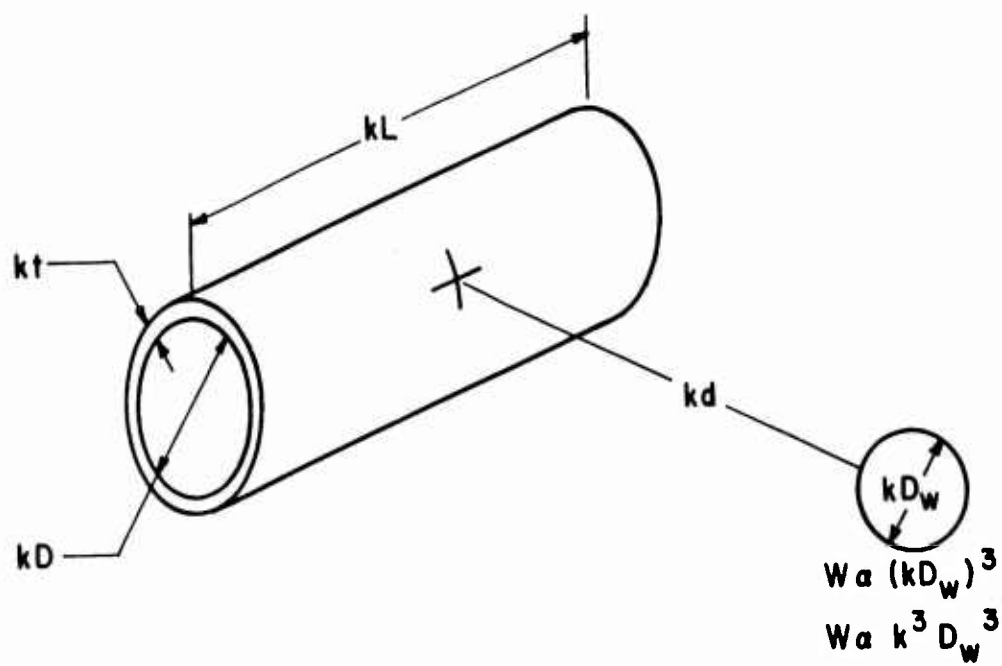
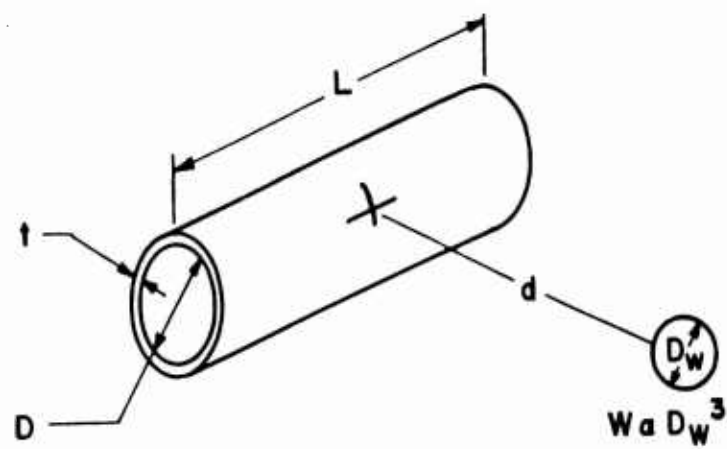


Fig. 4 Typical Lateral-Type Deformation



**FIG. 6 - SCALING PARAMETERS**

The correction factors for variations of these three parameters: diameter, thickness and charge weight are given in Figure 8. The required pressure would then be:

$$P_{cr} = p_i K_w K_t K_D$$

where

$P_{cr}$  - critical pressure

$p_i$  - Incident Pressure (Fig. 7)

$K_w$  - correction factor for charge weight (Figure 8)

$K_t$  - correction factor for thickness (Figure 8)

$K_D$  - correction factor for diameter (Figure 8)

As an example consider shell 16:

It is steel and  $L/D = 3.0$ ,  $p_i = 154$  psi

Also  $D = 6.0$   $D/3 \times 10 = 20$  and  $K_D = 0.57$

$t = 0.035$   $\frac{t}{0.019} \times 10 = \frac{0.035}{0.019} \times 10 = 18.4$  and  $K_t = 2.58$

$W = 389$   $K_w = 0.279$

Therefore  $P_{cr} = p_i K_w K_t K_D$

$$= (144) (0.279) (0.035) (0.57)$$

$$P_{cr} = 63.2 \text{ psi}$$

The actual pressure was  $p_i = 63.0$  psi. Therefore, the deviation of the predicted value from the actual value is 0.3%.

The average deviation between predicted and actual pressures is 6% with a spread of -20% to 46%.

## CONCLUSIONS

The first phase of an investigation of the response of thin walled cylinders exposed to blast loading has resulted in an empirical method of predicting the critical pressure required to cause permanent deformation. The correlation of predicted and actual pressures is good with an average deviation of 6%.

Further testing is planned. A series of 10 to 12 firings in the 1000 lb. to 30,000 lb. charge-weight region will be conducted at the Yuma Test Station the latter part of 1962. It is anticipated that additional data will be obtained by participation in the 500 ton firing to be conducted in Canada



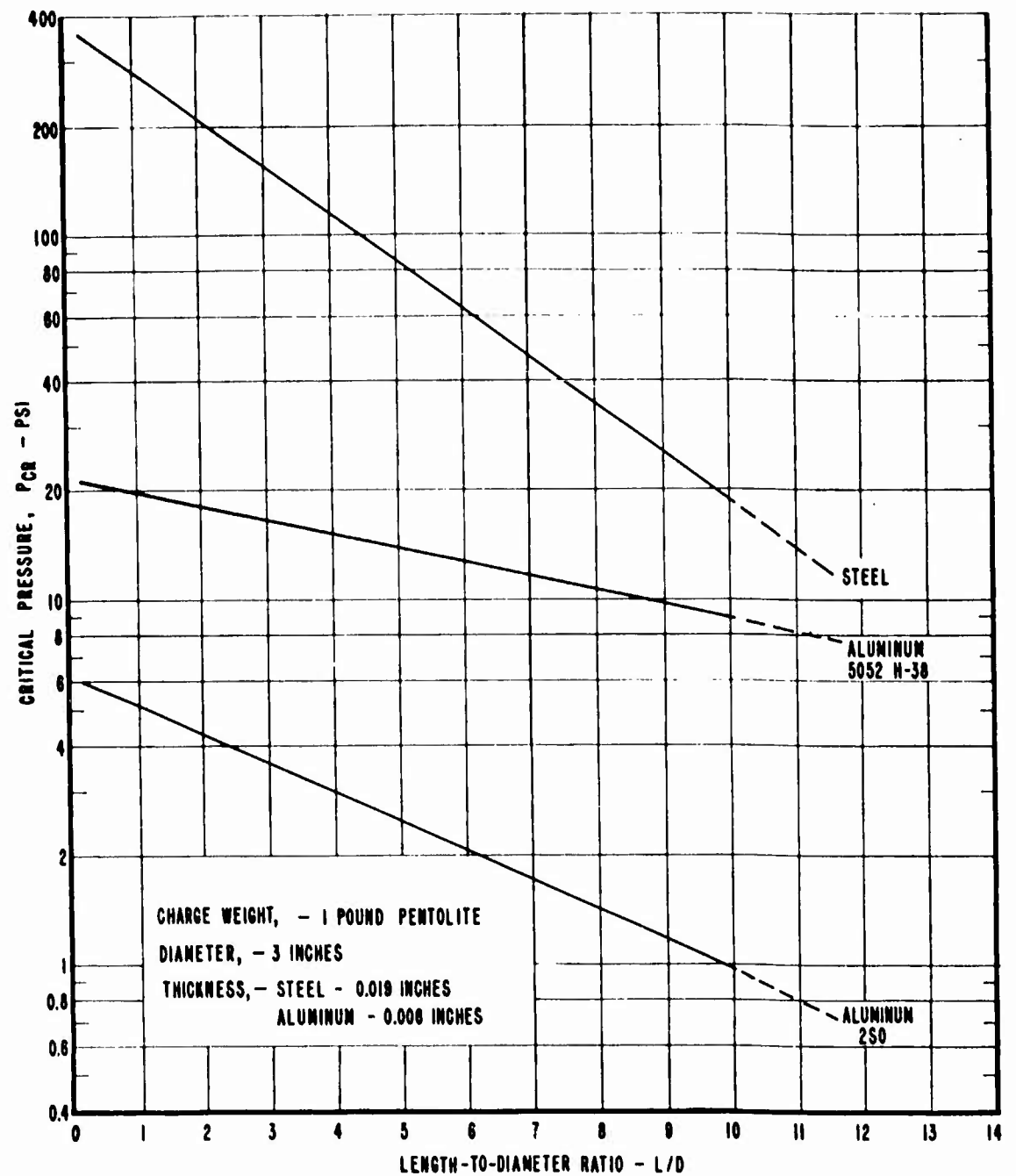
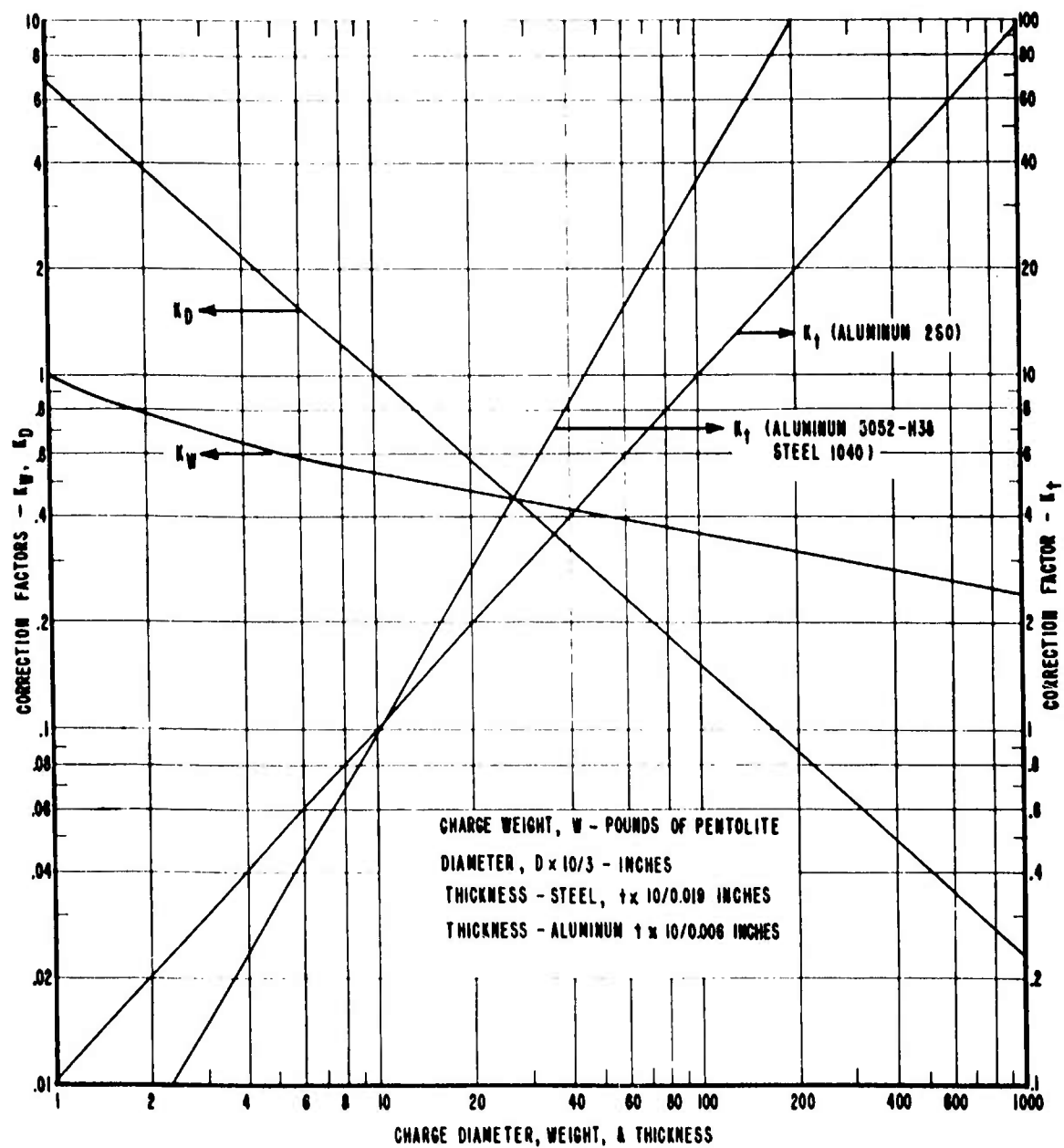


FIG. 7 - CRITICAL PRESSURE VS. DIAMETER-TO-LENGTH RATIO



**FIG. 8 - CORRECTION FACTORS FOR VARIATIONS  
IN CHARGE WEIGHT, DIAMETER, & THICKNESS**

during the summer of 1963. Some preliminary work has begun on instrumenting the shells with strain and pressure gages for more precise determinations of response and loading. These results will be used in the concurrent analytical studies.

This study is sponsored by the Defense Atomic Support Agency.

#### REFERENCES

1. Hodge, P. G. "Impact Pressure Loading of Rigid-Plastic Cylindrical Shells," Polytechnic Institute of Brooklyn Report No. 255, May 1954.

Hodge, P. G. "Ultimate Dynamic Load of a Circular Cylindrical Shell," Polytechnic Institute of Brooklyn Report No. 265, Nov. 1954.

Hodge, P. G. "The Influence of Blast Characteristics on the Final Deformation of Circular Cylindrical Shells," Polytechnic Institute of Brooklyn Report No. 266, Dec. 1954.

Sankaranarayanan, R. "Dynamic Response of Plastic Circular Cylindrical Shells Under Lateral and Hydrostatic Pressures," Polytechnic Institute of Brooklyn Report No. 573, June 1961.

2. Mindlin, R. D. and Bleich, H. H. "Response of an Elastic Cylindrical Shell to a Transverse Step Shock Wave," Technical Report No. 3, Contract NONR-266(08), Columbia University, March 1952.

Baron, M. L. and Bleich, H. H. "Further Studies of the Response of a Cylindrical Shell to a Transverse Shock Wave," Technical Report No. 10, Contract NONR-266(08), Columbia University, Dec. 1953.

Bleich, H. H. and Dimaggio, F. L. "Dynamic Buckling of Submerged Plates and Shells," Technical Report No. 12, Contract NONR-266(08), Columbia University, Sept. 1954.

3. Seide, P., Weingarten, V. I. and Morgan, E. J. "Final Report on the Development of Design Criteria for Elastic Stability of Thin Shell Structures," Space Technology Laboratories, AFBMD/TR-61-7, Dec. 1960. "Final Report on Buckling of Shells Under Dynamic Loads," Final Report, Contract NASr-56, Space Technology Laboratories, Oct. 1961.
4. Radkowski, P. P. et al "Studies on the Dynamic Response of Shell Structures and Materials to a Pressure Pulse," AVCO Corporation, AFSWC-TR-61-31 (II), July 1961.

5. Dellart, R. C. and Basdekas, N. L. "Response of Aircraft Fuselages and Missile Bodies to Blast Loading," Southwest Research Institute, ASD-TDR-62 - Preprint, Mar. 1962.
6. "Scientific Observations on the Explosion of a 20 Ton TNT Charge, Volume One, General Information and Measurements," Report No. 203, Suffield Experimental Station, Ralston, Alberta, Sept. 1961.

#### DISCUSSION

Francis B. Paca, U. S. Army ERDL, Ft. Belvoir, Va: I would hazard a guess that your higher pressures and your larger L/D rate shows that you have quite a differential pressure from the front to the end of the cylinder. Have you ever tried this same thing in the shock tube where there is no change in pressure?

Mr. Schuman: You are speaking about the longitudinal loading?

Mr. Paca: Yes, sir.

Mr. Schuman: We have done very little firing with longitudinal loading. Most of it has been done with lateral loading. We will probably run into a problem when we get into the longitudinal loading.

Ulric S. Lindholm, Southwest Research Institute: I have a two-part question. First, how did you manufacture the thin-walled cylinders? And secondly, what effect, if any, did eccentricity of the cylinder have on the buckling pressures?

Mr. Schuman: The steel cylinders we tested so far were cold-rolled and butt-welded. The aluminum ones, being very thin foil, were rolled and we used an army gun tape to hold them together. Since we were firing the lateral orientation, we have put the seam on the back side, away from the charge, and it did not effect our results. We have obtained, after many months, very thin seamless aluminum tubing. But it is quite a procurement problem to get it thin enough to be of practical use to us. We have not checked the eccentricity. We have conducted a fairly simple test for now and we were pleased that the results have turned out as well as they have. We hope when we get the instrumented test, that they will show as well.

## PHOTOELASTIC STUDIES OF DYNAMIC STRESSES IN LOW MODULUS MATERIALS

P. D. Flynn\*, J. T. Gilbert\*\*, A. A. Roll\*\*\*

### ABSTRACT

In 1960, the Frankford Arsenal began a new program in dynamic photoelasticity using low modulus materials subjected to either mechanical or explosive loads. High-speed photographic techniques were used to obtain full-image dynamic stress patterns at approximately 7500 pictures per second and exposures of 1.3  $\mu$ sec. Recently, a dual-polariscope was designed for obtaining simultaneous views of a specimen at normal and oblique incidence. This paper reviews the techniques developed for this work, discusses the results of fundamental studies on stress distributions under dynamic conditions, and outlines future plans.

### INTRODUCTION

When using high-speed photography in dynamic photoelasticity, the exposures must be short enough to "stop" the motion, and the exposure time required to prevent blurring of the image can be calculated from the speed of stress waves, e. g.,  $c = \sqrt{\frac{E}{\rho}}$  for longitudinal waves, where  $E$  is Young's modulus and  $\rho$  is the density. In order to resolve higher order fringes, monochromatic light must be used because white light and colored stress patterns "wash-out" for fringe orders greater than about five. These two requirements of dynamic photoelasticity, namely short exposures and monochromatic light, make it somewhat difficult to obtain satisfactory dynamic stress patterns.

In spite of these difficulties, there has been a good deal of interest and activity in dynamic photoelasticity over the past thirty-five years, and even a partial list of recent papers is rather extensive (1-8, 10-13). One approach is

---

\* P. D. Flynn, Physicist (Mechanics), Frankford Arsenal, Philadelphia, Pennsylvania.

to use "soft" or low modulus photoelastic materials in which the speed of stress waves is relatively slow ( $c \sim 0.002$  in/ $\mu$ sec) and conventional high-speed photography. Using a Fastax Camera, Perkins<sup>1</sup> photographed stress waves in photoelastic rubber and Dally, Riley, and Durelli<sup>2</sup> recommended urethane rubber for dynamic studies. Another approach is to use "hard" or high modulus photoelastic materials ( $c \sim 0.1$  in/ $\mu$ sec) and ultra-high-speed photography. Christie<sup>3</sup> and Wells and Post<sup>4</sup> used a multiple-spark, multiple-lens camera of the Granz-Schardin type; Feder, Gibbons, Gilbert, and Offenbacher<sup>5</sup> used the Beckman and Whitley high-speed framing camera; and Frocht and Flynn<sup>6,7</sup> employed the method of streak photography. A third approach is to use photoelastic coatings, and Cole, Quinlan, and Zandman<sup>8</sup> used this technique with the Beckman and Whitley 189 camera.

In general, the results obtained by dynamic photoelasticity have been limited mainly to free boundary stresses and to interior secondary maximum shears. The determination of the individual components of stress is a fundamental problem in photoelasticity, and the method of oblique incidence used by Drucker<sup>9</sup> to separate the principal stresses under static conditions is direct and promising for dynamic work because it requires only the measurement of fringe orders,<sup>10</sup>. This method was used by the authors to determine the principal stresses in a low modulus photoelastic material subjected to either mechanical or explosive loads,<sup>11,12,13</sup>.

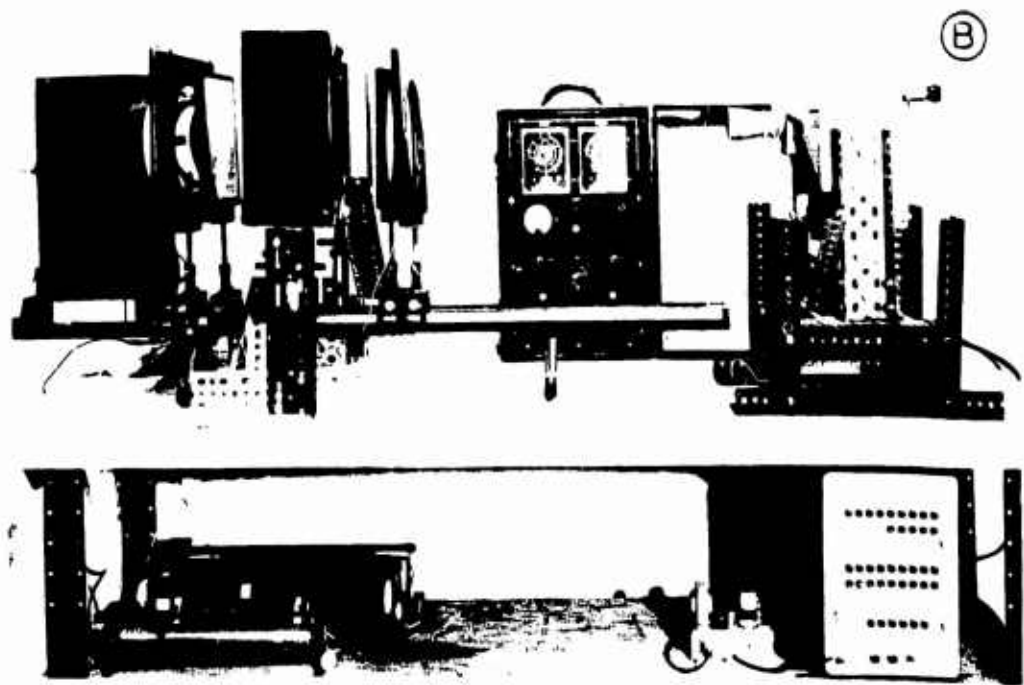
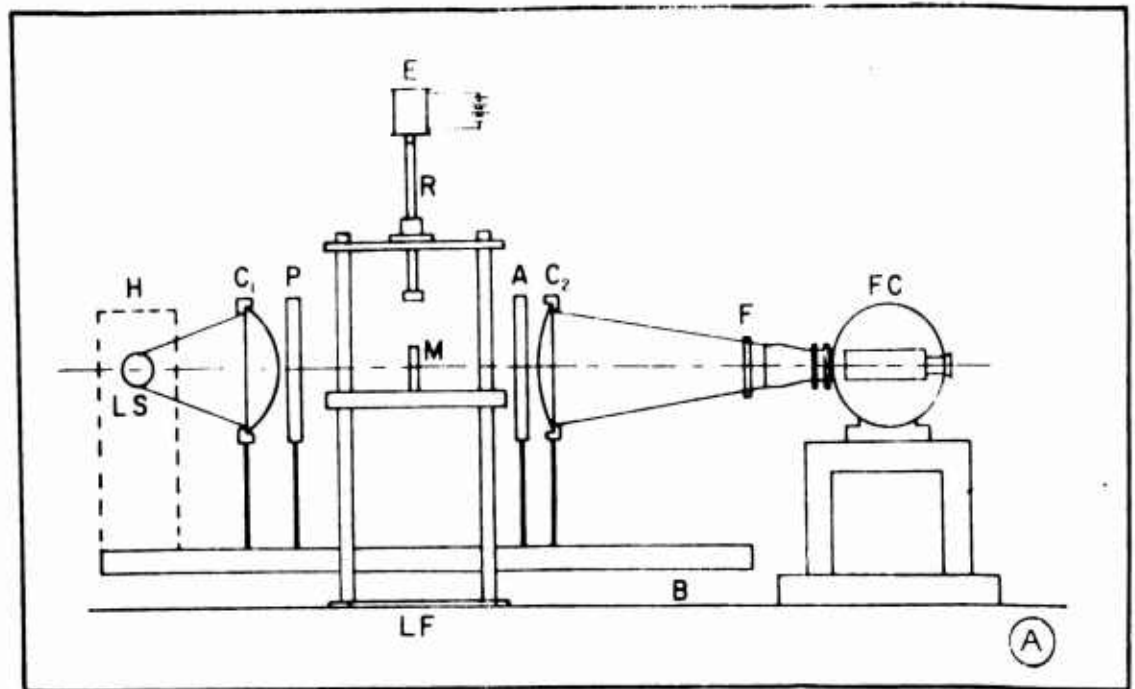
This paper deals with the results of basic research in dynamic photoelasticity and with studies of stress wave propagation and impact phenomena in two-dimensional configurations. The objectives were to develop new techniques in dynamic photoelasticity and high-speed photography and to obtain new information on stress distributions under dynamic conditions. A knowledge of such stresses is of fundamental importance in theories of strength and rational design.

## PART I

### NORMAL AND OBLIQUE INCIDENCE PHOTOGRAPHS FROM REPEATED TESTS

#### Equipment and Techniques

Polariscope. A lens-type polariscope was designed and assembled for this work. Figure 1(a) is a sketch showing the arrangement of the optical elements of the polariscope and the mechanical loading system, whereas Figure 1(b) is a photograph of the polariscope with the explosive loading system. The light source was a direct current (7.3 amps, 220 volts), small arc (4.5 x 2.3mm), 500 w. mercury lamp (Osram, Type HBO 500) which operated in series with a ballast resistor (22 ohms). The lamp was placed



78.271.52579.080.62.

at the focus of a condenser lens (8" diameter, 10" focal length) which gave a collimated field having an efficient use of the available light. The polarizer and analyzer were made from a sheet of plastic laminated circular polarizer (Polaroid, Type HNCP 37). A collector lens (8" diameter, 18" focal length) was used to converge the light into the camera lens, and in order to obtain a uniform field, the camera lens was placed at the focus of the collector lens. The camera lens (Wollensak, WF-100A, 25.4mm,  $f/2.3$ ) was chosen so that the image of the model filled the available frame in the camera.

Mechanical Loading System. The mechanical loading system sketched in Figure 1(a) consisted essentially of a platform to support the model and an impact rod for striking the specimen. The impact rod was guided by a vertical ball bushing, and the height of fall or drop was adjusted by changing the position of the electromagnet. Rods of different length and weight were used to vary the intensity of the loading. The striking end of the impact rod was designed to apply a uniform load across the full thickness of the model, and the design used depended on the configuration of the specimen under test. A typical impact rod is shown in Figure 2.

Explosive Loading System. Explosive loads were applied to a photoelastic model placed inside a metal firing box equipped with safety glass windows, Figure 1(b). The axis of symmetry of the photoelastic model was placed in line with the axis of the firing head assembly, and after aligning the model, the vertical position of the firing head was adjusted so that it was just in contact with the top of the specimen. Explosive loading was produced by a one grain M52A5 electric primer which was detonated by 135 volts D.C. Details of the firing head assembly are shown in Figure 2. The blast from the primer was transmitted directly to the model through a  $3/16$ " hole, and a slot  $1/16$ " wide and  $1/16$ " deep in the end-piece was used to distribute the load across the thickness of the specimen in order to obtain plane loading.

Camera. A Fastax high-speed motion picture camera (Wollensak, WF3, 16mm) equipped with a 0.003" slit aperture plate was used. The slit decreased the exposure time and also reduced the height of the frame by 50 percent. With a standard aperture plate, the exposure time is  $1/3$  of the interval between pictures, e.g., at 7500 pictures per second (pps), the interval is 133 $\mu$ sec and the exposure is 44 $\mu$ sec. With a slit aperture, the manufacturer gives the equivalent exposure in microseconds as  $1/BS$  where B is the camera ratio (100 for the 16mm camera with a 0.003" slit) and S is the camera speed in pps. For typical operating conditions of 7500 pps, exposures of 1.3 $\mu$ sec were obtained. Such short exposures were more than





36.231.50535.080.02

adequate for photographing stress waves in low modulus photoelastic materials. Dynamic stresses have also been photographed in hard materials by using slit apertures in the Fastax camera,<sup>11</sup>. A Fastax "goose" control (Model WF-301) was used to operate the camera and to synchronize the event.

Photographic Techniques. In order to obtain monochromatic light (5461Å), either Corning (No. 4-102) or Wratten (Nos. 58 and 77A) filters were placed in front of the camera lens, and essentially the same results were obtained with either type of filter. Kodak Double-X and Tri-X films were used, and for our lighting conditions, the film speeds were approximately equal. Double-X film may be preferable because of its finer grain characteristics, but Tri-X film also gives very good results. Development in either D-72 or D-76 gave satisfactory results, but D-72 is preferred when making measurements because it produces a higher contrast negative.

### Results and Discussion

Square Plate Models. Square plates resting on one edge and loaded at the center of the opposite edge were tested as shown in Figure 3. This figure also gives the notation for the coordinate axes and the principal stresses. For the results reported in Figures 4-7, the models were 5-1/2" square for the explosive loads and 6" square for the mechanical loads. The photoelastic models were made from 3/8" thick sheets of Hysol 8705, a urethane rubber compound supplied by the Hysol Corporation of Olean, New York.

Stress Patterns. Typical dynamic photoelastic stress patterns at normal and oblique incidence for both explosive and mechanical loading are given in Figure 4. The oblique incidence stress patterns were taken at an angle of incidence of  $45^\circ$ , and the angle between the refracted ray and the normal to the model was  $27.9^\circ$ . A Recordak Film Reader was used to study the individual frames, and these were enlarged twenty times and then viewed through a 2.5x magnifier. In the explosive loading, Figures 4(a) and 4(b), only the leading fringes could be resolved during the first few frames, and the full stress pattern did not become reasonably clear until the fifth frame. By the ninth frame the initial stress wave had crossed the plate and was being reflected from the support. For this type of loading only the first ten frames were analyzed. Figure 5 gives the fringe order distributions on the line of stress symmetry for the stress patterns in Figure 4(a). The stress patterns under mechanical loading, Figures 4(c) and 4(d), were relatively easy to read, and the first thirty frames were analyzed.

Fringe Order vs. Time Curves. The time at which the event began (i.e., time zero) was determined by plotting the position of the first half order fringe versus frame number, where Frame No. 0 was taken as the

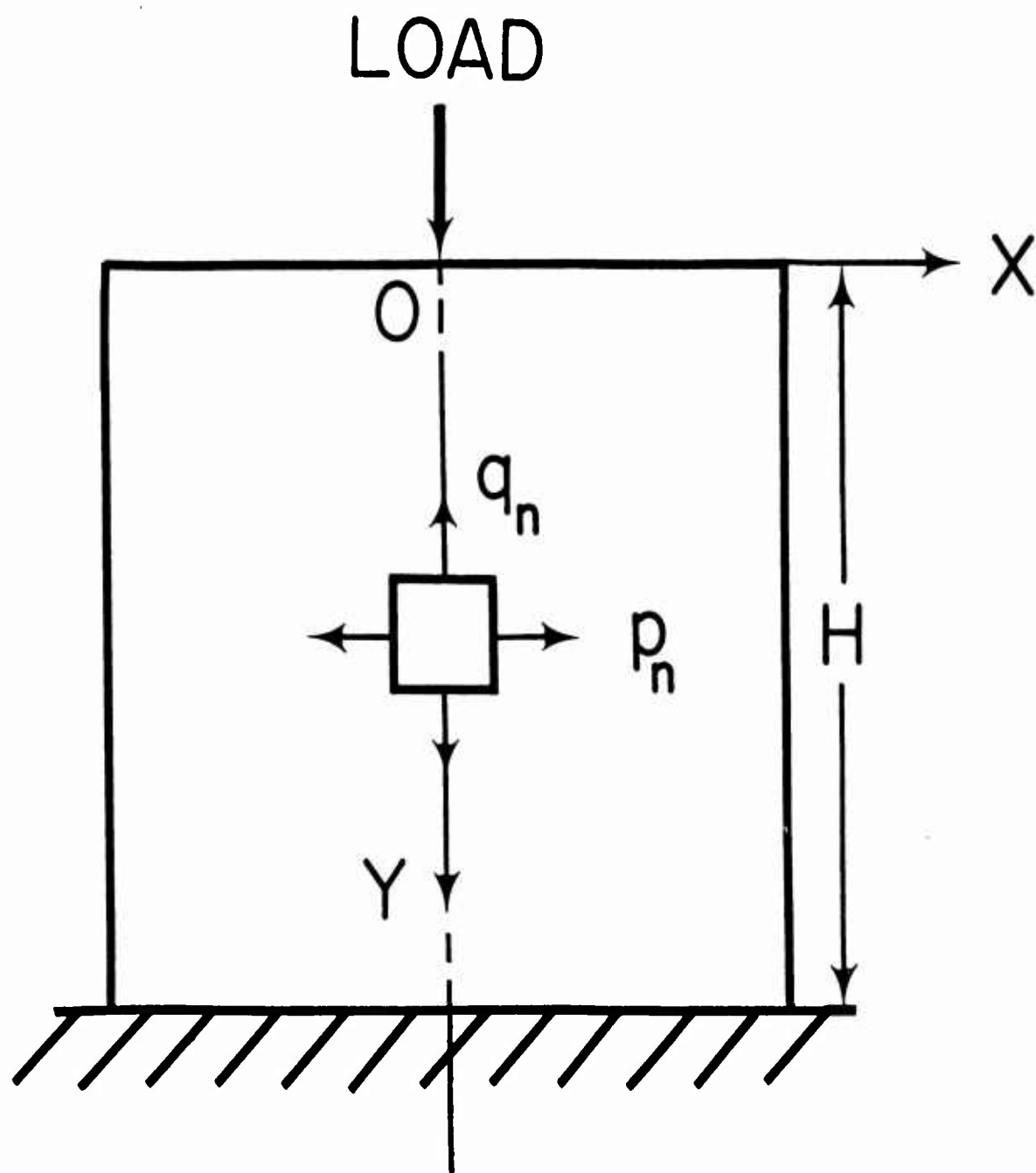
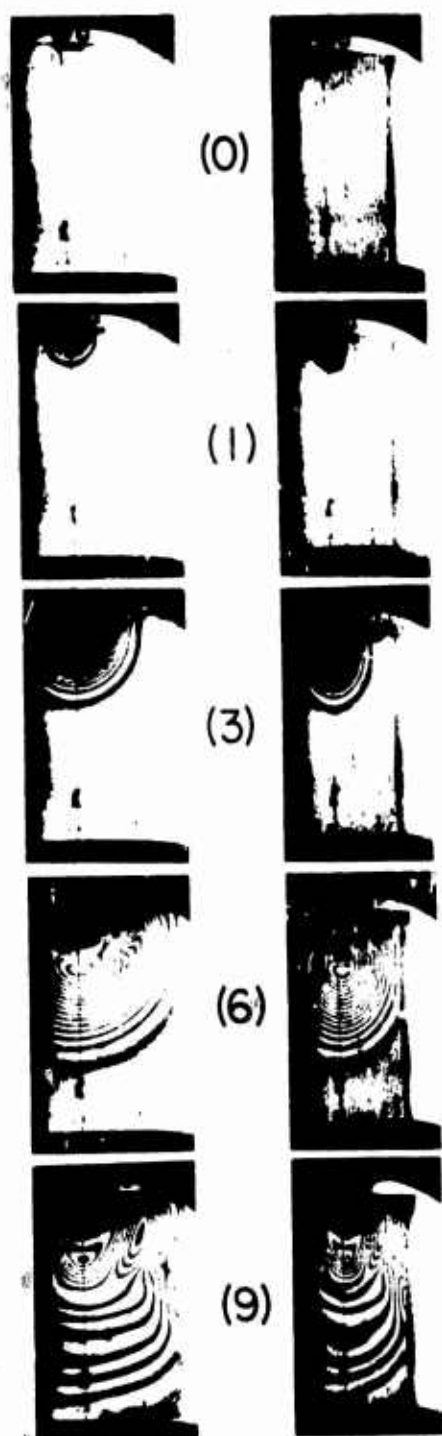


FIG. 3

Square Plate Models

# EXPLOSIVE

NORMAL OBLIQUE

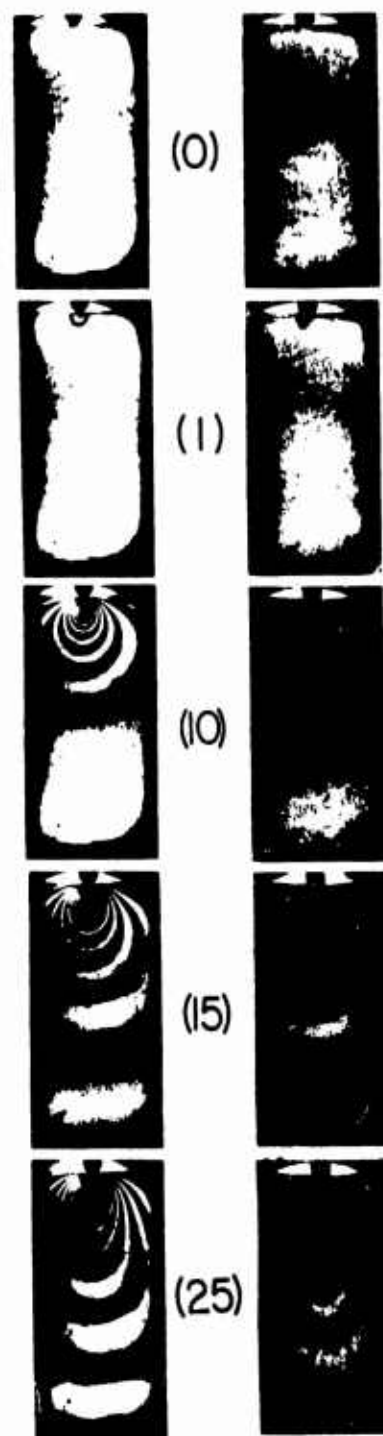


(A)

(B)

# MECHANICAL

NORMAL OBLIQUE



(C)

(D)

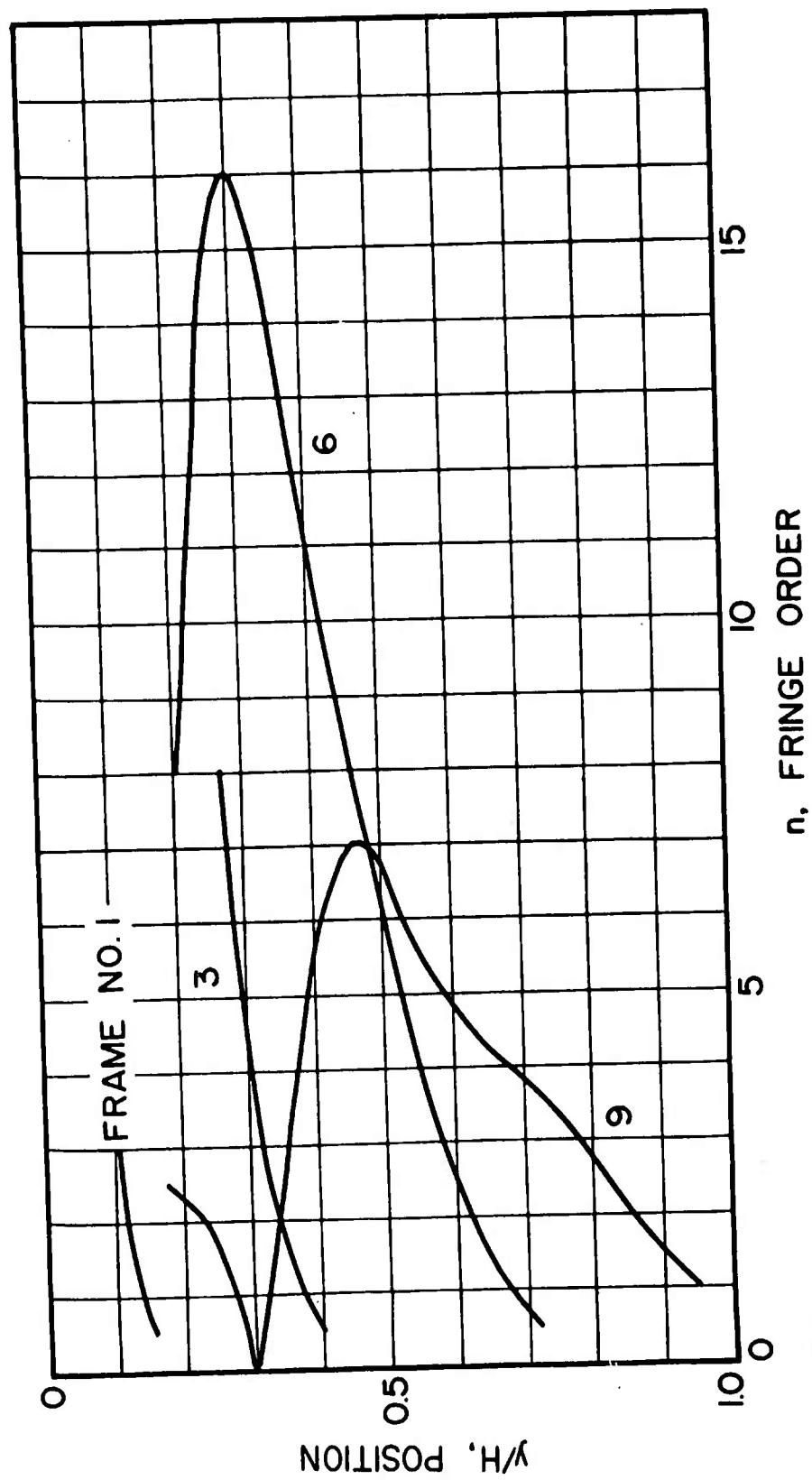


FIG. 5

Fringe Order Distributions Corresponding  
to Figure 4(a)

last picture without a stress pattern. Figure 6 gives the results for normal incidence for both explosive and mechanical loading. With explosive loading, it is seen that the leading fringe travels approximately twice as fast as it does with mechanical loading. Furthermore, under explosive loading the velocity of propagation of the leading fringe decreases somewhat with increasing frame number, whereas under mechanical loading the velocity is nearly constant.

Normal and oblique incidence photographs were obtained from repeated tests. For various points of interest on the line of stress symmetry, fringe order versus time curves were plotted by taking fringe order data from curves of the type shown in Figure 5 and by constructing a time scale starting at the beginning of the event and using the interval between frames as measured from timing marks. By combining the fringe orders determined from normal and oblique incidence at a given point and at the same time, it was then possible to separate the principal stresses.

Oblique Incidence Method. The principal stresses  $p_n$  and  $q_n$  in fringes were calculated from the equations:

$$P_n - Ctp = (n - n_\theta \cos \theta) / \sin^2 \theta \quad (1)$$

$$q_n = Ctp = (n \cos^2 \theta - n_\theta \cos \theta) / \sin^2 \theta \quad (2)$$

where  $C$  is the stress-optic coefficient,  $t$  is the thickness of the model,  $p$   $q$  are the principal stresses,  $n$  is the fringe order at normal incidence,  $n_\theta$  is the fringe order at oblique incidence, and  $\theta$  is the effective angle of oblique incidence. These equations are valid for a rotation about the  $q$ -stress, (10).

Principal Stresses in Square Plates. The principal stresses at the center of the square plates are given in Figure 7 for both explosive and mechanical loading. The stresses were calculated for the period of time that it took the initial stress wave to cross the plate and reflect from the supported edge. It is seen that the stresses due to explosive loads develop much more rapidly than those due to mechanical loads. From other tests, the duration of the one grain M52A5 electric primers was found to be approximately 350  $\mu$ sec. Thus the explosive loading time was short compared with the time for the passage of the stress wave across the plate, and peak stresses occurred during the passage of the first stress wave. The duration of the mechanical impact, i. e., the time that the impact rod was in contact with the model, was approximately 12.8 msec. Thus the mechanical loading time was long compared with the time for the passage of the stress wave, and the maximum stresses occurred at times later than those shown in

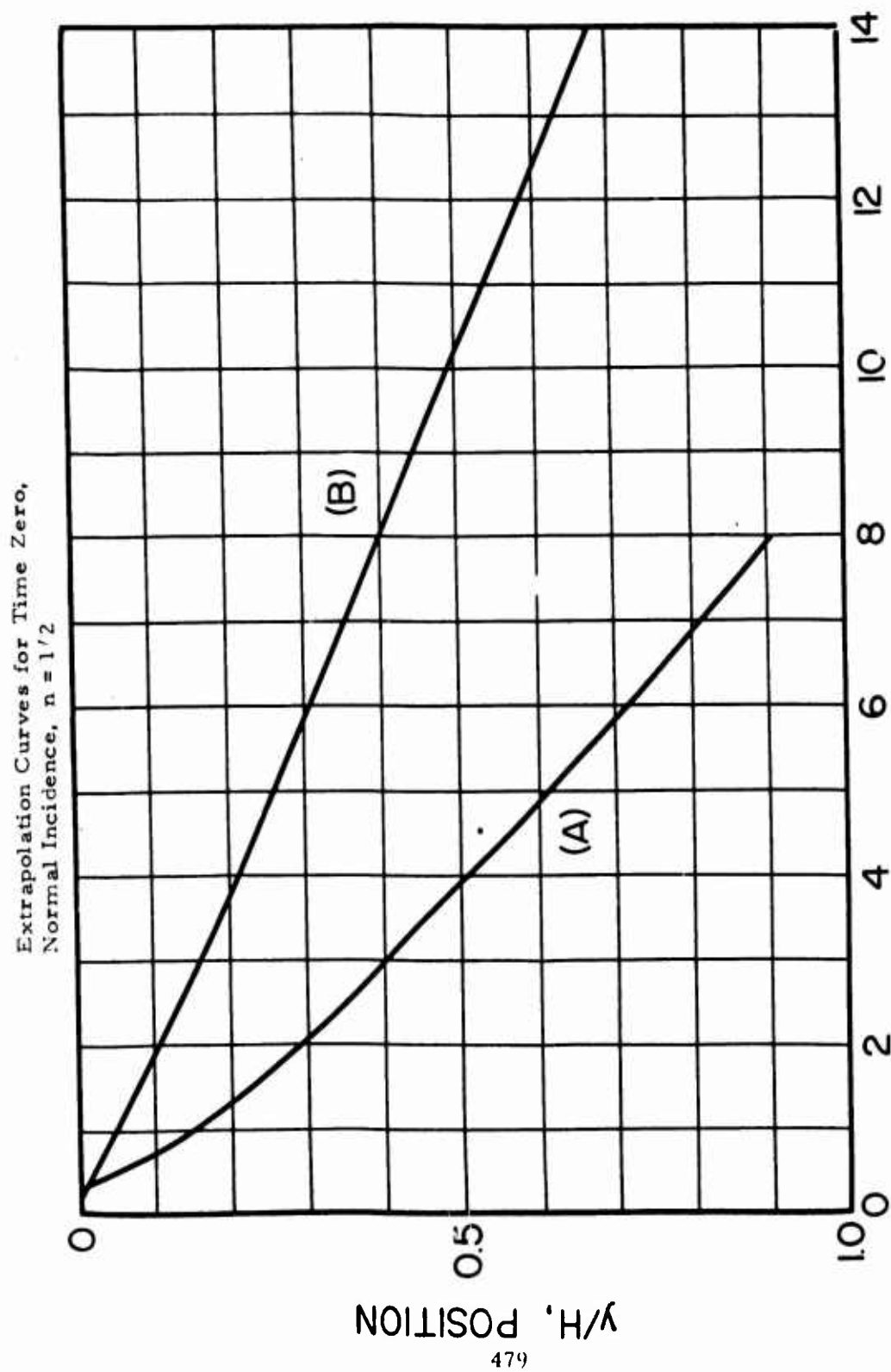


FIG. 6

FRAME NO.

- (a) Explosive Loading as in Figures 4(a) and 5
- (b) Mechanical Loading as in Figure 4(c)

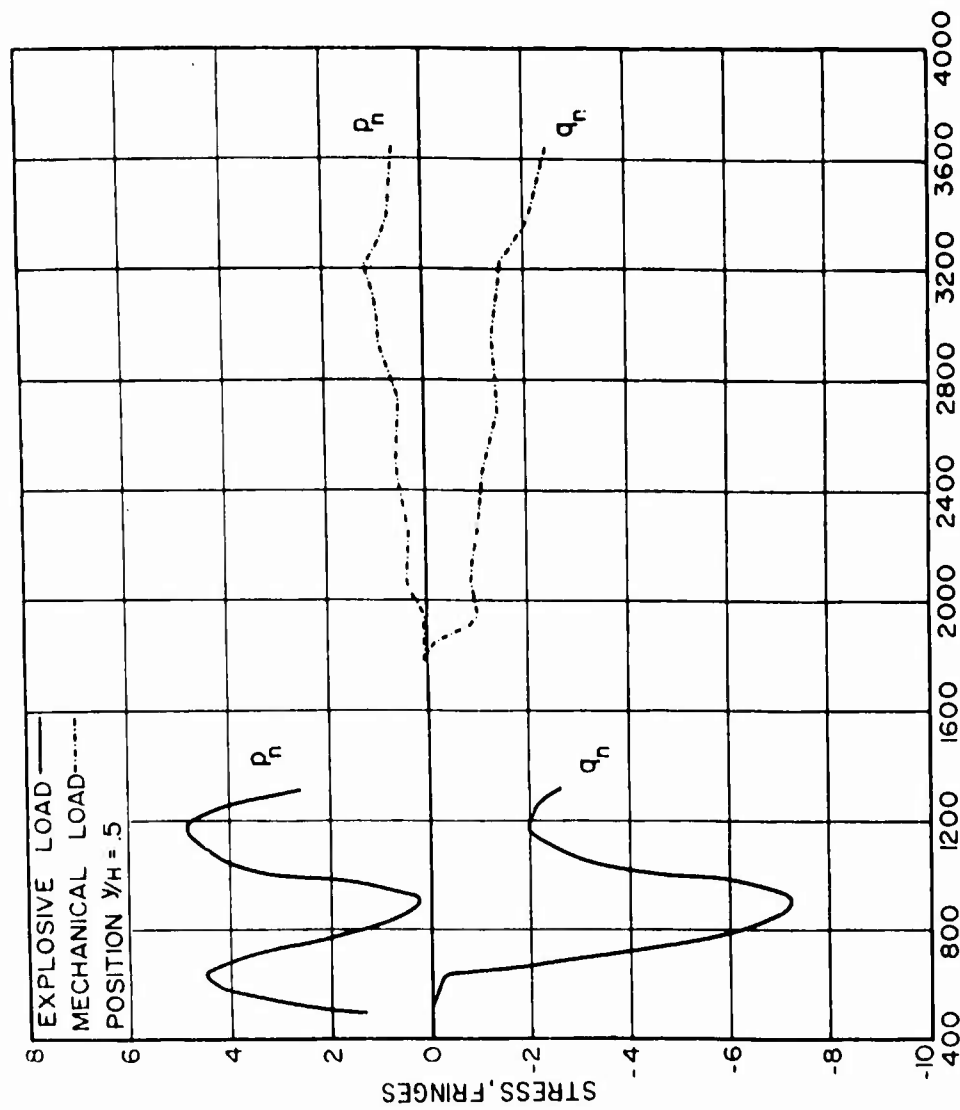


FIG. 7 Principal Stresses in Square Plates  
(Data from repeated tests as in Figure 4)



Figure 7. Additional results are given in (15).

Principal Stresses in Circular Disk and Rectangular Bar. A series of impact tests were made on a circular disk and a rectangular bar as sketched in Figure 8. The influence of the height of fall on the stresses at the center of the circular disk are shown in Figure 9. It is seen that the magnitudes of both  $p_n$  and  $q_n$  increase as the drop increases, and the duration of impact appears to be nearly independent of the height of fall. The effect of the weight of the impact rod on the stresses at the center of the rectangular bar are shown in Figure 10. The use of heavier impact rods and a fixed drop increases the magnitude of the  $q_n$  stresses and the duration of impact but has little effect on the average values of the  $p_n$  stresses. Additional results are given in (12).

## PART II

### SIMULTANEOUS NORMAL AND OBLIQUE INCIDENCE PHOTOGRAPHS

In the oblique incidence method, the equations for the principal stresses involve differences between quantities of the same magnitude so that small errors in the measurement of fringe orders may lead to large errors in the calculated stresses. When normal and oblique incidence stress patterns are photographed from repeated tests, the results are subject to errors due to lack of reproducibility in loading as well as difficulties in obtaining values of  $n$  and  $n_\theta$  at corresponding times. In order to eliminate these sources of error, a dual-polariscope was designed so that normal and oblique incidence stress patterns could be photographed simultaneously.

#### Dual-Polariscope

The dual-polariscope designed for photographing both normal and oblique incidence stress patterns from a single test on the same piece of film is shown in Figure 11. It consists essentially of two polariscopes whose optic axes intersect at 45 degrees and a system of mirrors for putting the projected images into a single camera, Figure 11(a). The condenser lenses ( $C_1$ , 8" diameter, 9" focal length) and the collector lenses ( $C_2$ , 8" diameter, 17.8" focal length) were made of plastic and were supplied by the Fostoria Corporation of Huntingdon Valley, Pennsylvania. A camera lens of shorter focal length (Wollensak, WF-142A, 13mm, f/1.6) was used in order to obtain both views of the specimen. The other optical elements and photographic techniques were the same as described in the work with the single polariscope.

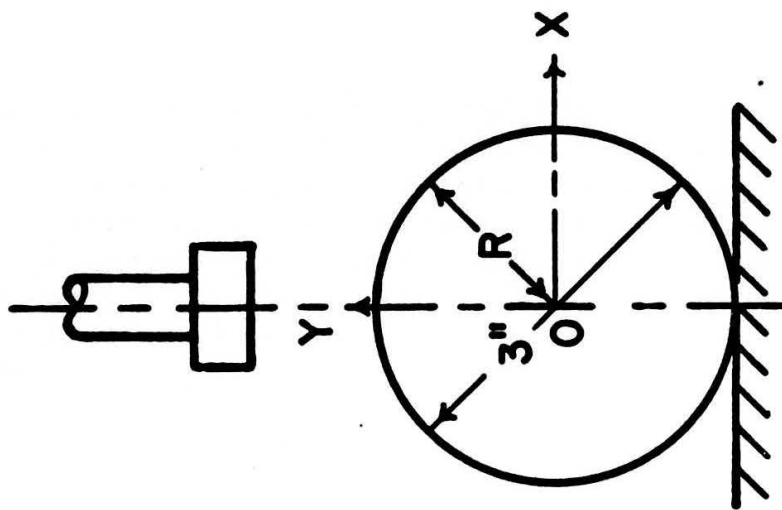
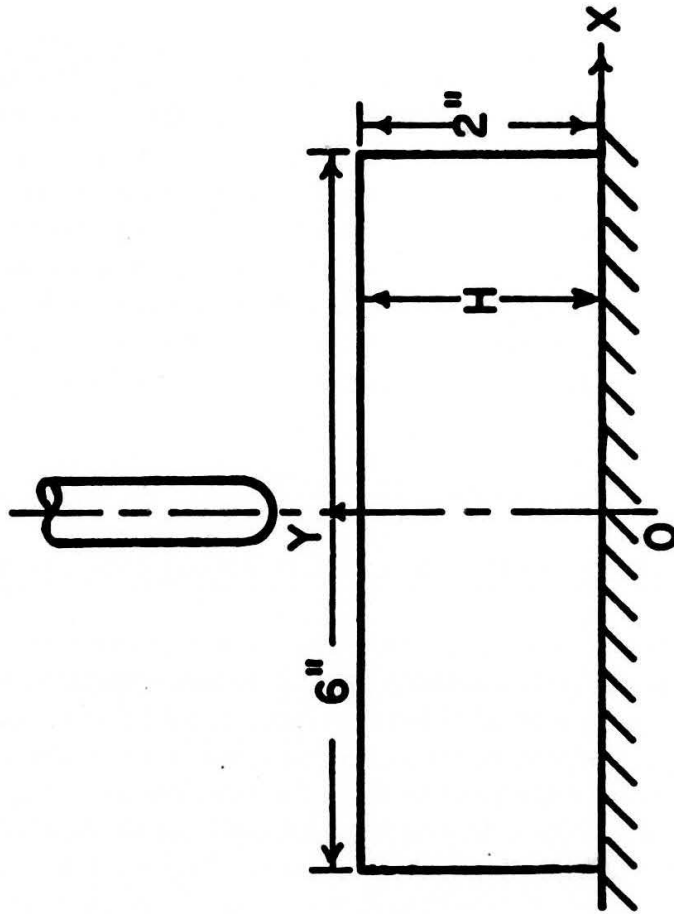


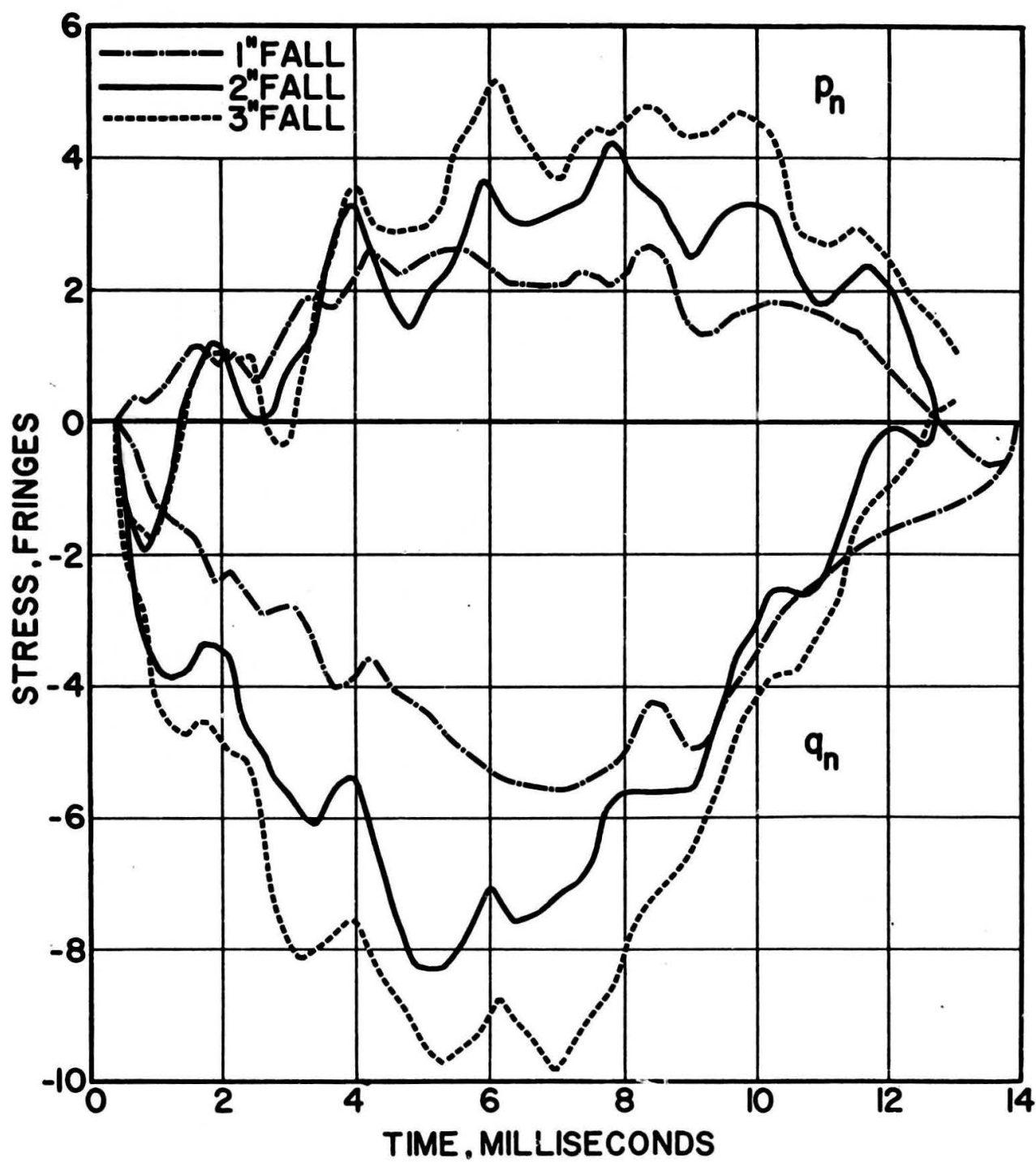
FIG. 8

(a)



(b)

Photoelastic Models  
(a) Circular Disk  
(b) Rectangular Bar



Principal Stresses in Circular Disk  
 $y/R = 0$ , 0.52 lb. impact rod

FIG. 9

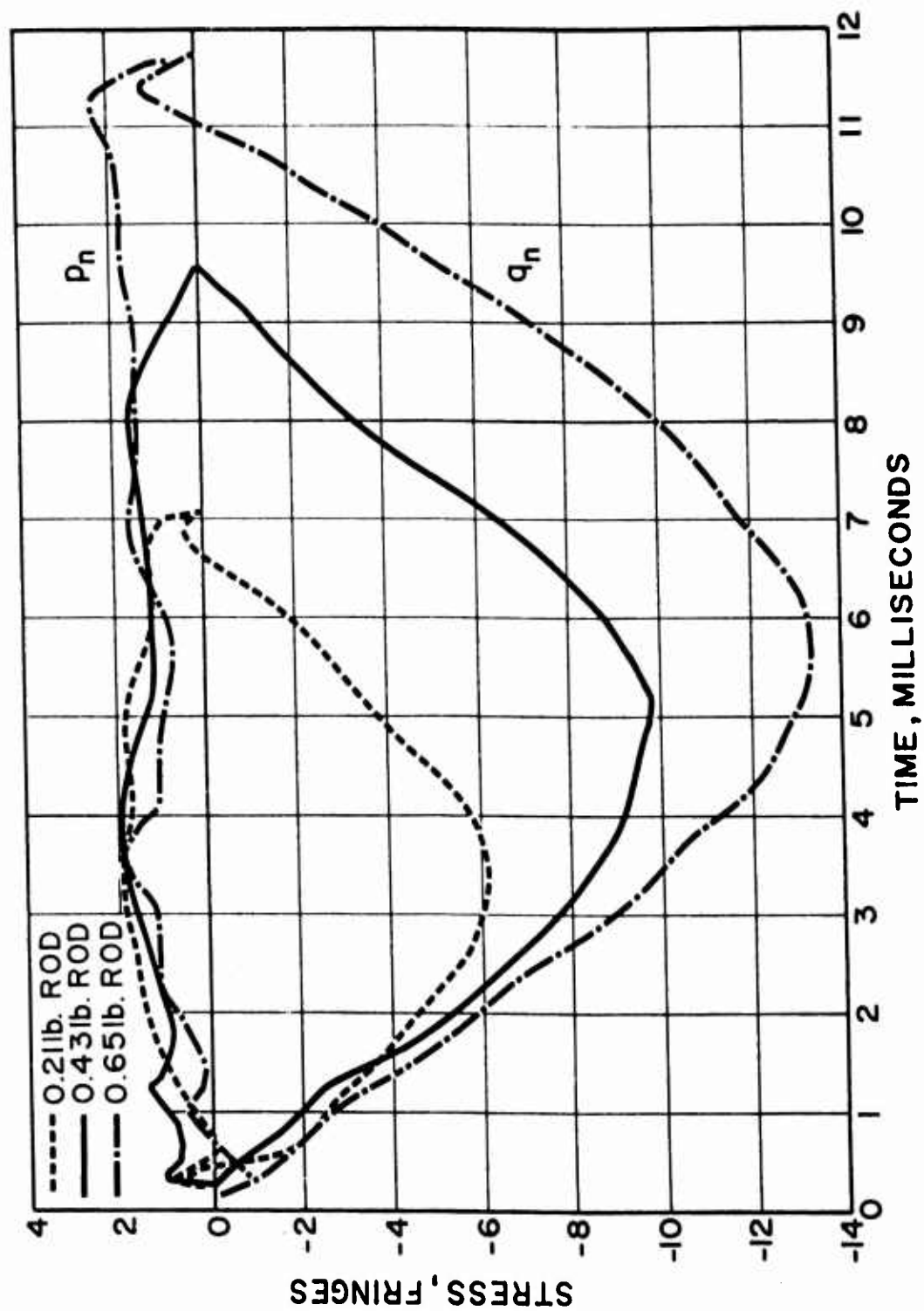
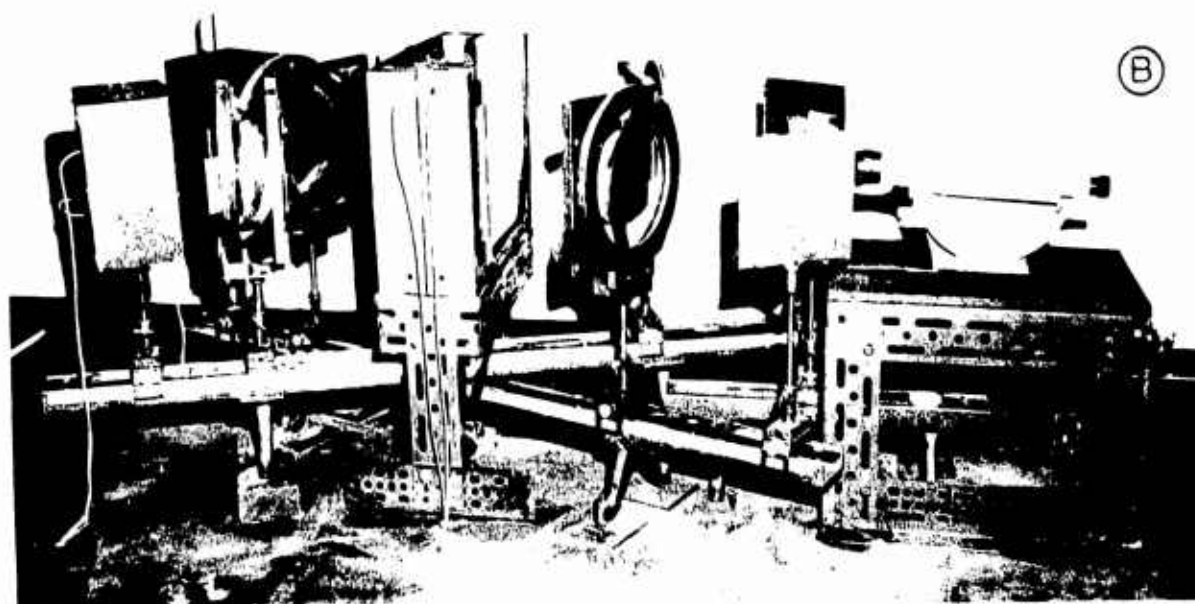
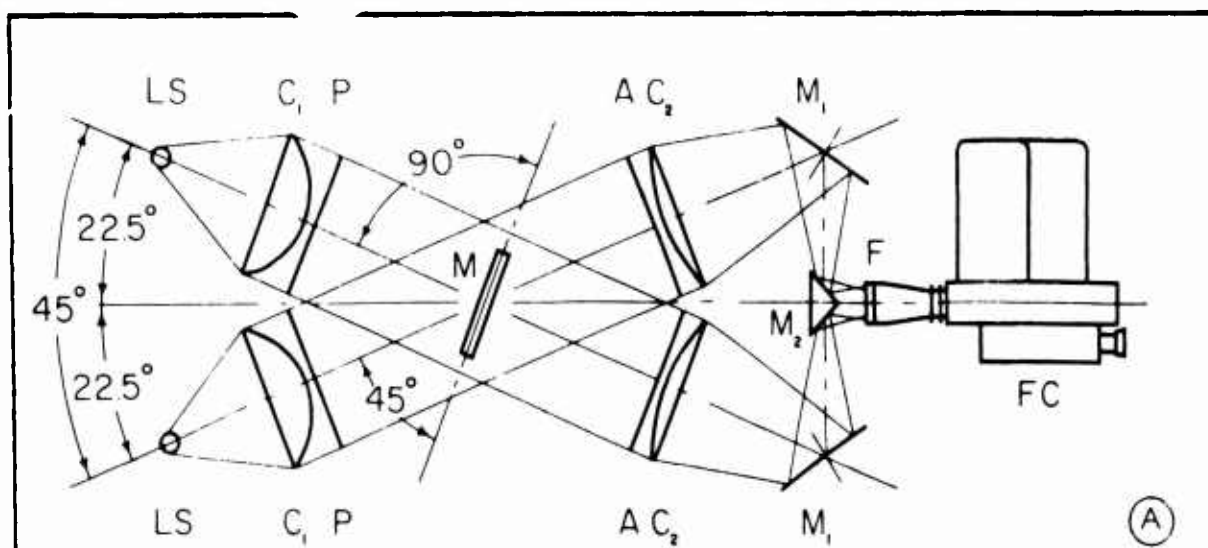


FIG. 10 Principal Stresses in Rectangular Bar  
 $y/H = 0.5$ , 2 in. drop



78.00152577.000000

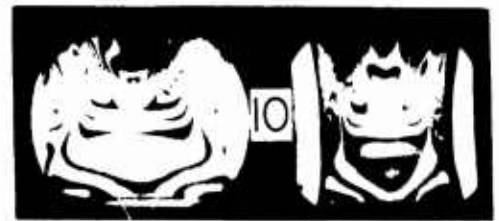
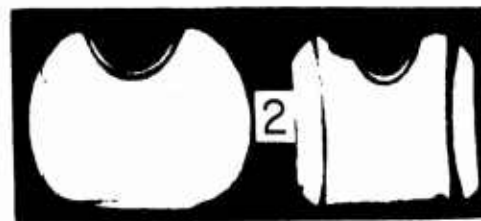
## Results and Discussion

Plates of Hysol 8705, 5" square as in Figure 3, were subjected to explosive loading, Figure 11(b), using one grain M52A5 electric primers as before. A complete sequence of simultaneous normal and oblique incidence stress patterns are given in Figure 12 for the period of time that it took the initial stress wave to cross the plate and reflect from the supported edge. For any pair of stress patterns, the fringe orders at corresponding points on the line of stress symmetry may be used directly in Equations (1, 2) to determine the principal stresses.

In order to compare the results obtained using simultaneous stress patterns with those obtained from repeated tests, several tests, several tests were made with the dual-polariscope under the same conditions shown in Figure 12. By using normal incidence data from one test and oblique incidence data from another test, the effect of repeated tests with a single polariscope was obtained.

Using Test 1 in Figure 13 as a reference, a time scale was constructed using time zero as determined from extrapolation and the interval between frames as measured from timing marks. For a given frame number, note that  $n_0 = 1/2$  has traveled farther into the specimen than  $n = 1/2$ . In previous work with the single polariscope, there was no way of observing this effect. In the extrapolation for zero time, both normal and oblique incidence data were used, but even so, the extrapolation may not be too accurate. In order to eliminate this as a possible source of error in establishing corresponding times, the position of  $n_0 = 1/2$  at Frame No. 2 was chosen arbitrarily in Test 1 to establish a reference point. An interpolation procedure was then used to correlate other tests with this reference point. Thus in Figure 13, Frame No. 2 of Test 2 occurred earlier than Frame No. 2 of Test 1 by an amount  $\Delta t$  as indicated.

Three tests were made for the conditions shown in Figure 12, and the first fifteen frames were analyzed in each test. Fringe order versus time curves at the center of the plate are given in Figure 14 for both normal and oblique incidence. It is seen that the spread in the values of either  $n$  or  $n_0$  is approximately one fringe. When the curves of  $n$  and  $n_0$  are compared, it is seen that their shapes are somewhat similar, and it is important to note that the curves from the three tests lie in the same relative position with respect to each other. It would thus appear that the intensity of loading (i.e., the output of the M52A5 electric primers) was somewhat different in these tests.



28 271 52500 000 62

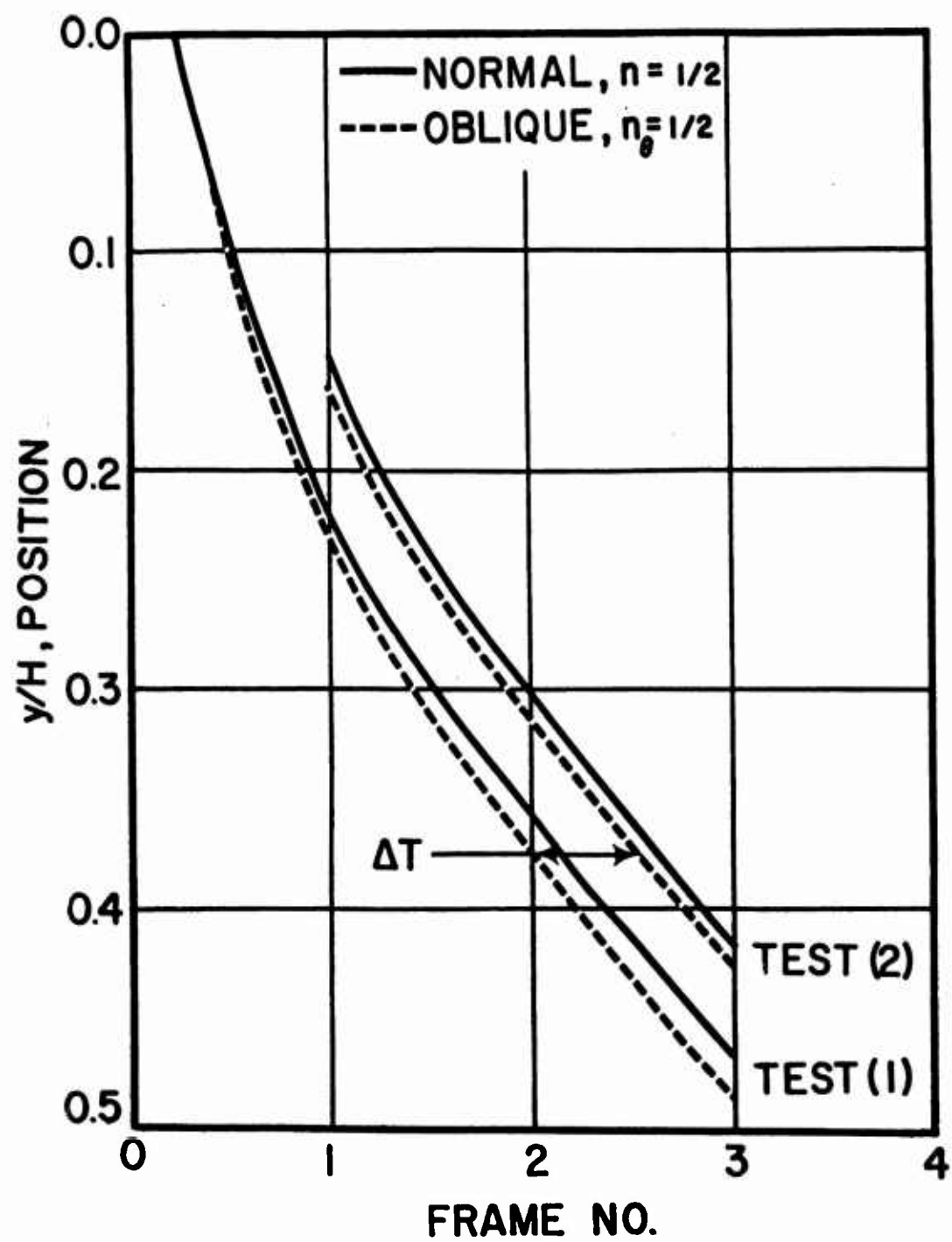


FIG. 13 Extrapolation for Time Zero,  
Interpolation for  $\Delta T$



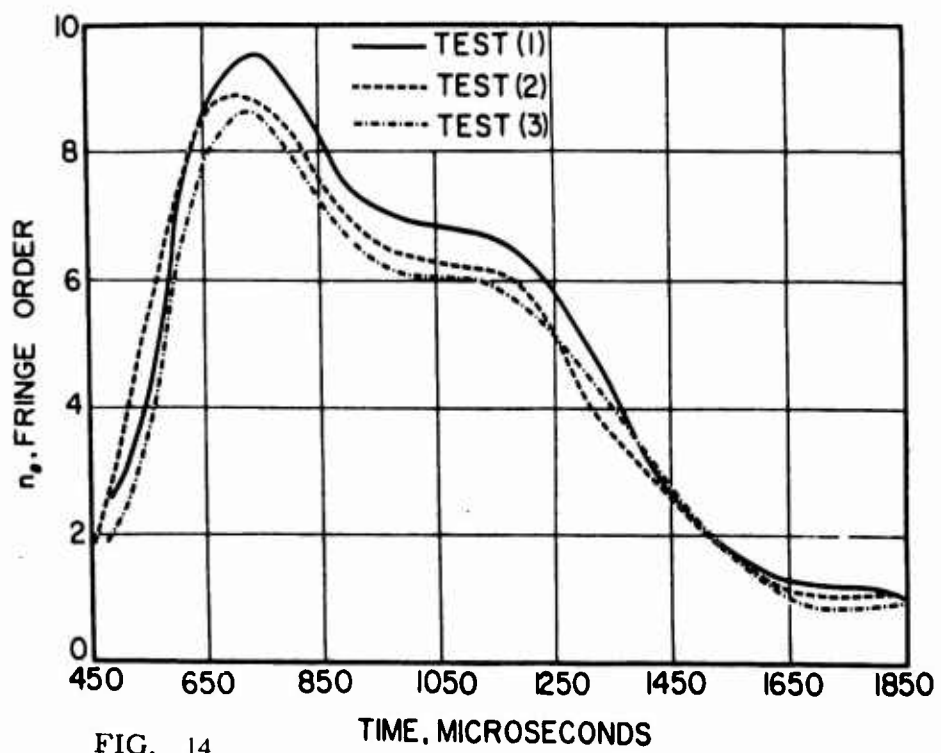
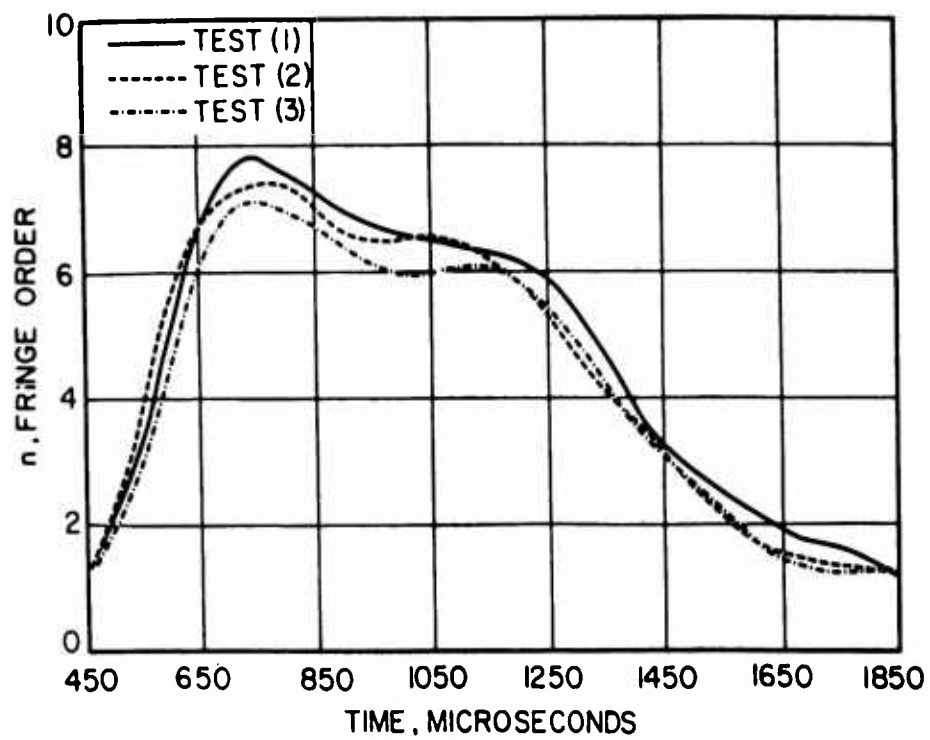


FIG. 14

Fringe Order vs. Time Curves  
 ( $n$  and  $n_0$ , three tests,  $y/H = 0.5$ )

The principal stresses were calculated for all three tests using simultaneous data, and the results from Tests 1 and 2 for the stresses at the center of the plate are shown in Figure 15. It is seen that both  $p_n$  and  $q_n$  are compressive initially, and that  $q_n$  is more than twice as large as  $p_n$ . After 800  $\mu$ sec,  $p_n$  becomes a tensile and reaches a maximum value approximately equal in magnitude to its earlier compressive value. The two tests are rather similar, and the differences between them are probably due to differences in the explosive loading.

When the results in Figure 15 from simultaneous data are compared with those in Figure 7 from repeated tests, it is seen that there is quite a difference, especially in the  $p_n$ -stress which is always tensile in Figure 7. This discrepancy would seem to be due primarily to the lack of reproducibility in the loading. For example, when the stresses are calculated from repeated tests using  $n$  from Test 1 and  $n_0$  from Test 3, Figure 16, the results are radically different from those in Figure 15. Although the results in Figure 16 do not agree with those in Figure 7, it is interesting to note that this procedure for calculating the stresses in Figure 16 nearly removed the initial compressive behavior of  $p_n$  shown in Figure 15, and it gave a tensile behavior somewhat similar to that shown in Figure 7.

#### Further Work

As previously noted, the equations for separating the principal stresses by means of the oblique incidence method are sensitive to small errors in the measurement of fringe orders. Even with simultaneous data, the use of photographs of dynamic stress patterns to determine fringe orders has its limitations, and further work should include a check on the accuracy of this method under dynamic conditions.

By reporting the principal stresses in units of fringes, it was possible to eliminate calibrating the material under dynamic conditions. Although the mechanical and optical properties of Hysol 8705 were studied by Dally, Riley, and Durelli (2) who found that the stress-optic coefficient was independent of the rate of loading over a wide range, it would seem that further work should be done on dynamic calibration before applying this result to the case of explosive loading.

The dual-polariscope can also be used to study dynamic stresses in high modulus photoelastic materials, and the only change necessary is that faster cameras will be required. An extension of this work from soft to hard materials is planned in order to study the influence of the physical properties on dynamic stress distributions. Such information will bear on the problem of transition from stresses in photoelastic materials to stresses in structural materials under dynamic conditions.

Principal Stresses in Square Plate  
(Simultaneous data, two tests,  $y/H = 0.5$ )

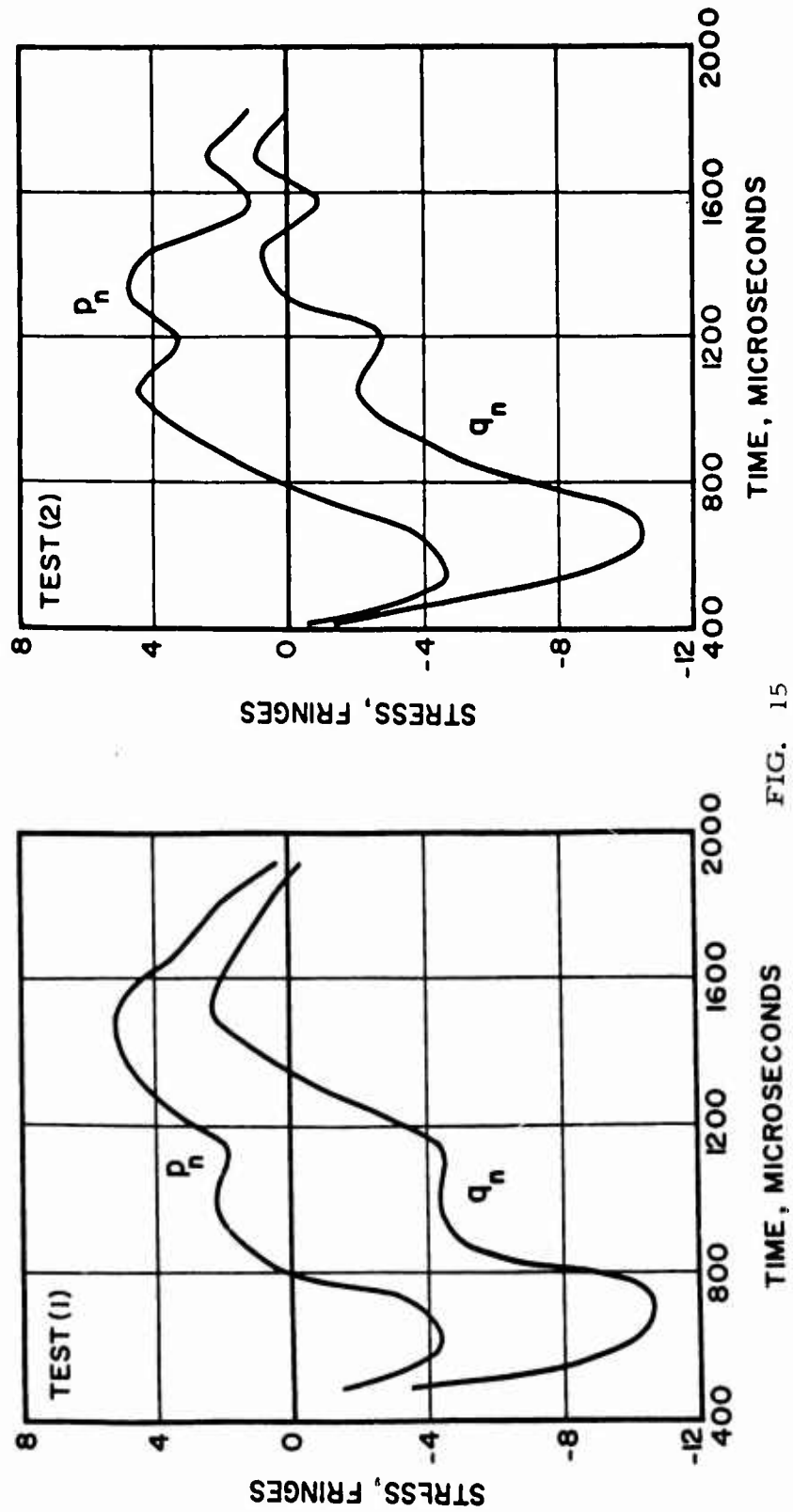
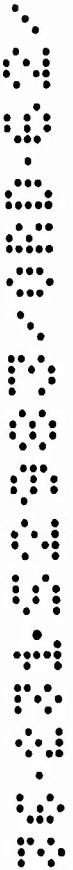


FIG. 15



Principal Stresses in Square Plate  
(Data from repeated tests,  $y/H = 0.5$ )

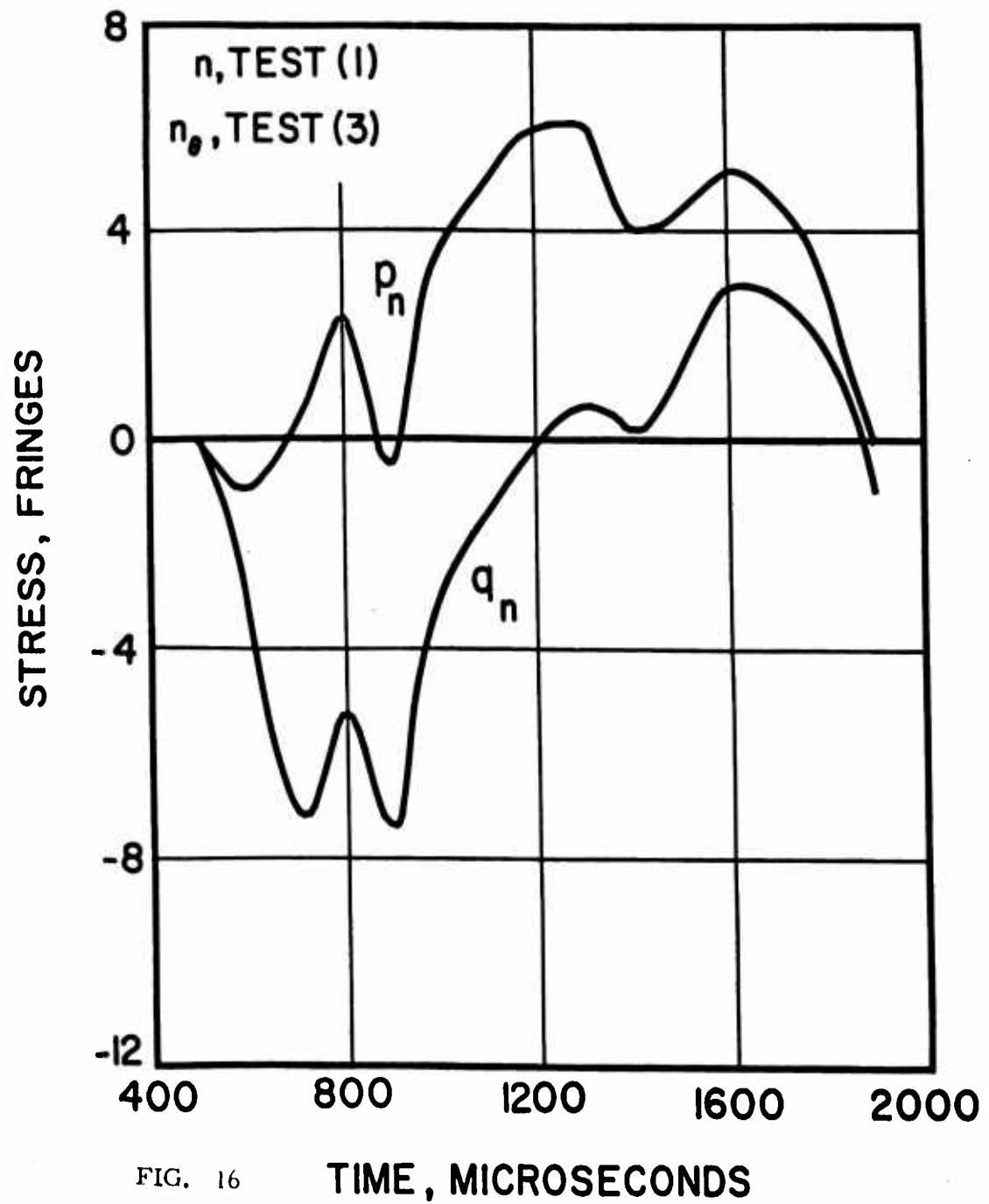


FIG. 16 TIME, MICROSECONDS

88-281-52982-080-62

## REFERENCES

1. Perkins, H. C., "Movies of Stress Waves in Photoelastic Rubber", J. Appl. Mech., Vol. 20, 1953, pp. 140-141.
2. Dally, J. W.; Riley, W. F.; Durelli, A. J., "A Photoelastic Approach to Transient Stress Problems Employing Low-Modulus Materials", J. Appl. Mech., Vol. 26, 1959, pp. 613-620.
3. Christie, D. G., "An Investigation of Cracks and Stress Waves in Glass and Plastics by High-Speed Photography", Trans. Soc. Glass Tech. Vol. 36, 1952, pp. 74-89.
4. Wells, A. A. and Post, D., "The Dynamic Stress Distribution Surrounding a Running Crack - A Photoelastic Analysis", Proc. SESA, Vol. XVI, No. 1, 1958, pp. 69-96.
5. Feder, J. C.; Gibbons, R. A.; Gilbert, J. T.; Offenbacher, E. L., "The Study of the Propagation of Stress Waves by Photoelasticity", Proc. SESA, Vol. XIV, No. 1, 1956, pp. 109-122.
6. Frocht, M. M. and Flynn, P. D., "Studies in Dynamic Photoelasticity", J. Appl. Mech., Vol. 23, 1956, pp. 116-122.
7. Frocht, M. M.; Flynn, P. D.; Landsberg, D., "Dynamic Photoelasticity by Means of Streak Photography", Proc. SESA, Vol. XIV, No. 2, 1957, pp. 81-90.
8. Cole, C. A.; Quinlan, J. F.; Zandman, F., "The Use of High-Speed Photography and Photoelastic Coatings for the Determination of Dynamic Strains", Proc. 5th Int'l Cong. High-Speed Phot., 1962, pp. 250-261.
9. Drucker, D. C., "Photoelastic Separation of Principal Stresses by Oblique Incidence", J. Appl. Mech., Vol. 10, 1943, pp. A-156-A-160.
10. Flynn, P. D. and Frocht, M. M., "On the Photoelastic Separation of Principal Stresses Under Dynamic Conditions by Oblique Incidence", J. Appl. Mech., Vol. 28, 1961, pp. 144-145. See also Technical Report No. 11 to OOR, Contract No. DA-11-022-ORD-1609, July 1960.
11. Flynn, P. D.; Feder, J. C.; Gilbert, J. T.; Roll, A. A., "Some New Techniques for Dynamic Photoelasticity", Experimental Mechanics, Vol. 2, 1962, pp. 159-160.

12. Flynn, P. D.; Feder, J. C.; Gilbert, J. T.; Roll, A. A., "Impact Stresses in Low Modulus Photoelastic Materials", presented at the International Symposium on Photoelasticity, Chicago, 1961, to be published.
13. Flynn, P. D.; Feder, J. C.; Gilbert, J. T.; Roll, A. A., "Stress Waves due to Explosive and Mechanical Loading of Low Modulus Photoelastic Materials", presented at the Second International Conference of Stress Analysis, Paris, 1962, to be published.

#### DISCUSSION

Carl A. Fenstermaker, National Bureau of Standards: I was wondering whether in setting up the experiment you had considered using an eight-sided prism in the FASTAX camera. This would effectively double your picture per second rate.

Mr. Roll: Are you thinking of the 8 millimeter camera?

Mr. Fenstermaker: No, this is in the 16 millimeter. It does cut your frame size, but it doubles your picture per second rate.

Mr. Roll: I hadn't heard of this before in the 16 millimeter FASTAX. It is interesting to note and I think we will look into it.

Fred W. Warner, White Sands Missile Range: Have you taken any color slides or color movies of these photo stress tests?

Mr. Roll: Under explosive loading as noted earlier, the fringe orders of greater than about five with colored film and color stress patterns wash out so we have been sticking straight to monochromatic light and using a circular polariscope with a light background.

Mr. Warner: I was interested in any other tests you might have done. We have a problem of taking color pictures on photostress rather than working with photoelastic models, and I thought you might have had some experience with that.

Mr. Roll: No, none at all.

# A PROPOSED METHOD FOR THE STUDY OF THE DYNAMIC STRENGTH OF HIGH STRENGTH MATERIALS

Francis B. Paca\*

## ABSTRACT

One of the problems which may face today's engineers is the determination of the response of various materials to dynamic loads. Currently there are several ways in which this can be done within specific limits or combinations of loading time, loading stress, and materials characteristics. However, serious problems arise when several types of different materials of very high strength are to be evaluated for dynamic response to short loads (i. e. , a few microseconds). Under these conditions, much of the current equipment cannot produce or accommodate one or more of the following: the short loading time, the mismatch of mechanical impedance or the propagation of a stress wave of the required intensity.

A method is proposed by which many of the above limitations can be overcome. In this method the samples of the material under study are formed into flat ended cylinders and subjected to guided impact against a massive high strength target block. The stress is calculated from impact velocity and the mechanical impedance of the sample.  $\sigma = V_o / (C\rho)$  The loading time is a function of the length of the sample and the elastic wave velocity. Test samples of a given length are fired (one time per sample) with increased velocity until failure occurs at the forward or impacting end. This determines V or stress.

The proposed method is not without limitations. These include: The mechanical impedance is assumed to remain constant over the entire range of Stress , only the stress is under study, and the number of samples will be large because for each test point the length of the sample (i. e. , loading time) and the impact velocity (i. e. , stress) must be in correct combination.

This proposed method is somewhat similar to that used by Taylor and Whiffin in England except that the impact velocity is substantially reduced. For example, a 300,000 psi steel bar would fail at less than 200 feet/sec. impact velocity.

---

\* Francis B. Paca, Chief, Applied Research Section, Mine Warfare and Barrier Branch, USAERDL, Fort Belvoir, Virginia.

(1) For electrically conducting materials, it appears possible to use the time of contact with the target block to determine the dynamic value of the elastic wave velocity, hence mechanical impedance.

(2) Taylor, G. I. "The use of flat ended projectiles for determining Dynamic Yield Stress" Proc of Royal Soc. (London) Vol. 194A - Sept 48.

---

In this paper I will review several of the methods for subjecting various materials to "so called" dynamic loads, and point out the limitations as relate to duration of loading, or material characteristics. A method will be proposed which can be used in many cases where other methods can not. This method is operationally cumbersome and, as usual, has its own limitations.

The basic objectives of dynamic loading tests are to subject a sample of a material to a known, predictable, or measurable force and be able to determine its effect in terms of stress, strain, or both. All of this must take place within a specific time frame; in this case, a few microseconds or milliseconds.

One of the early apparatus was that of Clark and Wood (1), Fig. 1. This consisted of an air driven ram which applies a load to the specimen. The time frame of load application is a function of the mass of the moving parts, the applied force, and the viscosity and velocity of the fluid. Stresses could be developed in 10 milliseconds and held for 6 seconds. No stress waves were propagated within the sample in this rapidly applied constant stress test. Samples of any material could be tested in this apparatus because there were no stress waves propagated and hence no reason to match the mechanical impedance of the material to that of the test apparatus. Stress, strain and time were capable of accurate measurement. The primary limitation of this method is the time frame of loading, which has been subsequently shortened to the 1 millisecond range by use of air or helium instead of the liquid (2).

An item of similar concept is driven by an electromagnet (3), Fig. 2. The stress, strain, and time are capable of accurate measurement within the 1/2 millisecond loading time. The limitations are the same as those of Wood's and Clark's device.

In order to obtain loading in the time frames shorter than 1 millisecond, several devices or methods have been evolved which depend upon the impact equations of Young (1807). These could be roughly separated into three classes, namely: the impact of one cylinder against another of the same diameter, the impact of a cylinder against a strong massive target, or combinations of the above. The impact equation states that the resulting stress is the product of the acoustic impedance times the impact velocity  $\sigma = \rho cv$ . One factor which must be measured as a transient is the effective impact velocity, as will be shown.



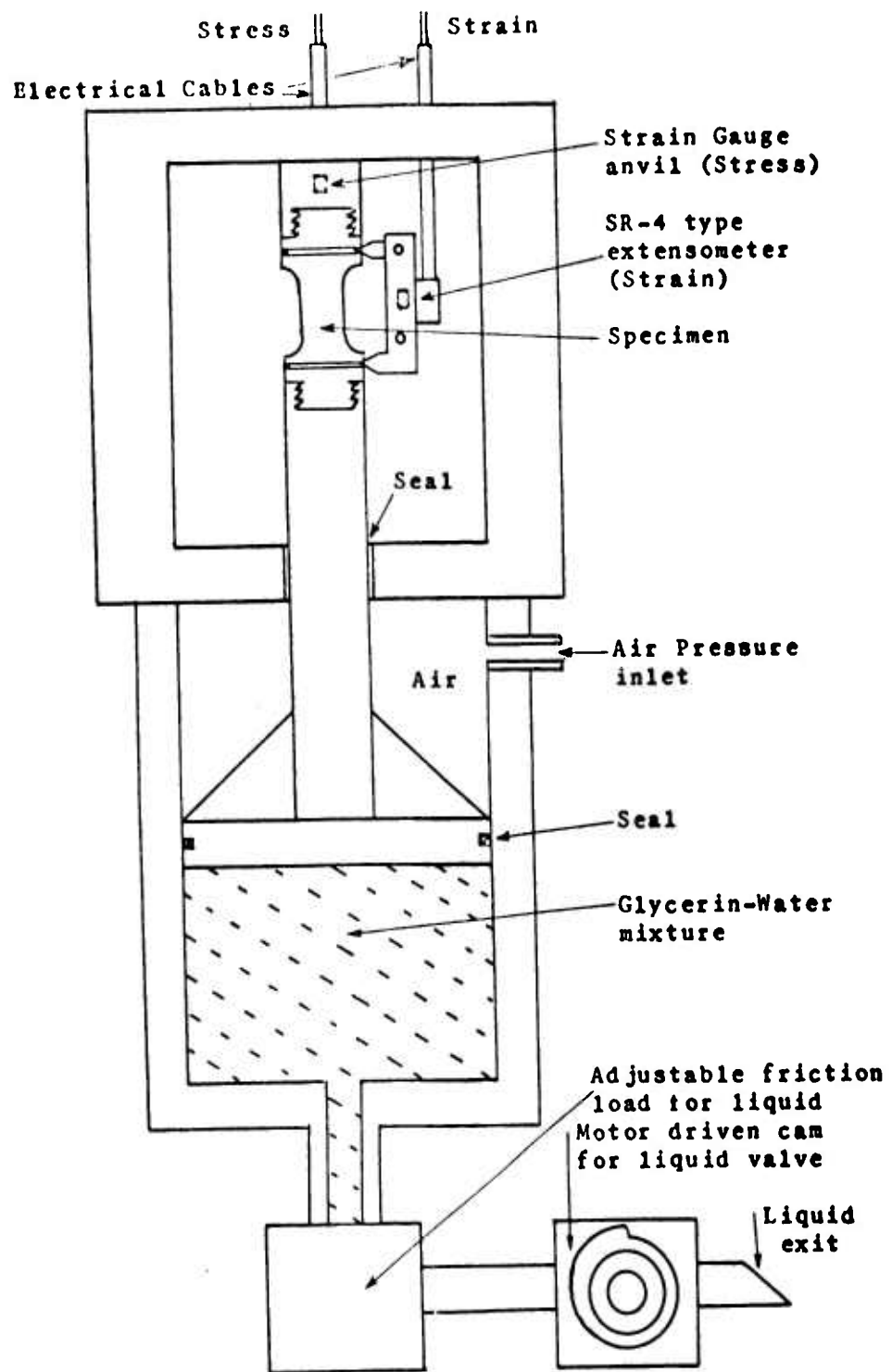


Fig. 1. Schematic diagram of apparatus used by Clark and Wood (1952) in their study of delay time.

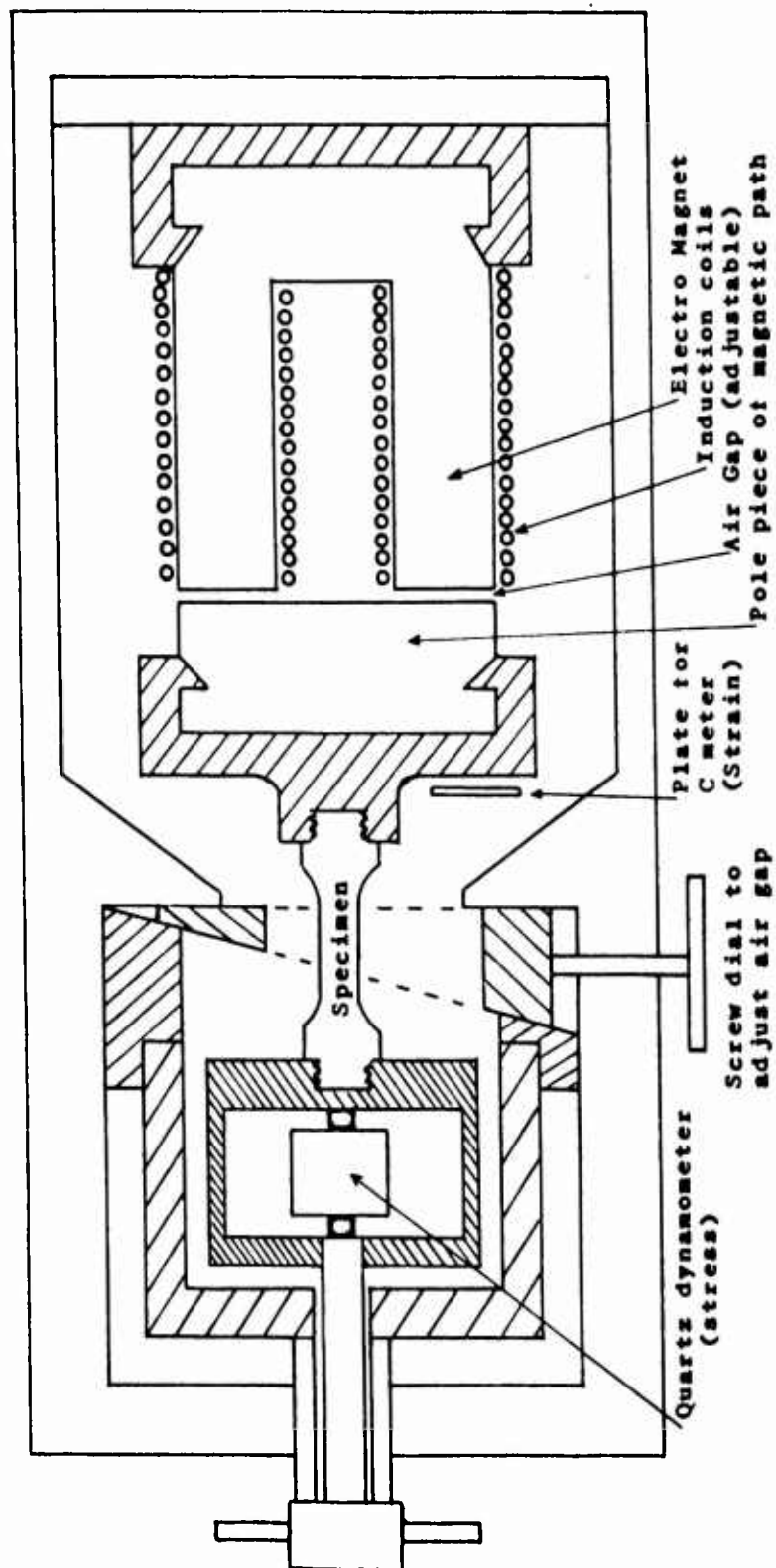


Fig. 2. Electromagnetic powered multiple impact apparatus of Ziembiski.

The apparatus used by Dr. Krafft of NRL is shown in Fig. 3. A steel rod is propelled and guided against a rod of the same diameter. Stress waves start at the point of impact and control the intensity and duration of stress. The impact stress, which was cut in half due to impact against a similar rod, is doubled or restored by a fixed end reflection against a heavy steel block. The stress then goes back thru the specimen until the other stress wave causes unloading. The load can be applied in a few microseconds and held for 1/2 millisecond or other values depending on the length of the impacting bar or failure of the specimen.

Another impact machine has been used by Campbell and Maiden (4) Fig. 4. The point of impact causes a stress wave to be propagated down bar portion A. The stress is increased by "semi-free end" reflections at the ends of portions A and B. After passing through the specimen the duration of the loading is controlled by the length of the "throw off" bar at the bottom. The characteristics of this device are similar to those of Dr. Krafft's.

The materials used in both of the above devices has been the same as that of the loading rods. The acoustic impedance of the specimen is the same as the load rod and no stress waves reflect from the specimen rod interface. Under this concept the limitations of this method are the type of material and its dynamic "strength" or response compared to the static strength of loading rods.

Materials which have acoustic impedance differing from the rod can also be used with this apparatus. In this case the specimen is made into a thin disk so that the time for stress waves to cross back and forward across the sample is very short compared to the loading time.

In any case the main limitation of these devices is not time, but the dynamic response of the material under test as compared to the static strength of the loading rods.

Thus a real question arises. What method can be used to dynamically test a material which is stronger than other materials? This material cannot be tested in the rapid loading devices of Clark and Wood because the time frame of loading may not be sufficiently short. The material cannot be used in the device of Krafft because it may be stronger than the apparatus used to test it.

In 1948 Taylor and Whiffin (5) devised a method for stress determination by firing flat ended cylinders against massive steel blocks. They derived a set of equations to determine the approximate dynamic yield strength from a measure of the original and final dimensions of the steel cylinder, its density and impact velocity. Figure 5 shows a schematic of their experiment. Their method involves an energy balance as is evidenced by a  $V_o^2$  term in their computations. The same sort of a system can be used to obtain data on stress directly in terms of  $V_o$  instead of  $V_o^2$ .

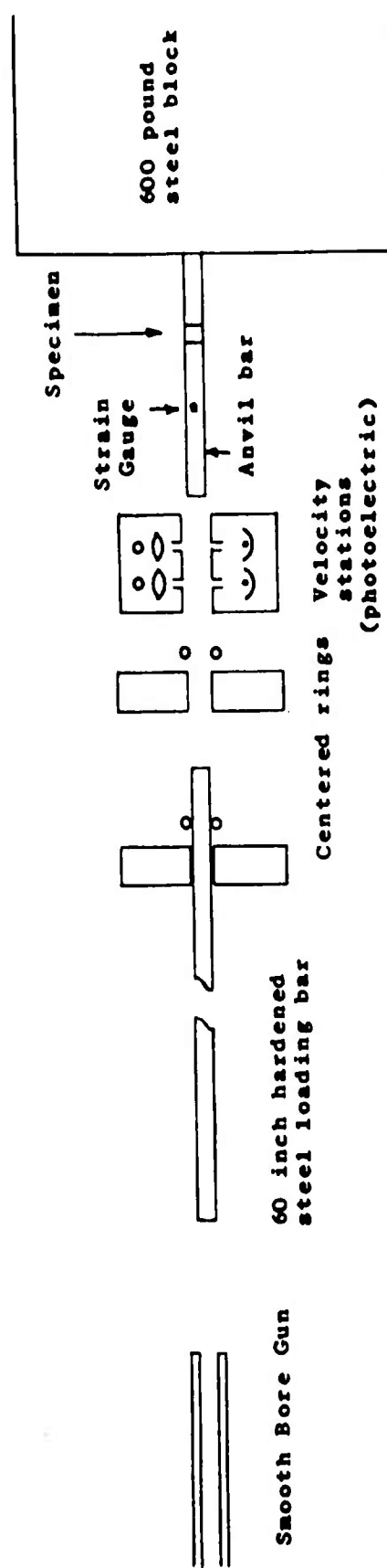


Fig. 3. Schematic drawing of apparatus used by Krafft in the study of delay time

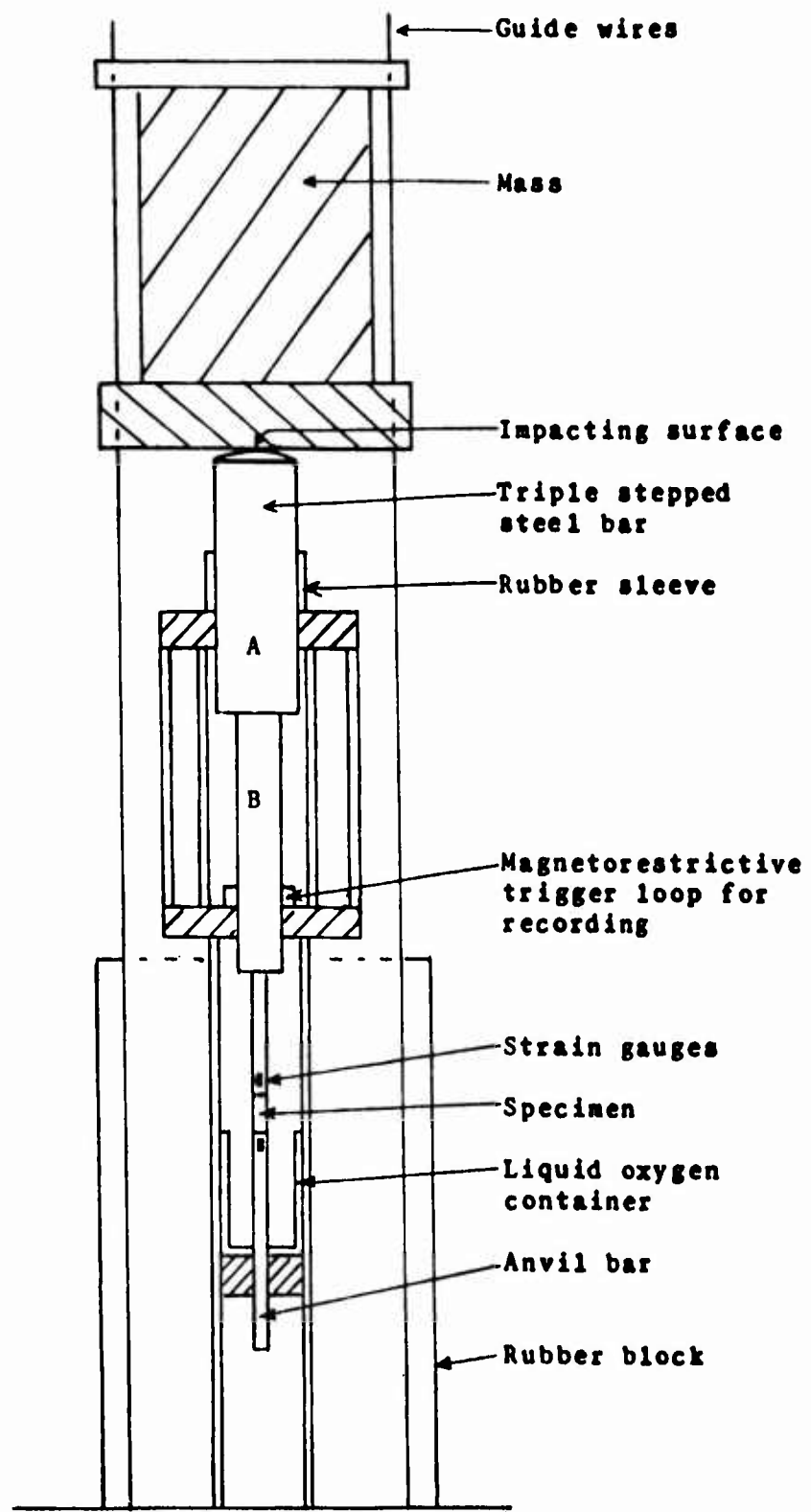


Fig. 4 Schematic diagram (exaggerated) of the mechanical impact apparatus of Campbell and Maiden

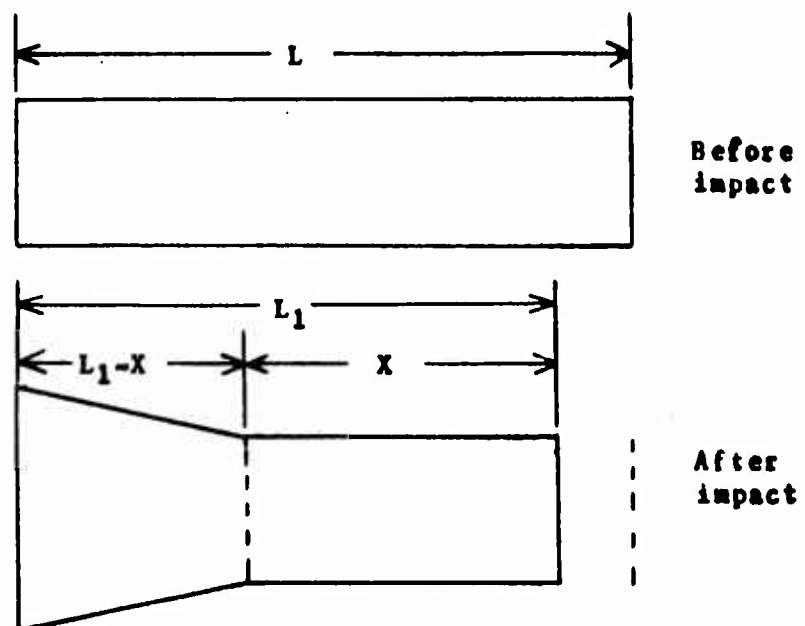
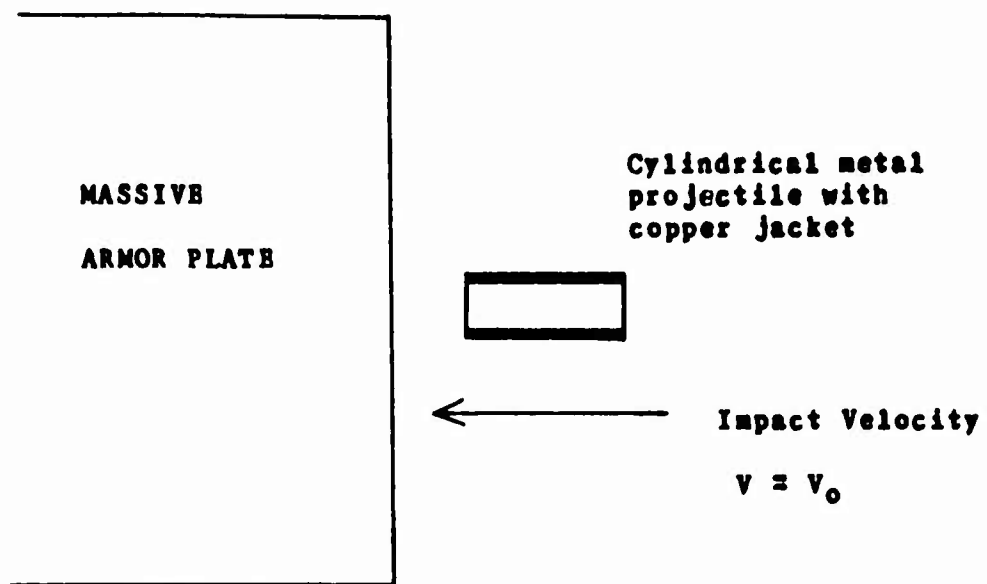


Fig. 5. Impact of a high speed metal projectile in determination of dynamic yield stress by Taylor and Whiffin

A simplified method is proposed which can accomplish the study of dynamic strength during short duration impact. It involves a system very similar in appearance to that of Taylor and Whiffin. The primary difference is that the impact velocity is reduced from the high impact speeds of Taylor (up to 2,500 feet per second) to lower speeds which cause a direct stress corresponding to Young's impact equation

$\sigma = C_0 \rho V$ . Under these conditions, the duration of a loading for the forward end of a non-yielding specimen can be calculated with a reasonable degree of accuracy and will be equal to  $2L/C_0$ .

A brief outline of this method is given below:

a. A flat-ended cylinder is subjected to a guided impact against a massive and strong target area (Armor steel) which has been grounded to a flat surface. The impact velocity is low and is calculated on the basis of Young's impact equation. For maximum versatility the target should be part of a ballistic pendulum of long radius.

b. The object of the method is to determine the highest impact velocity at which the specimen does not fail (neglecting pre-yield micro strain).

c. The time for loading for the forward end of a non-yielding cylinder is equal to  $2L/C_0$  where  $L$  is the length. Specimens of different length can be used to obtain variations in loading time.

d. In the event that a specimen does not fail on the first impact, the same specimen can be impacted repeatedly at the same velocity until failure. The number of impacts multiplied by the duration of impact can be used to estimate one point on the delay-time-versus-stress curve for materials which exhibit delay time.

e. The length and diameter of the specimen can be varied over a reasonable range ( $L$  from 0.5 to 5 inches and  $D$  from 0.1 to 0.5 inches). In order to guide the shorter projectiles it may be necessary to attach a bar of another material having low strength and acoustic impedance on the rear end of the projectile.

This method offers several advantages including the following:

a. The method is simple and uses a minimum of facilities and instrumentation. Impact velocity is the only transient event to be controlled and measured. The use of photo electric circuits or charged screens and high speed electronic chronographs should make accurate measurement possible.

b. Materials on any acoustic impedance can be investigated. The material of the specimen can be very strong, in fact, stronger than the impact area of the target mass due to the differences in stress distribution in the project as compared to stress distribution in the target.

c. The duration of impact of the forward end can be directly calculated to a reasonable accuracy.

d. A reasonable balance between the input and the pendulum response should be possible because the specimen does not yield excessively.

Apparent disadvantages include:

a. There are limits to the duration of loading to specimen length and number of multiple impacts. In general, the loading time will be short and generally less than 100 microseconds.

b. In the case of multiple impact and accrual of delay time, the impact velocity must be the same. It may be difficult to control the impact velocity to the required degree of accuracy.

c. For a test involving a single impact which appears inherently to be more reliable, the two factors of load duration and stress (which depend on projectile length and impact velocity) must be in the correct combination for a non-yielding specimen. If the specimen were projected at a slightly greater velocity, it would fail plastically. Many tests may have to be performed to "zero in" on the correct velocity for each length.

In this method we find stress in terms of impact velocity assuming that the acoustic impedance does not change ( $\sigma = C_0 \rho V_0$ ). We also can find  $\int F dt$  and  $\int m dv$  from the pendulum data assuming that  $dt$  is a function of the specimen length and  $C_0$ . Both of these assumptions involve  $C_0$ , which must also be measured in instances where materials of unusual or unknown characteristics are under study.

The value of  $C_0$  can be derived from the time which the specimen remains in contact with the target. For electrically conducting materials this might be done by electrical contacts. For non-conducting materials a separate apparatus might be required which is designed for this determination only. In any event we have not yet needed to use this method and have not yet built any equipment associated with it.

(The above material is contained in USAERDL Report 1643-TR--  
The Response of Materials to Dynamic Loads-- 20 July 60, ASTIA-AD  
243 547.)



## REFERENCES

1. Clark, D. S. and Wood, D. S. , "Time Delay for Initiation of Plastic Deformation at Rapidly Applied Constant Stress," Proc of ASTM, Vol. 49, p. 717 (1949).
2. Massard, J. M. and Collins, R. A. , "The Engineering Behavior of Structural Metals Under Slow and Rapid Loading," June 1958, University of Illinois, Contract N-Onr-1834(01).
3. Ziembinski, S. J. , "New Impact Tester Checks Metal Fatigue," Industrial Laboratories Magazine, May 1959.
4. Campbell, J. D. and Maiden, C. J. , "The Effect of Impact Loading on the Static Yield Strength of Medium Carbon Steel." June 1957, Jour of Mech and Physics of Solids, Vol 6 (London).
5. Whiffin, A. C. , "The Use of Flat Ended Projectiles for Determining Dynamic Yield Stress - Part II - Tests on Various Metallic Materials," Proc. of Royal Soc (London), Vol. 194A, Sept 1948.

## DISCUSSION

Dr. Bailey, U. S. Army Quartermaster Res & Eng Center: I wonder if you could describe the material itself in condition of delayed yield? Do you know anything about what changes have taken place in the material?

Mr. Paca: When you talk about dynamic strength and dynamic response in a material, you have to determine at first whether the material actually has strength or is this just a response. In delay yield, you probably all know, that if the delay in time is 100 microseconds, and if you only subject the material to 50 microseconds work, you have done 50 microseconds work of dislocation damage. It was found that if you run delayed yield tests under constant rate of strain loading and suddenly applied constant stress, these can be interchanged. There is a certain stress point at which you don't have any delayed yield. I think this is the activation energy at absolute zero or something like that. This is why the Taylor and Griffin experiments cannot handle material of delayed yield. Because when you impact something against a target at 25,000 fps, your stress far exceeds the activation energy at absolute zero.

## STRUCTURAL RESPONSE TO MISSILE THRUST

J. N. Crenshaw\*

### ABSTRACT

This paper presents a method for the evaluation of a so-called Dynamic Load Factor for use in the design of missile structures. In the general case one of the major shocks that the missile experiences is a result of the increase of the thrust vector as the motor is ignited.

Application of the technique to the problem of determining a design factor for use in missile structures is the objective of this study. This work is based on effort accomplished in the feasibility study stages of the SATURN vehicle by Dr. Rudolph Glaser, MSFC, NASA. Consideration of missile structures as mass-spring combinations may be used to provide a mathematical model for investigation. In the simplest case a single-spring, single-mass combination can be utilized. In the general case (for complex elastic structures)  $n$  mass-spring combinations are possible.

Initially, investigation develops a mathematical model for a thrust time history of a missile motor. Comparison of this theoretical model with measured firing test results is shown. Application of thrust as a forcing function on a single-mass spring model is accomplished. Using the ratio of a natural frequency of the spring mass to the frequency of the forcing function as a parameter, the response of the vehicle in terms of a multiple of the instantaneously impressed force is defined.

This investigation shows that use of a single spring-mass model results in dynamic load factor values which compare favorably with tests as found in a particular test case. Need for additional test measurement procedures and a clarification of the relationship of the actual structural mass distribution to the forces that are generated as a result of motion is necessary.

---

\* J. N. Crenshaw, Chief, Dynamics Analysis Branch, Structures and Mechanics Laboratory, Redstone Arsenal, Alabama.

Initially, it is pointed out that Dr. Rudolph Glaser of the Structures Branch, P&VD, Marshall Space Flight Center, Huntsville, Alabama is the originator of the basic analysis and simplification techniques utilized herein. From the time that man first understood the meaning of the word load, he has attempted to account for the response of the resisting structures by various methods. Consideration of all the types of loads allows us to distinguish two individual classifications--static (constant, time-independent) and dynamic (time-varying, time-dependent). For design requirements we must determine the maximum worst loading condition which the structure is expected to survive. Since a dynamic load is composed of two elements--the external force and the inertial force resulting from the motion of the masses themselves--it is necessary to consider the combined effect. The rapid burning of modern-day propellants imposes the dynamic condition on the thrust force utilized to propel missiles.

Any elastic structure may be modeled by a single mass-spring system. Assume that we impress the time-dependent external load,  $F(t)$ , on the mass and that damping is negligible. We may now express the equation of motion of this system as

$$m \ddot{x} + k x = F(t) \quad (1)$$

If we assume a load  $F(t)$  as shown in Fig. 1, we may approximate the function by a number of straight lines. The slopes of the straight line pieces are

$$a_i \quad i = 1, 2, \dots, n$$

and the time increments,

$$t_i \quad i = 1, 2, \dots, n+1$$

are the abscissas of the intersection points. Actually, the function which we consider here is composed of individual load elements (Fig. 2) with a particular slope:

$$a = \frac{F}{t_{n+1} - t_n}$$

Introduction of two separate load functions at time points,  $t_n$  and  $t_{n+1}$ , as shown in Fig. 3 allows representation of the total load element by superposition. For any straight line interval, i.e.  $t < t_{n+1}$ , we may express the differential equation resulting from the first load function as:

$$\begin{aligned} m \ddot{x} + k x &= a(t - t_n) \\ t &= t_n \\ x &= 0 \\ \dot{x} &= 0 \end{aligned} \quad (2)$$

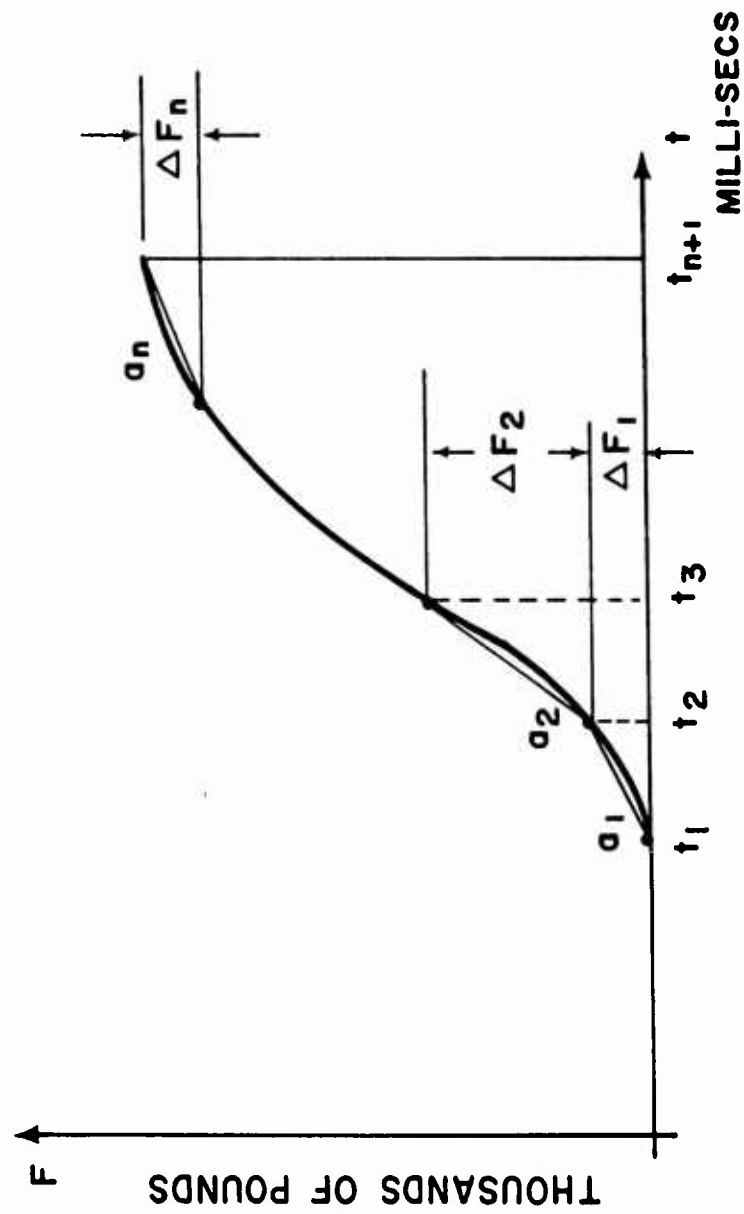


FIG. 1 LOAD AS A FUNCTION OF TIME

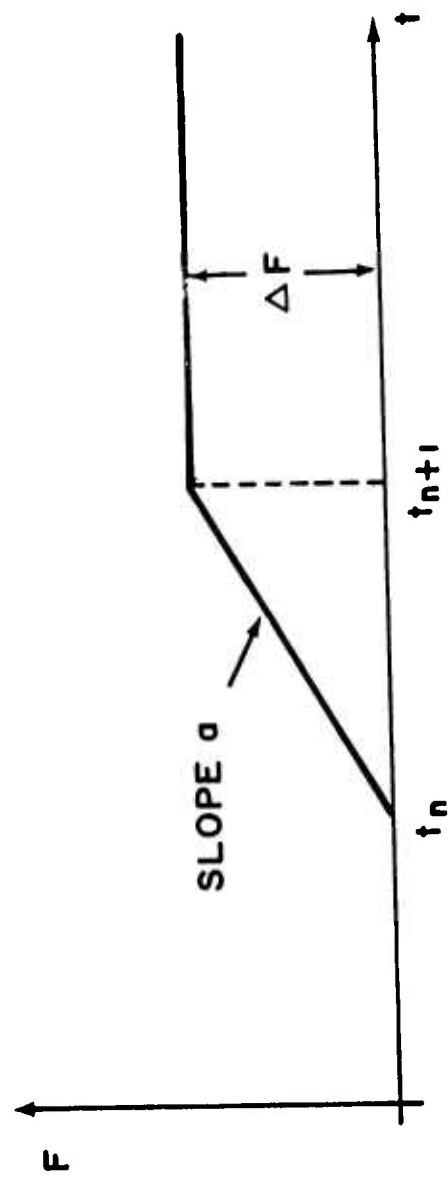


FIG. 2 LINEAR LOAD FUNCTION

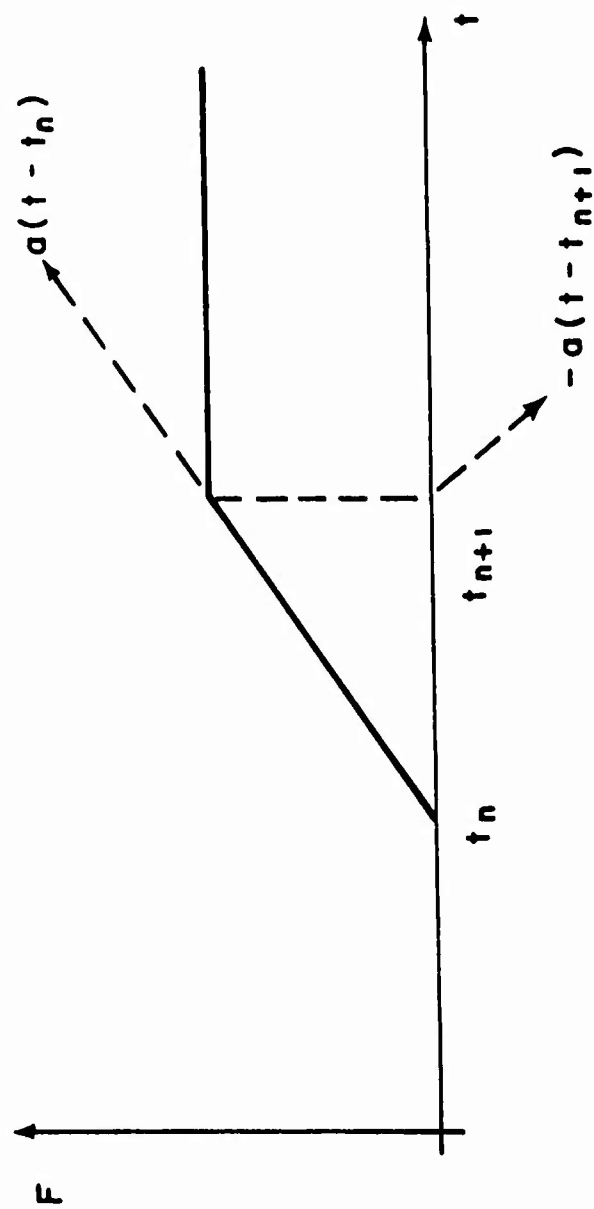


FIG. 3 SUPER POSITION OF TWO LINEAR LOAD  
FUNCTIONS

If we assume the initial conditions as shown, the solution of the equation is given by:

$$x = \frac{a}{k} (t - t_n) - \frac{a}{k \omega} \sin \omega (t - t_n) \quad (3)$$

Multiplying by  $k$  gives:

$$k x = a(t - t_n) - \frac{a}{\omega} \sin \omega (t - t_n) \quad (4)$$

where  $kx$  is the resulting spring force due to the vibration of the system. The term  $kx$  is usually called the "Dynamic Response". As shown by Equation (4), the response is a function which oscillates about the linear segment of the load function as shown in Fig. 4. Similarly, the response of the second load function of Fig. 3 is given by:

$$k x = -a(t - t_{n+1}) + \frac{a}{\omega} \sin \omega (t - t_{n+1}) \quad (5)$$

Use of a suitable time function such as:

$$A(t^*, t) = 1/2 \left[ |t - t^*| + (t - t^*) \right] \quad (6)$$

allows us to combine the superposed functions (4) and (5) because

$$A(t^*, t) = \begin{cases} 0 & t < t^* \\ t - t^* & t \geq t^* \end{cases} \quad (7)$$

It is possible to express the dynamic response of an external force approximated by straight lines as shown in Fig. 2 by a linear combination of expressions:

$$kx = \sum_{i=1}^n \left\{ a_i \left[ A(t_i, t) - A(t_{i+1}, t) \right] - \frac{a_i}{\omega} \sin \omega A(t_i, t) + \sin \omega A(t_{i+1}, t) \right\} \quad (8)$$

The first term in Equation (8) represents the external load and the second term represents the oscillating inertial forces of the moving structure as shown in Fig. 4. If for the considered time the internal inertial forces are less than maximum  $F$ , then instantaneous DLF equals the dynamic response,  $kx$ , divided by instantaneous forcing load. If we turn now to consideration of the time interval,  $t > t_{n+1}$ , and we consider the constant portion of the thrust-time curve, Equation (8) may be reduced to the following form:

$$k x = \max F - \sum_{i=1}^n \frac{a_i}{\omega} \left[ \sin \omega (t - t_n) - \sin \omega (t - t_{n+1}) \right] \quad (9)$$

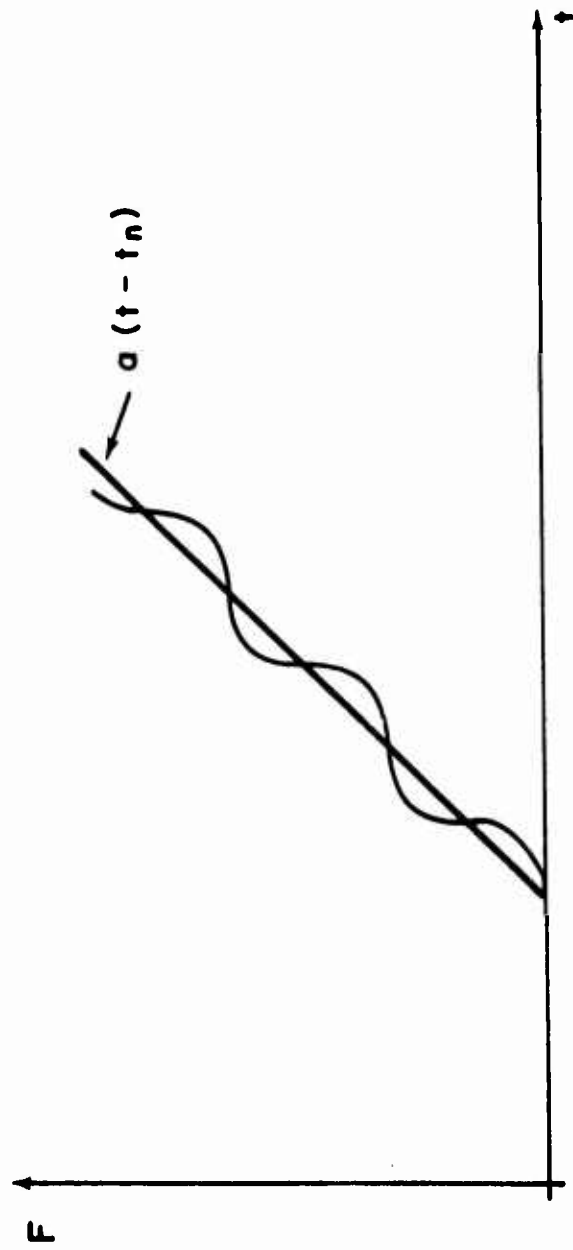


FIG. 4 DYNAMIC MODIFICATION OF A LINEAR LOAD  
FUNCTION



which may be expressed in two forms

$$k x = \max F - \tau_1 \cos \omega t + \tau_2 \sin \omega t \quad (10)$$

or

$$k x = \max F - A \cos (\omega t + \phi) \quad (11)$$

with constants:

$$\tau_1 = \frac{1}{\omega} \sum_{i=1}^n a_i (\sin \omega t_{i+1} - \sin \omega t_i) \quad (12)$$

$$\tau_2 = \frac{1}{\omega} \sum_{i=1}^n a_i (\cos \omega t_{i+1} - \cos \omega t_i) \quad (13)$$

and

$$\tau_1 = A \cos 0 \quad (14)$$

$$\tau_2 = A \sin 0 \quad (15)$$

$$A = \tau_1^2 + \tau_2^2 \quad (16)$$

$$\phi = \arctan \frac{\tau_1}{\tau_2} \quad (17)$$

Equation (11), which we use to represent the oscillation as shown in Fig. 4, denotes a sinusoidal vibration about the constant, instantaneous load, maximum  $F$ . If we consider a time interval  $t > t_{n+1}$ , Equation (8) becomes:

$$k x = \sum_{i=1}^n \frac{a_i}{\omega} \sin \omega(t - t_n) - \sin \omega(t - t_{n+1}) \quad (18)$$

Now if we consider again Fig. 2, we note that we have established a value of dynamic response for the linear load function over two separate time intervals, i.e.  $t_n$  through  $t_{n+1}$  and  $t_{n+1}$  through  $t_{n+2}$ . Utilizing Equations (9), (18), and the expressions for the forms shown in Equations (12), (13), (14), (15), (16), and (17), we may calculate the instantaneous value of dynamic response for any time point in the thrust-time history of the missile thrust.

If we can express our problem in a mathematical model for a single mass-spring arrangement, we may determine the effect of thrust variation on an elastic structure. A particular application for this technique is the problem of determining a Dynamic Load Factor for the design of a hold-down fixture for a missile. A very useful parameter is the ratio of

the natural frequency of the spring-mass to the frequency of the forcing function. It is possible with a known average thrust-time history for a given motor to show the relationship of DLF to the natural frequency of the structure. Parametric studies investigating this relationship enable us to arrive at realistic values of weight and stiffness for the structure at a point in preliminary analysis much earlier than otherwise.

#### DISCUSSION

Dr. Bailey, U. S. Army Quartermaster Res & Eng Center: Have you observed any malfunctioning of missiles due to this hold down thing?

Mr. Crenshaw: No, because to be quite honest, most of the current missile designs simply assume some dynamic load for the purpose of stress analysis. Of course, you have to look realistically at the whole design condition. I might point out one thing. The staggering of the engines on the Saturn, after studying the firing of the engines, was arrived at on the basis of this technique.

Herman P. Gay, APG-BRL: I think you might be interested to know that during the war sometime J. M. Franklin at the David Taylor Model Basin was interested in similar subjects, and published a report called "The Response of Simple Elastic Structures to Impact". He handled some functions like you indicated and I think he may have gotten an analytical solution in addition to some other work. It is a very interesting technique and very useful one. There was also some work done by Ayre on the West Coast and later followed up by R. E. D. Bishop in England, on a phase plane technique which is similar to and rather an extension of Franklin's work. It is always difficult in stepwise linear problems to approximate the force. Instead of approximating the force by series of ramp functions we approximated it by a series of step functions and it took some experience on the part of the operator to pick out the proper widths and heights of the steps. But we found that one can get quite good reproducible accuracy if one approximates  $Fdt$  by a series of sectors and from this calculates the corresponding forces and their duration.

Mr. Crenshaw: I would like to make one more comment. This approach does not claim to be anything more than just elementary mathematics. But it is a technique and it is surprising that it comes up with good answers. I have seen a number of other techniques. Convair, for example, developed an excellent one and used it on the Polaris. It was entirely different from this; and they came up with a useful result. What I am saying, gentlemen, is that I have gotten away from the dynamic behavior of materials and got into the realm of structural dynamics, the analysis of structural dynamics. Look at it in this light. You must have a technique which helps to obtain data for the designer to use when he puts his ideas on the board. I am sort of a

hybrid, half way between a scientist and an engineer, and I feel very strongly about this. You must have structural integrity, you must have numbers to prove it; you must be able to tell if these numbers are realistic by tests. I got real enthusiastic over this, and if anyone wishes to contribute his ideas on the subject, please do so.

Irwin Vigness, U. S. Naval Res Lab: First before I make any comment, I would like to thank the Army and the other persons who have made the arrangements and provided this very interesting meeting for us. As far as this particular paper is concerned, it has been most interesting to me also. The technique described is almost identical to what we call shock-spectra. And it is also almost the same as what was developed by Biot for the analysis of earthquake shocks. I would like to impress upon everyone that if you use the normal mode approach for the calculation of response of a complicated structure, you can break it down into any number of degrees of freedom that you wish and you may even consider it to be a distributed mass system. You do not have to break it down to mass spring system; the responses, as determined for the single degree of freedom system, may be placed in the equations which would be used for the solution of the more complicated case and give a direct answer so that no integrations need to be carried out in the more complicated case. And that is one reason that it has had such wide acceptance in a general field of shock and vibrations for determining the response of structures.

Dr. Hammer: I want to congratulate Mr. Crenshaw for his enthusiasm. I am also part scientist and part engineer and I would like to encourage you to keep up the good work. We, at Springfield Armory, are using the phase plane method for recoil analysis and our results greatly help the designers. As a matter of fact, we incorporated this technique into an academic presentation called "The Big Three - Analytical Design, Engineering Photo Analysis, Analog Computer", and used it for analyzing a 37mm AA weapon. We applied the method illustrated by you repeatedly and checked and double checked it with high speed motion pictures and analog computer. I am sorry that I did not know about this phase of your presentation because I would have been able to show slides which would indicate that there was excellent correlation between results established with the three mentioned techniques and the results were of great help to the designers. Keep up your enthusiasm and more power to you.

Mr. Crenshaw: Thank you, Dr. Hammer. No doubt, the presented technique was over-simplified but it could be used for solving more complex problems.

Dr. Hammer: In order to be accepted or be helpful, it is not necessary that the technique should be a complicated one. What the designer needs is the simple approach, not necessarily adorned with erudite mathematical manipulations. Do not apologize for your simple approach; the simpler the better.

ABSTRACTS FROM THE SYMPOSIUM  
ON  
STRUCTURAL DYNAMICS UNDER HIGH IMPULSE LOADING

Dayton, Ohio

17 - 18 September 1962

Co-sponsored by Aeronautical Systems Division

&

The Office of Aerospace Research

## PROJECTION TECHNIQUES

J. W. Gehring

Head, High Velocity Impact Gp, Flight Physics Laboratory  
General Motors Corporation Defense Research Laboratories  
General Motors Corporation, Box T  
Santa Barbara, California

This paper reviews the techniques used to accelerate projectiles to high velocity for impact and similar studies. Each type of projector is described briefly. The current capability of each is discussed as well as their potential for future improvement.

The type of projector used for a high velocity impact experiment is shown to depend critically upon the velocity and the projectile to be fired, in the sense that each projector has some unique features, which make it particularly applicable for certain experiments, but none are universally useful. The state-of-the-art is reviewed and it is pointed out that gas guns, explosive guns, and electric guns are the principal types of projectors, although only the first two have been developed to produce high velocity, except for microparticles. Current performance capabilities are discussed, and it is found that light-gas guns are capable of launching projectiles of known and controllable shape, mass, material, and orientation at velocities near 30,000 ft./sec., that explosive techniques can accelerate certain projectiles of less well defined shape and mass to a velocity of near 70,000 ft./sec., but that electric guns have not yet launched sizeable projectiles at even the relatively low velocity of 10,000 ft./sec.

The future potential of high velocity projectors is discussed. It is concluded that light-gas guns and explosive devices are the most promising types for sizeable projectiles and the electrostatic accelerators for microparticles. Performance estimates indicate that light-gas guns may be capable of firing at velocities of 40,000 ft./sec. and explosive devices at velocities of 80,000 ft./sec. and possibly as high as 100,000 ft./sec.

## DEFECTS IN SOLIDS AT HIGH VELOCITIES

A. N. Stroh

Associate Professor  
Massachusetts Institute of Technology  
Cambridge 39, Massachusetts

The behavior of dislocations moving at both subsonic and supersonic velocities is reviewed. At supersonic velocities energy is radiated and

a rather high stress is needed to maintain the motion. The properties of edge and screw dislocations which differ much more at high velocities than at low are contrasted. A major problem of dislocation dynamics is the nature of the resistive forces limiting the velocity and current ideas on this are discussed. The dependence of the dislocation velocity on the applied stress has been measured for several materials, but the relationship is not yet fully understood. Finally the production of point defects by rapidly moving dislocations is considered.

#### WAVE PROPAGATION IN UNIAXIAL STRAIN

John H. Percy  
Research Engineer  
Massachusetts Institute of Technology  
Cambridge 39, Massachusetts

Interest in this topic centers on the constitutive equation or behavior of materials under the extreme conditions of high impulse loading. Recent and current work in the field is treated generally and one area, the elastic-plastic behavior of aluminum at comparatively low pressures, is considered in detail. The outlook for future work is discussed.

#### STATIC FRACTURE

George R. Irwin  
Superintendent, Mechanics Division  
U. S. Naval Research Laboratory  
Washington 25, D. C.

This paper discusses the conditions governing the development of unstable progressive crack extension at normal speeds of stress application. Progress in this field has resulted from separating the topics of fracture initiation and crack extension. The relevance of laboratory tests to service behavior may then be represented for fracture initiation by flaw statistical analysis and for crack extension by fracture mechanics analysis. The concepts now at hand for fracture strength and for the ductile-brittle fracture mode transition will substantially assist the establishment of sound relationships between atomic and macroscopic properties. The impact of new viewpoints is expected to be of special practical interest in application to new fields such as composite materials, adhesive joints, and fatigue.

## TIME DEPENDENT FRACTURE

C. C. Hsiao

Associate Professor

University of Minnesota

Minneapolis 14, Minnesota

A brief account is given of some recent efforts here and abroad in studying the nature of rupture of solids. One of the important factors has been found to be the variation of time in the process of destruction of the solids. For a large variety of solids both in experiment and in theory the logarithm of time has shown to be linearly related with the applied uniaxial state of tensile breaking stress. This linear law has been established at least for some solids over a time range of a dozen decades from micro-seconds through months. Some suggestions are also given for future investigations on the time dependent fracture of solids.

## SOME PROBLEMS IN DYNAMIC RESPONSE OF TWO-DIMENSIONAL STRUCTURES

W. H. Hoppmann II

Professor of Mechanics

The Rensselaer Polytechnic Institute

Troy, New York

The paper presents a discussion of the problem of dynamical response of simple two-dimensional structures such as plates and shells to impulse loading. Consideration is given to the relationship between propagation of waves in the medium and the normal mode vibrations of the medium. Consideration is also given to the connection between the theory of dynamics of the three-dimensional continuum and that for the two-dimensional structures. The need for studies on one-dimensional bars is taken into account. The role of the constitutive equations and change of state of the material under load is briefly discussed. Finally motivations for various kinds of studies on the subject and also future needs are surveyed.

## HYPERVELOCITY IMPACT STATUS OF EXPERIMENTS

Walter Herrmann

Aeronautical Research Engineer

Massachusetts Institute of Technology

Cambridge 39, Massachusetts

A brief account of the development of hypervelocity impact experimentation is given, and the applicability of the presently available information to target design is discussed. Most of the available information refers to

cratering in effectively semi-infinite targets, or penetration of a single thin target, at velocities below 10 km/sec. This information is not directly applicable to hyperballistic penetration of complex built up targets, nor to penetration at meteoroid velocities. Dynamic measurements of quantities during crater formation, however, have led to a detailed qualitative understanding of cratering physics, which should ultimately lead to an adequate theory which will be useful as a design tool, and allow rational extrapolation to higher velocities.

DYNAMIC PROPERTIES OF MATTER  
UNDER HIGH STRESS-THERMODYNAMIC  
DESCRIPTIONS

Harold L. Brode  
Physicist  
The RAND Corporation  
Santa Monica, California

Although solids behave elastically at very low stress levels, and exhibit complex visco-elastic and plastic behavior at higher stress levels, when stresses in the megabar range are applied, it is generally more meaningful to ignore stress tensor descriptions and turn to thermodynamic and fluid dynamic descriptions. At high enough stress levels any material must be viewed as a compressible fluid.

Some empirical information is available in the regions of stress of a few kilobars to a few megabars from high explosive shock experiments. Static compression data are useful guides at lower stresses, but at the highest levels one finds the properties are reasonably well determined by atomic models such as a Fermi-Thomas-Dirac temperature dependent model. Theoretical calculations, numerical in nature, have provided the thermodynamic properties of all atomic elements. The properties of chemical mixtures as occur in natural materials can be constructed from suitable combinations of these elementary results. Successful use has been made of such results for calculations of dynamic response under high impulse loadings in a variety of applications.

DYNAMIC ANALYSIS IN VISCOELASTIC  
MEDIA

R. J. Arenz  
Research Assistant  
California Institute of Technology  
Pasadena, California

Distinguishing characteristics of viscoelastic media are reviewed with special reference to dynamic stress analysis. To circumvent the inherent computational difficulties in the usual transform type of solutions, an



extension of the Schapery method is proposed for approximating the viscoelastic strain distribution due to wave effects. From an experimental standpoint, the use of photoelastic materials to model the responses due to dynamic loading is discussed. It is emphasized that quantitative analysis depends upon knowing the birefringence as a function of strain rate and temperature. Certain characteristics pertinent to its measurement are therefore reviewed in order that dynamic photoviscoelasticity may be used in conjunction with the dynamic mechanical property characterization to complete a dynamic viscoelastic analysis. A method of correlating the approximate analysis with experimental results is pointed out.

#### SPALL FRACTURE

C. D. Lundergan

Chief, Physical Properties Division

Sandia Corporation

Albuquerque, New Mexico

The reported spall thresholds in copper, namely; ultimate, upper and lower fracture, and separation are discussed with relation to the stress-time history in the region of failure and to the experimental techniques used to induce the shock waves. The dynamic properties under uniaxial strain, and the geometry of the medium which influences the fracture and separation spall thresholds in polycrystalline metals are considered. Some suggestions are made as to the applicability of the various approaches of determining spall thresholds for obtaining more information about the microscopic and structural behavior of mediums subjected to short time intense impulsive loads.

#### UNIAXIAL STRESS CONDITIONS

Gordon L. Filbey, Jr.

University of Pennsylvania

Philadelphia, Pennsylvania

The propagation of waves of plastic deformation is experimentally studied in rods undergoing free flight impact with diffraction grating strain gages. Verification of the strain-rate-independent theory of Karman and Taylor has been demonstrated for several annealed fcc metals by Bell, using impact velocities up to 1100 inch/sec, and at 3000 inch/sec in experiments of the author with annealed aluminum. Aspects of dynamic overstress, initial development of the plastic wave, final strain distribution in finite rods and unloading phenomenon are discussed.

## ORIENTED SOLIDS

J. L. Ericksen  
Mechanics Department  
The Johns Hopkins University  
Baltimore, Maryland

Roughly, a continuum theory of oriented materials is one which ascribes a structure to a material point. This concept is useful for combining ideas concerning microscopic structure with thoughts concerning the macroscopic behavior of materials. Our purpose is to describe some theories of this type which show promise as theories to describe nonlinear mechanical behavior of solids.

## DISLOCATION CONCEPTS OF STRAIN RATE EFFECTS

J. E. Dorn and Frank Hanser  
University of California  
Berkeley, California

Whereas von Karman and Taylor independently based their analyses for plastic wave propagation on the deformation concept which assumes the deformation stress is exclusively a function of the plastic strain, Malvern believed that a viscoelastic type of behavior is more realistic, assuming the flow stress is a function of the strain rate as well as the strain. With relatively few exceptions, current investigators of plastic wave propagation phenomena are rather sharply divided into two camps, those that insist on the von Karman-Taylor type of formulation and those that adhere to the Malvern approach. It is the thesis of this paper that both concepts are substantially correct under appropriate circumstances. This thesis will be upheld not only in terms of new experimental evidence but also in terms of deductions arrived at from elementary dislocation theory.

ABSTRACTS FROM THE SYMPOSIUM  
ON  
DYNAMIC BEHAVIOR OF MATERIALS

University of New Mexico

Albuquerque, New Mexico

27 - 28 September 1962

Sponsored by the Civil Engineering Department, University of New Mexico

&

The Rock Mountain District  
of  
The American Society for Testing and Materials

## HIGH SPEED TENSILE TESTING OF SELECTED POLYMERS

R. R. Cosner

Union Carbide Chemicals Company  
South Charleston, West Virginia

Equipment and testing techniques for tensile testing with complete continuity of crosshead speeds from 0.02 to 12,000 inches per minute are described and discussed. Included are methods of actuation, load cells, velocity monitoring, and environmental chambers for  $-100^{\circ}\text{C}$  to  $+200^{\circ}\text{C}$ .

The effects of rate and temperature, as determined by these techniques, upon the mechanical behavior of high and low density polyethylene and plasticized vinyl are presented and discussed.

## HIGH SPEED COMPRESSION TESTING OF THERMOPLASTICS

Richard E. Ely

U. S. Army Ordnance Missile Command  
Redstone Arsenal, Alabama

Compressive properties for polyethylene, ethyl cellulose, and cellulose acetate butyrate are reported for stress rates ranging from static conditions to 1,000,000 psi/sec. and for several test temperatures. The cylindrical compression specimens had a slenderness ratio of 8, and the specimen ends were lubricated to reduce the effect of end constraint. Stresses at specific strain values and secant moduli are reported for over 330 tests. Tests were conducted with the aid of an Instron Tester and a pneumatic-type, high-speed compression machine which was developed for this study.

A second study was conducted to investigate the influence of specimen length and test method on the compressive properties of plastics. Room-temperature tests were conducted at constant strain rate by using a prescribed crosshead velocity with each length of specimen. Two strains rates and specimens with both dry and lubricated ends were employed. These results are utilized to interpret the data obtained at high loading rates.

IMPACT PERFORMANCE OF HIGH STRENGTH  
HT-1 AND NYLON PARACHUTE MATERIALS  
TO MACH 0.7

Robert J. Coskren, Chauncey C. Chu, Henry M. Morgan<sup>(1)</sup>  
Fabric Research Laboratories, Inc.  
Dedham, Massachusetts

A machine has been designed and constructed under the sponsorship of ASD<sup>(2)</sup> which is capable of evaluating parachute components of up to 10,000 pounds static breaking strength at impact velocities between 200 and 700 feet per second. The system consists mainly of a helium operated cannon for propelling various masses, together with photographic instrumentation for observing the impact. Force is measured from missile deceleration during impact. Extension is measured directly from changes in gage mark spacing on the test specimen. Energy absorption is calculated from the displacement of two ballistic pendulums.

Results reveal that, at impact speeds, force and strain waves are generated which cause rapid changes in the tensile response of the materials studied.

Energy measurements indicate a potential change in the stress-strain curves of the components during impact. The energy absorbing capacity of HT-1 materials, in particular, is reduced considerably at impact velocities in excess of 500 feet per second.

A color movie illustrating the operation of the equipment will be shown.

(1) Present address: KLH Research and Development Corporation,  
Cambridge, Massachusetts.

(2) Aeronautical Systems Division, U. S. A. F. Contract Nos. AF 33(616)-  
6321 and -7627.

REPORT ON ROUND ROBIN TESTING  
OF THERMOPLASTICS

ASTM Committee D-20 Task Group on High Speed Testing  
Gordon D. Patterson, Jr.  
E. I. du Pont de Nemours & Co., Inc.  
Wilmington 98, Delaware

In recognition of accelerating interest in the significance of the mechanical behavior of visco-elastic materials at high strain rates, ASTM Committee D-20 on Plastics has instituted a long-range inter-laboratory testing program. This work seeks to assess the effects of various techniques and equipment characteristics on the quantitative data obtained. Progress

is reported on four round robins wherein the data in part confirm certain theoretical suppositions and further suggest important test parameters requiring clarification.

#### AN INVESTIGATION OF THE DYNAMIC MECHANICAL PROPERTIES OF POLYETHYLENE

S. Matsuoka and C. J. Aloisio  
Bell Telephone Laboratories  
Murray Hill, New Jersey

The stress-strain properties of linear and branched polyethylenes with various thermal histories were investigated with Maxwell's dynamic tester<sup>(1)</sup> at frequencies from 0.01 to 100 cycles per second and at temperatures from -70 to +100°C. The "beta" peak in a loss tangent vs. log frequency curve for branched polyethylene was found to shift with temperature change in the Arrhenius manner rather than following the W-L-F equation.<sup>(2)</sup> Linear polyethylene does not exhibit the "beta" peak at corresponding temperatures and frequencies, but it was found to have a peak at about 70°C and 1 cycle per second. This peak was found to shift with temperature change similarly to the above mentioned "beta" peak in branched polyethylene. The experimental apparatus is described in detail. Relations between the dynamic properties of polymers and their behavior under actual use conditions are discussed.

(1) B. Maxwell, ASTM Bulletin No. 215, July 1956, p. 76 (TP132)

(2) M. L. Williams, R. F. Landel, and J. D. Ferry, J. American Chem. Soc. 77, 3701 (1955)

#### THE BEHAVIOR OF FILAMENTOUS MATERIALS SUBJECTED TO HIGH SPEED TENSILE IMPACT

Jack C. Smith  
National Bureau of Standards  
Washington 25, D. C.

When a filamentous material is subjected to an impact either transversely or longitudinally in tension, a strain wave is produced which propagates along the filament away from the point of impact. If this strain wave is sufficiently small the behavior of the material can be characterized by stress-strain and specific breaking energy data. A transverse-impact tester and a rotating disk impact tester, both operating at impact speeds up to 70 m/sec, are used for this purpose.

When the magnitude of the strain wave is large, the material may be characterized by its stress-strain data and critical breaking velocity.

These data are obtained by studying photographically the configurations and strain distributions in filaments struck transversely by rifle bullets at velocities up to 900 m/sec.

The impact behavior of several materials is illustrated with data obtained under various impact conditions. The results are interpreted theoretically and methods of improving the impact characteristics of these materials are discussed.

#### PRODUCTION OF STRONG SHOCKS IN PLASTICS BY ULTRA-SHORT IMPULSIVE LOADING

Dr. Arthur H. Guenther  
Air Force Special Weapons Center  
Kirtland AFB, New Mexico

Pressures in excess of 100 KB can be produced in plastics by the impact of high velocity thin plates. These plates, mainly mylar and lucite in the range of  $10^{-2}$  to .6 cm in thickness and areal dimensions to 7.5 cm square, have been accelerated by an exploding foil technique. Plates impacted at velocities approaching  $5 \times 10^5$  cm/sec have been used for the study of material dynamics at high transient pressures. Pulse lengths in the 0.1 to few microsecond region can be produced by this technique and the variation of the strength of materials with pulse length can be determined. A description of the technique and methods for analyzing the data will be presented including a short film depicting the construction of the transducer and photographic equipment used in the laboratory for the velocity determination. Variations of the technique as applied to equation of state and other methods for velocity determination will also be presented.

#### EXPERIMENTS ON THE MECHANISM OF SPALL

Donald W. Blincow and Donald V. Keller  
The Boeing Company  
Seattle, Washington

One-dimensional impulse loading experiments have been carried out on Lucite and aluminum to determine if the spall process occurs instantaneously upon the attainment of a critical tensile stress, or if there is a time delay between the attainment of a given tensile stress and spallation. The experiments involve the collision of two flat plates: a driver and a target. The velocity of the driver is adjusted until the threshold velocity for spall of the target is obtained. The experiment is repeated but with the thicknesses of the two plates scaled by some factor ( $\alpha$ ). The maximum tension is then unchanged, but the time over which it acts is changed by the factor ( $\alpha$ ).

In this manner the duration of tension was varied from  $2 \times 10^{-7}$  to  $50 \times 10^{-7}$  seconds for Lucite, and from  $10^{-7}$  to  $25 \times 10^{-7}$  seconds for aluminum. The threshold velocity for Lucite spall remained constant (60 meters/second) indicating that, over this time scale, the spall mechanism for Lucite is time independent and that a critical tensile stress exists ( $\sim 1$  kilobar). The threshold driver velocity for aluminum spall increased with decreasing driver thickness indicating a time dependent spall mechanism for this material, i.e. - a critical tensile stress does not exist.

#### ON EXPERIMENTAL SOLID DYNAMICS

George Gerard, Ralph Papirno and Herbert Becker  
New York University, New York, New York

There is a strong interdependence between the apparent dynamic properties of materials and the quantities measured by various experimental techniques. The principal task facing the investigator lies in the inference of stress from the measured quantities. In this report emphasis is placed upon the test technique and its influence upon the measured quantities rather than upon the correlation of data with theory. Three different types of solid dynamics experiments are reviewed from the standpoint of interpretation of stress: (1) One dimensional tension impact studies in which dynamic strain measurements are made simultaneously at several stations remote from the impact area, (2) Two dimensional studies on impulsively loaded diaphragms where dynamic strain and dynamic deflection are measured in an essentially wave free environment; (3) Dynamic photoelastic techniques employing stroboscopic lighting and repeated impacts where the minute details of a propagating wave can be investigated.

#### ON THE MEASUREMENT OF DYNAMIC STRESS-STRAIN CURVES WITH A UNIFORM UNIAXIAL STRESS SYSTEM

P. C. Johnson, B. A. Stein and R. S. Davis  
Arthur D. Little, Inc., Cambridge, Massachusetts

Past investigation of the strain rate dependence of the mechanical properties of solids have been carried out primarily through a study of the propagation characteristics of plastic waves down specimens in a rod or wire configuration. There are difficulties with experiments of this type because of the nonuniformity of stress and strain along the specimen at any instant of time. Moreover, in many cases the experimental techniques used are such as to impose constraints to lateral flow, which constitutes a departure from the true rod configuration.

We have designed an experimental technique which does not involve these difficulties and have used it for measurement of the strain rate dependence of the plastic flow behavior of metals. Specifically, we have observed the dynamic behavior of a freely expanding ring of the material under study.

The experimental technique used imparts to the ring an initial uniform radial velocity away from its center. The instant that the ring



begins to move, it separates from the energy source. Thereafter, the only force acting on the ring is its own circumferential or hoop stress. Since the ring cross-section is small relative to its diameter, there are no constraints to lateral flow, and the stress in the ring is homogeneous in any cross-section. The initial velocity of the ring is uniform so that the hoop stress is uniform, and there are, therefore, no plastic waves propagating along the circumference. The ring decelerates as a result of this uniform, uniaxial stress.

Strain measurements are carried out by high-speed photographic techniques. The instantaneous stress acting in the ring is given (exactly) by the equation

$$\sigma = -\rho r \ddot{r}$$

where  $\rho$  is the material density,  $r$  is the instantaneous radius of the ring, and  $\ddot{r}$  is the instantaneous deceleration.

The strain-time relationship is measured from the photographic record, and the stress corresponding to each level of strain is computed from the second differential of a curve analytically fitted to the strain-time data. It has also been possible to measure the uniform elongation before failure at high rates of strain for a number of materials under conditions of dynamic, uniform loading without constraints to lateral flow.

We have measured the stress-strain curves for 99.99% aluminum, annealed Armco iron, and annealed 304 stainless steel at initial strain rates from  $10^3$  to  $10^4$  per second.

#### THE METALLURGICAL EFFECTS OF EXPLOSIVE STRAINING OF SELECTED METAL ALLOYS\*

Louis Zernow, Irving Lieberman, John Wilkin and Erik Henriksen  
Aerojet-General Corporation  
Downey, California  
and  
W. B. McPherson  
Marshall Space Flight Center  
Huntsville, Alabama

A series of selected alloys have been subjected to both conventional and explosive straining in a study aimed at comparing their behavior and evaluating the metallurgical effects.

The alloys studied include 5456-0 aluminum alloy, AISI 301 stainless steel, 17-7 PH stainless steel and the two titanium alloys 6Al-4V and 13V-11Cr-3Al.

Both uniaxial and biaxial straining studies are being carried out. The early data indicates marked sensitivity of the mechanical properties of some of the materials to the higher strain rates.

\* This study is being supported under Contract NAS 8-2416.

#### THEORETICAL PREDICTION OF STRAIN DISTRIBUTION UNDER IMPACT LOADING

S. Rajnak, F. Hauser, and J. E. Dorn  
University of California  
Berkeley, California

A recent determination of the relation between stress, strain and strain-rate for polycrystalline pure aluminum under impact loading permits precise theoretical predictions to be made of the behavior of thin bars using a "Malvern" type system of equations. A computation was carried out to check the validity of Kolsky's "thin wafer" technique for determining the relation between stress, strain and strain-rate. A long tubular bar was impacted and the final strain distribution was predicted using the experimentally determined strain-rate function. Excellent agreement was obtained.

#### PLASTIC IMPACTS ON SHORT CYLINDRICAL SPECIMENS

E. A. Ripperger and C. H. Karnes  
The University of Texas  
Austin, Texas

During the past two decades, much effort has been devoted to the determination of the relationship between stress, strain, and strain rate for engineering materials. Experimental evidence is available which indicates that for a given material there is a strain-rate effect, and likewise, evidence is available which indicates that for the same material there is no effect. These conflicting results are evidence of the difficulty of the problem of determining dynamic stress-strain characteristics and of the need for further study of the problem. Interest in this aspect of material properties is generated to a large extent by a need for such information in the analysis of plastic wave propagation, and in the analysis of structures loaded dynamically.

Ideally, one would like to be able to measure stress, strain and strain-rate characteristics independently of all other considerations. Unfortunately, this does not appear to be possible where high strain-rates are involved. Application of the loading required is accompanied by stress wave propagation phenomena in which strain rates are apt to be high and to some extent indeterminate. It therefore appears that

stress, strain, strain-rate relationships should be investigated indirectly by studying the propagation of waves, and in particular the propagation of plastic waves. The problem is a difficult one so it should not be expected that it can be solved in a neat and simple manner. As E. H. Lee pointed out in 1960, more quantitative information is needed to determine the specific nature of an adequate material properties law. By this he means information concerning the variation of stress with time and distance from the point of load application. It is the purpose of this paper to present some information of the type to which Lee refers. Two well known theories of plastic wave propagation, or of dynamic material properties, have been used to calculate stresses and strains produced by impacts, and these calculated values have been compared with measured values.

In the first of these theories, referred to as the nonstrain-rate theory, the material is assumed to follow the same stress-strain relationship under dynamic loading as it follows under static loading. The second theory, referred to as the strain-rate theory is based upon the assumption that the stress is a function of the instantaneous stress and strain rate.

Short, copper specimens in compression impact have been used to make it possible to measure stresses with the pressure bar technique at a point where the strains are still in the plastic range. Strain is measured by resistance gages on the specimen. Comparisons of these measured stresses and strains with corresponding values predicted by theory form the essence of the paper.

#### THE THREE LOW PRESSURE SPALL THRESHOLDS IN COPPER

J. H. Smith

Sandia Corporation

Albuquerque, New Mexico

Distinct spall thresholds are found in copper at 6, 13, and 22 kilobars with a square shock pulse of 1.5 microsecond duration. These thresholds are somewhat dependent upon the pulse width and shape and upon the metallurgical condition of the sample.

The two lower thresholds have not been determined previously although they have been observed qualitatively.<sup>1</sup> The 22 kilobar threshold

---

1. J. L. O'Brien and R. S. Davis, "On the Fracture of Solids under Impulsive Loading Conditions," Response of Metals to High Velocity Deformation, Vol. 9, July 1960, pp 371-388.

corresponds to the 28 kilobar threshold in copper measured by Rinehart.<sup>2</sup> The elimination of edge effects, in the present work, accounts for the lowering of this threshold.

To determine these thresholds, a 4-inch diameter projectile is accelerated in an air gun to impact two copper plates together in an evacuated chamber. The target plate uses a special tapered plug design to eliminate edge effects until after spall occurs.

2. J. S. Rinehart, "Some Quantitative Data Bearing on the Scabbing of Metals under Explosive Attack," Journal of Applied Physics, Vol. 22, May 51, pp 555-560.

#### A SUBMICROSECOND TECHNIQUE FOR SIMULTANEOUS OBSERVATION OF INPUT AND PROPAGATED IMPACT STRESSES

W. J. Halpin, O. E. Jones, and R. A. Graham  
Sandia Corporation  
Albuquerque, New Mexico

By impacting a quartz gage on a disk-shaped specimen in a precisely controlled flat-faced projectile impact, the stress-time history of the specimen material at the impact surface is observed. In this manner the mechanical behavior of the material in one-dimensional strain can be studied separate from wave propagation effects for rise times as short as  $10^{-8}$  sec and for stress amplitudes up to 21 kbar. Simultaneously, the stress-time profile of the resulting wave after a finite propagation distance can be obtained from another quartz gage mounted on the opposite face of the specimen. The gages are X-cut quartz disks having a thickness such that wave transit time through the disk is much greater than time variations in stress. Under the conditions of usage the specimen-to-quartz interface stress is proportional to the instantaneous current output. Typical records of input and propagated stress-time profiles are shown for aluminum, mild steel, and barium titanate. The technique is particularly advantageous in studies of the dynamic yield behavior of materials.

#### FRACTURE OF SINGLE CRYSTALS UNDER EXPLOSIVE LOADING

C. M. Glass, S. K. Golaski, and J. J. Misey  
Ballistic Research Laboratories  
Aberdeen Proving Ground, Maryland

Experiments have been carried out on the high velocity deformation and fracture of metals. Copper single crystals and polycrystalline specimens have been subjected to explosive loading and the following results have been obtained:

1. Crystal orientation influences the reaction of the metal specimens at pressures of testing above 100 kilobars. The orientation factor causes a redistribution of flow in the reflected tensile wave.

2. The fracture of the specimen is not "instantaneous", but times between  $10^{-4}$  and  $10^{-6}$  seconds are required.

3. A measure of the theoretical strength of the metal has been obtained.

4. Crack velocities have been calculated.

5. The concept of an energy criteria for fracture, rather than a maximum stress criteria is implied from the data.

In addition, variations in metal reactions to the compressive wave are shown to follow a pattern best described by the assumption of shear deformation occurring during the compression cycle. Low rate testing has shown that, over a small distance in the metal, deformation is not uniform, but cyclic, and quite dependent on the preferred orientations present in the sample.

#### RESIDUAL TEMPERATURES OF SHOCK-LOADED IRON

R. G. McQueen, E. Zukas, and S. Marsh

Los Alamos Scientific Laboratory

Los Alamos, New Mexico

Iron specimens were shock loaded in vacuo by explosively-driven iron plates. The rarefaction pressure release waves subsequently destroyed the vacuum, exposing the shock-heated samples to air. An oxide coating formed on the surface of these samples, giving rise to the well known temper colors of iron. Comparison of the color of the shocked specimens with that of prepared standards established the residual temperature of the shocked iron.

Shock pressures were measured by the standard flash-gap technique, and ranged from about 500 to 750 kilobars. In this region it was found that the final temperature of the iron varied linearly from about  $500^{\circ}\text{K}$  to  $750^{\circ}\text{K}$ . The experimentally determined temperatures are in excellent agreement with those calculated.

Work performed under the auspices of the United States Atomic Energy Commission.

PARTICIPANTS  
IN THE  
U. S. ARMY CONFERENCE  
ON  
DYNAMIC BEHAVIOR OF MATERIALS AND STRUCTURES  
26 - 28 September 1962

Abbe, Earl H.	Springfield Armory, Springfield, Mass. R & D
Adam, Leslie H.	Frankford Arsenal, U. S. Army Munitions Command
	Pitman Dunn Labs, Philadelphia, Pa.
Agen, Mrs. Helen E.	Hq, QM R&E Cmd, Natick, Mass.
Albright, Allan A.	Watervliet Arsenal, Watervliet, N. Y.
Alexander, Max	U. S. Army Automotive Cmd, Centerline, Mich.
Allen, Frank J.	Aberdeen Proving Ground, Aberdeen, Md.
Allen, Thomas D.	Watervliet Arsenal, Watervliet, N. Y.
Andersen, Dr. A. G. H.	Watertown Arsenal, Watertown, Mass.
Arbuthnot, Guy L., Jr.	U. S. Army Engineer Waterways, Experiment Station, Vicksburg, Miss.
Audet, Norman	Hq, QM R&E Cmd, Natick, Mass.
Austin, Harold R.	Watertown Arsenal, R & D, Watertown, Mass.
Avakian, Ralph	Watervliet Arsenal, Watervliet, N. Y.
Bailey, Dr. S. D.	U. S. Army Natick Labs, Natick, Mass.
Barry, John	Hq, QM R&D Cmd, Natick, Mass.
Beeuwkes, Dr. Reinier, Jr.	Watertown Arsenal, AMRA, Watertown, Mass.
Bengtson, Colonel Nils	U. S. Army Research Office, Durham, N. C.
Britton, Major General F. H.	Director of R&D, U. S. Army Materiel Command, Washington 25, D. C.
Burdett, Colonel A. M., Jr.	U. S. Army Materiel Cmd, Washington, D. C.
Cadle, Hubert	Springfield Armory, Springfield, Mass. R&D
Clark, E. N.	Picatinny Arsenal, Dover, N. J.
Colby, Richard A.	Springfield Armory, Springfield, Mass. WDB, R&D
Coles, Harold	Hq, QM R&E Cmd, Natick, Mass.
Coogan, Prof. Charles H.	University of Connecticut, Storrs, Conn.
Corley, 1st Lt William G.	USAERDL, Ft. Belvoir, Va.
Crenshaw, J. N.	Redstone Arsenal, Huntsville, Ala.
Curl, Charles H.	Watertown Arsenal, AMRA, Watertown, Mass.
Daniel, J. N.	Transportation Res Cmd, Fort Eustis, Va.
Davids, Norman	Penn. State University, University Park, Pa.
Davidson, Thomas E.	Watervliet Arsenal, Watervliet, N. Y.
Demitrack, George	Picatinny Arsenal, Dover, N. J.
DeSisto, Thomas S.	Watertown Arsenal, AMRA, Watertown, Mass.
Donath, Dr. F. A.	Columbia University, New York, N. Y.
Dora, Joseph C., Jr.	Picatinny Arsenal, Dover, N. J.

Dorfman, Abraham L.  
Dubensky, Robert G.  
Duffy, Dr. Jacques  
Dusenberry, Robert B.

Ehrman, Oscar W., Jr.  
Ellington, Donal G.  
Emerson, Lt. Col. K. C.  
Esslinger, William H., Jr.

Fahey, N.  
Falcone, James  
Fenstermaker, Carl A.  
Fisher, Dr. Bruce S.  
Fitzpatrick, Miss Catherine  
Flanagan, James H.  
Frankowski, Charles S.  
Freeman, Harry

Gay, Herman P.  
Geldmacher, R. C.  
Gerard, George  
Gilbert, Joseph T.  
Glassman, N. S.  
Goodrich, William  
Grabarek, Chester  
Griffel, William  
Gudzent, Dietrich E.  
Guenther, Walter

Halvatgis, Capt. J. N.  
Hammer, Dr. Alexander  
Hanson, Dr. A. C.  
Hanson, J. C.  
Harvey, Earle M.  
Hawthorne, Herman F.  
Hirshman, Spencer S.  
Hoge, Harold  
Holmes, Henry A.  
Hultgren, 2/Lt Ronald  
Huss, Harry O.

Jarrett, William J.  
John, Frank K.  
Julian, C. Nelson

Picatinny Arsenal, Munition Cmd, Dover, N. J.  
Batelle Memorial Institute, Columbus, Ohio  
Brown University, Providence, R. I.  
Watervliet Arsenal, Watervliet, N. Y.

Frankford Arsenal, Philadelphia, Pa.  
Picatinny Arsenal, Dover, N. J.  
U. S. Army Materiel Cmd, Washington, D. C.  
U. S. Army Missile Cmd, Redstone Arsenal, Ala.

Watertown Arsenal, AMRA, Watertown, Mass.  
Springfield Armory, Springfield, Mass. R&D MRB  
National Bureau of Standards, Washington, D. C.  
Army Research Office, Washington, D. C.  
Rock Island Arsenal, Rock Island, Ill.  
Hq, QM R&E Cmd, Natick, Mass.  
Springfield Armory, Springfield, Mass. R&D  
Hq, QM R&E Cmd, Natick, Mass.

Aberdeen Proving Ground, BRL, Aberdeen, Md.  
New York University, New York, N. Y.  
Allied Research Association, Boston, Mass.  
Frankford Arsenal, Philadelphia, Pa.  
U. S. Army Materiel Cmd, Washington, D. C.  
Watertown Arsenal, Watertown, Mass.  
Aberdeen Proving Ground, BRL, Aberdeen, Md.  
Picatinny Arsenal, Dover, N. J.  
U. S. Army Missile Cmd, Redstone Arsenal, Ala.  
Springfield Armory, Springfield, Mass. AOD

Springfield Armory, Springfield, Mass. AOD  
Springfield Armory, Springfield, Mass. R&D, MRB  
Rock Island Arsenal, Rock Island, Ill.  
Rock Island Arsenal, Rock Island, Ill.  
Springfield Armory, Springfield, Mass. WDB, R&D  
Springfield Armory, Springfield, Mass. R&D  
Frankford Arsenal, Philadelphia, Pa.  
Hq, QM, R&D Cmd, Natick, Mass.  
Watertown Arsenal, Watertown, N. Y., R&D  
U. S. Army Weapons Cmd, Rock Island, Ill.  
Edgewood Arsenal, Md. - U. S. Army CBR  
Engineering Group

Springfield Armory, Springfield, Mass. R&D WDB  
Watervliet Arsenal, Watervliet, N. Y.  
Springfield Armory, Springfield, Mass. R&D  
R&ML

Kaye, George	Picatinny Arsenal, Dover, N. J.
Kendall, David P.	Watervliet Arsenal, Watervliet, N. Y.
Kiley, Dr. Marcus M.	Deputy Superintendent of Public Schools, Springfield, Mass.
Kottcamp, Lt. E.	Frankford Arsenal, Philadelphia, Pa.
Korytoski, Robert D.	Springfield Armory, Springfield, Mass. R&D R&ML
Kropf, C.	U. S. Army Tank-Auto Cmd, Centerline, Mich.
Kumar, Dr. Sudhir	U. S. Army Research Office, Durham, N. C.
Kundig, Konrad J. A.	Watervliet Arsenal, R&E Division, Design Engineering Branch, Watervliet, N. Y.
Larsen, Dr. Finn J.	Asst Secretary of Army R&D, U. S. Army Materiel Command, Washington, D. C.
Laselle, Ralph	Watervliet Arsenal, Watervliet, N. Y.
Latimer, Lawrence E.	Redstone Arsenal, U. S. Army Missile Cmd, Redstone Arsenal, Ala.
Ledoux, Robert	Springfield Armory, Springfield, Mass. R&D, MRB
Lindholm, Ulric S.	Southwest Research Institute, San Antonio, Texas
Lizza, Albert J.	Springfield Armory, Springfield, Mass. WDB, R&D
Lossnitzer von, O. H.	Springfield Armory, Springfield, Mass. R&D PP&CO
Luukkonen, V. A.	Springfield Armory, Springfield, Mass. Eng Div
Lynch, Harry F.	Springfield Armory, Springfield, Mass. Eng Div
MacLaughlin, Thomas F.	Watervliet Arsenal, Watervliet, N. Y.
Massa, Edmund J.	Springfield Armory, Springfield, Mass. Eng Div
McAbee, Miss E.	Picatinny Arsenal, Dover, N. J.
McCook, Dr. T. Joseph	Superintendent of Public Schools, Springfield, Mass.
Medinnis, Colonel C. L. P.	Commanding Officer, Springfield Armory, Springfield, Mass.
Melichar, Joseph F.	Aberdeen Proving Ground, BRL, Aberdeen, Md.
Mellor, C. C., Jr.	Batelle Memorial Institute, Columbus, Ohio
Menezes, Lauro D'A	Picatinny Arsenal, Dover, N. J.
Mielke, Lt. Leo G.	Watervliet Arsenal, Watervliet, N. Y.
Moritz, Edward W.	U. S. Army Tank Auto Cmd, Centerline, Mich.
Morrissey, John	Watertown Arsenal, Watertown, Mass.
Mulherin, J. H.	Frankford Arsenal, Philadelphia, Pa.
Murdock, Roland G.	Springfield Armory, Springfield, Mass. R&D, R&ML
Murray, James	U. S. Army Research Office, Durham, N. C.
Newcomb, Fred	Aberdeen Proving Ground, Human Eng Lab, Aberdeen, Md.
Nowakowski, Benedict J.	Springfield Armory, Springfield, Mass. R&D R&ML



O'Brien, John F., Jr.	Springfield Armory, Springfield, Mass. R&D WDB
O'Neil, James F.	Springfield Armory, Springfield, Mass. R&D MRB
Ouellette, Herve J.	Springfield Armory, Springfield, Mass. R&D WDB
Paca, Francis B.	U. S. Army ERDL, Ft. Belvoir, Va.
Packard, Charles F.	Springfield Armory, Springfield, Mass. WDB R&D
Pagano, Victor H.	U. S. Army Tank-Auto Cmd, Centerline, Mich.
Pape, Walter E.	Rock Island Arsenal, Rock Island, Ill.
Parsons, Gordon	Watertown Arsenal, Watertown, Mass.
Piergiovanni, Antonio J.	Springfield Armory, Springfield, Mass. AOD
Pilsworth, M. N., Jr.	Hq, QM R&E Cmd, Natick, Mass.
Pradko, F.	U. S. Army Tank-Auto Cmd, Centerline, Mich.
Preska, Victor R.	Watervliet Arsenal, Watervliet, N. Y.
Purtell, John P.	Watervliet Arsenal, Watervliet, N. Y.
Reinsmith, Gerald	U. S. Army Weapons Cmd, Rock Island, Ill.
Riechiazzi, A.	Aberdeen Proving Ground, BRL, Aberdeen, Md.
Ripperger, Eugene A.	University of Texas, Austin 5, Texas
Rizzo, George	Watertown Arsenal, Watertown, Massachusetts
Roach, Thomas M. Jr.	Picatinny Arsenal, Dover, N. J.
Rocha, John G.	Springfield Armory, Springfield, Mass. R&D WDB
Rolfes, Edward M.	Hq, QM R&E Cmd, Natick, Mass.
Roll, Arthur A.	Frankford Arsenal, Philadelphia, Pa.
Rose, Carol D.	U. S. Army Tank-Auto Cmd, Centerline, Mich.
Rose, Paul A.	Springfield Armory, Springfield, Mass. Eng Div
Rothfuss, Neal B.	The Bendix Corp., Utica Div., 211 Seward Ave., Utica, N. Y.
Ruffini, Sylvestro J.	Picatinny Arsenal, Dover, N. J.
Schmitt, F. H.	Picatinny Arsenal, Dover, N. J.
Schufrien, L.	Picatinny Arsenal, Dover, N. J.
Schuman, William	Aberdeen Proving Ground, BRL, Aberdeen, Md.
Schwartz, Robert M.	U. S. Army Munitions Cmd, Picatinny Arsenal, Dover, N. J.
Shea, Richard	Watertown Arsenal, AMRA, Watertown, Mass.
Sibley, Maj General A. K.	Commanding General, U. S. Army Mobility Cmd, Centerline, Mich.
Skeiber, Lt Col S. C.	Springfield Armory, Springfield, Mass. Eng Div
Skroski, Edward B.	Springfield Armory, Springfield, Mass. AOD
Smith, Troy A.	U. S. Army Missile Cmd, Redstone Arsenal, Ala.
Taylor, Glenn	Aberdeen Proving Ground, BRL, Aberdeen, Md.
Teichman, I. W.	Aberdeen Proving Ground, Aberdeen, Md. D&PS, Armor Branch Automotive Div

Vernet, Ralph	Hq, QM R&E Cmd, Natick, Mass.
Vigness, Irwin	U. S. Naval Research Laboratories, Washington, D. C.
Voorhees, John E.	Batelle Memorial Institute, Columbus, Ohio
Wallace, Dr. Lawrence W.	U. S. Army Weapons Cmd, OMETTA, Rock Island, Illinois
Ward, John F.	NASA, Langley Research Center, VTOL Br, ASM Div, Langley Field, Hampton Station, Va.
Warner, Fred W.	White Sands Missile Range, Las Cruces, N. M.
Weden, Capt. Gilbert	Transportation Research Cmd, Ft. Eustis, Va.
Weiss, Dr. Richard A.	U. S. Army Materiel Cmd, Washington, D. C.
Weitzler, Irving M.	Hq, QM R&E Cmd, Natick, Mass.
Whittlesey, Welsh C.	Hq, QM R&E Cmd, Natick, Mass.
Winfree, Clarence H.	U. S. Army Tank-Auto Cmd, Centerline, Mich.
Wood, Benjamin F.	Aberdeen Proving Ground, Human Eng Labs, Aberdeen, Md.
Zaroodny, Serge J.	Aberdeen Proving Ground, BRL, Aberdeen, Md.
Zavarella, A.	Springfield Armory, Springfield, Mass. R&ML R&D

List of Invitees \*  
Symposium on Structural Dynamics Under High Impulse Loading

Headquarters  
AERONAUTICAL SYSTEMS DIVISION  
Air Force Systems Command  
United States Air Force  
Wright-Patterson Air Force Base, Ohio

Abrahamson, Dr. G. R.	Stanford Resch Inst, Stanford University, Menlo Park, Cal.
Abramson, Mr. H. Norman	Southwest Resch Inst, 8500 Culebra Road, San Antonio 6, Texas
Adair, Mr. A. W.	ASD (ARZ) Wright-Patterson AFB, Ohio
Allen, Mr. W. A.	Hq Pacific Missile Range, Point Mugu, Cal.
Anderson, Mr. D. E.	Arnold Eng Development Center, ARO Inc., Tullahoma, Tennessee
Anderson, Dr. G. D.	Stanford Resch Inst, Stanford University, Menlo Park, Cal.
Anderson, Dr. Hoyt	Aerojet General Corporation, Terminal Ballistic Dept, Ord Div, Downey, Cal.
Ashley, Dr. H.	Massachusetts Inst of Tech, Dept of Aeronautics & Astronautics, Cambridge, Mass.
Askey, Dr. Charles M.	Hayes International Corporation, Birmingham, Ala.
Atkins, Capt. Marvin	AFSWC (BSRV) Kirtland AFB, New Mexico
Atkins, Dr. W. W.	Naval Resch Lab, Washington 25, D. C.
Atkinson, Lt/Col Ivan	AFOSR, Solids State Sciences Div., Washington 25, D. C.
Baird, Mr. E. R.	Gruman Aircraft Eng Corp, Bethpage, L. I., N. Y.
Baker, Lt T.	BSD (BSRV) Air Force Unit Post Office, Los Angeles 45, California
Barry, Dr. W. T.	General Electric Company, Aeroscience Lab. Philadelphia, Penn.
Beals, Mr. V.	North American Aviation, Inc., ATTN: Dynamics Section, Columbus 16, Ohio
Beard, Dr. D. B.	Lockheed, Aircraft Missile and Space Div, Sunnyvale, Cal.
Becker, Mr. Herbert	New York University, New York City, N. Y.
Bennett, Mr. Fredrick	BRL, Aberdeen Proving Ground, Aberdeen, Md.
Berry, Dr. J. P.	General Electric Company, Aeroscience Lab, Philadelphia, Penn.
Bilek, Mr. Andrew G.	APGC (PGWRT) Eglin AFB, Florida
Bingman, Mr. R. N.	ASD (ASRMDD-23) Wright-Patterson AFB, Ohio

\* Names present in the previous list have not been included here.

Bisplinghoff, Dr. Raymond	National Aeronautical and Space Admin., Advanced Resch Technology Section, Washington, D. C.
Bjork, Dr. R. L.	RAND Corporation, Santa Monica, Cal.
Blatz, Mr. P. J.	California Inst of Tech, Pasadena, Cal.
Bollard, Dr. R. J. H.	Dept of Aeronautical Eng, Univ. of Washington, Seattle, Washington
Brode, Dr. Harold L.	RAND Corp, Santa Monica, Cal.
Brown, Dr. Robert	Biological Science, AFOSR, Washington 25, D. C.
Bucciarrelli, Lt	AFIT (MCLI) Wright-Patterson AFB, Ohio
Bucknall, Prof. E. H.	Dept of Mechanical Eng, University of Texas, Austin 12, Texas
Budiansky, Dr. B.	Div of Eng & Applied Physics, Harvard University, Cambridge, Mass.
Bueche, Dr. A. M.	General Electric Company, Aeroscience Lab, Philadelphia, Penn.
Bull, Dr. G. V.	Dept of Mechanical Eng, McGill University, Montreal 2, P. Q., Canada
Cannon, Dr. Emerson	Utah Resch & Development Corp, Salt Lake City, Utah.
Catlin, Prof. C.	Dept of Petroleum Eng, University of Texas, Austin 12, Texas
Charters, Dr. A. C.	Ames Aeronautical Lab, Moffatt Field, Cal.
Chinn, Mr. Floyd	AFIT (MCLI), Wright-Patterson AFB, Ohio
Clark, Mr. D. S.	California Inst of Tech, Pasadena, Cal.
Cohen, Dr. Herbert M.	Dudley Observatory c/o AFCRL, Hanscom Field, Bedford, Mass.
Collier, Mr. K. I.	AFIT (MCLI), Wright-Patterson AFB, Ohio
Collins, Dr. R. D.	National Aeronautical and Space Administration, Washington 25, D. C.
Cook, Dr. Melvin	Explosives Resch Lab, University of Utah, Salt Lake City, Utah
Crandal, Dr. S.	Dept of Mech Eng, MIT, Cambridge 39, Mass.
Creel, Mr. Ralph	Bureau of Naval Weapons, Washington 25, D. C.
Crowley, Mr. J.	Office of Naval Resch, Washington 25, D. C.
Curtis, Dr. John	General Motors, Santa Barbara, Cal.
Czys, Mr. Paul	ASD (ASTEAH-1), Wright-Patterson AFB, Ohio
Dalton, Mr. D. D.	Corning Glass Works, Corning, N. Y.
D'Andrea, Mr. J. B.	ASD (ASTES), Wright-Patterson AFB, Ohio
Daniels, Mr. J.	Army Ordnance Missile Cmd, Redstone Arsenal, Huntsville, Ala.
Davids, Dr. Norman	Dept of Engineering Mechanics, Pennsylvania State University, State College, Penn.

Davies, Mr. Charles A. Davis, Major E.	ASD (RRIN), Wright-Patterson AFB, Ohio Office of Aerospace Resch (RROSA), Washington 25, D.C.
Davison, Mr. Elmer H.	National Aeronautical and Space Administration, Washington 25, D.C.
DeGraff, Mr. Raymond DeHart, Dr. R. C. Denke, Mr. Paul Dillon, Dr. O. Doran, Dr. Donald G.	AFSC (SC1AA) Bolling AFB, D.C. Southwest Resch Inst, San Antonio 6, Texas Douglas Airplane Company, Inc. Long Beach, Cal. Johns Hopkins University, Baltimore, Md. Stanford Resch Inst, Stanford University, Menlo Park, Cal.
Dorn, Dr. John E. Dow, Dr. N.	University of California, Berkeley, Cal. MSVD, Space Sciences Lab, General Electric Company, Valley Forge Space Tech Center, King of Prussia, Pennsylvania
Drucker, Dr. D. Drucker, Prof. Dan Dublin, Dr. M. Dudas, Mr. D. Duff, Dr. Durelli, Dr. A. J. Duvall, Dr. George	Cornell University, Ithaca, N. Y. Div of Eng, Brown University, Providence, R. I. AFCRL, Hanscom Field, Bedford, Mass. APGC (ASD Det 4), Eglin AFB, Florida Los Alamos Scientific Lab, Los Alamos, N. M. Catholic University, Washington, D. C. Stanford Resch Inst, Stanford University, Menlo Park, Cal.
Dyer, Dr. Ira	Bolt, Beranek, and Newman, Inc., Cambridge, Mass.
Edwards, Mr. H. Ericksen, Dr. J. L.	Vought Astronautics, Dallas, Texas Dept of Mechanics, Johns Hopkins University, Baltimore, Md.
Eringen, Dr. Cemal	School of Aeronautical and Eng Science, Purdue University, Lafayette, Indiana
Ernsberger, Mr. F. M.	Pittsburgh Plate Glass Co., One Gateway Center, Pittsburgh 22, Penn.
Eubanks, Dr. R.	Armour Resch Found, Illinois Inst of Tech, Chicago 16, Ill.
Filbey, Dr. Gordon	Dept of Mechanics, University of Pennsylvania, Philadelphia, Penn.
Florence, Dr. Alexander	Stanford Resch Inst, Stanford University, Menlo Park, California
Fowles, Mr. G. R.	Stanford Resch Inst, Stanford University, Menlo Park, California
Freitag, Capt. R. F.	Bureau of Naval Weapons, Washington 25, D. C.

Freudenenthal, Prof. A. M. Fuller, Dr. J. R.	Columbia University, New York City, N. Y. Boeing Company, Seattle, Washington
Garrick, Dr. I. E. Gehring, Mr. J. W. Gethine, Mr. Gordon L.	NASA Langley, Langley Field, Va. General Motors, Santa Barbara, Cal. General Dynamics/Convair, 3165 Pacific Highway, San Diego 12, Cal.
Gilman, Prof. J. J. Glass, Dr. Coy Goland, Mr. Martin Goldsmith, Dr. Werner	Brown University, Providence 12, R. I. Aberdeen Proving Ground, BRL, Aberdeen, Md. Southwest Resch Inst, San Antonio 6, Texas Dept of Mech Eng, University of California, Berkeley, Cal.
Griggs, Dr. Dave Griswold, Maj Truman	University of California, Los Angeles 24, Cal. AFSC (SC1AA) Bolling AFB, D. C.
Harwood, Mr. J. J. Head, Mr. A. L. Henricks, Mr.	ONR, Dept of the Navy, Washington, D. C. Chance-Vought Corporation, Dallas 22, Texas Army Ordnance Missile Command, Redstone Arsenal, Huntsville, Ala.
Henriques, Dr. F. C. Herrmann, Dr. Walter	Technical Operations Inc., Burlington, Mass. Aeroelastic and Structures Resch Lab, Dept of Aeronautics and Astronautics, MIT, Cambridge, Mass.
Hickmott, Mr. Robert L. Hirschfelder, Dr. J.	ASD (ASRCPR-1), Wright-Patterson AFB, Ohio Dept of Chem, University of Wisconsin, Madison, Wisc.
Hobbs, Dr. Norman Hoffmann, Mr. N. R. Holma, Mr.	AviDyne Resch, Inc., Burlington, Mass. ASD (ASNGD), Wright-Patterson AFB, Ohio Army Ordnance Missile Cmd, Redstone Arsenal, Huntsville, Ala.
Hook, Mr. R. E. Hsiao, Dr. C. C.	ASD (ARZ), Wright-Patterson AFB, Ohio Dept of Aeronautical Eng, University of Minne- sota, Minneapolis, Minn.
Hughes, Prof. D. S.	Dept of Physics, University of Texas, Austin 12, Texas
Hung, Dr. F. C.	North American Aviation, Inc., Space and Infor- mation Systems Div, Downey, Cal.
Irwin, Dr. George	Mechanical Div, Naval Resch Lab, Washington 25, D. C.
Jones, Dr. A. H.	Dept of Aeronautics and Astronautics, MIT, Cambridge, Mass.
Jones, Dr. O. E. Jordon, Mr. P. F.	Sandia Corporation, Albuquerque, N. M. The Martin Company, Baltimore 3, Md.

Ju, Dr. F.	Dept of Mech Eng, New Mexico University, Albuquerque, N. M.
Kaechle, Mr. L. E.	RAND Corporation, Santa Monica, Cal.
Kennard, Mr. D. C., Jr.	ASD (ASTE), Wright-Patterson AFB, Ohio
Kerper, Mr. Matthew	National Bureau of Standards, Washington, D. C.
Kies, Mr. J.	Naval Resch Lab, Washington 25, D. C.
Kinard, Mr. W. H.	NASA, Langley Resch Center, Langley Field, Va.
Kineke, Mr. J. H., Jr.	BRL, Aberdeen Proving Ground, Aberdeen, Md.
Knodel, Mr. D.	Allied Resch Associates, Boston 15, Mass.
Kolsky, Prof. H.	Brown University, Providence 12, R. I.
Kornhauser, Dr. M.	Missile and Ordnance Dept, General Electric Company, Philadelphia, Penn.
Kroman, Dr.	Martin Corporation, Baltimore, Md.
Kuo, Dr. Shan S.	Yale University, New Haven, Conn.
Laidlan, Dr. W. R.	North American Aviation, Inc., Space and Information Systems Div, Downey, Cal.
Lampert, Dr. Seymour	Aeromechanics Aeronutronic, A Div of Ford, Ford Road, Newport Beach, Cal.
Lee, Mr. E. H.	Brown University, Providence, R. I.
Levino, Mr. R. F.	Frankfort Arsenal, Philadelphia, Penn.
Lewis, Prof.	AFIT (Physics Dept), Wright-Patterson AFB, Ohio
Lieblein, Mr. Si	Flow Processes Branch, NASA Lewis Resch Center, Cleveland 35, Ohio
Lin, Dr. Hua	Boeing Company, Seattle 24, Washington
Lindberg, Mr. Herbert L.	Stanford Resch Inst, Stanford University, Menlo Park, Cal.
Lindsey, Mr. Frank	NASA, Langley Resch Center (SRD), Langley AFB, Va
Lipsitt, Dr. H. A.	ASD (ARZ), Wright-Patterson AFB, Ohio
Liu, Dr. H. W.	Firestone Flight Sciences Lab. California Inst of Tech, Pasadena, Cal.
Lowry, Maj E.	Hq USAF (AFRDR), Washington 25, D. C.
Lucey, Dr. Frank Allen	General Electric, Valley Forge, Penn.
Lulejian, Col N.	SSD AF Unit Post Office, Los Angeles 45, Cal.
Lundergan, Dr. C. D.	Sandia Corporation, Albuquerque, N. M.
Lunn, Miss Rose	North American Aviation, Inc., International Airport, Los Angeles 45, Cal.
Mahaffey, Mr. P. T.	General Dynamics/Fort Worth, Forth Worth, Texas
Mar, Prof. J.	Dept of Aeronautics and Astronautics, MIT, Cambridge, Mass.
Martin, Mr.	Watertown Arsenal, Watertown 12, Mass.

Matlock, Prof. Hudson	Dept of Civil Eng, University of Texas, Austin 12, Texas
Mazelsky, Mr. Boenard	Aerospace Resch Associates, West Covina, Cal.
McClintock, Dr.	Massachusetts Inst of Tech, Cambridge, Mass.
McGarry, Mr. F. J.	Massachusetts Inst of Tech, Cambridge, Mass.
Meshejian, Mr. John M.	The Hayes Corporation, Birmingham, Ala.
Meyerott, Dr. R. E.	Lockheed, Missile and Space Company, Palo Alto, Cal.
Miklowits, Mr. Julius	Div of Eng, California Inst of Tech, Pasadena, Cal.
Mindlin, Mr. R. D.	Columbia University, New York City, N. Y.
Mirourty, Mr. M. L.	McDonnell Aircraft Corporation, Municipal Airport, St. Louis 66, Mo.
Munson, Dr. D. E.	Sandia Corporation, Albuquerque, N. M.
Nash, Dr.	University of Florida, Gainesville, Fla.
Nadler, Maj M. R.	AFSWC (BSRV), Kirtland AFB, N. M.
Olshaker, Mr. A. E.	The RAND Corporation, Santa Monica, Cal.
Orowan, Mr. E.	Massachusetts Inst of Tech, Cambridge, Mass.
Onat, Prof. E. T.	Brown University, Providence 12, R. I.
Pao, Mr. C. L.	ASD (ASRMDD-23), Wright-Patterson AFB, Ohio
Papirno, Mr. Ralph	New York University, New York City, N. Y.
Partridge, Dr. W. S.	Utah Resch and Development Corporation, Salt Lake City, Utah
Pearson, Mr. John	Detonation Physics Grp, USNOTS, China Lake, Cal.
Percy, Dr. John	Aeroelastic and Structures Resch Lab, Dept of Aeronautics and Astronautics, MIT, Cambridge, Mass.
Pernini, Mr.	Armour Resch Foundation, Chicago, Ill.
Pfeifer, Mr. Jim	AFSC (SC TLS), Bolling AFB, D. C.
Pian, Prof	Dept of Aeronautics and Astronautics, MIT, Cambridge, Mass.
Pines, Mr. S.	Republic Aviation Corp, Resch and Development Div, Farmingdale, Long Island, N. Y.
Plass, Dr. H. J.	Dept of Mechanics, University of Texas, Austin, Texas
Pond, Prof. Robert B.	Johns Hopkins University, Baltimore, Md.
Poulter, Dr. T. C.	Stanford Resch Inst, Stanford University, Menlo Park, Cal.
Prager, Mr.	Brown University, Providence, R. I.

Preston, Dr. R. G.	Weapon Effects, Lawrence Radiation Lab, University of California, Livermore, Cal.
Prickett, Col D. I.	AFSWC (SWR), Kirtland AFB, N. M.
Promisel, Mr. N. E.	Bureau of Naval Weapons, Dept of the Navy, Washington, D. C.
Pugh, Dr. E. M.	Carnegie Inst of Tech, Pittsburgh, Penn.
Radkowski, Mr. Peter P.	Applied Mechs Section, Eng Dept, AVCO, Wilmington, Mass.
Regier, Mr. A.	National Aeronautical and Space Administra- tion, Langley Field, Va.
Reichert, Mr. C. E.	ASD (ASTE), Wright-Patterson AFB, Ohio
Rinehart, Dr. John S.	Colorado School of Mines, Golden, Colo.
Rish, Dr. F. L.	Dept of Structural Mechanics, North American Aircraft, Downey, Cal.
Roberts, Mr. W.	Northrop Corporation NORAIR Div, Hawthorne, Cal.
Rodden, Dr. William	Aerospace Corporation, El Segundo, Cal.
Rodriguez, Dr. David	Aeronutronic, A Div of Ford, Ford Road, Newport Beach, Cal.
Rogers, Mr. Randall L.	Springfield Armory, Springfield 21, Mass.
Rolsten, Dr. R. F.	Materials Lab, General Dynamics, Astronautics Div, San Diego, Cal.
Rosche, Mr. M.	National Aeronautics and Space Administra- tion, Washington 25, D. C.
Sachs, Dr. Donald	Aeronutronic, A Div of Ford, Ford Road, Newport Beach, Cal.
Salzberg, Mr. Leo F.	Physics Lab, ASD (ASRCP), Wright- Patterson AFB, Ohio
Schapery, Dr. R. A.	School of Aeronautical and Eng Sciences, Purdue University, Lafayette, Ind.
Scherrer, Mr. Victor E.	Technical Operations, Inc., Burlington, Mass.
Schjelderup, Dr. H. C.	National Engineering Science Company, Pasadena, Cal.
Schmid, Mr. C. J.	ASD (ASRMDS-11), Wright-Patterson AFB, Ohio
Scully, Dr. Charles N.	Aerospace Labs, North American Aviation, Inc., Downey, Cal.
Silk, Col J	AFSC (SCT), Bolling AFB, D. C.
Silverstein, Dr. A.	NASA Lewis Resch Center, Cleveland, Ohio
Singer, Mr. David	Aerospace Corporation, Los Angeles 45, Cal.
Singer, Lt/Col S.	DASA, Washington, D. C.
Smith, Dr. P.	Bolt, Beranek & Newman, Inc. Cambridge, Mass.
Smith, Mr. R.	ASD (ASTEAH-1), Wright-Patterson AFB, Ohio



Snyder, Mr. John	DASA, Washington, D. C.
Soelnger, Mr. E. E.	ASD (RRLN), Wright-Patterson AFB, Ohio
Sperrazza, Dr.	Ballistic Resch Labs, Aberdeen, Md.
Sternberg, Mr. E.	Brown University, Providence 12, R. I.
Stoker, Dr. J. J.	Institute of Mathematical Sciences, New York University, New York 3, N. Y.
Stroh, Dr. Allen N.	Dept of Mech Eng, MIT, Cambridge, Mass.
Summers, Dr. James L.	NASA Ames Research Center, Moffett Field, Cal.
Swedlow, Mr. J. L.	Firestone Flight Science Lab, California Inst of Tech, Pasadena, Cal.
Sweet, Mr. H.	North American Aviation, Inc., International Airport, Los Angeles 45, Cal.
Swift, Mr. H. F.	Naval Resch Lab, Washington 25, D. C.
Symonds, Prof. P. S.	Brown University, Providence 12, R. I.
Teutonico, Dr. Louis	Republic Aviation Corporation, Mineola, Long Island, N. Y.
Thompson, Prof. J. N.	Dept of Civil Eng, University of Texas, Austin 12, Texas
Thompson, Prof. M. J.	Dept of Aero-Space Eng, University of Texas, Austin 12, Texas
Torda, Dr. T. Paul	Fluid Dynamics and Systems Resch, Armour Resch Foundation, Chicago 16, Ill.
Trapp, Mr. Walter	ASD (ASRCMD), Wright-Patterson AFB, Ohio
Turner, Mr. M. J.	The Boeing Company, Aero Space Div, Seattle 24, Washington
Vossler, Maj Richard	ASD (ASRCPR), Wright-Patterson AFB, Ohio
Wasley, Mr. Richard J.	Chem Div, Lawrence Radiation Lab, University of California, Livermore, Cal.
Wendt, Dr. F.	MSVD, Space Sciences Lab, General Electric Company, Valley Forge Space Tech Center, King of Prussia, Penn.
Whipple, Dr. Fred	Harvard College Observatory, Cambridge, Mass.
White, Mr. Richard	Cornell Aeronautical Lab, Inc., Buffalo 21, N. Y.
Wiederhorn, Dr. Norman	Arthur D. Little, Inc., Cambridge, Mass.
Wilkov, Dr. M.	The Pennsylvania State University, Dept of Eng Mechanics, University Park, Penn.
Williams, Dr. Max L., Jr.	California Inst of Tech, Pasadena, Cal.
Wingerson, Capt	AFIT (MCLISE), Wright-Patterson AFB, Ohio
Winslow, Mr. Paul C.	National Aeronautical and Space Administration, Washington 25, D. C.

Witmer, Dr. Emmitt

Aeroelastic and Structures Lab, MIT,  
Cambridge 39, Mass.

Wood, Mr. D.S.

California Inst of Tech, Pasadena, Cal.

Zaid, Dr. M.

Technik, Inc., Garden City, Long Island,  
N. Y.

Zisfein, Mr. M.E.

Giannini Controls Corporation, Berwyn,  
Penn.

List of Registrants \*  
Symposium on Dynamic Behavior of Materials

Civil Engineering Department  
of  
University of New Mexico  
AND  
Rocky Mountain District  
American Society for Testing and Materials

Abbott, J. L.	USNWEF, Albuquerque, N. M.
Adam, H. P.	Douglas Aircraft Co., Santa Monica, Cal.
Adams, C. H.	Monsanto Chemical Co., Kirkwood 22, Missouri
Anderson, Brooke H.	Sandia Corporation, Albuquerque, N. M.
Arnold, Vernon E.	Sandia Corporation, Albuquerque, N. M.
Atkinson, Richard H.	Kirtland AFB, Albuquerque, N. M.
Aungst, R. C.	General Electric Co., Richland, Wash- ington
Austin, Arthur L.	Lawrence Radiation Lab., Berkeley, Cal.
Bailey, F. W.	Phillips Petroleum Co., Bartlesville, Okla.
Barba, Peter M.	Sandia Laboratory, Albuquerque, N. M.
Barker, Lynn M.	Sandia Corporation, Albuquerque, N. M.
Barton, James R.	University of New Mexico, Albuquerque, N. M.
Bass, Robert C.	Sandia Corporation, Albuquerque, N. M.
Becker, H.	Allied Resch Assoc., Aracon Labs, Boston, Mass.
Bild, Charles E.	Sandia Corporation, Albuquerque, N. M.
Black, J. T., Jr.	Sandia Corporation, Albuquerque, N. M.
Blincon, Donald W.	Boeing Co., Kent, Washington
Bobb, Franklin C.	Continental Can Co., Dolton, Ill.
Brinkman, George H.	Chemstrand Co., Gulf Breeze, Fla.
Brooks, William P.	Sandia Corporation, Albuquerque, N. M.
Bruce, Ralph S.	Rate Eng Corp, Waltham 54, Mass.
Burdick, Neal M.	NMIMT, Socorro, N. M.
Butchin, Barry M.	Sandia Corporation, Albuquerque, N. M.
Broughton, T. M.	Tinius Olsen Testing Machine Co., Willow Grove, Pa.
Cannon, Jack R.	Sandia Corporation, Albuquerque, N. M.
Cassity, C. R.	General Electric Co., Huntsville, Ala.
Cericola, Fred	Sandia Corporation, Albuquerque, N. M.
Chavez, David J.	Sandia Corporation, Albuquerque, N. M.

\* Names present in the previous two lists have not been repeated here.

Chown, W. H.  
Coskren, Robert J.  
Cosner, R. R.

Creech, Thomas F.  
Croeni, Jack G.  
Cronin, Herbert D.  
Crugnola, A. M.

Deal, William E., Jr.

D'Arcy, Gerald P.  
DeLollis, Nicholas J.  
Deveney, Joseph E.  
Dickey, D. D.  
Doverstike, Robert O.

Dunaway, Ernest Ray  
Dunbar, George R.

Eden, Charles H.  
Elsey, P. J.  
Ely, Richard E.

Fisher, Walter E.  
Fitzgerald, Roy G.  
Frye, Eugene R.

Gay, Neil  
Giclas, Henry  
Gittings, Elizabeth F.

Godshall, W. D.

Golaski, Stanley K.

Graham, Robert A.  
Grobeck, D. W.  
Guenther, A. H.

Halpin, Walter J.  
Hamada, Lt Harold  
Hargraves, Capt W. E., II  
Hartman, William F.  
Hauser, Frank E.

Sandia Corporation, Albuquerque, N. M.  
Fabrie Resch Lab., Inc., Dedham, Mass.  
Union Carbide Corporation, South  
Charleston, W. Va.

Kansas State University, Manhattan, Kans.  
U. S. Bureau of Mines, Corvallis, Oregon  
Black & Decker Mfg. Co., Baltimore, Md.  
QM R&E Cmd, U. S. Army, Natick, Mass.

Los Alamos Scientific Lab., Los Alamos,  
N. M.

Kirtland ARB, Albuquerque, N. M.  
Sandia Corporation, Albuquerque, N. M.  
Sandia Corporation, Albuquerque, N. M.  
U. S. Geological Survey, Arvada, Colo.  
Lockheed Missile & Space Co., Sunnydale,  
Cal.

Sandia Corporation, Albuquerque, N. M.  
Sandia Corporation, Livermore, Cal.

Western Electric Co., Inc., Omaha, Neb.  
University of Utah, Salt Lake City, Utah  
Army Missile Cmd, Huntsville, Ala.

AFSWC, Albuquerque, N. M.  
Sandia Corporation, Albuquerque, N. M.  
Sandia Corporation, Albuquerque, N. M.

Rexall Chemical Company, Odessa, Texas  
NMIMT, Socorro, N. M.  
Los Alamos Scientific Lab., Los Alamos,  
N. M.

USDA Forest Products Lab., Madison,  
Wisc.

Ballistic Resch Lab., Aberdeen Proving  
Ground, Aberdeen, Md.

Sandia Corporation, Albuquerque, N. M.  
Sandia Corporation, Albuquerque, N. M.  
Air Force Special Weapons Center,  
Albuquerque, N. M.

Sandia Corporation, Albuquerque, N. M.  
Kirtland AFB, Albuquerque, N. M.  
Kirtland AFB, Albuquerque, N. M.  
Sandia Corporation, Albuquerque, N. M.  
University of California, Berkeley, Cal.

Haycock, David A.  
Healy, William L.  
Herzog, Earl T.  
Hess, R. E.  
Hof, Gerrit J.  
Holmes, Harry R.  
Holland, J. Read

Ipson, Tom W.

Jackson, R. G.  
Jaffe, Edwin H.

Jacques, Charest  
Jahsman, H. E.  
Jeffers, Sam L.  
Johnson, Joe E.  
Johnson, Phillip C.

Kanipe, James F.  
Karnes, Charles H.  
Krieg, Raymond D.  
Kuchkuda, Roman W.

Lamberson, Donald L.  
Lacey, Robert M.  
LaMar, Frank W.  
Lang, Herman A.  
Lang, H. M.

Lepper, Kay K.  
Lindberg, Herbert E.  
Loree, Thomas R.

Mackay, Harold A.  
Malvern, L. E.

Marks, Robert E.

Marozick, R. B.

Marshall, T. A., Jr.  
Martinez, Jose E.  
Massengill, Earl B.

Kirtland AFB, Albuquerque, N. M.  
ASA, Arlington, Va.  
Sandia Corporation, Albuquerque, N. M.  
ASTM, Philadelphia, Pa.  
Sandia Corporation, Albuquerque, N. M.  
Sandia Corporation, Albuquerque, N. M.  
Sandia Corporation, Albuquerque, N. M.

University of Denver, Denver, Colo.

ACF Industries, Albuquerque, N. M.  
Aeronutronic Div., Ford Motor Co.,  
Costa Mesa, California  
Colorado School of Mines, Golden, Colo.  
Lockheed, Palo Alto, Cal.  
Sandia Corporation, Albuquerque, N. M.  
Kirtland AFB, Albuquerque, N. M.  
Arthur D. Little, Inc., Cambridge, Mass.

Kirtland AFB, Albuquerque, N. M.  
Texas University, Austin, Texas  
Sandia Corporation, Albuquerque, N. M.  
Celanese Polymer Co., Clark, N. J.

Kirtland AFB, Albuquerque, N. M.  
Sandia Corporation, Albuquerque, N. M.  
Bendix Corp., Kansas City, Mos.  
Aerospace Corp., El Segundo, Cal.  
Pan American Petroleum Corp.,  
Tulsa, Okla.  
University of California, Livermore, Cal.  
Stanford Resch Inst, Sunnydale, Cal.  
Los Alamos Scientific Lab., Los  
Alamos, N. M.

Sandia Corporation, Albuquerque, N. M.  
Michigan State University, East Lansing,  
Mich.

Lawrence Radiation Lab., Livermore,  
Cal.

Autonetic, Div. of N. A. A., Anaheim,  
Cal.

ASTM, Philadelphia, Pa.  
University of New Mexico, Albuquerque, N. M.  
U. S. Naval Weapons Evaluation Facility,  
Kirtland AFB, Albuquerque, N. M.

Mathews, Floyd H.	Sandia Corporation, Albuquerque, N. M.
Matsuoka, Shiro	Bell Telephone Lab., Millington, N. J.
Mauldin, Winford E.	Kirtland AFB, Albuquerque, N. M.
Markle, Lt D. H.	Kirtland AFB, Albuquerque, N. M.
McLain, John	NMIMT, Socorro, N. M.
Mebs, E. H.	Sandia Corporation, Albuquerque, N. M.
Milton, Osborne	Sandia Corporation, Albuquerque, N. M.
Misey, John J.	Ballistic Resch Lab., Baltimore, Md.
Moll, Robert E.	Sandia Corporation, Albuquerque, N. M.
Monsees, James E.	Kirtland AFB, Albuquerque, N. M.
Montgomery, Richard D.	West Virginia Pulp & Paper, Covington, Pa.
Murray, Mrs. Margaret H.	Time, Inc., Springdale, Conn.
Nelson, William E.	Lawrence Radiation Lab., Danville, Cal.
Neuer, Lt/Col John J.	Kirtland AFB, Albuquerque, N. M.
Overmier, David K.	University of New Mexico, Albuquerque, N. M.
Palmer, Edward P.	University of Utah, Salt Lake City, Utah
Papirno, Ralph	Allied Resch Associates, Concord, Mass.
Patterson, Gordon D., Jr.	E. I. DuPont de Nemours, Wilmington, Dela.
Potteiger, Lester A.	U.S. Naval Weapons Lab., Dahlgren, Va.
Rainhart, L. G.	Sandia Corporation, Albuquerque, N. M.
Recht, R. F.	University of Denver, Denver, Colo.
Robertson, Albert B.	Sandia Corporation, Albuquerque, N. M.
Rohrer, J. A.	Sandia Corporation, Albuquerque, N. M.
Russell, Donald H.	Atlantic Refining Co., Philadelphia, Pa.
Sebrell, Wayne A.	Sandia Corporation, Albuquerque, N. M.
Selig, E. T.	Armour Resch Foundation, Boston, Mass.
Shafer, Barry	University of New Mexico, Albuquerque, N. M.
Shaidnagle, Robert H.	Mar-Tec Electronics Co., Downey, Cal.
Silberberg, Melvin	Plas-Tech Equip. Corp., Natick, Mass.
Singer, D. B.	Aerospace Corp., Sepulveda, Cal.
Slobodzinski, Adolp E.	Picatinny Arsenal, Dover, N. J.
Smith, Jack C.	National Bureau of Standards, Washington 25, D. C.
Smith, Jimmie H.	Sandia Corporation, Albuquerque, N. M.
Sowell, R. R.	Sandia Corporation, Albuquerque, N. M.
Spanovick, Milan	University of New Mexico, Albuquerque, N. M.
Stanton, Philip	Sandia Corporation, Albuquerque, N. M.
Stein, Barry A.	Arthur D. Little, Inc., Cambridge, Mass.
Sweet, Fred R.	Sandia Corporation, Albuquerque, N. M.

Théberge, C. L.  
Towne, Thomas L.  
Traeger, R. K.

Tsai, Stephen W.

Walter, Eugene J.  
Wagner, Walter K.

Warren, William E.

Webb, Robert S.

Weeding, Gale

Weir, F. E.

Weis, Carl G.

Wentz, J. L.

Whittier, James S.

Wilcox, Dr. Paul

Williams, I. V.

Yao, James T. P.

Young, George A.

AVCO Corp., Wilmington, Mass.

Sandia Corporation, Albuquerque, N. M.

University of New Mexico, Albuquerque,  
N. M.

Ford Motor Co., Costa Mesa, Cal.

ACF Industries, Albuquerque, N. M.

Albuquerque Gravel Products Co.,

Albuquerque, N. M.

Sandia Corporation, Albuquerque, N. M.

Marbon Chemical, Parkersburg, W. Va.

University of Denver, Denver, Colo.

Shell Development, Emeryville, Cal.

U. S. Air Force, Albuquerque, N. M.

Sandia Corporation, Albuquerque, N. M.

Aerospace Corp., El Segundo, Cal.

Sandia Corporation, Albuquerque, N. M.

Bell Telephone Lab., Westfield, N. J.

University of New Mexico, Albuquerque,  
N. M.

University of New Mexico, Albuquerque,  
N. M.

CLOSING COMMENTS BY GENERAL CHAIRMAN,  
DR. SUDHIR KUMAR

Before the Conference is closed, I would like to express my very hearty and sincere appreciation to all the speakers for having taken great pain in preparing and presenting these papers here. I hope they will forgive the planning and review committee members for their continuous reminders and my almost annoying calls to get the manuscripts to AROD in time. I hope we did not hurt anybody's feelings in being too pressing in this direction. I also would like to thank all the Chairmen and Co-Chairmen for having helped to conduct the meetings so well. I am very happy to say that the time has been kept very well too, thanks to Chairmen like Dr. Bailey. We scheduled to finish at 12:00 and we still have five minutes to go. In the end, last but not the least, the utmost gratitude is felt for all the attendees who have done so much to make this Conference an outstanding success by their presence, by active participation in the discussions of the papers and by free exchange of ideas between engineers, designers and scientists from the different Commands. Thank you very much once again, and, of course, our deepest thanks go to our host, Springfield Armory, for organizing this Conference in a most excellent manner. And now, with these few comments, I will close the U. S. Army Conference on the "Dynamic Behavior of Materials and Structures".

Thank you.